frontiers | Research Topics

Horizontal gene transfer mediated bacterial antibiotic resistance, vol II

Edited by
Dongchang Sun, Xingmin Sun, Yongfei Hu and Yoshiharu Yamaichi

Published in
Frontiers in Microbiology

ISSN 1664-8714
ISBN 978-2-8325-2953-9
DOI 10.3389/978-2-8325-2953-9

About Frontiers

Frontiers is more than just an open access publisher of scholarly articles: it is a pioneering approach to the world of academia, radically improving the way scholarly research is managed. The grand vision of Frontiers is a world where all people have an equal opportunity to seek, share and generate knowledge. Frontiers provides immediate and permanent online open access to all its publications, but this alone is not enough to realize our grand goals.

Frontiers journal series

The Frontiers journal series is a multi-tier and interdisciplinary set of open-access, online journals, promising a paradigm shift from the current review, selection and dissemination processes in academic publishing. All Frontiers journals are driven by researchers for researchers; therefore, they constitute a service to the scholarly community. At the same time, the *Frontiers journal series* operates on a revolutionary invention, the tiered publishing system, initially addressing specific communities of scholars, and gradually climbing up to broader public understanding, thus serving the interests of the lay society, too.

Dedication to quality

Each Frontiers article is a landmark of the highest quality, thanks to genuinely collaborative interactions between authors and review editors, who include some of the world's best academicians. Research must be certified by peers before entering a stream of knowledge that may eventually reach the public - and shape society; therefore, Frontiers only applies the most rigorous and unbiased reviews. Frontiers revolutionizes research publishing by freely delivering the most outstanding research, evaluated with no bias from both the academic and social point of view. By applying the most advanced information technologies, Frontiers is catapulting scholarly publishing into a new generation.

What are Frontiers Research Topics?

Frontiers Research Topics are very popular trademarks of the *Frontiers journals series*: they are collections of at least ten articles, all centered on a particular subject. With their unique mix of varied contributions from Original Research to Review Articles, Frontiers Research Topics unify the most influential researchers, the latest key findings and historical advances in a hot research area.

Find out more on how to host your own Frontiers Research Topic or contribute to one as an author by contacting the Frontiers editorial office: frontiersin.org/about/contact

Horizontal gene transfer mediated bacterial antibiotic resistance, vol II

Topic editors

Dongchang Sun — Zhejiang University of Technology, China
Xingmin Sun — University of South Florida, United States
Yongfei Hu — China Agricultural University, China
Yoshiharu Yamaichi — UMR9198 Institut de Biologie Intégrative de la Cellule (I2BC), France

Citation

Sun, D., Sun, X., Hu, Y., Yamaichi, Y., eds. (2023). *Horizontal gene transfer mediated bacterial antibiotic resistance, vol II*. Lausanne: Frontiers Media SA. doi: 10.3389/978-2-8325-2953-9

Table of contents

frontiers | Frontiers in Microbiology

TYPE Editorial
PUBLISHED 23 June 2023
DOI 10.3389/fmicb.2023.1221606

OPEN ACCESS

EDITED AND REVIEWED BY
Rustam Aminov,
University of Aberdeen, United Kingdom

*CORRESPONDENCE
Dongchang Sun
✉ sundch@zjut.edu.cn
Xingmin Sun
✉ sun5@usf.edu
Yongfei Hu
✉ huyongfei@cau.edu.cn
Yoshiharu Yamaichi
✉ yoshiharu.yamaichi@i2bc.paris-saclay.fr

RECEIVED 12 May 2023
ACCEPTED 30 May 2023
PUBLISHED 23 June 2023

CITATION
Sun D, Sun X, Hu Y and Yamaichi Y (2023) Editorial: Horizontal gene transfer mediated bacterial antibiotic resistance, volume II. *Front. Microbiol.* 14:1221606. doi: 10.3389/fmicb.2023.1221606

Editorial: Horizontal gene transfer mediated bacterial antibiotic resistance, volume II

Dongchang Sun[1]*, Xingmin Sun[2]*, Yongfei Hu[3]* and Yoshiharu Yamaichi[4]*

[1]College of Biotechnology and Bioengineering, Zhejiang University of Technology, Hangzhou, China, [2]Department of Molecular Medicine, Morsani College of Medicine, University of South Florida, Tampa, FL, United States, [3]State Key Laboratory of Animal Nutrition, College of Animal Science and Technology, China Agricultural University, Beijing, China, [4]Université Paris-Saclay, CEA, CNRS, Institute for Integrative Biology of the Cell (I2BC), Gif-sur-Yvette, France

KEYWORDS

horizontal gene transfer (HGT), bacterial antibiotic resistance, antibiotic resistance genes (ARGs), plasmid, bacterial conjugation, mobile genetic elements (MGEs)

Editorial on the Research Topic
Horizontal gene transfer mediated bacterial antibiotic resistance, volume II

The issue of bacterial antibiotic resistance (BAR) has reached an alarming level in recent years. In 2019 alone, BAR was responsible for the deaths of approximately five million people globally, making it the third leading cause of death (Antimicrobial Resistance Collaborators, 2022). This figure surpasses the previous estimation (WHO, 2014), highlighting the severity of the situation. Bacteria can easily transfer antibiotic resistance genes (ARGs) through horizontal gene transfer (HGT), which can promote the development and spread of resistance within the bacterial population (Sun et al., 2019). Ten publications have recently been published on the topic of "Horizontal Gene Transfer Mediated Bacterial Antibiotic Resistance II," presenting the latest findings and advancements in this field. These publications could serve as new reference points to tackle BAR in the future.

In this Research Topic, three reports (Xin et al.; Zhang S. et al.; Yang et al.) demonstrated the high prevalence of ARGs in different regions of China, revealing the serious challenge of BAR in the country. By evaluating 4, 414 strains of enterococci from hospitals in 26 provinces in China, Xin et al. demonstrated the wide distribution of the fosfomycin resistance gene *fosX* in *E. faecium*, a human pathogen responsible for gastrointestinal tract infections. ARGs *tet(X)*, *bla*, and *mcr* threaten the efficacy of tigecycline, carbapenems, and colistin, which represent the three last-resort antibiotics. Zhang S. et al. summarized the distribution of *tet(X)* genes in China and demonstrated the presence of *tet(X)* genes in 24 provinces. Remarkably, *tet(X)* genes were identified not only in humans, livestocks, poultries and aquatic animals but also in wild animals and the environment, reflecting the fast spread of this ARG in the wild in China. Yang et al. reported not only the presence of bla_{NDM-5} and *mcr-8.1* in an animal breeding area in eastern China but also the clonal transfer of the two ARGs and their potential dissemination through horizontal gene transfer. These studies highlight the urgency of taking action to combat BAR in China.

Although observational studies have manifested the present situation of BAR, our understanding of this issue largely relies on retrospective analysis. A review article in this Research Topic summarized the recent progress of *in silico*, *in vitro*, and *in vivo* modeling of HGT, providing new perspectives and directions on understanding the plasmid-mediated transfer of ARGs in the gut of animals (Ott and Mellata). In nature, ARGs are often disseminated by vehicles (e.g., plasmid) and mobile genetic elements (MGEs). Guzman-Otazo et al. found that IncN plasmids can transmit ARGs via conjugation from environmental waterborne bacteria to *Escherichia coli*, which colonizes in the intestine of terrestrial animals, enabling the spread of ARGs across aquatic and terrestrial environments. Integrative and conjugative elements (ICEs) and integrons are MGEs that mediate the dissemination of ARGs. Two studies in this Research Topic investigated the roles of ICEs and integrons in facilitating the spread of ARGs. Through whole-genome analysis of 27 multidrug-resistant (MDR) *Proteus* strains, Li Y. et al. revealed that nine ICEs shared a common backbone structure, implicating the dissemination of ICEs in *Proteus* strains from livestocks and poultries and humans. Their study also revealed that ARGs were carried by MGEs of genetic diversity, highlighting the necessity of continuous monitoring. Bitar et al. analyzed 32 VIM metallo-β-lactamase producing Enterobacterales from Czech hospitals, and sequenced 19 isolates. Their work revealed that the spread of VIM-encoding integron In110 was more prevalent than other VIM-encoding integrons and that many new ARGs-carrying MGEs could be evolving.

Compared with that in non-pathogenic bacteria, the transfer of ARGs in pathogens is more threatening. Two studies in this Research Topic showed that the impact of HGT on the evolution of pathogens could be species-specific. Li P. et al. reported that outer membrane vesicles were able to incorporate DNA and deliver both virulence and antimicrobial-resistant plasmids. Their work provides new evidence supporting that HGT plays an important role in facilitating the evolution of carbapenem-resistant hypervirulent *Klebsiella pneumonia*. Whereas, Kandinov et al. discovered that the plasmid expressing $bla_{\mathrm{TEM-20}}$ reduced the viability of *Neisseria gonorrhoeae*. This could result from the expression of extended-spectrum β-lactamase, which may affect the structure of the peptidoglycan layer, providing an explanation for the absence of clinical isolates of extensive spectrum beta-lactamase-producing *N. gonorrhoeae*. Investigation of the transfer of ARGs in pathogens would not only explain co-evolutionary relationships between resistance and virulence but also provide guidance for the clinical use of antibiotics.

To be stably inherited, horizontally transferred ARGs need to be maintained in either a plasmid or the genome of the recipient bacteria through genetic recombination. Zhang G. et al. characterized an integrase of genomic island GI*sul2*, which mediated the integration of MGEs through site-specific recombination in *Shigella flexneri*. They found that GI*sul2* can excise and integrate GI*sul2* and the IS*CR*-related element CR2-*sul2* unit by site-specific recombination between the host chromosomal attachment sites, suggesting a potential role of GI*sul2* integrase homologs in the dissemination of GI*sul2* units.

In summary, articles of this Research Topic demonstrated the prevalence of ARGs, diverse mechanisms of transfer of ARGs under different settings, and novel ways of integration of MGEs carrying ARGs. Although remarkable advances in the knowledge of the dissemination of ARGs have been made in recent years, we still know little about associations between environmental cues and the HGT-driven spread of ARGs under different environmental conditions. More importantly, despite the severity of BAR being more serious than estimated, there is a lack of effective strategies to tackle this problem. To address this global crisis, collaboration among different fields from countries all over the world remains in high demand.

We would like to acknowledge all participating authors for their contributions, reviewers for their constructive comments, and our editorial team members for their great efforts.

Author contributions

All authors participated in editing manuscripts in this Research Topic, reviewed, and approved the final version of the editorial.

Conflict of interest

The authors declare that the research was conducted in the absence of any commercial or financial relationships that could be construed as a potential conflict of interest.

Publisher's note

References

Antimicrobial Resistance Collaborators. (2022). Antimicrobial resistance, global burden of bacterial antimicrobial resistance in 2019: a systematic analysis. *Lancet*. 399, 629–655. doi: 10.1016/S0140-6736(21)02724-0

Sun, D., Jeannot, K., Xiao, Y., and Knapp, C. W. (2019). Editorial: horizontal gene transfer mediated bacterial antibiotic resistance. *Front. Microbiol.* 10:1933. doi: 10.3389/fmicb.2019.01933

WHO (2014). *Antimicrobial Resistance Global Report on Surveillance*. World Health Organization. Available online at: https://www.who.int/publications-detail-redirect/9789241564748

frontiers | Frontiers in Microbiology

ORIGINAL RESEARCH
published: 20 June 2022
doi: 10.3389/fmicb.2022.896607

In vitro Susceptibility to β-Lactam Antibiotics and Viability of *Neisseria gonorrhoeae* Strains Producing Plasmid-Mediated Broad- and Extended-Spectrum β-Lactamases

Ilya Kandinov[1], Dmitry Gryadunov[1], Alexandra Vinokurova[1], Olga Antonova[1], Alexey Kubanov[2], Victoria Solomka[2], Julia Shagabieva[2], Dmitry Deryabin[2] and Boris Shaskolskiy[1]*

[1]Center for Precision Genome Editing and Genetic Technologies for Biomedicine, Engelhardt Institute of Molecular Biology, Russian Academy of Sciences, Moscow, Russia, [2]State Research Center of Dermatovenerology and Cosmetology, Russian Ministry of Health, Moscow, Russia

OPEN ACCESS

Edited by:
Dongchang Sun, Zhejiang University of Technology, China

Reviewed by:
Asad U. Khan, Aligarh Muslim University, India
Roberto Gustavo Melano, Public Health Ontario, Canada
Hui Lin, Zhejiang Academy of Agricultural Sciences, China

***Correspondence:**
Ilya Kandinov
ilya9622@gmail.com

Specialty section:
This article was submitted to Antimicrobials, Resistance and Chemotherapy, a section of the journal Frontiers in Microbiology

Received: *15 March 2022*
Accepted: *01 June 2022*
Published: *20 June 2022*

Citation:
Kandinov I, Gryadunov D, Vinokurova A, Antonova O, Kubanov A, Solomka V, Shagabieva J, Deryabin D and Shaskolskiy B (2022) In vitro Susceptibility to β-Lactam Antibiotics and Viability of Neisseria gonorrhoeae Strains Producing Plasmid-Mediated Broad- and Extended-Spectrum β-Lactamases. Front. Microbiol. 13:896607. doi: 10.3389/fmicb.2022.896607

Neisseria gonorrhoeae plasmids can mediate high-level antimicrobial resistance. The emergence of clinical isolates producing plasmid β-lactamases that can hydrolyze cephalosporins, the mainstay treatment for gonorrhea, may be a serious threat. In this work, *N. gonorrhoeae* strains producing plasmid-mediated broad- and extended-spectrum β-lactamases (ESBLs) were obtained *in vitro*, and their viability and β-lactam antibiotic susceptibility were studied. Artificial p*bla*$_{TEM-1}$ and p*bla*$_{TEM-20}$ plasmids were constructed by site-directed mutagenesis from a p*bla*$_{TEM-135}$ plasmid isolated from a clinical isolate. Minimum inhibitory concentration (MIC) values for a series of β-lactam antibiotics, including benzylpenicillin, ampicillin, cefuroxime, ceftriaxone, cefixime, cefotaxime, cefepime, meropenem, imipenem, and doripenem, were determined. The *N. gonorrhoeae* strain carrying the p*bla*$_{TEM-20}$ plasmid exhibited a high level of resistance to penicillins and second–fourth-generation cephalosporins (MIC ≥2 mg/L) but not to carbapenems (MIC ≤0.008 mg/L). However, this strain stopped growing after 6 h of culture. The reduction in viability was not associated with loss of the plasmid but can be explained by the presence of the plasmid itself, which requires additional reproduction costs, and to the expression of ESBLs, which can affect the structure of the peptidoglycan layer in the cell membrane. Cell growth was mathematically modeled using the generalized Verhulst equation, and the reduced viability of the plasmid-carrying strains compared to the non-plasmid-carrying strains was confirmed. The cell death kinetics of *N. gonorrhoeae* strains without the p*bla*$_{TEM-20}$ plasmid in the presence of ceftriaxone can be described by a modified Chick–Watson law. The corresponding kinetics of the *N. gonorrhoeae* strain carrying the p*bla*$_{TEM-20}$ plasmid reflected several processes: the hydrolysis of ceftriaxone by the TEM-20 β-lactamase and the growth and gradual death of cells. The demonstrated reduction in the viability of *N. gonorrhoeae* strains carrying the p*bla*$_{TEM-20}$ plasmid probably explains the absence of clinical isolates of ESBL-producing *N. gonorrhoeae*.

Keywords: *Neisseria gonorrhoeae*, β-lactamase-producing plasmids, *N. gonorrhoeae* viability, extended-spectrum β-lactamase, antimicrobal susceptibility

INTRODUCTION

The development of multidrug resistance in the pathogen *Neisseria gonorrhoeae* is a major problem worldwide. According to the World Health Organization (WHO), gonorrhea may become incurable due to the ineffectiveness of old antimicrobials and the lack of new drugs for its treatment (Tacconelli et al., 2018; Golparian and Unemo, 2022).

Currently, and possibly in future, antibiotics of the β-lactam group are the preferred drugs for treating gonococcal infection (Workowski and Bolan, 2015; WHO, 2016; Tacconelli et al., 2018; Unemo et al., 2020). This group of antibiotics includes the penicillin, cephalosporin, carbapenem, and monobactam classes. The mode of action of β-lactam antibiotics is to disrupt the synthesis of the peptidoglycan layer in bacterial cell walls, leading to bacterial cell death. In the mid-1940s, the discovery of the penicillins started a revolution in the treatment of gonococcal infection, and penicillins became the gold standard of treatment, resulting in cure after a single injection. However, by the end of the 20th century, most clinical isolates of *N. gonorrhoeae* showed reduced susceptibility or resistance to penicillins; thus, the use of penicillins was discontinued (Unemo and Shafer, 2014; Unemo and Jensen, 2017).

Currently, the preferred drugs for the treatment of gonococcal infections include another class of β-lactams—third-generation cephalosporins, i.e., ceftriaxone, cefotaxime and cefixime, which are used alone or in combination with the macrolide antibiotic azithromycin (Workowski and Bolan, 2015; WHO, 2016; Tacconelli et al., 2018; Unemo et al., 2020). However, the levels of gonococcal resistance to cephalosporins are increasing annually, and treatment failure with these drugs has already been reported in several countries (Unemo et al., 2012; Allen et al., 2013; Golparian et al., 2014; Attram et al., 2019). The next class of β-lactams that could replace cephalosporins if cephalosporin resistance spreads is the carbapenems (Unemo et al., 2020).

The resistance of *N. gonorrhoeae* to β-lactam antibiotics is associated with both chromosomal and plasmid determinants. Chromosomal mutations include substitutions in penicillin-binding proteins 1 and 2 (PBP1 and PBP2), mutations in the porin protein PorB that lead to a change in cell membrane permeability, and mutations that cause an increase in the expression level of the MtrCDE efflux pump (Unemo and Shafer, 2014; Unemo and Jensen, 2017; Unemo et al., 2019). In this resistance mechanism, the presence of the β-lactamase enzyme, which hydrolyzes the C-N bond in the β-lactam ring of the antibiotic and inactivates the drug, is particularly important. The proportion of *N. gonorrhoeae* clinical isolates carrying the p*bla*$_{\text{TEM}}$ plasmid is not very high; for example, in the Russian population, the percentage remains at ~5% of the total number of isolates (Kubanov et al., 2019). However, the presence of β-lactamases in gonococci causes a significant increase in the level of resistance to penicillins ($MIC_{pen} \geq 16$ mg/L) compared to that related to chromosomal mutations ($MIC_{pen} = 0.12–1.0$ mg/L; Shaskolskiy et al., 2019; Młynarczyk-Bonikowska et al., 2020). To date, clinical isolates of *N. gonorrhoeae* have been identified to produce only enzyme variants that are broad-spectrum β-lactamases (penicillinases), which cannot hydrolyze cephalosporins or carbapenems.

The following types of p*bla*$_{\text{TEM}}$ plasmids have been identified in gonococci: Asian (7,426 bp), African (5,599 bp), Toronto/Rio (5,154 bp), Nimes (6,798 bp), New Zealand (9,309 bp), Johannesburg (4,865 bp) and Australian (3,269 bp; Müller et al., 2011). The plasmid-encoded *bla* gene has a length of 861 bp. Most penicillinase-producing isolates of *N. gonorrhoeae* carry the plasmid containing the *bla*$_{\text{TEM-1}}$ gene, but recently, the *bla*$_{\text{TEM-135}}$ variant has been increasingly detected in the worldwide population of *N. gonorrhoeae* (Ohnishi et al., 2010; Nakayama et al., 2012; Muhammad et al., 2014; Cole et al., 2015; Tanaka et al., 2021). The *bla*$_{\text{TEM-1}}$ gene has been found in both African and Asian plasmids, while *bla*$_{\text{TEM-135}}$ is present mainly in Toronto/Rio and Asian plasmids (Cole et al., 2015; Yan et al., 2019). *bla*$_{\text{TEM-135}}$ differs from *bla*$_{\text{TEM-1}}$ in a single-nucleotide thymine-to-cytosine substitution at codon 182 (ATG → ACG). The resulting Met182Thr mutation is located far from the enzyme active site (17 Å) in the hinge region between two β-lactamase domains and leads to stabilization of the β-lactamase structure (Orencia et al., 2001). As previously noted (Cole et al., 2015; Yan et al., 2019), the increased enzyme stability may have contributed to the persistence of the TEM-135 β-lactamase variant in the *N. gonorrhoeae* population.

A large group of enzymes are related to bacterial β-lactamases. TEM-1 and TEM-135 are class A serine β-lactamases according to the Ambler classification (Bradford, 2001; Bush and Jacoby, 2010; Tooke et al., 2019). This class also includes extended-spectrum β-lactamases (ESBLs), such as TEM-20, which can hydrolyze both penicillins and cephalosporins. The *bla* gene variant encoding the TEM-20 β-lactamase can be produced by just a single-nucleotide substitution (GGT → AGT) in the *bla*$_{\text{TEM-135}}$ gene, which results in the Gly238Ser mutation (Arlet et al., 1999; Bradford, 2001). This substitution is associated with a change in the β-lactamase conformation, which increases the flexibility of the enzyme active site; as a result, the β-lactamase gains the ability to bind cephalosporins without losing its penicillin-hydrolyzing character (Orencia et al., 2001; Yan et al., 2019). Although *N. gonorrhoeae* clinical isolates carrying the p*bla*$_{\text{TEM-20}}$ plasmid have not been found in nature, just a single change could allow gonococci to encode an ESBL, which could end the therapeutic use of third-generation cephalosporins.

The goals of this work were to construct p*bla*$_{\text{TEM}}$ plasmids that contain different variants of the *bla* gene, to produce genetically engineered *N. gonorrhoeae* strains that contain p*bla*$_{\text{TEM}}$ plasmids, to study the properties of *N. gonorrhoeae* strains transformed with these plasmids and to assess the viability and β-lactam antibiotic (penicillins, cephalosporins and carbapenems) resistance of these strains. Particular attention was placed on constructing the p*bla*$_{\text{TEM-20}}$ plasmid and studying the properties of the *N. gonorrhoeae* strain carrying this plasmid. Such a strain may express the TEM-20 β-lactamase, which can hydrolyze both penicillins and cephalosporins. Studies on laboratory mutants generated by *in vitro* mutagenesis contribute to our understanding of evolutionary pathways and enable predictions of future events.

This research will allow the assessment of risks associated with the emergence and spread of *N. gonorrhoeae* clinical isolates with resistance to third-generation cephalosporins and the possibility to further use β-lactam antibiotics to treat gonococcal infections.

MATERIALS AND METHODS

All procedures and experiments with *N. gonorrhoeae*, including transforming cells, isolating plasmid DNA, electroporating cells, culturing cells on solid media, washing cells in Petri dishes and passaging them to other dishes, counting the colonies formed and assessing the number of viable bacteria (i.e., colony-forming units, CFU), were performed as described previously (Spence et al., 2008; Dillard, 2011).

All procedures with *N. gonorrhoeae* strains including transformation, estimation of susceptibility to antimicrobials and assessment of cell viability were conducted in biological safety cabinet (BSC) of the State Research Center of Dermatovenerology and Cosmetology, Russian Ministry of Health. The BSC was equipped with SafeFAST Elite class III microbiological safety cabinet (Faster, Italy). The laboratory room and equipment were carefully sterilized after each experiment using AntiseptiX decontamination reagents (Biomedical Innovations, Russia) and a UVR-Mi bactericidal air recirculator (Biosan, Latvia). Sterilization of culture vessels and disposable microbiological accessories was performed twice after each experiment at 130°C for 30 min using an autoclave (Tuttnauer, United States).

All strains were killed by heat inactivation after the experiments. Petri dishes with cells were autoclaved at 130°C for 30 min before disposing.

Isolation of the p*bla*$_{\text{TEM-135}}$ Plasmid From a Clinical Strain of *Neisseria gonorrhoeae* With Natural Resistance to Penicillins

We used an *N. gonorrhoeae* clinical isolate from the collection of the State Scientific Center of Dermatovenerology and Cosmetology of the Ministry of Health of the Russian Federation that was obtained in 2017 from the Chuvash Republic; this isolate carried a Toronto/Rio p*bla*$_{\text{TEM-135}}$ plasmid, and the associated minimum inhibitory concentration of penicillin (MIC_{pen}) was ≥32 mg/L (Shaskolskiy et al., 2019). The clinical isolate was seeded on GC chocolate agar (Thermo Fisher Scientific, United States) supplemented with IsoVitaleX Enrichment (Becton-Dickinson, United States) and 16 mg/L benzylpenicillin (Sigma–Aldrich, United States). The dish was incubated overnight at 37°C in 5% CO_2. Formed colonies were harvested using a culture loop in 100 µl of phosphate-buffered saline (PBS). Plasmid DNA was isolated with a Monarch Plasmid Miniprep Kit/T1010 (New England Biolabs, United Kingdom). The concentration and purity of the DNA preparations were determined using a Nanodrop 2000 spectrophotometer (Thermo Fisher Scientific, United States). Plasmid DNA was analyzed by PCR as described previously (Palmer et al., 2000; Shaskolskiy et al., 2019).

Construction of Plasmids With Different Variants of the *bla* Gene on the Basis of p*bla*$_{\text{TEM-135}}$ Isolated From a Clinical *Neisseria gonorrhoeae* Strain

The *bla* gene fragment was amplified by simultaneous site-directed mutagenesis, which ensured that the mutations were introduced into the gene. The primers 5′-TTACTTCTGACAAC GATCGGAGGACCGAAGG-3′-FOR and 5′-AATGATACCGCG AGAC CCACGCTCACTGGCT-3′-REV were used to obtain a PCR-amplified fragment of the *bla* gene that harbored the GGT → AGT mutation that results in the Gly238Ser substitution and is present in the TEM-20 ESBL (**Figure 1**). A PCR fragment corresponding to the sequence of the *bla* gene that encodes the TEM-1 broad-spectrum β-lactamase was produced by a similar method.

The PCR fragments and the p*bla*$_{\text{TEM-135}}$ plasmid were digested with the restriction endonucleases PvuI and BsaI. Then, the linearized p*bla*$_{\text{TEM-135}}$ plasmid and the PCR fragments with sticky ends were treated with a ligation mixture to generate the final p*bla*$_{\text{TEM-1}}$ and p*bla*$_{\text{TEM-20}}$ plasmids. The map of the resulting p*bla*$_{\text{TEM-20}}$ plasmid is shown in **Figure 1**.

Transformation of *Escherichia coli* Cells

The ready-to-use 10-beta competent *E. coli* strain DH10B (New England Biolabs, United Kingdom) was used for plasmid transformation. The puc19 (K+) vector was used as the transformation control, and a sample without DNA was used as the negative control. Cells were grown and subsequently reseeded on selective media. Medium containing 256–512 mg/L benzylpenicillin was used for transformation of *E. coli* with the p*bla*$_{\text{TEM-135}}$ and p*bla*$_{\text{TEM-1}}$ plasmids; medium containing 64 mg/L ceftriaxone (Sigma–Aldrich, United States) was used for transformation with the p*bla*$_{\text{TEM-20}}$ plasmid.

E. coli colonies formed on the selective media were collected with a culture loop in PBS, and plasmid DNA was isolated using a Plasmid Miniprep/BC021S Kit (Evrogen, Russia). The *bla* gene sequence and p*bla*$_{\text{TEM}}$ plasmid type were confirmed by PCR and Sanger sequencing.

Transformation of *Neisseria gonorrhoeae* Cells

We used *N. gonorrhoeae* strain ATCC 49226 (F-18, CDC 10, 001, P935), a reference strain for antimicrobial susceptibility testing.[1] *Neisseria gonorrhoeae* were transformed with the p*bla*$_{\text{TEM-1}}$, p*bla*$_{\text{TEM-135}}$ and p*bla*$_{\text{TEM-20}}$ plasmids, which were purified from *E. coli* cells, by electroporation.

The optimal condition for transformation was as follows. *Neisseria gonorrhoeae* cells were collected from the overnight culture inoculum with a sterile culture loop and resuspended in 0.3 M sucrose. The cells were precipitated at 12,000 rpm and resuspended in 0.3 M sucrose, and this procedure was repeated 2–3 times. For electroporation, 100–200 µl of the purified cell suspension and 50–100 ng of plasmid DNA

[1]https://www.culturecollections.org.uk/products/bacteria/detail.jsp?refId=NCTC+12700&collection=nctc

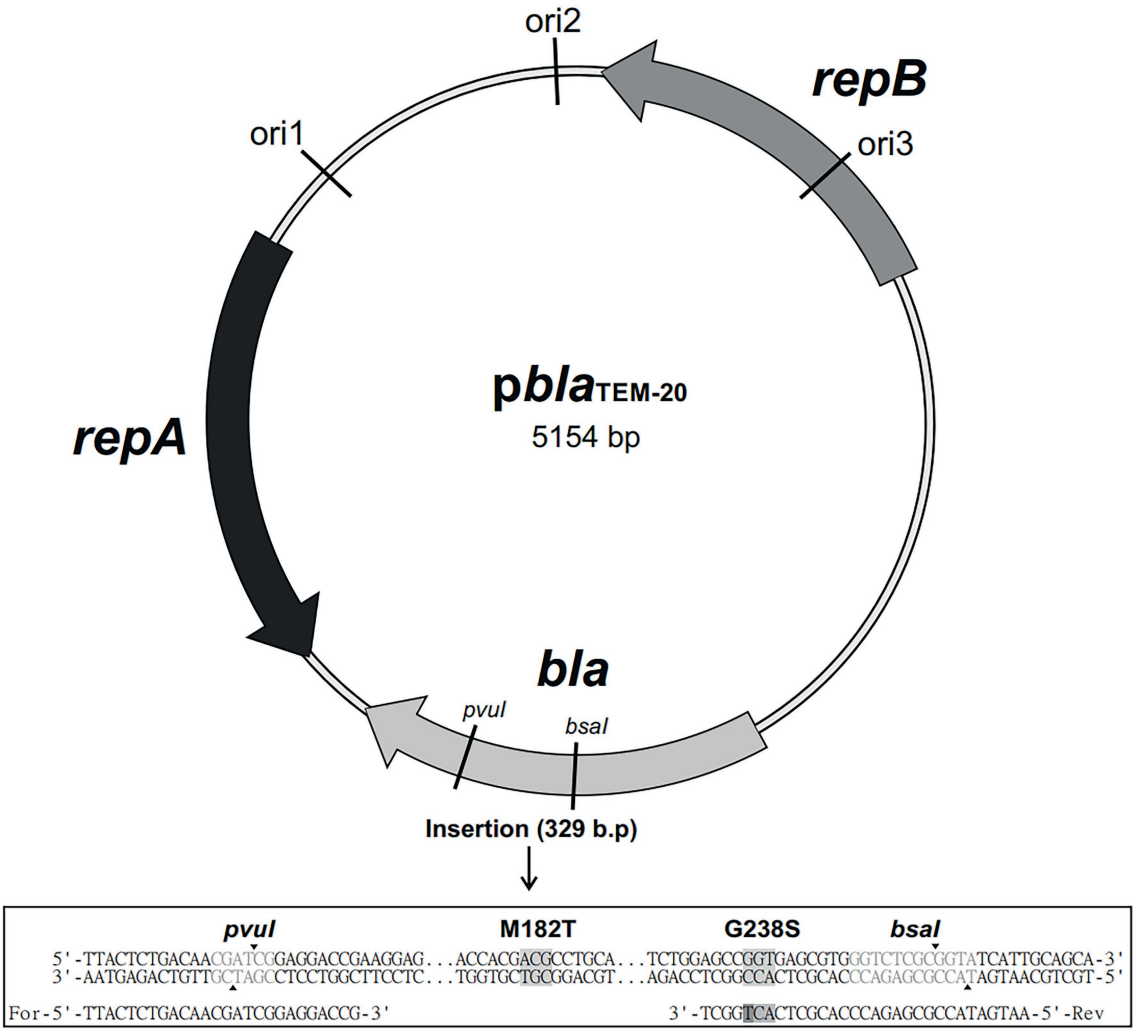

FIGURE 1 | Map of the p*bla*$_{TEM-20}$ plasmid (5,154 base pairs long) containing the *bla*$_{TEM-20}$ gene associated with resistance to β-lactam antibiotics, including penicillins and cephalosporins. The plasmid contained three replication origins (ori1, ori2, and ori3) compatible with Gram-negative bacteria and the *repA* and *repB* genes encoding replication initiation proteins. The nucleotide sequence alignment of a 329 bp insert that contained the portion of the *bla* gene with the GGT → AGT mutation, which resulted in the Gly → Ser substitution at codon 238, and the ATG → ACG mutation, which resulted in the Met→Thr substitution at codon 182, is shown below.

were put into 2 mm electroporation cuvettes. A suspension of cells without the addition of plasmid DNA was also subjected to electroporation and used as the "wild-type" strain in subsequent experiments. Electroporation was performed by applying single pulsed discharges of 2.5 kV, 200 Ω, and 25 μF. The cooled cell suspensions were plated on chocolate agar dishes, washed and subcultured on dishes with a selective antibiotic: for strains carrying the p*bla*$_{TEM-1}$ and p*bla*$_{TEM-135}$ plasmids, 2 mg/L penicillin was used, and for strains carrying the p*bla*$_{TEM-20}$ plasmid, 0.5 mg/L ceftriaxone was used.

The wild-type *N. gonorrhoeae* strain and the strains carrying the p*bla*$_{TEM-1}$ and p*bla*$_{TEM-135}$ plasmids were stored at −80°C in cryopreservation medium containing trypticase-soy broth and glycerol at a ratio of 4:1.

The expression of β-lactamases in transformed cells was checked using nitrocefin disks (Remel, United States), which qualitatively detect the presence of enzymes, including penicillinases and cephalosporinases, that are capable of destroying the β-lactam ring in the substrate (nitrocefin).

Estimation of the Susceptibility of *Neisseria gonorrhoeae* to β-Lactam Antibiotics

The following β-lactam antibiotics were used in this work: benzylpenicillin; ampicillin (extended-spectrum aminopenicillin); cefuroxime (second-generation cephalosporin); ceftriaxone, cefixime and cefotaxime (third-generation cephalosporins); cefepime (fourth-generation cephalosporin); and meropenem,

imipenem, and doripenem (carbapenems). All antibiotics were obtained from Sigma–Aldrich (United States).

The MICs of antibiotics for *N. gonorrhoeae* strains were measured by a serial dilution method. *Neisseria gonorrhoeae* cells were cultured on GC chocolate agar supplemented with IsoVitaleX Enrichment. Inocula (0.5 McFarland) of the wild-type *N. gonorrhoeae* strain (ATCC 49226) and the strains carrying the pbla_{TEM} plasmids were prepared. Microorganisms were seeded in Petri dishes containing selective medium supplemented with different concentrations of antibiotics. After 24 h of incubation at 37°C in 5% CO_2, the presence/absence of bacterial growth in the Petri dishes was assessed. Based on the measurement results, each strain was characterized in accordance with the established criteria of the European Committee on Antimicrobial Susceptibility Testing (EUCAST): S–susceptible, R–resistant.[2]

Assessment of *Neisseria gonorrhoeae* Cell Viability: Cell Growth and Death Studies

To estimate the effects of the plasmids on the survival of gonococci in the presence of antibiotics, the viability of *N. gonorrhoeae* cells carrying pbla_{TEM} plasmids was studied by constructing growth curves for cells cultured in the absence of antibiotics and death curves for cells cultured in the presence of ceftriaxone. The change in the number of viable cells (i.e., CFU) over time was determined by counting the number of colonies formed on solid medium.

All experiments conducted to study *N. gonorrhoeae* cell growth and death were performed immediately after transformation, allowing us to avoid cell storage. The avoidance of storage was important because of the low viability of *N. gonorrhoeae* cells carrying the p$bla_{\text{TEM-20}}$ plasmid.

To study cell growth, Petri dishes containing chocolate agar (10 ml) without the addition of antibiotics were used. An inoculum of cells (0.5 McFarland) was diluted to ~50 CFU/ml, and 1 ml of the cell suspension was plated in each dish, yielding nine dishes containing ~50 cells/dish for each *N. gonorrhoeae* strain. Every hour, the cultured cells were removed from every dish by washing as follows: 1 ml of a sterile 0.3 M sucrose solution was poured onto the agar surface, the cells were resuspended in the dish with a sterile plastic loop without disturbing the agar surface layer, and the resulting cell suspension was transferred to a new dish. Thus, the cells were cultured in dish No. 1 for 1 h, in dish No. 2 for 2 h, and so on. After the cultured cells were removed by washing, the dishes containing the removed cells were incubated for 24–48 h at 37°C in 5% CO_2, and the colonies formed were counted.

To study cell death in the presence of ceftriaxone, an inoculum of cells (0.5 McFarland) was diluted to ~1,000 CFU/ml, and 1 ml of the cell suspension was plated in each dish supplemented with ceftriaxone, yielding nine dishes containing ~1,000 cells/dish for each *N. gonorrhoeae* strain. Ceftriaxone concentrations of 0.03, 0.125, and 2 mg/L were used. Every hour, the cultured cells were removed from every dish by washing, and the resulting cell suspensions were transferred to new dishes without the addition of ceftriaxone. The dishes were incubated as described above, and the colonies formed were counted. All experiments conducted to study the growth and death of the obtained clones were performed in triplicate.

Mathematical Models of Cell Growth and Death

The generalized Verhulst equation was used to model cell growth for all strains under study (Peleg et al., 2007; Peleg and Corradini, 2011). To construct death curves for the strains not carrying the p$bla_{\text{TEM-20}}$ plasmid cultured in the presence of ceftriaxone, a modified Chick–Watson model (Jensen, 2010; Peleg, 2021) was used. The parameters were fit to the equation by determining the numerical solutions of the Cauchy problem using MATLAB 2021b software for different r, N_{asymp}, and α values for the Verhulst equation and for different k_{obs} values for the Chick–Watson law. Optimization of the obtained numerical solutions compared with the experimental results was carried out by the least squares method. The statistical significance of the difference between the mathematical models, which describe experimental results for different data series, was evaluated by Fisher's F test (F test) in accordance with a procedure described previously (Motulsky and Ransnas, 1987).

RESULTS

Production of the p$bla_{\text{TEM-1}}$, p$bla_{\text{TEM-135}}$, and p$bla_{\text{TEM-20}}$ Constructs

The p$bla_{\text{TEM-135}}$ plasmid obtained from the clinical *N. gonorrhoeae* isolate was used to construct the artificial p$bla_{\text{TEM-1}}$ and p$bla_{\text{TEM-20}}$ plasmids. Three 5,154 bp plasmids were constructed; these plasmids differed in the *bla* gene structure (**Figure 1**) as follows:

p$bla_{\text{TEM-1}}$, no mutations in codons 182 and 238;
p$bla_{\text{TEM-135}}$, the ATG → ACG substitution at codon 182 leading to the Met182Thr substitution, no mutation at codon 238; and
p$bla_{\text{TEM-20}}$, ATG → ACG substitution at codon 182 leading to the Met182Thr substitution and the GGT → AGT substitution at codon 238 leading to the Gly238Ser substitution.

These plasmids could replicate in both *E. coli* and *N. gonorrhoeae* cells due to the presence of replication origins compatible with gram-negative bacteria and replication initiation proteins.

Production of *Escherichia coli* and *Neisseria gonorrhoeae* Strains Carrying pbla_{TEM} Plasmids

E. coli and *N. gonorrhoeae* strains carrying the p$bla_{\text{TEM-1}}$, p$bla_{\text{TEM-135}}$, and p$bla_{\text{TEM-20}}$ plasmids were generated. *E. coli* strains carrying the pbla_{TEM} plasmids were grown on selective media with antibiotics and stored in Petri dishes at 4°C.

[2]https://www.eucast.org/clinical_breakpoints

The *N. gonorrhoeae* strains carrying the pbla_{TEM-1} and p$bla_{TEM-135}$ plasmids retained their viability after several (4–5) passages from dishes and after storage in cryopreservation medium. However, the *N. gonorrhoeae* strain carrying the pbla_{TEM-20} plasmid could not be stored in cryopreservation medium. In addition, cell viability was lost after 6 h of incubation on plates; colonies did not grow after subculture on medium with or without antibiotics (penicillin and ceftriaxone). The loss of viability cannot be explained by the loss of plasmids, since the test on nitrocefin disks produced positive results, indicating the presence of β-lactamases. Moreover, the presence of pbla_{TEM} plasmids with the introduced mutations in the β-lactamase gene was confirmed by both PCR and Sanger sequencing.

Antimicrobial Susceptibility Testing of *Neisseria gonorrhoeae* Strains Carrying Different pbla_{TEM} Plasmids

The susceptibility of *N. gonorrhoeae* strains carrying various pbla_{TEM} plasmids to several groups of β-lactam antibiotics was studied. The antibiotics included penicillins, which were previously used to treat gonococcal infections; cephalosporins, which are currently used for gonorrhea treatment; and carbapenems, which may replace cephalosporins if cephalosporin resistance spreads (Unemo et al., 2020). The MICs measured for these drugs are shown in **Table 1**.

After transformation of the wild-type *N. gonorrhoeae* strain with the pbla_{TEM-1} and p$bla_{TEM-135}$ plasmids, which contain genes encoding a broad-spectrum β-lactamase (penicillinase), the strain exhibited a sharp decrease in susceptibility to antibiotics from the penicillin class (MIC_{pen} = 16–32 mg/L, MIC_{amp} = 8 mg/L). The MICs measured on solid media confirmed that the TEM-1 and TEM-135 enzymes were unable to hydrolyze cephalosporins and carbapenems.

When incubated for 24 h on plates with antibiotics, the *N. gonorrhoeae* strain carrying the pbla_{TEM-20} plasmid exhibited visible growth, allowing us to determine the MICs of β-lactams (**Table 1**). Even if this strain stopped growing after 6 h of culture, we could record the numbers of colonies on the plates after 24 h and estimate the MICs of the antibiotics. The MICs for the strain containing the pbla_{TEM-20} plasmid confirmed that the expressed TEM-20 β-lactamase is an ESBL that can hydrolyze both penicillins and cephalosporins of different generations. The cephalosporin MICs were above the EUCAST breakpoint for susceptibility/resistance, which was established to be 0.125 mg/L (**Table 1**). For example, the MICs of the third- and fourth-generation cephalosporins were at least 4 mg/L. Thus, the MIC of the antibiotic for the strain carrying the pbla_{TEM-20} plasmid exceeded the breakpoint established for third- and fourth-generation cephalosporins by more than a fivefold dilution.

The measured MIC of carbapenems did not exceed 0.008 mg/L for any *N. gonorrhoeae* strain, i.e., all strains were susceptible to carbapenems, proving that the TEM-1, TEM-135, and TEM-20 β-lactamase variants cannot hydrolyze carbapenems (EUCAST breakpoints for carbapenems are not available).

Growth Curves of *Neisseria gonorrhoeae* Strains Carrying Different pbla_{TEM} Plasmids and the Mathematical Model of Cell Growth

Figure 2 shows the growth curves of the *N. gonorrhoeae* cells carrying the pbla_{TEM-1}, p$bla_{TEM-135}$, and pbla_{TEM-20} plasmids compared to the growth curve of the wild-type cells in the absence of antibiotics. Notably, in our experiments, we determined the number of viable cells by determining the number of colonies formed (i.e., CFU) in a dish. The wild-type strain and the strains carrying the pbla_{TEM-1} and p$bla_{TEM-135}$ plasmids exhibited growth throughout the 8 h of culture. However, the number of viable *N. gonorrhoeae* cells carrying the pbla_{TEM-20} plasmid began to decrease after 6 h of culture.

TABLE 1 | Susceptibility of *Neisseria gonorrhoeae* strains carrying different pbla_{TEM} plasmids to β-lactam antibiotics.

Antibiotic	EUCAST criteria	MIC, mg/L			
		WT*	**pbla_{TEM-1}**	**p$bla_{TEM-135}$**	**pbla_{TEM-20}**
Benzylpenicillin (PEN)	S: $MIC_{pen} \leq 0.06$ R: $MIC_{pen} > 1$	0.25	16 (R)	32 (R)	16 (R)
Ampicillin (AMP)	–	0.125	8	8	16
Cefuroxime (CXM)	–	0.008	0.004	0.004	2
Ceftriaxone (CRO)	S: $MIC_{cro} \leq 0.125$ R: $MIC_{cro} > 0.125$	0.03 (S)	0.015 (S)	0.03 (S)	4 (R)
Cefixime (CFM)	S: $MIC_{cfm} \leq 0.125$ R: $MIC_{cfm} > 0.125$	0.015 (S)	0.015 (S)	0.015 (S)	16 (R)
Cefotaxime (CTX)	S: $MIC_{ctx} \leq 0.125$ R: $MIC_{ctx} > 0.125$	0.015 (S)	0.008 (S)	0.015 (S)	8 (R)
Cefepime (FEP)	–	0.03	0.015	0.015	16
Meropenem (MEM)	–	0.002	0.002	0.002	0.004
Imipenem (IPM)	–	0.004	0.008	0.004	0.008
Doripenem (DOR)	–	0.002	0.002	0.002	0.002

*S–susceptible and R–resistant according to the EUCAST criteria (EUCAST, 2022). *WT–wild-type N. gonorrhoeae, ATCC 49226, not carrying the pbla_{TEM} plasmid.*

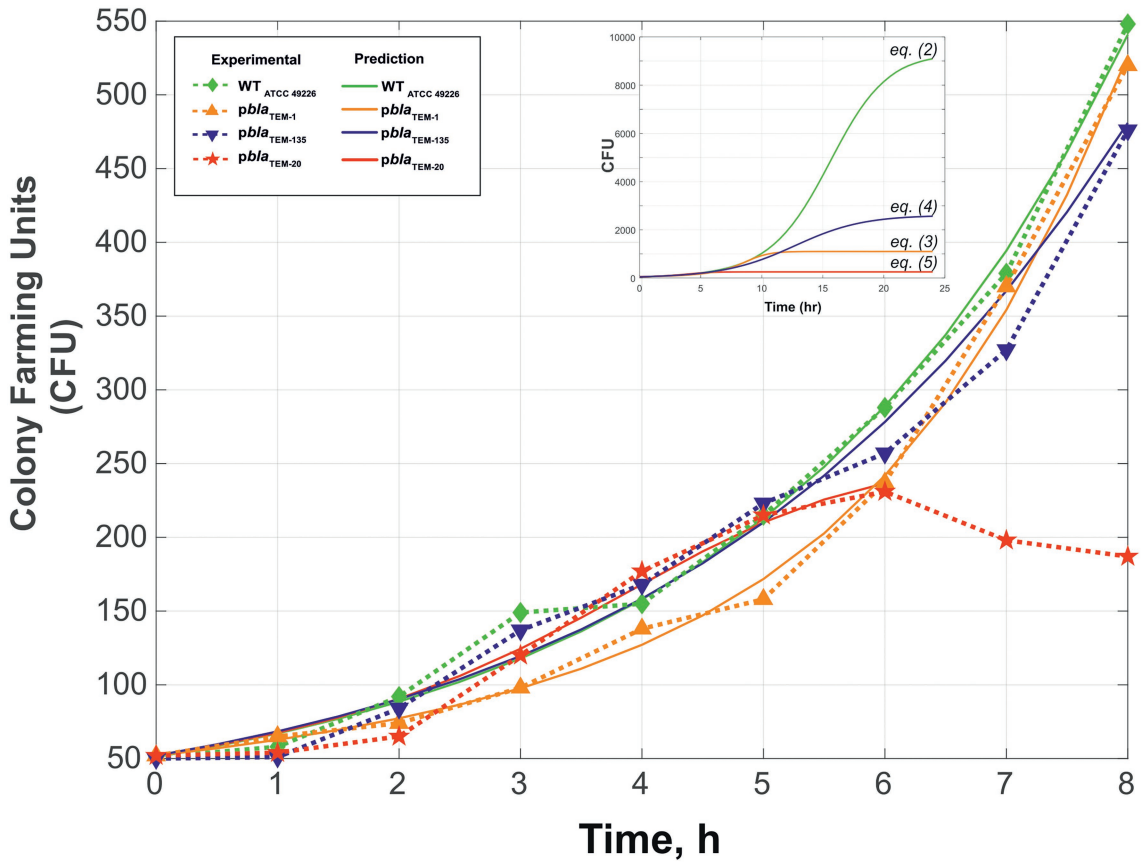

FIGURE 2 | Growth curves (change in CFU over time) of *Neisseria gonorrhoeae* strain ATCC 49226 not carrying plasmids (WT) and carrying p*bla*$_{TEM}$ plasmids, in the absence of antimicrobials (37°C, 5% CO_2). The experimental results are indicated by the dashed lines and dots, and the theoretical curves constructed using Eqs. (2)–(5) are indicated by the solid lines. The inset shows the theoretical curves for incubation periods of up to 24 h to reach N_{asymp}. In the graphs, the dots correspond to the mean CFU from three independent experiments (the initial CFU and the standard deviations are provided in **Supplementary Table S1**).

To compare the *N. gonorrhoeae* strains carrying different plasmids, we performed mathematical modeling of the cell growth kinetics. The generalized Verhulst equation [Peleg et al., 2007; Peleg and Corradini, 2011; Eq. (1)] was selected for modeling since it is the simplest and most universal equation for describing population growth dynamics until the transition to stationary phase.

$$\frac{dN(t)}{dt} = rN(t)^{\alpha}\left(1-\frac{N(t)}{N_{asymp}}\right) \quad (1)$$

where $dN(t)/dt$ is the growth rate at a given time, r is the proportionality coefficient, $N(t)$ is the number of cells at a given time, N_{asymp} is the maximum possible number of cells of a given type that can grow under the given experimental conditions, and α is the constant characterizing the growth specificity ($\alpha<1$ means that the organism does not achieve its potential for exponential growth, and $\alpha>1$ means that the organism exceeds this potential; Peleg et al., 2007).

Fitting of the parameters to Eq. (1) by determining the numerical solutions of the Cauchy problem for different r, N_{asymp}, and α values resulted in Eqs. (2)–(5), which describe the growth curves of cells carrying and not carrying plasmids (**Figure 2**).

N. gonorrhoeae cells not carrying plasmids (wild-type):

$$\frac{dN(t)}{dt} = 0.188\,N(t)^{1.093}\left(1-\frac{N(t)}{9300}\right) \quad (2)$$

N. gonorrhoeae cells carrying p*bla*$_{TEM\text{-}1}$:

$$\frac{dN(t)}{dt} = 0.018\,N(t)^{1.593}\left(1-\frac{N(t)}{1100}\right) \quad (3)$$

N. gonorrhoeae cells carrying p*bla*$_{TEM\text{-}135}$:

$$\frac{dN(t)}{dt} = 0.21\,N(t)^{1.071}\left(1-\frac{N(t)}{2600}\right) \quad (4)$$

N. gonorrhoeae cells carrying p*bla*$_{TEM\text{-}20}$ (up to 6 h of growth):

$$\frac{dN(t)}{dt} = 0.012\,N(t)^{1.819}\left(1-\frac{N(t)}{235}\right) \quad (5)$$

The R^2 values were 0.9916 for wild-type, 0.9958 for p$bla_{\text{TEM-1}}$, 0.9801 for p$bla_{\text{TEM-135}}$, and 0.9778 for p$bla_{\text{TEM-20}}$.

The statistical significance of the difference between the obtained models for describing the data (i.e., the value of p) was calculated using the Fisher criterion. The wild-type model outperformed the models for TEM-1, with $p = 0.02$, and TEM-135, with $p = 0.02$. The model for TEM-1 was superior to that of the wild-type and TEM-135 models, with $p = 0.01$. The model for TEM-135 was superior to that of the wild-type model, with $p = 0.05$, and the model for TEM-1, with $p = 0.06$. These results indicate that the developed models adequately describe cell growth for the corresponding strains.

The calculated value of N_{asymp} differed between wild-type *N. gonorrhoeae* cells and cells carrying the pbla_{TEM} plasmids: a maximum N_{asymp} of 9,300 CFU was observed for wild-type *N. gonorrhoeae*, lower values were observed for *N. gonorrhoeae* carrying the p$bla_{\text{TEM-135}}$ and p$bla_{\text{TEM-1}}$ plasmids (2,600 and 1,100 CFU, respectively), and a very low CFU of 235 was observed for *N. gonorrhoeae* carrying the p$bla_{\text{TEM-20}}$ plasmid. This means that cells carrying pbla_{TEM} plasmids had a reduced growth capacity compared to that of cells not carrying these plasmids, which can be explained by the additional energetic and metabolic costs of plasmid reproduction. Moreover, the strain carrying the p$bla_{\text{TEM-20}}$ plasmid expressing the β-lactamase with the Gly238Ser substitution showed a significantly reduced growth ability compared to that of the wild-type strain and the strains carrying the other plasmids. The reduced viability of the strain carrying the p$bla_{\text{TEM-20}}$ plasmid was also confirmed by the previously noted characteristics: the cells survived for no more than 6 h when stored on solid medium and did not survive when stored in cryopreservation medium.

Changes in the Numbers of Viable *Neisseria gonorrhoeae* Cells Carrying Different pbla_{TEM} Plasmids in the Presence of Ceftriaxone

The changes in the numbers of viable cells over time in the presence of various concentrations of ceftriaxone (0.03, 0.125 and 2 mg/L) are shown in **Figure 3**. Consistent with the protocol for the bacterial growth studies, the number of CFUs on solid medium (chocolate agar) under various culture conditions, rather than the total number of cells, was determined. As shown in **Figure 3A–C**, the strains that did not carry ceftriaxone resistance determinants rapidly lost viability in the presence of this antimicrobial agent (the ceftriaxone concentrations used in this experiment were equal to or greater than the MIC_{cro} for these strains, i.e., 0.015–0.03 mg/L; **Table 1**). After 2–8 h of incubation, the bacterial cells were completely eliminated.

Under our experimental conditions, the change in the concentration of ceftriaxone over time can be neglected since this concentration is much higher than that in the cells in the sample: [CRO] = 0.03–2.0 mg/L or $(0.045–3.030)\cdot10^{-6}$ M, $N_0 = 1{,}000$ cells (cells at the zero time point). The decrease in CFU over time evidenced in the curves in **Figures 3A–C** (strains not carrying plasmids and strains carrying p$bla_{\text{TEM-1}}$ and p$bla_{\text{TEM-135}}$) followed a logarithmic law, i.e., kinetic curves can be considered applicable for chemical reactions of the first (pseudo-first) order (**Scheme 1**).

A modified Chick–Watson model developed for disinfection curves (cell death under the action of a disinfecting agent) can be applied to describe the kinetic curves. According to Chick's law, the dependence of cell survival on time is described by the equations for a first-order chemical reaction [Jensen, 2010; Peleg, 2021; Eqs. (6) and (7)].

$$\frac{dN(t)}{dt} = -k_{obs}\,N(t) \quad (6)$$

$$\ln\frac{N_0}{N} = k_{obs}\,t \quad (7)$$

where $dN(t)/dt$ is the growth rate at a given time, $N(t)$ is the number of cells at a given time, and k_{obs} is the observed first-order rate constant.

Fitting the cell death curves (**Figures 3A–C**) using Eq. (7) made it possible to obtain the values of the observed first-order rate constants k_{obs} for all strains at different concentrations of the disinfecting agent, which in our experiment was ceftriaxone (pseudo-first-order rate constants). The dependence of k_{obs} on the concentration of ceftriaxone is shown in **Figure 4**.

According to the modified Chick–Watson model, the dependence of the cell death rate on the concentration of ceftriaxone is determined by the following equation:

$$\frac{dN(t)}{dt} = -k_d\,[CRO]^n\,N(t) \quad (8)$$

where [*CRO*] is the ceftriaxone concentration; n is the fitting coefficient, also called the coefficient of dilution; and k_{d} is the true rate constant of cell death.

Thus, the observed death rate constant is related to the true rate constant and the ceftriaxone concentration as follows:

$$\text{Viable cells} + \text{CRO} \xrightarrow{k_{obs}} \text{Nonviable cells} \quad \text{(Scheme 1)}$$

SCHEME 1 | Cell death under the action of ceftriaxone.

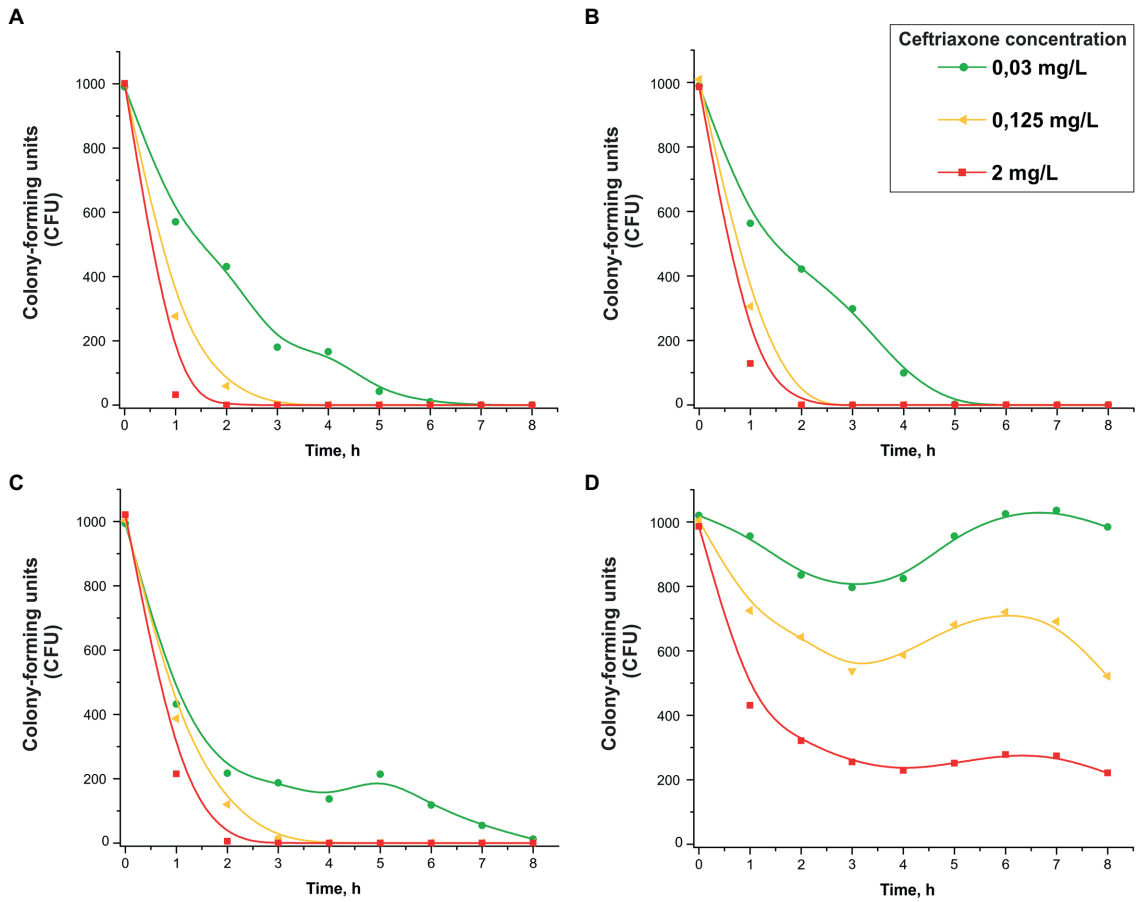

FIGURE 3 | Change in the CFU number vs. time in the presence of 0.03, 0.125, or 2 mg/L ceftriaxone for *Neisseria gonorrhoeae* strain ATCC 49226 not carrying plasmids **(A)**, carrying p*bla*$_{TEM-1}$ **(B)**, carrying p*bla*$_{TEM-135}$ **(C)**, and carrying p*bla*$_{TEM-20}$ (**D**; 37°C, 5% CO_2). The dots correspond to the mean CFU from three independent experiments (the initial CFU and the standard deviations are provided in **Supplementary Table S2**).

$$k_{obs} = k_d \left[CRO\right]^n \quad (9)$$

The dependence of k_{obs} on the concentration of ceftriaxone, shown in **Figure 4**, is approximated by the following power functions (R^2–approximation confidence value):

N. gonorrhoeae cells not carrying plasmids (wild-type):

$$k_{obs} = 2.71\left[CRO\right]^{0.44} \quad (10)$$

($R^2 = 0.9677$)

N. gonorrhoeae cells carrying p*bla*$_{TEM-1}$:

$$k_{obs} = 1.86\left[CRO\right]^{0.31} \quad (11)$$

($R^2 = 0.8461$)

N. gonorrhoeae cells carrying p*bla*$_{TEM-135}$:

$$k_{obs} = 1.44\left[CRO\right]^{0.22} \quad (12)$$

($R^2 = 0.9626$)

Thus, the equations describing the decrease in *N. gonorrhoeae* CFU over time under the influence of ceftriaxone are as follows:

N. gonorrhoeae cells not carrying plasmids (wild-type):

$$\frac{dN(t)}{dt} = -2.71\left[CRO\right]^{0.44} N(t) \quad (13)$$

N. gonorrhoeae cells carrying p*bla*$_{TEM-1}$:

$$\frac{dN(t)}{dt} = -1.86\left[CRO\right]^{0.31} N(t) \quad (14)$$

N. gonorrhoeae cells carrying p*bla*$_{TEM-135}$:

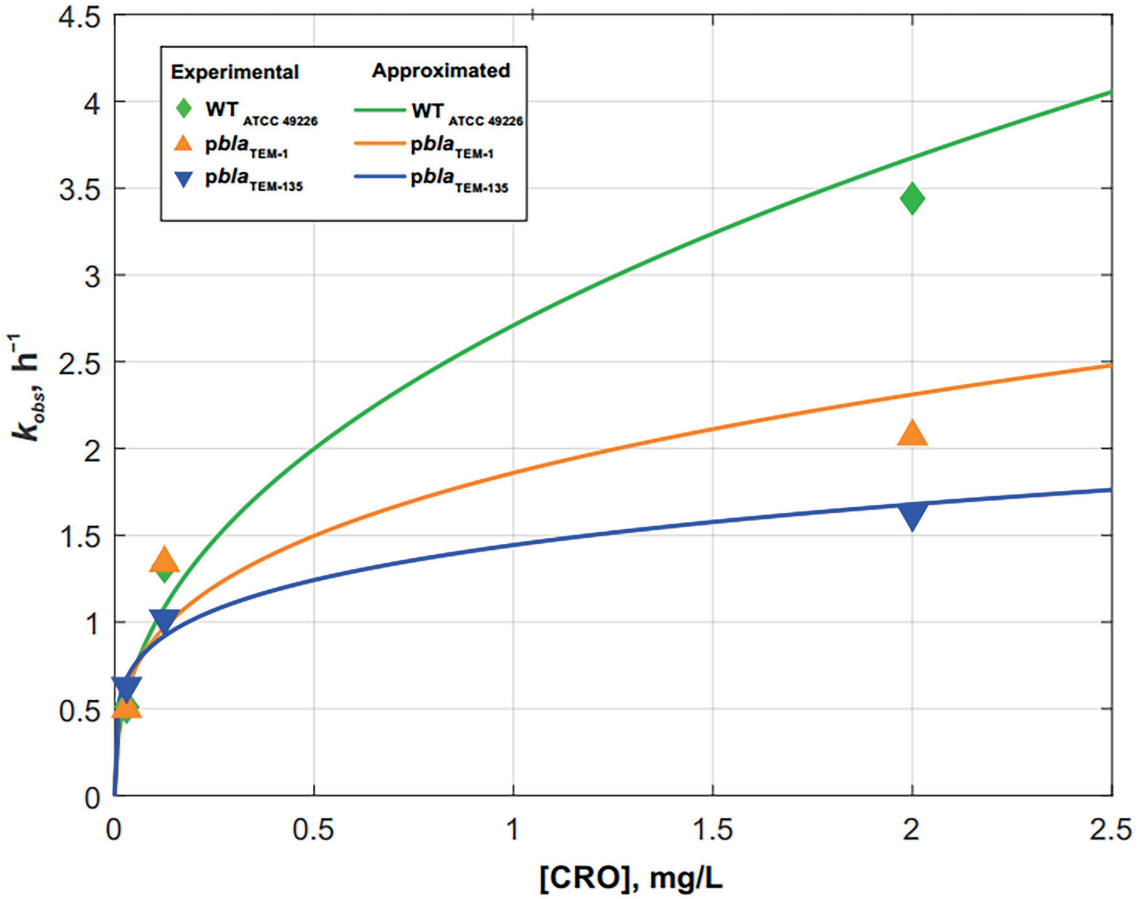

FIGURE 4 | Dependence of the cell death rate constant k_{obs} on the ceftriaxone concentration for *Neisseria gonorrhoeae* strains not carrying the plasmids and carrying pbla_{TEM-1} and p$bla_{TEM-135}$. The solid lines show the power approximation curves constructed according to Eqs. (10)–(12).

$$\frac{dN(t)}{dt} = -1.44[CRO]^{0.22} N(t) \quad (15)$$

The results showed that the patterns of *N. gonorrhoeae* cell death in the presence of ceftriaxone varied by strain. In the wild-type strain not carrying pbla_{TEM}, cell death occurred somewhat faster than in the strains carrying pbla_{TEM-1} and p$bla_{TEM-135}$, although the β-lactamases expressed by these plasmids were not capable of destroying cephalosporins.

However, the CFU reduction vs. time curves for the *N. gonorrhoeae* strain carrying the pbla_{TEM-20} plasmid that expresses an ESBL looked completely different (**Figure 3D**). The MIC of ceftriaxone for this strain was 4 mg/L (**Table 1**), and at ceftriaxone concentrations of 0.03–0.125 mg/L, the number of viable cells decreased in the first 3 h. Then, a short-term increase in CFU was observed over a period of 3–6 h, and this increase shifted to a reduction in CFU that was similar to the reduction observed in the *N. gonorrhoeae* strain carrying the pbla_{TEM-20} plasmid when cultured in the absence of the antibiotic (**Figure 2**, curve for the strain with the pbla_{TEM-20} plasmid). At a ceftriaxone concentration of 0.03 mg/L, i.e., a much lower concentration than the MIC_{cro} for the strain carrying pbla_{TEM-20}, a significant amount of the antibiotic seemed to be hydrolyzed in the first 3 h, and the number of cells was restored to its initial value during the next 3 h. Moreover, notably, the CFU vs. time curves for this strain did not obey the logarithmic law, and in this case, the Chick–Watson model was not applicable for describing the kinetic curves.

Obviously, the kinetic curves for cells carrying pbla_{TEM-20} reflected several processes: hydrolysis of ceftriaxone by the TEM-20 β-lactamase and the growth and gradual death of cells. Therefore, these curves could not be described by a simple Chick–Watson model for cell death in the presence of a disinfecting agent (here, ceftriaxone).

DISCUSSION

Currently, the threat of the emergence and spread of *N. gonorrhoeae* clinical isolates resistant to third-generation cephalosporins, such as ceftriaxone and cefixime, is a global problem. To date, a few isolates with chromosomal resistance to cephalosporins have been described. The typical ceftriaxone MICs for such isolates are 0.5–1.0 mg/L (Młynarczyk-Bonikowska et al., 2020; Shaskolskiy et al., 2021). However, the emergence

of ESBLs that can hydrolyze cephalosporins may lead to a several fold increase in the ceftriaxone MIC.

Although no ESBL-producing *N. gonorrhoeae* isolate has been detected worldwide, the massive use of cephalosporins for gonorrhea treatment in many countries creates the possibility of selecting new variants of TEM β-lactamases. Since the single Gly238Ser mutation could endow blaTEM-135 with the ability to encode an ESBL, such as TEM-20, this allele can be considered a possible precursor of an ESBL. Laboratory evaluation of *N. gonorrhoeae* strains obtained by *in vitro* mutagenesis that produce different types of plasmid β-lactamases, including TEM-20, allows the resistance level to different classes of β-lactam antibiotics to be estimated and the viability of such strains to be assessed. At the same time, such studies carry a high risk of creating a super resistant pathogen in the laboratory conditions. Therefore, special attention should be paid to controlling the safety of research and preventing the spread of the genetically engineered cells into the environment.

In this work, the artificial p$bla_{\text{TEM-1}}$ and p$bla_{\text{TEM-20}}$ plasmids were obtained by site-directed mutagenesis of the naturally occurring p$bla_{\text{TEM-135}}$ Toronto/Rio type plasmid. Efficient plasmid amplification occurred in *E. coli* cells due to the presence of specific replication origins (ori1, ori2, ori3) and the *repA* and *repB* genes encoding replication initiation proteins. The *N. gonorrhoeae* strain ATCC 49226 was transformed with these plasmids using electroporation to obtain individual strains, and the presence of the p$bla_{\text{TEM-1}}$, p$bla_{\text{TEM-135}}$, and p$bla_{\text{TEM-20}}$ plasmids in these strains was confirmed. All manipulations with obtained strains were carried out under strict conditions of biosafety level 3 laboratory. Cells were killed by heat inactivation after experiments.

As expected, benzylpenicillin susceptibility testing showed that compared to the wild-type strain, the strains carrying pbla_{TEM} plasmids exhibited high-level resistance ($\text{MIC}_{\text{pen}} \geq 16$ mg/L) to this antibiotic. For all cephalosporins, the MIC values for the strains carrying the p$bla_{\text{TEM-1}}$ or p$bla_{\text{TEM-135}}$ plasmid were similar to that for the wild-type strain, i.e., all strains displayed equivalent susceptibility to cephalosporins. However, very different MIC values were obtained for the strain carrying the p$bla_{\text{TEM-20}}$ plasmid. The MIC of ceftriaxone was 4 mg/L, twice the maximum MIC for the described clinical isolate HO41 with chromosomal ceftriaxone resistance (Ohnishi et al., 2011). The MIC values of the other third- and fourth-generation cephalosporins were as low as 8 mg/L, a pattern that can be explained only by the presence of an enzyme that effectively destroys these antibiotics in cells. Indeed, a single Gly238Ser amino acid substitution in the β-lactamase plasmid gene was sufficient to endow this enzyme with the ability to hydrolyze cephalosporins but retain the ability to hydrolyze penicillins. However, the *N. gonorrhoeae* strain carrying the p$bla_{\text{TEM-20}}$ plasmid showed substantially reduced viability; cell growth plateaued after 6 h of culture in either the absence or presence of the antibiotic. In addition, the cells did not grow after incubation on plates for more than 6 h or after freezing. Moreover, to determine the MICs, the colonies formed were counted after 24 h of incubation, a possible limitation of this study. The reduced viability of the strain carrying the p$bla_{\text{TEM-20}}$ plasmid most likely did not affect the measured MICs but decreased the number of proliferated cells.

Our results intersect with the work of Cole et al., 2018, in which genetically engineered *N. gonorrhoeae* strains of the widespread *N. gonorrhoeae* multiantigen sequence typing (NG-MAST) type 1,407, carrying African-type penicillinase-producing plasmids, were obtained. However, the strains described in Cole et al. were unable to retain plasmids in the absence of antibiotic selection, and the cells lost plasmids after even one passage in the absence of penicillin. In our work, the reduced viability of *N. gonorrhoeae* cells carrying the p$bla_{\text{TEM-20}}$ plasmid was not associated with loss of the plasmid during culture. Moreover, to exclude the effect of cell damage due to the electroporation procedure, all experiments for estimating the viability of the wild-type strain and the strains carrying the p$bla_{\text{TEM-1}}$, p$bla_{\text{TEM-135}}$ and p$bla_{\text{TEM-20}}$ plasmids were performed in triplicate.

The reduced viability of the strain carrying the p$bla_{\text{TEM-20}}$ plasmid that was demonstrated in this work can be explained by the following reasons: (a) the presence of the plasmid itself, which requires additional reproduction costs in cells and (b) the expression of an ESBL. The action of cephalosporins, like all β-lactam antibiotics, is aimed at inhibiting the synthesis of the bacterial cell wall *via* covalent inhibition of transpeptidase (PBP) activity. The main component of the cell wall is peptidoglycan, which is a macromolecular structure comprising peptide and sugar components. To protect themselves against β-lactam antibiotics, bacteria express β-lactamases, which are localized in the periplasmic space and hydrolyze the C–N bond in the β-lactam ring of the antibiotic, thereby inactivating the drug. Because peptidoglycan in gram-negative bacteria possesses a C-terminal motif in the acyl-D-Ala-D-Ala peptide chain that is structurally analogous to β-lactams, β-lactamases can induce changes in the peptidoglycan composition, thereby reducing the viability of bacterial cells. A change in the structure of the cell membrane leads to the suppression of cell division (bacteriostatic effect) or to the rupture of bacterial cells due to osmotic pressure (bactericidal activity; Sawa et al., 2020). A study published by Fernández et al. (2012) showed that a change in the peptidoglycan structure occurred in *E. coli* cells expressing certain β-lactamase variants: specifically, the level of crosslinked muropeptides was decreased, which negatively affected the viability of these strains.

Evaluation of the resistance of the *N. gonorrhoeae* strains carrying pbla_{TEM} plasmids to β-lactam antibiotics also showed that none of the obtained β-lactamase variants, including the ESBL TEM-20, were capable of hydrolyzing carbapenems. Thus, carbapenems remain among the β-lactams that can resist hydrolysis by *N. gonorrhoeae* lactamases, confirming that they are potential drugs for the treatment of gonococcal infections.

The cell growth kinetics were mathematically modeled using the generalized Verhulst equation (Peleg et al., 2007; Peleg and Corradini, 2011). The value of N_{asymp}, a parameter that characterizes the maximum possible number of cells that can grow under given conditions, was lower for strains carrying pbla_{TEM} plasmids than for strains not carrying these plasmids, i.e., the viability of plasmid-carrying strains was reduced compared to that of wild-type *N. gonorrhoeae*. N_{asymp} decreased in the order of

WT—p$bla_{TEM-135}$—pbla_{TEM-1}—pbla_{TEM-20}. The reduced viability of the strains carrying the pbla_{TEM} plasmids may explain why these strains have a lower incidence in the *N. gonorrhoeae* population than strains not carrying these plasmids. The higher viability of *N. gonorrhoeae* carrying p$bla_{TEM-135}$ than *N. gonorrhoeae* carrying pbla_{TEM-1} may be associated with the presence of the Met182Thr mutation in the β-lactamase, which leads to stabilization of the enzyme structure. As noted previously (Orencia et al., 2001; Cole et al., 2015; Yan et al., 2019), increased enzyme stability may have contributed to the persistence and spread of the TEM-135 β-lactamase variant in the *N. gonorrhoeae* population.

The decrease in the number of viable cells with culture time in the presence of ceftriaxone has been studied. The cell death kinetics of *N. gonorrhoeae* not carrying plasmids and *N. gonorrhoeae* carrying the pbla_{TEM-1} and p$bla_{TEM-135}$ plasmids, that lack ceftriaxone resistance determinants, can be described by a modified Chick–Watson law for modeling cell death in the presence of a disinfectant (Jensen, 2010; Peleg, 2021). The cell death rate of the wild-type *N. gonorrhoeae* strain in the presence of ceftriaxone was higher than that of the strains carrying the pbla_{TEM-1} and p$bla_{TEM-135}$ plasmids, although the strains carrying those plasmids were susceptible to ceftriaxone according to the EUCAST criteria.

In contrast, the CFU vs. time curves for the *N. gonorrhoeae* strain carrying the pbla_{TEM-20} plasmid that expresses an ESBL cannot be described by a simple Chick–Watson model. The cell death kinetic curves for this strain reflected several processes: hydrolysis of ceftriaxone by the TEM-20 β-lactamase, cell growth, and gradual cell death.

The obtained data on the reduced viability of *N. gonorrhoeae* strains carrying the pbla_{TEM-20} plasmid may explain the absence of *N. gonorrhoeae* clinical isolates producing ESBLs that hydrolyze cephalosporins of various generations.

DATA AVAILABILITY STATEMENT

The original contributions presented in the study are included in the article/**Supplementary Material**, and further inquiries can be directed to the corresponding author.

ETHICS STATEMENT

Ethical approval/written informed consent was not required for the study of animals/human participants in accordance with the local legislation and institutional requirements.

AUTHOR CONTRIBUTIONS

IK performed the experiments, analyzed the results, and wrote the manuscript. DG designed and supervised the project and wrote the manuscript. AV, OA, and JS carried out antimicrobial susceptibility testing. AK and VS supervised work with cell cultures. DD wrote the manuscript. BS directed the project, performed mathematical modeling, and wrote the manuscript. All authors contributed to the article and approved the submitted version.

FUNDING

This work was supported by the Russian Science Foundation, grant number 17-75-20039 (plasmid construction, susceptibility testing, mathematical modeling, and cell growth characteristics) and by the Ministry of Science and Higher Education of the Russian Federation to the EIMB Center for Precision Genome Editing and Genetic Technologies for Biomedicine under the Federal Research Program for Genetic Technologies Development for 2019-27, agreement number 075-15-2019-1660 (gene sequencing and analysis of sequence data). Work with cell cultures was performed according to the Ministry of Health of the Russian Federation, assignment number 056-03-2021-124.

SUPPLEMENTARY MATERIAL

The Supplementary Material for this article can be found online at: https://www.frontiersin.org/articles/10.3389/fmicb.2022.896607/full#supplementary-material

REFERENCES

Allen, V. G., Mitterni, L., Seah, C., Rebbapragada, A., Martin, I. E., Lee, C., et al. (2013). *Neisseria gonorrhoeae* treatment failure and susceptibility to Cefixime in Toronto, Canada. *JAMA* 309, 163–170. doi: 10.1001/jama.2012.176575

Arlet, G., Goussard, S., Courvalin, P., and Philippon, A. (1999). Sequences of the genes for the TEM-20, TEM-21, TEM-22, and TEM-29 extended-spectrum beta-lactamases. *Antimicrob. Agents Chemother.* 43, 969–971. doi: 10.1128/AAC.43.4.969

Attram, N., Agbodzi, B., Dela, H., Behene, E., Nyarko, E. O., Kyei, N. N. A., et al. (2019). Antimicrobial resistance (AMR) and molecular characterization of *Neisseria gonorrhoeae* in Ghana, 2012-2015. *PLoS One* 14:e0223598. doi: 10.1371/journal.pone.0223598

Bradford, P. A. (2001). Extended-Spectrum Beta-lactamases in the 21st century: characterization, epidemiology, and detection of this important resistance threat. *Clin. Microbiol. Rev.* 14, 933–951. doi: 10.1128/CMR.14.4.933-951.2001

Bush, K., and Jacoby, G. A. (2010). Updated functional classification of beta-lactamases. *Antimicrob. Agents Chemother.* 54, 969–976. doi: 10.1128/AAC.01009-09

Cole, M. J., Ison, C., and Woodford, N. (2018). Transfer of a Gonococcal β-lactamase plasmid into *Neisseria gonorrhoeae* belonging to the globally distributed ST1407 lineage. *J. Antimicrob. Chemother.* 73, 2576–2577. doi: 10.1093/jac/dky194

Cole, M. J., Unemo, M., Grigorjev, V., Quaye, N., and Woodford, N. (2015). Genetic diversity of blaTEM alleles, antimicrobial susceptibility and molecular epidemiological characteristics of Penicillinase-producing *Neisseria gonorrhoeae* from England and Wales. *J. Antimicrob. Chemother.* 70, 3238–3243. doi: 10.1093/jac/dkv260

Dillard, J. P. (2011). Genetic manipulation of *Neisseria gonorrhoeae*. *Curr. Protoc. Microbiol.* Chapter 4:Unit4A.2. doi: 10.1002/9780471729259.mc04a02s23

EUCAST (2022). The European committee on antimicrobial susceptibility testing. Breakpoint tables for interpretation of MICs and zone diameters. Version 12.0. Available at: http://www.eucast.org

Fernández, A., Pérez, A., Ayala, J. A., Mallo, S., Rumbo-Feal, S., Tomás, M., et al. (2012). Expression of OXA-type and SFO-1 β-lactamases induces changes in peptidoglycan composition and affects bacterial fitness. *Antimicrob. Agents Chemother.* 56, 1877–1884. doi: 10.1128/AAC.05402-11

Golparian, D., Ohlsson, A., Janson, H., Lidbrink, P., Richtner, T., Ekelund, O., et al. (2014). Four treatment failures of pharyngeal Gonorrhoea with ceftriaxone (500 mg) or Cefotaxime (500 mg), Sweden, 2013 and 2014. *Euro. Surveill.* 19:20862. doi: 10.2807/1560-7917.es2014.19.30.20862

Golparian, D., and Unemo, M. (2022). Antimicrobial resistance prediction in *Neisseria gonorrhoeae*: current status and future prospects. *Expert Rev. Mol. Diagn.* 22, 29–48. doi: 10.1080/14737159.2022.2015329

Jensen, J. N. (2010). Disinfection model based on excess inactivation sites: implications for linear disinfection curves and the Chick-Watson dilution coefficient. *Environ. Sci. Technol.* 44, 8162–8168. doi: 10.1021/es101818z

Kubanov, A., Solomka, V., Plakhova, X., Chestkov, A., Petrova, N., Shaskolskiy, B., et al. (2019). Summary and trends of the Russian Gonococcal antimicrobial surveillance Programme, 2005-2016. *J. Clin. Microbiol.* 57, e02024–e02018. doi: 10.1128/JCM.02024-18

Młynarczyk-Bonikowska, B., Majewska, A., Malejczyk, M., Młynarczyk, G., and Majewski, S. (2020). Multiresistant *Neisseria gonorrhoeae*: a new threat in second decade of the XXI century. *Med. Microbiol. Immunol.* 209, 95–108. doi: 10.1007/s00430-019-00651-4

Motulsky, H. J., and Ransnas, L. A. (1987). Fitting curves to data using nonlinear regression: a practical and nonmathematical review. *FASEB J.* 1, 365–374. PMID: 3315805. doi: 10.1096/fasebj.1.5.3315805

Muhammad, I., Golparian, D., Dillon, J. A., Johansson, A., Ohnishi, M., Sethi, S., et al. (2014). Characterisation of blaTEM genes and types of β-lactamase plasmids in *Neisseria gonorrhoeae*—the prevalent and conserved blaTEM-135 has not recently evolved and existed in the Toronto plasmid from the origin. *BMC Infect. Dis.* 14:454. doi: 10.1186/1471-2334-14-454

Müller, E. E., Fayemiwo, S. A., and Lewis, D. A. (2011). Characterization of a novel β-lactamase-producing plasmid in *Neisseria gonorrhoeae*: sequence analysis and molecular typing of host gonococci. *J. Antimicrob. Chemother.* 66, 1514–1517. doi: 10.1093/jac/dkr162

Nakayama, S., Tribuddharat, C., Prombhul, S., Shimuta, K., Srifuengfung, S., Unemo, M., et al. (2012). Molecular analyses of TEM genes and their corresponding Penicillinase-producing *Neisseria gonorrhoeae* isolates in Bangkok, Thailand. *Antimicrob. Agents Chemother.* 56, 916–920. doi: 10.1128/AAC.05665-11

Ohnishi, M., Ono, E., Shimuta, K., Watanabe, H., and Okamura, N. (2010). Identification of TEM-135 beta-lactamase in Penicillinase-producing *Neisseria gonorrhoeae* strains in Japan. *Antimicrob. Agents Chemother.* 54, 3021–3023. doi: 10.1128/AAC.00245-10

Ohnishi, M., Saika, T., Hoshina, S., Iwasaku, K., Nakayama, S., Watanabe, H., et al. (2011). Ceftriaxone-resistant *Neisseria gonorrhoeae*. Japan. *Emerg. Infect. Dis.* 17, 148–149. doi: 10.3201/eid1701.100397

Orencia, M. C., Yoon, J. S., Ness, J. E., Stemmer, W. P., and Stevens, R. C. (2001). Predicting the emergence of antibiotic resistance by directed evolution and structural analysis. *Nat. Struct. Biol.* 8, 238–242. doi: 10.1038/84981

Palmer, H. M., Leeming, J. P., and Turner, A. (2000). A multiplex polymerase chain reaction to differentiate beta-lactamase plasmids of *Neisseria gonorrhoeae*. *J. Antimicrob. Chemother.* 45, 777–782. doi: 10.1093/jac/45.6.777

Peleg, M. (2021). Modeling the dynamic kinetics of microbial disinfection with dissipating chemical agents -a theoretical investigation. *Appl. Microbiol. Biotechnol.* 105, 539–549. doi: 10.1007/s00253-020-11042-8

Peleg, M., and Corradini, M. G. (2011). Microbial growth curves: what the models tell us and what they cannot. *Crit. Rev. Food Sci. Nutr.* 51, 917–945. doi: 10.1080/10408398.2011.570463

Peleg, M., Corradini, M. G., and Normand, M. D. (2007). The logistic (Verhulst) model for sigmoid microbial growth curves revisited. *Food Res. Int.* 40, 808–818. doi: 10.1016/j.foodres.2007.01.012

Sawa, T., Kooguchi, K., and Moriyama, K. (2020). Molecular diversity of extended-Spectrum β-lactamases and Carbapenemases, and antimicrobial resistance. *J. Intensive Care* 8:13. doi: 10.1186/s40560-020-0429-6

Shaskolskiy, B., Dementieva, E., Kandinov, I., Filippova, M., Petrova, N., Plakhova, X., et al. (2019). Resistance of *Neisseria gonorrhoeae* isolates to beta-lactam antibiotics (benzylpenicillin and ceftriaxone) in Russia, 2015-2017. *PLoS One* 14:e0220339. doi: 10.1371/journal.pone.0220339

Shaskolskiy, B., Kandinov, I., Kravtsov, D., Filippova, M., Chestkov, A., and Solomka, V., et. al. (2021). Prediction of ceftriaxone MIC in *Neisseria gonorrhoeae* using DNA microarray technology and regression analysis. *J. Antimicrob. Chemother.* 76, 3151–3158. doi: 10.1093/jac/dkab308

Spence, J. M., Wright, L., and Clark, V. L. (2008). Laboratory maintenance of *Neisseria gonorrhoeae*. *Curr. Protoc. Microbiol.* Chapter 4:Unit 4A.1. doi: 10.1002/9780471729259.mc04a01s8

Tacconelli, E., Carrara, E., Savoldi, A., Harbarth, S., Mendelson, M., Monnet, D. L., et al. (2018). Discovery, research, and development of new antibiotics: the WHO priority list of antibiotic-resistant Bacteria and tuberculosis. *Lancet Infect. Dis.* 18, 318–327. doi: 10.1016/S1473-3099(17)30753-3

Tanaka, M., Furuya, R., Kobayashi, I., Ohno, A., and Kanesaka, I. (2021). Molecular characteristics and antimicrobial susceptibility of Penicillinase-producing *Neisseria gonorrhoeae* isolates in Fukuoka, Japan, 1996-2018. *J. Glob. Antimicrob. Resist.* 26, 45–51. doi: 10.1016/j.jgar.2021.04.014

Tooke, C. L., Hinchliffe, P., Bragginton, E. C., Colenso, C. K., Hirvonen, V. H. A., Takebayashi, Y., et al. (2019). β-Lactamases and β-lactamase inhibitors in the 21st century. *J. Mol. Biol.* 431, 3472–3500. doi: 10.1016/j.jmb.2019.04.002

Unemo, M., Golparian, D., Nicholas, R., Ohnishi, M., Gallay, A., and Sednaoui, P. (2012). High-level Cefixime- and ceftriaxone-resistant *Neisseria gonorrhoeae* in France: novel *penA* mosaic allele in a successful international clone causes treatment failure. *Antimicrob. Agents Chemother.* 56, 1273–1280. doi: 10.1128/AAC.05760-11

Unemo, M., and Jensen, J. S. (2017). Antimicrobial-resistant sexually transmitted infections: Gonorrhoea and *Mycoplasma genitalium*. *Nat. Rev. Urol.* 14, 139–152. doi: 10.1038/nrurol.2016.268

Unemo, M., Ross, J., Serwin, A. B., Gomberg, M., Cusini, M., and Jensen, J. S. (2020). 2020 European guideline for the diagnosis and treatment of Gonorrhoea in adults. *Int. J. STD AIDS* 956462420949126. doi: 10.1177/0956462420949126 [Epub ahead of print]

Unemo, M., Seifert, H. S., Hook, E. W. 3rd, Hawkes, S., Ndowa, F., and Dillon, J. R. (2019). Gonorrhoea. *Nat. Rev. Dis. Primers.* 5:79. doi: 10.1038/s41572-019-0128-6

Unemo, M., and Shafer, W. M. (2014). Antimicrobial resistance in *Neisseria gonorrhoeae* in the 21st century: past, evolution, and future. *Clin. Microbiol. Rev.* 27, 587–613. doi: 10.1128/CMR.00010-14

WHO (2016). WHO Guidelines for the Treatment of *Neisseria gonorrhoeae*. Available at: https://www.ncbi.nlm.nih.gov/books/NBK379221/

Workowski, K. A., and Bolan, G. A. (2015). Sexually transmitted diseases treatment guidelines, 2015. *MMWR Recomm. Rep.* 5, 1–137.

Yan, J., Zhang, J., and van der Veen, S. (2019). High prevalence of TEM-135 expression from the Asian plasmid in Penicillinase-producing *Neisseria gonorrhoeae* from Hangzhou, China. *Int. J. Antimicrob. Agents* 54, 361–366. doi: 10.1016/j.ijantimicag.2019.06.012

Conflict of Interest: The authors declare that the research was conducted in the absence of any commercial or financial relationships that could be construed as a potential conflict of interest.

Publisher's Note: All claims expressed in this article are solely those of the authors and do not necessarily represent those of their affiliated organizations, or those of the publisher, the editors and the reviewers. Any product that may be evaluated in this article, or claim that may be made by its manufacturer, is not guaranteed or endorsed by the publisher.

frontiers | Frontiers in Microbiology

REVIEW
published: 30 June 2022
doi: 10.3389/fmicb.2022.891548

Models for Gut-Mediated Horizontal Gene Transfer by Bacterial Plasmid Conjugation

Logan C. Ott[1,2] *and Melha Mellata*[1,2]*

[1]*Department of Food Science and Human Nutrition, Iowa State University, Ames, IA, United States,* [2]*Interdepartmental Microbiology Graduate Program, Iowa State University, Ames, IA, United States*

The emergence of new antimicrobial resistant and virulent bacterial strains may pose a threat to human and animal health. Bacterial plasmid conjugation is a significant contributor to rapid microbial evolutions that results in the emergence and spread of antimicrobial resistance (AR). The gut of animals is believed to be a potent reservoir for the spread of AR and virulence genes through the horizontal exchange of mobile genetic elements such as plasmids. The study of the plasmid transfer process in the complex gut environment is limited due to the confounding factors that affect colonization, persistence, and plasmid conjugation. Furthermore, study of plasmid transfer in the gut of humans is limited to observational studies, leading to the need to identify alternate models that provide insight into the factors regulating conjugation in the gut. This review discusses key studies on the current models for *in silico*, *in vitro*, and *in vivo* modeling of bacterial conjugation, and their ability to reflect the gut of animals. We particularly emphasize the use of computational and *in vitro* models that may approximate aspects of the gut, as well as animal models that represent *in vivo* conditions to a greater extent. Directions on future research studies in the field are provided.

Graphical Abstract Models for gut-mediated bacterial conjugation and plasmid transfer. Depiction of conjugative elements (Left, Top), current *in silico* models (Left, Middle), experimental *in vitro* models (Left, Bottom), and *in vivo* animal models (Right) for bacterial conjugation in the gut. Arthropods; spring tails (*Folsomia candida*), fleas (*Alphitobius diaperinus*), fruit flies (*Drosophila melanogaster*), house flies (*Musca domestica*), beetles (*Xenopsylla cheopis*); *Rhabditidae*; nematodes (*Caenorhabditis elegans*); *Phasianidae*; chickens (*Gallus gallus*). *Leporidae*; rabbits (*Oryctolagus cuniculus*). *Muridae*; mice (*Mus musculus*), rats (*Mus rattus*).

Keywords: horizontal gene transfer, plasmids, bacterial evolution, *in vivo*, *in vitro*, antimicrobial resistance

OPEN ACCESS

Edited by:
Yoshiharu Yamaichi, UMR9198 Institut de Biologie Intégrative de la Cellule (I2BC), France

Reviewed by:
Sebastien Rodrigue, Université de Sherbrooke, Canada
Brian Luna, University of Southern California, United States

***Correspondence:**
Melha Mellata
mmellata@iastate.edu

Specialty section:
This article was submitted to Antimicrobials, Resistance and Chemotherapy, a section of the journal Frontiers in Microbiology

Received: *07 March 2022*
Accepted: *07 June 2022*
Published: *30 June 2022*

Citation:
Ott LC and Mellata M (2022) Models for Gut-Mediated Horizontal Gene Transfer by Bacterial Plasmid Conjugation. Front. Microbiol. 13:891548. doi: 10.3389/fmicb.2022.891548

INTRODUCTION

The emergence and spread of antimicrobial resistance (AR) and virulence genes (VG) are of critical significance across the globe (Smillie et al., 2010; Devanga Ragupathi et al., 2019). Bacteria transmit genetic information either vertically from origin cell to progeny cells, or horizontally in the form of conjugation, transformation, or transduction (Smith, 2012; Juhas, 2015). Bacterial conjugation has shown to be the most significant route of horizontal gene transfer (HGT) in the context of the spread and emergence of AR in bacteria (Dolejska and Papagiannitsis, 2018). HGT

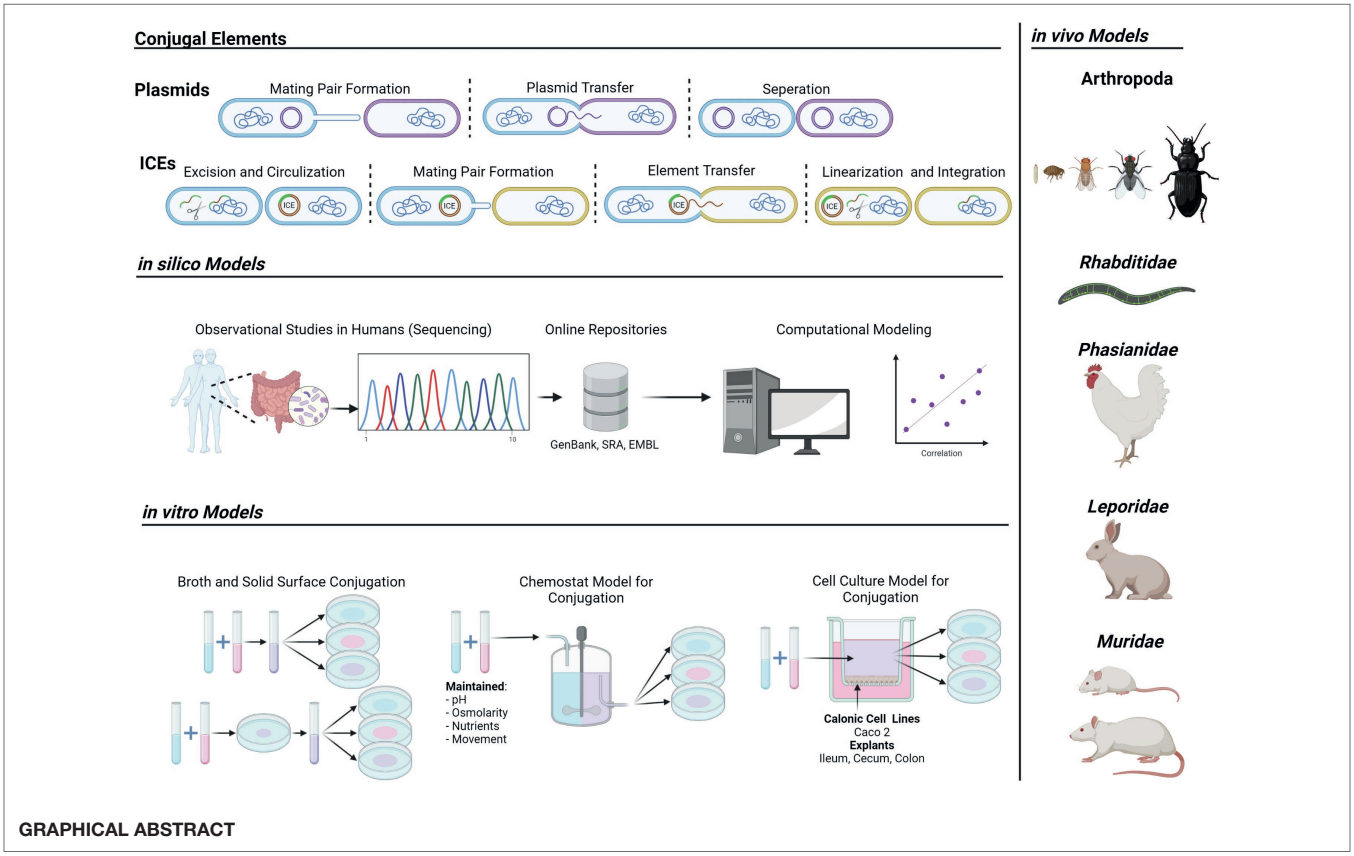

GRAPHICAL ABSTRACT

is prevalent in every environment, such as in soil, on surfaces, in clinical environments, as well as in the gut of animals (Guiyoule et al., 2001; Klümper et al., 2015; von Wintersdorff et al., 2016). HGT is a more significant means of evolution than that of random mutation, which results in slow alterations of genes already in a host bacterium. HGT, instead, results in the acquisition of entire genes, allowing for the rapid expression of new virulence, metabolic, and resistance phenotypes (Javadi et al., 2017). While bacterial evolution has been studied through the process of HGT, the primary concern in the context of human and animal health has been in AR, virulence, and the transfer of such from resistant bacterial strains to previously naïve bacteria that may function as reservoirs for transmission to other naive strains with the potential to become clinically and agriculturally important (Guiyoule et al., 2001; Klümper et al., 2015; von Wintersdorff et al., 2016).

The gut microbiota plays a critical role as a reservoir for AR genes (ARG) and HGT (McAllister et al., 1996; Salyers et al., 2004; Penders et al., 2013; Rolain, 2013). In mammals, as well as poultry, these reservoirs serve as sources for the emergence of novel AR strains with significance in both human and animal health (Balis et al., 1996; Salyers et al., 2004; Penders et al., 2013; Rolain, 2013; Nesme et al., 2014; Chen et al., 2016). However, to our knowledge, there are only few studies into the specific interactions of bacteria carrying one or more mobile plasmids and the host physiology resulting in HGT in humans. This is due to the inherent difficulty of conducting causal experiments in the human gastrointestinal tracts, and relies on either observational studies, or the use of *in vitro* and *in vivo* animal models to represent the human gut.

Many of the factors involved in the host–microbe interactions of gut-mediated HGT are not yet understood (Stecher et al., 2012; Ott et al., 2020). Limited *in vivo* studies have been conducted to determine the roles of factors such as host immunity, antibiotic treatment status, gut environmental conditions, and secretory molecules in the interactions of microbial HGT (Klimuszko et al., 1989; Thomas and Nielsen, 2005; Diaz et al., 2012; Stecher et al., 2012; Huddleston, 2014; Machado and Sommer, 2014; Getino et al., 2015; Zeng and Lin, 2017; Devanga Ragupathi et al., 2019; Ott et al., 2020). While there have been many publications reporting the transfer of AR plasmids *in vitro*, often in the context of soil or wastewater, there has been a stark lack of experiments that demonstrate the interactions of these bacteria *in vivo* (Macuch et al., 1967; Rang et al., 1996; Gevers et al., 2003; Card et al., 2017; Benz et al., 2020). In this review, we will present the current models for *in vitro*, *in silico*, and *in vivo* HGT experimentation regarding the gut environment, as well as survey of important findings demonstrated in these models.

CONJUGATIVE ELEMENTS

Classically, there are two forms of conjugative vectors: integrative and conjugative elements, and conjugative plasmids. They both

facilitate the transfer of genetic information between two bacterial cells but vary in the intracellular mechanism and maintenance within the cell. Regardless of genetic system, or mobile element involved, there are minimum requirement for both the physical interaction, recognition of recipient cells, and transfer of mobile DNA by donor and recipient cells. This is often mediated through the expression of type four secretion systems (T4SS) such as *tra*, *trw*, and *trb*. Each of these genes encode either intra or extracellular proteins for the assembly of a sex pilus for the attachment, retraction, and recruitment of recipient cells. Following pilus assembly and recipient recruitment, successful processing and trafficking of mobile DNA elements transfer encoded helicases, enzymes which unwind DNA and facilitate the nicking, replication, and trafficking of transfer DNA to the internal side of the conjugation machinery. Transfer strand DNA is then inserted and then transferred using ATP-dependent transferases to the recipient bacteria where it must be circularized, genes expressed, and mobile element replicated (Willetts and Wilkins, 1984; Johnson and Grossman, 2015).

Integrative Conjugative Elements

Integrative conjugative elements (ICE) are a unique form of insertable DNA vector that can be excised from the chromosome and transferred through conjugative sex between bacterial strains. ICE contain the genetic information that completely encodes for the machinery to enable its transmission. Unlike plasmids, ICE do not normally reside in the host cell as extrachromosomal genetic information. Instead, ICE are inserted sequences in the host chromosome and replicates as a passive element within the chromosome. Integration of ICE elements into target DNA sequences is dependent on the presence of sequence specific integration attachment (*att*) sites such as *attB* and a correlating recombination module encoded *att* site, such as *attP* (Wozniak and Waldor, 2010; Bauelos-Vazquez, 2017). Sequence binding between the *attP* and *attB* site by ICE vectors results in recombination and integration into the target DNA. This process results in duplicate flanking *att* sites on either end of the insertion increasing the total number of ATT sites in the target DNA sequence (Johnson and Grossman, 2015; Delavat et al., 2017). The prevalence of *att* sites varies in bacterial genomes; however, it is clear that ICE and associated *att* sites are widespread in bacteria so the specificity of ICE transfer and integration into bacterial hosts of varying backgrounds is not entirely clear (Cury et al., 2017; Guédon et al., 2017). Recently, examples of ICE that employ a site-independent integration using a separate DDE recombinases have been identified which has further added ambiguity to the host range of ICE vectors (Johnson and Grossman, 2015).

The mechanisms of ICE replication and transfer *in vivo* are still not completely understood, such as the steps of excision, maintenance, circularization, conjugative transfer, and integration in the gut environment (Pan et al., 2019). Thus, the continued observations and experimental studies of ICE are significantly important in the understanding, and prevention of, the spread of ARG both in the animal gut.

ICEs are typically modular, with weakly defined beginnings and ends as compared to other genetic vectors. ICE sequences are typically flanked by elements resembling transposons and viruses which allow them to randomly acquire new gene regions through recombination and inexact excision (Wozniak and Waldor, 2010). Davies et al. describe a novel ICE, ICEde3396 isolated from *Streptococcus dysgalactiae* (Davies et al., 2009). They determined through human isolate screening, that multiple *Streptococcus* isolates of group A, B, and G, possessed regions of the ICE, and some even contained all regions of the ICE. The authors then demonstrated by labeling the element with kanamycin resistance and *in vitro* mating that the element is conjugatively transferred from bacteria to bacteria, carrying the AR gene. They hypothesize that this integrative element can acquire DNA from each bacterial host that acquires it, and function as a vehicle for the dissemination of this information. While this was the observation of human isolates, it is not clear if this is true *in vivo* as it remains to be observed in the host.

There is anecdotal evidence that ICE are acting as vectors for modular evolutions where the dissemination of genetic information is facilitating the rapid adaption of bacterial strains to new metals and antibiotic substances. Davies et al. hypothesize that since β-hemolytic Streptococci have not developed resistance to penicillin, which is extensively used, by natural mutation, mobile genetic elements (MGE), such as ICE, are going to be the source of penicillin resistance acquisition in these bacteria (Davies and Davies, 2010). In *Enterobacteriaceae*, a prevalent family of bacteria implicated in the emergence and spread of antimicrobial resistance, ICE are highly prevalent such as in the pathogenicity islands of *Salmonella* with which also occurs in a large portion of non-*Salmonella Enterobacteriaceae* (Seth-Smith et al., 2012). Observational studies have shown the prevalence of MGE, including ICE, in bacterial strains isolated from populations of the human gut microbiotas, such as Actinobacteria, Bacteroidetes, Firmicutes, Proteobacterium, and Verrucomicrobium (Jiang et al., 2019). Furthermore, Coyne et al. reported evidence of extensive ICE transfer in the gut of humans. This study was observatory in nature and requires further experimental validation (Coyne et al., 2014).

In both human and animal host, *in vivo* examples of ICE gene transfer are almost exclusively observational. It is imperative to determine the *in vivo* roles of ICE experimentally. While reviews on the mechanisms and biology of ICE have been performed, a separate, detailed review of the *in vivo* models to study the transfer of ARG and VGs is desirable (Johnson and Grossman, 2015; Delavat et al., 2017; Botelho and Schulenburg, 2021), but outside the scope of this review.

Conjugative Plasmids

Conjugative plasmids are extrachromosomal circular DNA molecules replicated by the host during cellular division and periods of bacterial conjugation (Couturier et al., 1988; Grohmann et al., 2003; Smillie et al., 2010; Arutyunov and Frost, 2013). They can be mobile, mobilizable, or non-mobile in nature. Mobile plasmids, which encode all genes for replication, transfer initiation, and transfer machinery, and mobilizable plasmids

which encode the genes for replication and transfer initiation but not transfer machinery, are potent vectors for the exchange and transfer of genetic information. These genetic vectors often encode for virulence factors such as secretion systems, siderophores, and metabolic pathways, as well as ARG (Gibson et al., 1979; Goldstein et al., 1983; Wang et al., 2003; Diaz et al., 2012; Benzerara et al., 2017; Jamborova et al., 2017; Cabanel et al., 2018; Dolejska and Papagiannitsis, 2018). Recently, both mobile and mobilizable plasmids have been areas of major focus in the prevention of the emergence and spread of ARG in the context of agricultural and clinical environments (Marshall et al., 1981; Hoffmann et al., 1998; Lacey et al., 2017). While much research has been conducted on the mechanisms, rates, and inhibition of plasmid conjugation between bacteria in environments such as soil and wastewater treatment, there has been sparse research conducted on these topics in the context of the animal host.

Bacterial Plasmid Conjugation and the Human Gut

Although direct experimentation in humans is difficult due to the ethics related to this nature of research, many observational studies have been performed that demonstrate the capability of the human microbiota to be involved in the plasmid-mediated HGT of AR and VG. The presence of plasmid-mediated AR and VG in clinically isolated samples is well documented (Corliss et al., 1981; Balis et al., 1996; Oppegaard et al., 2001; Winokur et al., 2001; Salyers et al., 2004; Hong et al., 2009; Aguado-Urda et al., 2012; Diaz et al., 2012; Liu et al., 2012; McInnes et al., 2020). These plasmid-mediated ARG and VGs have been shown, anecdotally, to be involved in plasmid conjugation and the emergence of novel resistant bacterial strains in human healthcare (Balis et al., 1996; Guiyoule et al., 2001; Winokur et al., 2001; Ohana et al., 2005; Daini and Akano, 2009; Goldfarb et al., 2009; Mahmood et al., 2014; Schweizer et al., 2019). However, due to limitations in human microbial research related to the introduction of antimicrobial resistance plasmids into living hosts, there has been a limit to the understandings available surrounding the factors that participate in regulating the process of plasmid-mediated HGT in and on humans. Many studies have postulated hypothetical host-microbial interactions (HMI) involved in regulating the process of plasmid-mediated HGT in the animal microbiota, but few of these HMI have been experimentally demonstrated in an *in vivo* environment (Macuch et al., 1967; Dunkley et al., 2007; Ziv et al., 2013; Gresham and Hong, 2015; Card et al., 2017; Li et al., 2020).

Many of these studies, understandably, target the gut as the specific microbiota niche to study (Macuch et al., 1967; Gevers et al., 2003; Dunkley et al., 2007; Card et al., 2017; Oladeinde et al., 2019). While many surfaces in and on the human body are believed to maintain resident niche microbiotas, the gut significantly outweighs the others in importance, abundance, and effect on host physiology and biology (Huddleston, 2014; Zeng and Lin, 2017; Gould et al., 2018). To approximate this host environment, researchers in the fields of microbial evolution, emergent AR, and bacterial-host interactions have proposed both *in vitro* and *in vivo* models for the human gut and methods to use these models to study the role of the bacterial host interaction on HGT. Additionally, while integrative and conjugative elements and natural transformation with free DNA may play a role in the transfer of genes in the gut, the use of specific models to study these are not well developed and the contribution they make to the emergence of antimicrobial resistance and virulence spread is not clearly understood. As such, this review will focus on bacterial plasmid conjugation as the primary vector for horizontal gene transfer and describe the models used for study.

IN SILICO MODELS

Bacterial plasmid conjugation is inherently complex and relies on the interplay of a multitude of factors including both DNA and protein regulation, as well as intra and extracellular signaling and interactions (Willetts and Wilkins, 1984; Cabezón et al., 2014; Bragagnolo et al., 2020). Determining the significance of each individual factor in the incidence and rate of conjugation in complex environments is thus inherently difficult. However, the use of mathematical models to approximate conjugation in these environments, and to help elucidate the role and significance of these factors in conjugation has offered a potential way to unravel this complex interaction. For example, the roles of bacterial growth, self-regulatory elements, and mating pair stabilization proteins have been integrated using computational models. However, these models were experimentally informed by *in vitro* studies and do not currently incorporate all the confounding factors that potentially regulate plasmid conjugation in complex host associated environments such as in the animal gut (Haft et al., 2009; Merkey et al., 2011; Campos et al., 2020).

While *in vivo* experiments directly in the human gut are not feasible, mathematical, and computational models for conjugation do give us insight into the prevalence and impact of bacterial conjugation in these complex environments (Tepekule et al., 2019; Li et al., 2020; Techitnutsarut and Chamchod, 2021). Recently, Tepekule et al. described the impact of host antibiotic treatment history on plasmid-mediated resistance evolution in human gut microbiota by utilizing a composite model of resistance evolution and microbiota dynamics (Tepekule et al., 2019). Their model consisted of a set of ordinal differential equations that represent the growth and change in distribution of microbial phylums over time correlated with the incidence of antimicrobial treatment and recovery periods. Using this mathematical model to simulate treatment histories based on published microbiome data, they determined three crucial factors regulating HGT significance in the gut of antimicrobial-treated individuals. The first factor was total days of drug exposure, or the time that the patient was administered antimicrobial drugs during treatment. Secondly, the duration of the drug-free period after the last treatment, or the length of time for recovery of the gut microbiota. Finally, the center of mass of the treatment pattern, or the abundance and distribution of treatment.

The role or impact of antibiotics in bacterial plasmid transfer in the complex gut microbiota has been further modeled *in silico* by Klümper et al. whom used both direct experimentation in pig fecal extract experiments as well as in a mathematical model informed by results from the extract experiments and incorporated parameter vales for both susceptible and resistant populations, as well as for the microbial community (Klümper et al., 2019). This study demonstrated a time-discrete mathematical model to approximate the transfer of antimicrobial resistance plasmids in a complex microbiota environment compared to *in vitro* broth conditions. Using this model, the authors postulate two mechanisms for reduction in the minimum selective concentration, including the relative increased cost of resistance, and the protective effect of the microbiota community on the susceptible phenotype.

These *in silico* models have been beneficial in postulating novel mechanisms involved in the rate and incidence of plasmid transfer; however, mathematical modeling is burdened with inherent limitations due to the nature of mathematical modeling itself (Sørensen et al., 2005; Bakkeren et al., 2019). This approach is dependent on the quality and abundance of available source data; and is limited by the availability of metadata, or associated information about the data; coverage, or completeness of the data and the metadata; and diversity of the source data, or the number of real-world scenarios covered by the data.

In the case of bacterial conjugation in the human gut, many knowledge gaps may provide substantial variance that support or contradict mathematical modeling results when the observed trends are applied to real-world gut plasmid transfer. These factors need to be experimentally determined and characterized using the available *in vitro* and *in vivo* models available before they can be incorporated into *in silico* models. After which, a more refined and accurate model may be producible that would more accurately reflect real-world plasmid transfer in the gut. These models do, however, provide important preliminary insight and are helpful in postulating new research questions for further experimental exploration in both *in vitro* and *in vivo* models of the gut.

Furthermore, mathematical and *in silico* modeling of bacterial conjugation in the environment, such as in biofilms, wastewater, and *in vitro* laboratory conditions, however, modeling of conjugation in the *in vivo* environment of the animal gut is still limited, largely due to the lack of these priory data required for the construction of such models (Haft et al., 2009; Merkey et al., 2011; Campos et al., 2020; Sutradhar et al., 2021). As such, more effort to define and implement *in vivo* models to identify and characterize important *in vivo* factors is required before significant conclusions are achievable with *in silico* modeling.

IN VITRO MODELS

A significant task for *in vitro* studies is to identify environmental conditions measurable *in situ* that can approximate the conditions of the gut. The two most straightforward and common methods for *in vitro* conjugation assays are broth and solid surface conjugations. Broth conjugations include the growth of, and combination of, a donor and recipient strain at even or varying ratios (e.g., 1:1, 1,000:1, 1:1000, etc.) in either rich or defined media for a predetermined period (Fernandez-Lopez et al., 2005; García-Cazorla et al., 2018; Khajanchi et al., 2019; Ott et al., 2020; Jochum et al., 2021; Redweik et al., 2021). Further selective and differential plating of samples occurs for the selection and identification of donor, recipient, and transconjugant populations. Solid surface conjugation, likewise, involves the growth of donor and recipient strains in rich or defined media, these cultures are then placed onto the surface of either sterile agar or sterile filter paper applied to the surface of agar (Brown, 2016; Khajanchi et al., 2019). After a period, the cells are either scraped off the agar, or the filter paper is removed and vortexed in sterile buffer to generate a suspension. The resulting suspension is serially diluted and plated as in broth conjugations to enumerate each bacterial population of interest.

Both broth and surface methods work to approximate different conjugation environments in the context of the gut. Broth conjugations simulate the luminal conjugation between bacteria suspended in the heterogeneous matrix of intestinal material; while solid surface conjugation resembles, instead, the mucosal and epithelial niche environments where bacteria are stationary and anchored to a surface (Khajanchi et al., 2019). Although, these two methods can approximate the location and relation of bacterial cells in the gut during conjugations, they do not inherently represent the physiochemical, biochemical, and mechanical conditions of the gut environment. Confounding factors, such as pH, salinity, antimicrobial peptide (AMP) concentrations, antibodies, the host microbiota, and any number of yet characterized host factors potentially play a significant role in the efficacy of conjugations in the gut. The understanding of the basic mechanism by which these factors may or may not affect conjugation are significant to understand the emergence of novel antimicrobial resistant strains in human and animal health.

To understand these confounding factors more completely, much work has gone into developing more extensive *in vitro* models to simulate the human or animal guts. Incorporating factors such as pH, oxygen saturation, and metabolites may increase the insight garnered by these studies.

Chemostat Models

Chemostats are important *in vitro* models used by microbiologists to simulate the complex gut environment. They involve the automated, or manual, regulation of pH, osmolarity, nutrient availability, and homogenization of a bacterial suspension matrix in a built environment. These models are useful in approximating a limited set of gut factors and produce a limited approximation of the gut environment of a variety of hosts. However, chemostat models do not incorporate the entirety of the responsive host factors elicited by the microbiota in the gut environment, such as antimicrobial peptide secretion, reactive oxygen release, or even adaptive immune mediators such as IgA antibodies. Additionally, chemostats generally assume homogeneity in the systems they model, which is not the case in the gut environments where different sections of the gut have differing physiological characteristics.

This was assessed somewhat by Card et al. who used a six-stage fermentative chemostat to model the chicken gut environment. In their study, they describe the use of six individual 20 ml fermentation vessels that were maintained for pH, temperature, atmosphere, and matrix homogenization that represented separate segments of the gut (Card et al., 2017). Using the chemostat model, the authors were able to show the transfer of a multidrug resistance plasmid from *Salmonella* to commensal *E. coli* strains found within the chicken fecal microbiota. This study demonstrated the transfer of a multidrug resistance plasmid from a common gastrointestinal contaminant to the microbiota of chickens in a simulated chicken gut *in vitro*.

Human chemostat models are also in use to determine the role of human gut microbiota and host factors in the incidence and rate of conjugative plasmid transfer. Rooney et al. used a triple stage chemostat model of the human gut to demonstrate the transfer of carbapenem resistance (CRE) genes from *Klebsiella pneumoniae* to the microbiota of CRE-negative human feces (Rooney et al., 2019). The three vessels, V1 (proximal small intestine), V2 (distal small intestine), and V3 (large intestine), were controlled for pH and alkalinity. Additionally, V1 was supplemented with growth media to maintain nutrient availability. All three vessels were stirred for homogeneity and sparged with oxygen free nitrogen gas to maintain anaerobic conditions. This study demonstrated the colonization, clonal expansion, and transfer of CRE genes within the human gut microbiota.

However, chemostat models, such as those in Card et al. and Rooney et al. employ total vessel homogenization and fail to fully replicate the local segregation of physiochemical conditions found in each individual region of the gut compartment that each vessel represents. This is important because the intraluminal conditions of the gut contents are often significantly different than those found in the mucosal lining of the epithelia, and these differences result in distinct microbial communities between the two regains (Donaldson et al., 2015). Factors such as pH gradients, secretory proteins, and nutrient bioavailability vary between the epithelial surface and the luminal content, and this has been shown to significantly impact the overall growth and activity of gut microbes such as *Escherichia coli* (*E. coli*) and other *Enterobacteriaceae* that are important in the emergence and spread of antimicrobial resistance through bacterial conjugation indicating that the use of these models may mislead or provide an inaccurate representation of what may occur in the complex gut environment (Poulsen et al., 1995; Licht et al., 1999). Licht et al. demonstrated drastic differences between a homogeneous chemostat model and *in vivo* transfer of plasmids in a streptomycin treated mouse model (Licht et al., 1999). Instead, a fixed continuous flow biofilm culture better represented the results observed in the murine model but offered limitations such as cessation of plasmid transfer after an initial period of high incidence.

Further studies on the use of chemostats are warranted, as they provide meaningful insight into potential roles of various physiochemical factors identified in the gut environment; however, their results should be interpreted with an objective understanding of the limitation of this model to approximate the gut environment. Future studied implementing chemostats should further include the addition of either specific or combinations of additional host factors to hopefully increase the accuracy and impact of the results obtained from their use such as mechanisms to generate static regions of low homogeneity that may be able to rescue some characteristics of the epithelial and mucosal conditions found *in vivo*. Additionally, supplemental addition of individual factors such as purified antimicrobial peptides or isolated host immunoglobulin could help elucidate the specific role of those factors in conjugation in a less complex approximations of the gut environments.

EX VIVO MODELS

Limitations associated with simple *in vitro* studies, such as the lack of confounding host factors, has led to the need to identify and develop intermediate conditions that retain the ease of use and simplicity of traditional *in vitro* assays, but rescue a portion of complexity associated with host environments. To address this, a common practice in host-microbial interactions is to use host tissue *ex vivo*, or outside of the natural animal host (Bermudez-Brito et al., 2013; Machado and Sommer, 2014; Barrila et al., 2018; Stromberg et al., 2020). This approach offers advantages over traditional *in vitro* studies, such as maintaining a controlled environment while reincorporating the complex interactions associated with host tissues (Bermudez-Brito et al., 2013; Barrila et al., 2018).

Cell Culture Model

While studying plasmid transfer in the context of the *in vivo* human gastrointestinal tract is not feasible, the use of human- and animal-derived gastrointestinal cell lines does give us a glimpse at the host biology involved in host-microbial interactions. Machado et al. describe the use of the human gastrointestinal carcinoma cell line, Caco-2, as an *in vitro* model of the human gastrointestinal system (Machado and Sommer, 2014). The authors grew these immortal intestinal cells on the surfaces of sterile transwell membrane inserts allowing for the development of a differentiated cell monolayer and the separation of media to the basal and the apical sides, approximating the separation of space in the human epithelial layer. After adding bacterial donors and recipients to the apical media in co-culture, the authors showed conjugation. Furthermore, they showed the reduction in bacterial conjugation in the presence of the Caco-2 cells when compared to broth conjugation. Using this model, the authors demonstrated an unidentified protein factor that modulates bacterial conjugation in *in vitro* cell line co-culture. While the authors have not yet further characterized the factor that is regulating conjugation in the gut, this study shows the importance of human cell culture in providing an insight into the host-derived factors that regulate conjugation in the gut.

The cell culture model, inherently, does not incorporate confounding factors of the human host, such as mucosal barrier, innate and adaptive immune function, or further factors important in regulation of bacterial metabolic pathways or inter species interactions such as those observed in the microbial

fermentation of undigestible fibers into short chain fatty acids. However, many of these factors can be studied in more detail using this model by supplementing specific factors during conjugation. Cell culture serves as an important method for the future study of bacterial host interactions important in the regulation of bacterial conjugation and the emergence of novel antimicrobial resistant and virulent strains.

While cell culture provides an interesting model for the intestinal environment in conjugation events, it does not accurately represent healthy gastrointestinal tissue topology, biochemistry, nor diversity. Cell lines, such as Caco-2 cells, grow into monolayers and differentiate into complex cell surface topology; however, cell lines are typically cancerous or otherwise immortalized resulting in altered gene expressions and cellular response to stimuli and may vary even between cell lines of similar sources, e.g., Caco-2 and HT29 (Verhoeckx et al., 2015). As such, the use of healthy tissue is desirable. Explant tissue culture is currently used in numerous bacterial associations, pathology, and host response studies (Sunkara et al., 2011; Stromberg et al., 2018). However, there have not yet been any detailed studies using them as a model to demonstrate conjugation in association with healthy animal tissue *in vitro*. Studies in our laboratory are currently exploring this model to identify host responses in controlled *in vitro* assays (Ott et al., 2021).

IN VIVO MODELS

While *in vitro* models provide a glimpse into the role of individual factors of the gut environment in bacterial conjugation and a useful insight into the mechanism that may be involved, a wholistic model is required to better understand the real-world role of host and microbial factors on bacterial conjugation (Ott et al., 2020). Animal models that offer both a reduced gut complexity and express conserved functions from the animal gut have recently been used to model bacterial conjugation *in vivo* (Stecher et al., 2012; Ott et al., 2020, 2021). While they are not entirely representative of the natural gut environment of humans, they do incorporate compounding factors such as host immunity, diet, genetics, and microbiota; that are not well accounted for in *in vitro* and *in silico* models (Petridis et al., 2006; Stecher et al., 2012; Ott et al., 2020, 2021).

Arthropod Models

Arthropods are the most diverse and abundant group of animals on earth (Aguinaldo et al., 1997; Thomas et al., 2020). With significant co-occurrence in the environment with microbial communities, interaction between the two is a constant. The horizontal transfer of bacterial genetic information to arthropod hosts has previously been studied as a mechanism for both eukaryotic and prokaryotic evolution (Wybouw et al., 2016). However, the contribution of HGT between bacteria in the gut of arthropods resulting in the emergence of AR and virulent strains has not been extensively studied (Hoffmann et al., 1998; Fukuda et al., 2016, 2019). The mobility, and prevalence, of arthropod hosts in the environment, and specifically in the context of agricultural systems, make them an important reservoir for mobile AR and VG (Black et al., 2018; Fukuda et al., 2019). Furthermore, due to the dietary habits and lifecycles of many agricultural pests, exposure to populations of microbes sub-lethally exposed to antibiotics results in proliferate colonization of arthropod guts with bacterial strains harboring conjugatively transmissible elements, in the form of extrachromosomal plasmids (Hoffmann et al., 1998). As such, these complex gut-microbiota can function as reservoirs for the donation of these AR and virulence plasmids to pathogens and pathobionts resulting in the emergence of both human and agriculturally significant pathogens with novel phenotypes (Black et al., 2018; Fukuda et al., 2019).

The microarthropod *Folsomia candida* (Collembola), is important in this spread of mobilizable genetic material into microbial populations. Genetic information introduced into the gut microbiota of arthropod guts is further deposited by the host to soil and plant surfaces in agricultural environments (Hoffmann et al., 1998). This is significant if you consider the prevalence of HGT occurring on the surface of agricultural produce that participates in the colonization and spread of AR in the gut of humans (Maeusli et al., 2020). The arthropod endosymbionts of the genus *Rickettsia* have been shown to contain chromosomal and plasmid-encoded conjugation genes in addition to theoretical VGs involved in pathogenicity in humans (Weinert et al., 2009). However, it is not yet clear if this inherent plasmid conjugation is involved in the emergence of newly pathogenic bacteria that passage through these arthropod hosts and terminate as infections in humans.

While the significance of bacterial conjugation in these arthropod hosts in a clinical context is not clear, agriculturally significant strains are participating in conjugation. Poole et al. describe the transfer of a large AR plasmid from *Salmonella enterica* Serovar Newport to a laboratory *E. coli* (JM109) within the gut of the lesser mealworm beetle, *Alphitobius diaperinus* (Poole and Crippen, 2009). In this study, the authors demonstrated the *in vivo* transfer of AR from a commercially significant *Salmonella* pathogen to a laboratory strain *E. coli* after oral inoculation and colonization of the mealworm beetle, commonly associated with poultry litter and other poultry environments. These mealworms and other insects found in poultry environments are considered an important source for multi-drug resistance bacteria (McAllister et al., 1994, 1996; Wybouw et al., 2016; Fukuda et al., 2019).

The prevalence of HGT in the gut of arthropods is concerning as a source of novel resistance and virulence strains. The human pathogen, *Yersinia pestis*, the causative agent of the plague, has recently been shown to participate in high frequency conjugation with gut commensal *E. coli* donors *in vivo* in the midgut of the rat fleas *Xenopsylla cheopis* (Hinnebusch et al., 2002). The authors demonstrated the role of the gut microbiota of the alternate host as a source of additional AR plasmids in the emergence of novel plague strains with clinical significance. The model used in this study approximated the natural environment, and the authors hypothesize that the results may be like what could be seen in the wild. However, this has yet to be experimentally demonstrated and should be studied further to determine

the significance of arthropod host microbiota on the emergence of bacterial pathogens of human importance.

There have been few experimental studies yet that describe the bacterial host interactions that regulate the conjugation of plasmids and other MGEs in the gut of arthropod hosts. The common housefly *Musca domestica L.* was shown to facilitate the intestinal transfer of the pCF10 AR plasmid among *Enterococcus faecalis* (Akhtar et al., 2009). This model, however, has not yet been used to study in-depth any host-bacterial interactions that regulate the rate or presence of conjugation in the gut. Our laboratory has recently demonstrated the use of *Drosophila melanogaster* as a model organism for arthropods, humans, and other animals. Using this model, we hope to utilize the vast genetic toolbox and reduced gut complexity to identify specific mechanisms by which the host regulates bacterial conjugation. We have shown a potential role of plasmid Inc. type and host genetics on regulating conjugation in the gut (Ott et al., 2021). However, this model offers a significant amount of variability and requires significant increases in sample size due to the limited volume of the gut. We are further validating and optimizing this model for continued use.

Rhabditidae Model

The free-living nematode *Caenorhabditis elegans* (*C. elegans*) is extensively used to study genetics and cellular development due to its extreme simplicity and genetic tractability. Furthermore, due to its rapid multiplication time and ease of culture, they offer themselves as a desirable model for host bacterial interaction studies. Portal-Celhay et al. demonstrated *C. elegans* as a model for conjugative transfer of the R27 IncH1 plasmid (Portal-Celhay et al., 2013). The authors proposed a role of both age and genotype on the rate of intestinal conjugation between *E. coli* hosts. They identified age as a driver for an increased rate of conjugation with significant increases in older hosts (days 1–3 versus 4–7). Furthermore, they demonstrated that host genotype is a predictor for both conjugation frequency and transconjugant populations size within the gut of *C. elegans*.

However, the methods used in Portal-Celhay et al. study (Portal-Celhay et al., 2013) do not entirely rule out environmental conjugation, as the nematodes were grown on bacterial mats on the surface of growth agar, and conjugants could form outside of the host and then be subsequently ingested by the host. The role of environmental conjugation may be significant in the increase in conjugation identified with age as the transit time in the gut and volume of defecation varies with the age of nematodes (Portal-Celhay et al., 2013). The methods used with this model must be further refined to ensure that conjugation is occurring within the gastrointestinal tract of the animal host and not entering the gut through digestion.

Phasianidae Model

Avian sources are believed to be the largest contributors to foodborne illnesses (Economic Research Service, 2015). Additionally, Liu et al. recently showed that microbial contaminants on the surfaces of commercial poultry samples not only harbor AR but can be phylogenetically linked to urinary infections in humans (Liu et al., 2018). Acting as a significant host to foodborne illness, agricultural and healthcare industries are especially concerned with the formation of AR and the ability of such a resistance to being spread to other organisms or consumers (Smith, 1970; Teuber, 1999). The avian gastrointestinal tract has previously been approximated *in situ* and *in vitro* (Card et al., 2017). *In vitro* chemostat models have been described previously; however, these methods do not incorporate host factors such as avian immunology, dietary interactions, the mating pairs, or the role of the host microbiome (Card et al., 2017). As such, *in vivo* studies in the chicken gut are still desired to determine the holistic regulation of bacterial plasmid conjugation.

In 1970, Smith et al. stated that the transmission of an R factor-mediated AR occurred readily *in vitro*, and that many researchers previously used modified *in vivo* hosts, such as antibiotic knockdowns and gnotobiotic birds, to study plasmid transfer in a host, however, none studied the spread of AR in a non-modified normal microbiota host (Smith, 1970). As such, the authors conducted plasmid transfer between different strains of *E. coli* and *S. enterica subs*p. *enterica* Serovar Typhimurium in chickens. They concluded that not only was the resistance being transferred to the new bacterial hosts, but the organisms were also invading the tissue and were detectable in the liver. We have previously demonstrated the ability of large plasmids conferring both AR and virulence genes to normal gut microbiota members (Mellata et al., 2010). This is significant, as it shows transconjugant bacteria with acquired AR is transferring to areas of poultry tissues not automatically discarded at harvesting, such as is the intestines, in addition to the ready ability of poultry pathogens to spread AR and virulence genes to commensal organisms' (Oosterom et al., 1983; Mellata et al., 2010).

HGT in the agricultural environment has been considered a source of emergence and spread of AR; however, it is also as source of plasmid-mediated spread of virulence factors (Lacey et al., 2017). Identifying the mechanistic change in DNA associated with the emergence of virulent strains with medical significance to humans is important. While random mutations act as a source for the emergence of novel genes, in the commercial environment, the horizontal transfer of large plasmids encoding whole AR and VG are more concerning due to the rapid spread possible in a population. Lacey et al. demonstrated the prolific spread of virulence plasmids between strains of *Clostridium perfringens* within the gastrointestinal tract of chickens without selection under antibiotic pressure (Lacey et al., 2017). Furthermore, this cohort hypothesis that this conjugation-mediated HGT may play a significant role in pathogenesis and evolution on *Clostridium* sp. and this needs to be further studied for significance.

The role of host factors, such as DNA, RNA, secretory proteins, and other macromolecules, is not entirely clear; however, studies in chickens have begun to provide some introductory insight. We previously showed the implication of cecal small RNA (sRNA) in plasmid transfer in the gut (Redweik et al., 2021). In this study, we demonstrated that the concentration of cecal sRNA is affected by prophylactic treatments giving

to chicks and is proportional to the incidence of large plasmids in *E. coli* isolates from the ceca; *in vitro* assays showed a sRNA dose-dependent increases in bacterial conjugation in response to addition of isolated ceca small RNA. Further experimentation is required to better elucidate how cecal RNA populations may regulate bacterial conjugation and the incidence of large plasmids in the gut microbiota.

Leporidae Model

Rabbits provide a valuable experimental model analog for humans and other animals (Hershberger et al., 2000; Peng et al., 2015; Hirt et al., 2017). While rabbits have notable differences in physiology, such as being primarily fermentative in gastrointestinal digestion as compared to humans, they have been used extensively as a model for a plethora of human infections and diseases (Ericsson, 2019). Rabbits were, and continue to be, invaluable in the effort to make fundamental discoveries in immunity such as in the development of the rabies vaccine. The use of this model for human gut physiology has its limitations; however, rabbits may serve as a developed, more complex, intermediate between *in vitro* studies and human physiology.

For example, Hirt et al. used New Zealand White Rabbits in an endocarditis model of *E. faecalis*. Using this model, the authors showed stimulation of virulence and plasmid transfer of the sex pheromone plasmid pCF10 (Hirt et al., 2018). Through *in vivo* rabbit experiments and *in vitro* human and rabbit sera experiments, the authors showed that plasmid pCF10, which harbors the gene for aggregative substance molecules, not only increases vegetative mass of endocarditis but is important in the induction of plasmid transfer upon exposure to human and rabbit sera. This work shows that human and rabbit plasma function as an interference agent in the normal signaling of the sex pheromone and induce higher rates of plasmid transfer. While the authors do show this behavior *in vivo* in rabbits, they do not show that it is the case in humans *in vivo*. Rabbits are a valuable model for human diseases; however, it is still unclear if this is the same interaction that can be observed *in vivo* of human hosts. The significance of this work is evident when considering methods to prevent plasmid transfer. Defining an immune response to strains containing plasmids may not be sufficient to prevent HGT, in fact, it may exacerbate it by interfering with normal conjugation regulation.

Muridae Models

Observing plasmid transfer through conjugation in the mammalian gut proves to be difficult due to the variability in host factors, such as diet, environment, age, genetics, and microbiota. For example, the murine model for humans is difficult to use in the study of HGT as they confer a natural resistance to colonization by *Enterobacteriaceae* members, such as *E. coli* and *Salmonella* (Stecher et al., 2012; Ott et al., 2020). Both of which are significant contributors to the emergence and spread of novel AR plasmids as well as integrative elements (Stecher et al., 2012; Redondo-Salvo et al., 2020). Recently, Lasaro et al. demonstrated the isolation and use of an *E. coli* isolate for the colonization and replication in the gut of a murine model. While this does offer opportunities to use this *E. coli* strain as a recipient in *in vivo* conjugation experiments, it does not address the limitation of using alternate *Enterobacteriaceae* donors of interest such as human gastrointestinal pathogens (Lasaro et al., 2014). It is not clear what specific metabolic characteristics enable the reliable colonization and persistence in the gut microbiota, but the authors postulate that ability to participate in anaerobiosis and the expression of stress response regulators ArcA, CpxR, and RcsB are strong contributors to colonization. Identification of these pathways may lead to a better developed murine model for studies on conjugation in the gut and this warrant further exploration.

Mice can be conditioned chemically to prevent this natural resistance to *Enterobacteriaceae* colonization. The primary and most used method for this is the use of broad-spectrum antibiotics, such as streptomycin, to knock down the resident gut microbiota. Reduced microbial diversity and abundance in the gut permits colonization and persistence of *Enterobacteriaceae*, such as *E. coli* and *Salmonella*, within the gastrointestinal tract of mice. Alternatively, germ-free mice can be used to prevent the use of antibiotics and any associated effects of the drugs on the hosts physiology; however, both methods rely on ablating the natural gut microbiota that has a demonstrated role as crucial in normal host physiology and gut homeostasis (Stecher and Hardt, 2008; Round and Mazmanian, 2009; Broderick et al., 2014; Kim et al., 2014; Sannino et al., 2018; Lyte et al., 2019; Liao et al., 2020; Neil et al., 2021). For example, the gastrointestinal tissue of germ-free mice demonstrates significantly altered physiology and inflammation status than conventionally colonized mice (Brand et al., 2015). As a result, these models have a plethora of alternate effects such as altered gut brain axis function, diarrhea, increased gastrointestinal inflammation, and reduced macronutrient absorption (Brand et al., 2015; Lyte et al., 2019). These factors may interfere with observation of these studies or introduce additional variables that may be unaccounted for.

As a result of these limitations of chemical and germ-free models, an intermediate of germ-free and conventional microbiota is desirable for the observation of host and microbial interactions under non-selective host conditions. A model that rescues normal host physiology while offering a much less complex microbiota and allowing for stable colonization and persistence of *Enterobacteriaceae* species. To solve this issue, many studies have turned to using gnotobiotic mice, such as the Altered Schadler Flora (ASF) mice models (Brand et al., 2015; Lyte et al., 2019; Ott et al., 2020). ASF mice contain a defined set of eight bacterial species that approximate the gut of a healthy mouse while limiting the diversity of the gut (Brand et al., 2015). This host was recently shown to be a good model for *Enterobacteriaceae* colonization and *E. coli* pathology (Stromberg et al., 2018). Furthermore, this model was recently used by our team to show successful *E. coli* colonization of the gut as well as elucidate host factors important for the regulation of HGT between a foodborne *Salmonella enterica* subsp. *enterica* Serovar Kentucky and *E. coli* (Stecher et al., 2012; Ott et al., 2020). This model is desirable due to the control over inherently

complex host factors otherwise unaccounted for. ASF mice are isolated in sterile, flexible film barrier housing and fed irradiated standardized diets and subjected to regulated night day light cycles in a temperature-controlled room. The genetics of these animals can also be controlled using inbred mouse lines.

The use of the ASF mouse model is continuing to be explored as a controlled model to determine the effects of any number of host factors on conjugation in the gut. It may be used to further identify the role of host immunity and novel vaccine targets on conjugation, as well as other immune mediators such as antimicrobial peptides. It can also be used to determine the role of diet or the environment on the stability and efficiency of HGT in controlled settings, unlike the case with many other models where variability in starting hosts leads to uncertainty in experimental results.

Sub-lethal antibiotic exposure (SLAE) exhibits effects on bacteria beyond cell damage and death. SLAE initiates alternate gene expression in exposed cells, such as initiating the stress response pathways, reducing metabolic activity, and stimulating conjugative plasmid transfer (Beaber et al., 2004). Furthermore, antibiotic treatments affect the gut microbiota of mammals by significantly changing the abundance and the distribution of a complex network of microbes (Midtvedt et al., 1986; Pérez-Cobas et al., 2013; Modi et al., 2014; Tormo-Badia et al., 2014; Candon et al., 2015; Theriot et al., 2016; Yang et al., 2018). SLAE results in the change of gut homeostasis by, changing both host and bacterial metabolites, alterations in microbial signaling, antimicrobial peptide expression, and immunoregulation, disruption of gastrointestinal cell regulation, and systemic dysregulation of host immunity (Zhang et al., 2019).

SLAE results in an increased conjugative transfer of plasmids of the critically important extended-spectrum beta-lactamases (ESBL) and other AR (Liu et al., 2019). This may be due to the selection for, and proliferation of transconjugant and AR strains in the absence of competition resulting in the increase in densities of the donor strain, or it may also be the result of the clearance of the microbial community and reseeding of the gut with donor strains from the population of resistant persister cells; this is not yet clear and needs to be explicitly studied to determine the significance of either pathway in these events (Bakkeren et al., 2019). However, either methods would be significant due to the current prevalence of antibiotic use and misuse in non-susceptible infections.

A primary knowledge gap in bacterial conjugation is the role of bacterial strain differences and plasmid-encoded genes and the effect of these factors on conjugation *in vivo*. Few studies so far have characterized the role of the plasmid Inc. type and associated gene sequences with the regulation of conjugation in the gut of mammals. While this has been studied in the context of the natural and built environments, soil, and wastewater, respectively; it has yet to be characterized in depth using animal models (Klümper et al., 2015). It was recently demonstrated that ESBL-plasmid positive *E. coli* strains of differing Inc. groups conferred a variation in conjugation in a streptomycin treated murine gut model (Benz et al., 2020). These changes in conjugation efficiency were attributed to the presence of various *tra* genes, and associated proteins, involved in the structure and function of the conjugation machinery on the plasmids. Furthermore, the authors of this study also demonstrated the role of the native plasmids hosts in modulating conjugation efficiency by comparing native plasmids hosts with a transconjugant host plasmid in competition experiments.

Supporting this notion of plasmid-encoded factors that regulate conjugation, Neail et al. reported highly efficient transfer of an IncI2 plasmid in the gut of a streptomycin treated murine model (Neil et al., 2020). The authors isolated and characterized 13 plasmids from enteric bacteria and used a common modified *E. coli* Nissle donor to test incidence and rate of conjugation in the gut of the antibiotic treated murine host. They identified that the IncI2 plasmid TP114 demonstrated significantly greater levels of conjugation, with almost 100% conjugation efficiency, measured as the proportion of recipient population which receives the plasmid. The authors further postulate that the presence of a specific T4SS pilus present in the I-complex plays a crucial role in conjugation observed in the gut, and is likely crucial to mating pair stabilization.

It is not yet clear if these factors are consistent with plasmids of other classes as the authors only examined those of IncF and IncI subsets. Furthermore, the donor and recipient strains used in this study were primarily isolated from human clinical samples. While this does give some insight into the role of clinical strains in direct human health, it is not clear if this accurately represents environmental isolates that may be the source of these clinically relevant multidrug resistance plasmids. The authors do clarify that a larger study with a different experimental design would need to be conducted to determine if other host strain factors, such as restriction-modification, CIRSPR-Cas, or other systems, are essential in the variation in the conjugation efficiency seen between the various donor and the recipient strains (Benz et al., 2020).

Variations in host genetics play a significant role in the microbial populations in the gut, as well as the interactions of these microbes and the host. We showed that when compounding factors such as diet, environment, and microbiota are controlled, variations in host genetics significantly contribute to the levels of conjugation in the gut of a murine model (Ott et al., 2020). So far, the genetic host factors responsible for variation between host genetics have not yet been elucidated but may be the result in variations in; gut immunity (antimicrobial peptides, antibody excretion, etc.), gut metabolite availability, and microRNA regulation and microbe-host signaling. Further studies will be required to determine the important host genetic factors involved in the regulation of the gut-mediated HGT between bacteria.

Host inflammation results in significant immune regulation of gut microbes; however, bacterial species such as those of the *Enterobacteriaceae* family can persist, bloom, and elicit continued inflammation in the guts of mammalian hosts (Lupp et al., 2007). This increased Enterobacterial density was shown by Stecher et al. to increase plasmid transfer by conjugation based on an increase in donor/recipient density in a detergent-induced inflammation murine mouse model (Stecher et al., 2012). However, this observation was not found to be consistent with our study when examined using an *IL-10* knockout

chronic inflammation murine model compared to wildtype mice (Ott et al., 2020). Both studies used different donor and recipient strains so this relationship with host inflammation and conjugative plasmid transfer may be strain specific, or other compounding factors between model systems may not yet be known.

Future studies in mice of multiple inflammation types, as well as a greater number of donor and recipient strains, is needed to determine if this discrepancy between conjugation is strain-dependent or inflammation model-dependent interaction. The manifestation of inflammation between models can be mediated by different pathways and mechanisms and may be dependent on host genetics. For example, *IL-10* genetic knockout mice produce a chronic inflammation when exposed to bacterial stimuli, while the model in Stecher et al. was dependent on the use of CD8+ T cell injections targeting the hemagglutinin (HA) protein expressed on transgenic VILLIN-HA mice. These forms of inflammation differ in severity and pathology (Stecher et al., 2012; Ott et al., 2020).

In addition to mice, Rats have been used to demonstrate the role of dietary organism containing resistance plasmids in HGT in the gut. Jacobson et al. demonstrated the transfer of both *tet*(M) and *erm*(B) resistance plasmids from a food associated *Lactobacillus plantarum* to the pathogenic *E. faecalis* JH2-2 strain in the gut of gnotobiotic rats (Jacobsen et al., 2007). Furthermore, rats have been used to demonstrate both the absence and presence of transfer of dietary DNA in between the host diet and the gut microbiota (Kosieradzka et al., 2010; Nordgård et al., 2012).

CONCLUSION

The study of HGT in human and animal guts is of dire importance to combat the emergence and spread of mobile ARG and VG plasmids. However, due to limitations in the study of the human microbiota, alternate models are important to determine experimentally how host and bacterial factor interactions affect the occurrence of HGT in the gut. *In vitro* models have played a significant role in the controlled study of isolated factors in synthetic environments. These models have a specific role to fill; however, they do not allow for the study of HGT in complex environments like those found in the gut of animals. *In vitro* models do not incorporate the combination of microbial, and host secreted factors such as antimicrobial peptides, reactive oxygen species, immune mediates like IgA, or physiochemical factors such as pH and osmolarity. Thus *in vivo* models that approximate the human gut are desirable.

The ASF model accomplishes this feat by allowing for controlled incorporation of each of these host- and microbiota-derived factors. However, it has yet to be used to extensively study the varied factors involved in regulating HGT, with only a few mechanisms proposed thus far. Additional models with these qualities are desired, such as an arthropod model. An arthropod model of HGT in the gut would be beneficial due to the immense genetic toolbox available in arthropod models, such as *D. melanogaster*, as well as the significantly reduced gut complexity due to the absence of adaptive immunity. Using these models, we can better determine the specific role of host and bacterial factors on conjugation and HGT in complex gut environments. Doing so may aid in elucidating novel pathways and the mechanism to inhibit or prevent the emergence of AR and VGs in the human and animal guts.

AUTHOR CONTRIBUTIONS

LO and MM: conceptualization, writing—original draft preparation, writing—review and editing, visualization, and funding acquisition. MM: resources, supervision, and project administration. All authors contributed to the article and approved the submitted version.

FUNDING

Funding sources for this review were from the United States Department of Agriculture, National Institute of Food and Agriculture project IOW05679 (LO) and USDA Hatch project IOW04202 (MM). Figure was created with BioRender.

REFERENCES

Aguado-Urda, M., Gibello, A., Blanco, M. M., López-Campos, G. H., Cutuli, M. T., and Fernández-Garayzábal, J. F. (2012). Characterization of plasmids in a human clinical strain of *Lactococcus garvieae*. *PLoS One* 7:e40119. doi: 10.1371/journal.pone.0040119

Aguinaldo, A. M. A., Turbeville, J. M., Linford, L. S., Rivera, M. C., Garey, J. R., Raff, R. A., et al. (1997). Evidence for a clade of nematodes, arthropods and other moulting animals. *Nature* 387, 489–493. doi: 10.1038/387489a0

Akhtar, M., Hirt, H., and Zurek, L. (2009). Horizontal transfer of the tetracycline resistance gene *tetM* mediated by pCF10 Among *Enterococcus faecalis* in the house fly (*Musca domestica* L.) alimentary canal. *Microb. Ecol.* 58, 509–518. doi: 10.1007/s00248-009-9533-9

Arutyunov, D., and Frost, L. S. (2013). F conjugation: back to the beginning. *Plasmid* 70, 18–32. doi: 10.1016/J.PLASMID.2013.03.010

Bakkeren, E., Huisman, J. S., Fattinger, S. A., Hausmann, A., Furter, M., Egli, A., et al. (2019). *Salmonella* persisters promote the spread of antibiotic resistance plasmids in the gut. *Nature* 573, 276–280. doi: 10.1038/s41586-019-1521-8

Balis, E., Vatopoulos, A. C., Kanelopoulou, M., Mainas, E., Hatzoudis, G., Kontogianni, V., et al. (1996). Indications of *in vivo* transfer of an epidemic R plasmid from *Salmonella enteritidis* to *Escherichia coli* of the normal human gut flora. *J. Clin. Microbiol.* 34, 977–979. doi: 10.1128/jcm.34.4.977-979.1996

Barrila, J., Crabbé, A., Yang, J., Franco, K., Nydam, S. D., Forsyth, R. J., et al. (2018). Modeling host-pathogen interactions in the context of the microenvironment: three-dimensional cell culture comes of age. *Infect. Immun.* 86:11. doi: 10.1128/IAI.00282-18

Bauelos-Vazquez, L. A. (2017). Regulation of conjugative transfer of plasmids and integrative conjugative elements. *Plasmid* 91, 82–89. doi: 10.1016/J.PLASMID.2017.04.002

Beaber, J. W., Hochhut, B., and Waldor, M. K. (2004). SOS response promotes horizontal dissemination of antibiotic resistance genes. *Nature* 427, 72–74. doi: 10.1038/nature02241

Benz, F., Huisman, J. S., Bakkeren, E., Herter, J. A., Stadler, T., Ackermann, M., et al. (2020). Plasmid- and strain-specific factors drive variation in ESBL-plasmid spread *in vitro* and *in vivo*. *ISME J.* 15, 862–878. doi: 10.1038/s41396-020-00819-4

Benzerara, Y., Gallah, S., Hommeril, B., Genel, N., Decré, D., Rottman, M., et al. (2017). Emergence of plasmid-mediated fosfomycin-resistance genes among *Escherichia coli* isolates, France. *Emerg. Infect. Dis.* 23, 1564–1567. doi: 10.3201/eid2309.170560

Bermudez-Brito, M., Plaza-Díaz, J., Fontana, L., Muñoz-Quezada, S., and Gil, A. (2013). *In vitro* cell and tissue models for studying host–microbe interactions: a review. *Br. J. Nutr.* 109, S27–S34. doi: 10.1017/S0007114512004023

Black, E. P., Hinrichs, G. J., Barcay, S. J., and Gardner, D. B. (2018). Fruit flies as potential vectors of foodborne illness. *J. Food Prot.* 81, 509–514. doi: 10.4315/0362-028x.jfp-17-255

Botelho, J., and Schulenburg, H. (2021). The role of integrative and conjugative elements in antibiotic resistance evolution. *Trends Microbiol.* 29, 8–18. doi: 10.1016/J.TIM.2020.05.011

Bragagnolo, N., Rodriguez, C., Samari-Kermani, N., Fours, A., Korouzhdehi, M., Lysenko, R., et al. (2020). Protein dynamics in F-like bacterial conjugation. *Biomedicine* 8:362. doi: 10.3390/BIOMEDICINES8090362

Brand, M. W., Wannemuehler, M. J., Phillips, G. J., Proctor, A., Overstreet, A. M., Jergens, A. E., et al. (2015). The altered schaedler flora: continued applications of a defined murine microbial community. *ILAR J.* 56, 169–178. doi: 10.1093/ilar/ilv012

Broderick, N. A., Buchon, N., Lemaitre, B., Buchon, N., and Lemaitre, B. (2014). Microbiota-induced changes in *Drosophila melanogaster* host gene expression and gut morphology. *mBio* 5, 1–13. doi: 10.1128/mBio.01117-14

Brown, N. (2016). Conjugation on Filters [Online]. protocols.io, 1–2. Available at: https://protocols.io/view/Conjugation-on-filters-eqybdxw (Accessed June 13, 2022).

Cabanel, N., Bouchier, C., Rajerison, M., and Carniel, E. (2018). Plasmid-mediated doxycycline resistance in a *Yersinia pestis* strain isolated from a rat. *Int. J. Antimicrob. Agents* 51, 249–254. doi: 10.1016/j.ijantimicag.2017.09.015

Cabezón, E., Ripoll-Rozada, J., Peña, A., de la Cruz, F., and Arechaga, I. (2014). Towards an integrated model of bacterial conjugation. *FEMS Microbiol. Rev.* 39, 81–95. doi: 10.1111/1574-6976.12085

Campos, M., Millán, Á. S., Semper, J. M., Lanz, V. F., Coqu, T. M., Llorens, C., et al. (2020). Simulating the influence of conjugative-plasmid kinetic values on the multilevel dynamics of antimicrobial resistance in a membrane computing model. *Antimicrob. Agents Chemother.* 64:8. doi: 10.1128/AAC.00593-20

Candon, S., Perez-Arroyo, A., Marquet, C., Valette, F., Foray, A.-P., Pelletier, B., et al. (2015). Antibiotics in early life alter the gut microbiome and increase disease incidence in a spontaneous mouse model of autoimmune insulin-dependent diabetes. *PLoS One* 10:e0125448. doi: 10.1371/journal.pone.0125448

Card, R. M., Cawthraw, S. A., Nunez-Garcia, J., Ellis, R. J., Kay, G., Pallen, M. J., et al. (2017). An *in vitro* chicken gut model demonstrates transfer of a multidrug resistance plasmid from *Salmonella* to commensal *Escherichia coli*. *MBio* 8, 1–15. doi: 10.1128/mBio.00777-17

Chen, Y., Jian, S., Ping, L. X., Yang, S., Liang, L., Xing, F. L., et al. (2016). Impact of enrofloxacin and florfenicol therapy on the spread of *oqxAB* gene and intestinal microbiota in chickens. *Vet. Microbiol.* 192, 1–9. doi: 10.1016/j.vetmic.2016.05.014

Corliss, T. L., Cohen, P. S., and Cabelli, V. J. (1981). R-plasmid transfer to and from *Escherichia coli* strains isolated from human fecal samples. *Appl. Environ. Microbiol.* 41, 959–966. doi: 10.1128/aem.41.4.959-966.1981

Couturier, M., Bex, F., Bergquist, P. L., and Maas, W. K. (1988). Identification and classification of bacterial plasmids. *Microbiol. Rev.* 52, 375–395. doi: 10.1128/mr.52.3.375-395.1988

Coyne, M. J., Zitomersky, N. L., McGuire, A. M., Earl, A. M., and Comstock, L. E. (2014). Evidence of extensive DNA transfer between bacteroidales species within the human gut. *MBio* 5:3. doi: 10.1128/MBIO.01305-14

Cury, J., Touchon, M., and Rocha, E. P. C. (2017). Integrative and conjugative elements and their hosts: composition, distribution and organization. *Nucleic Acids Res.* 45, 8943–8956. doi: 10.1093/NAR/GKX607

Daini, O. A., and Akano, S. A. (2009). Plasmid-mediated antibiotic resistance in *Staphylococcus aureus* from patients and non patients. *Sci. Res. Essay* 4, 346–350. doi: 10.5897/SRE.9000736

Davies, J., and Davies, D. (2010). Origins and evolution of antibiotic resistance. *Microbiol. Mol. Biol. Rev.* 74, 417–433. doi: 10.1128/MMBR.00016-10

Davies, M. R., Shera, J., van Domselaar, G. H., Sriprakash, K. S., and McMillan, D. J. (2009). A novel integrative conjugative element mediates genetic transfer from group G *Streptococcus* to other β-hemolytic *streptococci*. *J. Bacteriol.* 191, 2257–2265. doi: 10.1128/JB.01624-08

Delavat, F., Miyazaki, R., Carraro, N., Pradervand, N., and van der Meer, J. R. (2017). The hidden life of integrative and conjugative elements. *FEMS Microbiol. Rev.* 41, 512–537. doi: 10.1093/FEMSRE/FUX008

Devanga Ragupathi, N. K., Muthuirulandi Sethuvel, D. P., Gajendran, R., Anandan, S., Walia, K., and Veeraraghavan, B. (2019). Horizontal transfer of antimicrobial resistance determinants among enteric pathogens through bacterial conjugation. *Curr. Microbiol.* 76, 666–672. doi: 10.1007/s00284-019-01676-x

Diaz, L., Kiratisin, P., Mendes, R. E., Panesso, D., Singh, K. V., and Arias, C. A. (2012). Transferable plasmid-mediated resistance to linezolid due to *cfr* in a human clinical isolate of *Enterococcus faecalis*. *Antimicrob. Agents Chemother.* 56, 3917–3922. doi: 10.1128/AAC.00419-12

Dolejska, M., and Papagiannitsis, C. C. (2018). Plasmid-mediated resistance is going wild. *Plasmid* 99, 99–111. doi: 10.1016/j.plasmid.2018.09.010

Donaldson, G. P., Lee, S. M., and Mazmanian, S. K. (2015, 2015). Gut biogeography of the bacterial microbiota. *Nat. Rev. Microbiol.* 14, 20–32. doi: 10.1038/nrmicro3552

Dunkley, K. D., Dunkley, C. S., Njongmeta, N. L., Callaway, T. R., Hume, M. E., Kubena, L. F., et al. (2007). Comparison of *in vitro* fermentation and molecular microbial profiles of high-fiber feed substrates incubated with chicken cecal inocula. *Poult. Sci.* 86, 801–810. doi: 10.1093/ps/86.5.801

Economic Research Service. (2015). Economic burden of major foodborne illness acquired in the United Stated. *Economic Information Bulletin Number 140 [Online]*. Available at: https://www.ers.usda.gov/publications/pub-details/?pubid=43987 (Accessed June 13, 2022).

Ericsson, A. C. (2019). The use of non-rodent model species in microbiota studies. *Lab. Anim* 53, 259–270. doi: 10.1177/0023677219834593

Fernandez-Lopez, R., Machón, C., Longshaw, C. M., Martin, S., Molin, S., Zechner, E. L., et al. (2005). Unsaturated fatty acids are inhibitors of bacterial conjugation. *Microbiology* 151, 3517–3526. doi: 10.1099/mic.0.28216-0

Fukuda, A., Usui, M., Okamura, M., Dong-Liang, H., and Tamura, Y. (2019). Role of flies in the maintenance of antimicrobial resistance in farm environments. *Microb. Drug Resist.* 25, 127–132. doi: 10.1089/mdr.2017.0371

Fukuda, A., Usui, M., Okubo, T., and Tamura, Y. (2016). Horizontal transfer of plasmid-mediated cephalosporin resistance genes in the intestine of houseflies (*Musca domestica*). *Microb. Drug Resist.* 22, 336–341. doi: 10.1089/mdr.2015.0125

García-Cazorla, Y., Getino, M., Sanabria-Ríos, D. J., Carballeira, N. M., de La Cruz, F., Arechaga, I., et al. (2018). Conjugation inhibitors compete with palmitic acid for binding to the conjugative traffic ATPase TrwD, providing a mechanism to inhibit bacterial conjugation. *J. Biol. Chem.* 293, 16923–16930. doi: 10.1074/jbc.RA118.004716

Getino, M., Sanabria-Ríos, D. J., Fernández-López, R., Campos-Gómez, J., Sánchez-López, J. M., Fernández, A., et al. (2015). Synthetic fatty acids prevent plasmid-mediated horizontal gene transfer. *MBio* 6, e01032–e01015. doi: 10.1128/mBio.01032-15

Gevers, D., Huys, G., and Swings, J. (2003). *In vitro* conjugal transfer of tetracycline resistance from *Lactobacillus* isolates to other Gram-positive bacteria. *FEMS Microbiol. Lett.* 225, 125–130. doi: 10.1016/S0378-1097(03)00505-6

Gibson, E. M., Chace, N. M., London, S. B., and London, J. (1979). Transfer of plasmid-mediated antibiotic resistance from *streptococci* to *lactobacilli*. *J. Bacteriol.* 137, 614–619.

Goldfarb, D., Harvey, S. B., Jessamine, K., Jessamine, P., Toye, B., and Desjardins, M. (2009). Detection of plasmid-mediated KPC-producing *Klebsiella pneumoniae* in Ottawa, Canada: evidence of intrahospital transmission. *J. Clin. Microbiol.* 47, 1920–1922. doi: 10.1128/JCM.00098-09

Goldstein, F. W., Labigne-Roljssel, A., Gerbaud, G., Carlier, C., Collatz, E., and Courvalrnt, P. (1983). Transferable plasmid-mediated antibiotic resistance in *Acinetobacter*. *Plasmid* 10, 130–147. doi: 10.1080/00480169.1971.33940

Gould, A. L., Zhang, V., Lamberti, L., Jones, E. W., Obadia, B., Korasidis, N., et al. (2018). Microbiome interactions shape host fitness. *Proc. Natl. Acad. Sci. U. S. A.* 115, E11951–E11960. doi: 10.1073/pnas.1809349115

Gresham, D., and Hong, J. (2015). The functional basis of adaptive evolution in chemostats. *FEMS Microbiol. Rev.* 39, 2–16. doi: 10.1111/1574-6976.12082

Grohmann, E., Muth, G., and Espinosa, M. (2003). Conjugative plasmid transfer in Gram-positive bacteria. *Microbiol. Mol. Biol. Rev.* 67, 277–301. doi: 10.1128/mmbr.67.2.277-301.2003

Guédon, G., Libante, V., Coluzzi, C., Payot, S., and Leblond-Bourget, N. (2017). The obscure world of integrative and mobilizable elements, highly widespread elements that pirate bacterial conjugative systems. *Genes* 8:337. doi: 10.3390/GENES8110337

Guiyoule, A., Gerbaud, G., Buchrieser, C., Galimand, M., Rahalison, L., Chanteau, S., et al. (2001). Transferable plasmid-mediated resistance to streptomycin in a clinical isolate of *Yersinia pestis*. *Emerg. Infect. Dis.* 7, 43–48. doi: 10.3201/eid0701.010106

Haft, R. J. F., Mittler, J. E., and Traxler, B. (2009). Competition favours reduced cost of plasmids to host Bacteria. *ISME J.* 3, 761–769. doi: 10.1038/ismej.2009.22

Hershberger, E., Coyle, E. A., Kaatz, G. W., Zervos, M. J., and Rybak, M. J. (2000). Comparison of a rabbit model of bacterial endocarditis and an *in vitro* infection model with simulated endocardial vegetations. *Antimicrob. Agents Chemother.* 44, 1921–1924. doi: 10.1128/AAC.44.7.1921-1924.2000

Hinnebusch, B. J., Rosso, M. L., Schwan, T. G., and Carniel, E. (2002). High-frequency conjugative transfer of antibiotic resistance genes to *Yersinia pestis* in the flea midgut. *Mol. Microbiol.* 46, 349–354. doi: 10.1046/j.1365-2958.2002.03159.x

Hirt, H., Greenwood-Quaintance, K. E., Karau, M. J., Till, L. M., Kashyap, P. C., Patel, R., et al. (2018). *Enterococcus faecalis* sex pheromone cCF10 enhances conjugative plasmid transfer *in vivo*. *MBio* 9:1. doi: 10.1128/mBio.00037-18

Hirt, H., Schlievert, P. M., and Dunny, G. M. (2017). *In vivo* induction of virulence and antibiotic resistance transfer in *Enterococcus faecalis* mediated by the sex pheromone-sensing system of pCF10. *Infect. Immun.* 70, 716–723. doi: 10.1128/IAI.70.2.716

Hoffmann, S., Maculloch, B., and Batz, M. (2015). Economic burden of major foodborne illnesses acquired in the United States economic burden of major foodborne illnesses acquired in the United States. *Economic Research Service*. doi: 10.1001/jamadermatol.2014.3593

Hoffmann, A., Thimm, T., Dröge, M., Moore, E. R. B., Munch, J. C., and Tebbe, C. C. (1998). Intergeneric transfer of conjugative and mobilizable plasmids harbored by *Escherichia coli* in the gut of the soil microarthropod *Folsomia candida* (*Collembola*). *Appl. Environ. Microbiol.* 64, 2652–2659. doi: 10.1128/aem.64.7.2652-2659.1998

Hong, B. K., Wang, M., Chi, H. P., Kim, E. C., Jacoby, G. A., and Hooper, D. C. (2009). *oqxAB* encoding a multidrug efflux pump in human clinical isolates of *Enterobacteriaceae*. *Antimicrob. Agents Chemother.* 53, 3582–3584. doi: 10.1128/AAC.01574-08

Huddleston, J. R. (2014). Horizontal gene transfer in the human gastrointestinal tract: potential spread of antibiotic resistance genes. *Infect. Drug Resist.* 7, 167–176. doi: 10.2147/IDR.S48820

Jacobsen, L., Wilcks, A., Hammer, K., Huys, G., Gevers, D., and Andersen, S. R. (2007). Horizontal transfer of *tet(M)* and *erm(B)* resistance plasmids from food strains of *Lactobacillus plantarum* to *Enterococcus faecalis* JH2-2 in the gastrointestinal tract of gnotobiotic rats. *FEMS Microbiol. Ecol.* 59, 158–166. doi: 10.1111/J.1574-6941.2006.00212.X

Jamborova, I., Dolejska, M., Zurek, L., Townsend, A. K., Clark, A. B., Ellis, J. C., et al. (2017). Plasmid-mediated resistance to cephalosporins and quinolones in *Escherichia coli* from American crows in the USA. *Environ. Microbiol.* 19, 2025–2036. doi: 10.1111/1462-2920.13722

Javadi, M., Bouzari, S., and Oloomi, M. (2017). "Horizontal gene transfer and the diversity of *Escherichia coli*," in *Escherichia coli - Recent Advances on Physiology, Pathogenesis and Biotechnological Applications*. ed. A. Samie (London: IntechOpen).

Jiang, X., Hall, A. B., Xavier, R. J., and Alm, E. J. (2019). Comprehensive analysis of chromosomal mobile genetic elements in the gut microbiome reveals phylum-level niche-adaptive gene pools. *PLoS One* 14:e0223680. doi: 10.1371/JOURNAL.PONE.0223680

Jochum, J. M., Redweik, G. A. J., Ott, L. C., and Mellata, M. (2021). Bacteria broadly-resistant to last resort antibiotics detected in commercial chicken farms. *Microorganisms* 9, 1–16. doi: 10.3390/microorganisms9010141

Johnson, C. M., and Grossman, A. D. (2015). Integrative and conjugative elements (ICEs): what they do and how they. *Work* 49, 577–601. doi: 10.1146/ANNUREV-GENET-112414-055018

Juhas, M. (2015). Horizontal gene transfer in human pathogens. *Crit. Rev. Microbiol.* 41, 101–108. doi: 10.3109/1040841X.2013.804031

Khajanchi, B. K., Kaldhone, P. R., and Foley, S. L. (2019). Protocols of conjugative plasmid transfer in *Salmonella*: plate, broth, and filter mating approaches. *Methods Mol. Biol.* 2016, 129–139. doi: 10.1007/978-1-4939-9570-7_12

Kim, C. H., Park, J., and Kim, M. (2014). Gut microbiota-derived short-chain fatty acids, T cells, and inflammation. *Immune Netw.* 14:277. doi: 10.4110/in.2014.14.6.277

Klimuszko, D., Szynkiewicz, Z. M., Piekarowicz, A., Binek, M., and Wrjcik, U. (1989). Transfer of plasmid Hly *in vivo* in pigs intestine. *Comp. Immunol. Microbiol. Infect. Dis.* 12, 29–38.

Klümper, U., Recker, M., Zhang, L., Yin, X., Zhang, T., Buckling, A., et al. (2019). Selection for antimicrobial resistance is reduced when embedded in a natural microbial community. *ISME J.* 13, 2927–2937. doi: 10.1038/s41396-019-0483-z

Klümper, U., Riber, L., Dechesne, A., Sannazzarro, A., Hansen, L. H., Sørensen, S. J., et al. (2015). Broad host range plasmids can invade an unexpectedly diverse fraction of A soil bacterial community. *ISME J.* 9, 934–945. doi: 10.1038/ismej.2014.191

Kosieradzka, I., Vasko, V., Szwacka, M., Przybysz, A., and Fiedorowicz, S. (2010). Evaluation of the possibility of horizontal gene transfer and accumulation of transgenic DNA from the diet in the bodies of rats. *J. Anim. Feed Sci.* 19, 307–315. doi: 10.22358/JAFS/66294/2010

Lacey, J. A., Keyburn, A. L., Ford, M. E., Portela, R. W., Johanesen, P. A., Lyras, D., et al. (2017). Conjugation-mediated horizontal gene transfer of *Clostridium perfringens* plasmids in the chicken gastrointestinal tract results in the formation of new virulent strains. *Appl. Environ. Microbiol.* 83, 1–13. doi: 10.1128/AEM.01814-17

Lasaro, M., Liu, Z., Bishar, R., Kelly, K., Chattopadhyay, S., Paul, S., et al. (2014). *Escherichia coli* isolate for studying colonization of the mouse intestine and its application to two-component signaling knockouts. *J. Bacteriol.* 196, 1723–1732. doi: 10.1128/JB.01296-13/ASSET/429112D2-F5DA-4A7E-A2F1-29559929A45C/ASSETS/GRAPHIC/ZJB9990931310007.JPEG

Li, Z., Liu, B., Li, S. H. J., King, C. G., Gitai, Z., and Wingreen, N. S. (2020). Modeling microbial metabolic trade-offs in a chemostat. *PLoS Comput. Biol.* 16:e1008156. doi: 10.1371/journal.pcbi.1008156

Liao, X., Shao, Y., Sun, G., Yang, Y., Zhang, L., Guo, Y., et al. (2020). The relationship among gut microbiota, short-chain fatty acids, and intestinal morphology of growing and healthy broilers. *Poult. Sci.* 99, 5883–5895. doi: 10.1016/j.psj.2020.08.033

Licht, T. R., Christensen, B. B., Krogfelt, K. A., and Molin, S. (1999). Plasmid transfer in the animal intestine and other dynamic bacterial populations: the role of community structure and environment. *Microbiology* 145, 2615–2622. doi: 10.1099/00221287-145-9-2615

Liu, G., Bogaj, K., Bortolaia, V., Olsen, J. E., and Thomsen, L. E. (2019). Antibiotic-induced, increased conjugative transfer is common to diverse naturally occurring ESBL plasmids in *Escherichia coli*. *Front. Microbiol.* 10, 2119. doi: 10.3389/fmicb.2019.02119

Liu, L., Chen, X., Skogerbø, G., Zhang, P., Chen, R., He, S., et al. (2012). The human microbiome: a hot spot of microbial horizontal gene transfer. *Genomics* 100, 265–270. doi: 10.1016/j.ygeno.2012.07.012

Liu, C. M., Stegger, M., Aziz, M., Johnson, T. J., Waits, K., Nordstrom, L., et al. (2018). *Escherichia coli* ST131-H22 as a foodborne uropathogen. *MBio* 9, 470–488. doi: 10.1128/mBio.00470-18

Lupp, C., Robertson, M. L., Wickham, M. E., Sekirov, I., Champion, O. L., Gaynor, E. C., et al. (2007). Host-mediated inflammation disrupts the intestinal microbiota and promotes the overgrowth of *Enterobacteriaceae*. *Cell Host Microbe* 2, 119–129. doi: 10.1016/j.chom.2007.06.010

Lyte, J. M., Proctor, A., Phillips, G. J., Lyte, M., and Wannemuehler, M. (2019). Altered schaedler flora mice: a defined microbiota animal model to study the microbiota-gut-brain axis. *Behav. Brain Res.* 356, 221–226. doi: 10.1016/j.bbr.2018.08.022

Machado, A. A. M. D., and Sommer, M. O. A. (2014). Human intestinal cells modulate conjugational transfer of multidrug resistance plasmids between clinical *Escherichia coli* isolates. *PLoS One* 9, 1–5. doi: 10.1371/journal.pone.0100739

Macuch, P., Seckarova, A., Parrakov, , Krcmerya, V., and Vymola, F. (1967). Transfer of tetracycline resistance from *Escherichia coli* to other *Enterobacteriaceae in vitro*. *Z Allg Mikrobiol.* 7, 159–162. doi: 10.1002/jobm.19670070212

Maeusli, M., Lee, B., Miller, S., Reyna, Z., Lu, P., Yan, J., et al. (2020). Horizontal gene transfer of antibiotic resistance from *Acinetobacter baylyi* to *Escherichia coli* on lettuce and subsequent antibiotic resistance transmission to the gut microbiome. *mSphere* 5:3. doi: 10.1128/mSphere.00329-20

Mahmood, K., Bal, B., and Banu, E. (2014). Transmission of antibiotic resistant *Enterobacteriaceae* between animals and humans gastrointestinal tract with the evidence of *in vivo* plasmid transfer. *Kahramanmaraş Sütçü İmam Üniversitesi Doğa Bilimleri Dergisi* 17:32. doi: 10.18016/ksujns.71116

Marshall, B., Schluederberg, S., Tachibana, C., and Levy, S. B. (1981). Survival and transfer in the human gut of poorly mobilizable (pBR322) and of transferable plasmids from the same carrier *E. coli*. *Gene* 14, 145–154. doi: 10.1016/0378-1119(81)90110-4

McAllister, J. C., Steelman, C. D., and Skeeles, J. K. (1994). Reservoir competence of the lesser mealworm (*Coleoptera: Tenebrionidae*) for *Salmonella Typhimurium* (*Eubacteriales: Enterobacteriaceae*). *J. Med. Entomol.* 31, 369–372. doi: 10.1093/jmedent/31.3.369

McAllister, J. C., Steelman, C. D., Skeeles, J. K., Newberry, L. A., and Gbur, E. E. (1996). Reservoir competence of *Alphitobius diaperinus* (*Coleoptera: Tenebrionidae*) for *Escherichia coli* (*Eubacteriales: Enterobacteriaceae*). *J. Med. Entomol.* 33, 983–987. doi: 10.1093/jmedent/33.6.983

McInnes, R. S., McCallum, G. E., Lamberte, L. E., and van Schaik, W. (2020). Horizontal transfer of antibiotic resistance genes in the human gut microbiome. *Curr. Opin. Microbiol.* 53, 35–43. doi: 10.1016/j.mib.2020.02.002

Mellata, M., Ameiss, K., Mo, H., and Curtiss III, R. (2010). Characterization of the contribution to virulence of three large plasmids of avian pathogenic *Escherichia coli* x7122 (O78:K80:H9). *Infect. Immun.* 78, 1528–1541. doi: 10.1128/IAI.00981-09

Merkey, B. V., Lardon, L. A., Seoane, J. M., Kreft, J. U., and Smets, B. F. (2011). Growth dependence of conjugation explains limited plasmid invasion in biofilms: an individual-based modelling study. *Environ. Microbiol.* 13, 2435–2452. doi: 10.1111/J.1462-2920.2011.02535.X

Midtvedt, T., Carlstedt-Duke, B., Høverstad, T., Lingaas, E., Norin, E., Saxerholt, H., et al. (1986). Influence of peroral antibiotics upon the biotransformatory activity of the intestinal microflora in healthy subjects. *Eur. J. Clin. Invest.* 16, 11–17. doi: 10.1111/j.1365-2362.1986.tb01300.x

Modi, S. R., Collins, J. J., and Relman, D. A. (2014). Antibiotics and the gut microbiota. *J. Clin. Investig.* 124, 4212–4218. doi: 10.1172/JCI72333

Neil, K., Allard, N., Grenier, F., Burrus, V., and Rodrigue, S. (2020). Highly efficient gene transfer in the mouse gut microbiota is enabled by the Incl2 conjugative plasmid TP114. *Commun. Biol.* 3:523. doi: 10.1038/s42003-020-01253-0

Neil, K., Allard, N., and Rodrigue, S. (2021). Molecular mechanisms influencing bacterial conjugation in the intestinal microbiota. *Front. Microbiol.*:1415. doi: 10.3389/FMICB.2021.673260

Nesme, J., Cécillon, S., Delmont, T. O., Monier, J.-M., Vogel, T. M., and Simonet, P. (2014). Large-scale metagenomic-based study of antibiotic resistance in the environment. *Curr. Biol.* 24, 1096–1100. doi: 10.1016/j.cub.2014.03.036

Nordgård, L., Brusetti, L., Raddadi, N., Traavik, T., Averhoff, B., and Nielsen, K. M. (2012). An investigation of horizontal transfer of feed introduced DNA to the aerobic microbiota of the gastrointestinal tract of rats. *BMC. Res. Notes* 5, 1–11. doi: 10.1186/1756-0500-5-170/TABLES/5

Ohana, S., Leflon, V., Ronco, E., Rottman, M., Guillemot, D., Lortat-Jacob, S., et al. (2005). Spread of a *Klebsiella pneumoniae* strain producing a plasmid-mediated ACC-1 AmpC β-lactamase in a teaching hospital admitting disabled patients. *Antimicrob. Agents Chemother.* 49, 2095–2097. doi: 10.1128/AAC.49.5.2095-2097.2005

Oladeinde, A., Cook, K., Lakin, S. M., Woyda, R., Abdo, Z., Looft, T., et al. (2019). Horizontal gene transfer and acquired antibiotic resistance in *Salmonella enterica* Serovar Heidelberg following *in vitro* incubation in broiler ceca. *Appl. Environ. Microbiol.* 85:22. doi: 10.1128/aem.01903-19

Oosterom, J., Notermans, S., Karman, H., and Engels, G. B. (1983). Origin and prevalence of *Campylobacter jejuni* in poultry processing. *J. Food Prot.* 46, 339–344.

Oppegaard, H., Steinum, T. M., and Wasteson, Y. (2001). Horizontal transfer of a multi-drug resistance plasmid between coliform bacteria of human and bovine origin in a farm environment. *Appl. Environ. Microbiol.* 67, 3732–3734. doi: 10.1128/AEM.67.8.3732-3734.2001

Ott, L. C., Engelken, M., Scott, S. M., McNeill, E. M., and Mellata, M. (2021). Drosophila model for gut-mediated horizontal transfer of narrow- and broad-host-range plasmids. *mSphere* 6:5. doi: 10.1128/mSphere.00698-21

Ott, L. C., Stromberg, Z. R., Redweik, G. A. J., Wannemuehler, M. J., and Mellata, M. (2020). Mouse genetic background affects transfer of an antibiotic resistance plasmid in the gastrointestinal tract. *mSphere* 5:1. doi: 10.1128/mSphere.00847-19

Pan, Z., Jin, L., Yue, Z., Shenshen, C., Jiale, M., Wenyang, D., et al. (2019). A novel integrative conjugative element mediates transfer of multi-drug resistance between *Streptococcus suis* strains of different serotypes. *Vet. Microbiol.* 229, 110–116. doi: 10.1016/j.vetmic.2018.11.028

Penders, J., Stobberingh, E. E., Savelkoul, P. H. M., and Wolffs, P. F. G. (2013). The human microbiome as a reservoir of antimicrobial resistance. *Front. Microbiol.* 4:87. doi: 10.3389/fmicb.2013.00087

Peng, X., Knouse, J. A., and Hernon, K. M. (2015). Rabbit models for studying human infectious diseases. *Comp. Med.* 65, 499–507. doi: 10.1016/j.dental.2008.11.005

Pérez-Cobas, A. E., Gosalbes, M. J., Friedrichs, A., Knecht, H., Artacho, A., Eismann, K., et al. (2013). Gut microbiota disturbance during antibiotic therapy: a multi-omic approach. *Gut* 62, 1591–1601. doi: 10.1136/gutjnl-2012-303184

Petridis, M., Bagdasarian, M., Waldor, M. K., and Walker, E. (2006). Horizontal transfer of Shiga toxin and antibiotic resistance genes among *Escherichia coli* strains in house fly (*Diptera: Muscidae*) gut. *J. Med. Entomol.* 43, 288–295. doi: 10.1603/0022-2585(2006)043[0288:HTOSTA]2.0.CO;2

Poole, T., and Crippen, T. (2009). Conjugative plasmid transfer between *Salmonella enterica* Newport and *Escherichia coli* within the gastrointestinal tract of the lesser mealworm beetle, *Alphitobius diaperinus* (Coleoptera: Tenebrionidae). *Poult. Sci.* 88, 1553–1558. doi: 10.3382/ps.2008-00553

Portal-Celhay, C., Nehrke, K., and Blaser, M. J. (2013). Effect of *Caenorhabditis elegans* age and genotype on horizontal gene transfer in intestinal Bacteria. *FASEB J.* 27, 760–768. doi: 10.1096/fj.12-218420

Poulsen, L. K., Licht, T. R., Rang, C., Krogfelt, K. A., and Molin, S. (1995). Physiological state of *Escherichia coli* BJ4 growing in the large intestines of streptomycin-treated mice. *J. Bacteriol.* 177, 5840–5845. doi: 10.1128/JB.177.20.5840-5845.1995

Rang, C. U., Kennan, R. M., Midtvedt, T., Chao, L., and Conway, P. L. (1996). Transfer of the plasmid RP1 *in vivo* in germ free mice and *in vitro* in gut extracts and laboratory media. *FEMS Microbiol. Ecol.* 19, 133–140. doi: 10.1111/j.1574-6941.1996.tb00206.x

Redondo-Salvo, S., Fernández-López, R., Ruiz, R., Vielva, L., de Toro, M., Rocha, E. P. C., et al. (2020). Pathways for horizontal gene transfer in bacteria revealed by a global map of their plasmids. *Nat. Commun.* 11:3602. doi: 10.1038/s41467-020-17278-2

Redweik, G. A. J., Horak, M. K., Hoven, R., Ott, L., Mellata, M., and Horak, M. K. (2021). Evaluation of live bacterial prophylactics to decrease IncF plasmid transfer and association with intestinal small RNAs. *Front. Microbiol.* 11, 1–10. doi: 10.3389/fmicb.2020.625286

Rolain, J.-M. (2013). Food And human gut as reservoirs of transferable antibiotic resistance encoding genes. *Front. Microbiol.* 4:173. doi: 10.3389/fmicb.2013.00173

Rooney, C. M., Sheppard, A. E., Clark, E., Davies, K., Hubbard, A. T. M., Sebra, R., et al. (2019). Dissemination of multiple carbapenem resistance genes in an *in vitro* gut model simulating the human Colon. *J. Antimicrob. Chemother.* 74, 1876–1883. doi: 10.1093/JAC/DKZ106

Round, J. L., and Mazmanian, S. K. (2009). The gut microbiota shapes intestinal immune responses during health and disease. *Nat. Rev. Immunol.* 9, 313–323. doi: 10.1038/nri2515

Salyers, A., Gupta, A., and Wang, Y. (2004). Human intestinal bacteria as reservoirs for antibiotic resistance genes. *Trends Microbiol.* 12, 412–416. doi: 10.1016/j.tim.2004.07.004

Sannino, D. R., Dobson, A. J., Edwards, K., Angert, E. R., and Buchon, N. (2018). The Drosophila *melanogaster* gut microbiota provisions thiamine to its host. *MBio* 9:2. doi: 10.1128/mBio.00155-18

Schweizer, C., Bischoff, P., Bender, J., Kola, A., Gastmeier, P., Hummel, M., et al. (2019). Plasmid-mediated transmission of KPC-2 carbapenemase in enterobacteriaceae in critically ill patients. *Front. Microbiol.* 10:276. doi: 10.3389/fmicb.2019.00276

Seth-Smith, H. M. B., Fookes, M. C., Okoro, C. K., Baker, S., Harris, S. R., Scott, P., et al. (2012). Structure, diversity, and mobility of the *Salmonella* pathogenicity island 7 family of integrative and conjugative elements within enterobacteriaceae. *J. Bacteriol.* 194, 1494–1504. doi: 10.1128/JB.06403-11/SUPPL_FILE/FIGS1-S3_TABLES1-S4.PDF

Smillie, C., Garcillán-Barcia, M. P., Francia, M. V., Rocha, E. P. C., and de la Cruz, F. (2010). Mobility of plasmids. *Microbiol. Mol. Biol. Rev.* 74, 434–452. doi: 10.1128/MMBR.00020-10

Smith, H. W. (1970). The transfer of antibiotic resistance between strains of enterobacteria in chicken, calves and pigs. *J. Med. Microbiol.* 3, 165–180. doi: 10.1099/00222615-3-1-165/CITE/REFWORKS

Smith, J. (2012). Tragedy of the commons among antibiotic resistance plasmids. *Evolution* 66, 1269–1274. doi: 10.1111/j.1558-5646.2011.01531.x

Sørensen, S. J., Bailey, M., Hansen, L. H., Kroer, N., and Wuertz, S. (2005). Studying plasmid horizontal transfer in situ: a critical review. *Nat. Rev. Microbiol.* 3, 700–710. doi: 10.1038/nrmicro1232

Stecher, B., Denzler, R., Maier, L., Bernet, F., Sanders, M. J., Pickard, D. J., et al. (2012). Gut inflammation can boost horizontal gene transfer between pathogenic and commensal *Enterobacteriaceae*. *Proc. Natl. Acad. Sci. U. S. A.* 109, 1269–1274. doi: 10.1073/pnas.1113246109

Stecher, B., and Hardt, W. D. (2008). The role of microbiota in infectious disease. *Trends Microbiol.* 16, 107–114. doi: 10.1016/j.tim.2007.12.008

Stromberg, Z. R., Masonbrink, R. E., and Mellata, M. (2020). Transcriptomic analysis of Shiga toxin-producing *Escherichia coli* during initial contact with cattle colonic explants. *Microorganisms* 8, 1–10. doi: 10.3390/microorganisms8111662

Stromberg, Z. R., van Goor, A., Redweik, G. A. J., Brand, M. J. W., Wannemuehler, M. J., and Mellata, M. (2018). Pathogenic and non-pathogenic *Escherichia coli* colonization and host inflammatory response in a defined microbiota mouse model. *Dis. Model. Mech.* 11:dmm035063. doi: 10.1242/dmm.035063

Sunkara, L. T., Achanta, M., Schreiber, N. B., Bommineni, Y. R., Dai, G., Jiang, W., et al. (2011). Butyrate enhances disease resistance of chickens by inducing antimicrobial host defense peptide gene expression. *PLoS One* 6:e27225. doi: 10.1371/journal.pone.0027225

Sutradhar, I., Ching, C., Desai, D., Suprenant, M., Briars, E., Heins, Z., et al. (2021). Computational model to quantify the growth of antibiotic-resistant bacteria in wastewater. *mSystems* 6:3. doi: 10.1128/mSystems.00360-21

Techitnutsarut, P., and Chamchod, F. (2021). Modeling bacterial resistance to antibiotics: bacterial conjugation and drug effects. *Adv. Differ. Equ.* 2021:290. doi: 10.1186/s13662-021-03423-8

Tepekule, B., Zur Wiesch, P. A., Kouyos, R. D., and Bonhoeffer, S. (2019). Quantifying the impact of treatment history on plasmid-mediated resistance evolution in human gut microbiota. *Proc. Natl. Acad. Sci. U. S. A.* 116, 23106–23116. doi: 10.1073/pnas.1912188116

Teuber, M. (1999). Spread of antibiotic resistance with food-borne pathogens. *Cell. Mol. Life Sci.* 56, 755–763. doi: 10.1007/s000180050022

Theriot, C. M., Bowman, A. A., and Young, V. B. (2016). Antibiotic-induced alterations of the gut microbiota alter secondary bile acid production and allow for *Clostridium difficile* spore germination and outgrowth in the large intestine. *mSphere* 1:1. doi: 10.1128/msphere.00045-15

Thomas, G. W. C., Dohmen, E., Hughes, D. S. T., Murali, S. C., Poelchau, M., Glastad, K., et al. (2020). Gene content evolution in the arthropods. *Genome Biol.* 21, 1–14. doi: 10.1186/S13059-019-1925-7

Thomas, C. M., and Nielsen, K. M. (2005). Mechanisms of, and barriers to, horizontal gene transfer between bacteria. *Nat. Rev. Microbiol.* 3, 711–721. doi: 10.1038/nrmicro1234

Tormo-Badia, N., Håkansson, Å., Vasudevan, K., Molin, G., Ahrné, S., and Cilio, C. M. (2014). Antibiotic treatment of pregnant non-obese diabetic mice leads to altered gut microbiota and intestinal immunological changes in the offspring. *Scand. J. Immunol.* 80, 250–260. doi: 10.1111/sji.12205

Verhoeckx, K., Cotter, P., López-Expósito, I., Kleiveland, C., Lea, T., Mackie, A., et al. (2015). in *The Impact of Food Bioactives on Health*. eds. K. Verhoeckx, P. Cotter, I. López-Expósito, C. Kleiveland, T. Lea and A. Mackieet al. (Cham: Springer International Publishing).

von Wintersdorff, C. J. H., Penders, J., van Niekerk, J. M., Mills, N. D., Majumder, S., van Alphen, L. B., et al. (2016). Dissemination of antimicrobial resistance in microbial ecosystems through horizontal gene transfer. *Front. Microbiol.* 7:173. doi: 10.3389/fmicb.2016.00173

Wang, M., Tran, J., and Jacoby, G. (2003). Plasmid-mediated quinolone resistance in clinical isolates of *Escherichia coli* from Shanghai, China. *Antimicrob. Agents Chemother.* 47, 2242–2248. doi: 10.1128/AAC.47.7.2242

Weinert, L. A., Welch, J. J., and Jiggins, F. M. (2009). Conjugation genes are common throughout the genus *Rickettsia* and are transmitted horizontally. *Proc. R. Soc. B Biol. Sci.* 276, 3619–3627. doi: 10.1098/rspb.2009.0875

Willetts, N., and Wilkins, B. (1984). Processing of plasmid DNA during bacterial conjugation. *Microbiol. Rev.* 48, 24. doi: 10.1128/MR.48.1.24-41.1984

Winokur, P. L., Vonstein, D. L., Hoffman, L. J., Uhlenhopp, E. K., and Doern, G. V. (2001). Evidence for transfer of CMY-2 AmpC β-lactamase plasmids between *Escherichia coli* and *Salmonella* isolates from food animals and humans. *Antimicrob. Agents Chemother.* 45, 2716–2722. doi: 10.1128/AAC.45.10.2716-2722.2001

Wozniak, R. A. F., and Waldor, M. K. (2010). Integrative and conjugative elements: mosaic mobile genetic elements enabling dynamic lateral gene flow. *Nat. Rev. Microbiol.* 8, 552–563. doi: 10.1038/nrmicro2382

Wybouw, N., Pauchet, Y., Heckel, D. G., and van Leeuwen, T. (2016). Horizontal gene transfer contributes to the evolution of arthropod Herbivory. *Genome Biol. Evol.* 8, 1785–1801. doi: 10.1093/gbe/evw119

Yang, J. J., Wang, J. T., Cheng, A., Chuang, Y. C., and Sheng, W. H. (2018). Impact of broad-spectrum antimicrobial treatment on the ecology of intestinal flora. *J. Microbiol. Immunol. Infect.* 51, 681–687. doi: 10.1016/j.jmii.2016.12.009

Zeng, X., and Lin, J. (2017). Factors influencing horizontal gene transfer in the intestine. *Anim. Health Res. Rev.* 18, 153–159. doi: 10.1017/S1466252317000159

Zhang, S., Chen, D. C., and Chen, L. M. (2019). Facing a new challenge: the adverse effects of antibiotics on gut microbiota and host immunity. *Chin Med J (Engl)* 132, 1135–1138. doi: 10.1097/CM9.0000000000000245

Ziv, N., Brandt, N. J., and Gresham, D. (2013). The use of chemostats in microbial systems biology. *J. Vis. Exp.* 80, 1–10. doi: 10.3791/50168

Conflict of Interest: The authors declare that the research was conducted in the absence of any commercial or financial relationships that could be construed as a potential conflict of interest.

Publisher's Note: All claims expressed in this article are solely those of the authors and do not necessarily represent those of their affiliated organizations, or those of the publisher, the editors and the reviewers. Any product that may be evaluated in this article, or claim that may be made by its manufacturer, is not guaranteed or endorsed by the publisher.

frontiers | Frontiers in Microbiology

ORIGINAL RESEARCH
published: 08 July 2022
doi: 10.3389/fmicb.2022.900185

High Prevalence and Overexpression of Fosfomycin-Resistant Gene *fosX* in *Enterococcus faecium* From China

Ling Xin[1,2], Xiaogang Xu[1,2], Qingyu Shi[1,2], Renru Han[1,2], Jue Wang[1,2], Yan Guo[1,2] and Fupin Hu[1,2]**

[1] Institute of Antibiotics, Huashan Hospital, Fudan University, Shanghai, China, [2] Key Laboratory of Clinical Pharmacology of Antibiotics, Ministry of Health, Shanghai, China

Enterococci are one of the main causes of gastrointestinal tract infections in the healthcare system and can develop resistance to fosfomycin through plasmid or chromosomally encoded fosfomycin resistance genes. To investigate the mechanisms of fosfomycin resistance, a total of 4,414 clinical isolates of non-replicated clinical enterococci collected from 62 hospitals in 26 provinces or cities in China were tested. Antibiotic susceptibility testing, detection of fosfomycin resistance genes, and cloning of the *fos*X gene were done. The PFGE, MLST, qRT-PCR, and next genome sequencing were carried out. The results revealed that the fosfomycin-resistant rate of enterococci was 3.5% (153/4,414), and the major resistance mechanism was *fos*X (101/153) and *fos*B (52/153) genes. The *fos*X gene could increase 4- fold fosfomycin MIC in *Enterococcus faecium* BM4105RF transformants, and the results of PFGE showed the 101 *E. faecium* carrying *fos*X were grouped into 48 pulse types. The multilocus sequence typing identified ST555 as the vast majority of STs, mostly distributed in Shanghai, China. Furthermore, the *fos*X gene expression was strongly related to the fosfomycin-resistant levels of *enterococci*. The present study was the first to describe the high prevalence presence of the *fos*X gene in *E. faecium* from China.

Keywords: *Enterococci*, fosfomycin, resistance, *fos*X, prevalence

OPEN ACCESS

Edited by:
Xingmin Sun,
University of South Florida,
United States

Reviewed by:
Balkiss Bouhaouala,
Pasteur Institute of Tunis, Tunisia
Xiucai Zhang,
Wenzhou Medical University, China

****Correspondence:***
Yan Guo
guoyan@fudan.edu.cn
Fupin Hu
hufupin@fudan.edu.cn

Specialty section:
This article was submitted to Antimicrobials, Resistance and Chemotherapy, a section of the journal Frontiers in Microbiology

Received: *20 March 2022*
Accepted: *16 June 2022*
Published: *08 July 2022*

Citation:
Xin L, Xu X, Shi Q, Han R, Wang J, Guo Y and Hu F (2022) High Prevalence and Overexpression of Fosfomycin-Resistant Gene fosX in Enterococcus faecium From China. Front. Microbiol. 13:900185. doi: 10.3389/fmicb.2022.900185

INTRODUCTION

Enterococci are significant opportunistic nosocomial pathogens of the gastrointestinal tract, occupying second place in the detection rate of Gram-positive bacteria (Fillgrove et al., 2003). Currently, clinically limited antibiotics are available for the treatment of enterococcal infections (Scortti et al., 2018). As a phosphoric acid antibiotic agent, fosfomycin showed broad-spectrum antibacterial activity and acted as the first step in the synthesis of bacterial peptidoglycan (Fillgrove et al., 2003; Chen et al., 2019; Zhang et al., 2020). With the widespread use of fosfomycin, the emergence of *enterococci* has become a major concern (Fillgrove et al., 2003; Scortti et al., 2018).

Fosfomycin resistance mechanisms have been proposed, including inherent the acquisition of chromosomal mutations and plasmid-encoded fosfomycin-modifying enzymes. Regarding the mechanisms of chromosomal mutations, it supported the replacement position of cysteine in the active site of the UDP-N-acetylglucosamine-3-enolpruvyltransferase (MurA), such as *Borrelia burgdorferi*, *Mycobacterium tuberculosis*, etc. (Fillgrove et al., 2003;

Clinical and Laboratory Standards Institute, 2020). Moreover, fosfomycin resistance is also mediated by reduced antimicrobial uptake by chromosomal mutations in the *glp*T and *uhp*T genes (Clinical and Laboratory Standards Institute, 2020). Different fosfomycin-modifying enzymes had been described, including metalloenzymes (FosA, FosB, and FosX) (Murray et al., 1990; Bernat et al., 1997; Xu et al., 2013; Chen et al., 2014) and fosfomycin kinases (FomA, FomB, and FosC) (Mendoza et al., 1980; Bernat et al., 1997; Sahni et al., 2013).

Fillgrove et al. (2003) found a related subfamily enzyme named FosX with 30–35% similarity to the sequences of FosA and FosB proteins in the microbial genome sequence database. Scortti et al. (2018) reported that the FosX-mediated resistance is epistatically suppressed by two members of the PrfA virulence regulon, *hpt* and *prf*A, which upon activation by host signals induce increased fosfomycin influx into the bacteria cell. Chen et al. (2019) found that the aminoglycosides resistance gene *rmt*B may be co-disseminated with bla_{KPC-2} and *fos*A3 genes through plasmid, which results in fosfomycin-resistance isolates difficult-to-treat pathogen due to limited treatment options. Zhang et al. (2020) reported that the coexistence of *van* series genes and *fos* genes simultaneously can greatly improve the transfer efficiency in *Enterococcus faecium*.

At present, most of the previous studies investigated the mechanism of fosfomycin resistance among Gram-negative bacteria, and only limited information about the resistance mechanism of Gram-positive, particularly *enterococci*, is available. In the published articles, *fos*A, *fos*C, and *fos*X genes were detected in gram-negative bacteria, while *fos*B genes were detected in gram-positive bacteria. In this study, we collected 4,414 clinical isolates of enterococci collected from 62 hospitals in 26 provinces or cities across China from 2017 to 2020 and aimed to survey the prevalence of fosfomycin resistance and the associated *fos*B, *fos*X, and *mur*A genetics in clinical isolates of enterococci in China.

MATERIALS AND METHODS

Bacterial Strains

The bacteria in this research were collected from 62 hospitals in 26 provinces or cities in China from 2017 to 2020. All 4,414 non-duplicated *enterococci* strains were collected by the CHINET surveillance system, including 2,316 *Enterococcus faecium* strains and 2,098 *Enterococcus faecalis* isolates, stored in 40% glycerol broth and frozen at −80°C. The hospitals in the CHINET surveillance system collect bacteria every year, and the staff numbers in hospitals randomly collect bacteria in the process. The distribution of 4,414 isolates was 1,222 in 2017, 1,411 in 2018, 1,277 in 2019, and 504 in 2020. All strains isolated from children and adults accounted for 1.6 and 98.4%, respectively. Among them, the main sources of specimens were urine (64.4%), bile (12.2%), pleural and ascites (12.2%), blood (8.5%), wounds (6.6%), and respiratory tract specimens (5.3%). *E. faecalis* ATCC 29212 was used as a quality control strain.

Antimicrobial Susceptibility Testing

The antimicrobial susceptibility to fosfomycin was determined using the agar dilution method by Mueller-Hinton agar (MHA) supplemented with 25 mg/L glucose-6-phosphate (G6P) and the results were interpreted by the Clinical and Laboratory Standards Institute (CLSI) M100 31th Edition guideline. To interpret the susceptibility of *E. faecium* to fosfomycin, values corresponded to the breakpoints of the urinary tract infection *E. faecalis* in CLSI (sensitivity $\leq$ 64 mg/L; resistant $\geq$ 256 mg/L) (Clinical and Laboratory Standards Institute, 2020).

Detection of Fosfomycin Resistance Genes

The fosfomycin resistance genes were detected and confirmed by polymerase chain reaction (PCR) using the primers listed in **Table 1**. The PCR products were sequenced by the MAP BIOTECH company (Shanghai, China) and the sequences were aligned by BLAST[1].

Cloning of *fos*X Gene

To further elucidate the function of *fos*X, we selected the *fos*X fragment from a fosfomycin-resistant *E. faecium* (MIC = 512 mg/L) for cloning and cloned it into the shuttle vector plasmid pIB166. The recombinant plasmid pIB166_*fos*X was transformed into *Escherichia coli* DH5α competent cells, selected with chloramphenicol (5 mg/L). Later, the resulting plasmids were electroporated from *E. coli* DH5α into *E. faecium* BM4105RF competent cells, selected with rifampin (50 mg/L) and chloramphenicol (5 mg/L). The presence of *fos*X in *E. coli* and *E. faecium* transformants were confirmed by PCR and sequenced by the MAP BIOTECH company (Shanghai, China).

[1]http://blast.ncbi.nlm.nih.gov/Blast.cgi

TABLE 1 | PCR primers of genes.

Gene primer	Sequences (5′→3′)	Product size (bp)	Tm (°C)
*fos*B-F	CAGAGATATTTTAGGGGCTGACA	312	53
*fos*B-R	CTCAATCTATCTTCTAAACTTCCTG		
*fos*X-F	TTGGGGGTGGGAAAGTTGATA	243	64
*fos*X-R	AACTGCAATCCAAAGGTCGT		
*mur*A-F	TCGCTTTATGCCGAAATCTT	1302	52
*mur*A-R	CGGCCACAAAAAGAAGGATA		
*fos*X-F-BamHI	CCC*GGATCC*ATGGAAGGAGAG GAAATGGAA		
*fos*X-R-XbaI	CGGCCCCC*TCTAGA*TTAATCTGTT GGTTCTTTTTGGTAG	243	64
qPCR-Primer			
*fos*X-F-RT	CTGTTGGTTCTTTTTGGTAGCGA		
*fos*X-R-RT	AAAGCTGGAGAAAAAGGGTT	130	60
purk-F-RT	TGGTGGCAGGAAATGGTCAA		
purk-R-RT	AGGCTCACTGCTTCTGCAAT	163	60

Tm, annealing temperature.

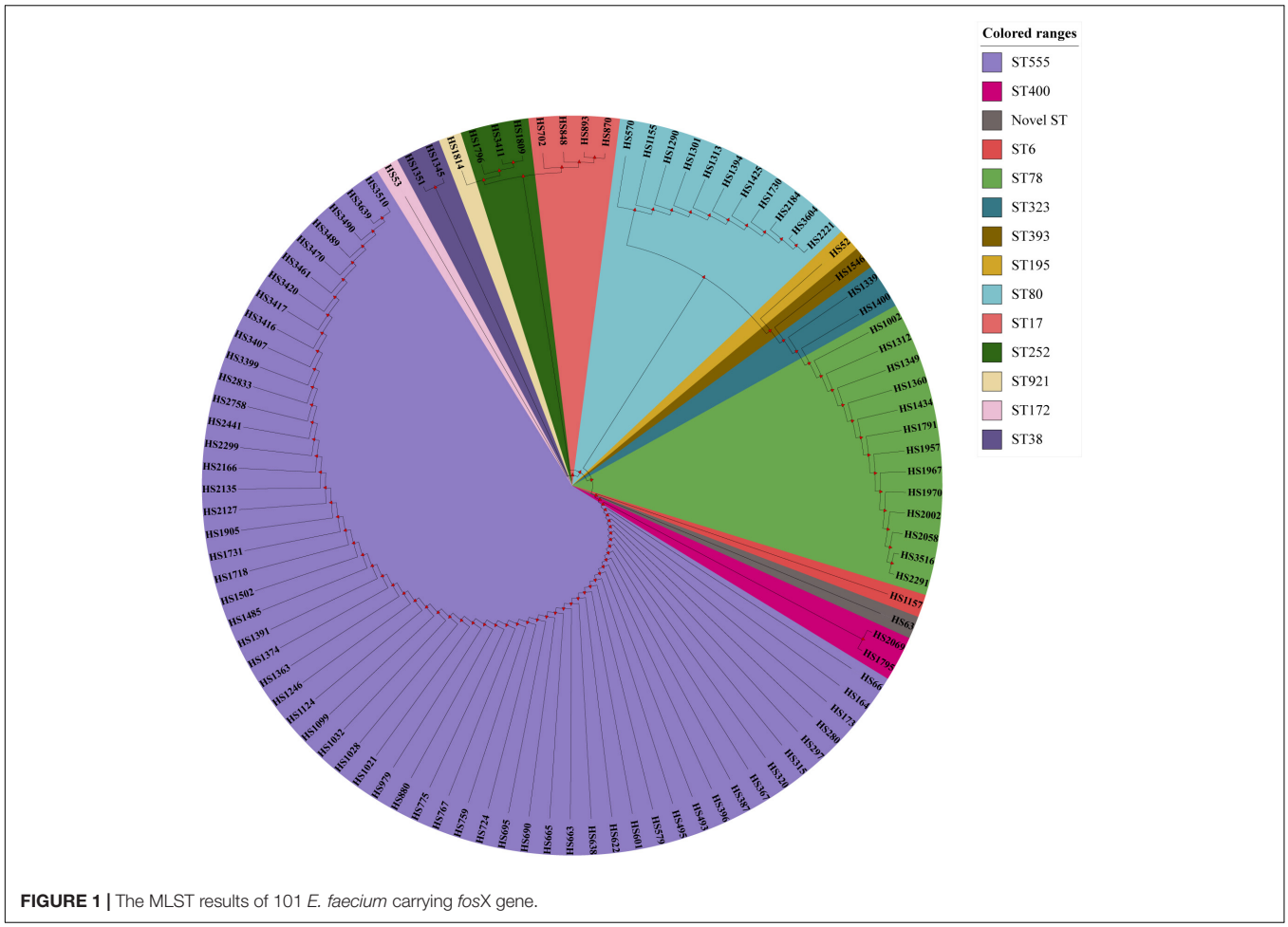

FIGURE 1 | The MLST results of 101 *E. faecium* carrying *fos*X gene.

Pulsed-Field Gel Electrophoresis

A pulsed-field gel electrophoresis analysis was performed using a CHEF mapper system (Bio-Rad, United States) (Murray et al., 1990). Agarose gel blocks were lysed with proteinase K at 20 mg/ml and digested with SmaI. The digested DNA was subjected to electrophoresis at 6 V/cm, 14°C, in a 1.0% agarose gel with pulse times of 1 to 20 s for 20 h. The banding patterns were interpreted using the criteria devised by Tenover et al. (Chen et al., 2014).

Multilocus Sequence Typing

Genomic DNAs of *enterococci* strains were subjected to whole-genome sequencing using Illumina (Illumina, San Diego, CA, United States) short-read sequencing (150 bp paired-end reads). To ensure the quality of information analysis, the raw data is filtered using FASTX-Toolkit software[2], assembled by the velvet V1.2.03 software[3], and used glimmer software[4] to predict genes. The functional annotation of genes was confirmed by searching the NCBI's nr library[5]. Isolates were screened using the following seven housekeeping genes: adenylate kinase (*adk*), ATP synthase-alpha subunit (*atpA*), D-alanine ligase (*ddl*), glyceraldehyde-3-phosphate dehydrogenase (*gyd*), glucose-6-phosphate dehydrogenase (*gdh*), phosphoribosylaminoimidazole carboxylase ATPase subunit (*pur*K), and phosphate ATP-binding cassette transporter (*pst*S). The alleles and sequence types (STs) were determined *via* the MLST database[6]. The phylogenetic tree was performed by MEGA_X and iTOL[7].

Total RNA Extraction and Quantitative Real-Time PCR

A single colony was selected from the blood agar plate and added to brain heart infusion broth and incubated for 18 h at 37°C with shaking at 180 rpm. The bacterial culture was centrifuged at 12,000 rpm for 5 min to collect the supernatant. Total RNA was extracted using a Life Real kit (Life Real, Hangzhou, China) according to the manufacturer's instructions. Thereafter, the RNAs were reverse transcribed to cDNA for qRT-PCR analysis in the light of the manufacturer's

[2]http://hannonlab.cshl.edu/fastx_toolkit
[3]https://www.ebi.ac.uk/~zerbino/velvet
[4]http://ccb.jhu.edu/software/glimmer/
[5]ftp://ftp.ncbi.nih.gov/blast/db
[6]http://efaecium.mlst.net/
[7]https://itol.embl.de/

manual of a commercial cDNA synthesis kit with a gDNA eraser (Takara, Dalian, China). The qPCR was performed on a Life Tech-ViiA7 qPCR multiplex reactions System (Life Technologies, United States) with specific primers (**Table 1**) for the PrimeScriptTM RT reagent Kit (Takara, Dalian, China). The relative expression levels of the *fos*X gene were normalized to the *pur*K reference gene. The quantification of the target genes was analyzed using the comparative threshold cycle $2^{-\Delta\Delta Ct}$ method (Zhang et al., 2020). All experiments were repeated in triplicate independently. The MIC range of the strains carrying the *fos*X gene to fosfomycin was 512–4,096 mg/L. Among them, the MICs of fosfomycin of HS2166, HS570, HS2069 and HS1440 were 512 mg/L, 1,024 mg/L, 2,048 mg/L, and 4,096 mg/L. The relative expression of the *fos*X gene of HS570, HS2069, and HS1440 isolates was normalized to that of the HS2166 strain.

Next Genome Sequencing

To evaluate the difference in antibiotic resistance of *enterococci* carrying the *fos*X gene with different levels of fosfomycin resistance, we extracted DNA from the HS2166, HS570, HS2069, and HS1440 strains and performed next genome sequencing according to the precious method (Xu et al., 2013). Raw sequences were filtered using FASTX-Toolkit (see text footnote 2) and assembled into contigs using the velvet V1.2.03 program. The Comprehensive Antibiotic Database[8] was used to identify antibiotic resistance genes. The replicon sequences were identified by PlasmidFinder 2.1[9]. The Virulence Factors Database[10] was used to identify virulence genes.

Ethics Statement

The study protocol was approved by the Institutional Review Board of Huashan Hospital, Fudan University (no. 2020-040).

RESULTS

Antimicrobial Susceptibility Testing and Detection of Fosfomycin Resistance Genes

Among the 4,414 isolates, the rate of fosfomycin-resistant *enterococci* was 3.5% (153/4414). Fosfomycin was very active against *enterococci* (MIC_{50} and MIC_{90} were both 50 mg/L; the median MIC value was 50 mg/L). Of 153 fosfomycin-resistant clinical isolates, *E. faecium* and *E. faecalis* accounted for 77.1% (117/153) and 23.5% (36/153), respectively. The MIC range of fosfomycin against 153 fosfomycin-resistant strains was 512–4,096 mg/L, of which MIC_{50} and MIC_{90} were 2,048 and 4,096 mg/L, and the median MIC value was 2,048 mg/L. The PCR results showed that the strains carrying the *fos*B and *fos*X genes were 33.8% (52/153) and 65.6% (101/153) in the current study, respectively.

Cloning of *fos*X Gene, Pulsed-Field Gel Electrophoresis, and Multilocus Sequence Typing

The *fos*X gene was cloned into *E. faecium* BM4105RF by cloning experiment, and the results revealed that the fosfomycin MICs of *E. faecium* BM4105RF transformant carrying *fos*X was 128 mg/L while the recipient and donor strains had fosfomycin MICs of 32 and 2,048 mg/L, indicating that *fos*X could be the expression in *E. faecium*. According to the results of PFGE, the *fos*X carrying *E. faecium* isolates were grouped into 48 pulse types. The top five pulse types were named ENT-27, ENT-15, ENT-29, ENT-8 and ENT-30, and the percentage were 8.9% (9/101), 5.9% (6/101), 4.9% (5/101), 4% (4/101), and 4% (4/101). The 101 *fos*X carrying *E. faecium* isolates in this study were categorized into fourteen different STs (ST555, ST6, ST17, ST38, ST78, ST 80, ST 172, ST195, ST252, ST323, ST393, ST400, ST921, and one novel ST). The top five STs were ST555, ST78, ST80, ST17, and ST252, and the percentage were 57.4% (58/101), 12.8% (13/101), 10.9% (11/101), 4% (4/101), and 3% (3/101). The minimum spanning tree analysis showed that seven groups were formed by *enterococci* STs by MEGA_X and iTOL analysis. The MIC of ST555, ST78, ST17, and ST252 *E. faecium* to Fosfomycin could reach 4,096 mg/L. 94% (95/101) of *E. faecium* belonged to the CC17 clonal complex, and the MIC of *E. faecium* to Fosfomycin can reach 4,096 mg/L. The fosfomycin MIC of 6% (6/101) of the *E. faecium* belonging to the non-CC17 clonal complex could reach 2,048 mg/L. In terms of geographical distribution, the distribution of 58 isolates of ST555 *E. faecium* was 44 in Shanghai, five strains in Beijing, two strains in Anhui, two strains in Hubei, two strains in Tianjin, one strain in Henan, one strain in Gansu, and one strain in Jiangsu province. Four ST17 *E. faecium* isolates were only distributed in Shanghai, and other types were scattered. The results of PFGE, MLST, and phylogenetic tree were summarized in supplement material and **Figure 1**.

Quantitative Real-Time PCR

Due to the presence of *fos*X in *E. faecium* with different fosfomycin MICs, we determined the relationship of *fos*X expression levels of different fosfomycin MICs of *fos*X carrying fosfomycin-resistant *E. faecium*. The fosfomycin MIC of four *E. faecium*, named HS2166, HS570, HS2069, and HS1440 were 512, 1,024, 2,048, and 4,096 mg/L. Interestingly, *fos*X expression of fosfomycin-resistant strain (HS2166, MIC = 512 mg/L) was lower than that of HS570, HS2069, and HS1440 isolates which showed fosfomycin MICs 1,024, 2,048, and 4,096 mg/L, and the *fos*X relative expression of HS570 and HS2069 strains showed no significant difference (**Figure 2**). Overall, the qPCR results showed that with the enhancement of the resistance to fosfomycin of *E. faecium*, the relative expression level of the *fos*X gene increased correspondingly.

[8]https://card.mcmaster.ca/analyze

[9]https://cge.food.dtu.dk/services/PlasmidFinder

[10]http://www.mgc.ac.cn/VFs

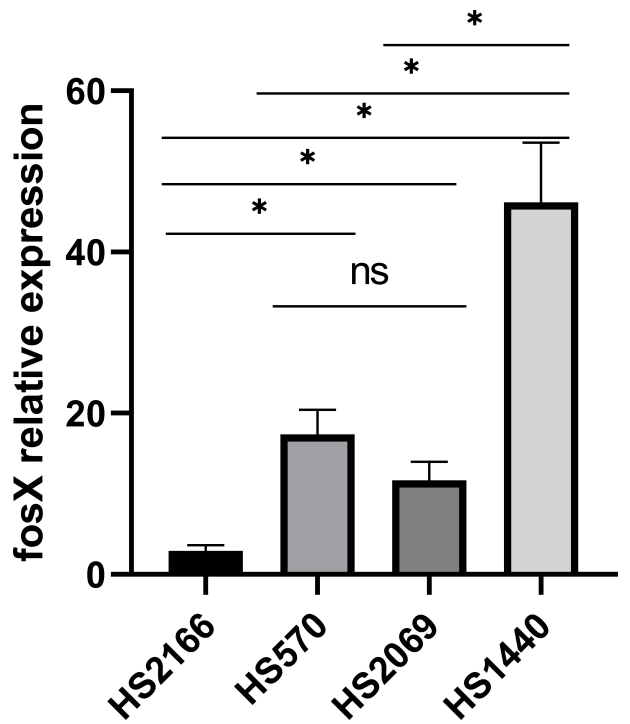

FIGURE 2 | The relative expression of *fos*X gene in HS2166, HS570, HS2069, and HS1440.

Next Genome Sequencing

The four next genome sequencing results of HS2166, HS570, HS2069, and HS1440 strains were listed in **Figure 3** and **Table 2**. The antibiotic resistance genes of the HS2166 strain with fosfomycin MIC of 512 mg/L were *aac(6')-Ii*, *erm*B, *dfr*G, *dfr*F, *inu*A, *efm*A, and *fos*X genes. There were *aac(6')-Ii*, *aph(3')-IIIa*, *efm*A, *erm*B, *tet*(45), *tet*U, and *fos*X genes in the HS570 strain with fosfomycin MIC of 1,024 mg/L. The drug resistance genes in the HS2069 strain with fosfomycin MIC of 2,048 mg/L were *aac(6')-Ii*, *bac*A, *isa*, *erm*B, and *fos*X genes. The resistance genes in HS1440 strain with fosfomycin resistance level of 4,096 mg/L were *aac(6')-Ii*, *ant*(6)-Ia, *efm*A, *dfr*G, *erm*B, *erm*T, *tet*(45), *inu*A, and *fos*X genes. The repUS15 and rep2 plasmids were present in all four strains, and the repIIa plasmid was present in HS2166, HS570, and HS2069. The plasmids in HS1400 isolate with fosfomycin MIC of 4,096 mg/L were repUS12, repUS15, repUS43, rep2, and rep29, and the virulence genes in the HS1400 strain were *has*B, *has*C, *cap*8D, and *kfi*D. Interestingly, no virulence gene was detected in the HS2166 strain with fosfomycin MIC of 512 mg/L. Only one virulence gene named *bop*D was detected in HS570 isolate with fosfomycin MIC of 1,024 mg/L.

DISCUSSION

Due to the unique mechanisms of action, fosfomycin exhibits significant antimicrobial activity against a broad spectrum of pathogens, including *enterococci* (Mendoza et al., 1980; Bernat et al., 1997). The fosfomycin resistance rate of *enterococci* isolated from South Africa was 1% (72/725) (Sahni et al., 2013). Zhang et al. (2020) reported that the fosfomycin resistance rate of *enterococci* isolated from China was 2.6% (20/761). The fosfomycin resistance rate of *enterococci* isolated from the United States was 1.3% (12/890) (Guo et al., 2017). In this study, 3.5% (153/4,414) of the *enterococci* were resistant to fosfomycin.

Little was known about the resistance mechanism of *enterococci* to fosfomycin in epidemiological research, and the most of genes that have been reported to be plasmid-mediated resistance to fosfomycin were *fosB*, with a G+C content of 27%, and were mainly distributed in *staphylococcus*, *enterococci*, and *bacillus* (Chen et al., 2014; Fu et al., 2016; Guo et al., 2017; Shinde et al., 2017; Ziwei et al., 2019; Xu et al., 2020). The *fos*B gene developed resistance to fosfomycin by encoding Mg^{2+}-dependent sulfhydryl transferase, while the *fos*X was by encoding Mn^{2+}-dependent epoxidase (Roberts et al., 2013). Recently, there are reports that the *fos*X gene was detected in *Acinetobacter baumannii, Klebsiella pneumoniae*, and *E. faecium* (Zhang et al., 2020; Kashefieh et al., 2021; Leite et al., 2021), indicating that the *fos*X gene is not unique to Gram-positive bacteria. The MICs of *fos*X-positive fosfomycin-resistant *A. baumannii* and *K. pneumoniae* were 128 and ≥ 200 mg/L, respectively (Kashefieh et al., 2021; Leite et al., 2021). Meanwhile, the MIC of fosfomycin-resistant *E. faecium* carrying the *fos*X gene was ≥ 512 mg/L (Zhang et al., 2020). In the current study, the MIC range of *fos*X-positive *E. faecium* was 512–4,096 mg/L.

Notably, in the report of Zhang et al., *fos*X, *fos*B genes, and *mur*A mutation can coexist in fosfomycin-resistant *enterococci* (Zhang et al., 2020). Mutation of MurA protein exists in *A. ba* carrying *fos*X gene with fosfomycin MIC of 128 mg/L (Leite et al., 2021). Unlike previous studies, the *fos*X gene was exclusively present on fosfomycin-resistant *E. faecium*. More importantly, this study was the first time to clone the *fos*X gene in *enterococci* and proved that the *fos*X gene can be expressed in *E. faecium*, which mediates the reduction of the bacteria's sensitivity to fosfomycin, indicating that these genes might be the primary factors mediating the resistance of *E. faecium* against fosfomycin.

As previously reported, the PFGE band patterns of 20 *fos*X-positive fosfomycin-resistant *enterococci* isolates showed 16 closely related isolates that exhibited ≥ 80% similarity (Zhang et al., 2020). In the current study, the PFGE patterns of 101 *enterococci* carrying the *fos*X gene showed 48 related strains that exhibited ≥ 80% similarity. A small number of isolates showed a high degree of homology, indicating that the possibility of genetic correlation between them was extremely small. The most frequent sequence type of enterococci carrying the *fos*X gene was the ST78 type in the previous studies (Zhang et al., 2020). Differently, ST555 (59/101) was the main clonal type in this study. The CC17 clonal complex *E. faecium*, which usually carries a virulence island and causes rapid dissemination in hospitals (Mancuso et al., 2021), belongs to a clonal complex closely related to nosocomial infection (Fiore et al., 2019). In this research, 94% (95/101) strains of *E. faecium* carrying the *fos*X gene belonged to the CC17 clonal complex, 57.4% (58/101) of the *E. faecium* belonged to the ST555 type, and most of them were isolated from Shanghai in China. Therefore, monitoring the ST555 type

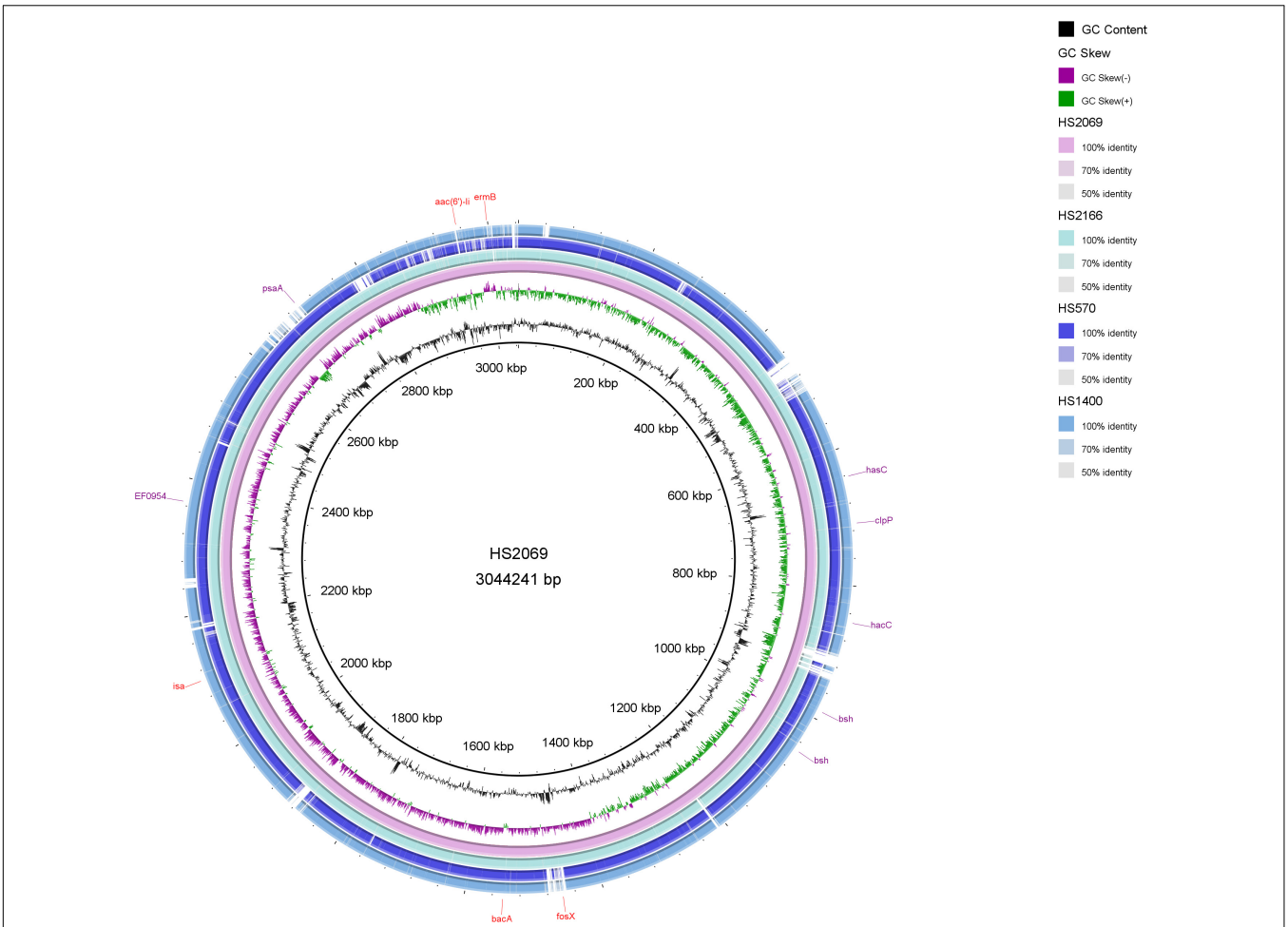

FIGURE 3 | The circle map of HS2069, HS2166, HS570, and HS1440.

TABLE 2 | The comparative genome sequences in HS2166, HS570, HS2069, and HS1440 strains.

Strain	HS2166 (Fosfomycin MIC 512 mg/L)	HS570 (Fosfomycin MIC 1024 mg/L)	HS2069 (Fosfomycin MIC 2048 mg/L)	HS1400 (Fosfomycin MIC 4096 mg/L)
Size (bp)	2982542	3043392	2905269	2982542
G+C (%)	37.7	37.5	37.8	37.7
No. of contigs	162	183	137	150
Median sequence size	8385	6551	7071	7065
N50 value	41952	42274	54021	47858
L50 value	20	23	16	16
Resistance genes	*aac(6')-Ii; ermB; dfrG,dfrF; lnuA; fosX; efm*A	*aac(6')-Ii,aph(3')-IIIa; efm*A*; ermB; tet*(45)*,tet(U)*	*aac(6')-Ii; bacA; fosX; ermB;lsa*	*aac(6')-Ii,ant*(6)*-Ia; efm*A*; dfrG; fosX; tet*(45)*; lnuA; ermB, ermT*
Replicon	repIIa; repUS15; rep2	repUS12; repUS15; rep14a; rep2; rep17; repIIa	repUS15; rep2; repIIa	repUS12; repUS15; repUS43; rep2; rep29
Virulence gene(s)	none	*bopD*	*hasC; clpP; EF0954; bsh; psaA*	*hasB; hasC; cap8D; kfiD;*

E. faecium is of great significance to curb the spread of antibiotic-resistant *enterococci*.

It was reported (Zhang et al., 2020) that the susceptibility to fosfomycin of *enterococci* carrying the *fosX* gene included resistance and sensitivity. However, the differences were that the *enterococci* carrying the *fosX* gene detected in this article were all fosfomycin-resistant strains. In addition, among the fosfomycin-resistant strains, the MIC of the isolates to fosfomycin is related to the expression level of the *fosX* gene, indicating that the function of the FosX resistance protein needs further verification.

In *enterococci*, the mobile genetic elements could account for 25% of the entire bacterial genome with strong plasticity (Hollenbeck and Rice, 2012). The fosfomycin resistance proteins FosX and FosA in pathogenic microorganisms are related to a catalytically promiscuous progenitor encoded in a *phn* operon in *Mesorhizobium loti* (Fillgrove et al., 2007). Chen et al. (2019) found that the *fos*A3 gene in clinical KPC-producing *Klebsiella pneumoniae* isolates collected from Zhejiang in China had an identical genetic background, *IS*26-*tet*R-*cad*C-*orf*1-*fos*A3-*IS*26, which is the same as that of the *fos*A3-positive plasmid pFOS18 in China. No other drug resistance genes have been reported in *E. faecium* carrying the *fos*X gene before. Parra-Flores et al. (2021) reported that ampicillin-resistant *Listeria monocytogenes* strains carried the *fos*X, *tet*A, and *tet*C resistance genes. In this study, *fos*X, *aac(6')-Ii*, and *erm*B resistance genes co-existed in the genomes of *E. faecium* strains. Through the expression of the *fos*X gene was previously reported to be associated with the virulence factors hpy and prfA (Scortti et al., 2018), no such virulence genes were found in this study. The *bop*D (biofilm formation) virulence gene belongs to the type III secreted protein and exists in the HS570 strain with fosfomycin MIC of 1,024 mg/L. A large number of gram-negative pathogenic bacteria secrete virulence factors *via* the type III secretion system during infection of host cells (Nogawa et al., 2004). The capsular genotype (*has*ABC) (Kaczorek et al., 2017), K5-specific UDP-glucose dehydrogenase (*kfi*D) (Muñoz et al., 1998), caseinolytic peptidase P (*clp*P) (Jing et al., 2022), bile resistance(*bsh*) (Parra-Flores et al., 2021), pneumococcal surface adhesion A (*psa*A) (Hu et al., 2021), and polysaccharide biosynthesis (*cap*8D) (Ali et al., 2016) were detected from *E. faecium* in this study. Unfortunately, the effect of virulence factors on fosfomycin-resistant bacteria is unclear and needs to be explored by researchers.

It was worth noting that the previous report of the *fos*X gene in *enterococci* had only appeared in Zhejiang, China, which reported that 20 *fos*X-positive fosfomycin-resistant *enterococci* were screened out of 790 *enterococci* isolates. This study was the first time to screen large-scale fosfomycin resistance genes in *enterococci* isolated from 62 hospitals in 26 provinces or cities in China and found 101 fosfomycin-resistant strains carrying the *fos*X gene among 4,414 *enterococci* clinical strains.

CONCLUSION

In summary, 153 fosfomycin-resistant strains were screened out of 4,414 *enterococci* clinical isolates, and mechanisms were explored. Our finding described that *fos*B and *fos*X genes were the major resistant mechanism of *enterococci* to fosfomycin. In addition, the *fos*X gene could increase the resistance of bacteria to fosfomycin in *E. faecium* bacteria. FosX overexpression was associated with high-level fosfomycin resistance in *E. faecium* clinical isolates. Moreover, the 101 *fos*X carrying *enterococci* showed no obvious clonal transmission by PFGE analysis, and the dominant sequence type in them was ST555. There were 14 groups of 101 *E. faecium* carrying *fos*X were formed by *E. faecium* STs by MEGA-X and iTOL analysis. Therefore, it is necessary to continuously monitor fosfomycin resistance and its mechanisms.

DATA AVAILABILITY STATEMENT

The datasets presented in this study can be found in online repositories. The names of the repository/repositories and accession number(s) can be found in the article/supplementary material.

AUTHOR CONTRIBUTIONS

FH and YG designed the study. LX, QS, and RH collected clinical samples. LX, XX, and JW performed the experiments. LX, YG, and FH analyzed the data and wrote the manuscript. All authors contributed to the article and approved the submitted version.

FUNDING

The publication was supported by Independent Medical Grants from Pfizer, the National Natural Science Foundation of China (81902100 and 81861138052), the National Key Research and Development Program of China (2021YFC2701803), 3-year Action Plan for the Construction of Shanghai Public Health System (GWV-10.2-XD02), and the China Antimicrobial Surveillance Network (Independent Medical Grants from Pfizer, 2018QD100).

ACKNOWLEDGMENTS

LX would like to thank his supervisor, FH, whose expertise was invaluable in formulating the research questions and methodology. LX would particularly like to acknowledge his team members, YG, XX, QS, RH, and JW, for their wonderful collaboration and patient support.

REFERENCES

Ali, L., Spiess, M., Wobser, D., Rodriguez, M., Blum, H. E., and Sakınç, T. (2016). Identification and functional characterization of the putative polysaccharide biosynthesis protein (CapD) of *Enterococcus faecium* U0317. *Infect. Genet. Evol.* 37, 215–224. doi: 10.1016/j.meegid.2015.11.020

Bernat, B. A., Laughlin, L. T., and Armstrong, R. N. (1997). Fosfomycin resistance protein (FosA) is a manganese metalloglutathione transferase related to glyoxalase I and the extradiol dioxygenases. *Biochemistry* 36, 3050–3055. doi: 10.1021/bi963172a

Chen, C., Xu, X., Qu, T., Yu, Y., Ying, C., Liu, Q., et al. (2014). Prevalence of the fosfomycin-resistance determinant, fosB3, in *Enterococcus faecium* clinical isolates from China. *J. Med. Microbiol.* 63, 1484–1489. doi: 10.1099/jmm.0.077701-0

Chen, J., Wang, D., Ding, Y., Zhang, L., and Li, X. (2019). Molecular epidemiology of plasmid-mediated fosfomycin resistance gene determinants in *Klebsiella pneumoniae* Carbapenemase-producing *Klebsiella pneumoniae* isolates in China. *Microb. Drug Resist.* 25, 251–257. doi: 10.1089/mdr.2018.0137

Clinical and Laboratory Standards Institute (2020). *Performance Standards for Antimicrobial Susceptibility Testing. M100-S30*. Wayne, PA: CLSI.

Fillgrove, K. L., Pakhomova, S., Newcomer, M. E., and Armstrong, R. N. (2003). Mechanistic diversity of fosfomycin resistance in pathogenic microorganisms. *J. Am. Chem. Soc.* 125, 15730–15731. doi: 10.1021/ja039307z

Fillgrove, K. L., Pakhomova, S., Schaab, M. R., Newcomer, M. E., and Armstrong, R. N. (2007). Structure and mechanism of the genomically encoded fosfomycin resistance protein, FosX, from *Listeria monocytogenes*. *Biochemistry* 46, 8110–8120. doi: 10.1021/bi700625p

Fiore, E., Van Tyne, D., and Gilmore, M. S. (2019). Pathogenicity of *Enterococci*. *Microbiol. Spectrum* 7:10.1128/microbiolspec.GPP3-0053-2018

Fu, Z., Liu, Y., Chen, C., Guo, Y., Ma, Y., Yang, Y., et al. (2016). Characterization of fosfomycin resistance gene, fosB, in methicillin-resistant *Staphylococcus aureus* isolates. *PLoS One* 11:e0154829. doi: 10.1371/journal.pone.0154829

Guo, Y., Tomich, A. D., McElheny, C. L., Cooper, V. S., Tait-Kamradt, A., Wang, M., et al. (2017). High-Level fosfomycin resistance in vancomycin-resistant *Enterococcus faecium*. *Emerg. Infect. Dis.* 23, 1902–1904. doi: 10.3201/eid2311.171130

Hollenbeck, B. L., and Rice, L. B. (2012). Intrinsic and acquired resistance mechanisms in enterococcus. *Virulence* 3, 421–433. doi: 10.4161/viru.21282

Hu, Y., Park, N., Seo, K. S., Park, J. Y., Somarathne, R. P., Olivier, A. K., et al. (2021). Pneumococcal surface adhesion a protein (PsaA) interacts with human Annexin A2 on airway epithelial cells. *Virulence* 12, 1841–1854. doi: 10.1080/21505594.2021.1947176

Jing, S., Ren, X., Wang, L., Kong, X., Wang, X., Chang, X., et al. (2022). Nepetin reduces virulence factors expression by targeting ClpP against MRSA-induced pneumonia infection. *Virulence* 13, 578–588. doi: 10.1080/21505594.2022.2051313

Kaczorek, E., Małaczewska, J., Wójcik, R., and Siwicki, A. K. (2017). Biofilm production and other virulence factors in *Streptococcus spp*. isolated from clinical cases of bovine mastitis in Poland. *BMC Vet. Res.* 13:398. doi: 10.1186/s12917-017-1322-y

Kashefieh, M., Hosainzadegan, H., Baghbanijavid, S., and Ghotaslou, R. (2021). The molecular epidemiology of resistance to antibiotics among *Klebsiella pneumoniae* isolates in azerbaijan. *Iran. J. Trop. Med.* 2021:9195184. doi: 10.1155/2021/9195184

Leite, G. C., Perdigão-Neto, L. V., Ruedas Martins, R. C., Rizek, C., Levin, A. S., and Costa, S. F. (2021). Genetic factors involved in fosfomycin resistance of multidrug-resistant *Acinetobacter baumannii*. *Infect. Genet. Evol.* 93:104943. doi: 10.1016/j.meegid.2021.104943

Mancuso, G., Midiri, A., Gerace, E., and Biondo, C. (2021). Bacterial antibiotic resistance: the most critical pathogens. *Pathogens (Basel, Switzerland)* 10:1310. doi: 10.3390/pathogens10101310

Mendoza, C., Garcia, J. M., Llaneza, J., Mendez, F. J., Hardisson, C., and Ortiz, J. M. (1980). Plasmid-determined resistance to fosfomycin in *Serratia marcescens*. *Antimicrobial Agents Chemotherapy* 18, 215–219. doi: 10.1128/AAC.18.2.215

Muñoz, R., García, E., and López, R. (1998). Evidence for horizontal transfer from *Streptococcus* to *Escherichia coli* of the kfiD gene encoding the K5-specific UDP-glucose dehydrogenase. *J. Mol. Evol.* 46, 432–436. doi: 10.1007/pl00006322

Murray, B. E., Singh, K. V., Heath, J. D., Sharma, B. R., and Weinstock, G. M. (1990). Comparison of genomic DNAs of different enterococcal isolates using restriction endonucleases with infrequent recognition sites. *J. Clin. Microbiol.* 28, 2059–2063. doi: 10.1128/jcm.28.9.2059-2063.1990

Nogawa, H., Kuwae, A., Matsuzawa, T., and Abe, A. (2004). The type III secreted protein BopD in *Bordetella bronchiseptica* is complexed with BopB for pore formation on the host plasma membrane. *J. Bacteriol.* 186, 3806–3813. doi: 10.1128/jb.186.12.3806-3813.2004

Parra-Flores, J., Holý, O., Bustamante, F., Lepuschitz, S., Pietzka, A., Contreras-Fernández, A., et al. (2021). Virulence and antibiotic resistance genes in *Listeria monocytogenes* strains isolated from ready-to-eat foods in chile. *Front. Microbiol.* 12:796040. doi: 10.3389/fmicb.2021.796040

Roberts, A. A., Sharma, S. V., Strankman, A. W., Duran, S. R., Rawat, M., and Hamilton, C. J. (2013). Mechanistic studies of FosB: a divalent-metal-dependent bacillithiol-S-transferase that mediates fosfomycin resistance in *Staphylococcus aureus*. *Biochem. J.* 451, 69–79. doi: 10.1042/BJ20121541

Sahni, R. D., Balaji, V., Varghese, R., John, J., Tansarli, G. S., and Falagas, M. E. (2013). Evaluation of fosfomycin activity against uropathogens in a fosfomycin-naive population in South India: a prospective study. *Future Microbiol.* 8, 675–680. doi: 10.2217/fmb.13.31

Scortti, M., Han, L., Alvarez, S., Leclercq, A., Moura, A., Lecuit, M., et al. (2018). Epistatic control of intrinsic resistance by virulence genes in *Listeria*. *PLoS Genet.* 14:e1007525. doi: 10.1371/journal.pgen.1007525

Shinde, D. B., Sangshetti, J. N., Moloney, M. G., Patil, R. H., and Joshi, S. S. (2017). Mur ligase inhibitors as anti-bacterials: a comprehensive review. *Curr. Pharmaceutical Des.* 23, 3164–3196. doi: 10.2174/1381612823666170214115048

Xu, W., Chen, T., Wang, H., Zeng, W., Wu, Q., Yu, K., et al. (2020). Molecular mechanisms and epidemiology of fosfomycin resistance in *Staphylococcus aureus* isolated from patients at a teaching hospital in China. *Front. Microbiol.* 11:1290. doi: 10.3389/fmicb.2020.01290

Xu, X., Chen, C., Lin, D., Guo, Q., Hu, F., Zhu, D., et al. (2013). The fosfomycin resistance gene fosB3 is located on a transferable, extrachromosomal circular intermediate in clinical *Enterococcus faecium* isolates. *PLoS One* 8:e78106. doi: 10.1371/journal.pone.0078106

Zhang, X., Bi, W., Chen, L., Zhang, Y., Fang, R., Cao, J., et al. (2020). Molecular mechanisms and epidemiology of fosfomycin resistance in enterococci isolated from patients at a teaching hospital in China, 2013-2016. *J. Global Antimicrobial Resistance* 20, 191–196. doi: 10.1016/j.jgar.2019.08.006

Ziwei, S., Xue, W., Xingchen, Z., Su, J., Yuanyuan, L., Owais, A., et al. (2019). Taxonomic distribution of FosB in human-microbiota and activity comparison of fosfomycin resistance. *Front. Microbiol.* 10:200. doi: 10.3389/fmicb.2019.00200

Conflict of Interest: The authors declare that the research was conducted in the absence of any commercial or financial relationships that could be construed as a potential conflict of interest.

Publisher's Note: All claims expressed in this article are solely those of the authors and do not necessarily represent those of their affiliated organizations, or those of the publisher, the editors and the reviewers. Any product that may be evaluated in this article, or claim that may be made by its manufacturer, is not guaranteed or endorsed by the publisher.

frontiers | Frontiers in Microbiology

TYPE Original Research
PUBLISHED 01 August 2022
DOI 10.3389/fmicb.2022.905865

OPEN ACCESS

EDITED BY
Yongfei Hu,
China Agricultural University, China

REVIEWED BY
Shiwei Wang,
Northwest University, China
Henan Li,
Peking University People's Hospital, China

*CORRESPONDENCE
Jie Feng
fengj@im.ac.cn

†PRESENT ADDRESS
Qinna Cui,
BioQuant Center of the University of Heidelberg, Heidelberg, Germany; Max-Planck-Institute for Terrestrial Microbiology, Marburg, Germany

‡These authors have contributed equally to this work

SPECIALTY SECTION
This article was submitted to Antimicrobials, Resistance and Chemotherapy, a section of the journal Frontiers in Microbiology

RECEIVED 28 March 2022
ACCEPTED 04 July 2022
PUBLISHED 01 August 2022

CITATION
Zhang G, Cui Q, Li J, Guo R, Leclercq SO, Du L, Tang N, Song Y, Wang C, Zhao F and Feng J (2022) The integrase of genomic island GI*sul2* mediates the mobilization of GI*sul2* and IS*CR*-related element CR2-*sul2* unit through site-specific recombination. *Front. Microbiol.* 13:905865. doi: 10.3389/fmicb.2022.905865

The integrase of genomic island GI*sul2* mediates the mobilization of GI*sul2* and IS*CR*-related element CR2-*sul2* unit through site-specific recombination

Gang Zhang[1‡], Qinna Cui[1,2†‡], Jianjuan Li[1,2], Ruiliang Guo[1,3], Sébastien Olivier Leclercq[4], Lifeng Du[5], Na Tang[1,2], Yuqin Song[1], Chao Wang[1], Fangqing Zhao[5] and Jie Feng[1*]

[1]State Key Laboratory of Microbial Resources, Institute of Microbiology, Chinese Academy of Sciences, Beijing, China, [2]College of Life Science, University of Chinese Academy of Sciences, Beijing, China, [3]School of Life Sciences, Zhengzhou University, Zhengzhou, China, [4]UMR ISP, INRAE, Université François Rabelais de Tours, Nouzilly, France, [5]Beijing Institutes of Life Science, Chinese Academy of Sciences, Beijing, China

In the worldwide health threat posed by antibiotic-resistant bacterial pathogens, mobile genetic elements (MGEs) play a critical role in favoring the dissemination of resistance genes. Among them, the genomic island GI*sul2* and the IS*CR*-related element CR2-*sul2* unit are believed to participate in this dissemination. However, the mobility of the two elements has not yet been demonstrated. Here, we found that the GI*sul2* and CR2-*sul2* units can excise from the host chromosomal attachment site (*attB*) in *Shigella flexneri*. Through establishing a two-plasmid mobilization system composed of a donor plasmid bearing the GI*sul2* and a trap plasmid harboring the *attB* in *recA*-deficient *Escherichia coli*, we reveal that the integrase of GI*sul2* can perform the excision and integration of GI*sul2* and CR2-*sul2* unit by site-specific recombination between *att* core sites. Furthermore, we demonstrate that the integrase and the *att* sites are required for mobility through knockout experiments. Our findings provide the first experimental characterization of the mobility of GI*sul2* and CR2-*sul2* units mediated by integrase. They also suggest a potential and unappreciated role of the GI*sul2* integrase family in the dissemination of CR2-*sul2* units carrying various resistance determinants in between.

KEYWORDS

integrase, genomic island (GI), mobilization, ISCR elements, site-specific recombination

Introduction

Mobile genetic elements (MGEs), including genomic islands (GIs), play a major role in the evolution of bacteria, and more specifically in the wide dissemination of antibiotic resistance genes (ARGs) (Juhas et al., 2009; Hall, 2010; Carraro and Burrus, 2014; Partridge et al., 2018; He et al., 2019; Halder et al., 2022; Li et al., 2022). Among them, GI*sul2* was proposed to participate in the dissemination of sulphonamide resistance gene *sul2* (Nigro and Hall, 2011; Harmer et al., 2017).

GI*sul2* was first detected in the chromosome of *Enterobacter cloacae* subspecies cloacae type strain ATCC 13047, in the chromosome of *Shigella flexneri* ATCC 700930 (also known as 2457T), and in the large conjugative plasmid pAB3 of *Acinetobacter baumannii* ATCC 17978 (Nigro and Hall, 2011). GI*sul2* was then also reported in the chromosome of *A. baumannii* ATCC 19606 and plasmids of several γ-proteobacteria (Hamidian and Hall, 2016; Harmer et al., 2017). GI*sul2* is usually inserted into the 3′ end of chromosomally-encoded *guaA* genes (GMP synthase) at the 5′-GAGTGGGA-3′ integration site (Harmer et al., 2017). GI*sul2* and its derivatives are also frequently found as part of antibiotic resistance island B (ARI-B) of IncC plasmids (Anantham et al., 2015; Harmer and Hall, 2015), but in this case, the integration site is limited to 5′-GGGA-3′, which may correspond to a secondary integration site (Harmer et al., 2017). According to the recent genomic description (Harmer et al., 2017), the element consists of genes putatively involved in mobilization (excision/integration, replication, and transfer), followed by a toxin–antitoxin system, an arsenic resistance operon, a CR2 element, and the *sul2* resistance gene (Figure 1).

The first common region (CR) element, CR1, was discovered in the 3′-conserved segment (3′-CS) of some class 1 integrons, where it is associated with antibiotic resistance genes not embedded in gene cassettes and is usually found between partial duplications of the 3′-CS (Stokes et al., 1993; Partridge and Hall, 2003). Other CR elements were later identified in numerous bacteria, especially in Gram-negative pathogens, and are frequently linked to diverse ARGs (Partridge and Hall, 2003; Toleman et al., 2006a; Schleinitz et al., 2010; Fang et al., 2019). CR2 is found downstream of the *sul2* gene in a head-to-head organization with a truncated *glmM* gene in between, a structure found at the 3′ end of GI*sul2*, and hereafter referred to as the CR2-*sul2* unit (Figure 1). More commonly, CR2-*sul2* units carry various other ARGs in between and locate on other MGEs. Recently, CR2 was also reported to likely contribute to the mobilization of the high-level tigecycline resistance gene *tet*(X) in *Escherichia coli* (Fang et al., 2019; He et al., 2019; Sun et al., 2019). CR elements are proposed to move by a process called rolling-circle replication because of the distant similarity of their encoded gene to the transposases of the IS*91* family insertion sequences, known to promote their own spread through this mechanism (Toleman et al., 2006b). Accordingly, the term IS*CR* was proposed for these elements (Toleman et al., 2006a). CR element boundaries, called *ter*IS and *ori*IS for 5′ and 3′ boundaries, respectively, were inferred from their genetic sequence for most elements, but not all (Toleman et al., 2006a; Lallement, 2018). The lack of experimental demonstration for a *rcr* (coding region of CR)-mediated rolling circle mechanism and the yet unclear boundaries of some CR elements make the hypothesis of CRs being IS elements still debatable. We therefore conservatively keep the CR denomination in this study to define these genetic elements.

Despite the numerous occurrences of GI*sul2* and CR2-*sul2* units in various bacteria, suggesting horizontal gene transfer, their mobility has not yet been demonstrated. GI*sul2* mobilization was tested in an *E. coli* genetic context, but no excised circular intermediate could be detected (Harmer et al., 2017). In the present study, we demonstrate that GI*sul2*-encoded integrase mediates (i) the excision of GI*sul2* and CR2-*sul2* from their original chromosomal location, (ii) the integration of GI*sul2* and CR2-*sul2* in two-plasmid mobilization assay system in *E. coli recA*-deficient mutant. All these reactions are site-specific and rely on the presence of GI*sul2* attachment (*att*) sites.

Results

GI*sul2* and CR2-*sul2* unit can excise from the chromosome of *S. flexneri*

By analyzing in detail the structure of GI*sul2* reported in the reference sequence of *S. flexneri* 2a 2457T (GenBank accession AE014073), we found that three putative *att* sites were present in this island. In addition, to the already described *attL* and *attR* located at the left and right end of the GI (Harmer et al., 2017), a third *att* site, termed *attLR*, lies 112–130 bp upstream of the *rcr2* gene (Figure 1A). The three sites are 19 bp-long and they all share the common central nucleotide motif 5′-GAGTGGGA-3′ (Figure 1B), previously proposed to be their core recombination site (Harmer et al., 2017). Interestingly, the putative *ter*IS proposed for CR2 (5′-GGGAGTGACGGGCACTGGC-3′), which is the putative 5′ boundary of the element (Toleman et al., 2006a), starts in the middle of the core recombination region of *attLR* (Figure 1B). According to the possible recombination events between the putative *att* sites, Figure 2A shows the three predicted circular intermediates that could be produced, namely, excised GI*sul2* (site-specific recombination between *attL* and *attR*), excised CR2-*sul2* (site-specific recombination between *attLR* and *attR*), and an excised 12-kb segment named GI12K (site-specific recombination between *attL* and *attLR*). We first tested whether any of these circular intermediates could be naturally excised from the chromosome of *S. flexneri* 51,575. This strain carries a single copy of GI*sul2* almost identical to that of *S. flexneri* 2a 2457T (GenBank accession number AZPD01000036, position 2,108–17,567), except for a 140-bp region in the *trbL* gene with several differences. GI*sul2* in *S. flexneri* 51,575 is also inserted in the 3′ end of *guaA* gene, resulting in the same three *att* sites as in Figure 1.

The presence of the junction region of each predicted circular intermediate was tested through PCR amplification on crude DNA extracts from overnight culture in standard conditions using a nested procedure because of the very low amplification yield after the first round of PCR. Two pairs of nested primers F1/R1 and Sul2-F/Int-R were used for the detection of the GI*sul2* circular form (805 bp), two pairs

of nested primers F1/R2 and Sul2-F/CR2-R were used for the detection of the CR2-*sul2* unit circular form (574 bp), and two pairs of nested primers tru-F1/R1 and tru-F2/Int-R were used for the detection of the GI12K circular form (767 bp; Figure 2A, Supplementary Table 1). These various PCR reactions resulted in only two target-size products (Figure 2B). The first corresponded to the junction in the circular form of GI*sul2*, resulting from the recombination between *attL* and *attR* sites. The second corresponded to the junction in the circular form of CR2-*sul2* unit, resulting from the recombination between *attLR* and *attR* sites. Sequencing of the amplified junctions confirmed that they consisted of *attL/attR* and *attLR/attR* hybrids, hereafter named $attP_{GIsul2}$ and $attP_{CR2-sul2}$, respectively (Figure 2C, Supplementary Figure 1), indicating that GI*sul2* and CR2-*sul2* units are naturally excised from the chromosome of *S. flexneri* 51575.

A donor plasmid bearing GI*sul2* can integrate into the chromosomal *attB* site downstream of *guaA* gene in *recA*-deficient *E. coli*

To avoid excision mediated by RecA-dependent homologous recombination and the difficulty of genetic operation in *Shigella*, pKDGItetWsul2 (24,157 bp) carrying a modified version of GI*sul2*, as a donor plasmid, was established and introduced into the *recA*-deficient strain, *E. coli* DH5α. pKDGItetWsul2 was constructed from pKD46, a temperature-sensitive plasmid that can be eliminated at 37 or 42°C (Datsenko and Wanner, 2000). pKDGItetWsul2 carries an ampicillin resistance marker and GI*sul2* in which Δ*glmM* between *rcr2* and *sul2* genes was replaced by a constitutively expressed *tetW* gene (tetracycline resistance; Figure 3A, Supplementary Table 2). PCR assays targeting $attP_{GIsul2}$ and $attP_{CR2-sul2}$ were then performed on *E. coli* DH5α (pKDGItetWsul2) as in Section Introduction, and the amplified products (validated by sequencing) confirmed that the excision of GI*tetWsul2* and CR2-*sul2* from donor plasmid can still occur in a $recA^-$ genetic context (Figure 3B).

Since *E. coli* DH5α carries a GI*sul2*-empty *attB* site at the 3′ end of its *guaA* gene, we tested the integration potential of the excised elements into this chromosomal position. *E. coli* DH5α (pKDGItetWsul2) culture was grown overnight at 42°C to discard pKDGItetWsul2 and then transferred at 42°C on fresh LB plates containing tetracycline to select for colonies bearing chromosomally integrated circular intermediates. Twelve randomly selected resistant colonies were tested using the same six pairs of primers as in Figure 3D, except that the primer GMP-R replaced the vector-specific primer

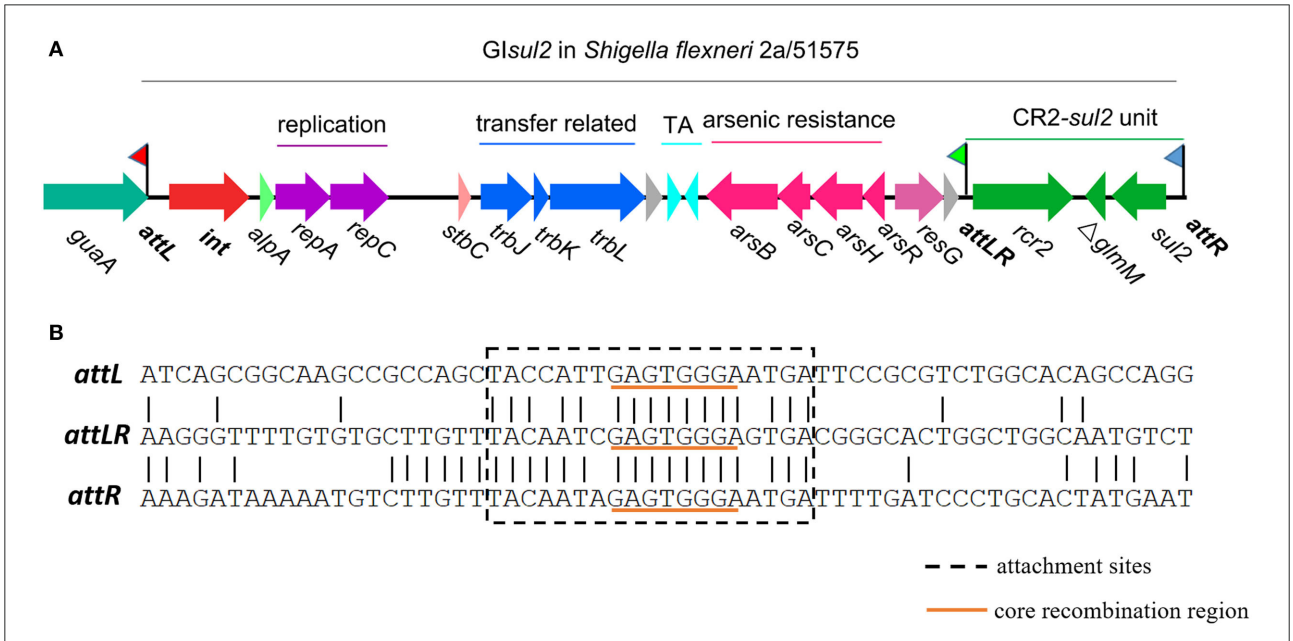

FIGURE 1
Genetic organization of genomic island GI*sul2* in *S. flexneri* 2a str. 2457T (accession AE014073) or *S. flexneri* 51575 (accession AZPD01000036, position 2108-17567). **(A)** Organization of the GI*sul2* element. The thick central line represents the backbone of the GI*sul2* with flags representing the three attachment sites (*attL/attLR/attR*). Horizontal arrows indicate the position, size, and orientation of ORFs with the names below. The *guaA* gene encoding a guanosine monophosphate synthetase (GMP) is shown in teal. The *int* gene encoding the integrase is represented in red. Bright green, light red, and pink ORFs denote *alpA*, *stbC*, and *resG* genes, respectively. Genes putatively involved in replication, transfer-related, toxin-antitoxin system, arsenic resistance, and the CR2-*sul2* unit are shown in purple, blue, cyan, pink and green, respectively. Gray ORFs encode hypothetical proteins. **(B)** Nucleotide alignment of *att* sites of GI*sul2*. The dotted box represents the expected *att* sites recognized by the integrase. The orange underlined motif indicates the putative core recombination region.

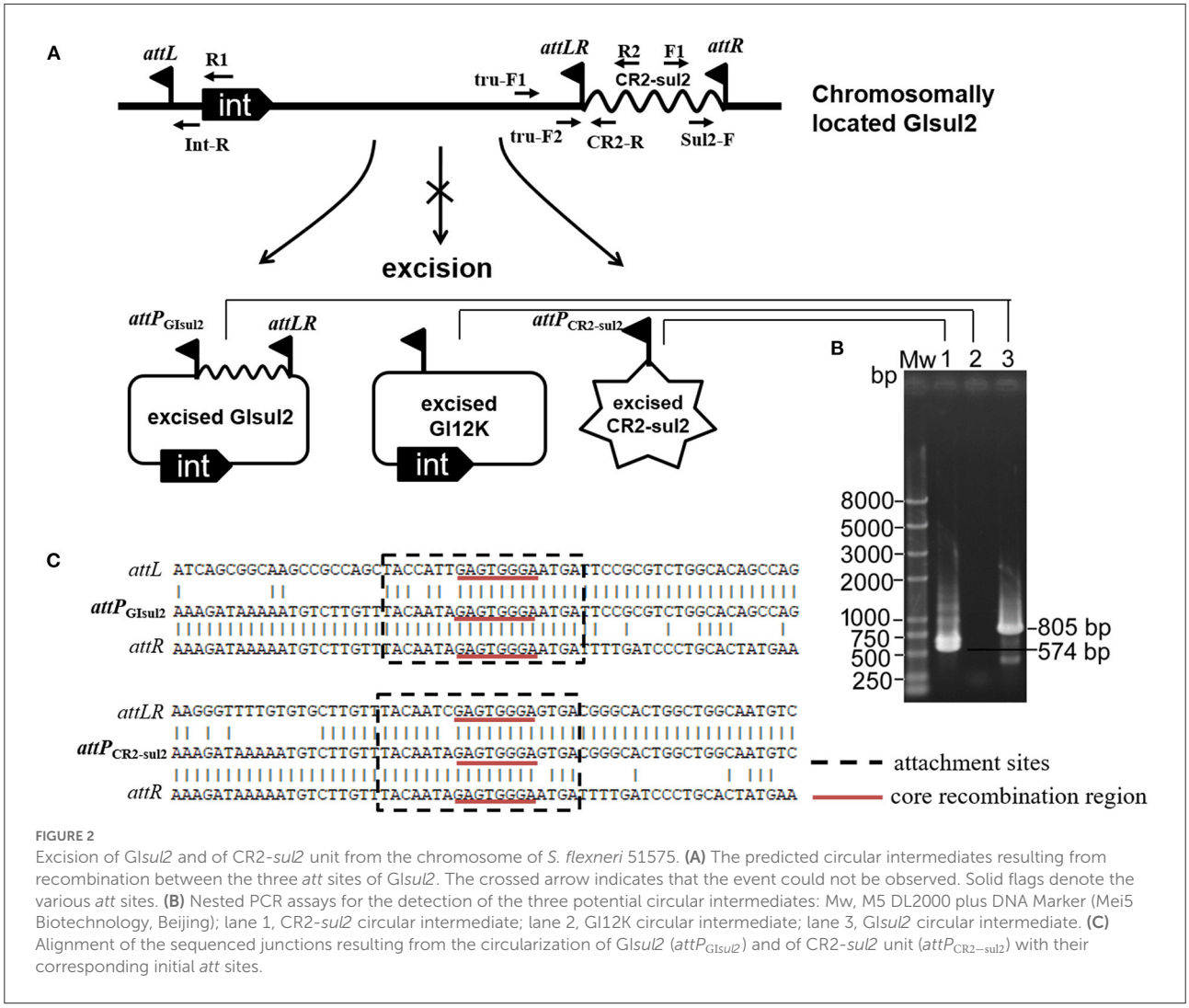

FIGURE 2
Excision of GI*sul2* and of CR2-*sul2* unit from the chromosome of *S. flexneri* 51575. **(A)** The predicted circular intermediates resulting from recombination between the three *att* sites of GI*sul2*. The crossed arrow indicates that the event could not be observed. Solid flags denote the various *att* sites. **(B)** Nested PCR assays for the detection of the three potential circular intermediates: Mw, M5 DL2000 plus DNA Marker (Mei5 Biotechnology, Beijing); lane 1, CR2-*sul2* circular intermediate; lane 2, GI12K circular intermediate; lane 3, GI*sul2* circular intermediate. **(C)** Alignment of the sequenced junctions resulting from the circularization of GI*sul2* ($attP_{GIsul2}$) and of CR2-*sul2* unit ($attP_{CR2-sul2}$) with their corresponding initial *att* sites.

M13-47 (Supplementary Figure 2). Only Sul2-F/GMP-R and GMP-F/pKD-R PCR reaction provided an amplification (Supplementary Figure 2). Successful amplification was obtained in all colonies for the primer pairs, corresponding to the recombination between *attR* of pKDGItetWsul2 and *attB*. Sequencing of the PCR products confirmed the expected junction. The observations indicate that the chromosomal *attB* site can recombine with a plasmidic *attR* site in a *recA*$^-$ genetic context, leading to donor plasmid carrying GI*sul2* integration into the chromosome.

The donor plasmid, GI*sul2*, and CR2-*sul2* unit can integrate into the *attB* site of a trap plasmid in *recA*-deficient *E. coli*

To clearly demonstrate the mobilization mechanism for GI*sul2* and CR2-*sul2* units, we applied a two-plasmid assay system consisting of the donor plasmid and trap plasmid. A similar strategy was also used for studying integration mechanisms of pathogenicity islands in *E. coli* 536 (Wilde et al., 2008). The trap plasmid, pKFattB (2843 bp), was constructed by cloning an uninterrupted *attB* region (811 bp) into the high copy vector pKF18k-2 (Supplementary Table 2). This plasmid bears a kanamycin resistance gene (kanR) as the selective marker. The two plasmids pKDGItetWsul2 and pKFattB were co-transformed into *E. coli* DH5α. The correct clones were performed using the two-plasmid mobilization assay. Based on the GI*sul2* and CR2-*sul2* excisions observed above, we speculated that there could be five types of integrations: integration of the GI*tetWsul2* circular intermediate into the trap plasmid (pKFattB-GItetWsul2 in Figure 3C), integration of the CR2-*sul2* intermediate (pKFattB-CR2sul2 in Figure 3C), and three possible integrations of the whole donor plasmid, one for each *att* site (cointegrate-attL/-attLR/-attR, Figure 3C).

First, we tested for the integration of the whole donor plasmid. There are three *att* sites in the donor plasmid, and we, therefore, designed six specific primer pairs (A to F) targeting

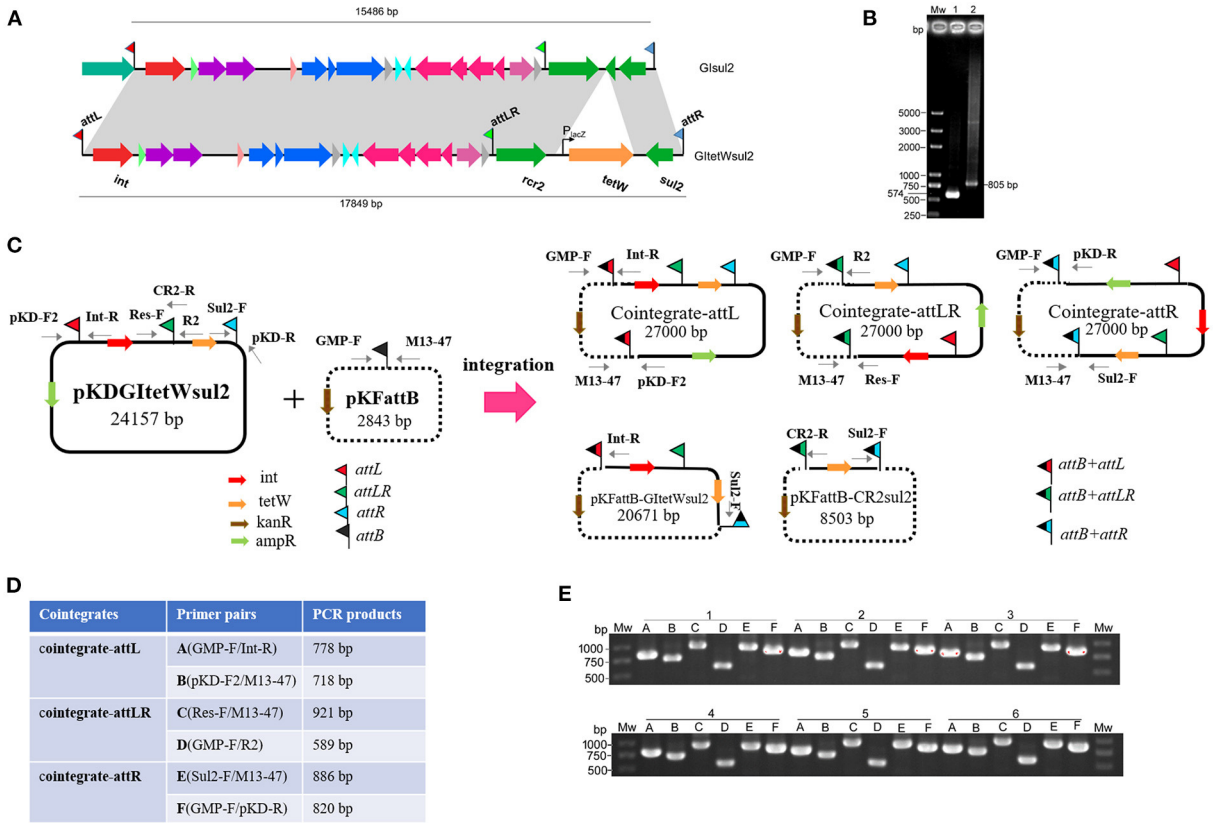

Cointegrates	Primer pairs	PCR products
cointegrate-attL	A(GMP-F/Int-R)	778 bp
	B(pKD-F2/M13-47)	718 bp
cointegrate-attLR	C(Res-F/M13-47)	921 bp
	D(GMP-F/R2)	589 bp
cointegrate-attR	E(Sul2-F/M13-47)	886 bp
	F(GMP-F/pKD-R)	820 bp

FIGURE 3
Co-integrate formation in *E. coli* DH5α through site-specific recombination at the *att* sites. **(A)** Construction of GI*tetWsul2*. The gray shadings denote 100% identity between GI*tetWsul2* and the original GI*sul2*. ORFs (horizontal arrows) are colored as in Figure 1. **(B)** Detection of circular intermediates excised from the donor plasmid pKDGItetWsul2 in *E. coli* DH5α. Mw, DNA size marker; lane 1, CR2-*sul2* unit circular intermediate; lane 2, GI*tetWsul2* circular intermediate. **(C)** Organization of the donor (pKDGItetWsul2) and trap (pFKattB) plasmids used in the two-plasmid integration experiment, and expected recombinant structures. Intervening ORFs are depicted with filled arrows while red, green, blue, and black flags denote *attL*, *attLR*, *attR*, and *attB*, respectively. The putative hybrid attachment sites resulting from site-specific recombination are represented by two-color flags. Primers used for the detection of the various structures are indicated. **(D)** Couples of primer pairs used to detect co-integrate structures in recombinant bacteria, and their expected amplification size. **(E)** PCR amplification using the six primer pairs from **(D)** on the plasmid extracts of six independent recombinant colonies. Colonies are labeled 1–6, with the six primer pairs amplification **(A–E)** displayed below each of them.

each of the possible recombined sites (junctions; Figure 3D). Gel bands corresponding to the PCR product of every junction were detected in all 12 randomly selected recombinant plasmid extracts used as templates (six shown, Figure 3E). Sequencing of the PCR products confirmed that the amplification indeed corresponded to the recombination between *attB* and each of the three *att* sites (*attL*, *attLR*, and *attR*). To understand which type of integration dominated in each colony, we used *Bam*HI to digest the recombinant plasmids. Two bands of 15.7 and 11.2 kb, respectively, corresponding to the digestion of the donor plasmid integration through *attR-attB* recombination, were observed for all colonies (Supplementary Figure 3). These results indicate that the integration of the donor plasmid into pKFattB mainly occurred in the *attR* site.

Second, we tested for the presence of structures matching the integration of the circular intermediates in the same 12 selected plasmid extracts. Primer pair Sul2-F/Int-R was used to detect pKFattB-GItetWsul2 structure, expected to produce an amplification size of 3,646 bp (Figure 3C). However, we only obtained bands around 10 kb which represented amplification of the donor plasmid from the cointegrates. We therefore digested the recombinant plasmids with *Nco*I restriction enzyme, which cuts only the backbone of the donor plasmid, resulting in digestion of the cointegrates. Using the *Nco*I digested products as a template, we obtain the expected 3,646 bp band for all six tested colonies (Figure 4A). Similarly, the primer pair Sul2-F/CR2-R was used for the detection of pKFattB–CR2sul2 structure after digestion of the cointegrates using *Nco*I. This PCR generated a product of the expected size (3,415 bp; Figure 4B), indicating that pKFattB-GItetWsul2 and pKFattB-CR2sul2 structures concurrently exist with cointegrate structures in the recombinant colonies.

We finally applied nanopore sequencing on the recombinant plasmids extracted from five colonies and digested them with

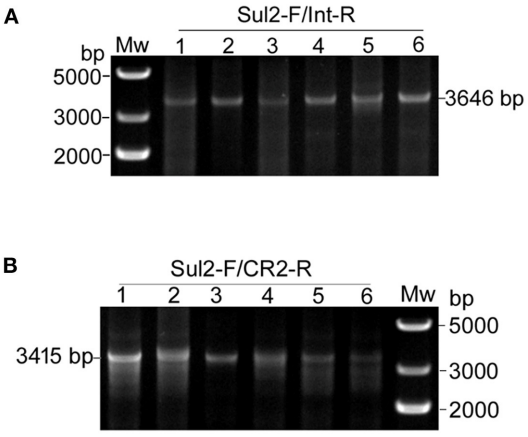

FIGURE 4
Detection of pKFattB-GItetWsul2 and pKFattB-CR2sul2 structures in recombinant colonies. PCR amplification using the primer pairs Sul2-F/Int-R and Sul2-F/CR2-R for the detection of GItetWsu2-pKFattB **(A)** and pKFattB-CR2sul2 **(B)** structures, respectively. PCR reactions were conducted on the same six recombinant colonies as in Figure 3E.

*Xba*I, which cuts only the trap plasmid pKF*attB*, and exactly once. The total number of reads ranged from 1,382,608 to 5,033,742 (Table 1, Supplementary Table 3) for all five samples, with most of them corresponding to the original trap plasmid pKFattB (80–88%), or to regions shared by two or more recombinant structures (ambiguous regions, 4–8% of the reads), or they did not properly map on any of the structures (∼10%). Nonetheless, 1,741–34,155 of the reads mapped unambiguously to the cointegrate-attR structure while only 1–225 and 5–471 reads mapped unambiguously to the cointegrate-attL and cointegrate-attLR structures, respectively. An additional 3–147 and 386–776 reads mapped unambiguously on the pKFattB-GItetWsul2 and pKFattB-CR2sul2 structures, respectively. The higher number of reads mapping to the pKFattB-CR2sul2 structure compared to other structures (except cointegrate-attR) should be treated with caution since unambiguous matches require reads long enough to map both junctions with pKFattB, which is easier to achieve for pKFattB-CR2sul2 (reads of at least 5.7-kb) than for pKFattB-GItetWsul2 (reads of at least 18-kb) or other cointegrates (reads of at least 24.2-kb). Despite this limitation, these results provided further evidence that all the five predicted structures are present, with high dominance of the cointegrate-attR structure.

The integrase and *att* sites of GI*sul2* are required for mobilization

To find out which genes or regions located in GI*sul2* are required for integration, several knockout plasmids were constructed from the donor plasmid pKDGItetWsul2. The deleted regions are *int*, *alpA/repA/C*, *resG*, *rcr2,* or the *att* sites (Supplementary Table 2). Integration of these constructs into pKFattB was tested using the same PCR detection strategy as for pKDGItetWsul2, except that the primers CRUp-R and IntUp-R replaced the primers CR2-R and Int-R, respectively, when testing for the pKFattB-CR2sul2 and pKFattB-GItetWsul2 structures because of the deletion of *rcr2 or int* in one of the constructs. The deletion of the *int* gene resulted in the complete loss of integration ability including cointegrations, GI*sul2*, and CR2-*sul2* integrations (Table 2). When the three *att* sites (*attL, attLR,* and *attR*) of pKDGItetWsul2 were deleted, only four colonies displayed the integration, but none of them carried any of the five expected recombinant structures (Table 2). A single type of integration was observed in all four clones involving the *attB* of pKFattB and a region 166 bp downstream of the deleted *attR* of pKDGItetWsul2, with the insertion site reduced to "TGGG" instead of "GAGTGGGA." Deletion of *rep, resG*, and *rcr2* regions had no effect on the recombination efficiency and the detection of the various structures. These results indicate that the integrase of GI*sul2* and its *att* sites are required for the integration of donor plasmid, GI*sul2*, and CR2-*sul2* unit into the trap plasmid, while *rcr2*-encoded putative transposase seemingly does not have any impact on the formation of recombination structures.

To confirm that no other factors encoded by GI*sul2* are required for integration, we constructed a minimal donor plasmid containing only the *int* gene, *attL*, and a chloramphenicol resistance determinant (*catR*) on the pKD46 backbone, designated pKDmini (6,498 bp; Supplementary Figure 4A) and tested its integration into pKFattB. After co-transformation of pKDmini and pKFattB into *E. coli* DH5α and temperature shift, transformants were plated on a medium supplemented with chloramphenicol and kanamycin, and six colonies were randomly selected. The *Xba*I restriction enzyme analysis revealed that all colonies harbored the expected 9.3-kb band corresponding to the cointegrate of pKDmini with pKFattB, and 2.8-kb band corresponding to residual pKFattB (Supplementary Figure 4B). PCR and sequencing also confirmed the result, which demonstrated that Int is sufficient for the integration through the site-specific recombination when relevant *att* sites are present.

Unambiguous observation of GI*sul2* and CR2-*sul2* mobilization through restriction analysis by the introduction of *sacB* into the donor plasmid and overexpression of *alpA*

Due to the dominance of *attR*-based cointegrate during two-plasmid mobilization experiments, the potential integration of circularized CR2-*sul2* or GI*tetWsul2* into the trap plasmid

TABLE 1 Number of nanopore reads unambiguously mapping on each possible recombinant structure described in Figure 3C, in five of the 12 randomly selected recombinant colonies.

Mapped structure	Colony ID				
	I	II	III	IV	V
Cointegrate-attL	225	1	3	5	23
Cointegrate-attLR	471	14	6	5	41
Cointegrate-attR	34,155	2,184	1,741	4,998	30,445
pKFattB-GItetWsul2	147	3	5	6	41
pKFattB-CR2sul2	460	389	776	386	686
pKFattB	1,114,689	2,528,150	1,800,859	2,147,060	4,398,420
Other reads	232,461	330,864	309,494	457,421	604,087
TOTAL	1,382,608	2,861,605	2,112,884	2,609,881	5,033,742

I–V represent the five first colonies of Figure 3E. "Other reads" include reads which mapped on regions shared by two or more structures (ambiguous reads, ~4–8% of the reads) and reads which could not map on any of the structures.

TABLE 2 Effect of deleting GI*sul2*-associated regions on integrations.

Recombinant structure	WT	Δ*int*	ΔDRs	Δ*rep*	Δ*resG*	Δ*rcr2*
Cointegrates	+	–	*–	+	+	+
pKFattB-GItetWsul2	+	–	–	+	+	+
pKFattB-CR2sul2	+	–	–	+	+	+

WT, wild-type (intact GItetWsul2). Δint, ΔDRs, Δrep, ΔresG, and Δrcr2 denote deleting int, attL/LR/R sites, alpA/repA/C, resG, and rcr2 in donor plasmid pKDGItetWsul2, respectively. + indicates the presence of the structure using PCR assays. *– Represents rare non-specific integration events. – Denotes no occurrence of integration events.

could not be observed distinctly through restriction enzyme digestions. The *sacB* gene, lethal for *E. coli* when expressed in the presence of sucrose, was therefore introduced into the backbone of pKDGItetWsul2, resulting in a new donor plasmid pKDGItetWsul2sacB (Supplementary Table 2). Cointegrates containing *sacB* are inhibited in the presence of sucrose, while colonies carrying only GI*tetWsul2* or CR2-*sul2* unit will be able to grow normally. The two-plasmid mobilization experiment was repeated using pKDGItetWsul2sacB as the donor plasmid and with the addition of 20% sucrose during the integration step, resulting in the successful growth of recombinant colonies from which 36 were randomly selected for plasmid extraction. *Xba*I digestion (cutting only pKFattB) resulted in an 8.5-kb band for all the tested colonies (6 are represented in Figure 5A), suggesting that all recombinant colonies carried the pKFattB-CR2sul2 structure. Additional digestion using the *Bam*HI enzyme (cutting CR2-*sul2* unit once) plus *Xba*I produced two bands of 6.5-kb and 2-kb, consistent with the presence of pKFattB-CR2sul2 structure (Figure 5B). These results indicate that integration of the circularized CR2-*sul2* unit into the trap plasmid can happen through site-specific recombination between the $attP_{CR2-sul2}$ site and the *attB* site. No colony carrying the pKFattB-GItetWsul2 structure could have been detected using the sucrose negative selection.

AlpA is deemed to improve the excision of circular intermediates during site-specific recombination (Kirby et al., 1994; Lesic et al., 2004), and thus can increase the integration frequency of genomic islands. However, *alpA* gene deletion in our experiment did not result in significant changes for integration (Table 2). We speculated that *alpA* gene may not be expressed or maybe expressed moderately due to the lack of an efficient promoter in GI*sul2*. In view of this point, we used the expression vector pCOLADGm and constructed the resultant plasmid pCOLADalpAGm (see Section Materials and methods), under the control of a strong T7 promoter induced by IPTG. pCOLADalpAGm, pKDGItetWsul2, and pKFattB were simultaneously transformed into the *recA*-deficient strain. The integration experiment was performed on the correct strain carrying the three plasmids. Then 20 randomly selected colonies were analyzed and six samples were exhibited in agarose gel. Their extracted plasmid DNA was cut using *Xba*I and the two recombinant plasmids displayed the significant 20.7-kb band (lanes 5, 6 of left panel in Figure 5C), corresponding to the size of pKFattB-GItetWsul2. We further cut the two recombinant plasmids using double restriction enzymes *Xba*I and *Sac*I and showed the correct expected bands, 13.3 and 7.4-kb (lanes 5 and 6 of right panel in Figure 5C). *Sac*I only exists in pKFattB-GItetWsul2 structure and can cut to different sizes of fragments with *Xba*I (the bottom in Figure 5C). The weak 4,023 bp band was residual pCOLADalpAGm that was only cut by *Xba*I, and the 2,843-bp band still existed, which was the remnant pKFattB. The restriction enzyme analysis strongly indicates that

10.3389/fmicb.2022.905865

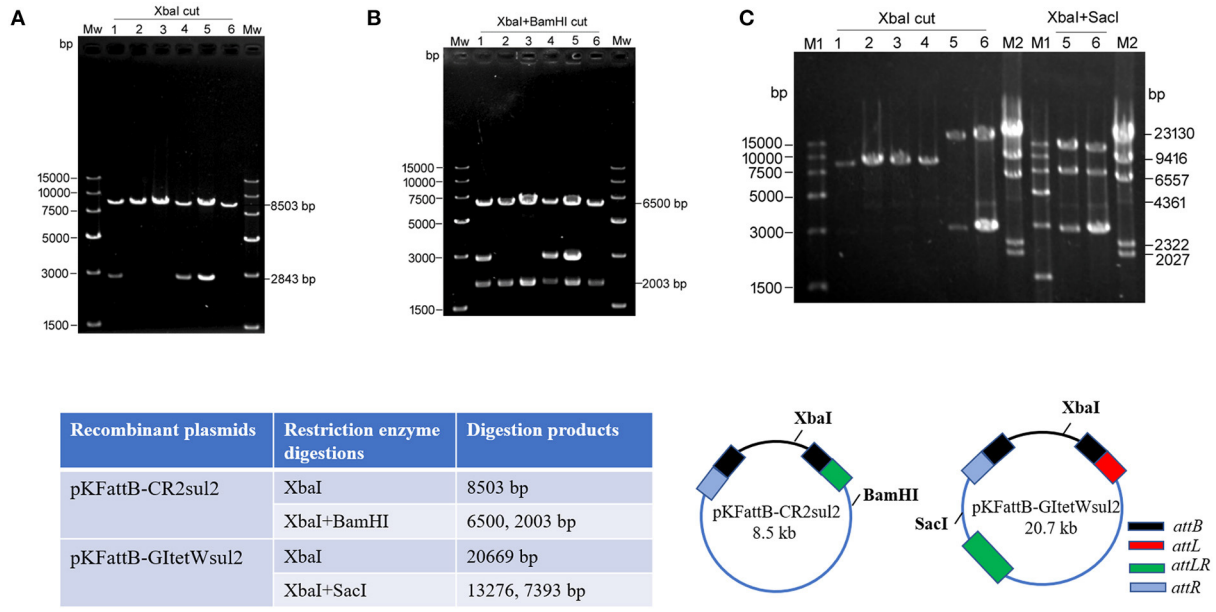

Recombinant plasmids	Restriction enzyme digestions	Digestion products
pKFattB-CR2sul2	XbaI	8503 bp
	XbaI+BamHI	6500, 2003 bp
pKFattB-GItetWsul2	XbaI	20669 bp
	XbaI+SacI	13276, 7393 bp

FIGURE 5
Integration of circular intermediates into the trap plasmid pKFattB under sucrose negative selection. **(A)** *Xba*I digestion of the plasmid extract from six independent recombinant colonies. Bands at 8,503 bp correspond to the recombinant plasmid pKFattB-CR2sul2 (CR2-*sul2* inserted into pKFattB) and bands at 2,843 bp correspond to original pKFattB copies. **(B)** *Xba*I and *Bam*HI double restriction of the same plasmid extracts. *Bam*HI cuts CR2-*sul2* unit once and not pKFattB, leading to the digestion of pKFattB-CR2sul2 into 6,500 and 2,003 bp bands. **(C)** Detection of GItetWsu2-pKFattB structure. Left panel, *Xba*I digestion of the plasmid extract from six independent recombinant colonies. M1, M2, different DNA markers. Right panel, *Xba*I and *Sac*I double restriction of plasmid extracts (number 5 and 6). *Sac*I cuts GI*tetWsu2* once and not pKFattB, leading to the digestion of GItetWsu2-pKFattB into 13,276 and 739 bp bands. The band at 2.8 kb is the residual pKFattB plasmid. The bottom schematics exhibit the locus of restriction enzymes and expected digestion sizes for restriction analysis.

GI*tetWsul2* movement occurred. Enzyme digestions of other recombinant plasmids also displayed the 8.5-kb band, indicative of CR2-*sul2* movement. These integration experiments clearly validated that GI*sul2* and CR2-*sul2* units can move into the trap plasmid.

GI*sul2* and CR2-*sul2* units are widely distributed in proteobacteria

To get a better insight into the distribution of GI*sul2*, CR2-*sul2* unit, and GI12K in bacterial species, we screened for their presence in the 169,991 complete bacterial genomes available in the NCBI GenBank database at the time of the study (see methods). The distribution of GI*sul2* shows that this element has disseminated in proteobacteria, essentially β- and γ-proteobacteria, although one instance has been detected in the α-proteobacteria *Sphingopyxis granuli* (Figure 6, Supplementary Table 4). Within γ-proteobacteria, it is restricted to two species of *Acinetobacter* (*A. baumannii* and *A. calcoaceticus*), in which eight instances were detected (6.6% of the total number of genomes for these two species), and to the *Enterobacterales* clade, in which it was sporadically found in six common pathogens (one to four instances per species, representing 0.3–33% of the species screened genomes). Within β-proteobacteria, GI*sul2* is mostly detected in species of the *Alcaligenecae* family, with eight instances distributed among five species. However, the total number of available β-proteobacterial genomes was much lower than those of γ-proteobacteria, leading to a comparatively higher prevalence of GI*sul2* in this cluster (15–100% of the species screened genomes, Supplementary Table 4). Only three of the 31 instances of GI*sul2* were detected on plasmid replicons of the complete genomes (Figure 6), consistent with its primary integration site at the 3′ end of the *guaA* gene.

CR2-*sul2* unit was detected in one Actinobacteria, one α-proteobacteria, and two β-proteobacteria, but it is widespread in γ-proteobacteria with 180 instances detected in 30 species (Figure 6). These species belong to 6 different taxonomic orders (Supplementary Table 4), including the *Aeromonadales*, *Oceanospirillales*, *Pasteurellales,* and *Vibrionales* in which no GI*sul2* was detected. The prevalence of CR2-*sul2* unit within species is also substantially higher than the prevalence of GI*sul2*; for instance, CR2-*sul2* unit was detected in 30.8, 17.8, 7.7, 6.6, and 5.4% of the *A. baumannii*, *Vibrio cholerae, K. pneumoniae*, *S. enterica,* and *E. coli* complete genomes, respectively, while GI*sul2* was detected in only 5.8, 0, 0, 0, and 0.3% of the same genomes. Contrary to GI*sul2*, CR2-*sul2*

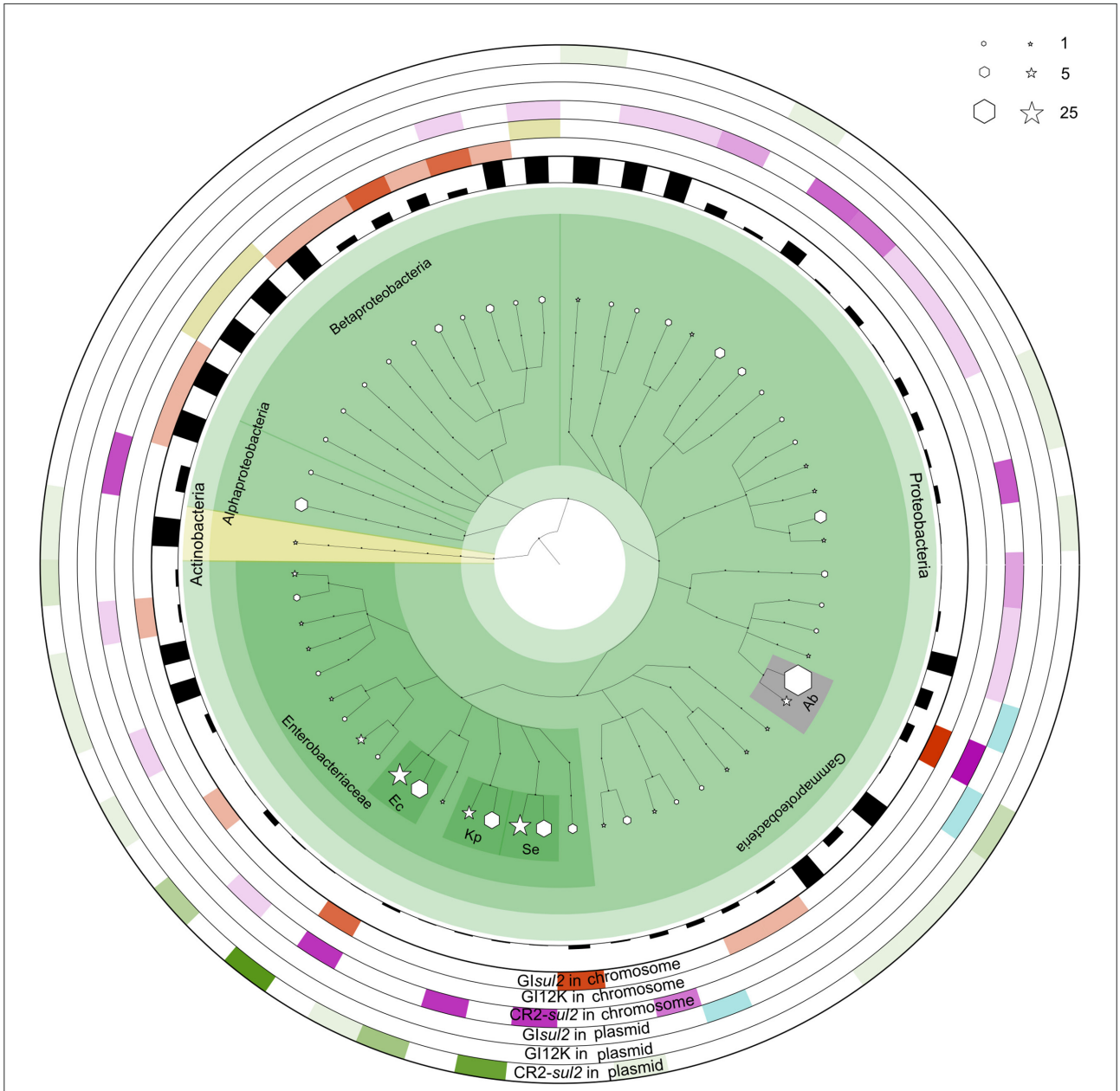

FIGURE 6
The distribution of GI*sul2*, CR2-*sul2* unit, and GI12K in chromosomes and plasmids of NCBI complete genome database. The internal species tree represent the host distribution of the three elements. The size of the hexagon and star markers denotes the number of genomes of each host carrying the corresponding elements in chromosomes or plasmids, respectively. The bar height in the inner circle represents the proportion of genomes carrying the elements among the total genome of the species in the database. The six outermost heatmaps represent each element's abundance, separated by chromosomal or plasmid localization. The color intensity corresponds to the proportion of the host in the total number of genomes carrying the given element. Orange, olive green, and purple heatmaps represent the distribution of GI*sul2*, GI12K, and the CR2-*sul2* unit in chromosomes, respectively. Blue and green heatmaps represent the dissemination of GI*sul2* and CR2-*sul2* units in the plasmids, respectively. Hosts with a total number of genomes >10 are highlighted and abbreviated as follows: Kp, *Klebsiella pneumoniae*; Ec, *Escherichia coli*; Se, *Salmonella enterica*; Ab, *Acinetobacter baumannii*.

unit is also widely present on plasmids with 42% of the detections, although these plasmid-borne instances are mostly found in *Enterobacteriaceae* and *A. baumannii* (Figure 6). The last investigated element, GI12K, was found only in three complete genomes, belonging to three different species from three different orders of β-proteobacteria, and always in a chromosomal location (Figure 6).

When the NCBI draft genomes database was investigated, similar results were obtained (Supplementary Table 4). GI*sul2* was found mostly in β-proteobacteria and γ-proteobacteria

with more than 10 instances detected, respectively, in *Bordetella bronchiseptica* (24% of the total genomes of the species), and *E. coli* and *A. baumannii* (0.41 and 0.97% of the total genomes). The CR2-*sul2* unit showed a wider distribution in γ-proteobacteria than GI*sul2*, but very few instances in β-proteobacteria. Its prevalence in draft genomes was similar to those in complete genomes with, e.g., 31 and 21% of the *A. baumannii* and *V. cholerae* genomes carrying it, respectively. The draft genome analysis revealed that GI12K was not restricted to β-proteobacteria since it was also detected in 19 γ-proteobacteria and one α-proteobacteria. However, its prevalence is usually extremely low in species with a sufficient number of available genomes (Supplementary Table 4). suggesting that these instances may be in fact GI*sul2* structures for which the CR2-*sul2* unit was incompletely sequenced or assembled.

Discussion

Although several studies showed that GI*sul2* is distributed in various γ- and β-proteobacterial species (Nigro and Hall, 2011; Hamidian and Hall, 2016; Harmer et al., 2017), its mobility has never been demonstrated. In this report, we investigated the mobilization capacity of GI*sul2* integrase to perform site-specific recombination at its cognate *att* sites. Contrary to most GIs studied to date, three related *att* sites were identified in GI*sul2*: the two expected *attL* and *attR* sites at the boundaries of the element and a third, termed *attLR*, lying upstream of the *rcr2* putative transposase. This atypical GI structure carries an important mobile element, the CR2-*sul2* unit, which can also be considered as an IS*CR2*-related element that plays an important role in transferring resistance determinants (Toleman et al., 2006a). But, the mobilization mechanism of IS*CR2* is still not revealed through biological experiments. In the present study, excisions involving either *attL-attR* or *attLR-attR* complexes were both detected in RecA$^+$ as well as in RecA$^-$ genetic backgrounds, indicating that the integrase can excise independently the GI*sul2* and CR2-*sul2* units (bounded by *attLR* and *attR*) from their respective insertion sites. However, detection of the circular intermediates required the use of nested PCR assays, suggesting that the excision process may be rare in standard culture conditions. This phenomenon was consistent with a previous report on the excision of high-pathogenicity island in *Yersinia pseudotuberculosis* (Lesic et al., 2004).

For most GI tyrosine integrases, the recombination process requires recombination directionality factors (RDFs). Notably, excision is usually controlled by excisionase proteins such as Xis in the phage λ model (Landy, 2014). The integrase gene of GI*sul2* is followed by a gene annotated as *alpA*, which was initially proposed to act as a transcriptional regulator of CP4-57 prophage integrase, leading to the efficient excision of the prophage (Kirby et al., 1994). Later studies demonstrated that Hef, a protein homologous to AlpA, induces the excision of the high-pathogenicity island (HPI) of *Y. pseudotuberculosis* through excisionase activity (Lesic et al., 2004). Therefore, AlpA of GI*sul2* likely also acts as an excisionase as previously suggested (Harmer et al., 2017), which may not be expressed or may be expressed slightly under standard culture conditions as is the case for excisionases of other integrative elements (Guédon et al., 2017). This speculation was verified by the introduction of *alpA* gene into expression vector pCOLADGm harboring T7 promoter during IPTG induction (Figure 6). Hence, we considered that the few observed circular intermediates could have arisen from expression leakage of the *alpA* gene or occasional AlpA-empty recombinations since excisionases are mostly helper proteins (Landy, 2014; Guédon et al., 2017). While the expression of Alp increased significantly, sufficient circular intermediates were supplied, and then GI*sul2* and CR2-*sul2* mobilization can be observed easily through restriction enzyme digestions.

Our findings are not consistent with the results of Harmer et al. (2017), who did not detect GI*sul2* circular intermediates in their *E. coli* experimental strain despite a nested PCR procedure similar to ours. In their experiment, GI*sul2* was not located in its typical integration site downstream of the *guaA* gene, but in an IncC-type plasmid in which the *attL* and *attR* sites were not conserved. We suspect that this unusual insertion site hampers the integrase-mediated excision because we showed that *att* sites are essential for proper integrase-mediated recombination. Despite its preferential chromosomal integration at the 3′-end of *guaA*, GI*sul2* has been sporadically detected on plasmids at unrelated insertion sites (8, 9, 12, Figure 6). Here, we showed that elements devoid of *att* sites could still integrate into the donor plasmid, but at a very low rate and in a recombination site with reduced specificity ("TGGG" instead of "GAGTGGGA"). This suggests that Int behaves like any other integrase, for which target specificity may be loosened when no proper integration site is present in the cell (Guédon et al., 2017). However, non-specific integrations are likely a dead-end for the dissemination of GI*sul2* because of the lack of proper excision when full-length *attL/R* sites are not present. GI*sul2* is more probably an integrative and mobilizable element (IME), which relies on a helper conjugative element to transfer between bacteria (Guédon et al., 2017). The presence of plasmid-related transfer proteins into the element strongly supports this hypothesis, and the reported amino-acid similarity of these proteins to those found in IncP plasmids suggests that members of this plasmid family would be the helper elements (Harmer et al., 2017).

Finally, we showed that when the dominant cointegrate recombinants are eliminated by sucrose negative selection, integration of circularized intermediates into *attB* can be detected. Notably, integration of GI*sul2* circular intermediate into the *attB* site of trap plasmid was observed through restriction enzyme analysis in *recA*$^-$ genetic context, indicating that the integrase can perform the final step of GI*sul2*

mobilization when molecular substrates are available. Even more interesting is our detection of CR2-*sul2* integration in the *attB* site of the trap plasmid. CR2 transposase is very often located in the vicinity of *sul2* with various ARGs in between, and several genomic evidences suggest that they represent independent mobile or mobilizable units (Leclercq et al., 2016; Xu et al., 2017). These CR2-*sul2* units are therefore recognized as vectors of dissemination of antibiotic resistance in environmental bacteria and important clinical pathogens such as *Vibrio* spp., *Pseudoalteromonas* spp., *Salmonella enterica*, *S. flexneri,* and *A. baumannii* (Beaber et al., 2002; Toleman et al., 2006a; Yau et al., 2010; Leclercq et al., 2016; Harmer et al., 2017; Xu et al., 2017; Shi et al., 2019; Wüthrich et al., 2019). Especially, plasmid-borne IS*CR2* carrying the high-level tigecycline resistance gene *tet(X)* has emerged in *E. coli* (Fang et al., 2019; He et al., 2019; Sun et al., 2019), which hints that we should pay close attention to the rise of this element. Interestingly, the boundaries of these transposons have been predicted to lie 119 bp upstream of the *rcr* gene and 304 bp upstream of *sul2* (Leclercq et al., 2016), which correspond to the middle of the core recombination region of *attLR,* and the 3′-end of *attR*, respectively. In another study conducted on *Aeromonas caviae*, two independent ARG-carrying CR2-*sul2* units are inserted in the *attR* core recombination region of a GI inserted in *guaA*. The GI harbors an integrase related to that of GI*sul2* (Shi et al., 2019). Both integrations recreated perfect *att* core recombination regions (Shi et al., 2019), and very likely functional *att* sites. These observations, together with the results presented here, suggest that the integrase of GI*sul2*, or other integrases of the same family, may be the main drivers of the wide dissemination of CR2-*sul2* units among proteobacteria. Future studies are need further to deeply investigate the influence of AlpA and possible host factors on integration or excision, providing a comprehensive understanding of mobilization.

Materials and methods

Bacterial strains and culture conditions

The genomic DNA of *S. flexneri* 51575 (kindly provided by Prof. Jianguo Xu from Chinese CDC) was extracted with the TIANamp Bacteria DNA Kit (TIANGEN BIOTECH, Beijing) and used to amplify the complete sequence region of GI*sul2*. *E. coli* DH5α deficient in *recA* was used for plasmid cloning and to perform all the integration experiments. IN-5 (KU736870) and IN-11 (KU736876) are, respectively *tetW*-containing and CR2-containing genomic regions cloned from pig manure's uncultured bacteria (Leclercq et al., 2016) and used for plasmid constructions. Unless otherwise stated, all strains were cultured at 37°C in a liquid LB medium. All plasmid constructions mentioned in this study are detailed in Supplementary Table 2.

PCR detection of circular intermediates

Detection of circular intermediates was performed using a nested PCR strategy on crude DNA from boiled overnight cultures (Lesic et al., 2004). To determine GI*sul2* circular intermediates, the primer pair F1/R1 was first used to amplify the junction. Then the Sul2-F/Int-R primer pair was used for the second round of PCR amplification using the first-round PCR product as the template. Similarly, to detect CR2-*sul2* unit and GI12K circular intermediates, a couple of primer pairs F1/R2 then Sul2-F/CR2-R, and tru-F1/R1 then tru-F2/Int-R were used, respectively. PCR conditions were as follows for both rounds: pre-denaturation at 95°C for 5 min; 30 cycles of denaturation at 94°C for 30 s, annealing at 55°C for 30 s, extension at 72°C for 1 min; and then a final extension at 72°C for 5 min. All PCR amplifications were performed using the ploymerase TransStart® FastPfu Fly DNA Polymerase, which is a hot start, ultra-high fidelity, and high-processivity DNA polymerase (TRANS, Beijing, China). These PCR amplicons could also have theoretically arisen from chromosomal tandem duplications of each of the elements, but the fact that a nested PCR procedure was necessary to produce visible bands, together with the absence of such duplication in the genome sequence of the used strain, makes this possibility highly unlikely.

Construction of a two-plasmid assay system

The donor plasmid pKDGItetWsul2 was constructed in a two-step process. The first step consisted of the construction of a CR2′-*tetW*-sul′ fragment containing a constitutively expressed *tetW* gene. The *tetW* gene (2,070 bp) was amplified from the DNA of the IN-05 clone by using tetW-F and tetW-R primers. The PCR product was digested together with plasmid pUC19 by *Pst*I and *Eco*RI enzymes and ligated using a T4 DNA ligase (New England Biolabs, Ipswich, MA, USA). The plasmid was termed pUC-*tetW*. The 3′ end of CR2 (1,156 bp) harboring the putative *ori* end was amplified from the IN-11 clone using G-UNIT-F/Rev-Pstv28cr2 primers. The *tetW* plus the P_{lacZ} promoter sequences (2,403 bp) were amplified from pUC-tetW using G-tetWF/Rev-tetW primers. The partial *sul2* sequence (789 bp) was amplified from IN-11 using Fwd-Pstv28cr2/G-UNIT-R primers. The above three fragments were assembled using the NEBuilder kit to obtain the CR2′-*tetW*-sul′ fragment (4,313 bp). The second step consisted of the aggregation of the CR2′-*tetW*-sul′ fragment with GI*sul2* in a pKD46 backbone, lacking *gam*, *bet,* and *exo* regions, from four genomic fragments. First, the pKD46 backbone segment (4,199 bp) was obtained by PCR amplification using G-PKD-F and G-PKD-R primers from an intact pKD46 template. Second, the G-UP-floRF11 and G-UP-R primers were used to amplify a 2,505 bp fragment

including the florfenicol resistance gene *floR* and the 5′ end of CR2 bearing *attLR* using the genomic DNA of the IN-11 clone as the template. The third fragment was the CR2′-*tetW*-sul′ constructed above. The fourth fragment included the 5′ end of *sul2* and its upstream sequence (1,005 bp), obtained using G-DOWN-F and G-DOWN-R11 primers with DNA of the IN-11 clone as the template. The above four fragments were assembled using NEBuilder HiFi DNA Assembly Cloning Kit, resulting in the plasmid pKD-tetW-CR2. The 12-kb sequence of GI*sul2* upstream of the CR2-*sul2* unit was amplified from the genomic DNA of *S. flexneri* 51575 using 15K-F/CRUp-R primers, resulting in a 12,256 bp fragment. The recombinant plasmid pKD-tetW-CR2 was digested by BbvC1 restriction enzyme, producing overlap sequences with the corresponding two terminal regions of the GI*sul2* 12-kb fragment. The two fragments were ligated using the NEBuilder HiFi DNA Assembly Cloning Kit, resulting in the donor plasmid pKDGItetWsul2.

To construct the trap plasmid pKFattB, the *attB* region (811 bp), including the *attB* site (19 bp) and its upstream (319 bp) and downstream (473 bp) regions, was amplified from the chromosome of *E. coli* DH5α with primers G-GMP-SF and G-GMP-SR. These *attB* upstream and downstream regions corresponded to the 3′ end of *guaA* (336 bp) and the 5′ end of a hypothetical protein (381 bp), respectively. The high copy plasmid pKF18k-2 (Takara Bio Inc., Kasatsu, Japan) was digested using *Xba*I/*Hind*III enzymes and the digestion product was assembled together with the amplified *attB* region using NEBuilder HiFi DNA Assembly Cloning Kit (New England Biolabs, Ipswich, MA, USA), resulting in the trap plasmid pKFattB.

Chromosomal integration and two-plasmid mobilization experiment in *recA*-deficient *E. coli*

pKDGItetWsul2 was transformed into *E. coli* DH5α, which was cultured on LB agar plates containing ampicillin (100 μg/ml) at 30°C. Single colonies (transformants) were selected and cultured at 30°C for 24 h in liquid medium containing tetracycline (20 μg/ml), then the temperature was increased to 42°C for 16 h to stop pKDGItetWsul2 replication. The resulting cultures were plated on LB medium containing tetracycline (20 μg/ml) at 42°C and then 12 colonies were selected and cultured in liquid LB at 42°C overnight. Crude DNA from these recombinant colonies was used as the template for PCR amplification.

The two-plasmid mobilization assay was performed according to a previous report (Wilde et al., 2008). pKDGItetWsul2 and pKFattB were co-transformed into *E. coli* DH5α, which was cultured on LB agar plates containing ampicillin (100 μg/ml) and kanamycin (50 μg/ml) at 30°C. The integration experiment was performed as in the chromosomal integration experiment, except that 50 μg/ml kanamycin was added to each medium. A total of 12 recombinant colonies were selected and their plasmids were extracted using TIANprep Mini Plasmid Kit (TIANGEN BIOTECH, Beijing). These recombinant plasmids were used as a template for PCR amplification and enzyme restriction analysis.

Nanopore sequencing and analysis

Five of the twelve recombinant plasmid extracts were digested with the *Xba*I restriction enzyme, cutting specifically the trap plasmid pKF*attB* 324 bp upstream of the *attB* site. The digestion products were sequenced using the PromethION platform (NextOmics, Wuhan, China). The raw reads data were demultiplexed and filtered with the Porechop v0.2.4 software (Wick, 2018). The quality control values were set as follows: (mean_qscore_template) ≥7 and sequence length ≥1,000 bp. Residual barcoding adapters were removed by trimming 100 bp on both sides of each read using cutadapt v2.9 (Martin, 2011). The filtered high-quality reads in fasta format were mapped against the pKF*attB* sequence and the sequence of each of the five expected recombinant structures using graphmap2 v0.6.3 (Sović et al., 2016) with the end-to-end owler parameter. The number of input structures mapped by each read was evaluated, and reads were categorized as unambiguous when they were properly mapped on only one structure and ambiguous when they were properly mapped on two or more structures.

Deletion of the *int* gene, *att* sites, and other mobility-associated genes or regions in GI*sul2*

Using pKDGItetWsul2 as a template, an *int*-deficient fragment of GI*sul2* (*int* completely deleted) was amplified using the delINT-F/R primers. The backbone of pKDGItetWsul2 segment including the temperature-sensitive replicon and the ampicillin resistance marker was obtained using primers V15K-F/R. The two fragments were assembled using the NEBuilder Assembly Tool to produce the pKDGItetWsul2-Δint donor. Using the same strategy, the pKDGItetWsul2-Δ*rcr2,* pKDGItetWsul2-Δ*resG,* and pKDGItetWsul2-Δ*rep* donor plasmids were constructed using the delCR2-F/R and V15K-F/R, del-ser-F/R and Res-F/R, del-repF/R and V15K-F/V-D-repR primer pairs, respectively. The *att*-depleted plasmid donor was constructed as follows: *attL*-/*attR*-deficient fragment and the vector backbone fragment were amplified by PCR using del-21bp-F/R and VPKD-F/R primers, respectively, with pKDGItetWsul2 as the template. The two fragments were assembled using NEBuilder Assembly Tool, resulting in the

attL/R-deficient plasmid. D-all21bpF/R and V-D-all21F/R primer pairs were then used to amplify two fragments devoid of *attLR* from the *attL/R*-deficient plasmid. The latter two fragments were assembled using NEBuilder Assembly Tool to construct the final *attL/LR/R*-deficient plasmid, named pKDGItetWsul2-Δatt. All primer sequences were designed according to the manufacturer's instructions (http://nebuilder.neb.com/), as shown in Supplementary Table 1. The constructed deletion plasmids served as donor plasmids for integration experiments using the two-plasmid mobilization system as described above.

Construction of pKDGItetWsul2sacB and pCOLADGm, and the mobilization assay

The *Mlu*I restriction enzyme (NEB) was used to cut pKDGItetWsul2 (24157 bp) and the *sacB* original vector pDM4 (7,104 bp). *Mlu*I cuts the araBAD promoter within pKDGItetWsul2 and cuts pDM4 twice, creating a 3.8-kb fragment that contains a chloramphenicol resistance gene and the *sacB* gene plus its promoter. The two fragments were purified and then ligated using a T4 DNA ligase (NEB). The ligation product was transformed into *E. coli* DH5α and cultured in LB containing tetracycline and chloramphenicol. Transformants were verified by *Mlu*I restriction analysis and sequencing. The new donor plasmid containing *sacB* was designated pKDGItetWsul2sacB and used for integration experiments with the trap plasmid pKFattB, as well as for the chromosomal integration experiment. Sucrose (20%) was used in addition to tetracycline and kanamycin in the LB medium used for the selection of the recombinant colonies.

To introduce *alpA* encoding region into the new two-plasmid system composed of pKDGItetWsul2sacB and pKFattB, pCOLADuet-1 (ColA origin, different from the origins of two-plasmid system) was used for overexpression of *alpA* gene under the control of IPTG. pCOLADuet-1 carries the kanamycin resistance determinant, similar to pKFattB. We used the gentamycin resistance gene derived from pEX18Gm to replace the kanamycin resistance gene. BspHI cut pCOLADuet-1 and pEX18Gm, respectively. Then using NEB T4 ligase ligated the two parts and then formed pCOLADGm. Amplification of *alpA* with primers alpANcoI-F and alpASalI-R was performed using the donor plasmid as the template. The PCR product was digested with NcoI and SalI restriction enzymes. The same double enzymes cut pCOLADGm. The two fragments were ligated by using T4 ligase. The resultant plasmid pCOLADalpAGm was constructed successfully through enzyme digestion and sequencing verification. pCOLADalpAGm, pKDGItetWsul2, and pKFattB were simultaneously transformed into the *recA*-deficient strain DH5α, and the LB agar plate containing tetracycline (10 μg/ml), kanamycin (50 μg/ml), and gentamycin (10 μg/ml) was screened at 30°C for 48 h. The correct strain was incubated in LB liquid culture carrying 20% sucrose, tetracycline (10 μg/ml), kanamycin (50 μg/ml), gentamycin (10 μg/ml), and IPTG (0.5 mM) at 30°C for 24 h. The culture dilution was plated LB harboring the same components as the liquid culture at 37°C for 48 h. Plasmids of the colonies extracted were the template, which was used for restriction enzyme analysis.

Bioinformatics methods and the distribution analysis of GI12K, GI*sul2,* and CR2-*sul2*

A total of 169,991 bacterial genomes were downloaded from the NCBI genome database [ftp://ftp.ncbi.nlm.nih.gov/genomes/genbank/] on 15 November 2018. The taxonomic lineage of each genome was retrieved from the NCBI taxonomy database. First, a search of regions matching the Int sequence with 95% amino acid identity and 98% coverage was performed. Preliminary results on the complete genomes database showed that the GI12K sequence coverage systematically exceeded 70% in genomes where a match on Int was detected with these parameters (Supplementary Figure 5). Hence, genomes returning a match to Int with 95% amino acid identity and 98% coverage were considered to carry GI12K. A search of the *rcr2* and *sul2* genes with a BLASTN cutoff of 95% nucleotide similarity was performed independently on all genomes, and genomes including both genes were considered as carrying the CR2-*sul2* element. Preliminary results on complete genomes indicated that it is indeed the case since all the CR2-*sul2* regions detected this way were surrounded by the typical 119 and 304 bp conserved regions ending at the core recombination sites of the *att* loci (Leclercq et al., 2016), despite inner structural variation. The distribution of the GI12K, GI*sul2,* and the CR2-*sul2* unit was then estimated as follows: when only the match to the integrase was satisfied, the genome was considered to carry GI12K; when only the match to *rcr2* and *sul2* regions was satisfied, the genome was considered to carry a CR2-*sul2* unit; finally, when all matches were satisfied, the genome was considered to carry GI*sul2.* This analysis was performed on the complete genome database and the draft genome database independently. The chromosomal or plasmid localization of the detected elements was returned only for the complete genome database, where the replicon type is known. Then, to illustrate the distribution of GI12K, GI*sul2,* and CR2-*sul2*, the bacterial taxonomic framework of the 169,991 bacterial genomes was built by using the software GraPhlAn based on the taxonomic lineage information (Asnicar et al., 2015), with the quantities for each GI being mapped to the taxonomic framework.

Data availability statement

The datasets presented in this study can be found in online repositories. The names of the repository/repositories

and accession number(s) can be found at: https://www.ncbi.nlm.nih.gov/genbank/, PRJNA608816.

Author contributions

GZ and QC designed and executed the work. GZ wrote the manuscript. JF and SL revised substantially the manuscript. JL and RG performed some detailed experiments. LD, NT, and FZ performed the distribution and drawn the relevant figure. YS and SL performed the bioinformatic analysis. CW did some figures. All authors contributed to the article and approved the submitted version.

Funding

This work was supported by the National Natural Science Foundation of China (grants 31870134, 32070075, 81861138053, and 31872632).

Conflict of interest

The authors declare that the research was conducted in the absence of any commercial or financial relationships that could be construed as a potential conflict of interest.

Publisher's note

Supplementary material

The Supplementary Material for this article can be found online at: https://www.frontiersin.org/articles/10.3389/fmicb.2022.905865/full#supplementary-material

References

Anantham, S., Harmer, C. J., and Hall, R. M. (2015). p39R861-4, A type 2 A/C2 plasmid carrying a segment from the A/C1 plasmid RA1. *Microb. Drug Resist.* 21, 571–576. doi: 10.1089/mdr.2015.0133

Asnicar, F., Weingart, G., Tickle, T. L., Huttenhower, C., and Segata, N. (2015). Compact graphical representation of phylogenetic data and metadata with GraPhlAn. *PeerJ* 3:e1029. doi: 10.7717/peerj.1029

Beaber, J. W., Hochhut, B., and Waldor, M. K. (2002). Genomic and functional analyses of SXT, an integrating antibiotic resistance gene transfer element derived from *Vibrio cholerae*. *J. Bacteriol.* 184:4259–4269. doi: 10.1128/JB.184.15.4259-4269.2002

Carraro, N., and Burrus, V. (2014). Biology of three ICE families: SXT/R391, ICEBs1, and ICESt1/ICESt3. *Microbiol. Spectr.* 2, 1–20. doi: 10.1128/microbiolspec.MDNA3-0008-2014

Datsenko, K. A., and Wanner, B. L. (2000). One-step inactivation of chromosomal genes in *Escherichia coli* K-12 using PCR products. *Proc. Natl. Acad. Sci. U.S.A.* 97, 6640–6645. doi: 10.1073/pnas.120163297

Fang, L. X., Chen, C., Yu, D. L., Sun, R. Y., Cui, C. Y., Chen, L., et al. (2019). Complete nucleotide sequence of a novel plasmid bearing the high-level tigecycline resistance gene tet(X4). *Antimicrob. Agents Chemother.* 63, e01373–e01319. doi: 10.1128/AAC.01373-19

Guédon, G., Libante, V., Coluzzi, C., Payot, S., and Leblond-Bourget, N. (2017). The obscure world of integrative and mobilizable elements, highly widespread elements that pirate bacterial conjugative systems. *Genes* 8:337. doi: 10.3390/genes8110337

Halder, U., Biswas, R., Kabiraj, A., Deora, R., Let, M., Roy, R. K., et al. (2022). Genomic, morphological, and biochemical analyses of a multi-metal resistant but multi-drug susceptible strain of Bordetella petrii from hospital soil. *Sci. Rep.* 12:8439. doi: 10.1038/s41598-022-12435-7

Hall, R. M. (2010). Salmonella genomic islands and antibiotic resistance in Salmonella enterica. *Fut. Microbiol.* 5, 1525–1538. doi: 10.2217/fmb.10.122

Hamidian, M., and Hall, R. M. (2016). *Acinetobacter baumannii* ATCC 19606 carries GIsul2 in a genomic island located in the chromosome. *Antimicrob. Agents Chemother.* 61, e01991–e01916. doi: 10.1128/AAC.01991-16

Harmer, C. J., and Hall, R. M. (2015). The A to Z of A/C plasmids. *Plasmid* 80, 63–82. doi: 10.1016/j.plasmid.2015.04.003

Harmer, C. J., Hamidian, M., and Hall, R. M. (2017). pIP40a, a type 1 IncC plasmid from 1969 carries the integrative element GIsul2 and a novel class II mercury resistance transposon. *Plasmid* 92, 17–25. doi: 10.1016/j.plasmid.2017.05.004

He, T., Wang, R., Liu, D., Walsh, T. R., Zhang, R., Lv, Y., et al. (2019). Emergence of plasmid-mediated high-level tigecycline resistance genes in animals and humans. *Nat Microbiol* 4, 1450–1456. doi: 10.1038/s41564-019-0445-2

Hem, S., Wyrsch, E. R., Drigo, B., Baker, D. J., Charles, I. G., Donner, E., et al. (2022). Genomic analysis of carbapenem-resistant comamonas in water matrices: implications for public health and wastewater treatments. *Appl. Environ. Microbiol.* 16:e0064622. doi: 10.1128/aem.00646-22

Juhas, M., van der Meer, J. R., Gaillard, M., Harding, R. M., Hood, D. W., and Crook, D. W. (2009). Genomic islands: tools of bacterial horizontal gene transfer and evolution. *FEMS Microbiol. Rev.* 33, 376–393. doi: 10.1111/j.1574-6976.2008.00136.x

Kirby, J. E., Trempy, J. E., and Gottesman, S. (1994). Excision of a P4-like cryptic prophage leads to Alp protease expression in *Escherichia coli*. *J. Bacteriol.* 176, 2068–2081. doi: 10.1128/jb.176.7.2068-2081.1994

Lallement, C. (2018). *Caractérisation des séquences d'insertions ISCR bactériennes impliquées dans la résistance aux antibiotiques* (Thesis). Université de Limoges, Limoges, France.

Landy, A. (2014). The λ integrase site-specific recombination pathway. *Microbiol. Spectr.* 3:MDNA3-0051-2014. doi: 10.1128/microbiolspec.MDNA3-0051-2014

Leclercq, S. O., Wang, C., Zhu, Y., Wu, H., Du, X., Liu, Z., et al. (2016). Diversity of the tetracycline mobilome within a chinese pig manure sample. *Appl. Environ. Microbiol.* 82, 6454–6462. doi: 10.1128/AEM.01754-16

Lesic, B., Bach, S., Ghigo, J. M., Dobrindt, U., Hacker, J., and Carniel, E. (2004). Excision of the high-pathogenicity island of *Yersinia pseudotuberculosis* requires the combined actions of its cognate integrase and Hef, a new recombination directionality factor. *Mol. Microbiol.* 52, 1337–1348. doi: 10.1111/j.1365-2958.2004.04073.x

Li, B., Chen, D., Lin, F., Wu, C., Cao, L., Chen, H., et al. (2022). Genomic Island-mediated horizontal transfer of the erythromycin resistance gene erm(X) among bifidobacteria. *Appl. Environ. Microbiol.* 88:e0041022. doi: 10.1128/aem.00410-22

Martin, M. (2011). Cutadapt removes adapter sequences from high-throughput sequencing reads. *EMBnet J.* 17, 10–12. doi: 10.14806/ej.17.1.200

Nigro, S. J., and Hall, R. M. (2011). GIsul2, a genomic island carrying the sul2 sulphonamide resistance gene and the small mobile element CR2 found in the *Enterobacter cloacae* subspecies cloacae type strain ATCC 13047 from 1890, *Shigella flexneri* ATCC 700930 from 1954 and *Acinetobacter baumannii* ATCC 17978 from 1951. *J. Antimicrob. Chemother.* 66, 2175–2176. doi: 10.1093/jac/dkr230

Partridge, S. R., and Hall, R. M. (2003). In34, a complex In5 family class 1 integron containing orf513 and dfrA10. *Antimicrob. Agents Chemother.* 47, 342–349. doi: 10.1128/AAC.47.1.342-349.2003

Partridge, S. R., Kwong, S. M., Firth, N., and Jensen, S. O. (2018). Mobile genetic elements associated with antimicrobial resistance. *Clin. Microbiol. Rev.* 31, e00088–e00017. doi: 10.1128/CMR.00088-17

Schleinitz, K. M., Vallaeys, T., and Kleinsteuber, S. (2010). Structural characterization of ISCR8, ISCR22, and ISCR23, subgroups of IS91-like insertion elements. *Antimicrob. Agents Chemother.* 54, 4321–4328. doi: 10.1128/AAC.00006-10

Shi, Y., Tian, Z., Leclercq, S. O., Zhang, H., Yang, M., and Zhang, Y. (2019). Genetic characterization and potential molecular dissemination mechanism of tet(31) gene in *Aeromonas caviae* from an oxytetracycline wastewater treatment system. *J. Environ. Sci.* 76, 259–266. doi: 10.1016/j.jes.2018.05.008

Sović, I., Šikić, M., Wilm, A., Fenlon, S. N., and Chen, S., Naragaran, N. (2016). Fast and sensitive mapping of nanopore sequencing reads with GraphMap. *Nat. Commun.* 7:11307. doi: 10.1038/ncomms11307

Stokes, H. W., Tomaras, C., Parsons, Y., and Hall, R. M. (1993). The partial 3'-conserved segment duplications in the integrons In6 from pSa and In7 from pDGO100 have a common origin. *Plasmid* 30, 39–50 doi: 10.1006/plas.1993.1032

Sun, J., Chen, C., Cui, C. Y., Zhang, Y., Liu, X., Cui, Z. H., et al. (2019). Plasmid-encoded tet(X) genes that confer high-level tigecycline resistance in *Escherichia coli*. *Nat. Microbiol.* 4, 1457–1464. doi: 10.1038/s41564-019-0496-4

Toleman, M. A., Bennett, P. M., and Walsh, T. R. (2006a). ISCR elements: novel gene-capturing systems of the 21st century? *Microbiol. Mol. Biol. Rev.* 70, 296–316. doi: 10.1128/MMBR.00048-05

Toleman, M. A., Bennett, P. M., and Walsh, T. R. (2006b). Common regions e.g. orf513 and antibiotic resistance: IS91-like elements evolving complex class 1 integrons. *J. Antimicrob. Chemother.* 58, 1–6. doi: 10.1093/jac/dkl204

Wick, R. (2018). Available online at: https://github.com/rrwick/Porechop

Wilde, C., Mazel, D., Hochhut, B., Middendorf, B., Le Roux, F., Carniel, E., et al. (2008). Delineation of the recombination sites necessary for integration of pathogenicity islands II and III into the *Escherichia coli* 536 chromosome. *Mol. Microbiol.* 68, 139–151. doi: 10.1111/j.1365-2958.2008.06145.x

Wüthrich, D., Brilhante, M., Hausherr, A., Becker, J., Meylan, M., and Perreten, V. (2019). A novel trimethoprim resistance gene, dfrA36, characterized from *Escherichia coli* from calves. *mSphere* 4, e00255–e00219. doi: 10.1128/mSphere.00255-19

Xu, Y., Wang, C., Zhang, G., Tian, J., Liu, Y., Shen, X., et al. (2017). ISCR2 is associated with the dissemination of multiple resistance genes among *Vibrio* spp. and Pseudoalteromonas spp. isolated from farmed fish. *Arch. Microbiol.* 199, 891–896. doi: 10.1007/s00203-017-1365-2

Yau, S., Liu, X., Djordjevic, S. P., and Hall, R. M. (2010). RSF1010-like plasmids in Australian *Salmonella enterica* Serovar Typhimurium and origin of their sul2-stra-strb antibiotic resistance gene cluster. *Microb. Drug Resist.* 16, 249–252. doi: 10.1089/mdr.2010.0033

frontiers | Frontiers in Microbiology

TYPE Original Research
PUBLISHED 24 August 2022
DOI 10.3389/fmicb.2022.977356

OPEN ACCESS

EDITED BY
Yongfei Hu,
China Agricultural University,
China

REVIEWED BY
Tieli Zhou,
First Affiliated Hospital of Wenzhou Medical University, China
Chang-Wei Lei,
Sichuan University, China
Michael P. Ryan,
University of Limerick,
Ireland

*CORRESPONDENCE
Luhua Zhang
zhluhua@swmu.edu.cn
Xiaoyi Dai
daixiaoyi@swmu.edu.cn

†These authors have contributed equally to this work

SPECIALTY SECTION
This article was submitted to Antimicrobials, Resistance and Chemotherapy, a section of the journal Frontiers in Microbiology

RECEIVED 24 June 2022
ACCEPTED 05 August 2022
PUBLISHED 24 August 2022

CITATION
Li Y, Liu Q, Qiu Y, Fang C, Zhou Y, She J, Chen H, Dai X and Zhang L (2022) Genomic characteristics of clinical multidrug-resistant *Proteus* isolates from a tertiary care hospital in southwest China. *Front. Microbiol.* 13:977356. doi: 10.3389/fmicb.2022.977356

Genomic characteristics of clinical multidrug-resistant *Proteus* isolates from a tertiary care hospital in southwest China

Ying Li[1,2†], Qian Liu[3†], Yichuan Qiu[1], Chengju Fang[1], Yungang Zhou[1], Junping She[1], Huan Chen[1], Xiaoyi Dai[1*] and Luhua Zhang[1*]

[1]The School of Basic Medical Science and Public Center of Experimental Technology, Southwest Medical University, Luzhou, Sichuan, China, [2]Immune Mechanism and Therapy of Major Diseases of Luzhou Key Laboratory, School of Basic Medical Science, Southwest Medical University, Luzhou, Sichuan, China, [3]Department of Clinical Laboratory, The Affiliated Traditional Chinese Medicine Hospital, Southwest Medical University, Luzhou, Sichuan, China

Multidrug-resistant (MDR) *Proteus*, especially those strains producing extended-spectrum β-lactamases (ESBL) and carbapenemases, represents a major public health concern. In the present work, we characterized 27 MDR *Proteus* clinical isolates, including 23 *Proteus mirabilis*, three *Proteus terrae*, and one *Proteus faecis*, by whole-genome analysis. Among the 27 isolates analyzed, SXT/R391 ICEs were detected in 14 strains, and the complete sequences of nine ICEs were obtained. These ICEs share a common backbone structure but also have different gene contents in hotspots and variable regions. Among them, ICE*Pmi*Chn2826, ICE*Pmi*Chn2833, ICE*Pmi*Chn3105, and ICE*Pmi*Chn3725 contain abundant antibiotic resistance genes, including the ESBL gene $bla_{CTX\text{-}M\text{-}65}$. The core gene phylogenetic analysis of ICEs showed their genetic diversity, and revealed the cryptic dissemination of them in *Proteus* strains from food animals and humans on a China-wide scale. One of the isolates, FZP3105, acquired an NDM-1-producing MDR plasmid, designated pNDM_FZP3105, which is a self-transmissible type 1/2 hybrid IncC plasmid. Analysis of the genetic organization showed that pNDM_FZP3105 has two novel antibiotic resistance islands bearing abundant antibiotic resistance genes, among which $bla_{NDM\text{-}1}$ is located in a 9.0kb ΔTn*125* bracketed by two copies of IS*26* in the same direction. In isolates FZP2936 and FZP3115, $bla_{KPC\text{-}2}$ was detected on an IncN plasmid, which is identical to the previously reported pT211 in Zhejiang province of China. Besides, a MDR genomic island PmGRI1, a variant of PmGRI1-YN9 from chicken in China, was identified on their chromosome. In conclusion, this study demonstrates abundant genetic diversity of mobile genetic elements carrying antibiotic resistance genes, especially ESBL and carbapenemase genes, in clinical *Proteus* isolates, and highlights that the continuous monitoring on their transmission and further evolution is needed.

KEYWORDS

***Proteus*, SXT/R391 ICEs, $bla_{NDM\text{-}1}$, $bla_{KPC\text{-}2}$, plasmid**

Introduction

Proteus spp., belonging to the family of Morganellaceae of the order Enterobacterales (Adeolu et al., 2016), are widespread in the environment, and also inhabit in the intestines of humans and animals (O'Hara et al., 2000). Currently, ten species were included in the genus *Proteus*, among which, *Proteus mirabilis* is the most frequently isolated from clinical samples, and represents a major cause of urinary tract infections (Schaffer and Pearson, 2015). *Proteus* are intrinsically resistant to polymyxins, nitrofurans, tigecycline, and tetracycline, and are naturally susceptible to aminoglycosides, fluoroquinolones, and trimethoprim-sulfamethoxazole (Korytny et al., 2016). Multidrug-resistant (MDR), to 3 or more classes of antimicrobial agents (Falagas and Karageorgopoulos, 2008) *Proteus* have been increasingly reported, which generally produce extended-spectrum β-lactamases (ESBLs) and AmpC-type cephalosporinase, and show co-resistance to fluoroquinolones, aminoglycosides, and sulfamethoxazole-trimethoprim (Tumbarello et al., 2012; Korytny et al., 2016). Carbapenems are one of the last-resort antibiotics to treat severe infections caused by MDR *Proteus*, while the identification of carbapenemases, such as KPC-2 (Hu et al., 2012), NDM-1 (He et al., 2021), OXA-48 (Fursova et al., 2015), OXA-23, and OXA-58 (Bonnin et al., 2020) in *Proteus* causes great clinical concern. Plasmid-mediated horizontal gene transfer plays an important role in the dissemination of carbapenemase genes in *Proteus* (Hua et al., 2020; Li et al., 2021).

Resistance genes on the chromosome are usually clustered into structures named genomic islands (GIs), which are distinct regions of a bacterial chromosome that have been acquired *via* horizontal transfer (Partridge et al., 2018). Integrating and conjugative elements (ICEs) are a specific GI with mobility functions that can be integrated into the host chromosome, and also excised as a circular intermediate to be self-transferred to a recipient cell *via* conjugation (Johnson and Grossman, 2015). The large SXT/R391 family ICEs are characterized by a conserved integrase, which catalyzes their integration into the 5′ end of the chromosomal *prfC* gene (encoding the peptide chain release factor 3) by site-specific recombination (Bioteau et al., 2018). SXT/R391 ICEs share 52 nearly identical core genes that mediate integration/excision, conjugative transfer, and regulation, and also contain variable DNA regions, dubbed hotspots (HS) 1–5 and variable regions (VR) I-IV (Wozniak et al., 2009), wherein SXT/R391 acquire new variable DNA sequences that confer element-specific phenotypes, such as resistance to antibiotics (Rodriguez-Blanco et al., 2012). Several SXT/R391 elements have been identified in *Proteus*, and they serve as vehicles of clinical important resistance genes, such as bla_{CMY-2} (Harada et al., 2010), bla_{NDM-1} (He et al., 2021), *tet*(X6) (Peng et al., 2020) and $bla_{CTX-M-65}$ (Lei et al., 2018), which constitutes a severe concern. At present, SXT/R391 ICEs have been widely studied in food-producing animals in China (Lei et al., 2016, 2018; Wang et al., 2021), while their prevalence and genetic characteristics in the clinical isolates are not well understood.

The present study was conducted to characterize MDR *Proteus* clinical isolates from a tertiary care hospital in Sichuan province, China. We performed whole-genome sequencing and analysis to investigate their genetic features about resistance determinants, with a focus on the diversity of genetic structure of SXT/R391 ICEs and the genetic contexts of carbapenemase-encoding genes. Also, the transfer capability of ICEs and carbapenemase-encoding plasmids were determined by conjugation assays.

Materials and methods

Bacterial isolates

Proteus isolates were isolated from clinical specimens of patients at the Affiliated Traditional Chinese Medicine Hospital of Southwest Medical University, in Sichuan Province, China, from January to December of 2021. This study was approved by the Ethics Committee of the Affiliated Traditional Chinese Medicine Hospital of Southwest Medical University. Written informed consent from the patients was exempted for this study, since the present study only focused on bacteria and the strains were isolated as a part of the routine hospital laboratory procedures. Species identification was carried out by 16S rRNA gene sequencing analysis (Lane, 1991). Antibiotic susceptibility testing was performed using the Biomerieux Vitek-2 system, and the results were interpreted by the clinical breakpoints defined by the Clinical and Laboratory Standards Institute standards for Enterobacterales (CLSI, M100). *Escherichia coli* strain ATCC 25922 was used as the quality control. The antibiotics used in this study was provided in Supplementary Table S1. The minimum inhibitory concentrations (MICs) of meropenem against the isolates were determined using the microdilution broth methods and the disk diffusion methods of Bauer and Kirby following recommendations of the CLSI. MDR strains were defined as non-susceptibility to at least one agent in three or more of the following antibiotic groups: β-lactam-β-lactam inhibitor combinations, cephalosporins, fluoroquinolones, aminoglycosides or sulfamethoxazole and trimethoprim (Korytny et al., 2016).

Genomic DNA sequencing and data analysis

Genomic DNA was prepared using the QIAamp DNA Mini Kit (Qiagen) following the manufacturer's guidelines. Whole genome sequencing was performed on the HiSeq 2000 (Illumina, San Diego, CA, United States) platform using a paired-end library with an insert size of 150 bp by the Beijing Tsingke Bioinformatics Technology Co. Ltd. Four isolates (FZP2936, FZP3115, FZP3105 and FZP2826) were additionally sequenced on the long-read MinION sequencer (Nanopore, Oxford, United Kingdom). Both the long MinION reads and short Illumina reads were *de novo*-assembled using Unicycler under the conservative mode

(Wick et al., 2017). Pilon was employed to correct the assembled contigs with Illumina reads (Walker et al., 2014). Annotation was carried out using the RAST tools (Aziz et al., 2008) combined with BLASTp/BLASTn searches against the UniProtKB/SwissProt database (Boutet et al., 2016).

The identification of *Proteus* species was performed by average nucleotide identity (ANI) analysis with JSpeciesWS.[1] Plasmid incompatibility types and multilocus sequence typing were identified using PlasmidFinder 2.1 (95%, minimum threshold for identity; 60%, minimum coverage) and pMLST 2.0 (Carattoli and Hasman, 2020). Antibiotic resistance genes (ARGs), insertion elements (ISs) and integrons were predicted using ResFinder (90%, minimum threshold for identity; 60%, minimum coverage; Bortolaia et al., 2020), ISfinder (Siguier et al., 2006) and INTEGRALL (Moura et al., 2009). The presence of SXT/R391 ICE was screened by targeting the conserved integrase gene (int_{SXT}) from the whole sequenced genomes. The contigs of SXT/R391 ICE were extracted and assembled against the reference ICE in the genome of FZP3105, with gaps between contigs closed by PCR and Sanger sequencing. Plasmids/ICEs similar to those in this study were identified by a BLASTn search in the GenBank database using whole plasmid/ICE sequences. Linear sequence alignment was performed using BLAST and visualized with Easyfig 2.2.3 (Sullivan et al., 2011).

Phylogenetic analysis

The genome sequences of other representative *Proteus* isolates in China from the literature were retrieved from the GenBank. Genetic relationship between the *Proteus* isolates in this study and these reference strains was assessed based on single nucleotide polymorphisms (SNPs) in their core genomes, as previously described with minor modification (Li et al., 2022). Briefly, Genomes were annotated using Prokka, and the generated GFF3 files were piped into Roary to create a core genome alignment. SNPs were extracted using snp-sites v2.3.2. A maximum-likelihood phylogenetic tree based on the SNPs was constructed using FastTree version 2.1.10 under the GTR model. Similarly, phylogenetic analysis of the ICEs in this study and other representative ICEs from the literature was carried out based on SNPs in their conserved regions. The presence of ARGs in the bacterial genomes was determined by ResFinder, and detailed information of isolates was annotated on the trees using iTOL.[2]

Transferability assay

Conjugation experiments were performed using broth-based method with the rifampin-resistant *E. coli* strain EC600, and azide-resistant *E. coli* strain J53 as the recipients, as described previously with minor modification (Li et al., 2021). After the donor strain and recipient were grown to exponential stage (the optical density at 600 nm reaches ~0.5), mix them at a ratio of 1:1, and incubate at 37°C for 24 h. Transconjugants were selected on Luria-Bertani (LB) agar plates containing 4 μg/ml meropenem, 16 μg/ml gentamicin or 2 μg/ml tigecycline plus 400 μg/ml rifampin or 150 μg/ml sodium azide. The presence of bla_{NDM-1}, or SXT/R391 ICE was confirmed by PCR using the primers bla_{NDM}-F 5′ -ATTTACTAGGCCTCGCATTTGC-3′ /bla_{NDM}-R 5′-GCCT CTGTCACATCGAAATCG-3′, and sxtintF 5′-TCGATGA TGGTCTCTAGCTG-3′ /5′-TCAGTTAGCTGGCTCGATGC-3′ (Sato et al., 2020), respectively, with the following conditions: 95°C for 5 min, and 30 cycles of amplification consisting of 30 s at 95°C, 30 s at 53°C, and 1 min 30 s at 72°C, followed by a final elongation step for 5 min at 72°C.

Results and discussion

Sources, resistance phenotype, and genotype of MDR *Proteus* isolates

54 *Proteus* strains were isolated from clinical specimens, and 27 of them were identified as MDR strains (Table 1). These MDR isolates were obtained from urine ($n = 13$, 48.1%), wound secretion ($n = 8$, 29.6%), sputum ($n = 2$, 7.4%), blood ($n = 2$, 7.4%), sanies ($n = 1$, 3.7%), and drainage ($n = 1$, 3.7%). ANI analysis indicated that 27 MDR *Proteus* strains belong to *P. mirabilis* ($n = 23$), *Proteus terrae* ($n = 3$), and *Proteus faecis* ($n = 1$). In addition to their intrinsic resistance profiles, these MDR *Proteus* isolates also showed high levels of resistance to ampicillin ($n = 27$, 100%), cefaloti ($n = 19$, 70.4%), ceftriaxone ($n = 17$, 63.0%), cefotaxime ($n = 19$, 70.4%), ampicillin/sulbactam ($n = 18$, 66.6%), sulfamethoxazole-trimethoprim ($n = 26$, 96.3%), moxifloxacin ($n = 18$, 66.6%), ciprofloxacin ($n = 21$, 77.7%), levofloxacin ($n = 18$, 66.6%), gentamicin ($n = 13$, 48.1%), and tobramycin ($n = 11$, 40.7%). Some MDR isolates were also resistant to aztreonam ($n = 6$, 22.2%), norfloxacin ($n = 9$, 33.3%), imipenem ($n = 5$, 18.5%), meropenem ($n = 3$, 11.1%), ceftazidime ($n = 2$, 7.4%), and piperacillin/tazobactam ($n = 2$, 7.4%; Table 1). Notably, all strains remained susceptible to amikacin.

We sequenced the genomes of all 27 MDR isolates on the Illumina platform (Supplementary Table S2). Genomic analysis revealed that 57 different ARGs were detected in the 27 MDR *Proteus* strains, and 23 (85.2%) of them carried at least 13 ARGs (Figure 1). Of the detected β-lactamase genes, $bla_{CTX-M-65}$, the only ESBL-producing gene, was the most prevalent ($n = 13$, 48.1%), followed by the non-ESBL bla_{OXA-1} ($n = 12$). Carbapenemase gene bla_{KPC-2} was found in two isolates, FZP2936 and FZP3115, in combination with bla_{TEM-1B}. bla_{NDM-1} was only detected in one isolate, FZP3105, which also harbors $bla_{CTX-M-65}$, bla_{OXA-1}, and bla_{OXA-10}. Accordingly, FZP2936, FZP3115, FZP3105, and one $bla_{CTX-M-65}$-positive isolate FZP2826 were selected for further

1 https://jspecies.ribohost.com/jspeciesws/#analyse

2 https://itol.embl.de/

TABLE 1 Microbiological and molecular characteristics of 27 MDR *Proteus* isolates.

Strain	Species	Specimen	Gender/age (year)	ICE/variants of PmGRI1	Resistance phenotype
FZP1665	*Proteus mirabilis*	Urine	F/49	PmGRI1	AMP, CIP, GEN, NIT, SXT, TCY, TGC
FZP2056	*Proteus mirabilis*	Urine	M/75	ICE	AMP, CIP, CZO, LVX, MFX, NIT, NOR, SAM, SXT, TCY, TGC
FZP2095	*Proteus terrae*	Wound secretion	M/56		AMP, ATM, CAZ, CIP, CRO, CTX, CXM, CZO, FEP, FOX, SAM, SXT, TGC
FZP2128	*Proteus mirabilis*	Wound secretion	M/41	PmGRI1	AMP, GEN, SAM, SXT, TOB
FZP2958	*Proteus mirabilis*	Urine	M/74	ICE	AMP, CEP, CIP, CPD, CRO, CTX, CXA, CXM, CZO, LVX, MFX, NIT, SAM, SXT, TCY, TGC
FZP3803	*Proteus mirabilis*	Urine	M/35	ICE	AMP, CEP, CIP, CPD, CRO, CTX, CXA, CXM, CZO, GEN, LVX, MFX, NIT, PIP, SAM, SXT, TCY, TGC, TOB
FZP4264	*Proteus mirabilis*	Urine	M/70	PmGRI1	AMC, AMP, ATM, CEP, CIP, CPD, CRO, CTX, CXA, CXM, CZO, CZX, FEP, GEN, LVX, MFX, NIT, NOR, PIP, SAM, SXT, TCY, TGC, TOB
FZP4280	*Proteus mirabilis*	Urine	M/80	ICE, PmGRI1	AMP, CEP, CIP, CPD, CRO, CTX, CXA, CXM, CZO, LVX, MFX, NIT, PIP, SXT, TCY, TGC
FZP4349	*Proteus terrae*	Wound secretion	F/58	ICE	AMP, CEP, CXA, CXM, CZO, NIT, SXT, TCY, TGC
FZP4423	*Proteus mirabilis*	Blood	M/82	ICE	AMC, AMP, CEP, CIP, CPD, CTX, CXA, CXM, CZO, CZX, GEN, IPM, LVX, MFX, NOR, PIP, SAM, SXT, TCY, TGC, TOB
FZP4515	*Proteus mirabilis*	Wound secretion	M/49	PmGRI1	AMP, CEP, CIP, CPD, CRO, CTX, CXA, CXM, CZO, GEN, LVX, MFX, NOR, PIP, SXT, TCY
FZP1097	*Proteus faecis*	Wound secretion	M/76		AMP, ATM, CIP, CRO, CTX, SXT
FZP1177	*Proteus mirabilis*	Sputum	F/67	PmGRI1	AMP, ATM, CIP, CRO, CTX, CXM, CZO, FEP, GEN, MFX, NOR, LVX, SXT, TOB
FZP1611	*Proteus mirabilis*	Sputum	M/66		AMP, ATM, CEP, CIP, CPD, CRO, CTX, CXA, CXM, CZO, CZX, FEP, GEN, LVX, MFX, NIT, PIP, SAM, SXT, TCY, TGC, TOB
FZP2024	*Proteus mirabilis*	Urine	M/77	ICE, PmGRI1	AMP, CIP, GEN, LVX, MFX, NIT, SXT, TCY, TGC
FZP2561	*Proteus mirabilis*	Urine	F/49	ICE	AMP, CEP, CPD, CRO, CTX, CXA, CXM, CZO, NIT, PIP, SXT, TCY
FZP2833	*Proteus mirabilis*	Drainage	F/49	ICE	AMP, CEP, CIP, CPD, CRO, CTX, CXA, CXM, CZO, LVX, MFX, PIP, SAM, SXT, TCY, TGC
FZP2937	*Proteus mirabilis*	Wound secretion	M/32	ICE, PmGRI1	AMC, AMP, CEP, CIP, CPD, CRO, CTX, CXA, CXM, CZO, LVX, MFX, NOR, PIP, SAM, SXT, TCY, TGC
FZP3043	*Proteus mirabilis*	Urine	F/37	ICE	AMC, AMP, ATM, CEP, CPD, CTX, CXA, CXM, CZO, CZX, NIT, SAM, SXT, TCY, TGC, TOB
FZP3105	*Proteus mirabilis*	Sanies	M/32	ICE, PmGRI1	AMC, AMP, CAZ, CEP, CIP, CPD, CRO, CTX, CXA, CXM, CZO, IPM, LVX, MFX, MEM， NOR, PIP, SAM, SXT, TCY, TGC
FZP3320	*Proteus mirabilis*	Urine	F/56		AMP, CIP, GEN, LVX, MFX, NIT, SAM, SXT, TCY, TGC
FZP3364	*Proteus terrae*	Wound secretion	F/82		AMP, CEP, CXA, CXM, CZO, TCY, TGC
FZP3406	*Proteus mirabilis*	Urine	F/52		AMC, AMP, CEP, CPD, CXA, CXM, CZO, GEN, NIT, SAM, SXT, TCY, TOB
FZP3725	*Proteus mirabilis*	Blood	M/81	ICE, PmGRI1	AMP, CEP, CIP, CPD, CRO, CTX, CXA, CXM, CZO, LVX, MFX, PIP, SAM, SXT, TCY, TGC
FZP2826	*Proteus mirabilis*	Urine	M/58	ICE	AMC, AMP, CEP, CIP, CPD, CRO, CTX, CXA, CXM, CZO, FEP, IPM, LVX, MFX, NIT, PIP, SAM, SXT, TCY, TGC, TOB
FZP2936	*Proteus mirabilis*	Urine	M/58	PmGRI1	AMC, AMP, CEP, CIP, CPD, CRO, CTT, CTX, CXA, CXM, CZO, ETP, GEN, IPM, LVX, MEM, MFX, NIT, NOR, PIP, SAM, SXT, TCY, TGC, TOB, TZP
FZP3115	*Proteus mirabilis*	Wound secretion	M/58	PmGRI1	AMC, AMP, CEP, CIP, CPD, CRO, CSL, CTT, CTX, CXA, CXM, CZO, ETP, GEN, IPM, LVX, MEM, MFX, NIT, NOR, PIP, SAM, SXT, TCY, TGC, TOB, TZP

AMC, amoxicillin/clavulanic acid; AMP, ampicillin; ATM, aztreonam; CIP, ciprofloxacin; CAZ, ceftazidime; CEP, cefalotin; CPD, cefpodoxime; CRO, ceftriaxone; CSL, cefoperazone/sulbactam; CTT, cefotetan; CTX, cefotaxime; CXA, cefuroxime axetil; CXM, cefuroxime; CZO, cefazolin; CZX, ceftizoxime; ETP, ertapenem; FEP, cefepime; FOX, cefoxitin; GEN, gentamicin; IPM, imipenem; LVX, levofloxacin; MEM, meropenem; MFX, moxifloxacin; NIT, nitrofurantoin; NOR, norfloxacin; PIP, piperacillin; SAM, ampicillin/sulbactam; SXT, trimethoprim/sulfamethoxazole; TCY, tetracycline; TGC, tigecycline; TOB, tobramycin; TZP, piperacillin/tazobactam.

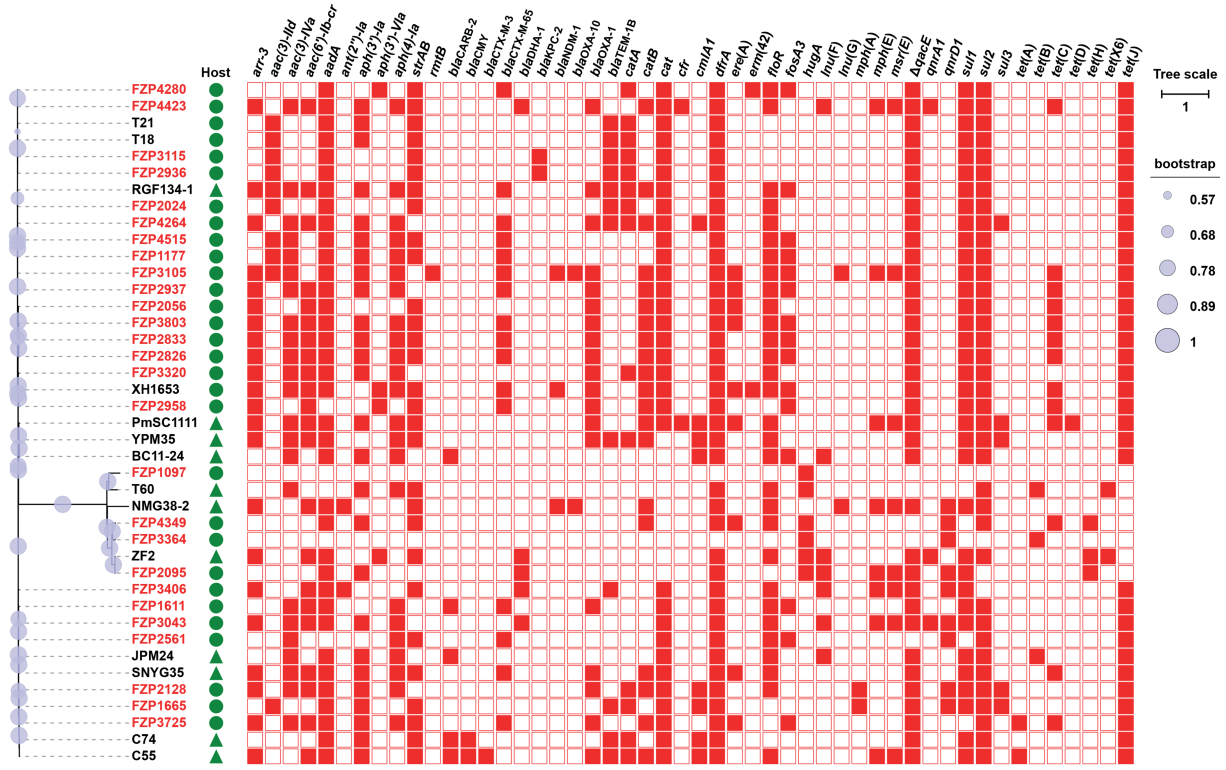

FIGURE 1
Phylogenetic analysis and antibiotic resistance gene (ARG) distribution of *Proteus* strains. Strains identified in this study are highlighted in red. The host of the isolate is indicated by triangles (animals) or circles (humans). The presence or absence of ARGs is indicated by filled or empty squares, respectively. The tree scale indicates substitutions per site. Detailed information of these strains is presented in Supplementary Table S4.

analyses by whole-genome sequencing using the Nanopore technology. Three different quinolone resistance genes were present: *aac(6′)-Ib-cr* (14/27, 51.9%), *qnrA1* (2/27, 7.4%), and *qnrD1* (8/27, 29.6%). Aminoglycoside resistance genes were commonly detected in these MDR *Proteus* strains, with *aadA1* (21/27, 77.7%), *aph(3″)-Ib* (17/27, 63.0%), and *aph(6)-Id* (17/27, 63.0%) being the most prevalent. All the isolates, except for FZP1097 and FZP3364, contained both *sul* and *dfrA* genes, conferring co-resistance to sulfamethoxazole-trimethoprim. Albeit only one known resistance gene *hugA* (encoding a class A β-lactamase conferring third-generation cephalosporin-resistance) was detected, FZP1097 was resistant to several antimicrobial agents, such as ciprofloxacin and sulfamethoxazole-trimethoprim in addition to cefotaxime, indicating that some unknown resistance mechanisms may be involved in its MDR phenotype.

Population structure analysis of MDR *Proteus* isolates

To understand the genetic relationship, the 27 MDR *Proteus* strains were compared to other *Proteus* isolates from different geographic locations in China, and a core genome-based phylogenetic tree was constructed, which revealed two distinct groups (Figure 1). The large group includes all the *P. mirabilis* strains with a high degree of whole-genome homogeneity (0–5,555 SNPs, Supplementary Table S3), and the other one consists of different non-*P. mirabilis* strains of the *Proteus* genus. From the phylogenetic tree, some isolates from different patients are tightly clustered, for example FZP2833/FZP3803 and FZP4349/FZP3364, hinting a common origin and cryptic transmission in this hospital. In addition, clonal relationship was also noticed between some isolates in this study and those from food animals or humans in other locations of China (Supplementary Table S4), for example FZP2958/XH1653 (*P. mirabilis*, humans, Zhejiang of China, 2015) and FZP2095/ZF2 (*P. terrae*, animals, Jiangsu of China, 2018), suggesting the possible circulation and clonal transmission of these MDR *Proteus* strains amongst animals and humans across China. Active monitoring the spread of MDR *Proteus* strains in the context of 'One Health' (environmental, animal, and human sectors) is an essential part in combating antimicrobial resistance.

Genetic features of ICE in MDR *Proteus* isolates

Fourteen out of the 27 *Proteus* strains were positive for the int_{SXT} gene (>97% identity to that of SXT), and all of these SXT/

R391 ICE-harboring isolates were *P. mirabilis*, except one *P. terrae* (Table 1). Based on the genome data, the complete sequences of nine SXT/R391 ICEs were successfully assembled, ranging in size from 83,975 bp to 130,923 bp, and five were fragmented in two or more contigs (Figure 2). Among them, ICE*Pmi*Chn2826 and ICE*Pmi*Chn2833 are almost identical, with only several different bases in variable regions. ICE*Pmi*Chn2024 and ICE*Pmi*Chn2561 are only differed by an insertion of a 1,063 bp truncated IS*Va2* between *traI* and *traD* in the former.

Analysis of genetic organization showed that the nine ICEs shared a common backbone structure with most SXT/R391 ICEs, but also contained DNA sequences that are relatively specific for individual elements, comprising five hotspots (HS1-5) and three variable regions (VRII, VRIII and VRIV; Figure 2), as described previously (Wozniak et al., 2009). Four ICEs (ICE*Pmi*Chn2024, ICE*Pmi*Chn2561, ICE*Pmi*Chn4280, and ICE*Pte*Chn4349) harbor a *mutL* gene (encoding a putative DNA mismatch repair protein) in the VRII (*xis-int*), and ICE*Pmi*Chn4280 solely has a *mer* operon in the VRIV (*traG-eex*). All nine ICEs harbored VRIII (disrupting the *rumB* gene), and three ICEs (ICE*Pmi*Chn2826, ICE*Pmi*Chn2833, and ICE*Pmi*Chn3803) have a MDR region bearing ARGs *floR*, *strB/A*, and *sul2*, conferring resistance to chloramphenicol, streptomycin, and sulfamethoxazole, respectively. Specially, ICE*Pmi*Chn4280 has a multi-drug resistance RND efflux pump gene cluster, *tmexCD3-toprJ3*, in VRIII (Wang et al., 2021). HS1 (*s043-traL*), HS2 (*traA-s054*), HS4 (*traN-s063*), and HS5 (*s026-traI*) were detected in all nine ICEs, while HS3 (*s073-traF*) was only found in ICE*Pmi*Chn2024 and ICE*Pmi*Chn2561, with inserted genes encoding an integrase, a dihydrofolate reductase-like protein and a hypothetical protein. Gene clusters encoding diverse restriction-modification (RM) systems conferring resistance to bacteriophages (Balado et al., 2013) are commonly found in HS5 in these ICEs, including the BREX phage resistance system (*brxA-brxB-brxC-pglX-pglZ-brxL*; Slattery et al., 2020). Additionally, genes encoding endonuclease, ATPase, methyltransferase, helicase, and the *mrr* restriction system are also detected in this region (Figure 2).

Abundant ARGs are present in HS4 in ICE*Pmi*Chn2826, ICE*Pmi*Chn2833, ICE*Pmi*Chn3105, and ICE*Pmi*Chn3725. Structural comparison showed that the four ICEs share similar gene contents in the HS4 region, which is also similar to that in ICE*Pmi*ChnXH1653 detected in a *P. mirabilis* strain from a urine sample of a patient in Zhejiang, China, in 2015 (He et al., 2021; Figure 3), indicating a common origin. Like the scenario in ICE*Pmi*ChnXH1653, the HS4 in ICE*Pmi*Chn3105 and ICE*Pmi*Chn3725 are also present as an IS*Ppu12*-mediated region, but the two tandem copies of a bla_{NDM-1}-bearing IS*CR1* element downstream of *sul1*, and two copies of IS*26* interrupting *tnpR* are not detected. It has been known that a second IS*26* preferentially inserted into adjacent positions of the existing IS*26*, and the recombination between the two copies of IS26 would cause deletion, insertion or translocation (Partridge et al., 2018). The

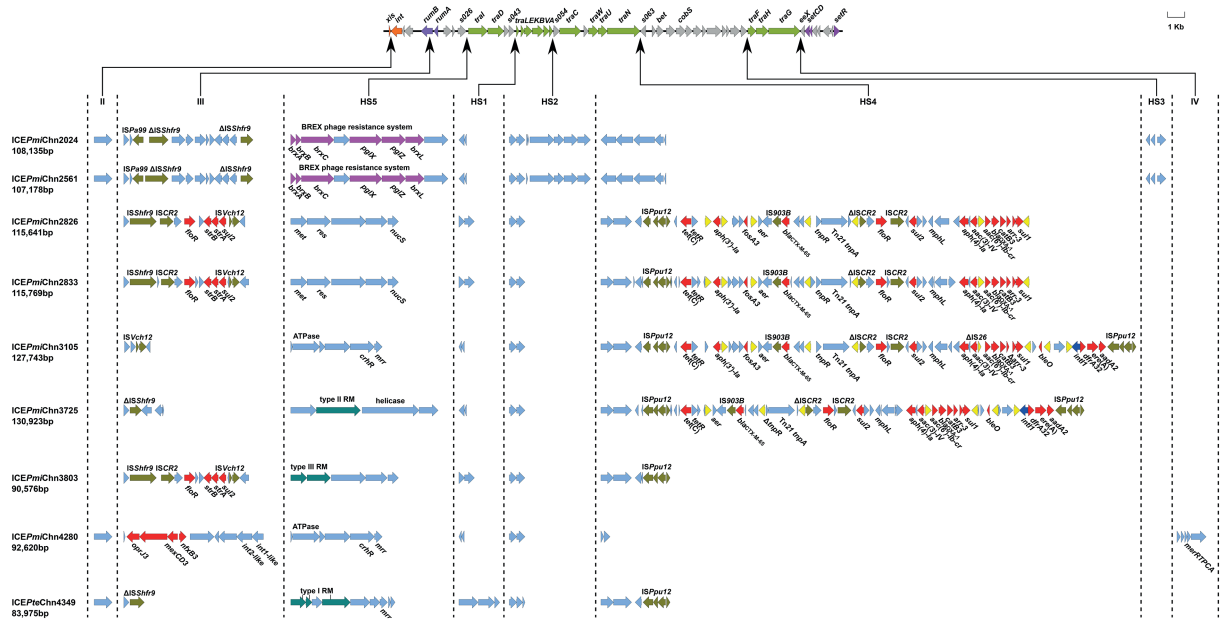

FIGURE 2
Genetic organization of the ICEs in this study. The upper line shows the backbone of SXT/R391 ICEs with conserved core genes. Arrows in orange, purple, green and amaranth indicate genes involved in site-specific excision and integration (*xis* and *int*), DNA repair (*rumAB*), conjugative transfer (*tra*) and regulation (*setCDR*). Other core genes are indicated by light gray arrows. Under the backbone, hotspots (HS1-HS5) and variable regions (II–IV) are shown, with thin arrows indicating the sites of their insertion. ARGs, insertion sequences, BREX phage resistance system, and restrictive modification systems are highlighted in red, olive, purple-red, and blue-green, respectively, except that IS*26* is highlighted in yellow. Other genes in the insertion regions are indicated by light blue arrows.

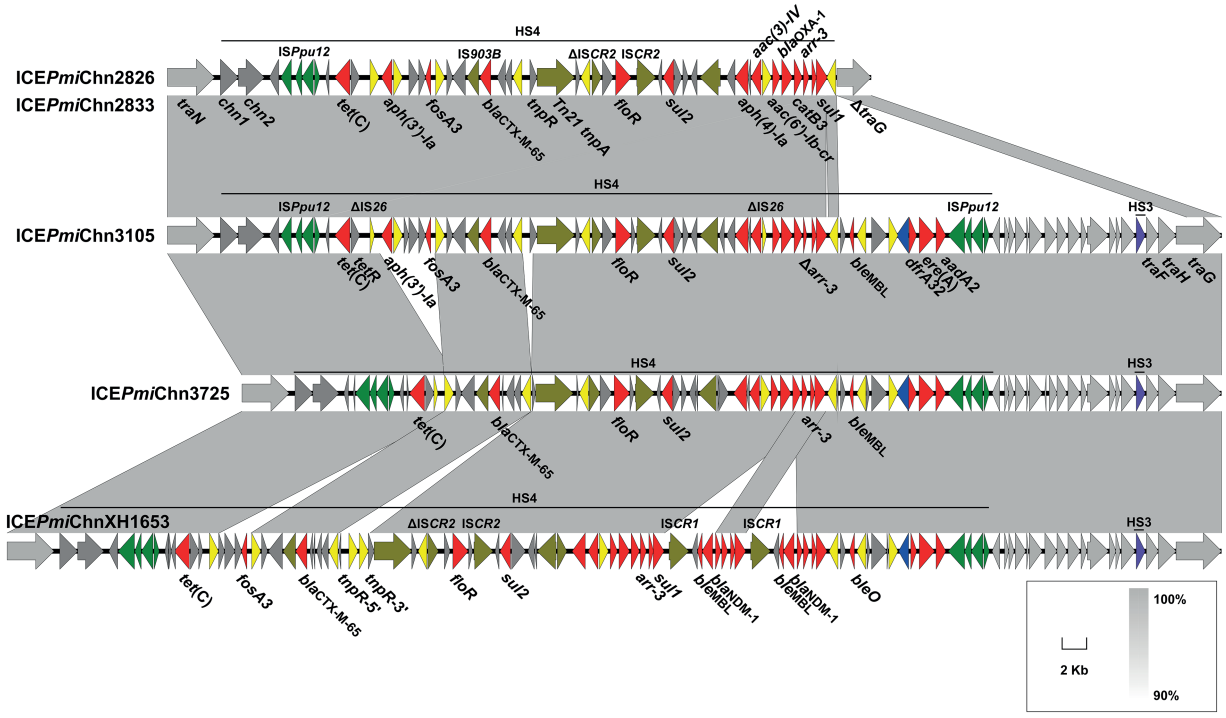

FIGURE 3
Genetic characteristics of HS4. The HS4-bearing region of ICE*Pmi*Chn2826 (ICE*Pmi*Chn2833), ICE*Pmi*Chn3105, and ICE*Pmi*Chn3725 is compared with that of ICE*Pmi*ChnXH1653 (accession no. CP065039). Genes are indicated by arrows, and those in HS4, HS3 and backbone are indicated in dark grey, purple and light grey, respectively. ARGs, integrase genes, IS*26*, IS*Ppu12*, and other transposase genes are highlighted in red, blue, yellow, green, and olive, respectively. Shared regions of >90% nucleotide sequence identity are indicated by grey shading.

HS4 in ICE*Pmi*Chn2826 (ICE*Pmi*Chn2833) seems to be a variant of ICE*Pmi*Chn3105 with the deletion of 9,781 bp HS4 region and 15,456 bp of adjacent backbone, very likely resulting from an insertion of the second IS*26* inside the *traG* and the subsequent recombination action of IS*26* (Figure 3). The HS4 in ICE*Pmi*Chn3105 and ICE*Pmi*Chn3725 are highly similar (99.97% nucleotide identity at 92% coverage), and an IS*26*-mediated excision of a 4,311 bp region bearing *aph(3′)-Ia* and *fosA3* downstream of *tetR*, and an 813 bp deletion upstream of *tnpR* represent two major modular differences of them (Figure 3). This finding suggests that these MDR ICEs are undergoing rapid evolution within healthcare environments.

By BLASTn analysis, the nine SXT/R391 ICEs exhibited similarity to many different ICEs recovering from food animals and humans in different locations of China (Supplementary Table S5), indicating wide spread of them. The core gene phylogenetic analysis showed that ICE*Pmi*Chn2826, ICE*Pmi*Chn2833, and ICE*Pmi*Chn3803 are closely related to the reference MDR ICEs, ICEPmiChn1 (*P. mirabilis*, chicken, Hubei of China), ICEPmiChnBCP11 (*P. mirabilis*, swine, Sichuan of China), and ICEPmiChnChSC1905 (*P. mirabilis*, swine, Sichuan of China; Figure 4; Supplementary Table S6). ICE*Pmi*Chn3105 is clustered with ICE*Pmi*ChnCC15031 that was detected in a *P. mirabilis* strain from a dog in Jilin, China. ICE*Pmi*Chn3725 is closely related, with only 1 SNP, to ICEPmiChn1701092 from a *P. mirabilis* strain recovered from the intestinal contents of humans in Zhejiang, China. The phylogenetic analysis indicated that ICE*Pte*Chn4349 serves as a potentially novel SXT/R391 element as it forms a distinct clade separated from other representative ICEs (Figure 4; Supplementary Table S6). ICE*Pmi*Chn2024, ICE*Pmi*Chn2561, and ICE*Pmi*Chn4280 are more distantly related to the ICEs in this study. ICE*Pmi*Chn4280 has the most closely genetic relationship with ICEPmiChnRGF134-1 (*P. mirabilis*, swine, Jiangsu of China), and ICE*Pmi*Chn2024 (ICE*Pmi*Chn2561) is closest to ICEPteChnS24-2-1 (*P. terrae*, Cacatua, Guangzhou of China), with 0 and 2 SNPs, respectively (Figure 4; Supplementary Table S6). These findings suggest the cryptic dissemination of these ICEs in *Proteus* strains on a China-wide scale.

According to the species tree (Figure 1), we found that strains FZP2024 and FZP2561 are little related, but share almost identical ICEs (ICE*Pmi*Chn2024 and ICE*Pmi*Chn2561). The closely related strains FZP2826 and FZP3803 bear ICEs (ICE*Pmi*Chn2826 and ICE*Pmi*Chn3803) with markedly different HS4 and HS5 contents. Besides, strains FZP4349 and FZP3364 are tightly clustered, and the latter is devoid of an SXT/R391 element on the chromosome while the former possesses the ICE*Pte*Chn4349. These findings suggest the independent acquisition and horizontal transmission of SXT/R391 ICEs across the *Proteus* population (Sato et al., 2020).

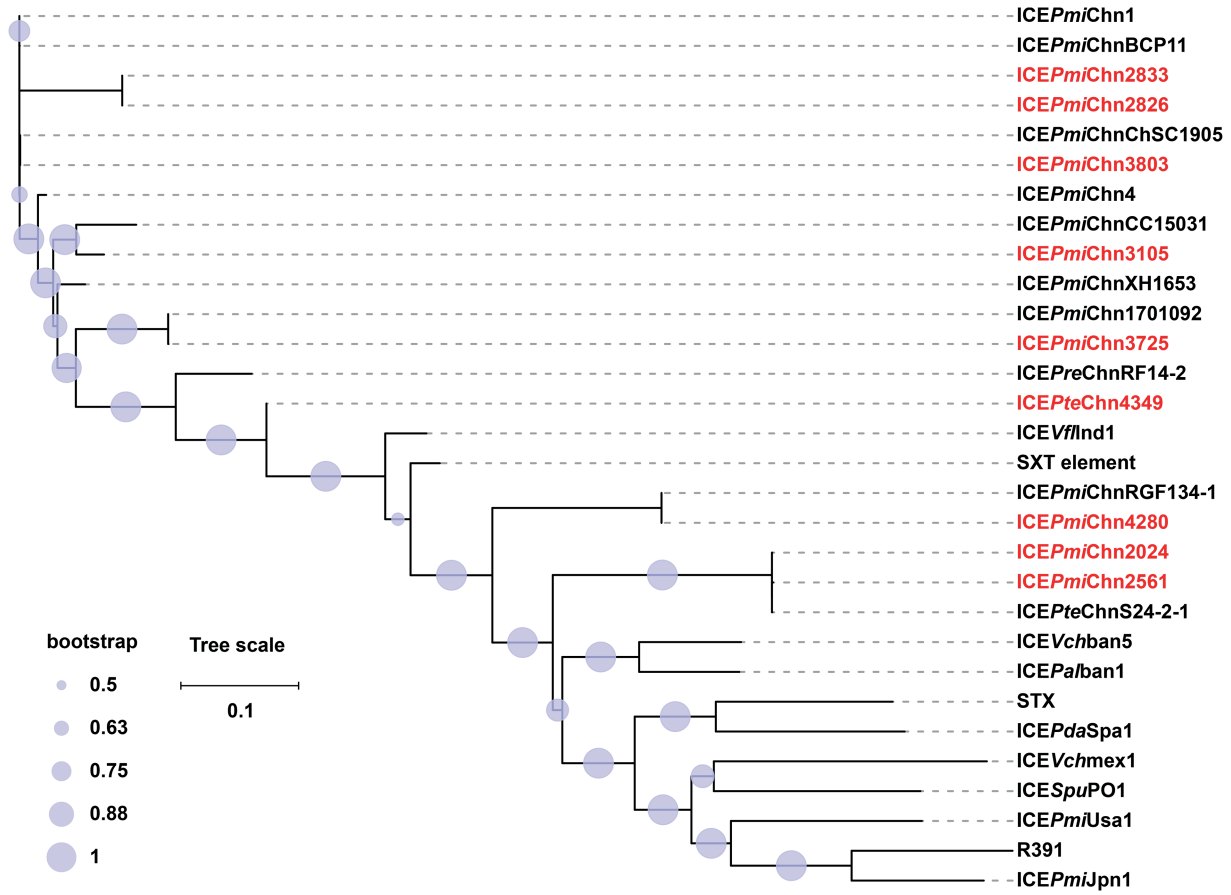

FIGURE 4
Phylogenetic analysis of ICEs in this study and 21 representative SXT/R391 ICEs. The phylogenetic tree of ICEs was constructed based on the SNPs in their conserved regions with the maximum-likelihood method in FastTree. ICEs in this study are highlighted in red. The tree scale indicates substitutions per site. Detailed information of these ICEs is presented in Supplementary Table S6.

We also detected the circular intermediate of ICEs by using the primers LE4 and RE4 as previously described (Lei et al., 2016). Results showed that the circular form of ICEs could be detected in all 14 ICE-harboring strains, revealing a potential transmission pattern of them. To determine the transfer ability of these ICEs, we selected three ICE-carrying isolates (FZP2826, FZP3725 and FZP4280) for the conjugation experiments. Results showed that ICE*Pmi*Chn3725 could be transferred to *E. coli* J53 at a frequency of $\sim 9 \times 10^{-5}$ transconjugants per recipient cell. Antimicrobial susceptibility analysis showed that the acquisition of ICE*Pmi*Chn3725 enables *E. coli* J53 to become resistant to gentamicin, cefotaxime, aztreonam, ampicillin/sulbactam, and trimethoprim/sulfamethoxazole (Supplementary Table S7), despite that resistance to aztreonam conferred by CTX-M-65 in FZP3725 remains within the sensitivity range. We hypothesize that the hydrolysis of aztreonam by CTX-M-65 is possibly inhibited in FZP3725 by an unknown regulatory mechanism, but it works normally in *E. coli* J53. The conjugation of ICE*Pmi*Chn2826 and ICE*Pmi*Chn4280 were failed despite repeated attempts, suggesting that both ICEs are not self-transmissible. The non-transferability of ICE*Pmi*Chn2826 may be caused by the truncated *traG,* and the deleted *traF* and *traH* (Figure 3).

Genetic features of the bla_{NDM-1}-harboring plasmid pNDM_FZP3105

P. mirabilis FZP2937 and FZP3105 were recovered from the same patient, and were sampled 18 days apart, from wound secretion and sanies, respectively. FZP2937 and FZP3105 are clonally related as they share identical core genomes (0 SNP). Despite that, the two strains exhibited different phenotypic resistance (Table 1), and the most noteworthy feature is that FZP3105 shows resistant to meropenem and ceftazidime, to which FZP2937 is susceptible. Genome data revealed that the later strain FZP3105 additionally acquired an NDM-1-producing MDR plasmid pNDM_FZP3105. This plasmid is 205,118 bp in size, and belongs to IncC ST3 (*A053-parA-parB-repA* allele number 1–2–2-2) incompatibility group. BLASTn analysis showed that it has >99.8% nucleotide identity (≥77% coverage) to pCMC307P_P2 (CP079626, *Klebsiella pneumoniae*, India), p13ARS_GMH0099

(LR697099, *K. pneumoniae*, United Kingdom), and pNDM-1_Dok01 (AP012208, *E. coli*, Japan; Figure 5A). pNDM_FZP3105 is a type 1/2 hybrid IncC plasmid, as it contains *orf1832* (characteristic of type 1) and Δ*rhs2* (characteristic of type 2), lacking of two additional sequences i1 and i2 (Harmer and Hall, 2014). The backbone of pNDM_FZP3105 is 112,618 bp in size with an average 51.05% G + C content. Nucleotide (nt) 56,193–126,943 of pNDM_FZP3105 showed 99.94% identity to that of type 1 IncC reference plasmid pR148 (JX141473, *Aeromonas hydrophila*, South Korea), and nt 1–2,522, 11,597–28,308, 163,334–165,885, and 185,018–205,098 showed 99.98% identity to that of type 2 IncC reference plasmid pR55 (JQ010984, *K. pneumoniae*, France; Supplementary Figure S1). Conjugation assays showed that pNDM_FZP3105 was able to conjugate into *E. coli* EC600, and the acquisition of pNDM_FZP3105 greatly increased meropenem resistance in EC600 by at least 8-fold (Supplementary Table S8).

pNDM_FZP3105 carries three accessory modules, namely the antibiotic resistance island (ARI)-A, ARI-B, and the IS*Cfr1-aac(3)-IId-tmrB* module. ARI-A (nt 127,160 to 163,333) is located immediately upstream of the 452 bp *rhs2* remnant (Figure 5B). Compared to the prototype ARI-A of a complex transposon structure bounded by 38-bp inverted repeats (IRs) of Tn*1696 tnp* and pDU *mer* modules interrupted by either IS*4321* or IS*5075* (Harmer and Hall, 2015), like the case in pRMH760 (KF976462, *K. pneumoniae*, Australia), ARI-A in pNDM_FZP3105 has only retained the IS*4321-tnpAR* structure, though it is interrupted by the Tn*6260* that is truncated by an IS*Pmi3* inside of *tnpA*. Instead of In*34* in ARI-A in pRMH760, an ΔIn*633*-like segment *intI1-dfrA14-arr-2-bla*$_{OXA-10}$*-aadA1-qacEΔ1-sul1*-IS*CR1* was present in pNDM_FZP3105, followed by a 6.5-kb region carrying an IS*Va9*, a DNA repair ATPase and three hypothetical proteins, and a 10.7-kb module IS*CR1*-IS*Ec28-rmtB*-IS*Ec29-msr*(E)-*mph*(E)-IS*15*. BLASTn analysis showed that ARI-A in pNDM_FZP3105 has 99.9% nucleotide identity at 59% coverage to plasmid unnamed5 (CP029118, *E. coli*, United States), but with genetic element insertions, deletions, and replacements (Figure 5B). These findings suggest that ARI-A in pNDM_FZP3105 is a novel MDR mosaic region. *Lnu*(G), which confers resistance to lincomycin by nucleotidylation, is commonly found on the chromosomes of Enterococcus, and also on the plasmids containing replicons of IncFIA(HI1), IncHI1A and IncHI1B(R27), or in combination with IncFII or IncX4 in Enterobacteriaceae (Li et al., 2021). To our knowledge, this is the first report of *lnu*(G) in an IncC plasmid.

bla$_{NDM}$ was found within ARI-B (nt 28,372–55,887) in pNDM_FZP3105, but not in ARI-A module as usually reported (Harmer and Hall, 2014; Wailan et al., 2016). When compared to pR55, ARI-B in pNDM_FZP3105 has gained two IS*26*-bracketed segments, a 9.0 kb *bla*$_{NDM-1}$-carrying ΔTn*125* and a 10.6 kb *aac(6′)-Ib-cr*-carrying region, causing the deletion of a 9.7 kb of the A/C2 backbone (immediately downstream of *orf312*), and the *int* end of GI*sul2*, but has retained a 2.4 kb *floR*-containing fragment and the last 2.8 kb of the *sul2* end of GI*sul2* (Figure 5C). Especially, the two copies of IS*26* surrounding ΔTn*125* have the potential to form a composite transposon to mobilize the intervening genetic components including *bla*$_{NDM-1}$. However, no 8-bp DRs were identified, indicating the occurrence of homologous recombination. Similar (>99.8% identity) IS*26*-ΔTn*125*-IS*26* unit was also found on several *Proteus* chromosomes and plasmids, suggesting an important role of IS*26* in the spread of *bla*$_{NDM-1}$ in *Proteus* species.

The IS*Cfr1-aac(3)-IId-tmrB* module, with the genetic structure *orf378*-IS*Cfr1*-ΔIS*Kox2*-IS*Aeme4-aac(3)-IId-tmrB*, is located 1,457 bp downstream of *repA*, breaking and truncating the *orf190* gene (encoding a hypothetical protein) downstream of *cysH* (Supplementary Figure S1). An insertion in this location is barely seen in IncC plasmids, and similar (>99% coverage, >99% identity) *aac(3)-IId-tmrB* module is only identified in pVFN3-blaOXA-193 K (CP089604, *Vibrio furnissii*, hospital sewage, China) by BLASTn analysis. The mobilization mechanism of the IS*Cfr1-aac(3)-IId-tmrB* module remains unknown.

Characteristics of *bla*$_{KPC-2}$-carrying *Proteus mirabilis* FZP2936 and FZP3115

FZP2936 and FZP3115 are two subsequent isolates from a single patient, from urine and wound secretion, respectively, 19 days apart. The two strains share identical core genomes as well as resistance profiles, showing the clonal nature of them. FZP2936 and FZP3115 both have a 4,245,458-bp circular chromosome and two closed plasmids. 15 ARGs were identified in both strains, and all of them, except *bla*$_{KPC-2}$, are located on the chromosome. *bla*$_{KPC-2}$ is present on 24,225-bp IncN plasmids pKPC_FZP2936 and pKPC_FZP3115, which are identical to the previously reported pT211(CP017083) from a clinical *P. mirabilis* strain T21 in 2013, in Zhejiang province (approximately 1,830 km apart in distance from Sichuan), China (Hua et al., 2020). The finding suggests the likelihood of a wide dissemination of the pT211-like *bla*$_{KPC-2}$-bearing plasmids in *proteus* in China, which warrant more surveillance. Given that FZP2936 and FZP3115 have close genetical relationship to strain T21 (7 SNPs; Figure 1), and that pT211 is not self-transferable as previously revealed (Hua et al., 2020), the diffusion of pT211-like plasmids is likely due to expansion of bacterial clones.

The *dfrA1-sat2-aadA1* gene cassettes in both strains are included in the Tn*7*-like transposon 20 bp downstream of the *glmS* gene on the chromosome, as described in *P. mirabilis* strain T21 (Hua et al., 2020). The remainder of the chromosomal ARGs were mainly clustered in a 64,829 bp MDR genomic island PmGRI1 (Lei et al., 2020), which was later identified as a variant of PmGRI1-YN9 (Ma et al., 2021; MW699445, *P. mirabilis*, animal, China) by BLASTn analysis. Compared to the configuration of PmGRI1-YN9, the PmGRI1 in FZP2936 (FZP3115) have two IS*26*-mediated excision situating 1,339 bp upstream and 533 bp downstream of *bla*$_{TEM-1B}$, with 14,053 bp and 20,022 bp in size, respectively, resulting in the loss of several ARGs (Figure 6). Besides, the

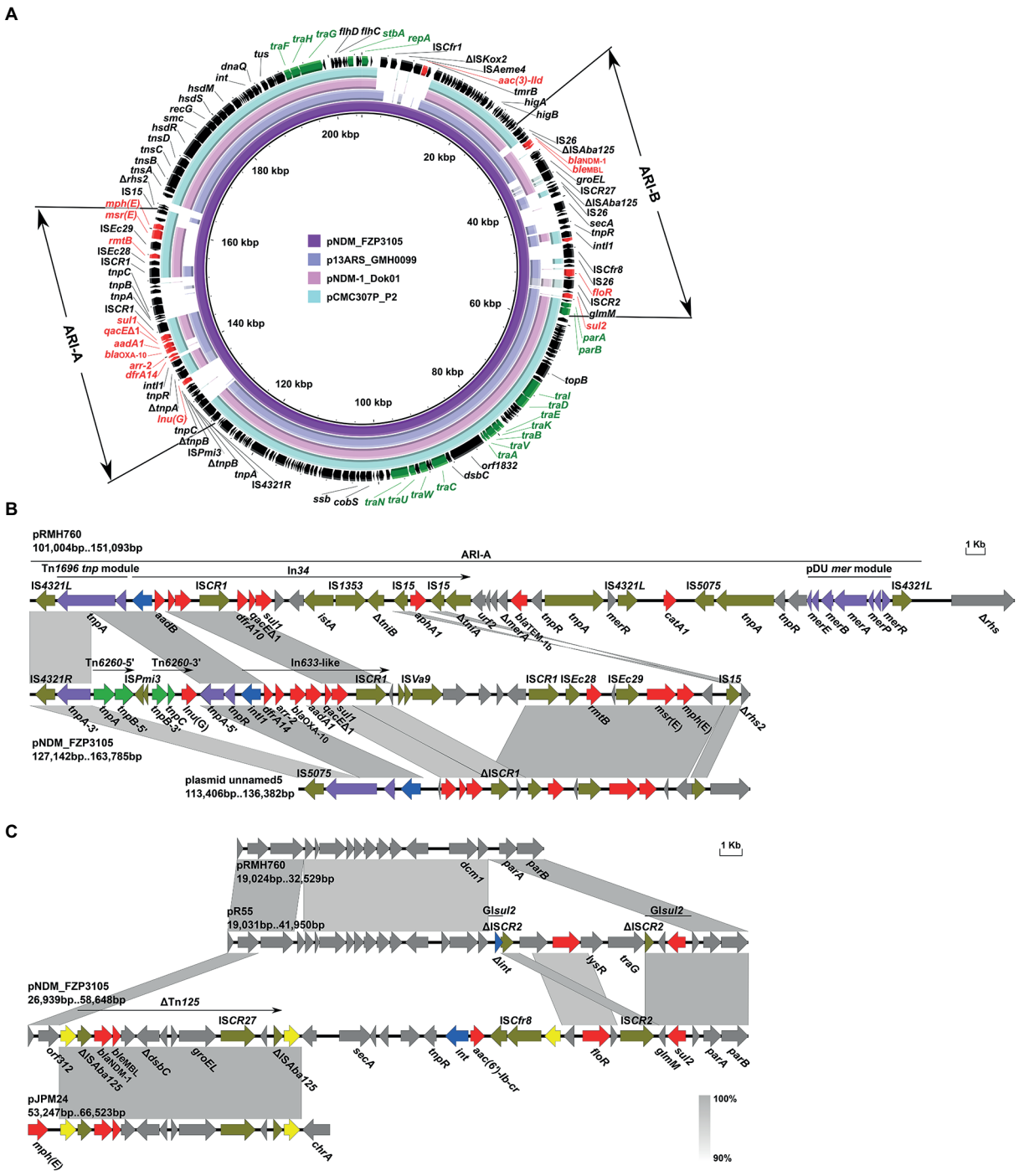

FIGURE 5
Genetic features of pNDM_FZP3105. **(A)** Circular comparison of pNDM_FZP3105 with pCMC307P_P2, p13ARS_GMH0099 and pNDM-1_Dok01. Arrows on the outer ring indicate deduced ORFs and their orientations. Genes for replication (*repA*), conjugal transfer (*tra*), and plasmid maintenance (*stbA*, *parAB*) are highlighted in green. ARGs are highlighted in red. Two antibiotic resistance islands, ARI-A and ARI-B, are indicated. **(B)** Organization of the ARI-A of pNDM_FZP3105, and comparisons to related regions. **(C)** Organization of the ARI-B of pNDM_FZP3105, and comparisons to related regions. Genes are denoted by arrows, and ARGs, integrase genes, IS*26*, and other transposase genes are highlighted in red, blue, yellow, and olive, respectively. The Tn*1696 tnp* and pDU *mer* modules are indicated in purple, and Tn6260 is in green. Regions of >90% identity are indicated by grey shading. Δ represents truncated genes.

PmGRI1 in this study was almost identical to that in *P. mirabilis* strain T21, except an IS*26*-mediated deletion of *aph(3′)-Ia* 1,491 bp downstream of $bla_{\text{TEM-1B}}$, and a *tnsB*-mediated reversal of a 7,275 bp region bearing a class I integron with the cassette array *dfrA17-addA5-qacEΔ1-sul1* (Figure 6). These results highlight the high plasticity of PmGRI1, and also reinforce the great ability of IS*26* to

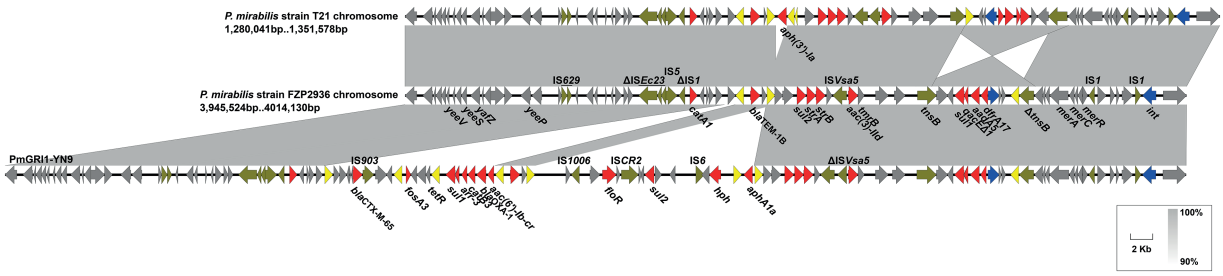

FIGURE 6
Genetic features of the multidrug-resistant genomic island in FZP2936. The genomic island in FZP2936 is compared with PmGRI1-YN9 and related region in *Proteus mirabilis* strain T21. Genes are denoted by arrows, and ARGs, integrase genes, IS*26*, and other transposase genes are highlighted in red, blue, yellow, and olive, respectively. Regions of >90% identity are indicated by grey shading. Δ represents truncated genes.

accumulate ARGs, and to promote the diversity of the multidrug resistance regions in mobile genetic elements (He et al., 2021).

PmGRI1 is a new GI carrying various resistance genes initially identified in a *P. mirabilis* strain from chicken in 2018 (Lei et al., 2020), and was later detected in several *P. mirabilis* isolates of swine and chicken origins in different locations of China (Ma et al., 2021). To determine the prevalence of PmGRI1 in *Proteus* isolates in the same hospital, we detected the PmGRI1 by searching the integrase gene *int* in the remaining 25 strains, and found that 10 of them were positive for the PmGRI1 integrase gene (Table 1). This finding indicates the possible prevalence of PmGRI1 variants in *Proteus* strains in both the animals and humans. More data is needed to better understand the epidemiology and dynamic evolution of PmGRI1 in China.

Conclusion

In this study, we demonstrated the genetic diversity of MDR *Proteus* strains and spotlighted the important roles of GIs, especially SXT/R391 ICEs, and plasmids in capturing and spreading ARGs in *Proteus*. Our study also raises concern that these MDR *Proteus* strains might be circulating and undergoing rapid evolution amongst animals and humans across China. From 'One Health' perspective, active surveillance for MDR *Proteus* in the environment is urgently needed.

Data availability statement

The datasets presented in this study can be found in online repositories. The names of the repository/repositories and accession number(s) can be found in the article/Supplementary material.

Author contributions

YL: conceptualization, formal analysis, and writing-original draft. QL, YQ, and HC: methodology, resources, and formal analysis. XD, CF, and LZ: methodology and software. YZ and JS: writing-review and editing. LZ: conceptualization, writing-review and editing, and supervision. All authors contributed to the article and approved the submitted version.

Funding

This work was supported by National Natural Science Foundation of China (31900125), Scientific and technological project in Sichuan Province (2022JDRC0144), the Joint Funds of the Luzhou and Southwest Medical University Natural Science Foundation (2019LZXNYDJ47 and 2020LZXNYDJ34), and Central Government Funds for Guiding Local Scientific and Technological Development of Sichuan Province (2021ZYD0084). The funders had no role in study design, data collection and interpretation, or the decision to submit the work for publication.

Conflict of interest

The authors declare that the research was conducted in the absence of any commercial or financial relationships that could be construed as a potential conflict of interest.

Publisher's note

All claims expressed in this article are solely those of the authors and do not necessarily represent those of their affiliated organizations, or those of the publisher, the editors and the reviewers. Any product that may be evaluated in this article, or claim that may be made by its manufacturer, is not guaranteed or endorsed by the publisher.

Supplementary material

The Supplementary material for this article can be found online at: https://www.frontiersin.org/articles/10.3389/fmicb.2022.977356/full#supplementary-material

References

Adeolu, M., Alnajar, S., Naushad, S., and Gupta, R. S. (2016). Genome-based phylogeny and taxonomy of the 'Enterobacteriales': proposal for Enterobacterales ord. nov. divided into the families Enterobacteriaceae, Erwiniaceae fam. nov., Pectobacteriaceae fam. nov., Yersiniaceae fam. nov., Hafniaceae fam. nov., Morganellaceae fam. nov., and Budviciaceae fam. nov. *Int. J. Syst. Evol. Microbiol.* 66, 5575–5599. doi: 10.1099/ijsem.0.001485

Aziz, R. K., Bartels, D., Best, A. A., DeJongh, M., Disz, T., Edwards, R. A., et al. (2008). The RAST server: rapid annotations using subsystems technology. *BMC Genomics* 9:75. doi: 10.1186/1471-2164-9-75

Balado, M., Lemos, M. L., and Osorio, C. R. (2013). Integrating conjugative elements of the SXT/R391 family from fish-isolated Vibrios encode restriction-modification systems that confer resistance to bacteriophages. *FEMS Microbiol. Ecol.* 83, 457–467. doi: 10.1111/1574-6941.12007

Bioteau, A., Durand, R., and Burrus, V. (2018). Redefinition and unification of the SXT/R391 family of integrative and conjugative elements. *Appl. Environ. Microbiol.* 84, e00485–18. doi: 10.1128/AEM.00485-18

Bonnin, R. A., Girlich, D., Jousset, A. B., Gauthier, L., Cuzon, G., Bogaerts, P., et al. (2020). A single *Proteus mirabilis* lineage from human and animal sources: a hidden reservoir of OXA-23 or OXA-58 carbapenemases in Enterobacterales. *Sci. Rep.* 10:9160. doi: 10.1038/s41598-020-66161-z

Bortolaia, V., Kaas, R. S., Ruppe, E., Roberts, M. C., Schwarz, S., Cattoir, V., et al. (2020). ResFinder 4.0 for predictions of phenotypes from genotypes. *J. Antimicrob. Chemother.* 75, 3491–3500. doi: 10.1093/jac/dkaa345

Boutet, E., Lieberherr, D., Tognolli, M., Schneider, M., Bansal, P., Bridge, A. J., et al. (2016). UniProtKB/Swiss-Prot, the manually annotated section of the UniProt KnowledgeBase: how to use the entry view. *Methods Mol. Biol.* 1374, 23–54. doi: 10.1007/978-1-4939-3167-5_2

Carattoli, A., and Hasman, H. (2020). PlasmidFinder and *in silico* pMLST: identification and typing of plasmid replicons in whole-genome sequencing (WGS). *Methods Mol. Biol.* 2075, 285–294. doi: 10.1007/978-1-4939-9877-7_20

Falagas, M. E., and Karageorgopoulos, D. E. (2008). Pandrug resistance (PDR), extensive drug resistance (XDR), and multidrug resistance (MDR) among Gram-negative bacilli: need for international harmonization in terminology. *Clin. Infect. Dis.* 46, 1121–1122. doi: 10.1086/528867

Fursova, N. K., Astashkin, E. I., Knyazeva, A. I., Kartsev, N. N., Leonova, E. S., Ershova, O. N., et al. (2015). The spread of bla OXA-48 and bla OXA-244 carbapenemase genes among *Klebsiella pneumoniae*, *Proteus mirabilis* and *Enterobacter* spp. isolated in Moscow, Russia. *Ann. Clin. Microbiol. Antimicrob.* 14:46. doi: 10.1186/s12941-015-0108-y

Harada, S., Ishii, Y., Saga, T., Tateda, K., and Yamaguchi, K. (2010). Chromosomally encoded bla_{CMY-2} located on a novel SXT/R391-related integrating conjugative element in a *Proteus mirabilis* clinical isolate. *Antimicrob. Agents Chemother.* 54, 3545–3550. doi: 10.1128/AAC.00111-10

Harmer, C. J., and Hall, R. M. (2014). pRMH760, a precursor of A/C(2) plasmids carrying bla_{CMY} and bla_{NDM} genes. *Microb. Drug Resist.* 20, 416–423. doi: 10.1089/mdr.2014.0012

Harmer, C. J., and Hall, R. M. (2015). The A to Z of A/C plasmids. *Plasmid* 80, 63–82. doi: 10.1016/j.plasmid.2015.04.003

He, J., Sun, L., Zhang, L., Leptihn, S., Yu, Y., and Hua, X. (2021). A novel SXT/R391 integrative and conjugative element carries two copies of the bla_{NDM-1} Gene in *Proteus mirabilis*. *mSphere* 6:e0058821. doi: 10.1128/mSphere.00588-21

Hu, Y. Y., Cai, J. C., Zhang, R., Zhou, H. W., Sun, Q., and Chen, G. X. (2012). Emergence of *Proteus mirabilis* harboring bla_{KPC-2} and *qnrD* in a Chinese hospital. *Antimicrob. Agents Chemother.* 56, 2278–2282. doi: 10.1128/AAC.05519-11

Hua, X., Zhang, L., Moran, R. A., Xu, Q., Sun, L., van Schaik, W., et al. (2020). Cointegration as a mechanism for the evolution of a KPC-producing multidrug resistance plasmid in *Proteus mirabilis*. *Emerg. Microbes. Infect.* 9, 1206–1218. doi: 10.1080/22221751.2020.1773322

Johnson, C. M., and Grossman, A. D. (2015). Integrative and conjugative elements (ICEs): what they do and how they work. *Annu. Rev. Genet.* 49, 577–601. doi: 10.1146/annurev-genet-112414-055018

Korytny, A., Riesenberg, K., Saidel-Odes, L., Schlaeffer, F., and Borer, A. (2016). Bloodstream infections caused by multi-drug resistant *Proteus mirabilis*: epidemiology, risk factors and impact of multi-drug resistance. *Infect. Dis.* 48, 428–431. doi: 10.3109/23744235.2015.1129551

Lane, D. J. (1991). "16S/23S rRNA sequencing," in *Nucleic Acid Techniques in Bacterial Systematic*. eds. E. Stackebrandt and M. Goodfellow (New York, NY: John Wiley and Sons), 115–175.

Lei, C. W., Chen, Y. P., Kang, Z. Z., Kong, L. H., and Wang, H. N. (2018). Characterization of a novel SXT/R391 integrative and conjugative element carrying *cfr*, $bla_{CTX-M-65}$, *fosA3*, and *aac(6′)-Ib-cr* in *Proteus mirabilis*. *Antimicrob. Agents Chemother.* 62, e00849–18. doi: 10.1128/AAC.00849-18

Lei, C. W., Yao, T. G., Yan, J., Li, B. Y., Wang, X. C., Zhang, Y., et al. (2020). Identification of *Proteus* genomic island 2 variants in two clonal *Proteus mirabilis* isolates with coexistence of a novel genomic resistance island PmGRI1. *J. Antimicrob. Chemother.* 75, 2503–2507. doi: 10.1093/jac/dkaa215

Lei, C. W., Zhang, A. Y., Wang, H. N., Liu, B. H., Yang, L. Q., and Yang, Y. Q. (2016). Characterization of SXT/R391 integrative and conjugative elements in *Proteus mirabilis* isolates from food-producing animals in China. *Antimicrob. Agents Chemother.* 60, 1935–1938. doi: 10.1128/AAC.02852-15

Li, Y., Qiu, Y., Gao, Y., Chen, W., Li, C., Dai, X., et al. (2022). Genetic and virulence characteristics of a *Raoultella planticola* isolate resistant to carbapenem and tigecycline. *Sci. Rep.* 12:3858. doi: 10.1038/s41598-022-07778-0

Li, Y., Qiu, Y., She, J., Wang, X., Dai, X., and Zhang, L. (2021). Genomic characterization of a *Proteus* sp. strain of animal origin co-carrying bla_{NDM-1} and *lnu (G)*. *Antibiotics* 10:1411. doi: 10.3390/antibiotics10111411

Ma, B., Wang, X., Lei, C., Tang, Y., He, J., Gao, Y., et al. (2021). Identification of three novel PmGRI1 genomic resistance islands and one multidrug resistant hybrid structure of Tn7-like transposon and PmGRI1 in *Proteus mirabilis*. *Antibiotics* 10:1268. doi: 10.3390/antibiotics10101268

Moura, A., Soares, M., Pereira, C., Leitao, N., Henriques, I., and Correia, A. (2009). INTEGRALL: a database and search engine for integrons, integrases and gene cassettes. *Bioinformatics* 25, 1096–1098. doi: 10.1093/bioinformatics/btp105

O'Hara, C. M., Brenner, F. W., and Miller, J. M. (2000). Classification, identification, and clinical significance of *Proteus*, *Providencia*, and *Morganella*. *Clin. Microbiol. Rev.* 13, 534–546. doi: 10.1128/CMR.13.4.534

Partridge, S. R., Kwong, S. M., Firth, N., and Jensen, S. O. (2018). Mobile genetic elements associated with antimicrobial resistance. *Clin. Microbiol. Rev.* 31, e00088–17. doi: 10.1128/CMR.00088-17

Peng, K., Li, R., He, T., Liu, Y., and Wang, Z. (2020). Characterization of a porcine *Proteus cibarius* strain co-harbouring *tet*(X6) and *cfr*. *J. Antimicrob. Chemother.* 75, 1652–1654. doi: 10.1093/jac/dkaa047

Rodriguez-Blanco, A., Lemos, M. L., and Osorio, C. R. (2012). Integrating conjugative elements as vectors of antibiotic, mercury, and quaternary ammonium compound resistance in marine aquaculture environments. *Antimicrob. Agents Chemother.* 56, 2619–2626. doi: 10.1128/AAC.05997-11

Sato, J. L., Fonseca, M. R. B., Cerdeira, L. T., Tognim, M. C. B., Sincero, T. C. M., Noronha do Amaral, M. C., et al. (2020). Genomic analysis of SXT/R391 integrative conjugative elements From *Proteus mirabilis* isolated in Brazil. *Front. Microbiol.* 11:571472. doi: 10.3389/fmicb.2020.571472

Schaffer, J. N., and Pearson, M. M. (2015). *Proteus mirabilis* and urinary tract infections. *Microbiol. Spectr.* 3, UTI-0017–2013. doi: 10.1128/microbiolspec.UTI-0017-2013

Siguier, P., Perochon, J., Lestrade, L., Mahillon, J., and Chandler, M. (2006). ISfinder: the reference centre for bacterial insertion sequences. *Nucleic Acids Res.* 34, D32–D36. doi: 10.1093/nar/gkj014

Slattery, S., Tony Pembroke, J., Murnane, J. G., and Ryan, M. P. (2020). Isolation, nucleotide sequencing and genomic comparison of a Novel SXT/R391 ICE mobile genetic element isolated from a municipal wastewater environment. *Sci. Rep.* 10:8716. doi: 10.1038/s41598-020-65216-5

Sullivan, M. J., Petty, N. K., and Beatson, S. A. (2011). Easyfig: a genome comparison visualizer. *Bioinformatics* 27, 1009–1010. doi: 10.1093/bioinformatics/btr039

Tumbarello, M., Trecarichi, E. M., Fiori, B., Losito, A. R., D'Inzeo, T., Campana, L., et al. (2012). Multidrug-resistant *Proteus mirabilis* bloodstream infections: risk factors and outcomes. *Antimicrob. Agents Chemother.* 56, 3224–3231. doi: 10.1128/AAC.05966-11

Wailan, A. M., Sidjabat, H. E., Yam, W. K., Alikhan, N. F., Petty, N. K., Sartor, A. L., et al. (2016). Mechanisms involved in acquisition of bla_{NDM} genes by IncA/C2 and IncFIIY plasmids. *Antimicrob. Agents Chemother.* 60, 4082–4088. doi: 10.1128/AAC.00368-16

Walker, B. J., Abeel, T., Shea, T., Priest, M., Abouelliel, A., Sakthikumar, S., et al. (2014). Pilon: an integrated tool for comprehensive microbial variant detection and genome assembly improvement. *PLoS One* 9:e112963. doi: 10.1371/journal.pone.0112963

Wang, Q., Peng, K., Liu, Y., Xiao, X., Wang, Z., and Li, R. (2021). Characterization of TMexCD3-TOprJ3, an RND-type efflux system conferring resistance to tigecycline in *Proteus mirabilis*, and its associated integrative conjugative element. *Antimicrob. Agents Chemother.* 65:e0271220. doi: 10.1128/AAC.02712-20

Wick, R. R., Judd, L. M., Gorrie, C. L., and Holt, K. E. (2017). Unicycler: resolving bacterial genome assemblies from short and long sequencing reads. *PLoS Comput. Biol.* 13:e1005595. doi: 10.1371/journal.pcbi.1005595

Wozniak, R. A., Fouts, D. E., Spagnoletti, M., Colombo, M. M., Ceccarelli, D., Garriss, G., et al. (2009). Comparative ICE genomics: insights into the evolution of the SXT/R391 family of ICEs. *PLoS Genet.* 5:e1000786. doi: 10.1371/journal.pgen.1000786

frontiers | Frontiers in Microbiology

TYPE Review
PUBLISHED 29 September 2022
DOI 10.3389/fmicb.2022.969769

OPEN ACCESS

EDITED BY
Xingmin Sun,
University of South Florida, United States

REVIEWED BY
Fangkun Wang,
Shandong Agricultural University, China
Li Yan,
Yangzhou University, China
Chaoyue Cui,
Wenzhou Medical University, China

*CORRESPONDENCE
Shaqiu Zhang
shaqiu86@hotmail.com
Anchun Cheng
chenganchun@vip.163.com

†These authors have contributed equally to this work and share first authorship

SPECIALTY SECTION
This article was submitted to Antimicrobials, Resistance and Chemotherapy, a section of the journal Frontiers in Microbiology

RECEIVED 15 June 2022
ACCEPTED 05 September 2022
PUBLISHED 29 September 2022

CITATION
Zhang S, Wen J, Wang Y, Wang M, Jia R, Chen S, Liu M, Zhu D, Zhao X, Wu Y, Yang Q, Huang J, Ou X, Mao S, Gao Q, Sun D, Tian B and Cheng A (2022) Dissemination and prevalence of plasmid-mediated high-level tigecycline resistance gene *tet* (X4). *Front. Microbiol.* 13:969769. doi: 10.3389/fmicb.2022.969769

Dissemination and prevalence of plasmid-mediated high-level tigecycline resistance gene *tet* (X4)

Shaqiu Zhang[1,2,3*†], Jinfeng Wen[1†], Yuwei Wang[4†], Mingshu Wang[1,2,3], Renyong Jia[1,2,3], Shun Chen[1,2,3], Mafeng Liu[1,2,3], Dekang Zhu[1,3], Xinxin Zhao[1,2,3], Ying Wu[1,2,3], Qiao Yang[1,2,3], Juan Huang[1,2,3], Xumin Ou[1,2,3], Sai Mao[1,2,3], Qun Gao[1,2,3], Di Sun[1,2,3], Bin Tian[1,2,3] and Anchun Cheng[1,2,3*]

[1]Avian Disease Research Center, College of Veterinary Medicine, Sichuan Agricultural University, Chengdu, China, [2]Institute of Preventive Veterinary Medicine, Sichuan Agricultural University, Chengdu, China, [3]Key Laboratory of Animal Disease and Human Health of Sichuan Province, Sichuan Agricultural University, Chengdu, China, [4]Mianyang Academy of Agricultural Sciences, Mianyang, China

With the large-scale use of antibiotics, antibiotic resistant bacteria (ARB) continue to rise, and antibiotic resistance genes (ARGs) are regarded as emerging environmental pollutants. The new tetracycline-class antibiotic, tigecycline is the last resort for treating multidrug-resistant (MDR) bacteria. Plasmid-mediated horizontal transfer enables the sharing of genetic information among different bacteria. The tigecycline resistance gene *tet*(X) threatens the efficacy of tigecycline, and the adjacent IS*CR2* or IS*26* are often detected upstream and downstream of the *tet*(X) gene, which may play a crucial driving role in the transmission of the *tet*(X) gene. Since the first discovery of the plasmid-mediated high-level tigecycline resistance gene *tet*(X4) in China in 2019, the *tet*(X) genes, especially *tet*(X4), have been reported within various reservoirs worldwide, such as ducks, geese, migratory birds, chickens, pigs, cattle, aquatic animals, agricultural field, meat, and humans. Further, our current researches also mentioned viruses as novel environmental reservoirs of antibiotic resistance, which will probably become a focus of studying the transmission of ARGs. Overall, this article mainly aims to discuss the current status of plasmid-mediated transmission of different *tet*(X) genes, in particular *tet*(X4), as environmental pollutants, which will risk to public health for the "One Health" concept.

KEYWORDS

antibiotic resistant bacteria, tigecycline resistance gene, plasmid-mediated, tet(X4), transmission, one health

Introduction

The discovery of antibiotics is a milestone event in human medicine. With the large-scale use of antibiotics, while reducing the morbidity and mortality of bacterial infections, strains carrying different antibiotic resistance genes (ARGs) appeared and spread rapidly (Davies and Davies, 2010; Ahmad and Khan, 2019). The global sales of antimicrobials are estimated to reach 104,079 tons in 2030, an increase of 11.5% since 2017 (Tiseo et al., 2020). Antimicrobial resistance (AMR) is one of the public health issues of widely concern around the world, and ARGs are regarded as new environmental pollutants (Plantinga et al., 2015; Zhang et al., 2020c). Tetracycline have many desirable properties of antibiotics, such as their excellent anti-bacterial activity and oral benefits. They have been widely used in the treatment of human and animal infections or as animal growth-promoting feed additives (Roberts, 2003). However, only a small part of tetracycline can be absorbed after entering the body, and more than 75% of tetracycline will be excreted in the form of a prototype or metabolite (Liao et al., 2021).

Tigecycline belonged to tetracycline-class drugs, is a new class of glycylcycline antibiotics, approved by the FDA in 2005 (Wenzel et al., 2005; Stein and Babinchak, 2013; Hirabayashi et al., 2021). It has broad-spectrum anti-bacterial activity, especially against multidrug-resistant (MDR) gram-negative bacteria (Zha et al., 2020). Tigecycline is also considered as a drug of last resort to combat bacterial infections, and which is mainly used for the treatment of infections within skin tissue, anti-tumor, bacterial pneumonia, and complex intra-abdominal (Olson et al., 2006; Kaewpoowat and Ostrosky-Zeichner, 2015; Zhao et al., 2021). Furthermore, it is a third-generation tetracycline-class antibiotic, which was improved by adding a 9-tert-butyl-glycylamido side-chain modification structure to the central framework of minocycline, and thereby forming a steric hindrance, overcoming normal mechanisms of resistance to tetracyclines, such as parts of the efflux pump mechanism[*tet*(A-E), *tet*(K)] and ribosome protection mechanism[*tet*(M)] (Chopra, 2002; Livermore, 2005; Linkevicius et al., 2016). Tigecycline can act on bacterial ribosomes and inhibit bacterial protein synthesis by interfering with aminoacyl-tRNA binding to ribosomes (Chopra and Roberts, 2001). We have gathered, appraised, and reviewed the accessible relevant literature from online sources, including Science Direct, PubMed, and Google Scholar. The keywords were included but not limited to *tet*(X) genes, *Escherichia coli* (*E. coli*), IS*CR2*, IS*26*, antibiotic resistant bacteria (ARB), AMR, ARGs, MDR, plasmids, environmental pollutants, public health, resistance contact, clinical and veterinary settings. Moreover, the cited references were also explored for further referencing. This article summarized the mechanisms of tigecycline resistance and the prevalence of the plasmid-mediated high-level tigecycline resistance gene *tet*(X4) among the environment, animals, and humans. In addition, the origin of the *tet*(X) and the importance of mobile genetic elements (MGEs) during the dissemination of the *tet*(X) are discussed. The purpose of this article is to collect and organize the information available so far in one platform, and to provide a bridge for readers to understand that the prevalence of plasmid-mediated high-level tigecycline resistance genes, which can contaminate the natural environment, and further risking to public health. Moreover, we also made a positive outlook for the transmission of ARGs by viruses.

Mechanism of tigecycline resistance

At present, the main mechanisms of bacterial resistance to tigecycline are efflux pump mechanism, cell membrane pore channel protein variation, ribosome protection mechanism, and drug-degrading enzyme mechanism (Figure 1).

Efflux pump mechanism

An active efflux pump is a protein transport system of bacteria, it can excrete antibiotics entering the bacteria from itself, reducing antibiotic concentration in bacteria, so as to promote the growth of ARB (Venter et al., 2015; Bankan et al., 2021). There are five main efflux pump families involved in the active efflux of antibiotics, one is the ATP binding cassette (ABC) superfamily, which is the "primary active" transporter that directly uses ATP binding and hydrolysis to drive the free efflux of drugs (Rempel et al., 2019). The other four families are secondary active transport proteins, which are energy-acquiring transporters with proton pumps, including the major facilitator super (MFS) family, multidrug and toxic compound extrusion (MATE) family, small multidrug resistance (SMR) family, and resistance modulation division (RND) superfamily (Kumar et al., 2016; Lamut et al., 2019). In Gram-negative bacteria, overexpression of MFS family and RND family efflux pumps plays a significant role in tigecycline resistance, such as Tet(A), AcrAB-TolC, OqxAB, and AdeABC (Ruzin et al., 2007; Zhong et al., 2014; Chen et al., 2017), Tet(A) and AcrAB-TolC efflux pumps have been studied relatively comprehensively (Munita and Arias, 2016), their coding genes can be located on chromosomes or plasmids and can be transmitted *via* plasmids or transposons (Sheykhsaran et al., 2019). As a tetracycline efflux pump gene, *tet*(A) has no effect on tigecycline sensitivity (Fluit et al., 2005), but studies showed the double frameshift mutation of *tet*(A) can make strains resistant to tigecycline at a low level (Hentschke et al., 2010; Akiyama et al., 2013). A new RND type efflux pump gene cluster, named *tmexCD1-toprJ1*, was first identified in *Klebsiella pneumoniae* (*K. pneumonia*) in 2020. *TmexCD1-toprJ1* is widely present in *K. pneumoniae*, leading to a 4–32 fold increase in the minimal inhibitory concentration (MIC) of *K. pneumoniae* to tigecycline and eravacycline (Lv L. et al., 2020).

Cell membrane porin variation

The 1-acyl-3-glycerol phosphatidyl transferase encoded by the *plsC* gene is located on the cell membrane of *E. coli*, and its

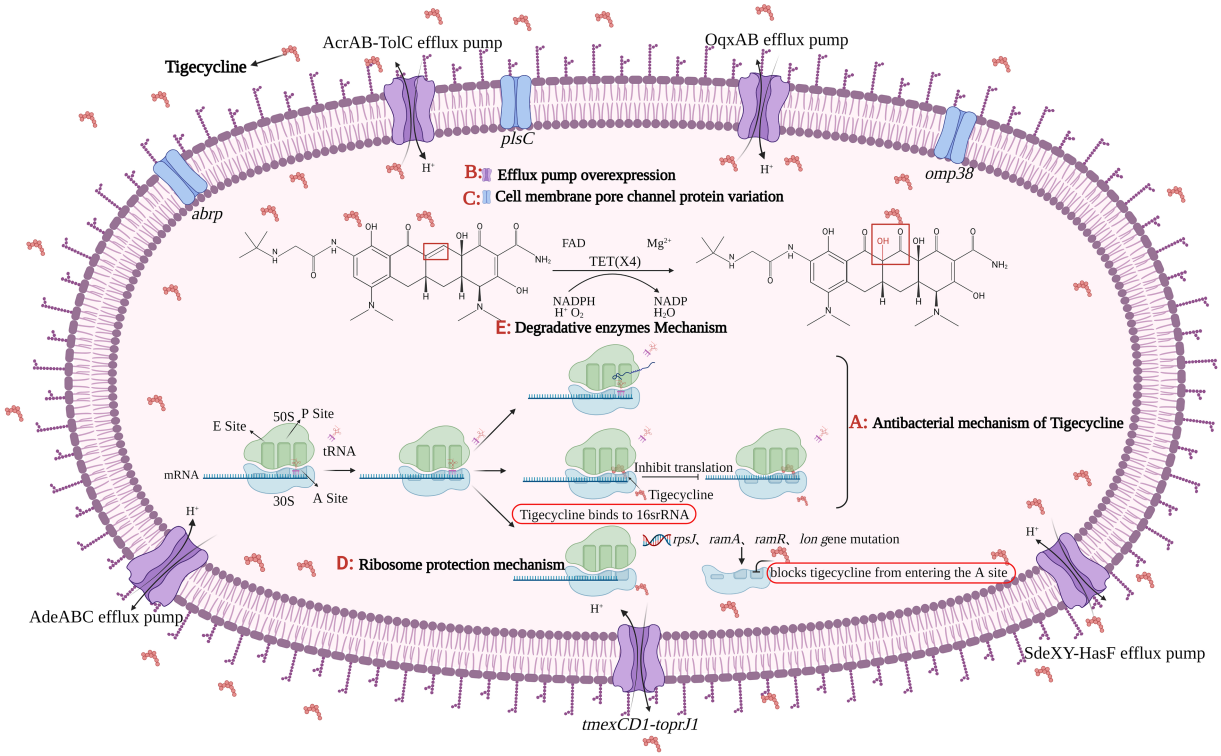

FIGURE 1
The figure was created with "BioRender.com" showing antibacterial mechanism and drug resistance mechanism of Tigecycline. **(A)** Tigecycline can act on bacterial ribosomes. After entering bacteria, tigecycline reversibly binds to the 16S rRNA in the 30S subunit of the ribosome, preventing tRNA from entering the A site, which eventually inhibits the process of transcription and translation in protein synthesis. There are four main tigecycline resistance mechanisms: **(B)** efflux pump overexpression; **(C)** cell membrane porin mutation; **(D)** ribosomal protection and **(E)** degrading enzyme mechanism. Among them, the expression product of plasmid-mediated *tet*(X4) gene belongs to the core member of degradative enzyme mechanism, and the Tet(X4) can catalyze the selective hydroxylation of tigecycline in the presence of FAD, Mg^{2+}, O_2 and NADPH, thus making tigecycline ineffective.

primary function is to catalyze the synthesis of phospholipids, and then participate in the biosynthesis of bacterial cell membranes (Lu et al., 2005). By inducing *Acinetobacter baumannii* (*A. baumannii*) to be resistant to tigecycline, the researchers performed whole-genome sequencing analysis of the strains before and after induction, and found three factors that could reduce the sensitivity of tigecycline, which were the frameshift mutation of *plsC* and *omp38* as well as SNP synonymous mutation (Li et al., 2015). A new *abrp* gene was found in *A. baumannii*, which encodes the C13 family of peptidases and makes the bacteria less sensitive to tigecycline (Li et al., 2016).

Ribosome protection mechanisms

The *rpsJ* gene can encode the production of the ribosomal structural protein S10. When there is a 12 bp deletion in *rpsJ*, the amino acid Rath at positions 53–56 of the S10 protein will be removed, resulting in a change in the binding site of tigecycline and bacteria, making bacteria resistant to tigecycline (Beabout et al., 2015; Bender et al., 2020). In addition to the S10 protein, mutations in the S3 and S13 proteins can also make bacteria resistant to tigecycline (Lupien et al., 2015). In *K. pneumoniae*, mutations in the *ramR* operon, *ramA*, *lon*, and *rpsJ* genes result in decreasing bacterial sensitivity to tigecycline (Fang et al., 2016). Mutation of *rpsJ* in *Enterococci* also leads to resistance to tigecycline (Cattoir et al., 2015). Mutations in the *rff*, *ropB* and *adeS* genes in *A. baumannii* can affect the normal function of the ribosome and thus confer tigecycline resistance to the strain (Hua et al., 2021).

Mechanism of drug enzymatic degradation

Tet(X) is a FAD-dependent monooxygenase that regioselectively hydroxylates tetracycline substrates, leading to the non-enzymatic breakdown of an unstable compound (Ghosh et al., 2015). Tet(X) can only produce effect in the presence of FAD, NADPH, Mg^{2+}, and O_2 at the same time (Moore et al., 2005). Researchers proved that tigecycline was a substrate of Tet(X) by X-ray crystallography (Volkers et al., 2011), and in fact, Tet(X) can effectively degrade almost all tetracycline antibiotics, making bacteria resistant to tetracycline (Ghosh et al., 2015; Xu et al.,

2022). *Tet*(X) gene was originally isolated from the anaerobic bacteria *Bacteroides fragilis* (Speer et al., 1991), however, according to recent reports, *tet*(X) appeared in *Riemerella anatipestifer* (*R. anatipestifer*) as early as the 1860s (Zhang et al., 2021a). In 2004, the *tet*(X) gene and its variant *tet*(X2) were discovered in anaerobic *Bacteroides*, then pointing out Tet(X) can degrade tigecycline, although it showed low levels of resistance to tigecycline, this phenomenon would still exist when *tet*(X) was transferred into *E. coli* (Guiney et al., 1984; Yang et al., 2004). Various *tet*(X) gene variants mediate different levels of tigecycline resistance. Compared with the Tet(X-X7), the enzymatic activity of the Tet(X4) has increased significantly. Researchers found five key residues (H231, M372, E43, R114, D308) could affect Tet(X4) enzyme activity in the tetracycline and FAD binding regions of the Tet(X4) (Xu et al., 2019). Subsequently, a new study has identified five mutants (L282S, A339T, D340N, V350I and K351E) in the structural domain of Tet(X2) when compared to Tet(X4), and demonstrated that the MIC of tigecycline increased 2–8 folds, when these five amino acid residues were mutated in the Tet(X2)-producing strain (Cui et al., 2021).

The plasmid-mediated tigecycline resistance genes *tet*(X3) and *tet*(X4) were first isolated from animal samples in 2019, which mediate high levels of antibiotic resistance to tigecycline, the MIC value can reach 32–64 mg/l (He et al., 2019). *Tet*(X4) is most commonly found in mobile plasmids and occasionally in chromosomes (Sun J. et al., 2019, 2020; Li et al., 2020b). Since the report of *tet*(X3/4), the degradative enzyme mechanism has gained more and more attention (He et al., 2019; Xu et al., 2022). At present, bismuth drugs and plumbagin can be used as Tet(X) inhibitors to improve the sensitivity of strains to tigecycline, which provides a new therapeutic strategy for the treatment of tigecycline-resistant bacterial infections (Deng et al., 2022; Xu et al., 2022).

Origin and spread of *tet*(X4)

Although, the *tet*(X) gene was first isolated from the anaerobic *Bacteroidetes*, the current study points the origin of the *tet*(X) to *R. anatipestifer*, the *tet*(X) and its variants share the same ancestry with the monooxygenase gene carried in the chromosomes of *Flavobacteriaceae* bacteria. In Zhu's study, 170 of 212 strains of *R. anatipestifer* carried the *tet*(X) gene (Zhu et al., 2018). Among 6,692 strains isolated from 13 different hospitals, almost all of the *tet*(X)-positive strains belonged to the *Flavobacteriaceae*. They then performed a phylogenetic analysis of the different evolutionary patterns of *tet*(X), in which one of the pathways involving the *Flavobacteriaceae* produced a major evolutionary branch, suggesting that it can be considered as the potential ancestral source of *tet*(X) (Zhang et al., 2020a). Umar et al. collect 57 non-repetitive sequences of *R. anatipestifer* in GenBank, of which *tet*(X) gene was detected in 47 genomes, and they have high similarity when compared with *tet*(X4) gene (Umar et al., 2021). The same finding was also reported in other study (Cui et al., 2021). When analyzing the evolutionary trajectory of the *tet*(X) gene, they found that most of the *tet*(X)-positive strains belonged to the *Flavobacteriaceae*, it has a higher detection rate than other species and is widely distributed in different clades of *tet*(X). Their latest study also inferred that the *tet*(X) gene originated in *Flavobacteriaceae* and can be transmitted to environmental and clinical strains such as *E. coli* and *Acinetobacter* with the help of the mobilization of IS*CR2* element (Chen et al., 2020).

The MGE such as IS*CR2* and IS*26* are essential for the spread of *tet*(X) gene. A 4608 bp element consisting of an IS*CR2*, a *tet*(X4) and a partner gene *catD* forms a canonical RC transposable unit (RC-TU) mediated by IS*CR2*, of which the 2,760 bp element of *catD-tet*(X4) is highly conserved. When transposition occurs, the IS*CR2-catD-tet*(X4)-IS*CR2* composite transposon structure is often generated, and the upstream or downstream of IS*CR2* element may be inserted and truncated by other IS elements, such as IS*26* (Chen et al., 2021; Liu et al., 2022). In addition, only single-copy IS*CR2* elements was sufficient to transpose adjacent DNA sequences through the process of rolling circle transposition (Poirel et al., 2009; Partridge et al., 2018). IS*26* was also often found in plasmids resistant to antibiotics, and it can participate in the progress of plasmid fusion and gene recombination (He et al., 2015; Du et al., 2020; Li et al., 2020b), and IS*26* can also be inserted into both ends of RC-TU, allowing IS*CR2* residues-*tet*(X4) to spread through a novel transmission mechanism (Liu et al., 2022). It has been found that the IS*CR2* element is frequent adjacent to *tet*(X4) or other *tet*(X) variants, which suggests IS*CR2* is more likely to participate in spread of *tet*(X) variants (Wang L. et al., 2019; Liu et al., 2020; Fu et al., 2021). In a conserved genetic environment and uncertain transferability among different bacteria, the co-action of IS*CR2* and IS*26* may be the main driving forces for the widespread of *tet*(X4; Dai et al., 2022; Zhang et al., 2022).

Prevalence of *tet*(X4)

Tetracycline resistance genes speculated to be of environmental origin but are now widely distributed in commensal and pathogenic bacteria (Thaker et al., 2010). The extensive use of first or second-generation tetracycline-class drugs played a major role in the emergance of tetracycline resistance genes, especially oxytetracycline, chlortetracycline, and doxycycline (Aminov, 2021). Since the discovery of the plasmid-mediated high-level tigecycline resistance genes *tet*(X3/X4) in 2019, reports of *tet*(X) have gradually increased around the world (Table 1). *Tet*(X4)-positive strains have spread globally and have been detected in animals, humans and the environment, which largely limited the use of tigecycline (Xu et al., 2022). The *tet*(X) gene and its variants were present in 23 countries on six continents (Pan et al., 2020; Wang J. et al., 2021), which are also widely present in various bacterial species, including *R. anatipestifer*, *E. coli*, *Acinetobacter*, *K. pneumoniae*, *Salmonella*, *Proteus*, *La Providencia bacteria*, *Bacteroides bacteria*, *Pseudomonas bacteria*, and *Aeromonas caviae* (Chen et al., 2019a, 2020). Moreover, most of the *tet*(X4) genes are located on different types of plasmids such as IncQ1, IncX1,

IncFIB, IncHI1, F-:A18:B-, ColE2-like, IncN, p0111 and hybrid plasmids (Fang et al., 2020), among which the IncX1 type is the most common (Cai et al., 2021; Cui et al., 2022). The Nomenclature Center[1] recommends that only *tet*(X) will be used in the future, because the *tet*(X) gene variant DNA similarity is in the range of 83–100% among *tet*(X2)-*tet*(X14), corresponding amino acid similarity is between 82 and 100%, which is greater than the standard of 79% amino acid similarity. In this article, for the convenience of description, the previous classification method is still used. This article also summarizes the prevalence of *tet*(X) gene and its variants in China in recent years as shown in Figure 2.

Prevalence of *tet*(X4) in animals

Antibiotics are commonly used in livestock production to maintain animal health and productivity. However, the absorption of antibiotics in the body is low, and most of them are excreted in the form of metabolites with feces and urine (Qiu et al., 2016). The antibiotic residues and ARGs carried in animal feces can be transmitted to the environment or humans, showing a potential source of ARGs (Ji et al., 2012; Van Boeckel et al., 2015). Tigecycline is currently approved for Human clinical use only, but the *tet*(X4) gene has been detected in food animals, retail meat, aquatic animals, and wild animals (Figure 3). Moreover, *tet*(X4) is currently detected in isolates from various animal origin samples, including pigs, ducks, geese, chickens, cattle, freshwater fish and shrimp, and migratory birds, with pig sources in particular predominating (Table 1). In a study based on a metagenomics approach, it was shown that among the abundant of ARGs in pig manure and its receiving environment (sewage, crops, soil, etc.), the tetracycline resistance genes were prevalent in pig farms (Tong et al., 2022). The same is true for pig slaughterhouses, suggesting that *tet*(X4)-carrying plasmids play an essential role in the spread of this drug related ARGs (Li et al., 2020b). Worth noting that the first isolation of plasmid mediated-*tet*(X4) was also obtained from the pig-derived sample (He et al., 2019). So far, 24 provinces in China have reported the emergence of *tet*(X), with Guangdong, Zhejiang, and Shandong having the largest number of positive strains (Figure 2). Li et al. (2021c) isolated 32 *tet*(X4)-positive strains from feces and anal swabs of pigs in Shanxi. At the same time, *tet*(X4)-positive *E. coli* were also detected in the sewage and soil of the pig farm environment. These isolates have different ST types, but their *tet*(X4)-carrying plasmids have the same replicon type, indicating that these plasmids are transferred horizontally among different reservoirs, and horizontal transfer maybe the main way for *tet*(X4) to spread in the surrounding environment (Sun J. et al., 2019). During 2016–2018, researchers isolated the *tet*(X)-positive *Acinetobacter* from pig, chicken, duck and goose feces in multi-regional farms of seven provinces, China (Guangdong, Hainan, Guangxi, Fujian, Shandong, Xinjiang, and Liaoning; Cui et al., 2020). Zhang et al. have detected 51 (17%) *tet*(X)-positive strains from 296 rectal swabs of healthy dairy cows, including the strains of *tet*(X3)-positive *Acinetobacter* and *tet*(X4)-positive *E. coli* (Zhang et al., 2020b). The prevalent range of *tet*(X) continues to expand, *tet*(X) and its variant genes have been detected in different reservoirs, and *tet*(X)-carrying plasmids have high mobility, which can be transmitted horizontally among different species.

The co-existence of *tet*(X4) with other important ARGs is noteworthy. Specifically, the *tet*(X) gene co-existed with the *flor* gene in most cases, the latter encoding chloramphenicol efflux pumps, which can be also co-transferred (Du et al., 2004; Fu et al., 2021). Further, ESBL genes and colistin resistance genes often co-existed with *tet*(X4) in *Enterobacteriaceae* (Table 1). In a retrospective study, five pig-derived *tet*(X4)-positive strains were detected in Sichuan, Henan, and Guangdong of China, and two of these *tet*(X4)-positive *E. coli* also carried the *mcr-1* gene (Sun C. et al., 2019). Tang et al. (2021) found eight *tet*(X4)-positive strains in two commercial pig farms in Sichuan, and three of them co-existed with the *cfr* gene in *E. coli*, and both ARGs were located on a novel hybrid plasmid, which could be transferred to the recipient bacteria. Li et al. (2020c) screened one strain of *tet*(X4)-positive *E. coli* and two strains of *tet*(X6)-positive *aspergillus* in different chicken farms, while the *tet*(X6) gene co-existed with the carbapenem resistance gene $bla_{\text{NDM-1}}$. The same situation also existed in other country, where the *tet*(X4) gene was detected to co-exist with the colistin resistance gene in Pakistan (Mohsin et al., 2021; Li et al., 2022). Specifically, Li et al. (2022) detected 36 *tet*(X4)-positive strains, of which 24 *tet*(X4)-positive strains co-carried the *mcr-1* gene. Mohsin et al. (2021) detected four *tet*(X4)-positive *E. coli* from farm animals and slaughterhouse effluents, and three *E. coli* contained the *mcr-1.1* gene. It should be noted that the resistance to tigecycline or colistin can be transferred by the transmission of plasmids, which posed an enormous threat to the clinical treatment of MDR bacterial infections (Ruan et al., 2020; Xu et al., 2021; Zhang et al., 2021b).

Food animals such as pigs and poultry are the primary source of high-quality protein for humans (Henchion et al., 2014), they have been slaughtered in slaughterhouses before entering the market, and *tet*(X) has also been detected in retail meat, which indicated that the slaughterhouse might be a potential reservoir for *tet*(X) (Homeier-Bachmann et al., 2021; Mohsin et al., 2021). There are also some reports on *tet*(X) from retail meat sources in Sichuan and Henan. In 2019, Sun et al. collected 311 retail meat samples from Sichuan province and detected 25 *tet*(X4)-positive *E. coli* strains, most of which were isolated from the raw pork (52%), chicken (40%), duck (4%), and beef (4%; Sun et al., 2021a). In addition, five *tet*(X4)-positive *E. coli* strains were isolated from retail chicken during routine monitoring of ARGs in the Sichuan market in 2020. Interestingly, one of the *tet*(X4)-carrying plasmids from retail chicken was 99% identity to the pig-derived *tet*(X4)-carrying plasmid, and others had the *tet*(X4) gene localized on hybrid plasmids (Lv H. et al., 2020). This phenomenon suggests that *tet*(X4)-carrying plasmids can spread among different animals, which lead to the dissemination of *tet*(X4) in the ecological environment.

1 http://faculty.washington.edu/marilynr/

TABLE 1 Global prevalence of different *tet*(X) genes in recent years.

Province/ Country	Years of samples	Source (Reference or NCBI database)	Sample sources	*Tet*(X) types	Localization of gene	Plasmid types	Sequence types	*Tet*(X)-positive isolates	ESBLs/*mcr* genes	Bacterial strains
Sichuan	2018–2020	(Bai et al., 2019; Sun C. et al., 2019, 2020; Li et al., 2021a; Tang et al., 2021; Feng et al., 2022)	Food animals	*tet*(X4)	Plasmid	IncQ1-IncY IncX1	ST48, ST4541, ST9772, ST972, ST410, ST10, ST195, ST3696, ST25, ST196	27	*cfr* *mcr-1* bla_{TEM-1B}	*E. coli* *Citrobacter freundii*
		(Li, 2020a; Lv H. et al., 2020; Sun et al., 2021b)	Retail meat	*tet*(X4)	Plasmid	IncFIA-IncHI1A-IncHI1B IncX1	ST4656, ST1788, ST871, ST48, ST1638, ST542, ST877, ST641, ST10, ST3858, ST195, ST515	31	bla_{NDM-5} bla_{SHV-12} $bla_{CTX-M-55}$ $bla_{CTX-M-14}$	*E. coli*
Guangdong	2016–2019	(He et al., 2019; Sun C. et al., 2019, Sun J. et al., 2019; Chen et al., 2020; Cheng et al., 2020; Cui et al., 2020; Sun et al., 2020; Zheng et al., 2020; Chen et al., 2021; Li et al., 2021a; Yu et al., 2021; Wu et al., 2022)	Food animals	*tet*(X/X2) *tet*(X3) *tet*(X4) *tet*(X5) *tet*(X6) *tet*(X14)	Plasmid Chromosome	IncFIA-IncHI1A-IncHI1B	ST4535, ST10, ST23, ST215, ST206, ST789, ST1196, ST2144, ST195, ST101, ST109, ST789, ST2064, ST980, ST355, ST542, ST8302	236	bla_{TEM-1B} bla_{NDM-1} bla_{OXA-58}	*E. coli* *Acinetobacter* *Citrobacter freundii* *Enterococcus faecalis* *Enterobacter cloacae*
		(Chen et al., 2019a; Cui et al., 2020; Sun et al., 2020; Wang Y. et al., 2020; Zheng et al., 2020; Chen et al., 2021; Yu et al., 2021; Gao et al., 2022)	Farm environment	*tet*(X) *tet*(X3) *tet*(X4) *tet*(X6)	Plasmid Chromosome	IncFIA-IncHI1A–IncHI1B	ST645, ST10, ST37	28	bla_{SHV-81} $bla_{SHV-110}$	*Acinetobacter* *E. coli* *K. pneumoniae* *Aeromonas cavive*

(Continued)

10.3389/fmicb.2022.969769

TABLE 1 (Continued)

Province/ Country	Years of samples	Source (Reference or NCBI database)	Sample sources	*Tet*(X) types	Localization of gene	Plasmid types	Sequence types	*Tet*(X)-positive isolates	ESBLs/*mcr* genes	Bacterial strains
		(Chen et al., 2019b)	Wild migratory birds	*tet*(X4)	Plasmid Chromosome	F-:A18:B-IncHI1	ST1196, ST6833, ST641	3	–	*E. coli*
		(Chen et al., 2020; Wang Y. et al., 2020; Cui et al., 2022)	Human	*tet*(X3) *tet*(X4)	Plasmid	IncX1, IncFIA, IncHIA, IncHIB	ST10, ST48, ST877, ST2144, ST101, ST515, ST542, ST871, ST4456, ST38, ST137, ST201, ST7176, ST10548, ST6984, ST46, ST1249, ST195, ST155, ST58, ST4014, ST7686, ST1114, ST7450, ST1684	51	*mcr-5.2* bla_{NDM} bla_{OXA} bla_{TEM} bla_{SHV} bla_{CTX-M}	*E. coli* *Acinetobacter*
Jiangsu	2015–2020	(He et al., 2019; Sun J. et al., 2019; Chen et al., 2020; Peng et al., 2020; Li et al., 2020b; He T. et al., 2020; Li et al., 2020c; Yu et al., 2021; Cheng et al., 2021a; Li et al., 2021b)	Food animals	*tet*(X3) *tet*(X4) *tet*(X6) *tet*(X15)	Plasmid Chromosome	IncHI1, IncFIB(K), IncX1, IncA/C2	ST3997, ST284, ST93, ST1286, ST155, ST327, ST1459, ST48, ST3944, ST10170, ST8302	137	bla_{CTX-M} *cfr* bla_{NDM-1} bla_{TEM-1B}	*E. coli* *Acinetobacter* *Proteus* *Citrobacter freundii* *Providencia*
		(Li et al., 2020b; Yu et al., 2021)	Farm environment	*tet*(X4)	Plasmid	–	–	21	–	*E. coli*

(Continued)

10.3389/fmicb.2022.969769

TABLE 1 (Continued)

Province/ Country	Years of samples	Source (Reference or NCBI database)	Sample sources	*Tet*(X) types	Localization of gene	Plasmid types	Sequence types	*Tet*(X)-positive isolates	ESBLs/*mcr* genes	Bacterial strains
		(Li et al., 2019)	Aquatic animal	*tet*(X2/3.2)	Plasmid	–	–	1	–	*Brevibacterium brevis*
Shanghai	2015–2019	(Chen et al., 2020; Sun et al., 2020; Wang J. et al., 2020; Li et al., 2021a; Wang J. et al., 2021)	Food animals	*tet*(X) *tet*(X3) *tet*(X)	Plasmid	IncFIA18-IncFIB(K)-IncX1 IncX1, IncQ	ST761, ST165, ST195, ST295, ST2144	41	bla_{OXA-58}	*E. coli* *Acinetobacter* *K. pneumoniae*
		(Wang J. et al., 2021)	Farm environment	*tet*(X)	Chromosome	–	–	1	–	*Proteus*
Henan	2013–2019	(Sun C. et al., 2019, 2020; Li et al., 2020d; Li et al., 2021a)	Food animals	*tet*(X4) *tet*(X6)	Plasmid Chromosome	IncX1 IncFIA-IncFIB(K)-IncX1	ST10, ST48, ST641, ST2345	11	*mcr-1*	*E. coli*
		(He D. et al., 2020)	Retail meat	*tet*(X6)	–	–	–	1	–	*Proteus*
Hebei	2019	(Li et al., 2021a)	Food animals	*tet*(X4)	Plasmid	IncX1, IncQ, IncFIA-IncHI1A-IncHI1B	ST48, ST10, ST4156, ST195, ST6833, ST515, ST2064, ST58	16	–	*E. coli* *K. pneumoniae*
	2017	(Wang L. et al., 2019)	Human	*tet*(X5)	Plasmid	–	–	1	–	*Acinetobacter*
Shandong	2017–2019	(Bai et al., 2019; He et al., 2019; Cui et al., 2020; Du et al., 2020; Liu et al., 2020; Li et al., 2021a; Yu et al., 2021)	Food animals	*tet*(X/X2) *tet*(X3) *tet*(X4) *tet*(X6)	Plasmid Chromosome	IncFII, IncFIA-IncHI1B-IncHI1A	ST761, ST746, ST101, ST10, ST847	83	bla_{TEM-1B} $bla_{CTX-M-55}$	*Acinetobacter* *Myroides* sp. *E. coli* *K. pneumoniae* *Proteus*

(Continued)

10.3389/fmicb.2022.969769

TABLE 1 (Continued)

Province/ Country	Years of samples	Source (Reference or NCBI database)	Sample sources	*Tet*(X) types	Localization of gene	Plasmid types	Sequence types	*Tet*(X)-positive isolates	ESBLs/*mcr* genes	Bacterial strains
Zhejiang	2015–2019	(Chen et al., 2020; Zhang et al., 2020b; Li et al., 2021a; Cheng et al., 2021b; Zheng et al., 2022)	Food animals	*tet*(X2) *tet*(X3) *tet*(X4) *tet*(X6) *tet*(X5.2) *tet*(X14)	Plasmid Chromosome	IncFIA-IncHI1B-IncHI1A IncFIA-IncHI1B-IncX1	ST10, ST773, ST1196, ST6883, ST641, ST515, ST767	100	bla_{OXA-58} bla_{NDM-1}	*Acinetobacter* *Enterococcus faecalis* *Proteus* *E. coli*
		(Cheng et al., 2021b)	Farm environment	*tet*(X2)	–	–	–	3	–	*Myroides* sp.
		(He et al., 2019; Ruan et al., 2020; Zeng et al., 2021)	Human	*tet*(X4)	Plasmid	IncX1	ST773	33	*mcr-1* $bla_{CTX-M-14}$	*E. coli*
Jiangxi	2015–2018	(Sun J. et al., 2019; Chen et al., 2020)	Food animals	*tet*(X4) *tet*(X3)	Plasmid Chromosome	IncQ1	ST761, ST515, ST871, ST8302	37	*mcr-1*, $bla_{CTX-M-14}$	*E. coli* *Acinetobacter*
Hainan	2017–2018	(Chen et al., 2020; Cui et al., 2020)	Food animals	*tet*(X) *tet*(X3)	Plasmid	–	–	43	bla_{NDM-1}	*Acinetobacter*
			Farm environment	*tet*(X)	Plasmid	–	–	5	bla_{OXA-58}	*Acinetobacter*
Guangxi	2017–2020	(Sun J. et al., 2019; Cui et al., 2020; Feng et al., 2022)	Food animals	*tet*(X) *tet*(X4)	Plasmid	–	ST1196, ST10, ST1415, ST34, ST109, ST48, ST195, ST799, ST2223, ST1244, ST3888, ST6404, ST641, ST677, ST452, ST1250	97	–	*Acinetobacter* *E. coli*
Fujian	2018	(Sun J.et al., 2019; Chen et al., 2020; Cui et al., 2020)	Food animals	*tet*(X) *tet*(X4)	Plasmid	–	ST8302, ST761, ST515, ST8338	26	–	*Acinetobacter*

(Continued)

10.3389/fmicb.2022.969769

TABLE 1 (Continued)

Province/ Country	Years of samples	Source (Reference or NCBI database)	Sample sources	*Tet*(X) types	Localization of gene	Plasmid types	Sequence types	*Tet*(X)-positive isolates	ESBLs/*mcr* genes	Bacterial strains
Qinghai	2015–2018	(Chen et al., 2020)	Wild migratory birds	*tet*(X4)	–	–	–	5	–	*Acinetobacter*
Xinjiang	2017–2018	(Cui et al., 2020)	Food animals	*tet*(X)	–	–	–	8	bla_{NDM-1}	*Acinetobacter*
			Farm environment	*tet*(X)	–	–	–	3	–	*Acinetobacter*
Liaoning	2018	(Cui et al., 2020)	Food animals	*tet*(X)	–	–	–	2	–	*Acinetobacter*
			Farm environment	*tet*(X)	–	–	–	3	–	*Acinetobacter*
Taiwan	2019–2020	(Hsieh et al., 2021; Wang et al., 2021a)	Human	*tet*(X)	Chromosome	–	ST793, ST723	7	bla_{OXA-72}	*Acinetobacter*
			Environment	*tet*(X10)				1		*Amniculibacterium aquaticum*
Shanxi	2018–2020	(Li et al., 2021a; Feng et al., 2022)	Food animals	*tet*(X4)	Plasmid	IncFIA-IncHI1B-IncHI1A IncX1	ST641, ST58, ST515, ST2064, ST6833, ST10, ST48, ST4156	11	–	*E. coli*
Gansu	2019	(Li et al., 2021a)	Food animals	*tet*(X4)	Plasmid	IncFII	ST540	1	–	*E. coli*
Anhui	2019	(Li et al., 2021a)	Food animals	*tet*(X4)	Plasmid	IncFIA-IncHI1B-IncHI1A IncFIA-IncFIB-IncX1 IncX1, IncFII	ST877, ST2035, ST218	8	–	*E. coli*
Beijing	2018	(Zhai et al., 2022)	Human	*tet*(X4)	Plasmid	IncFIIK	ST534	1	–	*K. pneumoniae*
		(Sun et al., 2020)	Food animals	*tet*(X4)	Plasmid	IncFIA-IncHI1B-IncHI1A	ST744	1	–	*E. coli*

(Continued)

10.3389/fmicb.2022.969769

TABLE 1 (Continued)

Province/ Country	Years of samples	Source (Reference or NCBI database)	Sample sources	*Tet*(X) types	Localization of gene	Plasmid types	Sequence types	*Tet*(X)-positive isolates	ESBLs/*mcr* genes	Bacterial strains
Shaanxi Ningxia	2018–2020	(Sun et al., 2020; Feng et al., 2022)	Food animals	*tet*(X4)	Plasmid	IncX1, IncN, IncR, IncY, IncFIA, IncFIB	ST877, ST2035, ST10392, ST10, ST7366, ST890, ST3580, ST442, ST278, ST4429, ST1602, ST746, ST48, ST189, ST8504, ST1437, ST7604	7,346	–	*E. coli*
Guizhou	2018	(Sun et al., 2020)	Food animals	*tet*(X4)	Plasmid	–	ST48, ST202, ST542, ST206, ST890	1	–	*E. coli*
Hunan	2015–2018	(Chen et al., 2020)	Food animals	*tet*(X3)	Plasmid	–	–	14	–	*Acinetobacter*
Vietnam	2021	(Dao et al., 2022)	River	*tet*(X4)	Chromosome	–	–	1	bla_{OXA-48}	*Shewanella Xiamen*
Sierra Leone	2010–2011	(Leski et al., 2013)	Human	*tet*(X)	–	–	–	11	–	*Enterobacter cloacae* *E. coli* *K. pneumoniae* *Pseudomonas* *Delftia acidovorans* *Comamonas testosteroni*
Singapore	2018	(Ding et al., 2020)	Human	*tet*(X4)	Plasmid	IncI1	ST73	2	*mcr-1*	*E. coli*
Japan	2012	(Usui et al., 2021)	Food animals	*tet*(X6)	Plasmid	IncW	–	1	–	*E. coli*
Chile	2010–2021	(Concha et al., 2021; Wang et al., 2021a)	Aquatic animals	*tet*(X) *tet*(X10)	–	–	–	3	–	*Epilithonimonas* *Chryseobacterium* sp.

(Continued)

10.3389/fmicb.2022.969769

TABLE 1 (Continued)

Province/ Country	Years of samples	Source (Reference or NCBI database)	Sample sources	*Tet*(X) types	Localization of gene	Plasmid types	Sequence types	*Tet*(X)-positive isolates	ESBLs/*mcr* genes	Bacterial strains
Pakistan	2018–2019	(Mohsin et al., 2021; Li et al., 2022)	Food animals Farm environment Human	*tet*(X4) *tet*(X7)	Plasmid	IncFII, IncQ	ST6726, ST694, ST4388 、ST224	41 1	*mcr-1*	*E. coli* *Pseudomonas aeruginosa*
United Kingdom	1966–2020	(Martelli et al., 2022)	Food animals Human Rainbow trout	*tet*(X4) *tet*(X12) *tet*(X4) *tet*(X7) *tet*(X6)	Plasmid – – –	IncX1-IncY – – –	ST1140 – – –	1 1 5 2 2	–	*E. coli* *Riemerella anatipestifer* *Salmonella* *Shigella soneii* *Enterobacter hormaechei* *Salmonella Typhimurium* *Chryseobacterium* sp.
Norway	–	(Marathe et al., 2021)	Wastewater treatment plants	*tet*(X4)	Plasmid	IncFIA/FIB	ST167	1	$bla_{CTX-M-14}$	*E. coli*
Belgium	2007–2017	LDIS01000001.1 SELG01000025.1	Food animals Musca domestica	*tet*(X10)	– –	– –	– –	1 1	– –	*Arcobacter thereius* *Apibacter muscae*
South Africa	2013	MKSZ01000121.1	Thiocyanate stock biobioreactor	*tet*(X10)	–	–	–	1	–	*Bacteroidales bacterium*
United States of America	2010–2018	(Wang et al., 2021a)	Human Environment	*tet*(X10) *tet*(X7) *tet*(X10)	– – –	– – –	– – –	47 1 2	– – –	*Bacteroides* sp. *E. coli* *Chryseobacterium* sp. *Bacteroides* sp.
Australia	2018	VSOP01000024.1	Mus musculus	*tet*(X10)	–	–	–	1	–	*Alistipes* sp.
Ireland	2017	VLSQ01000048.1 VLSR01000042.1 SMTB01000142.1	Environment Food animals	*tet*(X3) *tet*(X6)	– –	– –	– –	2 1	– –	*Acinetobacter* sp.
Bolivia	2016	PQTA01000018.1	Human	*tet*(X7)	–	–	–	1	–	*E. coli*
Turkey	2021	(Kürekci et al., 2022)	Wastewater	*tet*(X4)	Plasmid	IncFIA-IncHI1-IncFIB(K)	ST609	2	bla_{SHV-12}	*E. coli*

10.3389/fmicb.2022.969769

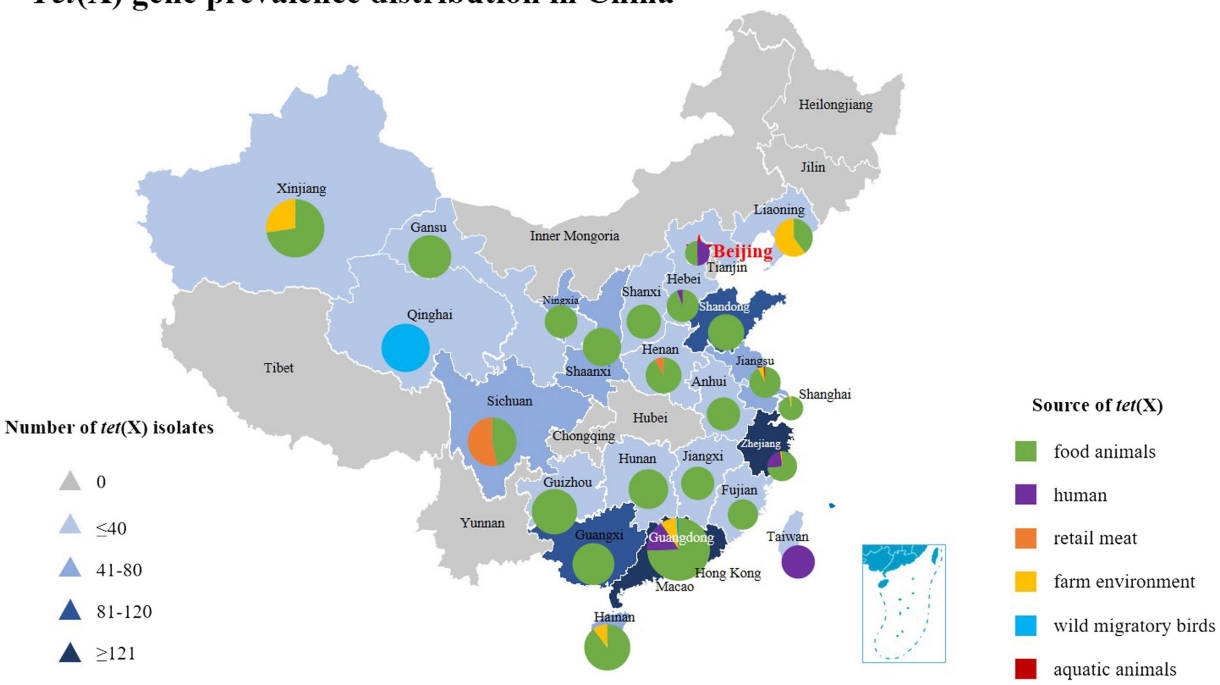

FIGURE 2
The distribution of *tet*(X) genes in different parts of China showing these genes have been found in 24 provinces from 2015 to 2022. The triangle in the figure indicates the number of *tet*(X)-positive strains isolated in each region of China, and the square indicates different sources of *tet*(X) genes, which corresponds to the pie chart in the figure. Furthermore, the different sources of *tet*(X) genes in the listed provinces can also be found, using color indication.

In addition to food animals, tigecycline resistance genes have also been detected in wild animals. In 2018, Chen et al. (2019b) isolated three strains of *tet*(X4)-positive *E. coli* from the feces of migratory birds in Guangdong, two of which were located on the plasmid, and the remaining one was located on the chromosome. The *tet*(X4)-carrying plasmid isolated from the migratory birds had a high degree of similarity with one plasmid isolated from human samples. In addition, five *tet*(X4)-positive *Acinetobacter* were also isolated from the bar-headed goose samples in Qinghai (Chen et al., 2020). In the latest report, researchers also detected the *tet*(X) variant genes in wild fish and shrimp (Li et al., 2019; Concha et al., 2021). Wild animals were not directly exposed to clinical antibiotics, but more and more ARGs were detected in them, indicating wild animals including migratory birds, were likely to be involved in the large-scale exchange of ARGs, especially long-distance transmission of cross species (Allen et al., 2010; Wang et al., 2017; Zeballos-Gross et al., 2021; Luo et al., 2022).

Prevalence of *tet*(X4) in humans

Tigecycline was approved for clinical use in 2005, and which was introduced in China in 2012. *Tet*(X) was detected in human clinical samples in 2013, with 11 *tet*(X) positive strains isolated from 52 samples, including stool, semen, blood, and urine in a Sierra Leonean hospital (Leski et al., 2013). Ding et al. (2020) conducted a retrospective screening study on 109 fecal samples, and detected *tet*(X4)-positive strains in the intestinal microflora of healthy human, with an isolation rate of 10.1%. Subsequently, *tet*(X4)-positive *E. coli* were also reported in clinical isolates from Guangdong, Hebei, Zhejiang, Beijing, Sichuan, and other places in China (Table 1). It can be seen that the *tet*(X) gene is not uncommon in hospital clinical isolates, and *tet*(X4) may be widely distributed in the human gut microflora, with great risk of transmission. In 2019, Cui et al. (2022) collected 1,001 stool samples from hospital inpatients in Guangdong Province of China, isolated 48 (4.8%) *tet*(X4)-positive *E. coli*. Notably, the hybrid plasmid was found to be prevalent in *tet*(X4)-positive strains of animal origin, with the characteristics of stable existence and horizontal transfer (Sun C. et al., 2019), which predicted this *tet*(X4)-carrying plasmid can be transmitted among humans, animals and the environment, thus facilitating the wide spread of *tet*(X4) in the ecosystem. The co-existence of *tet*(X4) with *mcr* and ESBL genes in the clinical setting is a great concern. Ruan et al. (2020) found one *E. coli* strain co-harboring *tet*(X4) with *mcr-1* on the same

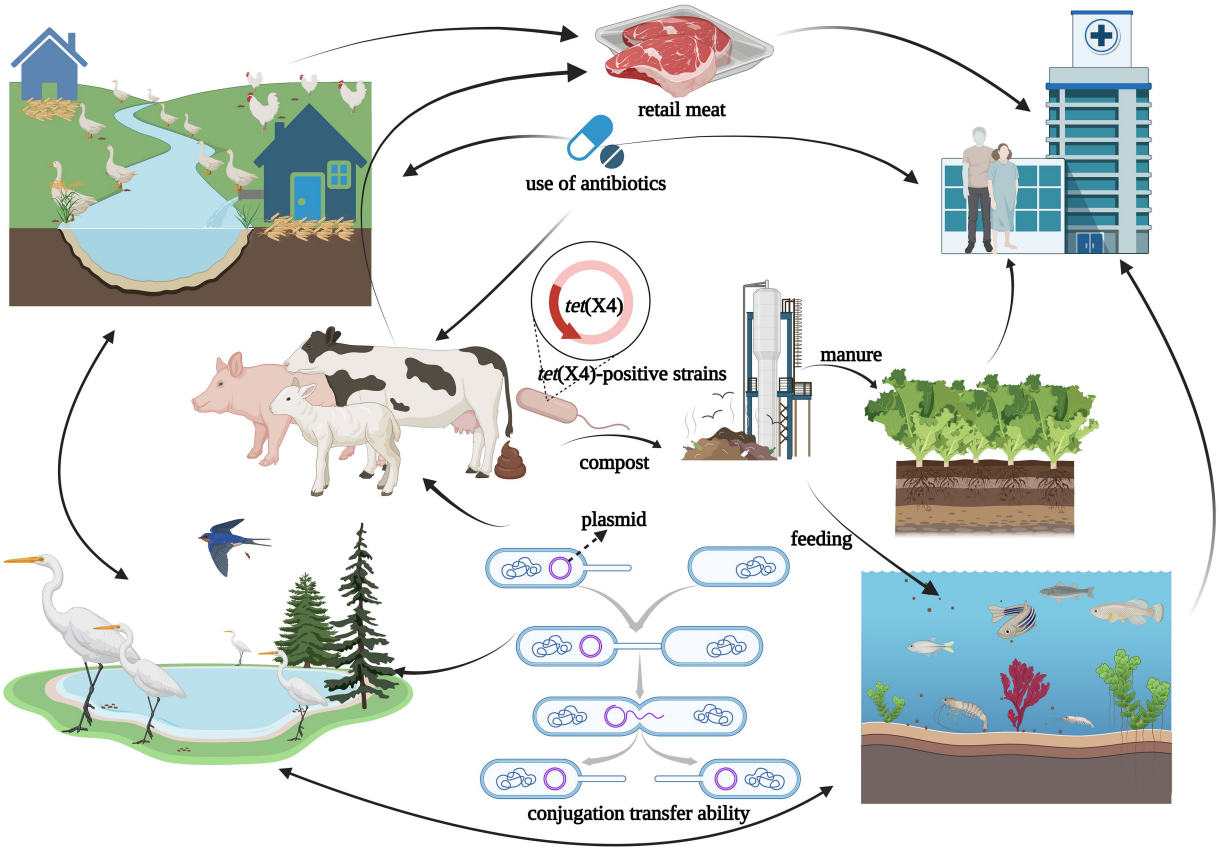

FIGURE 3
The figure was created with "BioRender.com" showing transmission routes illustration of *tet*(X4)-positive strains in natural environment. Possible dissemination routes of *tet*(X4)-positive strains showed by arrows among different reservoirs such as ducks, geese, migratory birds, chickens, pigs, cattle, aquatic animal, agricultural field, meat, and humans. The horizontal transmission of *tet*(X4) among reservoirs risked to public health for the "One Health" concept.

conjugative plasmid from the urine sample of a clinical patient in Zhejiang Province, China. Further, two *E. coli* strains carrying both *mcr-1* and *tet*(X4) were isolated in Singapore (Ding et al., 2020). Meanwhile, bla_{CTX}, bla_{OXA}, bla_{NDM}, and bla_{SHV} genes were also detected to be co-existence with *tet*(X) in one strain (Table 1). Tigecycline and colistin are the last resort for treating MDR bacteria, and the co-existence of *tet*(X) with *mcr* and ESBL genes limited the choice of clinical antibiotics, which subsequently poses a significant threat to public health.

ARB are persistent pollutants in the environment in which humans are in close contact (Kim and Aga, 2007). ARB can be transmitted to other hosts through human activities when conditions are favorable (Allen et al., 2010). Except for the hospital clinical environment, the live poultry market (LPM) is also a vast reservoir of ARGs (Wang Y. et al., 2019; Wang et al., 2021b). The *tet*(X3) and *tet*(X4) genes have been detected in the intestinal flora of LPM workers and the surrounding environment (Wang Y. et al., 2020), which indicated that the plasmid-mediated tigecycline resistance gene might exist in LPM for a long period. The ARGs are likely to be transmitted from live poultry to LPM staff, ecological environments or other animals.

Prevalence of *tet*(X4) in the environment

Antibiotics and ARGs were detected in various environments (Qiao et al., 2018). The humans, animals, and ecological environments are components of the "One health" concept, and they have important connections and can influence each other. Therefore, they can acquire ARGs through different pathways and achieve the flow of ARGs among different reservoirs (Anyanwu et al., 2021), including *tet*(X4) (Figure 3). In recent years, the environment has played an increasing role on the spread of antibiotic resistance (Finley et al., 2013; Bengtsson-Palme et al., 2014; Bondarczuk et al., 2016; Lerminiaux and Cameron, 2019). The ARGs and ARB existed in large numbers within the environment and can be transmit to reservoirs (Lin et al., 2021), such as rivers contaminated by animal manure, the soil around livestock farms, manure-irrigated agricultural fields, and sewage

treatment plants. The abuse use of antibiotics and the spread of antibiotic resistance caused by animal husbandry is one of the main concerns of sustainable agriculture(Manyi-Loh et al., 2018), where the use of first or second-generation tetracycline-class drugs was high, with subtherapeutic dosing in the forage (Yezli and Li, 2012). In animal husbandry, a wider range of antibiotic options lead to the spread of ARGs in agriculture to the human microbiota (Aminov, 2011). Animal manure as the valuable renewable fertilizer was often applied to the cropland (Zhou X. et al., 2019; Lima et al., 2020), which was found to contain different ARB and ARGs. Moreover, water as a good transport route for nutrients and contaminants was also a major reservoir for ARGs (Vaz-Moreira et al., 2014; Manaia et al., 2016; Miłobedzka et al., 2022). Specifically, macrogenomic analysis of wetland effluents and sediments in the Yangtze Delta region revealed a high abundance of the *tet*(X) gene (Du et al., 2022). *Tet*(X) and their variants were detected in farm soil, manure, and lettuce samples near chicken farms in Jiangsu, Jiangxi, and Sichuan provinces of China, and even in soil samples far from these farms (He et al., 2021). Cui et al. (2020) collected samples from some poultry farms in seven provinces across China, where *tet*(X)-positive strains from sewage and soil were isolated at 7.5% and 6.7%, respectively, and *tet*(X) was detected to be localized on the same plasmid with bla_{NDM-1}. These reports on identification and analysis of *tet*(X4) in the farm environment suggest that animal manure, sewage, and soil can influence with each other in this ecology. Moreover, *tet*(X4) can be transmitted among them, and the farm environment may be a massive reservoir of ARGs.

Discussion and prospects

The phenomenon of MDR of bacteria is a significant concern worldwide. Colistin and tigecycline are considered as the last resort drugs against carbapenem-resistant bacteria (Cunha et al., 2017; Zhou Y. et al., 2019). Either the global distribution of colistin-resistant *E. coli* or the rapid spread of the carbapenem-resistant *Enterobacteriaceae* have created enormous challenges for public health security. It is a more and more headache to solve the infection caused by MDR pathogens in human clinical treatment and animal husbandry (Gao et al., 2016; Potter et al., 2016; Rehman et al., 2020; Zhang et al., 2021b, 2021c). As a result, tigecycline has been recognized as the important antibiotic of last resort for the clinical treatment of certain bacterial infections. Through this article, we found that the *tet*(X) is prevalent on six continents around the world, with China having the highest prevalence, and most of *tet*(X4)-carrying plasmids can spread tigecycline resistance among different bacteria by means of horizontal transfer.

The mechanisms that cause antibiotic resistance to tigecycline are mainly overexpression of active efflux pump and ribosomal protection mechanisms. However, more and more *tet*(X4) has been detected in plasmids, and many different types of *tet*(X4)-carrying plasmids have strong ability of horizontal transfer, which means plasmids mediated transmission of tigecycline resistance genes may gradually increase, risking to public health (Pereira et al., 2021). The widespread use of antimicrobial drugs in domestic animals is an important reason for the rapid increase of AMR. The researchers reported the AMR monitoring results of *E. coli* in China's pig farms from 2018 to 2019, showing that multidrug resistance was detected in 91% of isolates (1871 in total), and resistance to last resort drugs including tigecycline, colistin and carbapenem was found (Peng et al., 2022). Recent studies have also found the antibiotic resistance of livestock has increased from 1970 to 2019, indicating that if the use of antibiotics is not restricted, it may not be able to effectively protect the livestock. By testing the sensitivity of several recent strains of *E. coli* to various antibiotics, researchers found their resistance was far higher than that of the strains in the 1970s. In addition, the researchers also pointed out although the specific antibiotics used to treat bacterial infections may be different, the types are often the same, so the rapid rise in drug resistance will eventually affect human beings (Yang et al., 2022). Surprisingly, the potential spread of virus-mediated ARGs is likely to exacerbate AMR, including tetracycline resistance and harm to public health (Calero-Cáceres et al., 2019; Debroas and Siguret, 2019; Shi et al., 2022), which needs our wider attention. Moreover, viruses might be linked to *Enterobacteriaceae* or *Vibrionaceae* and were considered as gene shuttles in ARGs transfer, like plasmids. This indicates that viruses and bacteria may have a synergistic effect on the transmission of ARGs. Therefore，we should look at AMR from a holistic perspective that includes humans, animals as well as the environment, and develop a plan for rational use of antibiotics to reduce the long-term and single use of tigecycline in the clinical environment, avoiding reduced clinical efficacy and increased mortality (Yahav et al., 2011). Controlling the "spillover effect" of ARGs is also important from "One Health" concept (Collignon, 2015; Tyrrell et al., 2019; Olesen et al., 2020; Aslam et al., 2021). In-depth studies of tigecycline resistance or transmission mechanisms, and continuous monitoring of *tet*(X) prevalence are urgent needed to determine the precise transmission route of ARB and ARGs, so as to provide reference for designing more effective public health intervention strategies. However, due to the limitation of the length of the article, we did not summarize the current methods and strategies of various countries or regions to limit the transmission of *tet*(X4)-positive strains, and what beneficial substances (like probiotics, prebiotics and antimicrobial peptide) can replace use of specific antibiotics in the post-antibiotic era to avoid the spread of tigecycline resistance.

Author contributions

SZ and JW wrote this manuscript. JW, YuW, and SZ contributed to the design of this manuscript. MW, XO, QY, YiW, RJ, ML, DZ, SC, and QG provided ideas for the conception of this manuscript.

BT, DS, XZ, SM, and JH helped to create figures and tables. SZ and AC modified this manuscript, and acquired funding. All authors contributed to the article and approved the submitted version.

Funding

This work was supported by the NSFC (31902267), the earmarked fund for China Agriculture Research System (CARS-42-17), the funds of Key Laboratory of Livestock and Poultry Provenance Disease Research in Mianyang, Sichuan Veterinary Medicine and Drug Innovation Group of China Agricultural Research System (SCCXTD-2022-18), and the Applied Basic Research Programs of Science and Technology Department of Sichuan Province (2019YJ0410).

Conflict of interest

The authors declare that the research was conducted in the absence of any commercial or financial relationships that could be construed as a potential conflict of interest.

Publisher's note

References

Ahmad, M., and Khan, A. (2019). Global economic impact of antibiotic resistance: a review. *J. Glob. Antimicrob. Resist.* 19, 313–316. doi: 10.1016/j.jgar.2019.05.024

Akiyama, T., Presedo, J., and Khan, A. (2013). The tetA gene decreases tigecycline sensitivity of *Salmonella enterica* isolates. *Int. J. Antimicrob. Agents* 42, 133–140. doi: 10.1016/j.ijantimicag.2013.04.017

Allen, H., Donato, J., Wang, H., Cloud-Hansen, K., Davies, J., and Handelsman, J. (2010). Call of the wild: antibiotic resistance genes in natural environments. *Nat. Rev. Microbiol.* 8, 251–259. doi: 10.1038/nrmicro2312

Aminov, R. (2011). Horizontal gene exchange in environmental microbiota. *Front. Microbiol.* 2:158. doi: 10.3389/fmicb.2011.00158

Aminov, R. (2021). Acquisition and spread of antimicrobial resistance: a *tet*(X) case study. *Int. J. Mol. Sci.* 22:3905. doi: 10.3390/ijms22083905

Anyanwu, M., Okpala, C., Chah, K., and Shoyinka, V. (2021). Prevalence and traits of mobile colistin resistance gene harbouring isolates from different ecosystems in Africa. *Biomed. Res. Int.* 2021, 1–20. doi: 10.1155/2021/6630379

Aslam, B., Khurshid, M., Arshad, M., Muzammil, S., Rasool, M., Yasmeen, N., et al. (2021). Antibiotic resistance: one health one world outlook. *Front. Cell. Infect. Microbiol.* 11:771510. doi: 10.3389/fcimb.2021.771510

Bai, L., Du, P., Du, Y., Sun, H., Zhang, P., Wan, Y., et al. (2019). Detection of plasmid-mediated tigecycline-resistant gene *tet*(X4) in *Escherichia coli* from pork, Sichuan and Shandong provinces, China, February 2019. *Euro Surveill.* 24. doi: 10.2807/1560-7917.ES.2019.24.25.1900340

Bankan, N., Koka, F., Vijayaraghavan, R., Basireddy, S., and Jayaraman, S. (2021). Overexpression of the *ade B* efflux pump gene in Tigecycline-resistant *Acinetobacter baumannii* clinical isolates and its inhibition by (+)Usnic acid as an adjuvant. *Antibiotics* 10:1900340. doi: 10.3390/antibiotics10091037

Beabout, K., Hammerstrom, T., Perez, A., Magalhães, B., Prater, A., Clements, T., et al. (2015). The ribosomal S10 protein is a general target for decreased tigecycline susceptibility. *Antimicrob. Agents Chemother.* 59, 5561–5566. doi: 10.1128/AAC.00547-15

Bender, J., Klare, I., Fleige, C., and Werner, G. (2020). A nosocomial cluster of Tigecycline-and vancomycin-resistant enterococcus faecium isolates and the impact of *rps J* and *tet* (M) mutations on tigecycline resistance. *Microb. Drug Resist.* 26, 576–582. doi: 10.1089/mdr.2019.0346

Bengtsson-Palme, J., Boulund, F., Fick, J., Kristiansson, E., and Larsson, D. (2014). Shotgun metagenomics reveals a wide array of antibiotic resistance genes and mobile elements in a polluted lake in India. *Front. Microbiol.* 5:648. doi: 10.3389/fmicb.2014.00648

Bondarczuk, K., Markowicz, A., and Piotrowska-Seget, Z. (2016). The urgent need for risk assessment on the antibiotic resistance spread via sewage sludge land application. *Environ. Int.* 87, 49–55. doi: 10.1016/j.envint.2015.11.011

Cai, W., Tang, F., Jiang, L., Li, R., Wang, Z., and Liu, Y. (2021). Histone-like nucleoid structuring protein modulates the fitness of *tet*(X4)-bearing Inc X1 plasmids in gram-negative bacteria. *Front. Microbiol.* 12:763288. doi: 10.3389/fmicb.2021.763288

Calero-Cáceres, W., Ye, M., and Balcázar, J. L. (2019). Bacteriophages as environmental reservoirs of antibiotic resistance. *Trends Microbiol.* 27, 570–577. doi: 10.1016/j.tim.2019.02.008

Cattoir, V., Isnard, C., Cosquer, T., Odhiambo, A., Bucquet, F., Guérin, F., et al. (2015). Genomic analysis of reduced susceptibility to tigecycline in *Enterococcus faecium*. *Antimicrob. Agents Chemother.* 59, 239–244. doi: 10.1128/AAC.04174-14

Chen, C., Chen, L., Zhang, Y., Cui, C., Wu, X., He, Q., et al. (2019a). Detection of chromosome-mediated tet(X4)-carrying *Aeromonas caviae* in a sewage sample from a chicken farm. *J. Antimicrob. Chemother.* 74, 3628–3630. doi: 10.1093/jac/dkz387

Chen, C., Cui, C., Wu, X., Fang, L., He, Q., He, B., et al. (2021). Spread of *tet* (X5) and *tet*(X6) genes in multidrug-resistant *Acinetobacter baumannii* strains of animal origin. *Vet. Microbiol.* 253:108954. doi: 10.1016/j.vetmic.2020.108954

Chen, C., Cui, C., Yu, J., He, Q., Wu, X., He, Y., et al. (2020). Genetic diversity and characteristics of high-level tigecycline resistance *Tet*(X) in *Acinetobacter* species. *Genome Med.* 12:111. doi: 10.1186/s13073-020-00807-5

Chen, C., Cui, C., Zhang, Y., He, Q., Wu, X., Li, G., et al. (2019b). Emergence of mobile tigecycline resistance mechanism in *Escherichia coli* strains from migratory birds in China. *Emerg. Microbes Infect.* 8, 1219–1222. doi: 10.1080/22221751.2019.1653795

Chen, Y., Hu, D., Zhang, Q., Liao, X., Liu, Y., and Sun, J. (2017). Efflux pump overexpression contributes to tigecycline heteroresistance in *Salmonella enterica* serovar Typhimurium. *Front. Cell. Infect. Microbiol.* 7:37. doi: 10.3389/fcimb.2017.00037

Cheng, Y., Chen, Y., Liu, Y., Guo, Y., Zhou, Y., Xiao, T., et al. (2020). Identification of novel tetracycline resistance gene *tet*(X14) and its co-occurrence with *tet*(X2) in a tigecycline-resistant and colistin-resistant *Empedobacter stercoris*. *Emerg. Microbes Infect.* 9, 1843–1852. doi: 10.1080/22221751.2020.1803769

Cheng, Y., Chen, Y., Liu, Y., Song, J., Chen, Y., Shan, T., et al. (2021a). Detection of a new *tet*(X6)-encoding plasmid in *Acinetobacter towneri*. *J. Glob. Antimicrob. Resist.* 25, 132–136. doi: 10.1016/j.jgar.2021.03.004

Cheng, Y., Liu, Y., Chen, Y., Huang, F., Chen, R., Xiao, Y., et al. (2021b). Sporadic dissemination of *tet*(X3) and *tet*(X6) mediated by highly diverse plasmidomes among livestock-associated *Acinetobacter*. *Microbiol. Spectr.* 9:e0114121. doi: 10.1128/Spectrum.01141-21

Chopra, I. (2002). New developments in tetracycline antibiotics: glycylcyclines and tetracycline efflux pump inhibitors. *Drug Resist. Updat.* 5, 119–125. doi: 10.1016/S1368-7646(02)00051-1

Chopra, I., and Roberts, M. (2001). Tetracycline antibiotics: mode of action, applications, molecular biology, and epidemiology of bacterial resistance. *Microbiol. Mol. Biol. Rev.* 65, 232–260; second page, table of contents. doi: 10.1128/MMBR.65.2.232-260.2001

Collignon, P. (2015). Antibiotic resistance: are we all doomed? *Intern. Med. J.* 45, 1109–1115. doi: 10.1111/imj.12902

Concha, C., Miranda, C., Santander, J., and Roberts, M. (2021). Genetic characterization of the tetracycline-resistance gene *tet*(X) carried by two *Epilithonimonas* strains isolated from farmed diseased rainbow trout, *Oncorhynchus mykiss* in Chile. *Antibiotics* 10:1051. doi: 10.3390/antibiotics10091051

Cui, C., Chen, C., Liu, B., He, Q., Wu, X., Sun, R., et al. (2020). Co-occurrence of plasmid-mediated tigecycline and carbapenem resistance in *Acinetobacter* spp. from waterfowls and their neighboring environment. *Antimicrob. Agents Chemother.* 64:e02502-19. doi: 10.1128/AAC.02502-19

Cui, C., He, Q., Jia, Q., Li, C., Chen, C., Wu, X., et al. (2021). Evolutionary trajectory of the Tet(X) family: critical residue changes towards high-level Tigecycline resistance. *mSystems* 6:e00050-21. doi: 10.1128/mSystems.00050-21

Cui, C., Li, X., Chen, C., Wu, X., He, Q., Jia, Q., et al. (2022). Comprehensive analysis of plasmid-mediated tet(X4)-positive *Escherichia coli* isolates from clinical settings revealed a high correlation with animals and environments-derived strains. *Sci. Total Environ.* 806:150687. doi: 10.1016/j.scitotenv.2021.150687

Cunha, B., Baron, J., and Cunha, C. (2017). Once daily high dose tigecycline – pharmacokinetic/pharmacodynamic based dosing for optimal clinical effectiveness: dosing matters, revisited. *Expert Rev. Anti-Infect. Ther.* 15, 257–267. doi: 10.1080/14787210.2017.1268529

Dai, S., Liu, D., Han, Z., Wang, Y., Lu, X., Yang, M., et al. (2022). Mobile tigecycline resistance gene *tet*(X4) persists with different animal manure composting treatments and fertilizer receiving soils. *Chemosphere* 307:135866. doi: 10.1016/j.chemosphere.2022.135866

Dao, T., Kasuga, I., Hirabayashi, A., Nguyen, D., Tran, H., Vu, H., et al. (2022). Emergence of mobile tigecycline resistance gene *tet*(X4)-harbouring *Shewanella xiamenensis* in a water environment. *J. Glob. Antimicrob. Resist.* 28, 140–142. doi: 10.1016/j.jgar.2021.12.022

Davies, J., and Davies, D. (2010). Origins and evolution of antibiotic resistance. *Microbiol. Mol. Biol. Rev.* 74, 417–433. doi: 10.1128/MMBR.00016-10

Debroas, D., and Siguret, C. (2019). Viruses as key reservoirs of antibiotic resistance genes in the environment. *ISME J.* 13, 2856–2867. doi: 10.1038/s41396-019-0478-9

Deng, T., Jia, Y., Tong, Z., Shi, J., Wang, Z., and Liu, Y. (2022). Bismuth drugs reverse Tet(X)-conferred tigecycline resistance in gram-negative bacteria. *Microbiol. Spectr.* 10:e0157821. doi: 10.1128/spectrum.01578-21

Ding, Y., Saw, W., Tan, L., Moong, D., Nagarajan, N., Teo, Y., et al. (2020). Emergence of tigecycline-and eravacycline-resistant Tet(X4)-producing *Enterobacteriaceae* in the gut microbiota of healthy Singaporeans. *J. Antimicrob. Chemother.* 75, 3480–3484. doi: 10.1093/jac/dkaa372

Du, J., Xu, T., Guo, X., and Yin, D. (2022). Characteristics and removal of antibiotics and antibiotic resistance genes in a constructed wetland from a drinking water source in the Yangtze River Delta. *Sci. Total Environ.* 813:152540. doi: 10.1016/j.scitotenv.2021.152540

Du, P., Liu, D., Song, H., Zhang, P., Li, R., Fu, Y., et al. (2020). Novel IS*26*-mediated hybrid plasmid harbouring *tet*(X4) in *Escherichia coli*. *J. Glob. Antimicrob. Resist.* 21, 162–168. doi: 10.1016/j.jgar.2020.03.018

Du, X., Xia, C., Shen, J., Wu, B., and Shen, Z. (2004). Characterization of florfenicol resistance among calf pathogenic *Escherichia coli*. *FEMS Microbiol. Lett.* 236, 183–189. doi: 10.1111/j.1574-6968.2004.tb09645.x

Fang, L., Chen, Q., Shi, K., Li, X., Shi, Q., He, F., et al. (2016). Step-wise increase in tigecycline resistance in *Klebsiella pneumoniae* associated with mutations in *ram R*, *lon* and *rpsJ*. *PLoS One* 11:e0165019. doi: 10.1371/journal.pone.0165019

Fang, L., Chen, C., Cui, C., Li, X., Zhang, Y., Liao, X., et al. (2020). Emerging high-level tigecycline resistance: novel tetracycline destructases spread via the Mobile *Tet*(X). *BioEssays* 42:e2000014. doi: 10.1002/bies.202000014

Feng, J., Su, M., Li, K., Ma, J., Li, R., Bai, L., et al. (2022). Extensive spread of *tet*(X4) in multidrug-resistant *Escherichia coli* of animal origin in western China. *Vet. Microbiol.* 269:109420. doi: 10.1016/j.vetmic.2022.109420

Finley, R., Collignon, P., Larsson, D., Mcewen, S., Li, X., Gaze, W., et al. (2013). The scourge of antibiotic resistance: the important role of the environment. *Clin. Infect. Dis.* 57, 704–710. doi: 10.1093/cid/cit355

Fluit, A., Florijn, A., Verhoef, J., and Milatovic, D. (2005). Presence of tetracycline resistance determinants and susceptibility to tigecycline and minocycline. *Antimicrob. Agents Chemother.* 49, 1636–1638. doi: 10.1128/AAC.49.4.1636-1638.2005

Fu, Y., Chen, Y., Liu, D., Yang, D., Liu, Z., Wang, Y., et al. (2021). Abundance of tigecycline resistance genes and association with antibiotic residues in Chinese livestock farms. *J. Hazard. Mater.* 409:124921. doi: 10.1016/j.jhazmat.2020.124921

Gao, R., Hu, Y., Li, Z., Sun, J., Wang, Q., Lin, J., et al. (2016). Dissemination and mechanism for the *MCR-1* Colistin resistance. *PLoS Pathog.* 12:e1005957. doi: 10.1371/journal.ppat.1005957

Gao, X., He, X., Lv, L., Cai, Z., Liu, Y., and Liu, J. (2022). Detection of *Tet*(X4)-producing *Klebsiella pneumoniae* from the environment and wide spread of Inc FIA-Inc HI1A-Inc HI1B plasmid carrying *tet*(X4) in China. *J. Glob. Antimicrob. Resist.* 30, 130–132. doi: 10.1016/j.jgar.2022.05.028

Ghosh, S., Lapara, T., and Sadowsky, M. (2015). Transformation of tetracycline by Tet X and its subsequent degradation in a heterologous host. *FEMS Microbiol. Ecol.* 91:fiv059. doi: 10.1093/femsec/fiv059

Guiney, D. Jr., Hasegawa, P., and Davis, C. (1984). Expression in *Escherichia coli* of cryptic tetracycline resistance genes from bacteroides R plasmids. *Plasmid* 11, 248–252. doi: 10.1016/0147-619X(84)90031-3

He, D., Wang, L., Zhao, S., Liu, L., Liu, J., Hu, G., et al. (2020). A novel tigecycline resistance gene, *tet*(X6), on an SXT/R391 integrative and conjugative element in a *Proteus* genomospecies 6 isolate of retail meat origin. *J. Antimicrob. Chemother.* 75, 1159–1164. doi: 10.1093/jac/dkaa012

He, S., Hickman, A., Varani, A., Siguier, P., Chandler, M., Dekker, J., et al. (2015). Insertion sequence IS26 reorganizes plasmids in clinically isolated multidrug-resistant bacteria by replicative transposition. *MBio* 6:e00762. doi: 10.1128/mBio.00762-15

He, T., Li, R., Wei, R., Liu, D., Bai, L., Zhang, L., et al. (2020). Characterization of *Acinetobacter* indicus co-harbouring *tet*(X3) and bla_{NDM-1} of dairy cow origin. *J. Antimicrob. Chemother.* 75, 2693–2696. doi: 10.1093/jac/dkaa182

He, T., Wang, R., Liu, D., Walsh, T., Zhang, R., Lv, Y., et al. (2019). Emergence of plasmid-mediated high-level tigecycline resistance genes in animals and humans. *Nat. Microbiol.* 4, 1450–1456. doi: 10.1038/s41564-019-0445-2

He, T., Wei, R., Zhang, L., Gong, L., Zhu, L., Gu, J., et al. (2021). Dissemination of the tet(X)-variant genes from layer farms to manure-receiving soil and corresponding lettuce. *Environ. Sci. Technol.* 55, 1604–1614. doi: 10.1021/acs.est.0c05042

Henchion, M., Mccarthy, M., Resconi, V., and Troy, D. (2014). Meat consumption: trends and quality matters. *Meat Sci.* 98, 561–568. doi: 10.1016/j.meatsci.2014.06.007

Hentschke, M., Christner, M., Sobottka, I., Aepfelbacher, M., and Rohde, H. (2010). Combined ram R mutation and presence of a Tn1721-associated tet(A) variant in a clinical isolate of *Salmonella enterica* serovar Hadar resistant to tigecycline. *Antimicrob. Agents Chemother.* 54, 1319–1322. doi: 10.1128/AAC.00993-09

Hirabayashi, A., Dao, T., Takemura, T., Hasebe, F., Trang, L., Thanh, N., et al. (2021). A transferable Inc C-Inc X3 hybrid plasmid cocarrying bla_{NDM-4}, *tet*(X), and *tmex CD3-topr J3* confers resistance to carbapenem and tigecycline. *mSphere* 6:e0059221. doi: 10.1128/mSphere.00592-21

Homeier-Bachmann, T., Heiden, S., Lübcke, P., Bachmann, L., Bohnert, J., Zimmermann, D., et al. (2021). Antibiotic-resistant *Enterobacteriaceae* in wastewater of abattoirs. *Antibiotics* 10:568. doi: 10.3390/antibiotics10050568

Hsieh, Y., Wu, J., Chen, Y., Quyen, T., Liao, W., Li, S., et al. (2021). An outbreak of *tet*(X6)-carrying tigecycline-resistant *Acinetobacter baumannii* isolates with a new capsular type at a hospital in Taiwan. *Antibiotics* 10:1239. doi: 10.3390/antibiotics10101239

Hua, X., He, J., Wang, J., Zhang, L., Zhang, L., Xu, Q., et al. (2021). Novel tigecycline resistance mechanisms in *Acinetobacter baumannii* mediated by mutations in *ade S*, *rpo B* and *rrf*. *Emerg. Microbes Infect.* 10, 1404–1417. doi: 10.1080/22221751.2021.1948804

Ji, X., Shen, Q., Liu, F., Ma, J., Xu, G., Wang, Y., et al. (2012). Antibiotic resistance gene abundances associated with antibiotics and heavy metals in animal manures and agricultural soils adjacent to feedlots in Shanghai; China. *J. Hazard. Mater.* 235–236, 178–185. doi: 10.1016/j.jhazmat.2012.07.040

Kaewpoowat, Q., and Ostrosky-Zeichner, L. (2015). Tigecycline: a critical safety review. *Expert Opin. Drug Saf.* 14, 335–342. doi: 10.1517/14740338.2015.997206

Kim, S., and Aga, D. (2007). Potential ecological and human health impacts of antibiotics and antibiotic-resistant bacteria from wastewater treatment plants. *J. Toxicol. Environ. Health B Crit. Rev.* 10, 559–573. doi: 10.1080/10937390600975137

Kumar, S., He, G., Kakarla, P., Shrestha, U., Ranjana, K., Ranaweera, I., et al. (2016). Bacterial multidrug efflux pumps of the major facilitator superfamily as targets for modulation. *Infect. Disord. Drug Targets* 16, 28–43. doi: 10.2174/1871526516666160407113848

Kürekci, C., Lu, X., Celil, B., Disli, H., Mohsin, M., Wang, Z., et al. (2022). Emergence and characterization of tigecycline resistance gene tet(X4) in ST609 *Escherichia coli* isolates from wastewater in Turkey. *Microbiology Spectrum* 10, e00732–e00722. doi: 10.1128/spectrum.00732-22

Lamut, A., Peterlin Mašič, L., Kikelj, D., and Tomašič, T. (2019). Efflux pump inhibitors of clinically relevant multidrug resistant bacteria. *Med. Res. Rev.* 39, 2460–2504. doi: 10.1002/med.21591

Lerminiaux, N., and Cameron, A. (2019). Horizontal transfer of antibiotic resistance genes in clinical environments. *Can. J. Microbiol.* 65, 34–44. doi: 10.1139/cjm-2018-0275

Leski, T., Bangura, U., Jimmy, D., Ansumana, R., Lizewski, S., Stenger, D., et al. (2013). Multidrug-resistant *tet*(X)-containing hospital isolates in Sierra Leone. *Int. J. Antimicrob. Agents* 42, 83–86. doi: 10.1016/j.ijantimicag.2013.04.014

Li, B. (2020a). Investigation of tigecycline resistant *Escherichia coli* from raw meat reveals potential transmission among food-producing animals. *Food Control* 121:107633. doi: 10.1016/j.foodcont.2020.107633

Li, R., Li, Y., Peng, K., Yin, Y., Liu, Y., He, T., et al. (2021a). Comprehensive genomic investigation of tigecycline resistance gene *tet*(X4)-bearing strains expanding among different settings. *Microbiol. Spectr.* 9:e0163321. doi: 10.1128/spectrum.01633-21

Li, R., Liu, Z., Peng, K., Liu, Y., Xiao, X., and Wang, Z. (2019). Co-occurrence of two *tet*(X) variants in an *Empedobacter brevis* of shrimp origin. *Antimicrob. Agents Chemother.* 63:e01636-19. doi: 10.1128/AAC.01636-19

Li, R., Lu, X., Munir, A., Abdullah, S., Liu, Y., Xiao, X., et al. (2022). Widespread prevalence and molecular epidemiology of *tet*(X4) and *mcr-1* harboring *Escherichia coli* isolated from chickens in Pakistan. *Sci. Total Environ.* 806:150689. doi: 10.1016/j.scitotenv.2021.150689

Li, R., Lu, X., Peng, K., Liu, Z., Li, Y., Liu, Y., et al. (2020b). Deciphering the structural diversity and classification of the mobile tigecycline resistance gene *tet*(X)-bearing plasmidome among bacteria. *mSystems* 5:e00134-20. doi: 10.1128/mSystems.00134-20

Li, R., Peng, K., Li, Y., Liu, Y., and Wang, Z. (2020c). Exploring *tet*(X)-bearing tigecycline-resistant bacteria of swine farming environments. *Sci. Total Environ.* 733:139306. doi: 10.1016/j.scitotenv.2020.139306

Li, X., Liu, L., Ji, J., Chen, Q., Hua, X., Jiang, Y., et al. (2015). Tigecycline resistance in *Acinetobacter baumannii* mediated by frameshift mutation in *pls C*, encoding 1-acyl-sn-glycerol-3-phosphate acyltransferase. *Eur. J. Clin. Microbiol. Infect. Dis.* 34, 625–631. doi: 10.1007/s10096-014-2272-y

Li, X., Quan, J., Yang, Y., Ji, J., Liu, L., Fu, Y., et al. (2016). *Abrp*, a new gene, confers reduced susceptibility to tetracycline, glycylcine, chloramphenicol and fosfomycin classes in *Acinetobacter baumannii*. *Eur. J. Clin. Microbiol. Infect. Dis.* 35, 1371–1375. doi: 10.1007/s10096-016-2674-0

Li, Y., Peng, K., Yin, Y., Sun, X., Zhang, W., Li, R., et al. (2021b). Occurrence and molecular characterization of abundant *tet*(X) variants among diverse bacterial species of chicken origin in Jiangsu, China. *Front. Microbiol.* 12:751006. doi: 10.3389/fmicb.2021.751006

Li, Y., Wang, Q., Peng, K., Liu, Y., Li, R., and Wang, Z. (2020d). Emergence of carbapenem- and tigecycline-resistant *Proteus cibarius* of animal origin. *Front. Microbiol.* 11:1940. doi: 10.3389/fmicb.2020.01940

Li, Y., Wang, Q., Peng, K., Liu, Y., Xiao, X., Mohsin, M., et al. (2021c). Distribution and genomic characterization of tigecycline-resistant *tet*(X4)-positive *Escherichia coli* of swine farm origin. *Microb. Genom.* 7:000667. doi: 10.1099/mgen.0.000667

Liao, Q., Rong, H., Zhao, M., Luo, H., Chu, Z., and Wang, R. (2021). Interaction between tetracycline and microorganisms during wastewater treatment: a review. *Sci. Total Environ.* 757:143981. doi: 10.1016/j.scitotenv.2020.143981

Lima, T., Domingues, S., and Da Silva, G. (2020). Manure as a potential hotspot for antibiotic resistance dissemination by horizontal gene transfer events. *Vet. Sci.* 7:110. doi: 10.3390/vetsci7030110

Lin, Z., Yuan, T., Zhou, L., Cheng, S., Qu, X., Lu, P., et al. (2021). Impact factors of the accumulation, migration and spread of antibiotic resistance in the environment. *Environ. Geochem. Health* 43, 1741–1758. doi: 10.1007/s10653-020-00759-0

Linkevicius, M., Sandegren, L., and Andersson, D. (2016). Potential of tetracycline resistance proteins to evolve tigecycline resistance. *Antimicrob. Agents Chemother.* 60, 789–796. doi: 10.1128/AAC.02465-15

Liu, D., Wang, T., Shao, D., Song, H., Zhai, W., Sun, C., et al. (2022). Structural diversity of the IS*CR2*-mediated rolling-cycle transferable unit carrying *tet*(X4). *Sci. Total Environ.* 826:154010. doi: 10.1016/j.scitotenv.2022.154010

Liu, D., Zhai, W., Song, H., Fu, Y., Schwarz, S., He, T., et al. (2020). Identification of the novel tigecycline resistance gene tet(X6) and its variants in Myroides, Acinetobacter and *Proteus* of food animal origin. *J. Antimicrob. Chemother.* 75, 1428–1431. doi: 10.1093/jac/dkaa037

Livermore, D. (2005). Tigecycline: what is it, and where should it be used? *J. Antimicrob. Chemother.* 56, 611–614. doi: 10.1093/jac/dki291

Lu, B., Jiang, Y., Man, M., Brown, B., Elias, P., and Feingold, K. (2005). Expression and regulation of 1-acyl-sn-glycerol-3-phosphate acyltransferases in the epidermis. *J. Lipid Res.* 46, 2448–2457. doi: 10.1194/jlr.M500258-JLR200

Luo, Y., Tan, L., Zhang, H., Bi, W., Zhao, L., Wang, X., et al. (2022). Characteristics of wild bird resistomes and dissemination of antibiotic resistance genes in interconnected bird-habitat systems revealed by similarity of bla_{TEM} polymorphic sequences. *Environ. Sci. Technol.* doi: 10.1021/acs.est.2c01633

Lupien, A., Gingras, H., Leprohon, P., and Ouellette, M. (2015). Induced tigecycline resistance in *Streptococcus pneumoniae* mutants reveals mutations in ribosomal proteins and rRNA. *J. Antimicrob. Chemother.* 70, 2973–2980. doi: 10.1093/jac/dkv211

Lv, H., Huang, W., Lei, G., Liu, L., Zhang, L., and Yang, X. (2020). Identification of novel plasmids containing the tigecycline resistance gene *tet*(X4) in *Escherichia coli* isolated from retail chicken meat. *Foodborne Pathog. Dis.* 17, 792–794. doi: 10.1089/fpd.2020.2822

Lv, L., Wan, M., Wang, C., Gao, X., Yang, Q., Partridge, S., et al. (2020). Emergence of a plasmid-encoded resistance-nodulation-division efflux pump conferring resistance to multiple drugs, including tigecycline, in *Klebsiella pneumoniae*. *MBio* 11:e02930-19. doi: 10.1128/mBio.02930-19

Manaia, C., Macedo, G., Fatta-Kassinos, D., and Nunes, O. (2016). Antibiotic resistance in urban aquatic environments: can it be controlled? *Appl. Microbiol. Biotechnol.* 100, 1543–1557. doi: 10.1007/s00253-015-7202-0

Manyi-Loh, C., Mamphweli, S., Meyer, E., and Okoh, A. (2018). Antibiotic use in agriculture and its consequential resistance in environmental sources: potential public health implications. *Molecules* 23:150689. doi: 10.3390/molecules23040795

Marathe, N., Svanevik, C., Ghavidel, F., and Grevskott, D. (2021). First report of mobile tigecycline resistance gene *tet*(X4)-harbouring multidrug-resistant *Escherichia coli* from wastewater in Norway. *J. Glob. Antimicrob. Resist.* 27, 37–40. doi: 10.1016/j.jgar.2021.07.019

Martelli, F., Abuoun, M., Cawthraw, S., Storey, N., Turner, O., Ellington, M., et al. (2022). Detection of the transferable tigecycline resistance gene tet(X4) in *Escherichia coli* from pigs in the United Kingdom. *J. Antimicrob. Chemother.* 77, 846–848. doi: 10.1093/jac/dkab439

Miłobedzka, A., Ferreira, C., Vaz-Moreira, I., Calderón-Franco, D., Gorecki, A., Purkrtova, S., et al. (2022). Monitoring antibiotic resistance genes in wastewater environments: the challenges of filling a gap in the one-health cycle. *J. Hazard. Mater.* 424:127407. doi: 10.1016/j.jhazmat.2021.127407

Mohsin, M., Hassan, B., Martins, W., Li, R., Abdullah, S., Sands, K., et al. (2021). Emergence of plasmid-mediated tigecycline resistance *tet*(X4) gene in *Escherichia coli* isolated from poultry, food and the environment in South Asia. *Sci. Total Environ.* 787:147613. doi: 10.1016/j.scitotenv.2021.147613

Moore, I., Hughes, D., and Wright, G. (2005). Tigecycline is modified by the flavin-dependent monooxygenase *Tet* X. *Biochemistry* 44, 11829–11835. doi: 10.1021/bi0506066

Munita, J., and Arias, C. (2016). Mechanisms of antibiotic resistance. *Microbiol. Spectr.* 4:VMBF-0016-2015. doi: 10.1128/microbiolspec.VMBF-0016-2015

Olesen, S., Lipsitch, M., and Grad, Y. (2020). The role of "spillover" in antibiotic resistance. *Proc. Natl. Acad. Sci. U. S. A.* 117, 29063–29068. doi: 10.1073/pnas.2013694117

Olson, M., Ruzin, A., Feyfant, E., Rush, T. 3rd, O'connell, J., and Bradford, P. (2006). Functional, biophysical, and structural bases for antibacterial activity of tigecycline. *Antimicrob. Agents Chemother.* 50, 2156–2166. doi: 10.1128/AAC.01499-05

Pan, Y., Awan, F., Zhenbao, M., Zhang, X., Zeng, J., Zeng, Z., et al. (2020). Preliminary view of the global distribution and spread of the *tet*(X) family of tigecycline resistance genes. *J. Antimicrob. Chemother.* 75, 2797–2803. doi: 10.1093/jac/dkaa284

Partridge, S., Kwong, S., Firth, N., and Jensen, S. (2018). Mobile genetic elements associated with antimicrobial resistance. *Clin. Microbiol. Rev.* 31:e00088-17. doi: 10.1128/CMR.00088-17

Peng, K., Li, R., He, T., Liu, Y., and Wang, Z. (2020). Characterization of a porcine *Proteus cibarius* strain co-harbouring *tet*(X6) and *cfr*. *J. Antimicrob. Chemother.* 75, 1652–1654. doi: 10.1093/jac/dkaa047

Peng, Z., Hu, Z., Li, Z., Zhang, X., Jia, C., Li, T., et al. (2022). Antimicrobial resistance and population genomics of multidrug-resistant *Escherichia coli* in pig farms in mainland China. *Nat. Commun.* 13:1116. doi: 10.1038/s41467-022-28750-6

Pereira, A., Paranhos, A., De Aquino, S., and Silva, S. (2021). Distribution of genetic elements associated with antibiotic resistance in treated and untreated animal husbandry waste and wastewater. *Environ. Sci. Pollut. Res. Int.* 28, 26380–26403. doi: 10.1007/s11356-021-13784-y

Plantinga, N., Wittekamp, B., Van Duijn, P., and Bonten, M. (2015). Fighting antibiotic resistance in the intensive care unit using antibiotics. *Future Microbiol.* 10, 391–406. doi: 10.2217/fmb.14.146

Poirel, L., Mugnier, P., Toleman, M., Walsh, T., Rapoport, M., Petroni, A., et al. (2009). IS*CR2*, another vehicle for bla_{VEB} gene acquisition. *Antimicrob. Agents Chemother.* 53, 4940–4943. doi: 10.1128/AAC.00414-09

Potter, R., D'souza, A., and Dantas, G. (2016). The rapid spread of carbapenem-resistant *Enterobacteriaceae*. *Drug Resist. Updat.* 29, 30–46. doi: 10.1016/j.drup.2016.09.002

Qiao, M., Ying, G., Singer, A., and Zhu, Y. (2018). Review of antibiotic resistance in China and its environment. *Environ. Int.* 110, 160–172. doi: 10.1016/j.envint.2017.10.016

Qiu, J., Zhao, T., Liu, Q., He, J., He, D., Wu, G., et al. (2016). Residual veterinary antibiotics in pig excreta after oral administration of sulfonamides. *Environ. Geochem. Health* 38, 549–556. doi: 10.1007/s10653-015-9740-x

Rehman, M., Yang, H., Zhang, S., Huang, Y., Zhou, R., Gong, S., et al. (2020). Emergence of *Escherichia coli* isolates producing NDM-1 carbapenemase from waterfowls in Hainan island, China. *Acta Trop.* 207:105485. doi: 10.1016/j.actatropica.2020.105485

Rempel, S., Stanek, W., and Slotboom, D. (2019). ECF-type ATP-binding cassette transporters. *Annu. Rev. Biochem.* 88, 551–576. doi: 10.1146/annurev-biochem-013118-111705

Roberts, M. (2003). Tetracycline therapy: update. *Clin. Infect. Dis.* 36, 462–467. doi: 10.1086/367622

Ruan, Z., Jia, H., Chen, H., Wu, J., He, F., and Feng, Y. (2020). Co-existence of plasmid-mediated tigecycline and colistin resistance genes *tet*(X4) and *mcr-1* in a community-acquired *Escherichia coli* isolate in China. *J. Antimicrob. Chemother.* 75, 3400–3402. doi: 10.1093/jac/dkaa317

Ruzin, A., Keeney, D., and Bradford, P. (2007). Ade ABC multidrug efflux pump is associated with decreased susceptibility to tigecycline in *Acinetobacter* calcoaceticus-*Acinetobacter baumannii* complex. *J. Antimicrob. Chemother.* 59, 1001–1004. doi: 10.1093/jac/dkm058

Sheykhsaran, E., Baghi, H., Soroush, M., and Ghotaslou, R. (2019). An overview of tetracyclines and related resistance mechanisms. *Rev. Med. Microbiol.* 30, 69–75. doi: 10.1097/MRM.0000000000000154

Shi, L. D., Dong, X., Liu, Z., Yang, Y., Lin, J. G., Li, M., et al. (2022). A mixed blessing of viruses in wastewater treatment plants. *Water Res.* 215:118237. doi: 10.1016/j.watres.2022.118237

Speer, B., Bedzyk, L., and Salyers, A. (1991). Evidence that a novel tetracycline resistance gene found on two *Bacteroides* transposons encodes an NADP-requiring oxidoreductase. *J. Bacteriol.* 173, 176–183. doi: 10.1128/jb.173.1.176-183.1991

Stein, G., and Babinchak, T. (2013). Tigecycline: an update. *Diagn. Microbiol. Infect. Dis.* 75, 331–336. doi: 10.1016/j.diagmicrobio.2012.12.004

Sun, C., Cui, M., Zhang, S., Liu, D., Fu, B., Li, Z., et al. (2020). Genomic epidemiology of animal-derived tigecycline-resistant *Escherichia coli* across China reveals recent endemic plasmid-encoded *tet*(X4) gene. *Commun. Biol.* 3:412. doi: 10.1038/s42003-020-01148-0

Sun, C., Cui, M., Zhang, S., Wang, H., Song, L., Zhang, C., et al. (2019). Plasmid-mediated tigecycline-resistant gene tet(X4) in *Escherichia coli* from food-producing animals, China, 2008–2018. *Emerg. Microbes Infect.* 8, 1524–1527. doi: 10.1080/22221751.2019.1678367

Sun, H., Wan, Y., Du, P., Liu, D., Li, R., Zhang, P., et al. (2021a). Investigation of tigecycline resistant *Escherichia coli* from raw meat reveals potential transmission among food-producing animals. *Food Control* 121:107633. doi: 10.1016/j.foodcont.2020.107633

Sun, H., Zhai, W., Fu, Y., Li, R., Du, P., and Bai, L. (2021b). Co-occurrence of plasmid-mediated resistance genes *tet*(X4) and bla_{NDM-5} in a multidrug-resistant *Escherichia coli* isolate recovered from chicken in China. *J. Glob. Antimicrob. Resist.* 24, 415–417. doi: 10.1016/j.jgar.2021.02.010

Sun, J., Chen, C., Cui, C., Zhang, Y., Liu, X., Cui, Z., et al. (2019). Plasmid-encoded *tet*(X) genes that confer high-level tigecycline resistance in *Escherichia coli*. *Nat. Microbiol.* 4, 1457–1464. doi: 10.1038/s41564-019-0496-4

Tang, Y., Lai, Y., Kong, L., Wang, X., Li, C., Wang, Y., et al. (2021). Characterization of three porcine *Escherichia coli* isolates co-harbouring *tet*(X4) and *cfr*. *J. Antimicrob. Chemother.* 76, 263–264. doi: 10.1093/jac/dkaa384

Thaker, M., Spanogiannopoulos, P., and Wright, G. (2010). The tetracycline resistome. *Cell. Mol. Life Sci.* 67, 419–431. doi: 10.1007/s00018-009-0172-6

Tiseo, K., Huber, L., Gilbert, M., Robinson, T., and Van Boeckel, T. (2020). Global trends in antimicrobial use in food animals from 2017 to 2030. *Antibiotics* 9:918. doi: 10.3390/antibiotics9120918

Tong, C., Xiao, D., Xie, L., Yang, J., Zhao, R., Hao, J., et al. (2022). Swine manure facilitates the spread of antibiotic resistome including tigecycline-resistant *tet*(X) variants to farm workers and receiving environment. *Sci. Total Environ.* 808:152157. doi: 10.1016/j.scitotenv.2021.152157

Tyrrell, C., Burgess, C. M., Brennan, F., and Walsh, F. (2019). Antibiotic resistance in grass and soil. *Biochem. Soc. Trans.* 47, 477–486. doi: 10.1042/BST20180552

Umar, Z., Chen, Q., Tang, B., Xu, Y., Wang, J., Zhang, H., et al. (2021). The poultry pathogen *Riemerella anatipestifer* appears as a reservoir for *Tet*(X) tigecycline resistance. *Environ. Microbiol.* 23, 7465–7482. doi: 10.1111/1462-2920.15632

Usui, M., Fukuda, A., Suzuki, Y., Nakajima, C., and Tamura, Y. (2021). Broad-host-range Inc W plasmid harbouring *tet*(X) in *Escherichia coli* isolated from pigs in Japan. *J. Glob. Antimicrob. Resist.* 28, 97–101. doi: 10.1016/j.jgar.2021.12.012

Van Boeckel, T., Brower, C., Gilbert, M., Grenfell, B., Levin, S., Robinson, T., et al. (2015). Global trends in antimicrobial use in food animals. *Proc. Natl. Acad. Sci. U. S. A.* 112, 5649–5654. doi: 10.1073/pnas.1503141112

Vaz-Moreira, I., Nunes, O., and Manaia, C. (2014). Bacterial diversity and antibiotic resistance in water habitats: searching the links with the human microbiome. *FEMS Microbiol. Rev.* 38, 761–778. doi: 10.1111/1574-6976.12062

Venter, H., Mowla, R., Ohene-Agyei, T., and Ma, S. (2015). RND-type drug efflux pumps from gram-negative bacteria: molecular mechanism and inhibition. *Front. Microbiol.* 6:377. doi: 10.3389/fmicb.2015.00377

Volkers, G., Palm, G., Weiss, M., Wright, G., and Hinrichs, W. (2011). Structural basis for a new tetracycline resistance mechanism relying on the *Tet* X monooxygenase. *FEBS Lett.* 585, 1061–1066. doi: 10.1016/j.febslet.2011.03.012

Wang, J., Ma, Z., Zeng, Z., Yang, X., Huang, Y., and Liu, J. (2017). The role of wildlife (wild birds) in the global transmission of antimicrobial resistance genes. *Zool. Res.* 38, 55–80. doi: 10.24272/j.issn.2095-8137.2017.003

Wang, J., Wang, Y., Wu, H., Wang, Z., Shen, P., Tian, Y., et al. (2020). Coexistence of bla_{OXA-58} and *tet*(X) on a novel plasmid in *Acinetobacter* sp. from pig in Shanghai, China. *Front. Microbiol.* 11:578020. doi: 10.3389/fmicb.2020.578020

Wang, J., Wu, H., Mei, C., Wang, Y., Wang, Z., Lu, M., et al. (2021). Multiple mechanisms of tigecycline resistance in *Enterobacteriaceae* from a pig farm, China. *Microbiol. Spectr.* 9:e0041621. doi: 10.1128/Spectrum.00416-21

Wang, L., Liu, D., Lv, Y., Cui, L., Li, Y., Li, T., et al. (2019). Novel plasmid-mediated *tet* (X5) gene conferring resistance to tigecycline, eravacycline, and omadacycline in a clinical *Acinetobacter baumannii* isolate. *Antimicrob. Agents Chemother.* 64:e01326-19. doi: 10.1128/AAC.01326-19

Wang, Y., Hu, Y., Cao, J., Bi, Y., Lv, N., Liu, F., et al. (2019). Antibiotic resistance gene reservoir in live poultry markets. *J. Infect.* 78, 445–453. doi: 10.1016/j.jinf.2019.03.012

Wang, Y., Liu, F., Xu, X., Huang, H., Lyu, N., Ma, S., et al. (2021a). Detection of plasmid-mediated tigecycline resistance gene *tet*(X4) in a *Salmonella enterica* serovar Llandoff Isolate. *Infect. Microb. Dis.* 3, 198–204. doi: 10.1097/IM9.0000000000000077

Wang, Y., Liu, F., Zhu, B., and Gao, G. (2020). Discovery of tigecycline resistance genes *tet*(X3) and *tet*(X4) in live poultry market worker gut microbiomes and the surrounded environment. *Sci. Bull.* 65, 340–342. doi: 10.1016/j.scib.2019.12.027

Wang, Y., Lyu, N., Liu, F., Liu, W., Bi, Y., Zhang, Z., et al. (2021b). More diversified antibiotic resistance genes in chickens and workers of the live poultry markets. *Environ. Int.* 153:106534. doi: 10.1016/j.envint.2021.106534

Wenzel, R., Bate, G., and Kirkpatrick, P. (2005). Tigecycline. *Nat. Rev. Drug Discov.* 4, 809–810. doi: 10.1038/nrd1857

Wu, Y., He, R., Qin, M., Yang, Y., Chen, J., Feng, Y., et al. (2022). Identification of plasmid-mediated tigecycline-resistant gene *tet*(X4) in *Enterobacter cloacae* from pigs in China. *Microbiol. Spectr.* 10:e0206421. doi: 10.1128/spectrum.02064-21

Xu, L., Zhou, Y., Niu, S., Liu, Z., Zou, Y., Yang, Y., et al. (2022). A novel inhibitor of monooxygenase reversed the activity of tetracyclines against *tet*(X3)/*tet*(X4)-positive bacteria. *EBioMedicine* 78:103943. doi: 10.1016/j.ebiom.2022.103943

Xu, Y., Liu, L., Zhang, H., and Feng, Y. (2021). Co-production of *Tet*(X) and *MCR-1*, two resistance enzymes by a single plasmid. *Environ. Microbiol.* 23, 7445–7464. doi: 10.1111/1462-2920.15425

Xu, Y., Liu, L., Sun, J., and Feng, Y. (2019). Limited distribution and mechanism of the *Tet* X4 tetracycline resistance enzyme. *Sci. Bull.* 64, 14–17. doi: 10.1016/j.scib.2019.08.024

Yahav, D., Lador, A., Paul, M., and Leibovici, L. (2011). Efficacy and safety of tigecycline: a systematic review and meta-analysis. *J. Antimicrob. Chemother.* 66, 1963–1971. doi: 10.1093/jac/dkr242

Yang, L., Shen, Y., Jiang, J., Wang, X., Shao, D., Lam, M., et al. (2022). Distinct increase in antimicrobial resistance genes among *Escherichia coli* during 50 years of antimicrobial use in livestock production in China. *Nat. Food* 3, 197–205. doi: 10.1038/s43016-022-00470-6

Yang, W., Moore, I., Koteva, K., Bareich, D., Hughes, D., and Wright, G. (2004). *Tet* X is a flavin-dependent monooxygenase conferring resistance to tetracycline antibiotics. *J. Biol. Chem.* 279, 52346–52352. doi: 10.1074/jbc.M409573200

Yezli, S., and Li, H. (2012). Antibiotic resistance amongst healthcare-associated pathogens in China. *Int. J. Antimicrob. Agents* 40, 389–397. doi: 10.1016/j.ijantimicag.2012.07.009

Yu, Y., Cui, C., Kuang, X., Chen, C., Wang, M., Liao, X., et al. (2021). Prevalence of *tet*(X4) in *Escherichia coli* from duck farms in Southeast China. *Front. Microbiol.* 12:716393. doi: 10.3389/fmicb.2021.716393

Zeballos-Gross, D., Rojas-Sereno, Z., Salgado-Caxito, M., Poeta, P., Torres, C., and Benavides, J. (2021). The role of gulls as reservoirs of antibiotic resistance in aquatic environments: a scoping review. *Front. Microbiol.* 12:703886. doi: 10.3389/fmicb.2021.703886

Zeng, Y., Lu, J., Liu, C., Ling, Z., Sun, Q., Wang, H., et al. (2021). A method for screening tigecycline-resistant gene *tet*(X) from human gut. *J. Glob. Antimicrob. Resist.* 24, 29–31. doi: 10.1016/j.jgar.2020.11.010

Zha, L., Pan, L., Guo, J., French, N., Villanueva, E., and Tefsen, B. (2020). Effectiveness and safety of high dose tigecycline for the treatment of severe infections: a systematic review and meta-analysis. *Adv. Ther.* 37, 1049–1064. doi: 10.1007/s12325-020-01235-y

Zhai, W., Tian, Y., Lu, M., Zhang, M., Song, H., Fu, Y., et al. (2022). Presence of mobile tigecycline resistance gene tet(X4) in clinical *Klebsiella pneumoniae*. *Microbiol. Spectr.* 10:e0108121. doi: 10.1128/spectrum.01081-21

Zhang, R., Dong, N., Shen, Z., Zeng, Y., Lu, J., Liu, C., et al. (2020a). Epidemiological and phylogenetic analysis reveals *Flavobacteriaceae* as potential

ancestral source of tigecycline resistance gene *tet*(X). *Nat. Commun.* 11:4648. doi: 10.1038/s41467-020-18475-9

Zhang, R., Dong, N., Zeng, Y., Shen, Z., Lu, J., Liu, C., et al. (2020b). Chromosomal and plasmid-borne tigecycline resistance genes *tet*(X3) and *tet*(X4) in dairy cows on a Chinese farm. *Antimicrob. Agents Chemother.* 64:e00674-20. doi: 10.1128/AAC.00674-20

Zhang, R., Sun, J., Sun, R. Y., Wang, M., Cui, C., Fang, L., et al. (2021a). Source tracking and global distribution of the Tigecycline non-susceptible *tet*(X). *Microbiol. Spectr.* 9:e0116421. doi: 10.1128/Spectrum.01164-21

Zhang, S., Abbas, M., Rehman, M. U., Huang, Y., Zhou, R., Gong, S., et al. (2020c). Dissemination of antibiotic resistance genes (ARGs) via integrons in *Escherichia coli*: a risk to human health. *Environ. Pollut.* 266:115260. doi: 10.1016/j.envpol.2020.115260

Zhang, S., Abbas, M., Rehman, M. U., Wang, M., Jia, R., Chen, S., et al. (2021b). Updates on the global dissemination of colistin-resistant *Escherichia coli*: an emerging threat to public health. *Sci. Total Environ.* 799:149280. doi: 10.1016/j.scitotenv.2021.149280

Zhang, S., Chen, S., Rehman, M. U., Yang, H., Yang, Z., Wang, M., et al. (2021c). Distribution and association of antimicrobial resistance and virulence traits in *Escherichia coli* isolates from healthy waterfowls in Hainan, China. *Ecotoxicol. Environ. Saf.* 220:112317. doi: 10.1016/j.ecoenv.2021.112317

Zhang, Z., Zhan, Z., and Shi, C. (2022). International spread of Tet(X4)-producing *Escherichia coli* isolates. *Foods* 11:2010. doi: 10.3390/foods11142010

Zhao, E., Wang, X., Ji, J., Wang, Z., Wang, Y., and Cui, H. (2021). Anti-tumor activity of tigecycline: a review. *Sheng Wu Gong Cheng Xue Bao* 37, 3031–3041. doi: 10.13345/j.cjb.200630

Zheng, X., Ma, J., Lu, Y., Sun, D., Yang, H., Xia, F., et al. (2022). Detection of *tet*(X6) variant-producing *Proteus terrae* subsp. *cibarius* from animal cecum in Zhejiang, China. *J. Glob. Antimicrob. Resist.* 29, 124–130. doi: 10.1016/j.jgar.2022.02.011

Zheng, X., Zhu, J., Zhang, J., Cai, P., Sun, Y., Chang, M., et al. (2020). A novel plasmid-borne *tet*(X6) variant co-existing with bla_{NDM-1} and bla_{OXA-58} in a chicken *Acinetobacter baumannii* isolate. *J. Antimicrob. Chemother.* 75, 3397–3399. doi: 10.1093/jac/dkaa342

Zhong, X., Xu, H., Chen, D., Zhou, H., Hu, X., and Cheng, G. (2014). First emergence of acr AB and oqx AB mediated tigecycline resistance in clinical isolates of *Klebsiella pneumoniae* pre-dating the use of tigecycline in a Chinese hospital. *PLoS One* 9:e115185. doi: 10.1371/journal.pone.0115185

Zhou, X., Qiao, M., Su, J. Q., Wang, Y., Cao, Z., Cheng, W., et al. (2019). Turning pig manure into biochar can effectively mitigate antibiotic resistance genes as organic fertilizer. *Sci. Total Environ.* 649, 902–908. doi: 10.3389/fmicb.2019.02957

Zhou, Y., Liu, P., Zhang, C., Liao, X., Sun, J., and Liu, Y. (2019). Colistin combined with tigecycline: a promising alternative strategy to combat *Escherichia coli* harboring bla_{NDM-5} and *mcr-1*. *Front. Microbiol.* 10:2957. doi: 10.3389/fmicb.2019.02957

Zhu, D., Luo, H., Liu, M., Zhao, X., Jia, R., Chen, S., et al. (2018). Various profiles of tet genes addition to *tet*(X) in *Riemerella anatipestifer* isolates from ducks in China. *Front. Microbiol.* 9:585. doi: 10.3389/fmicb.2018.00585

frontiers | Frontiers in Microbiology

TYPE Original Research
PUBLISHED 19 October 2022
DOI 10.3389/fmicb.2022.1030490

OPEN ACCESS

EDITED BY
Dongchang Sun,
Zhejiang University of Technology,
China

REVIEWED BY
Biao Tang,
Zhejiang Academy of Agricultural Sciences,
China
Xiaofei Jiang,
Fudan University,
China

*CORRESPONDENCE
Xianjun Ma
18560087567@163.com
Xuewen Li
lxw@sdu.edu.cn

SPECIALTY SECTION
This article was submitted to Antimicrobials, Resistance and Chemotherapy, a section of the journal Frontiers in Microbiology

RECEIVED 29 August 2022
ACCEPTED 04 October 2022
PUBLISHED 19 October 2022

CITATION
Yang C, Han J, Berglund B, Zou H, Gu C, Zhao L, Meng C, Zhang H, Ma X and Li X (2022) Dissemination of bla_{NDM-5} and *mcr-8.1* in carbapenem-resistant *Klebsiella pneumoniae* and *Klebsiella quasipneumoniae* in an animal breeding area in Eastern China. *Front. Microbiol.* 13:1030490. doi: 10.3389/fmicb.2022.1030490

Dissemination of bla_{NDM-5} and *mcr-8.1* in carbapenem-resistant *Klebsiella pneumoniae* and *Klebsiella quasipneumoniae* in an animal breeding area in Eastern China

Chengxia Yang[1], Jingyi Han[2], Björn Berglund[3], Huiyun Zou[1], Congcong Gu[1], Ling Zhao[1], Chen Meng[1], Hui Zhang[1], Xianjun Ma[4]*and Xuewen Li[1]*

[1]Department of Environment and Health, School of Public Health, Cheeloo College of Medicine, Shandong University, Jinan, Shandong, China, [2]Department of Thoracic Surgery, Qilu Hospital of Shandong University, Jinan, Shandong, China, [3]Department of Clinical and Experimental Medicine, Linköping University, Linköping, Sweden, [4]Department of Blood Transfusion, Qilu Hospital of Shandong University, Jinan, Shandong, China

Animal farms have become one of the most important reservoirs of carbapenem-resistant *Klebsiella* spp. (CRK) owing to the wide usage of veterinary antibiotics. "One Health"-studies observing animals, the environment, and humans are necessary to understand the dissemination of CRK in animal breeding areas. Based on the concept of "One-Health," 263 samples of animal feces, wastewater, well water, and human feces from 60 livestock and poultry farms in Shandong province, China were screened for CRK. Five carbapenem-resistant *Klebsiella pneumoniae* (CRKP) and three carbapenem-resistant *Klebsiella quasipneumoniae* (CRKQ) strains were isolated from animal feces, human feces, and well water. The eight strains were characterized by antimicrobial susceptibility testing, plasmid conjugation assays, whole-genome sequencing, and bioinformatics analysis. All strains carried the carbapenemase-encoding gene bla_{NDM-5}, which was flanked by the same core genetic structure (IS*5*-bla_{NDM-5}-ble_{MBL}-*trpF*-*dsbD*-IS*26*-IS*Kox3*) and was located on highly related conjugative IncX3 plasmids. The colistin resistance gene *mcr-8.1* was carried by three CRKP and located on self-transmissible IncFII(K)/IncFIA(HI1) and IncFII(pKP91)/IncFIA(HI1) plasmids. The genetic context of *mcr-8.1* consisted of IS*903*-*orf*-*mcr-8.1*-*copR*-*baeS*-*dgkA*-*orf*-IS*903* in three strains. Single nucleotide polymorphism (SNP) analysis confirmed the clonal spread of CRKP carrying-bla_{NDM-5} and *mcr-8.1* between two human workers in the same chicken farm. Additionally, the SNP analysis showed clonal expansion of CRKP and CRKQ strains from well water in different farms, and the clonal CRKP was clonally related to isolates from animal farms and a wastewater treatment plant collected in other studies in the same province. These findings suggest that CRKP and CRKQ are capable of disseminating *via* horizontal gene transfer and clonal expansion and may pose a significant threat to public health unless preventative measures are taken.

KEYWORDS

carbapenem-resistant *Klebsiella* spp., animal breeding area, bla_{NDM-5}, *mcr-8.1*, plasmid, clonal expansion

Introduction

The prevalence of antibiotic-resistant bacteria (ARB) and antibiotic-resistant genes (ARGs) has the potential to cause a global health crisis in the 21st century. Carbapenem-resistant *Klebsiella* spp. (CRK) are especially concerning owing to their resistance to carbapenems, one of the last resort antibiotics used against gram-negative bacteria, and ability to cause a variety of community- or hospital-acquired infections such as pneumonia, urinary tract infections, bloodstream infections, and septic shock. Carbapenem-resistant *Klebsiella pneumoniae* (CRKP), which is widely reported in Europe, Asia, Africa, and other regions (Navon-Venezia et al., 2017), is listed in the critical priority tier of pathogens and was recognized as the highest priority in new antibiotic development by the World Health Organization (WHO) in 2017 (Tacconelli et al., 2018). However, according to the China Antimicrobial Surveillance Network (CHINET),[1] the prevalence of clinical meropenem resistance in *K. pneumoniae* has increased rapidly in China, from 2.9% in 2005 to 24.4% in 2021, posing a massive challenge to public health.

China is the largest consumer of veterinary antimicrobials, accounting for 45% of global use in 2017, and is expected to remain the largest consumer in 2030 (Tiseo et al., 2020). Thus, ARB and ARGs have been widely spread in animal farms, such as in animal feces (Tang et al., 2019), groundwater (Gu et al., 2022), aerosol (Yang et al., 2021), and animal foods (Wang et al., 2022). Although carbapenems are not approved for use on animal farms in China, the widespread use of other antibiotics such as fluoroquinolones, sulfonamides, and tetracyclines can co-select carbapenem-resistant bacteria (BIOHAZ, 2013). In China, CRK has been detected in animal farms, such as in animal feces and raw milk in dairy cattle farms in Jiangsu province (He et al., 2017), chicken cloaca and environment (sewage trenches, corridor floors, drooping boards, feeding troughs, and nipple drinkers) in broiler farms in Hebei province (Zhai et al., 2020), duck feces in Guangdong province (Ma et al., 2020), and pig anal swabs from a pig farm in Hunan province (Zhao et al., 2021b). However, most CRK studies on animal farms in China have two major shortcomings. First, the studies mainly focused on a single type of animal farms (He et al., 2017; Ma et al., 2020; Zhao et al., 2021b). Objectively understanding the true prevalence of CRK on different types of animal farms is difficult. Second, the studies are mostly limited to animals and the environment (Zhai et al., 2020; Gu et al., 2022), and the CRK transmission among animals, the environment, and humans is not entirely clear.

Thus, our study randomly selected 60 animal farms, including 20 chicken, 20 pig, and 20 bovine farms, in a typical region of the animal farming industry with a long breeding time and stable animal breeding patterns in Shandong province in July 2019. Based on the perspective of "One-Health," animal feces, wastewater (excluding chicken farms), well water, and human feces were collected from each farm to screen for CRK. This study aimed to characterize CRK in terms of antimicrobial susceptibility, antibiotic resistance genes, virulence genes and multilocus sequence typing (MLST), investigate the prevalence of CRK in different types of farms in the same animal breeding area, and explore the transmission of CRK among animals, the environment, and humans.

Materials and methods

Sampling site and collection samples

The study site is in Eastern China, has a population of approximately 1,194,365, covers an area of 2,414 km^2, and has a long breeding time and stable animal breeding patterns. The primary animal husbandry in this area consists of breeding chickens, pigs, and bovines. We selected 60 livestock and poultry farms (Figure 1), including pig farms ($n=20$), chicken farms [($n=20$); laying hen farms ($n=11$) and broiler farms ($n=9$)], and bovine farms [($n=20$); dairy cattle farms ($n=13$) and beef farms ($n=7$)]. In July 2019, a total of 263 samples were collected, with 75 from chicken farms, 86 from pig farms, and 102 from bovine farms. The following samples types were collected: 66 animal feces, 37 wastewater, 107 worker feces, and 53 well water samples. The number and type of samples are summarized in Supplementary Table S1. Worker feces was collected using a Copan Liquid Amies Elution Swab (ESwab; Copan, Brescia, Italy). Well water (500 ml) from each farm well and wastewater (500 ml) from each farm sewage outlet (excluding chicken farms) were collected in sterile glass bottles. Approximately 30 g of each fresh animal fecal sample was collected in a sterile plastic bottle with a sterile spoon. All samples were temporarily placed in iceboxes (4–8°C) upon collection and transported to the laboratory at the end of the sampling day. The well water and wastewater samples were filtered through 0.45 μm sterile membrane filters (Millipore, Billerica, United States). After filtration, the membranes were placed in 5 ml of sterile brain heart infusion broth (BHI; Oxoid, Basingstoke, United Kingdom) with 20% glycerin. 2.0 g of each animal fecal sample was homogenized in 5 ml of sterile BHI broth (Oxoid, Basingstoke, United Kingdom) with 20% glycerin. All samples were stored at −80°C until cultivation.

Isolation and identification for carbapenem-resistant *Klebsiella* spp.

For all samples, a pre-enrichment step in the BHI broth (Oxoid, Basingstoke, United Kingdom) was performed in a constant temperature shaker (Boxun, Shanghai, China) at 37°C overnight. Enriched solutions (50 μl) were evenly spread on MacConkey agar (Landbridge, Beijing, China) supplemented with 2 mg/l meropenem (Meilun, Dalian, China) to screen for carbapenem-resistant isolates. Colonies were selected based on colony morphotypes and repeatedly streaked on the MacConkey agar to obtain pure isolates (Zhao et al., 2021a). The isolates were

1 http://www.chinets.com/

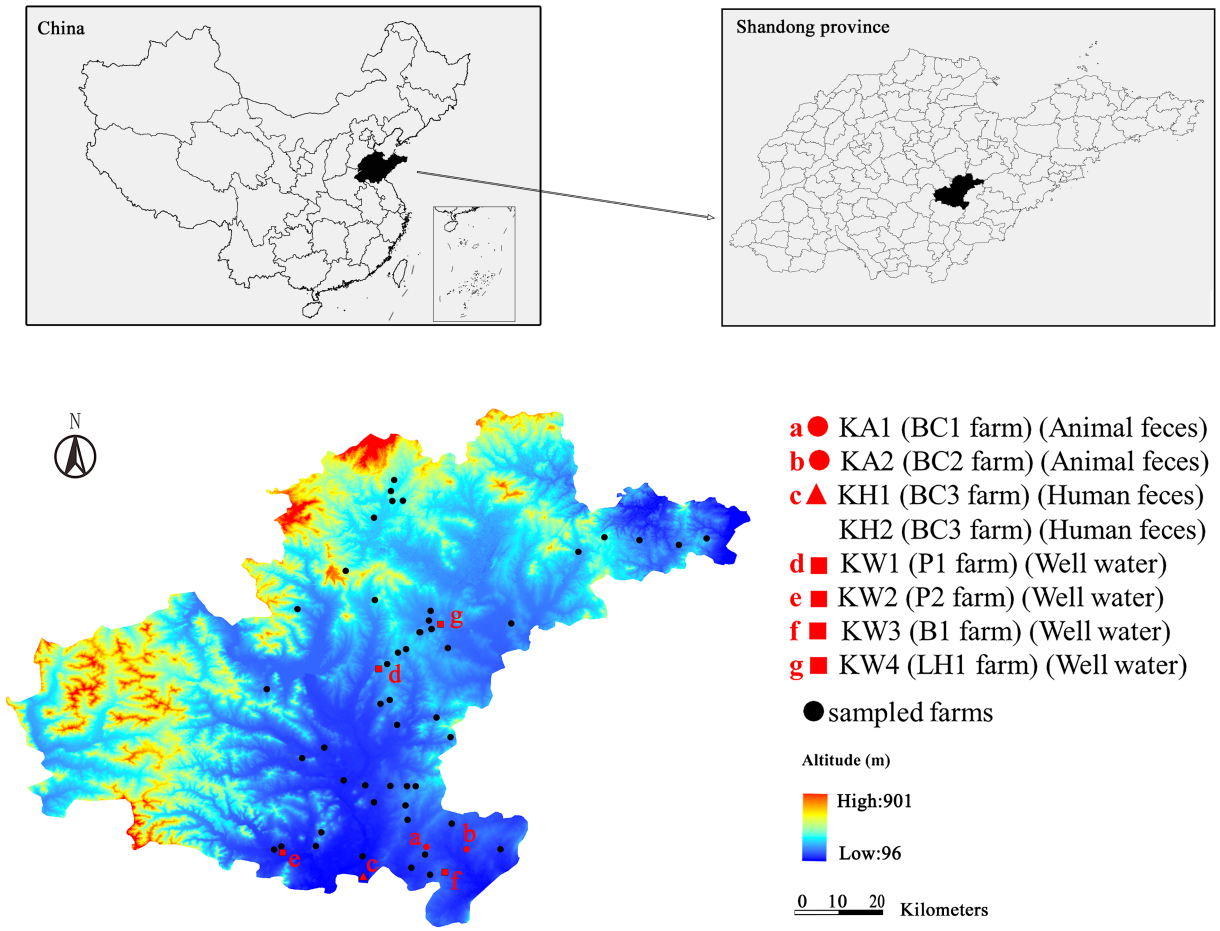

FIGURE 1
Map showing the location of the CRK-negative farms (denoted by black dots) and CRK-positive farms (denoted by red dots). The farms denoted "a" and "b" represent the farms in which CRK was isolated from animal feces. The red triangles (c) represent the farm in which CRK was isolated from human feces. Red squares (d, e, f, and g) represent the farms in which CRK was isolated from well water. BC1, BC2 and BC3 are broiler chicken farms; P1 and P2 are pig farms; B1 is a beef farm; LH1 is a laying hen farm.

tested for the presence of bla_{NDM}, bla_{KPC}, bla_{OXA-48}, bla_{VIM} and bla_{IMP} carbapenemase genes using PCR, as previously described (Poirel et al., 2011). The PCR products were verified using Sanger sequencing (Biosune, Shanghai, China). Matrix-assisted laser desorption/ionization time-of-flight mass spectrometry (MALDI-TOF/MS; Bruker Daltonik GmbH, Bremen, Germany) was used to identify the carbapenem-resistant isolates. The CRK isolates were selected for further research.

Antimicrobial susceptibility testing

The minimum inhibitory concentrations (MICs) of the 12 antibiotics were determined for CRK. 12 antibiotics were tested at a series of concentrations, and the maximum concentrations of amoxicillin/clavulanate, piperacillin/tazobactam, cefotaxime, ceftazidime, meropenem, imipenem, amikacin, ciprofloxacin, tetracycline, tigecycline, colistin and nitrofurantoin were 128/64 mg/l, 128/4 mg/l, 256 mg/l, 256 mg/l, 256 mg/l, 256 mg/l, 256 mg/l, 64 mg/l, 128 mg/l, 32 mg/l, 64 mg/l, 128 mg/l, respectively; the minimum concentrations were 0.0625 mg/l for 12 antibiotics. The MICs of tigecycline and colistin were determined using the broth microdilution method, and others were determined using the agar dilution method according to the Clinical Laboratory Standards Institute (CLSI). The results were interpreted according to the CLSI (document M100-S31), excluding tigecycline, for which MICs were interpreted following the ecological cut-off (ECOFF) of the European Committee on Antimicrobial Susceptibility Testing (EUCAST) SOP 10.2. *Escherichia coli* ATCC 25922 was used as the quality control strain. Multidrug resistance was defined as non-susceptibility to at least one agent in three or more antimicrobial categories (Magiorakos et al., 2012).

The transmissibility of plasmids

Sodium azide-resistant *E. coli* J53 was used as the recipient strain, and CRK was used as the donor strain to evaluate the

horizontal transferability of the plasmids mediating carbapenem resistance, colistin resistance, and tigecycline resistance by filter mating. The donor strain and recipient strain were mixed at a ratio of 2:1 and incubated at 37°C for 12 h. Transconjugants carrying carbapenemase gene, colistin resistance gene, and tigecycline resistance gene were selected by cultivation on LB agar supplemented with 100 mg/l sodium azide and 2 mg/l meropenem, 100 mg/l sodium azide and 2 mg/l colistin, 100 mg/l sodium azide and 4 mg/l tigecycline for 18 h at 37°C, respectively. Transconjugants carrying resistance genes were verified using PCR. Moreover, plasmids of tigecycline-resistant strain (KA2) were extracted using the M5 BAC/PAC large plasmid extraction kit (Mei5, Beijing, China) according to the manufacturer's instructions. XL10-Gold chemically competent *E. coli* cells (Angyu, Shanghai, China) were used as the recipient strain to evaluate the transformation of plasmids that mediate tigecycline resistance using the heat shock method, as previously described (Hassan et al., 2022). Transformants were selected by cultivation on LB agar supplemented with 4 mg/l tigecycline for 18 h at 37°C.

Whole-genome sequencing

All CRK were subjected to whole-genome sequencing on the Illumina NovaSeq 6,000-PE150 platform (Illumina, San Diego, United States) combined with the PacBio Sequel platform (Berry Genomics Co. Ltd.). Hybrid genome assembly with both short and long reads was performed using Unicycler v0.5.0 (Wick et al., 2017). The sequences were annotated using Prokka v1.12 (Seemann, 2014) and RAST v2.0 (Aziz et al., 2008). Antibiotic resistance genes, plasmid replicons, and MLST were identified at the Center for Genomic Epidemiology[2] using ResFinder 4.1, PlasmidFinder 2.1, and MLST 2.0, respectively. Virulence genes were analyzed using the VFDB analyzer[3] and capsule polysaccharide-based serotyping (K-type) was performed using the BIGSdb Klebsiella Pasteur MLST database.[4] The Basic Local Alignment Search Tool (BLAST) at the National Center for Biotechnology Information (NCBI)[5] was used to analyze the plasmid alignments. Alignment analysis of amino acid sequences of DNA gyrase (*gyrA* and *gyrB*) and topoisomerase IV (*parC* and *parE*) was performed using Clustal Omega (Sievers et al., 2011). Genetic relatedness of the isolates was determined by single nucleotide polymorphism (SNP) analysis using CSI Phylogeny 1.4 at the Center for Genomic Epidemiology (Kaas et al., 2014). A distance of ≤15 SNPs was defined as clonally related strains (Schürch et al., 2018). Visualization of the genome comparison of the plasmids harboring bla_{NDM-5} and *mcr-8.1* was performed using BLAST Ring Image Generator (BRIG; Alikhan et al., 2011). All genome sequences in this study have been deposited in NCBI Genome database under BioProject PRJNA834640. The bla_{NDM-5}-carrying plasmids of strains KA1, KA2, KH1, KH2, KW1, KW2, KW3, and KW4 have been deposited into GenBank under accession nos. CP102896.1, CP102875.1, CP102881.1, CP102887.1, CP102900.1, CP102890.1, CP102892.1, and CP102905.1, respectively. The *mcr-8.1*-carrying plasmids of strains KA2, KH1 and KH2 have been deposited into GenBank under accession nos. CP102872.1, CP102880.1, and CP102886.1, respectively.

2 http://www.genomicepidemiology.org/services/
3 http://www.mgc.ac.cn/cgi-bin/VFs/v5/main.cgi
4 https://bigsdb.pasteur.fr/klebsiella/
5 https://blast.ncbi.nlm.nih.gov/Blast.cgi

Results

Prevalence of carbapenem-resistant *Klebsiella* spp.

Eight CRK were isolated from 263 samples, five of which were *K. pneumoniae* and three were *K. quasipneumoniae*. Five CRK (KA1, KA2, KH1, KH2, and KW4) were isolated from chicken farms (6.7%, 5/75), two (KW1 and KW2) from pig farms (2.3%, 2/86) and one (KW3) from bovine farms (0.98%, 1/102). KH1 and KH2 were isolated from the same chicken farm, whereas the other strains were obtained from different farms. In terms of sample types, four CRK (KW1-KW4) were isolated from well water, two (KA1 and KA2) from animal feces, two (KH1 and KH2) from human feces, and no CRK was isolated from wastewater (Supplementary Table S1).

Phenotypic and genotypic antibiotic resistance

Antibiotic susceptibility testing showed that all CRK were multidrug-resistant and resistant to amoxicillin-clavulanic acid, piperacillin/tazobactam, cefotaxime, ceftazidime, meropenem, imipenem, and tetracycline. Most isolates were resistant to ciprofloxacin (62.5%), whereas resistance to colistin (50%), amikacin (37.5%), nitrofurantoin (37.5%), and tigecycline (12.5%) was observed to a lesser degree (Table 1). Eight CRK harbored the carbapenemase gene bla_{NDM-5}, accounting for high-level resistance to meropenem (≥128 mg/l) and imipenem (≥64 mg/l). In addition to the carbapenemase gene, CKR carried various classes of resistance genes and the most prevalent ARGs (prevalence ≥50%), including *oqxAB* ($n = 8$), *fosA* ($n = 8$), *tet* (A) ($n = 6$), *aadA2* ($n = 5$), *floR* ($n = 5$), *qnrS1* ($n = 4$), and *aac(6′)-Ib-cr* ($n = 4$; Supplementary Table S2). Three strains (KA2, KH1, and KH2) carried the colistin resistance *mcr-8.1* and *armA* genes which encode a 16S rRNA-methylase, accounting for high-grade aminoglycoside resistance. KH1 and KH2 were resistant to all tested antibiotics except tigecycline, and KA2 was resistant to all tested antibiotics, including tigecycline. However, no known tigecycline resistance genes were not found on KA2 strain. Plasmid conjugation assay and transformation assay found that

TABLE 1 Antimicrobial susceptibility profiles of carbapenem-resistant *Klebsiella* spp. strains from animal farms in Shandong, China.

Isolate	Species	Farm[a]	Source	Minimal inhibitory concentration (mg/L)											
				AMC	TZP	CTX	CAZ	MEM	IPM	AMK	CIP	TE	TGC	CL	F
KA1	*K. quasipneumoniae*	BC1	Animal feces	**32/16**	**>128/4**	**>256**	**>256**	**128**	**64**	4	**8**	**128**	1	1	32
KA2	*K. pneumoniae*	BC2	Animal feces	**32/16**	**>128/4**	**>256**	**>256**	**128**	**64**	**>256**	**8**	**>128**	**8**	**>64**	**>128**
KH1	*K. pneumoniae*	BC3	Human feces	**32/16**	**>128/4**	**>256**	**>256**	**256**	**256**	**>256**	**>64**	**128**	1	**4**	**>128**
KH2	*K. pneumoniae*	BC3	Human feces	**32/16**	**>128/4**	**>256**	**>256**	**128**	**128**	**>256**	**>64**	**128**	1	**4**	**>128**
KW1	*K. quasipneumoniae*	P1	Well water	**32/16**	**>128/4**	**>256**	**>256**	**128**	**128**	16	**4**	**128**	1	**4**	32
KW2	*K. pneumoniae*	P2	Well water	**32/16**	**>128/4**	**>256**	**>256**	**128**	**64**	2	0.25	**128**	0.5	1	64
KW3	*K. pneumoniae*	B1	Well water	**64/32**	**>128/4**	**>256**	**>256**	**128**	**64**	2	0.25	**64**	0.25	2	64
KW4	*K. quasipneumoniae*	LH1	Well water	**64/32**	**>128/4**	**>256**	**>256**	**128**	**64**	2	0.5	**128**	0.25	1	16
ATCC 25922	*E. coli*			8/4	1/4	0.06	0.25	0.03	0.5	2	0.03	1	0.5	1	4

[a]BC1, BC2 and BC3 are broiler chicken farms; P1 and P2 are pig farms; B1 is a beef farm; LH1 is a laying hen farm.
AMC, amoxicillin/clavulanate; TZP, piperacillin/tazobactam; CTX, cefotaxime; CAZ, ceftazidime; MEM, meropenem; IPM, imipenem; AMK, amikacin; CIP, ciprofloxacin; TE, tetracycline; TGC, tigecycline; CL, colistin; F, nitrofurantoin. Resistance is indicated in bold, intermediate resistance is indicated by underlined.

the plasmids pKA2-2, pKA2-3-mcr8.1, pKA2-5, and pKA2-6-NDM5 could be successfully transferred from KA2 to the recipient strain *E. coli* J53, while the transconjugants and transformants were remain sensitive to tigecycline, indicating a novel or more complex resistant mechanism in this strain.

As the strains showed a high resistance rate (62.5%, 5/8) to ciprofloxacin, the resistance mechanisms of ciprofloxacin were analyzed. Comparison of the amino acid sequence of DNA gyrase (*gyrA* and *gyrB*) and topoisomerase IV (*parC* and *parE*) between the CRK isolated in this study and the reference sequence in the NCBI database showed that the amino acid substitutions of quinolone resistance-determining regions (QRDRs) were observed at position 83 (Ser→IIe) of *gyrA* and position 80 (Ser→IIe) of *parC* in KA2, KH1, and KH2 (Supplementary Table S3). Three strains were resistant to ciprofloxacin, two of which had high-level ciprofloxacin resistance (MICs >64 mg/l). Several studies have confirmed that amino acid co-substitution in the QRDRs of *gyrA* and *parC* in *Klebsiella* spp. were associated with high-level resistance to ciprofloxacin (Minarini and Darini, 2012; Kareem et al., 2021; Zhan et al., 2021), which is consistent with our results. Additionally, all CRK, including ciprofloxacin-resistant strains, carried three or more fluoroquinolone resistance genes, including *oqxAB* (100%, 8/8), *qnrS* (50%, 4/8), *qnrB* (50%, 4/8), and *aac(6′)-Ib-cr* (50%, 4/8; Supplementary Table S3). Even in the absence of QRDRs mutations, one strain carrying the fluoroquinolone resistance genes *qnrB2*, *aac(6′)-Ib-cr,* and *oqxAB*, and another strain carrying *qnrS1* and *oqxAB* showed non-susceptibility to ciprofloxacin. The *qnr* genes encode proteins belonging to the pentapeptide repeat protein family that play a role in binding and protecting topoisomerase IV and DNA gyrase from repression by ciprofloxacin (Kim et al., 2009). The *aac(6′)-Ib-cr* gene encodes a variant aminoglycoside acetyltransferase that reduces the activity of ciprofloxacin by N-acetylation at the amino nitrogen on its piperazinyl substituent (Robicsek et al., 2006). Mirzaii et al. (2018), Zhan et al. (2021), and Reo et al. (2022) reported that *Klebsiella* spp. strains carrying fluoroquinolone resistance genes, but without mutations in the QRDRs, were resistant to ciprofloxacin. These findings indicate that fluoroquinolone resistance genes can mediate ciprofloxacin resistance in *Klebsiella* spp.

Virulence genes of carbapenem-resistant *Klebsiella* spp.

In this study, all strains possessed the type 1 fimbrial gene cluster *fimABCDEFGHI*, type 3 fimbrial gene cluster *mrkABCDFHIJ*, enterobactin-encoding genes *entABCDEFS* and its transport protein-encoding genes *fepABCDG*, and salmochelin-encoding gene *iroE*, but carried no genes related to hypervirulent *Klebsiella*, such as *iroB, iucA, rmpA and rmpA2* (Thomas et al., 2018; Supplementary Table S2).

Genotypic characterization of carbapenem-resistant *Klebsiella* spp.

The silico analysis of the general molecular characteristics of the isolates are summarized in Supplementary Table S2. The eight strains belonged to four different sequence types (ST): ST526 (KA1, KW1, and KW4), ST37 (KH1 and KH2), ST766 (KW2 and KW3), and ST495 (KA2). Three types of capsular serotypes KL22KL37-*wzi*385, KL28-*wzi*84, and KL15KL17KL51KL52-*wzi*50 were identified in KH1 and KH2, KW1 and KW4, and KW2 and KW3, respectively, and KA1 and KA2 had poor match confidence against any known serotype and were determined to

be non-typeable (Supplementary Table S2). The genome of each strain possessed a circular chromosome with sizes ranging from 5,225,745 bp to 5,320,447 bp. Furthermore, the genomes of KA1, KA2, KH1, KH2, KW1, KW2, KW3, and KW4 contained four, seven, five, five, four, one, one, and five circular plasmids, respectively. As shown in Supplementary Table S2, various classes of resistance genes were detected on the chromosomes and plasmids of the strains. Incompatible IncX3 type plasmids (45,122–52,085 bp) carrying bla_{NDM-5} were found on all strains. A hybrid incompatible IncFII(pKP91)/IncFIA(HI1) plasmid carrying *mcr-8.1* was detected on KA2, and IncFII(K)/IncFIA(HI1) plasmids carrying *mcr-8.1* were detected on KH1 and KH2.

Characterization and comparative genomics of plasmids carrying bla_{NDM-5} and *mcr-8.1*

bla_{NDM-5}-carrying IncX3 plasmids were successfully transferred from all strains to the recipient strain *E. coli* J53 *via* conjugation assays. bla_{NDM-5} was located on the 46,161 bp IncX3 plasmid among strains KA1, KW2, and KW3, designated pKA1-3-NDM5, pKW2-1-NDM5, and pKW3-1-NDM5, respectively. Plasmid sequence comparison showed that the three IncX3 plasmids shared 100% nucleotide identity and 100% coverage with each other, and were identical to several other IncX3 plasmids found in *Enterobacteriaceae* isolates in China, such as the plasmid pNDM5_IncX3 (GenBank: KU761328.1) from *K. pneumoniae* isolated from a patient in Suzhou city, pNDM-SCCRK18-72 (GenBank: MN565271.1) from an *E. coli* isolated from chicken in Sichuan province, and pEC24-NDM-5 (GenBank: CP060888.1) from an *E. coli* isolated from a patient in Zhejiang province. bla_{NDM-5} was flanked by the same genetic structure as that of Tn*3*-IS*3000*-IS*Aba125*-IS*5*-bla_{NDM-5}-ble_{MBL}-*trpF*-*dsbD*-IS*26*-IS*Kox3* (Figure 2A). In strains KA2, KW1, and KW4, bla_{NDM-5} was located on 45,244, 45,122 and 45,122 bp IncX3 plasmids, designated pKA2-6-NDM5, pKW1-2-NDM5, and pKW4-2-NDM5, respectively. The three IncX3 plasmids showed 97% coverage and 99.99% nucleotide identity with pKA1-3-NDM5. Tn*3*, IS*3000*, and IS*5* were located upstream of bla_{NDM-5}, whereas ble_{MBL}, *trpF*, *dsbD*, IS*26*, and IS*Kox3* were located downstream (Figure 2A). KH1 and KH2 contained a 52,085 bp IncX3 plasmid carrying bla_{NDM-5}, which shared 99.99% nucleotide identity and 97% coverage with pKA1-3-NDM5. The environment of bla_{NDM-5} was same with strains KA2, KW1, and KW4 (Figure 2B). Although the size and structure of IncX3 plasmids carrying bla_{NDM-5} differed slightly among strains, all IncX3 plasmids contained a highly conserved region around bla_{NDM-5}, consisting of IS*5*-bla_{NDM-5}-ble_{MBL}-*trpF*-*dsbD*-IS*26*-IS*Kox3*.

The *mcr-8.1* harboring plasmids were successfully transferred into the recipient strain *E. coli* J53 from three CRKP *via* conjugation assays. In strain KA2, *mcr-8.1* was located on a 118,931 bp plasmid, designated pKA2-3-mcr8.1, which contained IncFII(pKP91) and IncFIA(HI1) replicons. In addition to *mcr-8.1*, resistance genes bla_{TEM-1B}, $bla_{CTX-M-1}$, and ble_{O} were identified on the plasmid. The plasmid BLAST query in the GenBank database showed that the plasmid pKA2-3-mcr8.1 exhibited the highest degree of sequence homology with plasmids pKP19-3,138-3 (GenBank: CP090619.1) from *K. pneumoniae* and pKP46-mcr8 (GenBank: CP088125.1) from *K. pneumoniae*, with over 99% identity and 81% coverage (Figure 3A). In strains KH1 and KH2, *mcr-8.1* was located on 100,448 bp plasmids, designated pKH1-3-mcr8.1 and pKH2-3-mcr8.1, both of which harbor

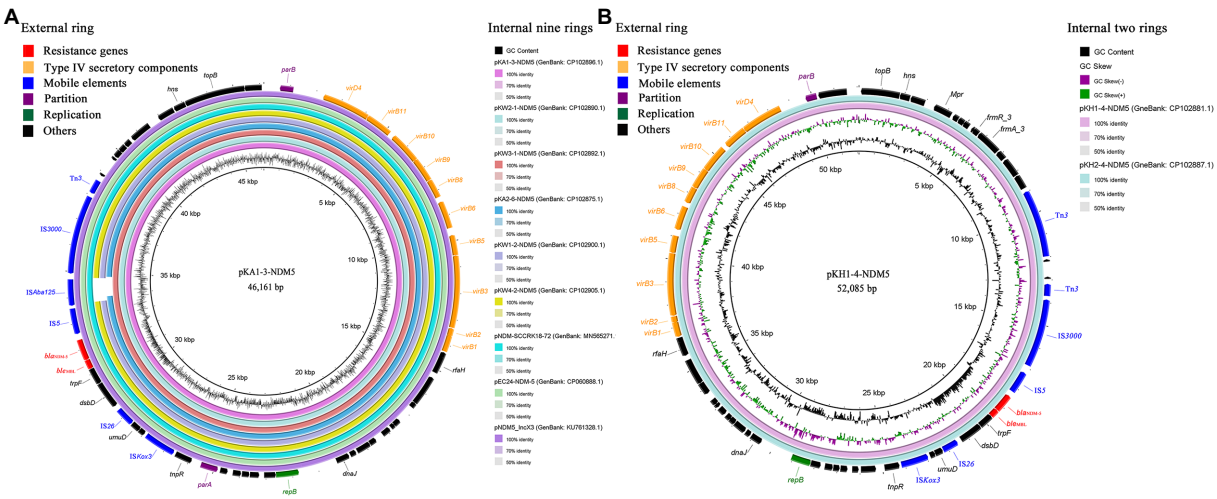

FIGURE 2
The blast and annotation of bla_{NDM-5}-carrying IncX3 plasmid genomes (constructed by BRIG). Genes are color-coded depending on functional annotations. **(A)** The nine internal rings represent different bla_{NDM-5}-carrying IncX3 plasmids from this study and GenBank database. The external ring represents the annotation of plasmid pKA1-3-NDM5. **(B)** The two internal rings represent plasmid pKH1-4-NDM5 and pKH2-4-NDM5. The external ring represents the annotation of plasmid pKH1-4-NDM5.

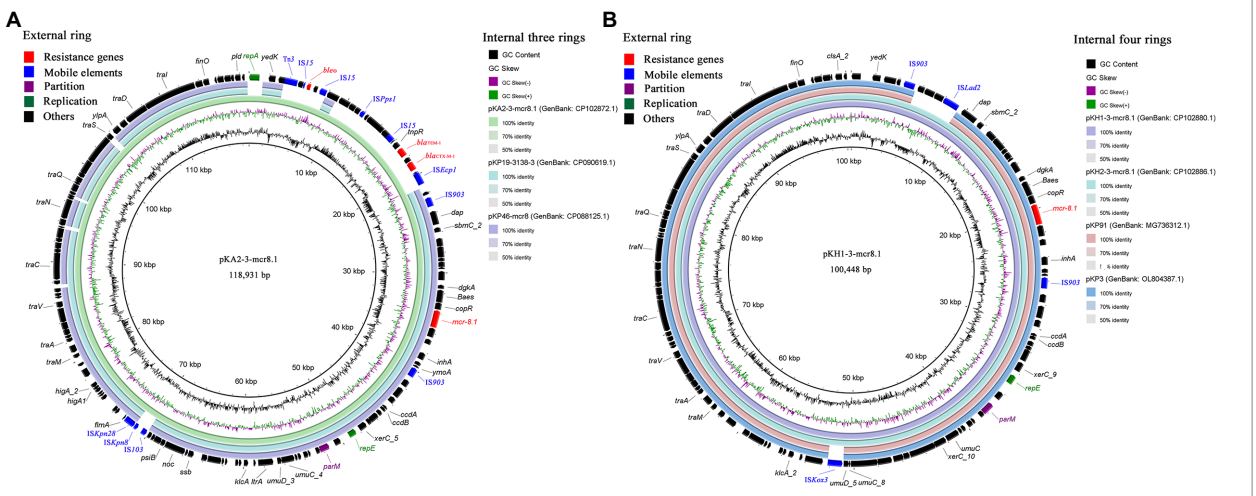

FIGURE 3
The blast and annotation of *mcr-8.1*-carrying plasmid genomes (constructed by BRIG). Genes are color-coded depending on functional annotations. **(A)** The three internal rings represent plasmids pKA2-3-mcr8.1, pKP19-3,138-3 (GenBank: CP090619.1) and pKP46-mcr8 (GenBank: CP088125.1). The external ring represents the annotation of plasmid pKA2-3-mcr8.1. **(B)** The four internal rings represent different *mcr-8.1*-carrying plasmids from this study and GenBank database. The external ring represents the annotation of plasmid pKH1-3-mcr8.1.

IncFII(K) and IncFIA(HI1) replicons. The two plasmids shared over 99% nucleotide identity and 94% coverage with the plasmids pKP3 (GenBank: OL804387.1) and pKP91 (GenBank: MG736312.1), which were isolated from chicken anal swab and pig feces, respectively, in Shandong province, China (Figure 3B), indicating that this type of plasmid may have been widely spread in this region. The genetic context of *mcr-8.1* in the isolates was similar and was composed of *IS903-orf-mcr-8.1-copR-baeS-dgkA-orf-IS903*. *mcr-8.1* was flanked by the complete insertion sequence IS*903*, which may facilitate the transmission of *mcr-8.1* among animals, the environment, and humans in this animal breeding area. Additionally, the *mcr-8.1*-carrying IncFII(pKP91)/IncFIA(HI1) and IncFII(K)/IncFIA(HI1) plasmids carried two genes coding the response regulator transcription factor *CopR* and HAMP domain-containing histidine kinase *Baes*. The combination of these two protein families usually constitutes a two-component system involved in colistin resistance in *Enterobacteriaceae*.

Genetic relationship analysis

SNP-based phylogenetic analysis revealed that the eight CRK were grouped into four clusters. The first cluster included KW2 and KW3, isolated from the well water of farms P2 and B1, respectively, with four SNPs differences. The second cluster consisted of KA1, KW1, and KW4, among which KW1 and KW4 differed by only six SNPs and were isolated from the well water of farms P1 and LB1. The third cluster included only KA2. The fourth cluster included KH1 and KH2 isolated from two human fecal samples in farm BC3, with two SNPs differences (Figure 4; Supplementary Table S4).

Moreover, the genetic relationships between these strains, and 72 CRKP and 20 carbapenem-resistant *Klebsiella quasipneumoniae* (CRKQ) stains from the GenBank database were characterized (Figure 4). The sample identifier (ID), location, collection date, and source were indicated for each strain. The results suggest that CRKP and CRKQ were wide spread among humans, animals, and different environmental media (well water, sewage, sludge, river water, and river sediment) in multiple countries, and humans were the most common hosts of CRKP and CRKQ. KW2 and KW3 were clonally related to four CRKP from sludge and sewage in a wastewater treatment plant (WWTT), including *K. pneumoniae* strains SDWK15, SDWK18, SDWK19, and SDWK20, and two CRKP (*K. pneumoniae* strains SW03 and SW04) from well water in two animal breeding areas (differed by 4–6 SNPs). KW1 and KW4 were similar to *K. quasipneumoniae* strain KE1661 from a human rectal swab in Germany (differed by 89 and 87 SNPs, respectively) and *K. quasipneumoniae* strain SDWK24 from the abovementioned WWTT (differed by 91 and 91 SNPs, respectively; Supplementary Table S4). The WWTT and animal breeding areas are in different counties of Shandong province, more than 200 km and 150 km from this study site, respectively.

Discussion

As animal farms have become one of the most important reservoirs of CRK, it is important to investigate the prevalence and dissemination of CRK in animal breeding areas. In this study, a total of eight bla_{NDM-5}-carrying CRK were isolated from animal feces, well water, and worker feces from seven animal farms. Four CRK were isolated from animal feces and human feces in chicken farms,

whereas no CRK was isolated from animal feces and human feces in pig and bovine farms. A possible explanation for this may be the use of antibiotics on the farms. Antibiotics are usually used to prevent and treat diseases in larger quantities and at higher frequencies in chicken farms than in pig and bovine farms, because of the higher breeding density and shorter production cycles of chicken farms, especially broiler farms (Zhao et al., 2010). Several studies have shown results consistent with our research. For example, Gu et al. observed that the carbapenem-resistant *Enterobacteriaceae* (CRE) detection rate in animal fecal samples was higher in chicken farms compared to bovine and pig farms in northern China (Gu et al., 2022). Qian et al. found that the diversity and abundance of ARGs were higher in chicken feces than in bovine feces sampled from the Shaanxi province in China (Qian et al., 2018). In this study, four CRK were isolated from well water in chicken, pig, and bovine farms, suggesting that groundwater has been contaminated by CRK in this animal breeding area and groundwater may have become a potential CRK reservoir. In addition to CRK, other carbapenem-resistant *Enterobacteriaceae* species have been detected in well water in animal breeding areas in China. Sun et al. isolated one bla_{KPC-2}-carrying *Raoultella ornithinolytica* from well water in a pig breeding area in Shandong province (Sun et al., 2017). Zou et al. detected one bla_{NDM-1}-carrying *Raoultella ornithinolytica* in well water in Weifang city of Shandong province (Zou et al., 2020). Gu et al. conducted a large-scale study in animal breeding areas of six countries in Inner Mongolia and Shandong province, and detected several CRE from well water, including *K. pneumoniae*, *Enterobacter* spp., *Citrobacter sedlakii*, and *K. michiganensis* (Gu et al., 2022). The results indicate that the groundwater in animal breeding areas is vulnerable to CRE contamination, and it is necessary to strengthen the groundwater monitoring and control of CRE in breeding areas.

Since the IncX3 plasmid pNDM-MGR194 carrying bla_{NDM-5} was first identified in *K. pneumoniae* from a patient in India (Krishnaraju et al., 2015), pNDM-MGR194-like plasmids have been found in *Enterobacteriaceae* worldwide (Alexander et al., 2015; Tian et al., 2020; Chakraborty et al., 2021; Costa et al., 2021). Additionally, previous studies have shown a high capacity of the IncX3 plasmid to mediate the dissemination of bla_{NDM-5} in *Enterobacteriaceae* in various environments. Tian et al. reported that the horizontal gene transfer (HGT) of bla_{NDM-5} among different *Enterobacteriaceae* species was mainly mediated by IncX3 plasmids in a pediatric hospital in Shanghai (Tian et al., 2020). Gu et al. confirmed that bla_{NDM-5}-carrying IncX3 plasmids are widely disseminated among different *Enterobacteriaceae* genera among animals and the environment in animal breeding areas in Inner Mongolia and Shandong province (Gu et al., 2022). Zhao et al. reported that bla_{NDM-5} could disseminate among humans and the environment *via* IncX3 plasmids in an intensive vegetable cultivation area in Shandong province (Zhao et al., 2021a). In this study, bla_{NDM-5} was located on highly related conjugative IncX3 plasmids among all strains and flanked by the same core genetic structure: IS*5*-bla_{NDM-5}-ble_{MBL}-*trpF*-*dsbD*-IS*26*-IS*Kox3*, which confirms that the IncX3 plasmid may serve as a major vehicle for the bla_{NDM-5} dissemination among animals, the environment, and humans in this animal breeding area.

KH1 and KH2 from two fecal samples from workers at farm BC3 and KA2 from animal feces at farm BC2 carried the colistin resistance gene *mcr-8.1* and were resistant to colistin. Colistin is effective against most gram-negative bacteria and is considered a last-resort antibiotic for treating serious infections caused by multidrug-resistant bacteria, particularly CRE (Li et al., 2006; Petrosillo et al., 2019). However, with the emergence and prevalence of CRE, extensive use of colistin has led to the emergence of colistin resistance. In 2016, Liu et al. reported the plasmid-mediated colistin resistance gene *mcr-1* in *Enterobacteriaceae* isolated from animals and humans in China (Liu et al., 2016). In the past 5 years, *mcr* gene variants (*mcr-1* to *mcr-10*) have been identified in different bacteria isolated from animals, the environment, and humans worldwide (Hussein et al., 2021; Portes et al., 2022). Since Wang et al. reported that *mcr-8.1* is located on a conjugative IncFII-type plasmid in *K. pneumoniae* in 2018 (Wang et al., 2018), *K. pneumoniae* has become one of the main hosts of *mcr-8.1* in animals and humans. Plasmids are considered to play an important role in the dissemination of *mcr-8.1* genes, because the majority of *mcr-8.1* carriers are on plasmids. *Mcr-8.1* has been reported to be located on various plasmids replicon types, especially IncFII, IncFIA, IncFIB, IncQ, IncR, and IncA/C replicon plasmids in *Enterobacteriaceae* (Hadjadj et al., 2019; Farzana et al., 2020; Wu et al., 2020). In this study, *mcr-8.1* was located on the hybrid incompatible plasmid groups IncFII(pKP91)/IncFIA(HI1) and IncFII(K)/IncFIA(HI1), supporting the notion that plasmids are the main factor in disseminating *mcr-8.1*.

Clonal spread of colistin-resistant CRKP has been reported most frequently in hospitals (Battikh et al., 2016; Jonathan et al., 2017; Rocha et al., 2022). However, several studies have reported the clonal spread of colistin-resistant CRKP in animal farms. For example, Zhai et al. and Sun et al. reported the clonal spread of colistin-resistant CRKP among chickens and the environment in a poultry farm in Hebei province, China and among chickens in a chicken farm in Shandong province, China, respectively (Sun et al., 2020; Zhai et al., 2020). In this study, SNP analysis confirmed the clonal spread of ST37 *K. pneumoniae* carrying bla_{NDM-5} and *mcr-8.1* between human workers in the same chicken farm. However, because the types of samples were limited, the route of dissemination could not be determined in this study, and further research should clarify the route of clonal spread and provide effective control strategies for the dissemination of colistin-resistant CRKP in animal farms. Additionally, two pairs of clonally related CRKP and CRKQ were isolated from well water in four different farms located at a distance of more than 20 km, revealing that clonal spread also has significant implications for the dissemination of bla_{NDM-5} in the animal breeding area. Unexpectedly, the pair of clonal CRKP was clonally related to six strains from animal farms and a WWTT collected in other studies in the same province, suggesting that bla_{NDM-5}-carrying *K. pneumoniae* are capable of disseminating within or between

10.3389/fmicb.2022.1030490

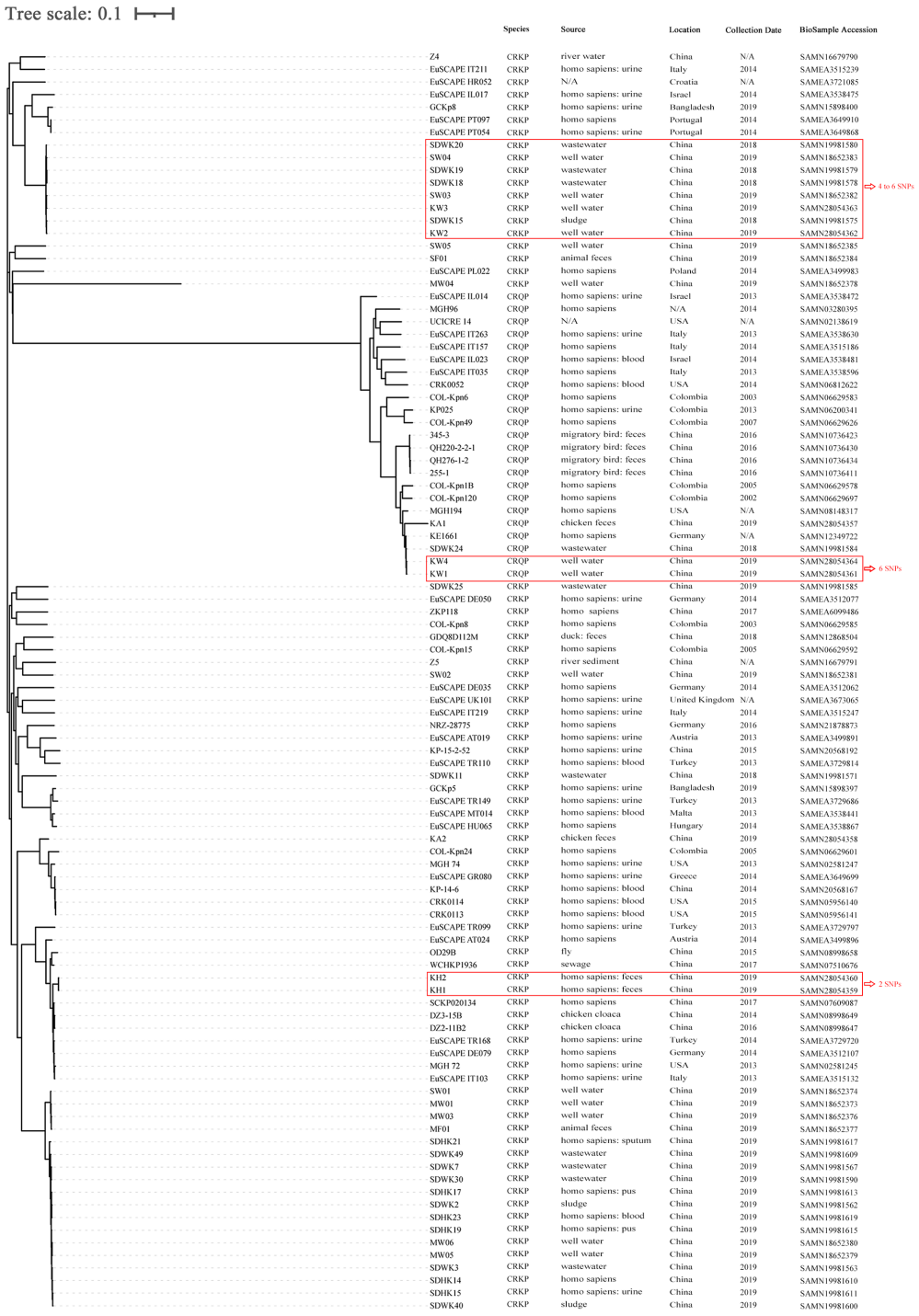

FIGURE 4
SNP-based phylogenetic tree of 8 carbapenem-resistant *Klebsiella* spp. isolated from animal breeding area in this study, and another 72 carbapenem-resistant *Klebsiella pneumoniae* (CRKP) and 20 carbapenem-resistant *Klebsiella quasipneumoniae* (CRKQ) in NCBI database. The sample identifier, location, collection date and source were indicated for each isolate. The number of SNPs denoted in red outside the rectangles indicate the number of SNPs differing between the isolates. *K. pneumoniae* MGH 78578 (GenBank: NC_009648.1) genome sequence was used as reference for construction of the phylogenetic trees based on SNP differences. N/A, not available.

farms in the same county, even in different counties within a province, *via* clonal expansion. Although the exact route of long-distance transmission of CRKP is uncertain, population movement and travel (Schwartz and Morris, 2018), migration of birds (Wang et al., 2017), and the live poultry trade (Wang et al., 2019) may promote the cross-regional transmission of CRKP.

Conclusion

In this study, we investigated the prevalence of CRK by randomly selecting 20 chicken, 20 pig, and 20 bovine farms from a typical region of the animal farming industry in China. Based on the "One-Health" concept, the transmission of CRK among animals, the environment and humans were discussed. All CRK carried bla_{NDM-5}, which was located on highly related conjugative IncX3 plasmids. *Mcr-8.1* was carried by three CRK and located on self-transmissible IncFII(K)/ IncFIA(HI1) and IncFII(pKP91)/IncFIA(HI1) plasmids. Two pairs of clonal CRK from well water and one pair of clonal colistin-resistant CRK from human workers were identified. Thus, both HGT *via* plasmids and clonal expansion play a significant role in disseminating bla_{NDM-5} and *mcr-8.1* among animals, the environment, and humans in the animal breeding area. The results highlight that systematical monitoring and large-scale investigation of the prevalence and spread of CRK with a "One Health"-perspective in animal breeding areas in Eastern China are urgently needed to enable effective measures for controlling the further spread of CRK.

Data availability statement

The datasets presented in this study can be found in online repositories. The names of the repository/repositories and accession number(s) can be found in the article/Supplementary material.

Ethics statement

Ethical approval to conduct this study was granted by the Ethics Committee for Shandong University [Ethics permission number: 20191202]. The patients/participants provided their written informed consent to participate in this study. Ethical review and approval was not required for the animal study because We only collected animal feces from the animal farms and did not contact animals.

Author contributions

CY: sampling, experiments conducting, data formal analysis, and writing—original draft preparation. BB and JH: writing—reviewing and editing. HZo, CG, LZ, CM, and HZh sampling. XM and XL: conceptualization, supervision, and writing-reviewing. All authors contributed to the article and approved the submitted version.

Funding

This work was supported by the National Key Research and Development Program of China [2020YFC1806904] and the National Natural Science Foundation of China (grant nos. 8197120700 and 41771499).

Conflict of interest

The authors declare that the research was conducted in the absence of any commercial or financial relationships that could be construed as a potential conflict of interest.

Publisher's note

All claims expressed in this article are solely those of the authors and do not necessarily represent those of their affiliated organizations, or those of the publisher, the editors and the reviewers. Any product that may be evaluated in this article, or claim that may be made by its manufacturer, is not guaranteed or endorsed by the publisher.

Supplementary material

The Supplementary material for this article can be found online at: https://www.frontiersin.org/articles/10.3389/fmicb.2022.1030490/full#supplementary-material

References

Alexander, M. W., David, L. P., Caffery, M., Sowden, D., and Hanna, E. S. (2015). Draft genome sequence of NDM-5-producing Escherichia coli sequence type 648 and genetic context of blaNDM-5 in Australia. *Genome Announc.* 3, e00194–e00115. doi: 10.1128/genomeA.00194-15

Alikhan, N.-F., Petty, N. K., Ben Zakour, N. L., and Beatson, S. A. (2011). BLAST ring image generator (BRIG): simple prokaryote genome comparisons. *BMC Genomics* 12:402. doi: 10.1186/1471-2164-12-402

Aziz, R. K., Bartels, D., Best, A. A., DeJongh, M., Disz, T., Edwards, R. A., et al. (2008). The RAST server: rapid annotations using subsystems technology. *BMC Genomics* 9:75. doi: 10.1186/1471-2164-9-75

Battikh, H., Harchay, C., Dekhili, A., Khazar, K., Kechrid, F., Zribi, M., et al. (2016). Clonal spread of Colistin-resistant Klebsiella pneumoniae coproducing KPC and VIM Carbapenemases in neonates at a Tunisian university hospital. *Microb. Drug Resist.* 23, 468–472. doi: 10.1089/mdr.2016.0175

BIOHAZ (2013). Scientific opinion on Carbapenem resistance in food animal ecosystems. *EFSA J.* 11:501. doi: 10.2903/j.efsa.2013.3501

Chakraborty, T., Sadek, M., Yao, Y., Imirzalioglu, C., Stephan, R., Poirel, L., et al. (2021). Cross-border emergence of Escherichia coli producing the Carbapenemase NDM-5 in Switzerland and Germany. *J. Clin. Microbiol.* 59, e02238–e02220. doi: 10.1128/JCM.02238-20

Costa, A., Figueroa-Espinosa, R., Gaudenzi, F., Lincopan, N., Fuga, B., Ghiglione, B., et al. (2021). Co-occurrence of NDM-5 and RmtB in a clinical isolate of Escherichia coli belonging to CC354 in Latin America. *Front. Cell. Infect. Microbiol.* 11:852. doi: 10.3389/fcimb.2021.654852

Farzana, R., Jones Lim, S., Barratt, A., Rahman Muhammad, A., Sands, K., Portal, E., et al. (2020). Emergence of Mobile Colistin resistance (mcr-8) in a highly successful Klebsiella pneumoniae sequence type 15 clone from clinical infections in Bangladesh. *mSphere* 5, e00023–e00020. doi: 10.1128/mSphere.00023-20

Gu, C., Li, X., Zou, H., Zhao, L., Meng, C., Yang, C., et al. (2022). Clonal and plasmid-mediated dissemination of environmental carbapenem-resistant Enterobacteriaceae in large animal breeding areas in northern China. *Environ. Pollut.* 297:118800. doi: 10.1016/j.envpol.2022.118800

Hadjadj, L., Baron, S. A., Olaitan, A. O., Morand, S., and Rolain, J.-M. (2019). Co-occurrence of variants of mcr-3 and mcr-8 genes in a Klebsiella pneumoniae isolate from Laos. *Front. Microbiol.* 10:720. doi: 10.3389/fmicb.2019.02720

Hassan, A. M., Johar, A. A., Kassem, I. I., and Eltai, N. O. (2022). Transmissibility and persistence of the plasmid-borne Mobile Colistin resistance gene, mcr-1, harbored in poultry-Associated E. coli. *Antibiotics* 11:774. doi: 10.3390/antibiotics11060774

He, T., Wang, Y., Sun, L., Pang, M., Zhang, L., and Wang, R. (2017). Occurrence and characterization of blaNDM-5-positive Klebsiella pneumoniae isolates from dairy cows in Jiangsu, China. *J. Antimicrob. Chemother.* 72, 90–94. doi: 10.1093/jac/dkw357

Hussein, N. H., Al-Kadmy, I. M. S., Taha, B. M., and Hussein, J. D. (2021). Mobilized colistin resistance (mcr) genes from 1 to 10: a comprehensive review. *Mol. Biol. Rep.* 48, 2897–2907. doi: 10.1007/s11033-021-06307-y

Jonathan, A. O., Doumith, M., Davies, F., Mookerjee, S., Dyakova, E., Gilchrist, M., et al. (2017). Emergence and clonal spread of colistin resistance due to multiple mutational mechanisms in carbapenemase-producing Klebsiella pneumoniae in London. *Sci. Rep.* 7:12711. doi: 10.1038/s41598-017-12637-4

Kaas, R. S., Leekitcharoenphon, P., Aarestrup, F. M., and Lund, O. (2014). Solving the problem of comparing whole bacterial genomes across different sequencing platforms. *PLoS One* 9:e104984. doi: 10.1371/journal.pone.0104984

Kareem, S. M., Al-Kadmy, I. M., Kazaal, S. S., Mohammed Ali, A. N., Aziz, S. N., Makharita, R. R., et al. (2021). Detection of gyrA and parC mutations and prevalence of plasmid-mediated quinolone resistance genes in Klebsiella pneumoniae. *Infect. Drug Resist.* 14, 555–563. doi: 10.2147/idr.s275852

Kim, H. B., Park Chi, H., Kim Chung, J., Kim, E.-C., Jacoby George, A., and Hooper David, C. (2009). Prevalence of plasmid-mediated quinolone resistance determinants over a 9-year period. *Antimicrob. Agents Chemother.* 53, 639–645. doi: 10.1128/AAC.01051-08

Krishnaraju, M., Kamatchi, C., Jha, A., Devasena, N., Vennila, R., Sumathi, G., et al. (2015). Complete sequencing of an IncX3 plasmid carrying blaNDM-5 allele reveals an early stage in the dissemination of the blaNDM gene. *Indian J. Microbiol.* 33, 30–38. doi: 10.4103/0255-0857.148373

Li, J., Nation, R. L., Turnidge, J. D., Milne, R. W., Coulthard, K., Rayner, C. R., et al. (2006). Colistin: the re-emerging antibiotic for multidrug-resistant gram-negative bacterial infections. *Lancet Infect. Dis.* 6, 589–601. doi: 10.1016/S1473-3099(06)70580-1

Liu, Y.-Y., Wang, Y., Walsh, T. R., Yi, L.-X., Zhang, R., Spencer, J., et al. (2016). Emergence of plasmid-mediated colistin resistance mechanism MCR-1 in animals and human beings in China: a microbiological and molecular biological study. *Lancet Infect. Dis.* 16, 161–168. doi: 10.1016/S1473-3099(15)00424-7

Ma, Z., Liu, J., Yang, J., Zhang, X., Chen, L., Xiong, W., et al. (2020). Emergence of blaNDM-carrying IncX3 plasmid in Klebsiella pneumoniae and Klebsiella quasipneumoniae from duck farms in Guangdong Province, China. *J. Glob. Antimicrob. Resist.* 22, 703–705. doi: 10.1016/j.jgar.2020.07.001

Magiorakos, A. P., Srinivasan, A., Carey, R. B., Carmeli, Y., Falagas, M. E., Giske, C. G., et al. (2012). Multidrug-resistant, extensively drug-resistant and pandrug-resistant bacteria: an international expert proposal for interim standard definitions for acquired resistance. *Clin. Microbiol. Infect.* 18, 268–281. doi: 10.1111/j.1469-0691.2011.03570.x

Minarini, L. A. R., and Darini, A. L. C. (2012). Mutations in the quinolone resistance-determining regions of gyrA and parC in Enterobacteriaceae isolates from Brazil. *Braz. J. Microbiol.* 43, 1309–1314. doi: 10.1590/S1517-83822012000400010

Mirzaii, M., Jamshidi, S., Zamanzadeh, M., Marashifard, M., Malek Hosseini, S. A. A., Haeili, M., et al. (2018). Determination of gyrA and parC mutations and prevalence of plasmid-mediated quinolone resistance genes in Escherichia coli and Klebsiella pneumoniae isolated from patients with urinary tract infection in Iran. *J. Glob. Antimicrob. Resist.* 13, 197–200. doi: 10.1016/j.jgar.2018.04.017

Navon-Venezia, S., Kondratyeva, K., and Carattoli, A. (2017). Klebsiella pneumoniae: a major worldwide source and shuttle for antibiotic resistance. *FEMS Microbiol. Rev.* 41, 252–275. doi: 10.1093/femsre/fux013

Petrosillo, N., Taglietti, F., and Granata, G. (2019). Treatment options for Colistin resistant Klebsiella pneumoniae: present and future. *J. Clin. Med.* 8:934. doi: 10.3390/jcm8070934

Poirel, L., Walsh, T. R., Cuvillier, V., and Nordmann, P. (2011). Multiplex PCR for detection of acquired carbapenemase genes. *Diagn. Microbiol. Infect. Dis.* 70, 119–123. doi: 10.1016/j.diagmicrobio.2010.12.002

Portes, A. B., Rodrigues, G., Leitão, M. P., Ferrari, R., Conte Junior, C. A., and Panzenhagen, P. (2022). Global distribution of plasmid-mediated colistin resistance mcr gene in salmonella: a systematic review. *J. Appl. Microbiol.* 132, 872–889. doi: 10.1111/jam.15282

Qian, X., Gu, J., Sun, W., Wang, X.-J., Su, J.-Q., and Stedfeld, R. (2018). Diversity, abundance, and persistence of antibiotic resistance genes in various types of animal manure following industrial composting. *J. Hazard. Mater.* 344, 716–722. doi: 10.1016/j.jhazmat.2017.11.020

Reo, O., Shigemura, K., Osawa, K., Yang, Y.-M., Maeda, K., Tanimoto, H., et al. (2022). Impact on quinolone resistance of plasmid-mediated quinolone resistance gene and mutations in quinolone resistance-determining regions in extended spectrum beta lactamase-producing Klebsiella pneumoniae isolated from urinary tract infection patients. *Pathog. Dis.* 80:ftac030. doi: 10.1093/femspd/ftac030

Robicsek, A., Strahilevitz, J., Jacoby, G. A., Macielag, M., Abbanat, D., Hye Park, C., et al. (2006). Fluoroquinolone-modifying enzyme: a new adaptation of a common aminoglycoside acetyltransferase. *Nat. Med.* 12, 83–88. doi: 10.1038/nm1347

Rocha, V. F. D., Barbosa, M. S., Leal, H. F., Silva, G. E. O., Sales, N. M. M. D., Monteiro, A. D. S. S., et al. (2022). Prolonged outbreak of Carbapenem and Colistin-resistant Klebsiella pneumoniae at a large tertiary Hospital in Brazil. *Front. Microbiol.* 13:770. doi: 10.3389/fmicb.2022.831770

Schürch, A. C., Arredondo-Alonso, S., Willems, R. J. L., and Goering, R. V. (2018). Whole genome sequencing options for bacterial strain typing and epidemiologic analysis based on single nucleotide polymorphism versus gene-by-gene–based approaches. *Clin. Microbiol. Infect.* 24, 350–354. doi: 10.1016/j.cmi.2017.12.016

Schwartz, K. L., and Morris, S. K. (2018). Travel and the spread of drug-resistant bacteria. *Curr. Infect. Dis. Rep.* 20, 1–10. doi: 10.1007/s11908-018-0634-9

Seemann, T. (2014). Prokka: rapid prokaryotic genome annotation. *Bioinformatics* 30, 2068–2069. doi: 10.1093/bioinformatics/btu153

Sievers, F., Wilm, A., Dineen, D., Gibson, T. J., Karplus, K., Li, W., et al. (2011). Fast, scalable generation of high-quality protein multiple sequence alignments using Clustal omega. *Mol. Syst. Biol.* 7:539. doi: 10.1038/msb.2011.75

Sun, P., Bi, Z., Nilsson, M., Zheng, B., Berglund, B., Stålsby Lundborg, C., et al. (2017). Occurrence of blaKPC-2, blaCTX-M, and mcr-1 in Enterobacteriaceae from well water in rural China. *Antimicrob. Agents Chemother.* 61, e02569–e02516. doi: 10.1128/AAC.02569-16

Sun, S., Gao, H., Liu, Y., Jin, L., Wang, R., Wang, X., et al. (2020). Co-existence of a novel plasmid-mediated efflux pump with colistin resistance gene mcr in one plasmid confers transferable multidrug resistance in Klebsiella pneumoniae. *Emerg. Microbes Infect.* 9, 1102–1113. doi: 10.1080/22221751.2020.1768805

Tacconelli, E., Carrara, E., Savoldi, A., Harbarth, S., Mendelson, M., Monnet, D. L., et al. (2018). Discovery, research, and development of new antibiotics: the WHO priority list of antibiotic-resistant bacteria and tuberculosis. *Lancet Infect. Dis.* 18, 318–327. doi: 10.1016/S1473-3099(17)30753-3

Tang, B., Chang, J., Cao, L., Luo, Q., Xu, H., Lyu, W., et al. (2019). Characterization of an NDM-5 carbapenemase-producing Escherichia coli ST156 isolate from a poultry farm in Zhejiang, China. *BMC Microbiol.* 19:82. doi: 10.1186/s12866-019-1454-2

Thomas, A. R., Olson, R., Fang, C.-T., Stoesser, N., Miller, M., MacDonald, U., et al. (2018). Identification of biomarkers for differentiation of Hypervirulent Klebsiella pneumoniae from Classical K. pneumoniae. *J. Clin. Microbiol.* 56, e00776–e00718. doi: 10.1128/JCM.00776-18

Tian, D., Wang, B., Zhang, H., Pan, F., Wang, C., Shi, Y., et al. (2020). Dissemination of the blaNDM-5 gene via IncX3-type plasmid among Enterobacteriaceae in children. *mSphere* 5, e00699–e00619. doi: 10.1128/mSphere.00699-19

Tiseo, K., Huber, L., Gilbert, M., Robinson, T. P., and Van Boeckel, T. P. (2020). Global trends in antimicrobial use in food animals from 2017 to 2030. *Antibiotics* 9:918. doi: 10.3390/antibiotics9120918

Wang, Y., Hu, Y., Cao, J., Bi, Y., Lv, N., Liu, F., et al. (2019). Antibiotic resistance gene reservoir in live poultry markets. *J. Infect.* 78, 445–453. doi: 10.1016/j.jinf.2019.03.012

Wang, J., Tang, B., Lin, R., Zheng, X., Ma, J., Xiong, X., et al. (2022). Emergence of mcr-1- and blaNDM-5-harbouring IncHI2 plasmids in Escherichia coli strains isolated from meat in Zhejiang, China. *J. Glob. Antimicrob. Resist.* 30, 103–106. doi: 10.1016/j.jgar.2022.06.002

Wang, X., Wang, Y., Zhou, Y., Li, J., Yin, W., Wang, S., et al. (2018). Emergence of a novel mobile colistinresistance gene, mcr-8, in NDM-producing Klebsiella pneumoniae. Emerg. *Microbes Infect.* 7, 1–9. doi: 10.1038/s41426-018-0124-z

Wang, Y., Zhang, R., Li, J., Wu, Z., Yin, W., Schwarz, S., et al. (2017). Comprehensive resistome analysis reveals the prevalence of NDM and MCR-1 in Chinese poultry production. *Nat. Microbiol.* 2:16260. doi: 10.1038/nmicrobiol.2016.260

Wick, R. R., Judd, L. M., Gorrie, C. L., and Holt, K. E. (2017). Unicycler: resolving bacterial genome assemblies from short and long sequencing reads. *PLoS Comput. Biol.* 13:e1005595. doi: 10.1371/journal.pcbi.1005595

Wu, B., Wang, Y., Ling, Z., Yu, Z., Shen, Z., Zhang, S., et al. (2020). Heterogeneity and diversity of mcr-8 genetic context in chicken-associated Klebsiella pneumoniae. *Antimicrob. Agents Chemother.* 65, e01872–e01820. doi: 10.1128/AAC.01872-20

Yang, F., Gao, Y., Zhao, H., Li, J., Cheng, X., Meng, L., et al. (2021). Revealing the distribution characteristics of antibiotic resistance genes and bacterial communities in animal-aerosol-human in a chicken farm: from one-health perspective. *Ecotoxicol. Environ. Saf.* 224:112687. doi: 10.1016/j.ecoenv.2021.112687

Zhai, R., Fu, B., Shi, X., Sun, C., Liu, Z., Wang, S., et al. (2020). Contaminated in-house environment contributes to the persistence and transmission of NDM-producing bacteria in a Chinese poultry farm. *Environ. Int.* 139:105715. doi: 10.1016/j.envint.2020.105715

Zhan, Q., Xu, Y., Wang, B., Yu, J., Shen, X., Liu, L., et al. (2021). Distribution of fluoroquinolone resistance determinants in Carbapenem-resistant Klebsiella pneumoniae clinical isolates associated with bloodstream infections in China. *BMC Microbiol.* 21:164. doi: 10.1186/s12866-021-02238-7

Zhao, Q., Berglund, B., Zou, H., Zhou, Z., Xia, H., Zhao, L., et al. (2021a). Dissemination of blaNDM-5 via IncX3 plasmids in carbapenem-resistant Enterobacteriaceae among humans and in the environment in an intensive vegetable cultivation area in eastern China. *Environ. Pollut.* 273:116370. doi: 10.1016/j.envpol.2020.116370

Zhao, L., Dong, Y. H., and Wang, H. (2010). Residues of veterinary antibiotics in manures from feedlot livestock in eight provinces of China. *Sci. Total Environ.* 408, 1069–1075. doi: 10.1016/j.scitotenv.2009.11.014

Zhao, Y., Liu, L., Wang, S., Tian, M., Qi, J., Li, T., et al. (2021b). Draft genome sequence analysis of a novel MLST (ST5028) and multidrug-resistant Klebsiella quasipneumoniae subsp. similipneumoniae (Kp4) strain 456S1 isolated from a pig farm in China. *J. Glob. Antimicrob. Resist.* 24, 275–277. doi: 10.1016/j.jgar.2021.01.006

Zou, H., Berglund, B., Xu, H., Chi, X., Zhao, Q., Zhou, Z., et al. (2020). Genetic characterization and virulence of a carbapenem-resistant Raoultella ornithinolytica isolated from well water carrying a novel megaplasmid containing blaNDM-1. *Environ. Pollut.* 260:114041. doi: 10.1016/j.envpol.2020.114041

frontiers | Frontiers in Microbiology

TYPE Original Research
PUBLISHED 26 October 2022
DOI 10.3389/fmicb.2022.997849

OPEN ACCESS

EDITED BY
Yoshiharu Yamaichi,
UMR 9198 Institut de Biologie Intégrative de la Cellule (I2BC), France

REVIEWED BY
Krista Kaster,
University of Stavanger, Norway
Veronica Maria Jarocki,
University of Technology Sydney, Australia

*CORRESPONDENCE
Enrique Joffré
enrique.joffre@ki.se
Åsa Sjöling
asa.sjoling@ki.se

SPECIALTY SECTION
This article was submitted to Antimicrobials, Resistance and Chemotherapy, a section of the journal Frontiers in Microbiology

RECEIVED 19 July 2022
ACCEPTED 10 October 2022
PUBLISHED 26 October 2022

CITATION
Guzman-Otazo J, Joffré E, Agramont J, Mamani N, Jutkina J, Boulund F, Hu YOO, Jumilla-Lorenz D, Farewell A, Larsson DGJ, Flach C-F, Iñiguez V and Sjöling Å (2022) Conjugative transfer of multi-drug resistance IncN plasmids from environmental waterborne bacteria to *Escherichia coli*. *Front. Microbiol.* 13:997849. doi: 10.3389/fmicb.2022.997849

Conjugative transfer of multi-drug resistance IncN plasmids from environmental waterborne bacteria to *Escherichia coli*

Jessica Guzman-Otazo[1,2,3], Enrique Joffré[2,3]*, Jorge Agramont[1], Nataniel Mamani[1], Jekaterina Jutkina[4,5], Fredrik Boulund[2,3], Yue O. O. Hu[2,3], Daphne Jumilla-Lorenz[6], Anne Farewell[5,6], D. G. Joakim Larsson[4,5], Carl-Fredrik Flach[4,5], Volga Iñiguez[1] and Åsa Sjöling[2,3,6]*

[1]Institute of Molecular Biology and Biotechnology, Universidad Mayor de San Andrés, La Paz, Bolivia, [2]Department of Microbiology, Tumor and Cell Biology, Karolinska Institutet, Stockholm, Sweden, [3]Centre for Translational Microbiome Research, Karolinska Institutet, Stockholm, Sweden, [4]Department of Infectious Diseases, Institute of Biomedicine, Sahlgrenska Academy, University of Gothenburg, Göteborg, Sweden, [5]Centre for Antibiotic Resistance Research (CARe), University of Gothenburg, Göteborg, Sweden, [6]Department of Chemistry and Molecular Biology, University of Gothenburg, Göteborg, Sweden

Watersheds contaminated with municipal, hospital, and agricultural residues are recognized as reservoirs for bacteria carrying antibiotic resistance genes (ARGs). The objective of this study was to determine the potential of environmental bacterial communities from the highly contaminated La Paz River basin in Bolivia to transfer ARGs to an *Escherichia coli* lab strain used as the recipient. Additionally, we tested $ZnSO_4$ and $CuSO_4$ at sub-inhibitory concentrations as stressors and analyzed transfer frequencies (TFs), diversity, richness, and acquired resistance profiles. The bacterial communities were collected from surface water in an urban site close to a hospital and near an agricultural area. High transfer potentials of a large set of resistance factors to *E. coli* were observed at both sites. Whole-genome sequencing revealed that putative plasmids belonging to the incompatibility group N (IncN, IncN2, and IncN3) were predominant among the transconjugants. All IncN variants were verified to be mobile by a second conjugation step. The plasmid backbones were similar to other IncN plasmids isolated worldwide and carried a wide range of ARGs extensively corroborated by phenotypic resistance patterns. Interestingly, all transconjugants also acquired the class 1 integron *intI1*, which is commonly known as a proxy for anthropogenic pollution. The addition

of $ZnSO_4$ and $CuSO_4$ at sub-inhibitory concentrations did not affect the transfer rate. Metal resistance genes were absent from most transconjugants, suggesting a minor role, if any, of metals in the spread of multidrug-resistant plasmids at the investigated sites.

KEYWORDS

waterborne bacteria, horizontal gene transfer, multi-drug resistance, *Escherichia coli*, IncN plasmid, copper sulfate, zinc sulfate, conjugative plasmid transfer

Introduction

During the last decades, infections caused by antibiotic-resistant bacteria have escalated worldwide, positioning antibiotic resistance as one of the worst health-threatening problems for mankind (Fauci and Marston, 2014; Petchiappan and Chatterji, 2017). Insufficient hygiene, use, misuse, and over-use of antibiotics, and the release of selective agents to the environment have further potentiated the occurrence and dispersion of antibiotic resistance (Andersson and Hughes, 2014; Aubertheau et al., 2017; Tan et al., 2018). Water bodies and soils receive discharges of pathogenic and non-pathogenic bacteria, antibiotics, biocides, metals, and other chemical residues from hospital and community settings as well as from agriculture and animal husbandry (Andersson and Hughes, 2014; Singer et al., 2016; Pal et al., 2017). Therefore, contaminated water bodies and aquatic sediments may facilitate the emergence and dissemination of pollutant- and antibiotic-resistant bacteria (ARB) (Finley et al., 2013; Marti et al., 2014; Bengtsson-Palme et al., 2018; Larsson and Flach, 2022). In Bolivian cities such as La Paz, the lack of wastewater treatment and discharges from hospitals, industries, and households directly into the La Paz River basin have significantly contributed to the pollution of river water, which is often used for irrigation of agricultural areas located downstream. Several studies have found large numbers of pathogenic and resistant bacteria isolated from river water, soil, and vegetable samples from the La Paz River basin (Poma et al., 2016; Guzman-Otazo et al., 2019; Medina et al., 2021).

Antibiotic-resistant bacterias can emerge by mutations in target genes or by acquiring genes by horizontal gene transfer (HGT). Bacterial conjugation is one of the most common HGT mechanisms for antibiotic resistance dispersion (Andersson and Hughes, 2017). Moreover, multi-drug resistance in bacteria has evolved at least partly by co-selection through co- and cross-resistance mechanisms (multiple resistance genes within a mobile genetic element (MGE) versus the presence of resistance genes with a broad substrate range) (Marti et al., 2014; Pal et al., 2014, 2015).

Several stressors affecting transfer of ARGs have been identified; for instance, different kinds of metals such as Cu, Zn, and Hg might influence the occurrence and mobilization of ARGs in the environment since antibiotic and metal resistance genes often co-exist in the same MGE (Ji et al., 2012; Pal et al., 2015). These metals can be found in downstream water from mining and industrial areas (Rogozin and Gavrilkina, 2008; Agramont et al., 2020). In Bolivia, lakes and rivers located upstream of the La Paz River basin have been shown to be highly impacted by acid mining drainage discharges due to the intensive mining activity carried out during the last century (Agramont et al., 2020). The transfer of antibiotic resistance from bacterial communities in natural and contaminated environments in the absence/presence of stressors different from antibiotics needs to be further studied (Finley et al., 2013; Marti et al., 2014; Zhang et al., 2018a).

This study aimed to determine the potential of environmental waterborne bacterial communities from urban and agricultural areas in the contaminated La Paz River basin to transfer genetic elements carrying multi-drug resistance into an *E. coli* lab strain as a recipient model. In addition, the effect of $ZnSO_4$ and $CuSO_4$ at sub-inhibitory concentrations as stressors during conjugation experiments was evaluated.

Materials and methods

Recipient strain and minimum inhibitory concentration determination

The strain *E. coli* CV601, characterized by the expression of the *gfp* gene (green fluorescent protein) and kanamycin (KAN) and rifampicin (RIF) resistance as selection markers (Heuer et al., 2002) was used as the recipient for conjugation experiments. The minimum inhibitory concentration (MIC) for sulfamethoxazole-trimethoprim (SMX/TMP) was tested prior to experiments using Etest® (BioMérieux SA, Marcy l'Etoile, France) and was found to be 0.304–0.016 mg/L. *Escherichia coli* ATCC 25922 was used as a susceptibility control.

The MIC for the metal salts $ZnSO_4 \times 7H_2O$ (Merck, Darmstadt, Germany) and $CuSO_4 \times 5H_2O$ (Merck, Darmstadt, Germany) was determined by the agar dilution MIC determination method for metals (Aarestrup and Hasman, 2004) with some minor modifications. Briefly, Mueller-Hinton media was used to prepare series of two-fold dilutions of

$ZnSO_4 \times 7H_2O$ (from 0.5 to 16 mM) and $CuSO_4 \times 5H_2O$ (from 0.5 to 32 mM). The pH of the media was adjusted to 5.5 and 7.0, respectively. Plates were inoculated with spots of 2 μL of bacterial suspensions adjusted to 0.5 McFarland standard. Plates were incubated for 48 h at 37°C, and the MIC concentration was established as the minimum concentration of metal salt where bacterial growth was not detectable (Wiegand et al., 2008). *Escherichia coli* ATCC 25922 was used as a control and for comparison purposes. MIC determination tests were conducted in triplicate. The MIC of the CV601 recipient strain was calculated as 4 mM for $ZnSO_4 \times 7H_2O$ and 16 mM for $CuSO_4 \times 5H_2O$.

Growth kinetics of the recipient strain in the presence of metals

Growth kinetic experiments were performed to test the effect of $ZnSO_4 \times 7H_2O$ and $CuSO_4 \times 5H_2O$ at two selected sub-inhibitory concentrations (0.5 and 1 mM) on the growth rate of the recipient strain. *Escherichia coli* CV601 recipient and *E. coli* ATCC 25922 (control) were cultured in Luria-Bertani (LB) broth (Sigma-Aldrich, St. Louis, MO, USA) for 3 h at 37°C, and the OD_{600} of each culture was adjusted to 1. Bacterial suspensions were added in aliquots of 20 μl to 96 well plates containing 180 μl of LB broth (negative control) or LB broth supplemented with $ZnSO_4 \times 7H_2O$ or $CuSO_4 \times 5H_2O$ at 0.5 and 1 mM. Plates were incubated overnight at 37°C, and the OD_{600} was measured using an automatic spectrophotometer (SpectraMax® i3x, Molecular Devices, San Jose, CA, USA) every 30 mins. Growth kinetic experiments were performed twice with three replicates. The effect of metal addition on the growth rate of *E. coli* CV601 was taken into account for TF calculations by adjusting the recipient counts.

Recipient and donor preparation prior conjugation experiments

Escherichia coli CV601 was grown in LB broth supplemented with KAN 50 mg/L at 37°C overnight. The culture was diluted 1:10 with LB broth without antibiotics and grown at 37°C for 2–3 additional hours. The recipient suspension was washed twice with PBS, pelleted, and finally resuspended in LB broth to an OD_{600} of 1–1.2 ($\approx 1 \times 10^9$ CFU/mL).

The collection of water samples from the highly contaminated La Paz River basin in Bolivia was carried out three times on different occasions and used as a source of donor communities for conjugation experiments. The first and second experiments were performed in July and August 2016, respectively, and the third experiment was performed in April 2018. The specific area and sampling sites are described elsewhere (Poma et al., 2016; Guzman-Otazo et al., 2019). An urban site located in the Choqueyapu River in La Paz city, where the river receives the discharge from hospitals and industries, and a downstream agricultural site where river water is used for crop irrigation were selected for water sampling. A total of three samples of water per site were collected to obtain 1 L of water, which was mixed, and subsequently an aliquot of 300 ml was taken and filtered through 0.45 μm pore size filters (Millipore Corporation, Bedford, MA, USA). The filters were cut, placed in tubes containing PBS and 5 mm glass beads (Supelco, Merck, Darmstadt, Germany), and vigorously vortexed to release the bacteria from the filters (donors). The donor suspension was decanted, washed twice with PBS, pelleted, and subsequently resuspended at an OD_{600} of 1–1.2. Water samples and donor suspensions were kept at 4°C at a maximum of 24 h before conjugation experiments.

Conjugation assays

Conjugation assays were performed according to the protocol by Jutkina et al. (2016) with some minor modifications. Briefly, donor suspensions from each sampling point were mixed 1:1 with the recipient. Aliquots of 100 μL of donor-recipient suspensions were spread on a membrane of mixed cellulose esters (MCE) MF-Millipore™ with a 0.22 μm pore size and a diameter of 47 mm (Millipore Corporation, Bedford, MA, USA) and placed on LB media plates for mating. In the case of testing metal salts as stressors during conjugation experiments, donor-recipient mating filters were placed on LB media supplemented with $ZnSO_4 \times 7H_2O$ and $CuSO_4 \times 5H_2O$ at 0.5 and 1 mM. Control filters containing only the donor or the recipient suspensions on LB media plates were incubated and treated under the same conditions as the donor-recipient mating filters. After 3 h of incubation at 30°C, mating and control filters were transferred to tubes containing PBS and glass beads. The tubes were vortexed, and the contents serially diluted ten-fold. Plating of 100 μL of every dilution was performed on CHROMagar™ MH Orientation (CHROMagar, Paris, France), or standard Mueller Hinton Agar (MHA) (Sigma-Aldrich, St. Louis, MO, USA) supplemented with KAN (50 mg/L), RIF (50 mg/L), and the chosen selective antibiotic SMX/TMP (150/30 mg/L). This antibiotic combination was selected due to the high variety of donors and conjugative and transferable genetic elements characterized to carry sulfamethoxazole resistance genes (Jutkina et al., 2016). In addition, the mix of sulfamethoxazole/trimethoprim, commercially known as Cotrimoxazole, is frequently used to treat gastrointestinal and urinary tract infections in the Bolivian population, suggesting that the associated resistance genes are circulating in the population and surrounding environments (Duwig et al., 2014; Archundia et al., 2017, 2018). Control plates with recipients were plated onto MHA supplemented with KAN (50 mg/L) and RIF (50 mg/L), and control plates for donors

onto CHROMagar™ Orientation or LB media. For counting and visualizing recipients and transconjugants, the plates were incubated at 37°C for 48 h. In the case of donors, plates were incubated at 30°C. Transfer frequencies (TFs) were calculated as the ratio between the number of transconjugants obtained from each specific condition and the number of recipients on the control plates.

Three independent experiments were performed. Every independent experiment included collecting water samples at the two sites and two mating replicates for each donor-recipient combination. Plating of bacterial dilutions was always performed in triplicate.

A second transconjugation experiment was performed using four selected transconjugants to verify that the acquired genetic elements were mobile. Transconjugation was performed as described above using four transconjugants with each type of IncN plasmid on an *E. coli* CV601 background as donors and *E. coli* HA4 (BW25113) (Alalam et al., 2020) as recipient. The mating efficiency was calculated as the ratio of transconjugant to donor colonies.

Selection and confirmation of transconjugants

Transconjugants were identified based on growth in selective media and confirmed by *gfp* phenotype under UV light. For additional verification, selected transconjugants were tested by PCR to confirm the presence of the *gfp* gene construct as a marker of the recipient strain (Jutkina et al., 2016). Transconjugants were also tested by PCR for the presence of sulfamethoxazole resistance genes *sul1* and *sul2* to confirm the transfer of MGEs carrying resistance to the chosen selective antibiotic (Flach et al., 2015).

Characterization of multi-drug resistant patterns obtained from conjugation experiments

A total of 150 randomly selected transconjugants, including 50 from each independent experiment and five from each of the ten sampling site-experimental condition combinations, were evaluated for phenotypic antibiotic resistance using the Kirby-Bauer Disk Disks (Oxoid/Thermo Fisher Scientific, Basingstoke, UK) Diffusion Susceptibility Test (Hudzicki, 2009). Disks for 13 antibiotics were tested: Ampicillin (10 μg), Tetracycline (30 μg), Ciprofloxacin (5 μg), Chloramphenicol (30 μg), Cefotaxime (5 μg), Meropenem (10 μg), Doripenem (10 μg), Ertapenem (10 μg, Imipenem (10 μg), Nalidixic Acid (30 μg), Gentamicin (10 μg), Streptomycin (10 μg), and Piperacillin-Tazobactam (110 μg). When possible, EUCAST guidelines[1] were applied to interpret inhibition zones and categorize transconjugants as resistant, intermediate, or susceptible to the different antibiotics tested. CSLI guidelines[2] were alternatively used when needed.

Every different combination of antibiotic susceptibility, resistance, or intermediate response to the 13 antibiotics tested was considered as a single MDRP. All transconjugants were classified as resistant to SMX/TMP as they were isolated from the conjugation assay using this antibiotic combination as the selection factor.

The multiple antibiotic resistance index (MAR) was calculated for each transconjugant as the ratio between the number of antibiotics to which the transconjugant is resistant and the total number of antibiotics tested. The Shannon diversity index (H') for MDRPs was calculated using the Excel template developed by Klaus D. Goepel.[3]

Evaluation of metal tolerance in selected transconjugants

Fifty randomly selected transconjugants representing both donor sites, all treatments, and all observed MDRPs were examined for tolerance to $ZnSO_4 \times 7H_2O$ and $CuSO_4 \times 5H_2O$. In the case of MDRPs that were repeatedly found at different sites and treatments, more than one transconjugant was included in the analysis. In the case of unique MDRPs, only one transconjugant was available per site. Agar dilution MIC determination method for metals (Aarestrup and Hasman, 2004) was applied with some minor modifications as mentioned above. The acquired tolerance to metals was defined as an increase in the MIC value for the tested transconjugants compared to the MIC of the original recipient strain *E. coli* CV601. The strain of *E. coli* ATCC 25922 was also included as a control. Metal tolerance evaluation was conducted in triplicate.

DNA extraction and whole-genome sequencing

DNA was extracted individually from 47 of the 50 selected transconjugants used in the metal tolerance test (representing the 28 different MDRPs identified in this study) and *E. coli* CV601 using the QIAamp Fast DNA Stool Mini Kit (Qiagen, Hilden, Germany). The DNA was eluted in Milli-Q water, and 50 ng of DNA were used for sequencing library preparation. Sequencing libraries were prepared using the TruSeq Nano kit (Illumina, San Diego, CA, USA) with a mean fragment

1 http://www.eucast.org/
2 https://clsi.org/
3 http://bpmsg.com

length of 900 bp. Libraries were sequenced on the MiSeq platform using v3 chemistry, 2 × 300 bp, generating coverage of > 100× for all strains.

Sequencing data analysis

Sequencing data were processed using the BACTpipe assembly and annotation pipeline (v. 2.6.1) (Kirangwa et al., 2017). To find and subtract the acquired genes, the annotated genomes of the transconjugants were compared with the genome of the original recipient *E. coli* CV601. Contigs containing the acquired, transferred DNA were manually analyzed to identify antibiotic resistance genes (ARGs), other relevant genes (ORGs) conferring possible advantage to the host (biofilm and persister formation, survival under stress conditions, resistance to disinfectants, solvents or antimicrobial peptides and virulence), conjugation machinery (*tra* genes) and plasmid maintenance associated genes (toxin antitoxin systems), *etc.*, using ResFinder (Camacho et al., 2009; Bortolaia et al., 2020). The similarity of plasmid-like structures found in transconjugants with other previously reported plasmids was analyzed by NCBI BLAST (Altschul et al., 1990, 1997; Johnson et al., 2008). We further examined the content of the acquired genetic material in transconjugants by performing plasmid finding, plasmid sequence typing, antibiotic resistance gene finding, and virulence gene finding following the Bacterial Analysis Pipeline (Thomsen et al., 2016) in assembled genomes. Finally, metal and biocide resistance genes were searched for on the assembled genomes using DIAMOND BLASTx search (v. 0.9.25) (Buchfink et al., 2015) against the BacMet experimentally confirmed resistance gene database (v. 2.0) (Pal et al., 2014). The settings for BacMet analysis included "more-sensitive," e-value > 10^{-5}, amino acid identity > 90%, and the default alignment length cutoff.

Statistical analysis

One- and two-way ANOVA in IBM SPSS Statistics (v. 22.0) with a significance level of 95% ($p < 0.05$) was used to test the effect of metal salts on the growth kinetics of *E. coli* CV601 and the effect of donor source and metal treatment on the number of transconjugants, TF, richness, diversity, and number of unique MDRPs per site when comparing multiple groups. *T*-test and Mann-Whitney *U* test were used when appropriate to compare variables between two groups. Non-metric multidimensional analysis NMDS was performed using R (v. 3.5.0). The "ecodist" (v. 2.0.1) R package was used to calculate Euclidean distances, and "vegan" R package was used to conduct NMDS and anosim analyses.

Data availability

All of the genomes determined in this study are available at NCBI under BioProject no. PRJEB33390. The sequences and strain features are deposited in the European Nucleotide Archive under the accession number PRJEB33390.

Results

Culturable bacterial donor communities in the La Paz River basin

Water samples from the two sites at the La Paz River basin were plated on CHROMagar orientation media to characterize the culturable fraction of donor communities. Bacteria culturable on CHROMagar were abundant at both the urban (9.6×10^5 CFU/ml on average) and agricultural (4.3×10^5 CFU/ml on average) sites (**Supplementary Figure 1**). No statistically significant difference was found between bacterial counts from the two sites. The bacterial genera were classified solely based on the appearance of observed colonies[4] and included: *E. coli*, *Enterococcus*, *Klebsiella, Enterobacter, Serratia*, *Staphylococcus aureus*, *and Pseudomonas aeruginosa*, with no apparent differences in composition between sampling sites (**Supplementary Figure 1**). It is important to note that donors were prepared directly from water filters and without any prior culture step, so donor communities from the La Paz River basin included culturable and non-culturable bacteria for mating experiments.

Bacterial communities from urban and agricultural areas in the La Paz River basin have the potential to transfer antibiotic resistance to *Escherichia coli*

Conjugation experiments in LB media using bacterial communities from the two sites at the La Paz River basin as donors and *E. coli* CV601 as the recipient were performed. The number of transconjugants and TFs were calculated from three independent experiments. When combining all three experiments, significantly higher numbers of SMX-TMP resistant transconjugants were obtained using donor communities from the urban area (7×10^4 CFUs) compared to the agricultural area (1.5×10^4 CFUs) (Mann-Whitney $U = 21$, $p = 0.003$ two-tailed). Significantly higher TFs were obtained using donor communities from the urban site compared to the agricultural area (Mann-Whitney $U = 32.5$, $p = 0.02$ two-tailed; **Figure 1**). Hence, the urban site might contain higher levels of

4 www.CHROMagar.com

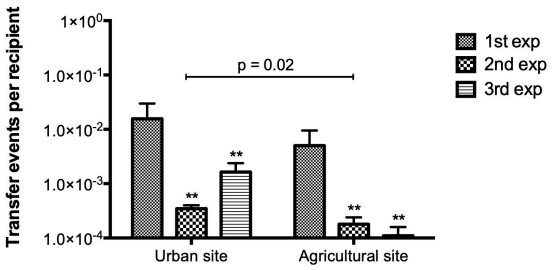

FIGURE 1
Transfer frequencies (TFs) obtained from conjugation experiments in LB media using aquatic donor communities from urban and agricultural areas of the La Paz River basin and *E. coli* CV601 (recipient). Bars represent mean values obtained from three independent conjugation experiments. Error bars represent the standard deviation of the mean from the two mating replicates included in each independent experiment. A higher number of transfer events per recipient was obtained using bacterial donors from the urban site (Mann-Whitney *U* Test, $p = 0.02$). For both sampling sites, TFs varied significantly between independent experiments. Asterisks (**) show the significantly between difference from the first independent experiment (1st exp) by Brown-Forsythe ANOVA $p = 0.03$, *post hoc* Tukey test. There was no significant difference in TF between the second and third independent experiments.

suitable donors. Additionally, a statistically significant difference in TF between independent experiments was observed in both sampling sites (Brown-Forsythe ANOVA F = 5.97, $p = 0.03$; Figure 1).

Transfer of antibiotic resistance from waterborne bacterial communities to *Escherichia coli* in the presence of stressors $ZnSO_4$ and $CuSO_4$

Donors from the two sites along the La Paz River basin were also used for conjugation experiments in LB media supplemented with sub-MIC levels of $ZnSO_4 \times 7H_2O$ and $CuSO_4 \times 5H_2O$ to test if stressors might influence the transfer of resistance determinants. The selected concentrations were 0.5 and 1 mM for both metals, since the objective was to exert stress on donors and recipients but not kill them during mating experiments. For this reason, the selected concentrations were under the MIC but higher than the expected concentrations in watersheds. Information about the metal content in the La Paz River basin is scarce.

We monitored the growth of the recipient *E. coli* CV601 and control *E. coli* ATCC 25922 in the presence of $ZnSO_4 \times 7H_2O$ and $CuSO_4 \times 5H_2O$ at 0.5 and 1 mM overnight. Since conjugation experiments were performed with incubation of 3 h, this time point was selected for statistical analysis and further interpretation. Growth was not significantly affected in the presence of 0.5 mM and 1 mM $ZnSO_4$ or by 0.5 mM $CuSO_4$, while $CuSO_4$ at 1 mM caused a reduction of 29% in the bacterial growth of the recipient (One-Way ANOVA $p < 0.001$) at 3 h of incubation at 37°C (Supplementary Figure 2). This effect was continuously observed up to 6 h after incubation (One-Way ANOVA $p < 0.001$; Supplementary Figure 2). Comparable growth kinetic results were observed for the control strain of *E. coli* ATCC 25922. The reduction in growth produced by $CuSO_4$ at 1 mM was included in the TF calculations.

Adding $ZnSO_4$ and $CuSO_4$ at 0.5 and 1 mM to conjugation experiments did not cause any significant change in the number of SMX-TMP resistant transconjugants and TFs compared to conjugation experiments in LB media without the addition of metals for both sampling sites (Figure 2). Hence, the sub-MIC metal levels evaluated in this study did not significantly affect the TF of antibiotic resistance.

Multi-drug resistance profiles were acquired from conjugation experiments using waterborne bacterial donors and metal salts as stressors

Even if the addition of stressors did not affect the total number of transconjugants or TFs, it might cause selective pressure on the transferred resistome. To determine the transposable genetic elements of the two sampling sites with and without stressors, 150 randomly selected transconjugants from experiments in the absence and presence of metals were analyzed using the Kirby-Bauer Disk Diffusion Susceptibility Test for 13 different antibiotics. Considering that SMX-TMP plates were used to select transconjugants, resistance to this combination of antibiotics was found in every MDRP (Supplementary Table 1). After classification of each transconjugant as susceptible, intermediate, or resistant to each antibiotic tested, a total of 28 different phenotypic MDRPs among the 150 isolates tested were identified. Each profile represented a specific combination of susceptibility, intermediate resistance, and resistance to the group of antibiotics tested (Figure 3 and Supplementary Table 1). As shown in the clustering analysis in Figure 3, MDRPs obtained using SMX-TMP resistance as the selection marker for transconjugants were found to commonly include resistance to ampicillin, nalidixic acid, and streptomycin, and less frequent to tetracycline and cefotaxime. Resistance to ciprofloxacin and chloramphenicol was rarely found in the MDRPs obtained in this study. Intermediate resistance to piperacillin-tazobactam was identified in two transconjugants. Resistance to gentamicin and carbapenems was not detected in any MDRP (Figure 3 and Supplementary Table 1).

The Shannon index of diversity (H') and richness (R) of MDRPs obtained from conjugation experiments with and without the addition of $ZnSO_4$ and $CuSO_4$ were calculated.

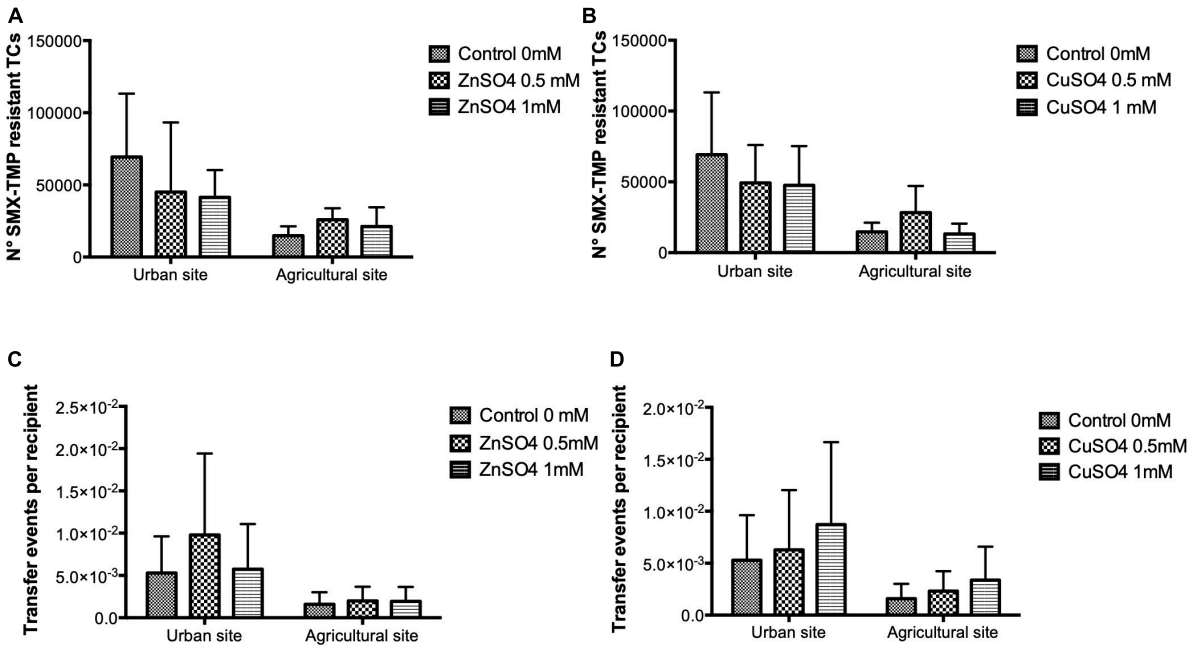

FIGURE 2
The number of transconjugants and transfer frequencies (TFs) obtained from conjugation experiments in LB media supplemented with $ZnSO_4$ and $CuSO_4$ at 0.5 and 1 mM. Conjugation experiments used waterborne bacterial donor communities from two La Paz River basin sites and *E. coli* CV601 as the recipient strain. The bars represent mean values of the number of SMX-TMP resistant transconjugants **(A,B)** and transfer events per recipient **(C,D)** in the presence of $ZnSO_4$ and $CuSO_4$. Data were obtained from three independent conjugation experiments. The error bars represent the standard deviation of the mean. For both sampling sites, the number of SMX-TMP-resistant transconjugants and TFs did not differ significantly between the experiments performed in LB media and LB media supplemented with metals.

When conjugation experiments were performed in the absence of metals, the diversity and richness of MDRPs did not vary significantly between the two sampling sites since a richness of six and seven different MDRPs was identified, respectively (Table 1). Some of these profiles like P1 (STX/TMP), P6 (STX/TMP, AMP, and NA), P14 (STX/TMP, AMP, TET, and STR), and P16 (STX/TMP, AMP, NA, and STR) were found from both sampling sites (Table 1, Supplementary Table 1, and Figure 4). Unique profiles per site were defined as profiles detected only once among all transconjugants tested per sampling site. When metals were added to the conjugation experiments and data from both metal treatments was analyzed as a group, a tendency of variation in the richness of MDRPs between sampling sites was observed (Mann-Whitney $U = 40$ $p = 0.052$; Table 1). In addition, a statistically significant difference between the two sites was observed for the percentage of unique MDRPs per site in the presence of metals (Mann-Whitney $U = 36.5$ $p = 0.026$; Table 1). Thus, with the addition of metals to the conjugation media, the La Paz River donor bacteria from the agricultural site transferred more diverse MDRPs than bacterial donors from the urban point (Table 1 and Figure 4). Notwithstanding that, the TFs obtained from the agricultural area were markedly lower compared to the TFs obtained from the urban site (Figure 2).

The analysis was also performed per individual sampling point for diversity, richness, and unique MDRPs in the absence and presence of metals. When the urban site was used as a donor source, no significant differences were observed in the diversity, richness, and unique MDRPs between conjugation experiments in the absence and presence of metal treatment (Table 1). However, when the agricultural site was used as the source of donors, a significantly higher diversity (t-test, $p = 0.028$), richness (Mann-Whitney $U = 3$ $P = 0.021$), and percentage of unique MDRPs (Mann-Whitney $U = 3$, $p = 0.023$) was obtained from conjugation experiments in the presence of metals compared to LB only (Table 1).

The multiple antibiotic resistance index (MAR) varied slightly between sampling sites and treatments, with a small range of 0.22–0.27 (Table 1). Only 7% of the transconjugants acquired resistance to more than five antibiotics, and this was only found in transconjugants from the agricultural site obtained from conjugation experiments in the presence of 0.5 M $ZnSO_4$ (Table 1).

The number of resistant transconjugants to each of the 13 antibiotics tested, and the number of transconjugants carrying each of the 28 different MDRPs were compared between sampling sites and metal treatments. In the absence of metal treatment, no significant differences were observed between the sampling sites. When metals ($ZnSO_4$ and $CuSO_4$)

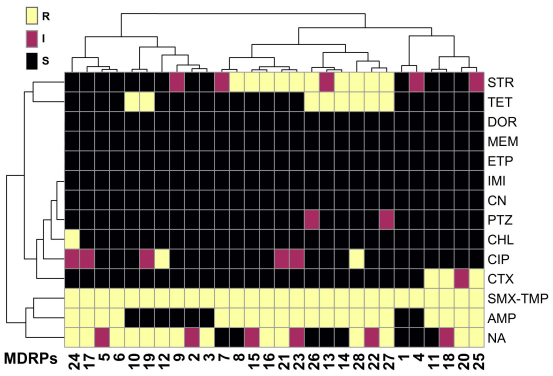

FIGURE 3
Heatmap of the phenotypic characterization of the main multi-drug resistance profiles (MDRPs) identified by the Kirby-Bauer Disk Diffusion Susceptibility Test in randomly selected transconjugants. A total of 28 different phenotypic MDRPs were transferred from bacterial communities from the two sites in the La Paz River basin to *E. coli* CV601 recipients. A single profile was defined as the unique combination of susceptibility, intermediate resistance, or resistance to the 13 antibiotics included in the analysis. Color code: black = susceptible (S), magenta = intermediate (I), and yellow = resistant (R). Antibiotics: AMP, ampicillin; TET, tetracycline; CIP, ciprofloxacin; CHL, chloramphenicol; CTX, cefotaxime; MEM, meropenem; DOR, doripenem; ETP, ertapenem; IMI, imipenem; NA, nalidixic acid; CN, gentamicin; STR, streptomycin; PTZ, piperacillin-tazobactam; SMX/TMP, sulfamethoxazole/trimethoprim. All MDRPs include resistance to SMX/TMP because all transconjugants were selected from conjugation experiments using plates supplemented with this specific combination of antibiotics. Correlation was used as the clustering method. The pheatmap R program was used to generate the heatmap.

were added to the conjugation media, transconjugants with intermediate resistance to piperacillin-tazobactam were only found in the agricultural area. Transconjugants expressing intermediate resistance to streptomycin (STR) were significantly enriched on the agricultural site compared to the urban site (Mann-Whitney $U = 42$, $p = 0.028$). Transconjugants carrying the STX/TMP, AMP, STR resistance profile (P8) were significantly more often present in the agricultural area (Mann-Whitney $U = 48$, $p = 0.032$), while P14 (STX/TMP, AMP, TET, and STR) was significantly enriched in the urban site (Mann-Whitney $U = 35.5$, $p = 0.028$; **Figure 4**). Finally, the number of transconjugants resistant to streptomycin was significantly higher in conjugation experiments with metal treatment (Mann Whitney $U = 5$, $p = 0.046$), and P6 (STX/TMP, AMP, and NA) was significantly enriched in experiments in the absence of metals (Mann Whitney $U = 30$, $p = 0.022$; **Figure 4**).

The origin of the sample and the presence of metals determined the acquisition of specific antibiotic resistance genes

Similarities between transconjugants obtained from experiments in the absence and presence of metals were evaluated according to the occurrence and abundance of specific MDRPs using a non-metric multidimensional scaling (NMDS) analysis. The results shown in **Figure 5** showed that transconjugants obtained from the urban site (US) and the agricultural site (AS) clustered separately in the space, meaning that transconjugants obtained from these two places acquired different combinations and abundance of MDRPs (**Figure 5**). Moreover, transconjugants obtained from conjugation experiments in the presence of metals (B: LB + 0.5 mM $ZnSO_4$, C: LB + 1 mM $ZnSO_4$, D: LB + 0.5 mM $CuSO_4$, and E: LB + 1 mM $CuSO_4$) (**Supplementary Table 2**) clustered together and separately from transconjugants obtained in the absence of metals (A: LB) (**Figure 5**). An exception was observed for transconjugants obtained from the agricultural site and 1 mM $ZnSO_4$ (ASC). This group of transconjugants was located far from the other groups of transconjugants obtained in the presence of metals (**Figure 5**).

Tolerance to $ZnSO_4$ and $CuSO_4$ in transconjugants from conjugation experiments in the absence and presence of metals

Since the results suggested that adding $ZnSO_4$ and $CuSO_4$ might influence the transfer/uptake of different pools of MGEs compared to conjugation experiments in the absence of metals, we next determined if the transconjugants had obtained increased metal tolerance. A subgroup of 50 transconjugants representing all MDRP types obtained from conjugation experiments in LB media with and without the addition of $ZnSO_4$ and $CuSO_4$ was evaluated for increased tolerance to both metal salts compared to those obtained to the recipient strain of *E. coli* CV601. All tested transconjugants presented the same MIC values as the recipient: 4 mM for $ZnSO_4$ and 16 mM for $CuSO_4$. An increased metal tolerance was not obtained for the presence of the sub-MIC metal levels used in this study.

TABLE 1 Number of multi-drug resistance profiles (MDRPs) obtained from conjugation experiments in the absence and presence of $ZnSO_4$ and $CuSO_4$ at two different concentrations.

	Transconjugants							AR profiles		
Treatment	**1A (%)[a]**	**2A (%)[a]**	**3A (%)[a]**	**4A (%)[a]**	**5A (%)[a]**	**6A (%)[a]**	**MAR[b]**	**R[c] (U%)[d]**	**H'[e]**	**H'[e] (R)[c]**
Urban site										
Control 0 mM	1 (7)	1 (7)	8 (53)	5 (33)	0 (0)	0 (0)	0.22	6 (0)	1.53	1.53 (6)
$ZnSO_4$ 0.5 mM	0 (0)	0 (0)	3 (20)	12 (80)	0 (0)	0 (0)	0.27	6 (33)	1.53	1.89 (10)
$ZnSO_4$ 1 mM	3 (20)	0 (0)	4 (27)	8 (53)	0 (0)	0 (0)	0.22	8 (25)	1.89	
$CuSO_4$ 0.5 mM	1 (7)	2 (13)	5 (33)	7 (47)	0 (0)	0 (0)	0.23	8 (25)	1.89	1.79 (9)
$CuSO_4$ 1 mM	0 (0)	0 (0)	7 (47)	8 (53)	0 (0)	0 (0)	0.25	5 (20)	1.40	
Agricultural site										
Control 0 mM	2 (13)	0 (0)	7 (47)	6 (40)	0 (0)	0 (0)	0.22	7 (0)	1.77	1.77 (7)
$ZnSO_4$ 0.5 mM	1 (7)	2 (13)	5 (33)	6 (40)	0 (0)	1 (7)	0.24	12 (33)	2.40	2.67 (19)
$ZnSO_4$ 1 mM	1 (7)	2 (13)	7 (47)	5 (33)	0 (0)	0 (0)	0.22	10 (50)	2.08	
$CuSO_4$ 0.5 mM	2 (13)	1 (7)	7 (47)	5 (33)	0 (0)	0 (0)	0.21	10 (30)	2.21	2.50 (15)
$CuSO_4$ 1 mM	1 (7)	0 (0)	7 (47)	6 (40)	1 (7)	0 (0)	0.24	10 (40)	2.18	

[a]Number and percentage of transconjugants with resistance to 1, 2, 3, 4, 5, and 6 different antibiotics.
[b]Multiple antibiotic resistance index (MAR) calculated as the ratio between the number of antibiotics to which the transconjugant is resistant and the total number of antibiotics tested.
[c]Richness or number of different antibiotic susceptibility profiles observed.
[d]Percentage of unique profiles observed in transconjugants obtained from a specific treatment and per sampling point. [e]Shannon Diversity Index (H').

Genomic profiling of antibiotic resistance genes, other relevant genes, and plasmids among representative multi-drug resistant patterns

The antibiotic disc diffusion test and the NMDS analysis indicated that site-specific MGEs might be present at the two sites analyzed in the present study. To determine the transferred MGEs, we performed WGS of 47 selected transconjugants, representing all MDRPs and the recipient strain of *E. coli* CV601 (**Supplementary Table 2**). The assembled and annotated CV601 genome was subtracted from the transconjugant genomes to identify the acquired MGEs. To get a more comprehensive characterization of the ARGs, the ResFinder (Bortolaia et al., 2020) database was used to annotate and identify the resistance genes within the transconjugants' genomes. In general, several ARGs acquired by this group of transconjugants were correlated with the observed phenotypic resistance (**Figures 3**, **4** and **Supplementary Table 1**). However, some exceptions were observed. For example, P2 and P18 showed intermediate resistance to nalidixic acid (NA), but no apparent plasmid-borne quinolone resistance genes or mutations in the nucleotide sequence of DNA gyrase subunit B (*gyrB*) were identified. Conversely, P1-P2 and P8 profiles displayed susceptibility to streptomycin despite the presence of *aadA2/strAB* genes (**Figures 4**, **6** and **Supplementary Table 1**).

Unique MDRPs P11, P18, P20, P25, and P28 carried extended-spectrum B-lactamases (ESBLs) such as $bla_{CTX\text{-}M\text{-}15}$, $bla_{SHV\text{-}129}$, and $bla_{OXA\text{-}9}$ were only obtained from conjugation experiments in the presence of metals and using the agricultural site as the source of donors (**Figure 6**). After ARGs identification, we identified other relevant genes (ORGs) in the MGEs acquired by transconjugants that might favor the host. We found genes encoding multi-drug transporters (*yedA, Rv1258c*), genes conferring resistance to other agents such as disinfectants (*qacA, emrE1,* or *qac*Δ*E1*), solvents (*srpC1*) or antimicrobial peptides (*sapA*), genes encoding metal transporters (*nhaA, srpC2*), genes involved in biofilm and persister formation (*hha, yafQ*) as well as survival in stress conditions (*groL, ynaI*), toxin anti-toxin system genes (*dinJ, ldrD*, *mazE,* and *mazF*) and virulence genes (*pld, ptlE*) among others. The transconjugants also carried higher varieties of ORGs involved in resistance to disinfectants and solvents, metal transporters, biofilm formation, survival in stress conditions, and virulence were mainly obtained from conjugation experiments in the presence of metals (**Figure 6**). Using VirulenceFinder (Joensen et al., 2014; Malberg Tetzschner et al., 2020) only two virulence genes, glutamate decarboxylase (*gad)* and increased serum survival (*iss)*, were found equally present in the recipient strain and all transconjugants. In addition, we were able to identify that the transconjugants also acquired the class 1 integron-integrase gene, *intl1*, which is an a proxy for anthropogenic pollution (Gillings et al., 2015). This gene was found in all transconjugants (**Supplementary Table 2**).

By comparing the genomes size of the transconjugants against the recipient *E. coli* CV601 genomes, we were able to get information on the size of genomic DNA transferred from waterborne bacterial communities to *E. coli* CV601. The size of the transferred genomic DNA ranged from 38 Mbp (ASE-3-8) to 164 Mbp (ASE-3-3). No significant difference was observed in the approximate number of base pairs

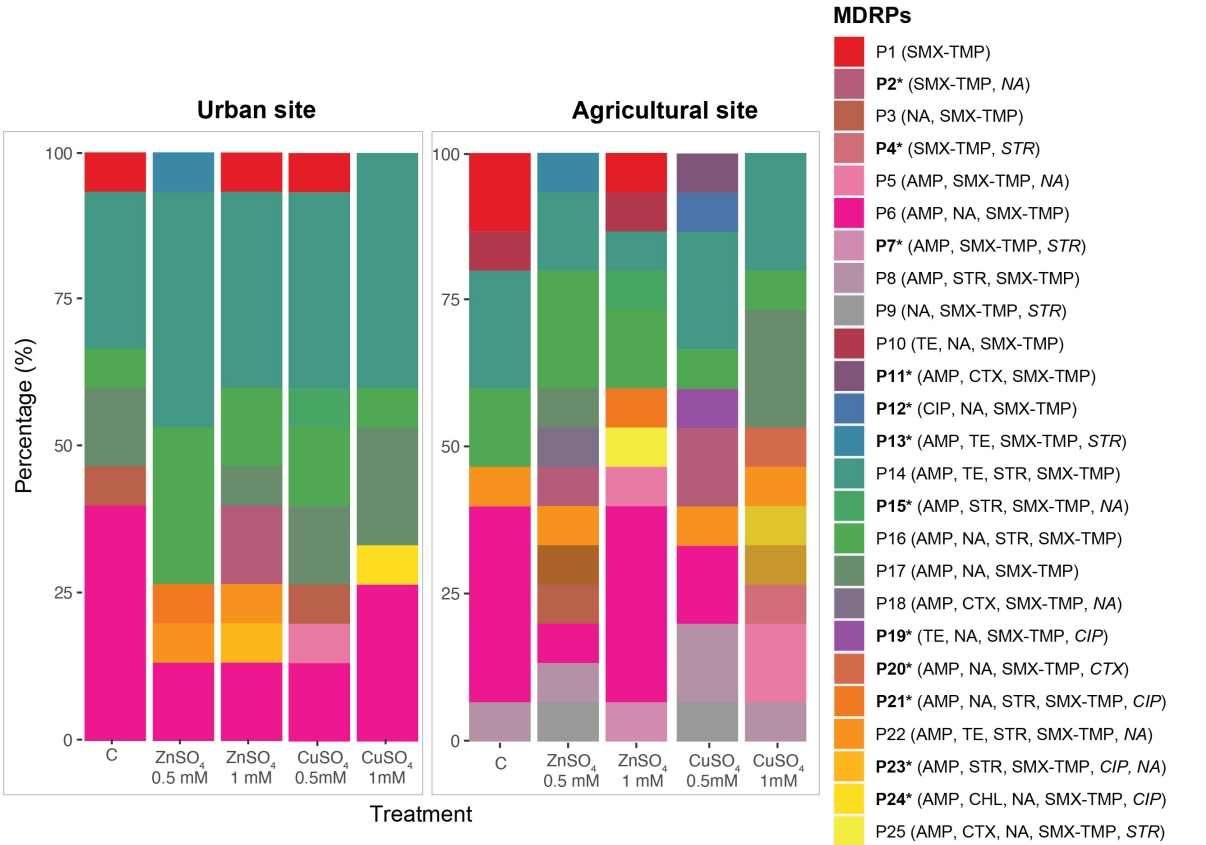

FIGURE 4
Distribution and abundance of MDRPs obtained from conjugation experiments in the absence (C) and presence of $ZnSO_4$ and $CuSO_4$ at 0.5 and 1 mM. Urban and agricultural areas in the La Paz River basin were used as the source of bacterial donor communities. A total of 28 MDRPs (P1–P28) were identified in 150 randomly selected transconjugants analyzed by the Kirby-Bauer Disk Diffusion Susceptibility Test to 13 antibiotics. Each identified profile was labeled with a distinctive color followed by the antibiotic resistance profile. Antibiotics whose transconjugants exhibited intermediate resistance are written in italics. Unique MDRPs per site are marked with a star (*), and they were only found with the addition of metals in conjugation experiments.

acquired by transconjugants from both sampling sites and in the absence or presence of metals (**Supplementary Table 1**). The transferred genomic DNA was most likely plasmids and profiling of the plasmid multi-locus sequence types (pMLSTs) and plasmid incompatibility groups (Inc group) of the acquired genome identified that all transconjugants acquired at least one plasmid from the IncN group (IncN, Inc2, and IncN3). pMLST analysis showed that the IncN plasmids belonged to ST5, ST6 or an unknown type. The resistance gene *sul1* was carried mainly by IncN2 and IncN3 plasmids, while *sul2* was always located in IncN plasmids (**Supplementary Table 2**). Further characterization of the methylation-related genes that play a role in the bacterial restriction-modification system (RM) and plasmid transfer efficiency identified five different methylation-associated genes that encode MTases such as Dcm (*dcm*), HsdM (*hsdM*) genes, and *EC*ORII (*ecoRIIM*), and Reases as HsdR (*hsdR*), and *klcA2*. IncN plasmids carried *ecoRIIM*, *dcm,* and some carried *klcA2*, IncN2 plasmids carried *hsdM/hsdR*, and IncN3 plasmids carried *klcA2* (**Supplementary Table 1**).

Additionally, sequence analysis using the BacMet database (Pal et al., 2014) revealed the presence of 131 biocide- and metal-resistance genes in the recipient *E. coli* CV601 (**Supplementary Table 3**). Compared to the recipient, only two extra biocide resistance genes (*qacE* and *qacEΔ1*) conferring resistance to quaternary ammonium compounds (QACs) were found in more than half of sequenced transconjugants, which were also characterized to carry the sulfonamide resistance gene *sul1* (**Supplementary Tables 1**, **3**). Alignment and sequence analysis revealed that *qacEΔ1* was located adjacent to *sul1*, and in the same contig and plasmid as the class 1 integron integrase intI1 (**Figures 7A,B**).

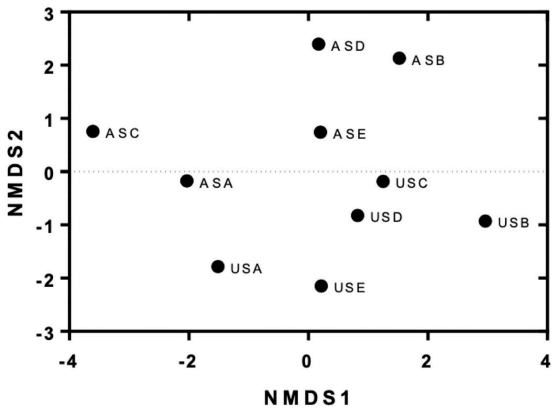

FIGURE 5
Non-metric multidimensional scaling (NMDS) of obtained transconjugants from conjugation experiments in the absence and presence of metals. The results show the ordination of different groups of transconjugants in two dimensions according to the similarities in their MDRPs. US: transconjugants were obtained using the urban site as the donor source. AS: Transconjugants were obtained using the agricultural site as the donor source. Treatments: A = without the addition of metals, B and C = 0.5 and 1 mM ZnSO4, respectively, D and E = 0.5 and 1 mM CuSO4, respectively.

Analysis of the genetic context of ARGs, ORGs and class 1 integron revealed that both were often found together in the same contigs within transconjugant isolates, indicating co-transfer on the same MGE or plasmid (**Figures 7A,B**). Contigs were found to be up to 55 kb and contained transferred genes. In addition, we found that several of the transconjugants with similar or identical MDRPs contained the same acquired genes with conserved gene order on identical contigs. Manual inspection of all contigs containing acquired genetic material verified that only four different and complete plasmid backbones with variations mainly in MGEs carrying ARGs were repeatedly identified among transconjugants from the river water microbial community. Since all four backbones were identified in transconjugants from urban and agricultural sites and from experiments in the absence and presence of metals, they were further studied (**Figures 7A,B**). The four plasmid backbones were classified according to the RSGs and Inc group. Backbone #1 was characterized to only carry the anti-restriction protein gene *klcA2* (IncN3), backbone #2 carried a combination of restriction-methylase genes *hsdR-hsdM* (IncN2), backbone #3 harbored a different combination of restriction-methylase genes *ECORII-dcm* (IncN) *and* finally, backbone #4 carried three different restriction system genes *klcA2-ECORII-dcm* (IncN) (**Figure 7A**).

In order to determine from the short-read assembles whether the acquired DNA was associated with AMR plasmids, the extra contigs were subjected to NCBI BLAST. The results showed that the four plasmid-like backbones were highly similar (85–95%) and covered a large proportion of the nucleotide sequences (75–90%) of AMR plasmids' sequences found in the NCBI database and belonged to several bacterial pathogens such as *Klebsiella pneumoniae* (*K. pneumoniae*), *Enterobacter*, *Citrobacter,* and *Shigella*. For instance, the plasmid-like backbone #1 was found to be 93% similar to AMR IncN plasmid found in a clinical strain of *K. pneumoniae* JIE137 (EF219134.3) carrying $bla_{\text{CTX-M-62}}$ isolated in Australia as well as in a clinical isolate of *E. coli* (EF219134.3) (Zong et al., 2008). Also, the plasmid-like backbone #1 was 95% similar to a 53.129 kb (77% coverage) MDR plasmid found in *Enterobacter hormaechei* (*E. hormaechei*) subsp. Steigerwaltti (CP010382.1) isolated from patients at different health care institutions in New York, USA. Although this plasmid was reported to carry several *bla* genes ($bla_{\text{KPC-4}}$, $bla_{\text{TEM-1A}}$, and $bla_{\text{OXA-1}}$), they were not present in our transconjugants (Chavda et al., 2016). The comparison of the plasmid-like backbone #2 yielded MDR plasmids with an identity of almost 100% and coverage of 88% found in *E. coli* (pEC448_OXA163: CP015078.1) isolated from Argentina carrying an OXA-163 that was not acquired by our recipient strain. Similarly to plasmid-like backbone #1, plasmid-like backbone #2 was highly similar to a plasmid in *E. coli* p17511_70 (MN583554), which also carried a $bla_{\text{OXA-48}}$ gene. Other hits for backbone #2 included *Citrobacter farmer* (*C. farmer*), a serially isolated KPC-2 producer from a single patient. The contig corresponding to the plasmid-like backbone #3 shared the highest coverage and pairwise nucleotide identity with other reported plasmids such as pD17KP0013-2 in *K. pneumoniae* (CP052348.1), pAR-04232-1 in *S. flexneri* AR-0423 (CP044159.1), pEclE3-3 in *E. hormaechei* strain Eho-E3 (CP049024.1). Although *K. pneumoniae* and *S. flexneri* were clinical isolates, *E. hormaechei* was recovered from sewage water samples from Ontario, Canada (Kohler et al., 2020). Lastly, plasmid-like backbone #3 and plasmid-like backbone #4 shared a highly similar DNA sequence with related plasmids from diverse bacterial species, and both plasmid-like backbones #3 and 4 are identical to pD17KP0013-2 found in *K. pneumoniae* and *E. hormaechei* strain Eho-E3 with the exception that plasmid-like backbone #4 is ∼12 kb larger than backbone #3 (**Figure 7A**).

A detailed comparison of the four plasmid-like backbones is shown in **Figure 7B**, where all backbones presented conserved regions containing mainly plasmid maintenance genes. All ARG positive contigs contained T4SS genes indicating the presence of the complete Tra-operon, including conjugation-associated genes *traD* and *traI*. Variable regions containing different combinations of ARGs, ORGs, metabolic and hypothetical genes were also identified in the four putative plasmid structures. Differences in the variable regions containing ARGs of the four plasmid-like structures determined the observed differences in phenotype and genotype of analyzed transconjugants. We confirmed that all identified backbones were mobile by a second transconjugation using four selected transconjugants representing #1–4 as donors and *E. coli* HA4 as the recipient.

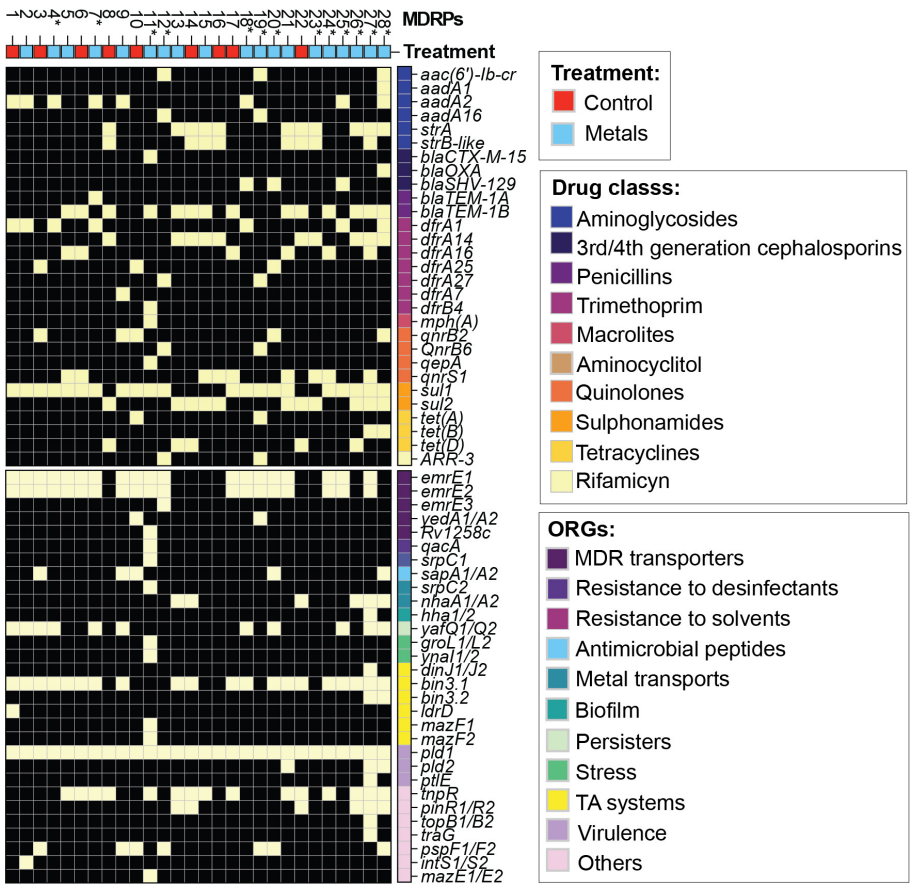

FIGURE 6
Genomic characterization of representative transconjugants with unique MDRP. Heatmap based on the presence (yellow)/absence (black) of ARGs annotated using the ResFinder database (Bortolaia et al., 2020). ARGs were classified according to the drug class they belong to. Other relevant genes (ORGs) were labeled based on their biological function. Unique MDRPs are marked with (*).

Discussion

The potential of waterborne bacteria from the contaminated La Paz River basin to transfer antibiotic resistance determinants to *E. coli* was evaluated. Two different sampling sites in the river were used as a donor source, one urban site located after the city center of La Paz and close to several hospitals, and another rural agricultural site located downstream in the river where water is used for irrigation of crops. After 3 h of mating experiments on solid media without adding stressors, SMX/TMP resistant transconjugants were retrieved at high frequencies from both sites in the La Paz River. Donors from the urban site generated more than three times higher TFs than the agricultural site (5.3×10^{-3} and 1.6×10^{-3} transfer events per recipient, respectively). Previous studies using waterborne donors and *E. coli* CV601 as the recipient reported transconjugants at frequencies of 1×10^{-4} transfer events per recipient in a lake in India (Flach et al., 2015) and 2×10^{-6} and 3×10^{-5} after 3- and 16-h mating experiments, respectively, using bacteria from a Swedish sewage treatment plant (Jutkina et al., 2016). Compared to these studies, bacterial donors from the La Paz River transferred SMX-associated MGEs to *E. coli* at very high frequencies after only 3 h of mating, suggesting that higher levels of bacterial contamination, particularly in the urban site, were associated with higher TFs of antibiotic resistance. Supporting these results, we reported in a previous study high bacterial loads of diarrheagenic *E. coli* (DEC), *Salmonella enterica*, *K. pneumoniae,* and *Shigella* spp., at different points in the La Paz River basin, including the urban and agricultural sites used in the present study. High water conductivity and the highest number of total enterobacteria (7×10^6 *gapA* gene copies per 100 ml of river water) were observed at the urban site, confirming the high level of anthropogenic fecal contamination in the river and a high number of suitable donors for HGT experiments (Guzman-Otazo et al., 2019).

In the present study, the addition of metal salts such as $ZnSO_4$ and $CuSO_4$ at 0.5 and 1 mM in mating experiments did not cause a significant effect on the number of SMX-TMP resistant transconjugants and TFs. Previous studies on

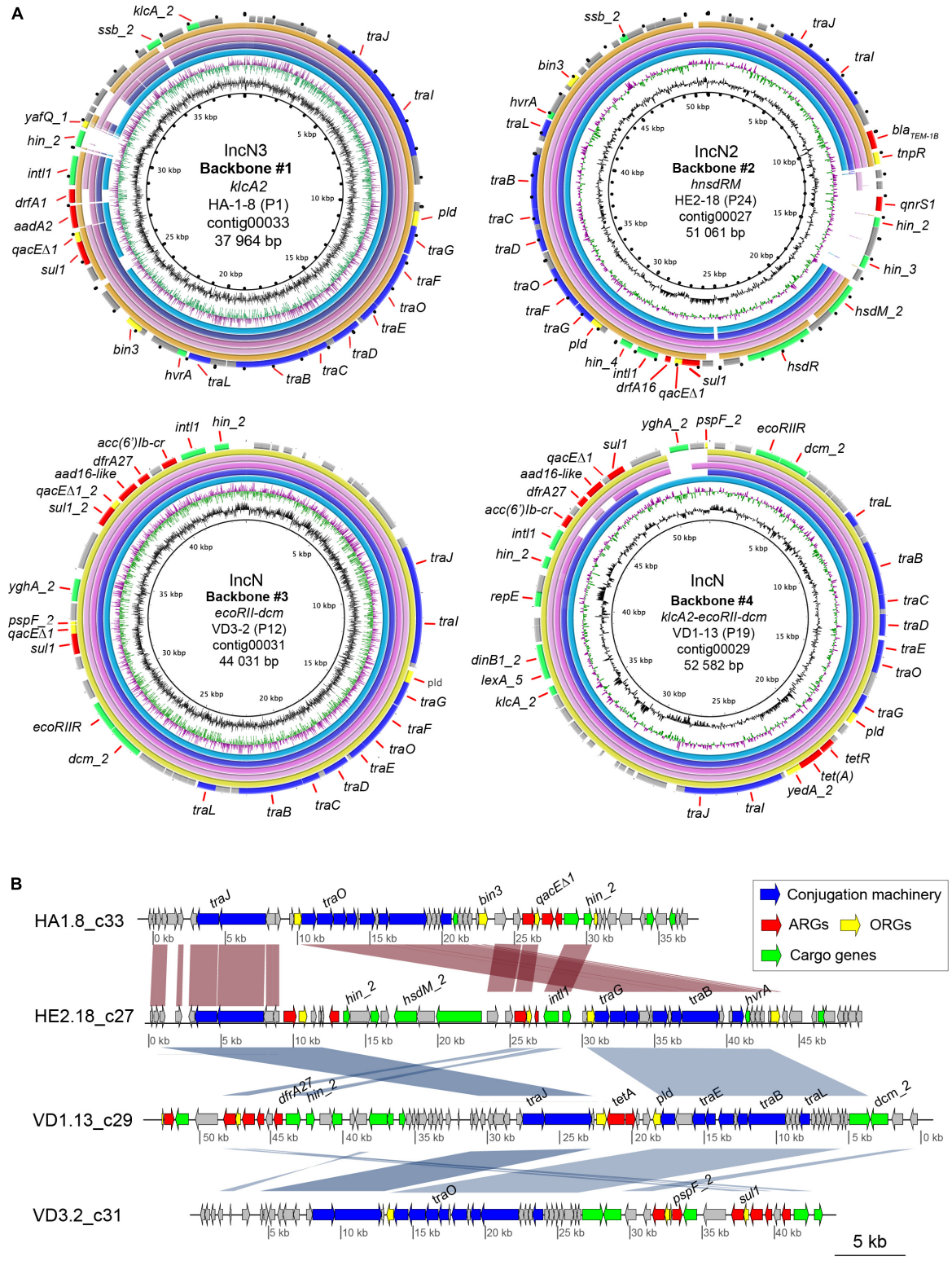

FIGURE 7
Comparison between the IncN plasmid-like backbones repeatedly identified in transconjugants from river water using blastn. **(A)** The top five plasmid genomes with the highest percentage of identity (>70%) and query cover were included in the comparison. A plasmid-like backbone was used as the reference sequence (outer ring). The genes present in the reference genome are shown as black dots in the rings that represent the five genomes. The color code for the annotations is listed at the bottom of the figure. The two inner rings depict GC content in black and

(Continued)

FIGURE 7 (Continued)
GC Skew- in purple, and GC Skew + in green. The figures were generated using BRIG36 (v0.95, http://brig.sourceforge.net/). #1: *K. pneumoniae* isolate JIE137 plasmid pJIE137 (EF219134.3) (light blue); *E. coli* I23 plasmid pEcI23 (MH713706.1) (purple); *K. pneumoniae* N11 plasmid pKpnN11 (MH782635.1) (magenta); *E. hormaechei* subsp. hormaechei strain 34983 plasmid p34983-59.134kb (CP010378.1) (pink); *E. coli* strain M17224 plasmid p17511_70 (MN583554.1) (yellow). Backbone #2: *E. coli* strain Ecol_448 plasmid pEC448_OXA163 (CP015078.1) (light blue); *E. coli* strain M17224 plasmid p17511_70 (MN583554.1) (purple); *K. pneumoniae* N11 plasmid pKpnN11 (MH782635.1) (magenta); *E. coli* I23 plasmid pEcI23 (MH713706.1) (pink); *C. farmeri* strain CCRI-24236 plasmid pCCRI24236-2 (CP081316.1) (yellow). Backbone #3: *K. pneumoniae* strain D17KP0013 plasmid pD17KP0013-2 (CP052348.1) (light blue); *Shigella flexneri* strain AR-0423 plasmid pAR-0423-1 (CP044159.1) (purple); *Enterobacter hormaechei* (*E. hormaechei*) strain Eho-E3 plasmid pEclE3-3 (CP049024.1) (magenta); *E. hormaechei* strain Eho-E4 plasmid pEclE4-3 (CP048699.1) (pink); *E. coli* strain RHBSTW-00822 plasmid pRHBSTW-00822_3 (CP056317.1) (yellow). Backbone #4: *K. pneumoniae* strain D17KP0013 plasmid pD17KP0013-2 (CP052348.1) (light blue); *K. pneumoniae* strain D16KP0144 plasmid pD16KP0144-3 (CP052359.1) (purple); *Salmonella enterica* subsp. enterica serovar Typhimurium strain STM3224 plasmid pUY_STM62 (MN241904.1) (magenta); *E. coli* strain Ec19397 plasmid pEc19397-131, complete sequence (MG878866.1) (pink); *E. hormaechei* strain EH_316 plasmid pEH_316-3 (CP078058.1) (yellow). **(B)** Comparison of the plasmid-like backbones of IncN plasmids. The MAUVE-based progressive multi-alignment shows the similarity between the genetic structure of the different IncN plasmid-like obtained during conjugation experiments. VD1.13_c29 nucleotide sequence was reversed to improve visualization of the comparison. The scale bar represents the sequence length. Protein annotations colored by putative functions are shown as arrows for each contig. BLAST similarity values greater than 95% between contigs are shown in red if they are oriented in the same direction and blue if they are in the reverse direction.

the effect of metals on conjugative transfer rates have shown contradictory results that are highly dependent on the type of metal and concentration tested. Suzuki et al. (2012) reported that vanadium at 0.5 and 1 mM significantly increased the conjugative transfer rate of oxytetracycline resistance plasmids from *Photobacterium damselae* strain 04Ya311 to *E. coli* JM109. However, other metals, such as zinc and copper, up to 0.5 mM caused a decrease in the conjugation rate of this study model. In another study, Zhang et al. (2018b) reported that very low concentrations of copper (0.005, 0.01, and 0.05 mg/L), silver (0.01 and 0.02 mg/L), and chromium (0.1 mg/L) but not zinc, significantly increased the conjugation frequency of a multi-drug resistance plasmid between two *E. coli* isolates in water conjugation experiments. It is important to note that the positive copper concentrations used by the authors were more than 100 times lower than the concentrations tested in our study. This might suggest that metals like copper are more likely to exert a promoting effect on conjugation rate at low concentrations. Metal nanoparticles have also been studied for their effect on bacterial conjugation. Zinc nanoparticles up to 10 mg/L increased the conjugative transfer of the resistance plasmid RP4 between *E. coli* isolates (24.3-fold increase) and between donor *E. coli* isolates and indigenous water bacteria as recipients (8.3-fold increase). Zinc nanoparticles did also increase transformation efficiency. Nevertheless, this effect was nanoparticle-dependent since $Zn(NO_3)_2$ in equivalent concentrations did not increase conjugation frequency or transformation efficiency in the model proposed by the authors (Wang et al., 2018). Similar conjugation experiments showed that copper nanoparticles and $CuSO_4$ at 20 and 50 mg/L could reduce the conjugation frequency of catabolic plasmids among *Cupriavidus pinatubonensis*, *Pseudomonas putida,* and *Pseudomonas* sp. isolates by 10% (Parra et al., 2019).

The transconjugants obtained from mating experiments in the presence of $ZnSO_4$ and $CuSO_4$ did not acquire increased tolerance to any of these metal salts compared to the original recipient strain *E. coli* CV601. These results suggest that our experiments did not involve the co-transfer of ARGs and copper/zinc resistance genes. Additionally, WGS analysis of transconjugants revealed the acquisition of only two genes encoding lithium (*nhaA*) and chromate (*srpC2*) transporters. This indicates a low potential for metals to promote the spread of antibiotic resistance plasmids compatible with *E. coli* in these waterways. Supporting these findings, Pal et al. (2015) reported patterns of genetic co-occurrence of ARGs and biocide/metal resistance genes in bacterial genomes and plasmids from different taxa and environments. The authors identified genes conferring resistance to mercury (*mer* genes), quaternary ammonium compounds (*qacEΔ1*) and the class 1 integron integrase intI1 gene, *intl1* as the most common co-occurrence with a wide variety of ARGs in plasmids implying the high probability for co-selection of antibiotic resistance. These results reinforce the findings of several studies that suggest that the presence of *intl1* gene could serve as a marker for anthropogenic pollutants due to its widely spread among pathogenic and commensal bacteria of humans or domestic animals, often located in mobile genetic elements and commonly associated with ARGs, disinfectants and heavy metals (Stalder et al., 2012; Gillings et al., 2015; Agramont et al., 2020; Zheng et al., 2020; Baltazar et al., 2022). The authors reported that cadmium and zinc resistance genes (*cadD*) only co-occurred with aminoglycoside and macrolide resistance genes. According to Pal et al. (2015), silver, copper, and arsenic resistance genes were less likely to co-localize and co-select for other ARGs. The co-occurrence of biocide/metal resistance genes and ARGs was more commonly found in clinical isolates, while this genetic co-localization was less common in plasmids of environmental isolates (<0.7%) (Pal et al., 2015). Finally, the authors showed that plasmids carrying biocide/metal and antibiotic resistance genes tended to be conjugative and carry toxin-antitoxin system genes, promoting the persistence of bacteria and plasmids. In our study, although transconjugants did not acquire zinc and copper resistance genes, many of them acquired multi-drug resistance plasmids carrying ARGs

co-localized with genes conferring resistance to biocides such as QACs (*qacA* and *qacEΔ1*) and toxin-antitoxin system genes (*dinJ, ldrD*, *mazE,* and *mazF)*.

Most conjugation experiments to test the effect of metals on antibiotic resistance transfer are performed between one specific donor strain (carrying a specific plasmid) and one recipient. To our extent of knowledge, this is the first study of metals at sub-lethal concentrations as stressors in conjugation experiments between complex waterborne bacterial communities as donors and *E. coli* as the recipient. In that way, we were able to evaluate not only the conjugative transfer rate but also the diversity and richness of phenotypic MDRPs and identify the transferred genes and plasmids in the absence and presence of metals by WGS of transconjugants. Significantly higher diversity and richness and unique MDRPs carrying ESBLs such as $bla_{\text{CTX-M-15}}$, $bla_{\text{SHV-129}}$, and $bla_{\text{OXA-9}}$ were obtained only from the agricultural site when metals were added to mating experiments. The agricultural area in the La Paz River is characterized by the production of lettuce, chard, and chamomile, among other crops irrigated with contaminated water from the river. Furthermore, farmers use river sediments as manure for crops. In a previous study, we reported the presence of different categories of diarrheagenic *E. coli* (DEC), *S. enterica*, *K. pneumoniae,* and *Shigella* spp. in soil samples and vegetables from the agricultural area in the La Paz River. *E. coli* isolates carrying ARGs for macrolides and quinolones and ESBLs were also recovered from soil samples (Guzman-Otazo et al., 2019). Soils are considered important reservoirs of antibiotic-resistant bacteria (ARB) and ARGs. In agricultural soils, the continuous discharge of reused wastewater for irrigation, manure, and biosolids promotes the enrichment of antibiotics, ARB, and ARGs, which might be transported vertically deeper into the soil layers or horizontally entering the environment in watersheds and other compartments (Christou et al., 2017). Our results suggest that bacterial donors from the agricultural area in the La Paz River carry higher diversity and richness of transferable MGEs and ARGs than donors from the urban area.

All plasmid-like structures identified in this study belonged to the incompatibility group N (IncN, IncN2, and IncN3). Plasmids belonging to the IncN group are commonly found in and mobilized between, members of the Enterobacterales (Rada et al., 2020; Yamagishi et al., 2020; Sellera et al., 2021). This group of plasmids tends to be self-conjugative, and they are highly associated with antibiotic resistance dispersion since they commonly carry ESBLs, oxacillinases, carbapenemases, quinolone, aminoglycoside, and sulfonamide resistance genes, among others (Carattoli, 2009; Garcia-Fernandez et al., 2011; Dolejska et al., 2013). Several studies of tranconjugation between resident waterborne bacteria using *E. coli* CV601 as recipient identified a dominance of IncN plasmids (Flach et al., 2015; Hutinel et al., 2022) corroborating the results of the present study. However, IncF, IncA/C, IncP, IncN, and other plasmids are commonly found in bacteria from water sources, and the reason for the sole isolation of IncN plasmids in this study needs further analysis.

Transconjugants carrying a high number and varieties of ORGs associated with resistance mechanisms to disinfectants and solvents, metal transporters, biofilm formation, survival in stress conditions, and virulence were mainly obtained from conjugation experiments in the presence of $ZnSO_4$ and $CuSO_4$. Bacteria and other microorganisms have developed metabolic advantages in the presence of low concentrations of metals. For example, bacteria have mechanisms to transform metals from insoluble to soluble forms and take advantage of metals such as zinc and copper that participate in redox reactions and in the electron transport chain to synthesize more energy molecules and benefit bacterial metabolism (Nguyen et al., 2019). However, heavy metals can also produce oxidative stress, and this has been proposed to be the main mechanism by which metals can promote the spread of antibiotic resistance. The generation of reactive oxygen species (ROS), the activation of SOS response, and the increased permeability of bacterial membranes might promote the horizontal transfer and acquisition of MGEs (Zhang et al., 2018b). Although this study did not show a significant difference in the conjugative transfer rate in the absence and presence of metals, higher diversity, and richness of MDRPs, ARGs, and ORGs were observed in the presence of metals. We might speculate that an energetic and metabolic advantage or the oxidative stress caused by sub-inhibitory concentrations of $ZnSO_4$ and $CuSO_4$ may favor the transfer/acquisition of a higher diversity of ARGs and ORGs. Assuming that low concentrations of metals promote stress conditions and a significant increase in membrane permeability, this might influence the acquisition of bigger MGEs carrying a higher number and diversity of relevant genes that at the same time confer an advantage to the host in stress conditions. This is the case of unique MDRP P27 and P28 obtained from metal treatment, which contains the highest number of ARGs and ORGs observed in this study. Although the approximate number of base pairs acquired by transconjugants did not significantly differ between sites and treatments, contigs carrying ARGs and ORGs obtained from metal treatment showed an apparent bigger size in base pairs.

In conclusion, this study shows the high potential for a large set of resistance factors to be transferred from polluted bacterial communities in the La Paz River basin to *E. coli*. Metal stressors such as $ZnSO_4$ and $CuSO_4$ at the sub-lethal

concentrations tested in this study did not affect transfer frequencies of antibiotic resistance. However, the presence of metal salts influenced the transfer/acquisition of higher diversity, richness, and unique MDRPs in *E. coli*. This study found the highest diversity of phenotypic MDRPs, ARGs, and ORGs in transconjugants obtained from agricultural water samples in the presence of metal salts during conjugation experiments. Hence, agricultural ecosystems might represent important reservoirs of ARGs and MGEs, posing a risk of transmission of antibiotic resistance to the community by consuming contaminated vegetables. ESBLs and ORGs associated with resistance to disinfectants and antimicrobial peptides, multi-drug transporters, biofilm formation and persisted state in bacteria, survival in stress conditions, virulence determinants and markers for anthropogenic pollution such as the class 1 integron integrase intI1 were also transferred from waterborne bacteria to *E. coli* making evident that contaminated watersheds and ARGs reservoirs in the environment represent a risk for human health.

Data availability statement

The datasets presented in this study can be found in online repositories. The names of the repository/repositories and accession number(s) can be found in the article/**Supplementary material**.

Author contributions

ÅS, DL, VI, and C-FF contributed to the conception and design of the study. JG-O, JA, NM, and VI were involved in the sample collection. JG-O, JJ, and JA performed the experiments. JG-O, EJ, and JA analyzed the data, performed the statistical analysis and visualization. FB and YH performed the bioinformatic analysis. EJ curated the data. JG-O, DL, VI, and ÅS wrote the first draft of the manuscript. AF, DL, EJ, and JA wrote sections of the manuscript. AF, DJ-L, C-FF, and DL edited the manuscript. All authors contributed to manuscript revision, read, and approved the submitted version.

Acknowledgments

This study was supported by the Swedish International Development Cooperation Agency (Sida) to VI and ÅS, JG-O acknowledges the financial support from the International Science Program (ISP). C-FF acknowledges support from the Swedish Research Council Formas. DL would like to thank the EU and Swedish Research Council for funding in the frame of the collaborative international consortium (BIOCIDE) financed under the ERA-NET AquaticPollutants Joint Transnational Call (GA n^{a}869178). ÅS and EJ would like to thank the collaborative international consortium (PARRTAE) under the same call for funding. This ERA-NET is an integral part of the activities developed by the Water, Oceans, and AMR Joint Programming Initiatives. AF acknowledges financial support from the Centre for Antibiotic Resistance Research (CARe) at the University of Gothenburg and JPIAMR (2016-06503_3). Support was also obtained from the Swedish Research Council Dnrs 2014-02639, 2018-01874, and 2019-04202, and Swedish Research Links Dnr 2017-05423 to ÅS. Sequencing was performed with the support of the Centre for Translational Microbiome Research (CTMR), a collaboration between Karolinska Institutet, Science for Life Laboratory, and Ferring Pharmaceuticals.

Conflict of interest

The authors declare that the research was conducted in the absence of any commercial or financial relationships that could be construed as a potential conflict of interest.

Publisher's note

Supplementary material

The Supplementary Material for this article can be found online at: https://www.frontiersin.org/articles/10.3389/fmicb.2022.997849/full#supplementary-material

References

Aarestrup, F. M., and Hasman, H. (2004). Susceptibility of different bacterial species isolated from food animals to copper sulphate, zinc chloride and antimicrobial substances used for disinfection. *Vet. Microbiol.* 100, 83–89. doi: 10.1016/j.vetmic.2004.01.013

Agramont, J., Gutiérrez-Cortez, S., Joffré, E., Sjöling, Å, and Calderon Toledo, C. (2020). Fecal pollution drives antibiotic resistance and class 1 integron abundance in aquatic environments of the bolivian andes impacted by mining and wastewater. *Microorganisms* 8:1122. doi: 10.3390/microorganisms8081122

Alalam, H., Graf, F. E., Palm, M., Abadikhah, M., Zackrisson, M., Boström, J., et al. (2020). A high-throughput method for screening for genes controlling bacterial conjugation of antibiotic resistance. *mSystems* 5, e1226–e1220. doi: 10.1128/mSystems.01226-20

Altschul, S. F., Gish, W., Miller, W., Myers, E. W., and Lipman, D. J. (1990). Basic local alignment search tool. *J Mol Biol* 215, 403–410. doi: 10.1016/S0022-2836(05)80360-2

Altschul, S. F., Madden, T. L., Schäffer, A. A., Zhang, J., Zhang, Z., Miller, W., et al. (1997). Gapped BLAST and PSI-BLAST: A new generation of protein database search programs. *Nucleic Acids Res.* 25, 3389–3402. doi: 10.1093/nar/25.17.3389

Andersson, D. I., and Hughes, D. (2014). Microbiological effects of sublethal levels of antibiotics. *Nat. Rev. Microbiol.* 12, 465–478. doi: 10.1038/nrmicro3270

Andersson, D. I., and Hughes, D. (2017). Selection and transmission of antibiotic-resistant bacteria. *Microbiol. Spectr.* 5. doi: 10.1128/microbiolspec.MTBP-0013-2016

Archundia, D., Boithias, L., Duwig, C., Morel, M. C., Flores Aviles, G., and Martins, J. M. F. (2018). Environmental fate and ecotoxicological risk of the antibiotic sulfamethoxazole across the katari catchment (Bolivian Altiplano): Application of the GREAT-ER model. *Sci. Total Environ.* 622-623, 1046–1055. doi: 10.1016/j.scitotenv.2017.12.026

Archundia, D., Duwig, C., Lehembre, F., Chiron, S., Morel, M. C., Prado, B., et al. (2017). Antibiotic pollution in the katari subcatchment of the Titicaca Lake: Major transformation products and occurrence of resistance genes. *Sci. Total Environ.* 576, 671–682. doi: 10.1016/j.scitotenv.2016.10.129

Aubertheau, E., Stalder, T., Mondamert, L., Ploy, M. C., Dagot, C., and Labanowski, J. (2017). Impact of wastewater treatment plant discharge on the contamination of river biofilms by pharmaceuticals and antibiotic resistance. *Sci. Total Environ.* 579, 1387–1398. doi: 10.1016/j.scitotenv.2016.11.136

Baltazar, M., Bourgeois-Nicolaos, N., Larroudé, M., Couet, W., Uwajeneza, S., Doucet-Populaire, F., et al. (2022). Activation of class 1 integron integrase is promoted in the intestinal environment. *PLoS Genet* 18, e1010177. doi: 10.1371/journal.pgen.1010177

Bengtsson-Palme, J., Kristiansson, E., and Larsson, D. G. J. (2018). Environmental factors influencing the development and spread of antibiotic resistance. *FEMS Microbiol. Rev.* 42:fux053. doi: 10.1093/femsre/fux053

Bortolaia, V., Kaas, R. S., Ruppe, E., Roberts, M. C., Schwarz, S., Cattoir, V., et al. (2020). ResFinder 4.0 for predictions of phenotypes from genotypes. *J. Antimicrob. Chemother.* 75, 3491–3500. doi: 10.1093/jac/dkaa345

Buchfink, B., Xie, C., and Huson, D. H. (2015). Fast and sensitive protein alignment using DIAMOND. *Nat. Methods* 12, 59–60. doi: 10.1038/nmeth.3176

Camacho, C., Coulouris, G., Avagyan, V., Ma, N., Papadopoulos, J., Bealer, K., et al. (2009). BLAST+: Architecture and applications. *BMC Bioinform.* 10:421. doi: 10.1186/1471-2105-10-421

Carattoli, A. (2009). Resistance plasmid families in *Enterobacteriaceae*. *Antimicrob. Agents Chemother.* 53, 2227–2238. doi: 10.1128/AAC.01707-08

Chavda, K. D., Chen, L., Fouts, D. E., Sutton, G., Brinkac, L., Jenkins, S. G., et al. (2016). Comprehensive genome analysis of carbapenemase-producing *Enterobacter* spp.: New insights into phylogeny, population structure, and resistance mechanisms. *mBio* 7, e2093–e2016. doi: 10.1128/mBio.02093-16

Christou, A., Aguera, A., Bayona, J. M., Cytryn, E., Fotopoulos, V., Lambropoulou, D., et al. (2017). The potential implications of reclaimed wastewater reuse for irrigation on the agricultural environment: The knowns and unknowns of the fate of antibiotics and antibiotic resistant bacteria and resistance genes - A review. *Water Res.* 123, 448–467. doi: 10.1016/j.watres.2017.07.004

Dolejska, M., Villa, L., Hasman, H., Hansen, L., and Carattoli, A. (2013). Characterization of IncN plasmids carrying bla CTX-M-1 and qnr genes in *Escherichia coli* and *Salmonella* from animals, the environment and humans. *J. Antimicrob. Chemother.* 68, 333–339. doi: 10.1093/jac/dks387

Duwig, C., Archundia, D., Lehembre, F., Spadini, L., Morel, M., Uzu, G., et al. (2014). Impacts of anthropogenic activities on the contamination of a sub watershed of Lake Titicaca. Are antibiotics a concern in the Bolivian Altiplano? *Procedia Earth Planet. Sci.* 10, 370–375. doi: 10.1016/j.proeps.2014.08.062

Fauci, A. S., and Marston, L. D. (2014). The perpetual challenge of antimicrobial resistance. *Jama* 311, 1853–1854. doi: 10.1001/jama.2014.2465

Finley, R. L., Collignon, P., Larsson, D. G. J., Mcewen, S. A., Li, X.-Z., Gaze, W. H., et al. (2013). The scourge of antibiotic resistance: The important role of the environment.(Report). *Clin. Infect. Dis.* 57:704. doi: 10.1093/cid/cit355

Flach, C. F., Johnning, A., Nilsson, I., Smalla, K., Kristiansson, E., and Larsson, D. G. (2015). Isolation of novel IncA/C and IncN fluoroquinolone resistance plasmids from an antibiotic-polluted lake. *J. Antimicrob. Chemother.* 70, 2709–2717. doi: 10.1093/jac/dkv167

Garcia-Fernandez, A., Villa, L., Moodley, A., Hasman, H., Miriagou, V., Guardabassi, L., et al. (2011). Multilocus sequence typing of IncN plasmids. *J. Antimicrob. Chemother.* 66, 1987–1991. doi: 10.1093/jac/dkr225

Gillings, M. R., Gaze, W. H., Pruden, A., Smalla, K., Tiedje, J. M., and Zhu, Y.-G. (2015). Using the class 1 integron-integrase gene as a proxy for anthropogenic pollution. *ISME J.* 9, 1269–1279. doi: 10.1038/ismej.2014.226

Guzman-Otazo, J., Gonzales-Siles, L., Poma, V., Bengtsson-Palme, J., Thorell, K., Flach, C. F., et al. (2019). Diarrheal bacterial pathogens and multi-resistant *enterobacteri*a in the Choqueyapu River in La Paz, Bolivia. *PLoS One* 14:e0210735. doi: 10.1371/journal.pone.0210735

Heuer, H., Krogerrecklenfort, E., Wellington, E. M., Egan, S., Van Elsas, J. D., Van Overbeek, L., et al. (2002). Gentamicin resistance genes in environmental bacteria: Prevalence and transfer. *FEMS Microbiol. Ecol.* 42, 289–302. doi: 10.1111/j.1574-6941.2002.tb01019.x

Hudzicki, J. (2009). Kirby-Bauer disk diffusion susceptibility test protocol. *Am. Soc. Microbiol.* Available online at: https://asm.org/Protocols/Kirby-Bauer-Disk-Diffusion-Susceptibility-Test-Pro

Hutinel, M., Larsson, D. G. J., and Flach, C.-F. (2022). Antibiotic resistance genes of emerging concern in municipal and hospital wastewater from a major Swedish city. *Sci. Total Environ.* 812:151433. doi: 10.1016/j.scitotenv.2021.151433

Ji, X., Shen, Q., Liu, F., Ma, J., Xu, G., Wang, Y., et al. (2012). Antibiotic resistance gene abundances associated with antibiotics and heavy metals in animal manures and agricultural soils adjacent to feedlots in Shanghai; China.(Report). *J. Hazard. Mater.* 235:178. doi: 10.1016/j.jhazmat.2012.07.040

Joensen, K. G., Scheutz, F., Lund, O., Hasman, H., Kaas, R. S., Nielsen, E. M., et al. (2014). Real-time whole-genome sequencing for routine typing, surveillance, and outbreak detection of verotoxigenic *Escherichia coli*. *J. Clin. Microbiol.* 52, 1501–1510. doi: 10.1128/JCM.03617-13

Johnson, M., Zaretskaya, I., Raytselis, Y., Merezhuk, Y., Mcginnis, S., and Madden, T. L. (2008). NCBI BLAST: A better web interface. *Nucleic Acids Res.* 36, W5–W9. doi: 10.1093/nar/gkn201

Jutkina, J., Rutgersson, C., Flach, C.-F., and Joakim Larsson, D. G. (2016). An assay for determining minimal concentrations of antibiotics that drive horizontal transfer of resistance. *Sci. Total Environ.* 548-549, 131–138. doi: 10.1016/j.scitotenv.2016.01.044

Kirangwa, J., Alvarez-Carretero, S., Boulund, F., and Thorell, K. (2017). *BBACTpipe: Bacterial whole-genome sequence assembly and annotation pipeline v.2.6.1*. Available online at: https://github.com/ctmrbio/BACTpipe

Kohler, P., Tijet, N., Kim, H. C., Johnstone, J., Edge, T., Patel, S. N., et al. (2020). Dissemination of verona integron-encoded Metallo-β-lactamase among clinical and environmental *Enterobacteriaceae* isolates in Ontario, Canada. *Sci. Rep.* 10:18580.

Larsson, D. G. J., and Flach, C.-F. (2022). Antibiotic resistance in the environment. *Nat. Rev. Microbiol.* 20, 257–269. doi: 10.1038/s41579-021-00649-x

Malberg Tetzschner, A. M., Johnson, J. R., Johnston, B. D., Lund, O., and Scheutz, F. (2020). In silico genotyping of *Escherichia coli* isolates for extraintestinal virulence genes by use of whole-genome sequencing data. *J. Clin. Microbiol.* 58, e1269–e1220. doi: 10.1128/JCM.01269-20

Marti, E., Variatza, E., and Balcazar, J. L. (2014). The role of aquatic ecosystems as reservoirs of antibiotic resistance. *Trends Microbiol.* 22, 36–41. doi: 10.1016/j.tim.2013.11.001

Medina, C., Ginn, O., Brown, J., Soria, F., Garvizu, C., Salazar, Á, et al. (2021). Detection and assessment of the antibiotic resistance of *Enterobacteriaceae* recovered from bioaerosols in the Choqueyapu river area, La Paz–Bolivia. *Sci. Total Environ.* 760:143340. doi: 10.1016/j.scitotenv.2020.143340

Nguyen, C., Hugie, C., Kile, M., and Navab-Daneshmand, T. (2019). Association between heavy metals and antibiotic-resistant human pathogens in environmental

reservoirs: A review. *Front. Environ. Sci. Eng.* 13, 1–17. doi: 10.1007/s11783-019-1129-0

Pal, C., Asiani, K., Arya, S., Rensing, C., Stekel, D. J., Larsson, D. G. J., et al. (2017). Metal Resistance and its association with antibiotic resistance. *Adv. Microb. Physiol.* 70, 261–313. doi: 10.1016/bs.ampbs.2017.02.001

Pal, C., Bengtsson-Palme, J., Kristiansson, E., and Larsson, D. G. (2015). Co-occurrence of resistance genes to antibiotics, biocides and metals reveals novel insights into their co-selection potential. *BMC Genomics* 16:964. doi: 10.1186/s12864-015-2153-5

Pal, C., Bengtsson-Palme, J., Rensing, C., Kristiansson, E., and Larsson, D. G. J. (2014). BacMet: Antibacterial biocide and metal resistance genes database. *Nucleic Acids Res.* 42:D737. doi: 10.1093/nar/gkt1252

Parra, B., Tortella, G. R., Cuozzo, S., and Martinez, M. (2019). Negative effect of copper nanoparticles on the conjugation frequency of conjugative catabolic plasmids. *Ecotoxicol. Environ. Saf.* 169, 662–668. doi: 10.1016/j.ecoenv.2018.11.057

Petchiappan, A., and Chatterji, D. (2017). Antibiotic resistance: Current perspectives. *ACS Omega* 2, 7400–7409. doi: 10.1021/acsomega.7b01368

Poma, V., Mamani, N., and Iñiguez, V. (2016). Impact of urban contamination of the La Paz River basin on thermotolerant coliform density and occurrence of multiple antibiotic resistant enteric pathogens in river water, irrigated soil and fresh vegetables. *Springerplus* 5, 1–11. doi: 10.1186/s40064-016-2132-6

Rada, A. M., De La Cadena, E., Agudelo, C., Capataz, C., Orozco, N., Pallares, C., et al. (2020). Dynamics of bla(KPC-2) Dissemination from Non-CG258 *Klebsiella pneumoniae* to Other *Enterobacter*ales via IncN plasmids in an area of high endemicity. *Antimicrob. Agents Chemother.* 64, e1743–e1720. doi: 10.1128/AAC.01743-20

Rogozin, A. G., and Gavrilkina, S. V. (2008). Causes for high concentration of copper and zinc in the water of some lakes in the Southern Urals. *Water Resour.* 35, 701–707. doi: 10.1134/S0097807808060092

Sellera, F. P., Fuga, B., Fontana, H., Esposito, F., Cardoso, B., Konno, S., et al. (2021). Detection of IncN-pST15 one-health plasmid harbouring bla(KPC-2) in a hypermucoviscous *Klebsiella pneumoniae* CG258 isolated from an infected dog. Brazil. *Transbound Emerg. Dis.* 68, 3083–3088. doi: 10.1111/tbed.14006

Singer, A. C., Shaw, H., Rhodes, V., and Hart, A. (2016). Review of antimicrobial resistance in the environment and its relevance to environmental regulators. *Front. Microbiol.* 7:1728. doi: 10.3389/fmicb.2016.01728

Stalder, T., Barraud, O., Casellas, M., Dagot, C., and Ploy, M. C. (2012). Integron involvement in environmental spread of antibiotic resistance. *Front. Microbiol.* 3:119. doi: 10.3389/fmicb.2012.00119

Suzuki, S., Kimura, M., Agusa, T., and Rahman, H. M. (2012). Vanadium accelerates horizontal transfer of tet(M) gene from marine photobacterium to *Escherichia coli*. *FEMS Microbiol. Lett.* 336:52. doi: 10.1111/j.1574-6968.2012.02653.x

Tan, L., Li, L., Ashbolt, N., Wang, X., Cui, Y., Zhu, X., et al. (2018). Arctic antibiotic resistance gene contamination, a result of anthropogenic activities and natural origin. *Sci. Total Environ.* 621, 1176–1184. doi: 10.1016/j.scitotenv.2017.10.110

Thomsen, M. C., Ahrenfeldt, J., Cisneros, J. L., Jurtz, V., Larsen, M. V., Hasman, H., et al. (2016). A bacterial analysis platform: An integrated system for analysing bacterial whole genome sequencing data for clinical diagnostics and surveillance. *PLoS One* 11:e0157718. doi: 10.1371/journal.pone.0157718

Wang, X., Yang, F., Zhao, J., Xu, Y., Mao, D., Zhu, X., et al. (2018). Bacterial exposure to ZnO nanoparticles facilitates horizontal transfer of antibiotic resistance genes. *Nanoimpact* 10, 61–67. doi: 10.1016/j.impact.2017.11.006

Wiegand, I., Hilpert, K., and Hancock, R. E. (2008). Agar and broth dilution methods to determine the minimal inhibitory concentration (MIC) of antimicrobial substances. *Nat. Protoc.* 3, 163–175. doi: 10.1038/nprot.2007.521

Yamagishi, T., Matsui, M., Sekizuka, T., Ito, H., Fukusumi, M., Uehira, T., et al. (2020). A prolonged multispecies outbreak of IMP-6 carbapenemase-producing *Enterobacter*ales due to horizontal transmission of the IncN plasmid. *Sci. Rep.* 10:4139. doi: 10.1038/s41598-020-60659-2

Zhang, Q. Q., Tian, G. M., and Jin, R. C. (2018a). The occurrence, maintenance, and proliferation of antibiotic resistance genes (ARGs) in the environment: Influencing factors, mechanisms, and elimination strategies. *Appl. Microbiol. Biotechnol.* 102, 8261–8274. doi: 10.1007/s00253-018-9235-7

Zhang, Y., Gu, A. Z., Cen, T., Li, X., He, M., Li, D., et al. (2018b). Sub-inhibitory concentrations of heavy metals facilitate the horizontal transfer of plasmid-mediated antibiotic resistance genes in water environment. *Environ. Pollut.* 237, 74–82. doi: 10.1016/j.envpol.2018.01.032

Zheng, W., Huyan, J., Tian, Z., Zhang, Y., and Wen, X. (2020). Clinical class 1 integron-integrase gene - A promising indicator to monitor the abundance and elimination of antibiotic resistance genes in an urban wastewater treatment plant. *Environ. Int.* 135:105372. doi: 10.1016/j.envint.2019.105372

Zong, Z., Partridge, S. R., Thomas, L., and Iredell, J. R. (2008). Dominance of blaCTX-M within an Australian extended-spectrum beta-lactamase gene pool. *Antimicrob. Agents Chemother.* 52, 4198–4202. doi: 10.1128/AAC.00107-08

frontiers | Frontiers in Microbiology

TYPE Original Research
PUBLISHED 01 December 2022
DOI 10.3389/fmicb.2022.945972

OPEN ACCESS

EDITED BY
Dongchang Sun,
Zhejiang University of Technology, China

REVIEWED BY
Tieli Zhou,
First Affiliated Hospital of Wenzhou Medical University, China
Yanqin Huang,
Harvard Medical School,
United States
Yawei Zhang,
Peking University People's Hospital, China

*CORRESPONDENCE
Yang Liu
ly13767160474@sina.com
Wei Zhang
zhangweiliuxin@163.com

†These authors have contributed equally to this work and share first authorship

SPECIALTY SECTION
This article was submitted to Antimicrobials, Resistance and Chemotherapy, a section of the journal Frontiers in Microbiology

RECEIVED 17 May 2022
ACCEPTED 19 October 2022
PUBLISHED 01 December 2022

CITATION
Li P, Luo W, Xiang T-X, Jiang Y, Liu P, Wei D-D, Fan L, Huang S, Liao W, Liu Y and Zhang W (2022) Horizontal gene transfer *via* OMVs co-carrying virulence and antimicrobial-resistant genes is a novel way for the dissemination of carbapenem-resistant hypervirulent *Klebsiella pneumoniae*. *Front. Microbiol.* 13:945972. doi: 10.3389/fmicb.2022.945972

Horizontal gene transfer *via* OMVs co-carrying virulence and antimicrobial-resistant genes is a novel way for the dissemination of carbapenem-resistant hypervirulent *Klebsiella pneumoniae*

Ping Li[1,2,3†], Wanying Luo[1,2†], Tian-Xin Xiang[4], Yuhuan Jiang[5], Peng Liu[5], Dan-Dan Wei[5], Linping Fan[5], Shanshan Huang[5], Wenjian Liao[1,2], Yang Liu[5,6*] and Wei Zhang[1,2*]

[1]Department of Pulmonary and Critical Care Medicine, The First Affiliated Hospital of Nanchang University, Nanchang University, Nanchang, China, [2]Jiangxi Institute of Respiratory Disease, The First Affiliated Hospital of Nanchang University, Nanchang, China, [3]Yichun People's Hospital, Yichun, China, [4]Department of Infectious Diseases, The First Affiliated Hospital of Nanchang University, Nanchang University, Nanchang, China, [5]Department of Clinical Laboratory, Medical Center of Burn Plastic and Wound Repair, The First Affiliated Hospital of Nanchang University, Nanchang University, Nanchang, China, [6]National Regional Center for Respiratory Medicine, China-Japan Friendship Jiangxi Hospital, Nanchang, China

Introduction: The rapidly increased isolation rate of CR-HvKP worldwide has brought great difficulties in controlling clinical infection. Moreover, it has been demonstrated that the transmission of drug-resistant genes among bacteria can be mediated by outer membrane vesicles (OMVs), which is a new way of horizontal gene transfer (HGT). The transmission of virulence genes among bacteria has also been well studied; however, it remains unclear whether virulence and drug-resistant genes can be co-transmitted simultaneously. Co-transmission of virulence and drug-resistant genes is essential for the formation and prevalence of CR-HvKP.

Methods: First, we isolated OMVs from CR-HvKP by cushioned-density gradient ultracentrifugation (C-DGUC). TEM and DLS were used to examine the morphology and size of bacterial OMVs. OMV-mediated gene transfer in liquid cultures and the acquisition of the carbapenem gene and virulence gene was confirmed using colony-PCR. Antimicrobial susceptibility testing, mCIM and eCIM were conducted for the resistance of transformant. Serum killing assay, assessment of the anti-biofilm effect and galleria mellonella infection model, mucoviscosity assay, extraction and quantification of capsules were verified the virulence of transformant. Pulsed-field gel electrophoresis (PFGE), S1 nuclease-pulsed-field gel electrophoresis (S1-PFGE), Southern blotting hybridization confirmed the plasmid of transformant.

Results: Firstly, OMVs were isolated from CR-HvKP NUHL30457 (K2, ST86). TEM and DLS analyses revealed the spherical morphology of the vesicles. Secondly, our study demonstrated that CR-HvKP delivered genetic material, incorporated DNA within the OMVs, and protected it from degradation by extracellular exonucleases. Thirdly, the vesicular lumen DNA was delivered to the recipient cells after determining the presence of virulence and carbapenem-resistant genes in the CR-HvKP OMVs. Importantly, S1-PFGE and Southern hybridization analysis of the 700603 transformant strain showed that the transformant contained both drug-resistant and virulence plasmids.

Discussion: In the present study, we aimed to clarify the role of CRHvKP-OMVs in transmitting CR-HvKP among *K. pneumoniae*. Collectively, our findings provided valuable insights into the evolution of CR-HvKP.

KEYWORDS

outer membrane vesicles, carbapenem-resistant hypervirulent *Klebsiella pneumoniae*, horizontal gene transfer, virulence genes, antimicrobial-resistant genes

Introduction

As a human commensal and opportunistic pathogenic species, *K. pneumoniae* infection can result in acute hospital-acquired diseases (Paczosa and Mecsas, 2016). Moreover, it is also a clinical strain with extraordinarily high multidrug resistance and hypervirulence-encoding mobile genetic components (Yang et al., 2021). The uninterrupted evolution of plasmids encoding carbapenem resistance or hypervirulence leads to the emergence of new *K. pneumoniae* strains, which can be carbapenem-resistant and hypervirulent simultaneously. Therefore, much attention has been paid to the recent outbreak of carbapenem-resistant and hypervirulent *K. pneumoniae* (CR-HvKP) strains since these pathogens may lead to acute infections in comparatively healthy populations. Furthermore, such infections are hard to treat with currently available antibiotic regimens. Consequently, the prevalence of CR-hvKP has trended upward since 2010. CR-hvKP is primarily prevalent in Asia, especially China. At the same time, it has also been reported worldwide, such as in India, Singapore, Japan, Iran, the United Kingdom, Germany, the United States, Canada, Argentina, and Russia (Lan et al., 2021). In China, the prevalence of CR-hvKP infections is 0 ~ 25.8%, with large numbers of infections found in Henan and Shandong Provinces (Zhang et al., 2020). Mechanisms for the emergence of CR-hvKP can be summarized into three patterns: (i) CRKP acquiring a hypervirulent phenotype; (ii) hvKP acquiring a carbapenem-resistant phenotype; and (iii) *K. pneumoniae* acquiring both a carbapenem resistance and hypervirulence hybrid plasmid. Since mobile genetic elements transmit virulence genes and antibiotic resistance genes, the CR-hvKP strains are widely found (Zhang et al., 2016; Lee et al., 2017; Zhan et al., 2017). With their global dissemination, such organisms have the potential to be the next 'superbug', and public health efforts have thus emphasized the containment of CR-hvKP.

CR-HvKP outbreaks have been reported worldwide, suggesting that it does not affect the transmission potential of the host strain when acquiring resistance genes or a resistance-encoding plasmid (Zhang et al., 2016; Mohammad Ali Tabrizi et al., 2018). However, ten potentially conjugative virulence plasmids have been identified, among which only one has been demonstrated to have transferability by experiments (Yang et al., 2021). PLVPK-like virulence plasmids are not conjugative. Their transmission may need help from conjugative elements in other plasmids, while this theory has not yet been validated.

Horizontal gene transfer (HGT) is the primary type of genetic information delivery among microbes (Daubin and Szöllősi, 2016; Husnik and McCutcheon, 2018). It is well known that genetic material is exchanged between bacteria *via* HGT through three widely described pathways: transformation, conjugation, and transduction (Turnbull et al., 2016; Redondo-Salvo et al., 2020). Recent evidence has indicated that HGT processes may also be promoted by outer membrane vesicles (OMVs) (Schwechheimer and Kuehn, 2015; Kalra et al., 2016; Wang et al., 2019). OMVs are released into the extracellular environment by Gram-negative bacteria. OMVs are enriched with bioactive proteins, toxins, and virulence factors, playing a fundamental role in the bacteria-bacteria and bacteria-host interactions. Many investigations have recognized these vesicles as vectors of HGT (Schwechheimer and Kuehn, 2015). Moreover, the luminal DNA is not affected by DNases within the OMVs, thus favoring the HGT of DNA and probably conferring extra merits to OMV-releasing microbes (Yaron et al., 2000; Kalra et al., 2016). HGT has been reported in *E. coli, Acinetobacter baumannii, Acinetobacter baylyi, Porphyromonas gingivalis, P. aeruginosa,* and *Thermus thermophilus* (Yaron et al., 2000; Kalra et al., 2016; Soler and Forterre, 2020). In *Acinetobacter*, OMVs can transfer the bla_{NDM-1} gene (Chatterjee et al., 2017). OMVs can spread carbapenem-resistant genes in *A. baumannii* strains (Rumbo et al.,

2011). In addition, OMVs are efficient vehicles for disseminating the $bla_{CTX\text{-}M\text{-}15}$ gene among *Enterobacteriaceae* (Bielaszewska et al., 2020).

OMVs derived from CR-HvKP strains promote the HGT of mobile virulence elements among bacteria, resulting in drug-resistant HvKP strains (Hua et al., 2022). Furthermore, Federica et al. have modified *K. pneumoniae* OMVs through genetic engineering, which is used as carriers for transmitting drug-resistant genes in microbial communities (Dell'Annunziata et al., 2021). However, it remains unclear whether CR-HvKP-derived OMVs can simultaneously transmit virulence and drug-resistant genes, resulting in the production of new CR-HvKP strains and the further spread of CR-HvKP. Our work first showed that CR-HvKP OMVs contained both virulence and drug-resistant genes. The CR-HvKP OMVs could transfer virulence and drug-resistant genes to the ATCC *K. pneumoniae* strain to produce CR-HvKP, resulting in the phenotype with increased drug resistance and virulence. In conclusion, our data revealed the simultaneous transmission of virulence and drug-resistant genes by CR-HvKP OMVs and we clarified the potential mechanism underlying the transmission of the CR-HvKP strain.

Materials and methods

Bacterial strains, antibiotic susceptibility, and growth conditions

The CR-HvKP strain NUHL30457, co-producing virulence and antimicrobial-resistant genes, was extracted from the wound of a burn patient with a severe nosocomial infection and a fatal outcome at a hospital in Jiangxi Province, China, in May 2017. The species was identified using biochemical testing with the VITEK 2 compact system (bioMérieux) and 16S rRNA sequencing. The capsular serotype was determined by the nucleotide sequence of the *wzc* gene. The isolate belonged to ST86 and K2 capsular serotype. The molecular characterization of NUHL30457 has been previously reported (Liu et al., 2019), and 42 antibiotic-resistant genes were identified in the NUHL30457 genome.

Genome statistics and comparative genomic analysis revealed that as a single chromosome of 5,302,595 bp in length, the NUHL30457 genome contained four plasmids: p30457-1(215,697 bp), p30457-2 (126,149 bp), p30457-3 (89,247 bp), and p30457-4 (49,215 bp). The genome sequence of *K. pneumoniae* NUHL30457 was submitted to GenBank under accession numbers CP026586.1 (NUHL30457 chromosome) and CP026587.1-CP026590.1 (plasmids p30457-1-p30457-4). p30457-1, a virulence plasmid containing various virulence genes, including *iroBCDN*, *iucABCD*, *rmpA*, *rmpA2*, and *iutA*, was located in the *IncHI1*/*IncFIB* plasmid p30457-1, while no antimicrobial-resistant gene was identified. The β-lactamase-resistant genes in the NUHL30457 genome were $bla_{SHV\text{-}1}$ in the chromosome, $bla_{CTX\text{-}M\text{-}65}$ and $bla_{KPC\text{-}2}$ in plasmid p30457-3, $bla_{NDM\text{-}1}$ in plasmid p30457-4, and $bla_{CTX\text{-}M\text{-}30}$ in plasmid p30457-2. The other antimicrobial-resistant genes on the chromosome were associated with MDR mechanisms, including efflux pumps, MDR tripartite systems, the MDR MAR locus, and the mdtABCD MDR cluster. MICs of the widely used antimicrobial agents were calculated using the microdilution method according to CLSI guidelines (document M100-S30). *Escherichia coli* ATCC 25922 and *K. pneumoniae* ATCC700603 were used as quality control reference strains for antimicrobial susceptibility testing.

For all experiments, CR-HvKP NUHL 30457 strain was grown in Luria-Bertani (LB) (Difco, Detroit, MI, United States) at 37°C with shaking (180 rpm) in the presence of meropenem (8 mg/l). *K. pneumoniae* ATCC700603 was used as the recipient for transformation experiments. The strain was also maintained in LB at 37°C with shaking.

Purification of OMVs

OMVs were purified from liquid cultures of the CR-HvKP strain NUHL30457 using a previously reported method with minor modifications (Chutkan et al., 2013; Li et al., 2018). First, 2.5 ml of overnight (O/N) bacterial culture was inoculated in 250 ml of LB supplemented with 8 mg/l imipenem. The bacterial inoculum was maintained at 37°C, and the culture was orbitally shaken (180 rpm) for 8–12 h until the OD600 nm of 1.0 was achieved. The culture medium was centrifuged at 11,000 × *g* for 20 min twice at 4°C in a 50-mL centrifugal tube, and the supernatant was collected. The low-speed supernatant was transferred into a new tube, followed by centrifugation at 13,000 × g for 20 min at 4°C, and the mid-speed supernatant was harvested. The supernatants were filtered using a polyethersulfone (PES) top filter with pore sizes of 0.45 μm and 0.22 μm (Millipore, Burlington, MA, United States) to deflect remaining bacteria and cell debris. Subsequently, 23 ml cell-free supernatant was added into an ultracentrifuge tube (Beckman Coulter NO. 355618), and the medium was carefully underlaid with 2 ml of 60% iodixanol using Hamilton blunt point 4-inch needles. Then the cell-free culture supernatant was centrifuged at ultra-high speed (150,000× g, centrifuge Optima XPN-100 Beckman Coulter and rotor 70Ti) at 4°C for 1.5 h. The blunt-end needles were carefully used to collect 3 ml from the bottom of the ultracentrifuge tubes containing 2 ml iodixanol cushion and 1 ml medium, resulting in a mixture of 40% iodixanol. OptiPrep (60% iodixanol; Sigma-Aldrich) density gradient solutions with 5, 10, and 20% density gradients were prepared and distributed into discrete 5–20% density gradient layers. Subsequently, 3 ml 40% iodixanol solution containing nanoparticles was placed at the bottom of the discontinuous gradient and centrifuged at 150,000 g for 16 h at 4°C with an SW40 Ti rotor. Subsequently, phosphate-buffered saline (PBS) was used to resuspend the OMV layer, the suspension was filtered through a 0.22-μm membrane filter, and 10 μl was transferred onto an LB plate to test the bacterial growth. Bacteria-negative preparations were adopted for further analyses. The isolated OMVs were preserved at-80°C.

Transmission electron microscopy

A transmission electron microscope (Hitachi H-7800, Japan) was used to examine the morphology and size of bacterial OMVs. Briefly, 20 μl of exosomal suspension, viral suspension, nanomaterial suspension, or other suspensions was dropped onto the copper grid with carbon film for 3–5 min. Then the excess liquid was absorbed using filter paper. Subsequently, 2% phosphotungstic acid was dropped on the copper grid to stain for 1–2 min, then the excess liquid was absorbed using filter paper, and the copper grid was dried at room temperature. The cuprum grids were examined under TEM, and images were acquired.

Size characterization of OMVs by dynamic light scattering

Vesicle diameter size (Z-ave) and polydispersity index (PDI) analysis were performed using Zetasizer NanoZS 90 (Malvern Instruments, Worcestershire, United Kingdom). For DLS, 40 μl of OMV aliquots were gently mixed and transferred to sterile cuvettes. PBS was adopted as the dispersing solvent. All analyses were carried out at 25°C, and each purification had three replicates. All measurements were carried out 12 times per sample. DLS data were analyzed using Zetasizer software (V 7.11) supplied by Malvern Panalytical (Malvern, United Kingdom).

Sodium dodecyl sulphate-polyacrylamide gel electrophoresis

The protein concentration of OMVs was determined using the Bradford assay (Bradford). Equal amounts of proteins were subjected to 12% SDS-PAGE. The gel was subjected to Coomassie brilliant blue staining. Protein molecular weight standards (size range 11–180 kDa, Bio-Rad).

OMV-mediated gene transfer in liquid cultures and PCR screening

For gene transfer experiments through OMVs from CR-HvKP strain NUHL30457, OMV preparations were exposed to 50 mg/l proteinase K to digest phage coats (if present) and 2 U of DNase I (Sigma-Aldrich) to eliminate extravehicular DNA (Rumbo et al., 2011; Bielaszewska et al., 2020). The mixtures were maintained at 37°C for 20 min, followed by DNase digestion (65°C, 10 min) (Bielaszewska et al., 2020).

OMV-mediated transformation experiments were conducted as previously described (Chatterjee et al., 2017). The recipient strain *K. pneumoniae* ATCC700603 was inoculated in LB broth and grown until the OD600 nm was 0.4. Cells were diluted in cold LB at a final concentration of 107 CFU/ml. Bacterial suspensions (60 μl) were incubated with 20 μg and 50 μg of CR-HvKP OMVs statically for 4 h at 37°C, followed by incubation for 4 h under orbital shaking (180 rpm) at 37°C. Next, 10 ml of fresh LB medium was supplemented to each bacterial suspension, followed by incubation overnight under orbital shaking (180 rpm) at 37°C. Two additional experiments were carried out to further validate whether OMVs mediated the plasmid transfer: (i) free plasmid and (ii) OMVs pre-lysed with Triton X-100. On the following day, the bacterial pellet was resuspended in 1 ml of LB broth, and 10-fold dilutions were incubated overnight on LB agar (to determine total bacterial counts) or LB agar containing 2 mg/l imipenem and 5 mg/l potassium tellurite to select transformants carrying both carbapenem gene and virulence gene. The frequency of OMV-mediated transfer was determined as the number of transformants (CFU/mL on LB agar containing imipenem and potassium tellurite) in the total bacterial count (CFU/mL on LB agar). For DNA extraction, vesicles were lysed at 100°C for 10 min. The acquisition of the carbapenem gene and virulence gene was confirmed using colony-PCR. A region of the carbapenem gene and virulence gene was amplified, and the amplicon was subjected to agarose gel electrophoresis. Table 1 lists all primer sequences.

TABLE 1 Sequences of primers.

Primer	Sequence, 5′ → 3′	Gene	Product size (bp)
KPC-Fw	CGTCTAGTTCTGCTGTCTTG	bla_{KPC}	798
KPC-Rev	CTTGTCATCCTTGTTAGGCG		
NDM-Fw	GGTTTGGCGATCTGGTTTTC	bla_{NDM}	621
NDM-Rev	CGGAATGGCTCATCACGATC		
rmpA-Fw	ACGACTTTCAAGAGAAATGA	*rmpA*	434
rmpA-Rev	CATAGATGTCATAATCACAC		
rmpA2-Fw	CTTTATGTGCAATAAGGATGTT	*rmpA2*	452
rmpA2-Rev	CCTCCTGGAGAGTAAGCATT		
SHV-Fw	GCCTTTATCGGCCTTCACTCAAG	bla_{SHV}	898
SHV-Rev	TTAGCGTTGCCAGTGCTCGATCA		
aac(6′)-Ib-cr-Fw	TTAGGCATCACTGCGTGTTC	*acc(6′)-Ib-cr*	508
aac(6′)-Ib-cr-Rev	TGACCTTGCGATGCTCTATG		
CTX-M-9 group-Fw	ATGGTGACAAAGAGAGTGCAAC	$bla_{CTX-M-9\ group}$	876
CTX-M-9 group-Rev	TTACAGCCCTTCGGCGATGATT		
iroB-Fw	ATCTCATCATCTACCCTCCGCTC	*iroB*	235
iorB-Rev	GGTTCGCCGTCGTTTTCAA		
iutA-Fw	ACCTGGGTTATCGAAAACGC	*iutA*	1,115
iutA-Rev	GATGTCATAGCCTGATTGC		
silS-Fw	CATAGCAAACCTTCCAGGC	*silS*	803
silS-Rev	ATCGGCAGAGAAATTGGC		

Resistance assessment of transformant

Antimicrobial susceptibility testing

Antimicrobial susceptibility testing was conducted for transformant strain using Vitek 2 automated systems following CLSI guidelines. Results were interpreted according to the Clinical and Laboratory Standards Institute (M100-S30).

mCIM and eCIM

The EDTA-CIM (eCIM) and modified carbapenem inactivation method (mCIM) were conducted as previously described (Tsai et al., 2020). The mCIM test could identify the bacteria that produced all carbapenemases, while the eCIM test was performed to differentiate MBL producers from the serine carbapenemases. To perform mCIM, 1 µl loopful of the isolates was emulsified in 2 ml of tryptone soy broth (TSB). Then, one meropenem disc was immersed in the suspension at 37°C for 4 h. The MHA plate was inoculated by 0.5-McFarland standard *E. coli* ATCC25922. Meropenem disc was removed from the suspension, and excess liquid was expelled. Meropenem disc was placed on the inoculated plate and incubated at 37°C for 24 h. An inhibition zone with a diameter of 6–15 mm or the appearance of pinpoint colonies within a 16–18 mm zone around the imipenem disc indicated the presence of carbapenemase. eCIM test was carried out when the mCIM test was positive. This test was done similarly, except that 20 µl of 0.5 M EDTA was added to the TSB after the test isolate was added. Then the meropenem disc was immersed. Meropenem discs of eCIM and mCIM tests were placed on one plate and analyzed simultaneously. An increase of ≥ 5 mm in the inhibition zone for eCIM versus mCIM was considered MBL positive. In contrast, no change in zone diameter or an increase of ≤ 4 mm indicated the presence of carbapenemase.

Virulence assessment of transformant

Serum killing assay

Serum bactericidal activity was determined as previously described (Liu et al., 2017). Briefly, serum was isolated from healthy controls and preserved at-80°C. An inoculum containing 106 CFU mid-log phase bacteria was reacted with 75% pooled human serum. The final mixture was maintained at 37°C, and viable counts were determined at 0, 1, 2, and 3 h. The reaction to serum killing in terms of viable counts was scored using six grades. Grade 1 refers to viable counts <10% of the inoculum after 1 and 2 h and < 0.1% after 3 h. Grade 2 refers to viable counts of 10–100% of the inoculum after 1 h and < 10% after 3 h. Grade 3 refers to viable counts that exceeded those of the inoculum after 1 h but <100% after 2 and 3 h. Grade 4 refers to viable counts >100% of the inoculum after both 1 and 2 h but <100% after 3 h. Grade 5 refers to viable counts >100% of the inoculums 1, 2, and 3 h, which was decreased during the third hour. Grade 6 refers to viable counts that exceeded those of the inoculum after 1, 2, and 3 h, and they were increased throughout this period. Each strain was tested at least three times, and the mean results were expressed as percent inoculums. The results were expressed as a percentage of inoculation, and the responses regarding viable counts were graded from 1 to 6 as previously described (Pomakova et al., 2012). A strain was categorized as serum sensitive (grade 1 or 2), intermediately sensitive (grade 3 or 4), or serum resistant (grade 5 or 6).

Assessment of the anti-biofilm effect

The anti-biofilm effect was assessed using a reported approach (Xu et al., 2022). Briefly, overnight cultures of OD600 nm of 0.1 were incubated with shaking (180 rpm). Cells adherent to the wells were subjected to staining using 0.1% crystal violet for 30 min. A Thermo Scientific Multiskan FC Microplate photometer was adopted to record the absorbance of each well at 540 nm. The ability of the test organisms to form biofilm was assessed using a reported approach (Extremina et al., 2011). The mean OD values of ATCC700603 and 700,603 transformants were determined, and the ODC was determined as the sum of the average OD of the negative control (ODNC) and three standard deviations of negative control (SDNC) [ODC = average ODNC + (3SDNC)]. The ability of strains to develop biofilms was divided into the following categories: OD% ODC = non biofilm producer; ODC < OD % 23ODC = weak biofilm producer; 23ODC < OD % 43ODC = moderate biofilm producer; 43ODC < OD = strong biofilm producer.

Galleria mellonella infection model

The Galleria mellonella infection model was adopted to assess toxicity for virulence testing (McLaughlin et al., 2014). A total of 10 larvae weighing between 250 and 350 mg (purchased from Tianjin Huiyude Biotech Company, Tianjin, China) were employed to explore the virulence level of each isolate. The insects were inoculated by injecting 1×10^6 CFU per 10 µl aliquot into the hemocoel *via* the rear left pro leg, followed by a recording of the survival rate every 12 h for 3 days. All experiments were carried out three times. The recent assessment of a range of *K. pneumoniae* isolates suggests that the parameters for the Galleria model to define hypervirulence are based on a calculation of the LD50 value (Shi et al., 2018). The HvKP strain NTUH-K2044 and *K. pneumoniae* strain ATCC700603 were used as controls of high and low virulence strains, respectively. Statistical analyses were performed and visualized with GraphPad Prism 8.0.

Mucoviscosity assay

The mucoviscosity of the capsule of the test strains was evaluated using a sedimentation assay (Palacios et al., 2018). Briefly, cultures were maintained in LB broth overnight and then subcultured to an OD600 nm of 0.2 in fresh medium, followed by incubation at 37°C. After 6 h, cultures were normalized to an OD600 nm of 1.0 ml^{-1} and centrifuged for 5 min at 1,000 g. The supernatant was gently removed without disturbing the pellet to measure the OD600 nm. A string test was performed by stretching the bacterial colonies on sheep blood agar plates using an inoculation loop (Shon et al., 2013). Results were presented as the mean and SD of three independent experiments. The analysis was performed with Prism 8.

Extraction and quantification of capsules

Uronic acid was purified and quantified using a reported method (Palacios et al., 2018). Briefly, 500 μl of bacterial culture grown for 6 h and tested in the microviscosity assay was mixed with 100 μl of 1% ZWITTERGENT 3–14 detergent in 100 mM citric acid, and the mixture was incubated at 50°C for 20 min. Cells were then pelleted, and 300 μl of the supernatant was added to 1.2 ml of absolute ethanol. The mixture was incubated at 4°C for 20 min, followed by centrifugation at the maximum speed for 5 min. The pellet was resuspended in 200 μl of distilled water, to which 1.2 ml of 12.5 mM sodium tetraborate in sulfuric acid was added. The mixture was incubated at 100°C for 5 min minutes and then left on ice for 10 min. Subsequently, 20 μl of 0.15% 3-phenylphenol in 0.5% NaOH was then added. The mixture was incubated at room temperature for 5 min, followed by the absorbance measurement at 520 nm. A standard curve of glucuronic acid was generated to determine the content of glucuronic acid, which was expressed as μg OD unit−1. Data were expressed as the mean and SD of three independent experiments. Statistical analysis was carried out with Prism 8.

Pulsed-field gel electrophoresis

Clonal relatedness was established using XbaI-PFGE (Taraka). The isolates sharing >80% similarity were defined as the same PFGE cluster (Tenover et al., 1995). The molecular marker was Salmonella serotype Braenderup strain H9812. DNA fragments were separated with a CHEF DR III apparatus (Bio-Rad; Richmond, CA, United States).

S1 nuclease-pulsed-field gel electrophoresis

S1-PFGE was conducted to determine the plasmid location of transformants (Du et al., 2020). Briefly, total DNA was embedded in agarose gel plugs. The plugs were digested with S1 nuclease (Taraka) at 37°C for 45 min and then separated by electrophoresis. S1-PFGE was performed to confirm the acquisition of plasmids by transformant strain.

Southern blotting hybridization

Southern blotting hybridization was performed to determine the plasmid location of bla_{NDM-1}-carrying plasmid and virulence plasmid (Du et al., 2020). Briefly, total DNA was embedded in agarose gel plugs. The plugs were digested with S1 nuclease (Taraka) at 37°C for 30 min and then separated by electrophoresis. Labeling of the probes and hybridized with the DIG-High Prime DNA Labeling and Detection Starter Kit II according to the manufacturer's instructions (Roche, Basle, Switzerland).

Growth curve measurements

Overnight cultures of transformant strains were diluted until an OD600 nm of 0.05 was achieved, and the diluents were incubated at 37°C for 12 h with vigorous aeration (180 pm). Growth curves in LB medium were performed in triplicate using standard protocols.

Plasmid stability experiments

Plasmid stability experiments were conducted as previously described (De Gelder et al., 2007). Briefly, the integrate plasmid-carrying 700,603 transformant was propagated by serial passaging for 14 days in antibiotic-free LB broth. Every 12 h, 5 μl of each culture was transferred to 5 ml of fresh LB broth. The proportion of plasmid-containing cells was determined every 24 h, and the number of colonies growing on antibiotic-free and antibiotic-containing plates was counted. Next, the integrate-carrying strain 700,603 transformants were passaged for 14 days under meropenem and potassium tellurite selection.

Results

Characterization of OMVs derived from CR-HvKP

A CR-HvKP strain (NUHL30457) (Liu et al., 2019) was grown in LB broth supplemented with 8 mg/l imipenem, and the culture supernatants were collected after 12 h of incubation. CR-HvKP OMVs were purified from culture supernatants by cushioned-density gradient ultracentrifugation (C-DGUC) and characterized concerning morphology and size. TEM showed that CR-HvKP-derived vesicles had spherical bilayered structures (Figure 1A), consistent with findings about OMVs from other Gram-negative bacteria (Dell'Annunziata et al., 2020). DLS showed that the diameters of CR-HvKP OMVs were 50–250 nm (median size of 132 nm). In contrast, we rarely found relatively large-sized vesicles with diameters >200 nm and small-sized vesicles with diameters of 50 nm (Figure 1C). This finding suggested that CR-HvKP produced and secreted OMVs into the extracellular milieu during *in vitro* culture. The protein content of OMVs was 502 ± 26 μg/ml using the Bradford assay. The protein sample of NUHL30457 OMVs was subjected to SDS-PAGE, followed by Coomassie brilliant blue staining. In the 35–48 kDa range, two major bands were detected in the OMVs (Figure 1B), which was the marker location for the ompA protein. We did not find bacterial growth on the LA plate, suggesting that the OMVs were pure. Meanwhile, no bacteria were found under the microscope.

CR-HvKP OMVs are enriched in bacterial genetic elements

Polymerase chain reaction (PCR) results showed that carbapenemases genes and virulence genes were packaged into OMVs of NUHL30457, indicating that OMVs could contain the

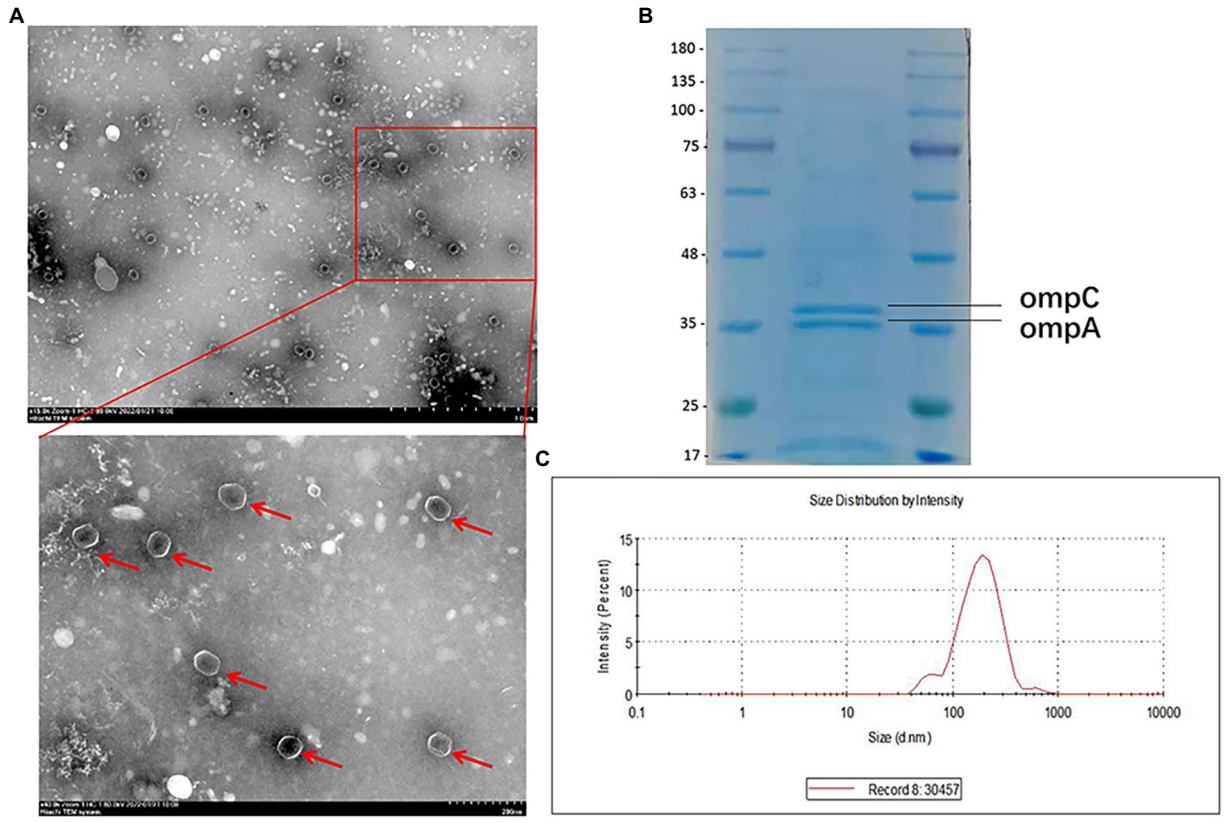

FIGURE 1
Characterization of OMVs derived from CR-HvKP. **(A)** Transmission electron microscopy (TEM) showed that CR-HvKP-derived vesicles had spherical bilayered structures. OMVS marked with red arrow. **(B)** Coomassie-stained SDS-PAGE (12%) protein profiles of CR-HvKP-derived vesicles. In the 35–48kDa range, two major bands were detected in the OMVs. The molecular mass marker (MW) is expressed in kilodaltons (kDa). **(C)** DLS intensity-weighed distribution of OMVs derived from CRHvKP-derived vesicles.

genetic information of strains and various virulence and drug-resistant genes (Table 2).

CR-HvKP OMVs mediate virulence and antimicrobial-resistant gene transfer to *Klebsiella pneumoniae* ATCC 700603 strain

Transformation experiments were performed by isolating OMVs from CR-HvKP NUHL30457 to determine whether CR-HvKP OMVs could transfer virulence and antimicrobial-resistant genes. The transformation experiments were successful in *K. pneumoniae* ATCC 700603 using different amounts (20 and 50 μg) of purified OMVs (Table 3; Figure 2). After 24 h, treated cells were plated on LB agar containing 2 mg/l imipenem and 5 mg/l potassium tellurite to detect the transformant's resistance marker in the recipient bacteria. No transformants were found when the free plasmid isolated from the clinical strain CR-HvKP NUHL30457 was incubated with the ATCC 700603 strain or with different amounts (20 and 50 μg) of OMVs pre-lysed with Triton X-100. Colonies were obtained on LB agar plates at each dose of purified OMVs when ATCC700603 was transformed after incubation with OMVs purified from *K. pneumoniae* NUHL30457 (Table 3). Colony-PCR achieved the amplification of bla_{NDM-1} and *rmpA2* from transformants (Figure 3). One of the successful transformants was selected for further experiments.

Characterization of ATCC700603 transformant

CR-HvKP OMVs enhance the antimicrobial resistance-associated features of *Klebsiella pneumoniae* ATCC strains

We evaluated the phenotypic effect correlated to the genotypic resistance through antibiotic susceptibility testing. Table 4 shows the detailed antimicrobial resistance profiles. The antibiotic susceptibility test showed that the 700,603 transformant was resistant to carbapenem drugs, such as imipenem, ertapenem, and meropenem. The EDTA-CIM (eCIM) and modified carbapenem inactivation method (mCIM) were used to demonstrate that the acquired resistance was associated with the plasmid containing the carbapenemase gene. The inhibition zone diameter of mCIM was 6 mm,

TABLE 2 Presence of antibiotic resistance and virulence genes in OMVs of NUHL30457 strain and 700,603 transformant.

Gene	Results of PCRs performed with the following templates					
	PK/DNase+ OMVs intact[a]	OMVs Lysed with TritonX-100 + [b]	Purified DNA Of Omvs	700,603 transformant	Total DNA 30457	Total DNA 700603
bla_{KPC}	+[c]	-[c]	+	+	+	–
bla_{NDM}	+	–	+	+	+	–
rmpA	–	–	–	–	+	–
rmpA2	+	–	+	+	+	–
bla_{SHV}	–	–	–	–	+	–
acc(6′)-Ib	–	–	–	–	+	–
$bla_{CTX\text{-}M\text{-}9\ group}$	+	–	+	+	+	–
iroB	+	–	+	+	+	–
iutA	+	–	+	+	+	–
silS	+	–	+	+	+	–

a, OMVs treated by PK/DNase (to remove phage coats and extravesicular DNA) and left intact. b, OMVs lysed with Triton X-100. + indicates presence of amplicon; – indicates absence of amplicon.

TABLE 3 Different treatments of vesicle-mediated transformation.

Group	treatment	Amount (ug)	transformation		
			cfu/ml of transformants	Transformation frequency	Percentage of transformants
1	OMVs previously lysed with Triton X-100	20	0	0	0
2	OMVs previously lysed with Triton X-100	50	0	0	0
3	the free plasmid of 30,457	6	0	0	0
4	OMVs treated with DNase I and proteinase K	20	$[(2.8 \pm 0.03)x10^{8}]^{a}$	$[(1.4 \pm 0.02)x10^{-4}]^{a}$	$[(1.4 \pm 0.03)x10^{-2}]^{a}$
5	OMVs treated with DNase I and proteinase K	50	$[(3.79 \pm 0.02)x10^{8}]^{a}$	$[(7.58 \pm 0.05)x10^{-4}]^{a}$	$[(7.58 \pm 0.05)x10^{-2}]^{a}$

The data were expressed as mean ± standard deviation (SD) of three measurements; Means with lowercase letter "a" in the same column are significantly different at $p < 0.05$.

indicating the presence of carbapenemases. Meropenem discs of eCIM and mCIM tests were placed on one plate and analyzed simultaneously. The inhibition zone diameter of eCIM was 19 mm, which was MBL positive (Figure 4). The results showed that the transformant exhibited drug sensitivity and phenotype resistance to carbapenems.

CR-HvKP OMVs improve the virulence level of *Klebsiella pneumoniae* ATCC strains

Mucoviscosity assay, uronic acid production, serum killing assay, anti-biofilm effect, and Galleria mellonella infection model were carried out on donors, receptors, and transformants to verify whether the virulence level was changed.

1. To verify whether the transformant obtained the virulence gene, the expression of high viscosity phenotype was detected in the transformant. The results showed that acquisition of CR-HvKP OMVs by the ATCC 700603 strain significantly increased microviscosity and production of capsular polysaccharide (uronic acid) to a level similar to the CR-HvKP NUHL30457 strains (Figures 5A,B). In addition, string tests were favorable compared with the recipient strains, showing a markedly increased length by stretching colonies of 700,603 transformant strains (Figure 5C).
2. Serum resistance level of the CR-HvKP NUHL30457 strain, ATCC 700603 strain, and 700,603 transformant strain. The CR-HvKP NUHL30457 strain, HvKP BD2411, and 700,603 transformant strain exhibited grade 6 and grade 5 responses, respectively, whereas ATCC 700603 exhibited a grade 1 response (Figure 6A).
3. Biofilm plays a primary role in expressing the resistance and virulence phenotypes of CR-HvKP. Therefore, we investigated the ability of the 700,603 transformant strain and ATCC 700603 to form biofilm by crystal violet assay. The cut-off value (ODC) was 0.12, and the final absorbance of 700,603 T and ATCC700603 biofilm was 0.4293 ± 0.0166 and 0.2470 ± 0.0028, respectively (Figure 6B). Moreover, the two tested strains (ODtest) were considered moderate biofilm producers (2*ODC < ODtest % 4*ODC) after 24 h of incubation (Extremina et al., 2011).
4. The Galleria mellonella model showed that the 700,603 transformant strain had toxicity for virulence testing. The virulence of 700,603 T was markedly different compared

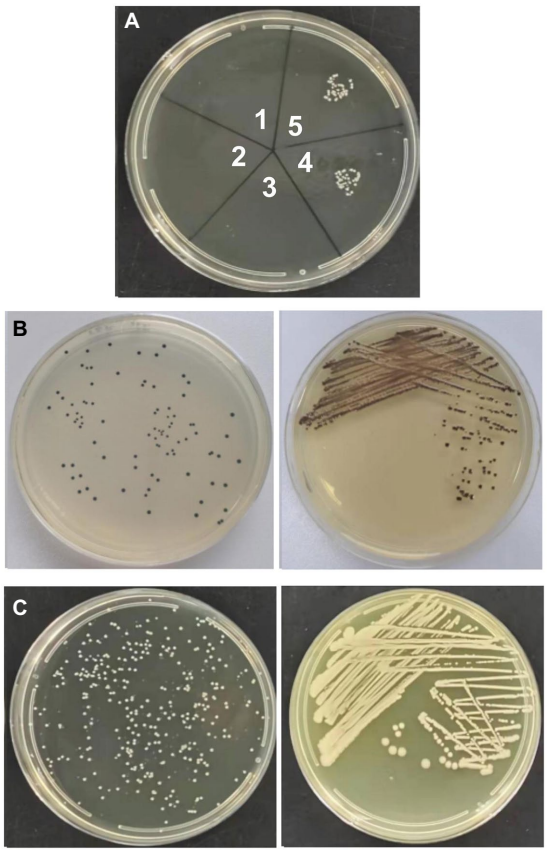

FIGURE 2
Vesicle-mediated transformation. **(A)** transformants in LB plate with 2mg/l imipenem and 5mg/l potassium tellurite. Note: 1. 20ug of CR-HvKP-OMVs previously lysed with Triton X-100; 2. 50ug of CR-HvKP-OMVs previously lysed with Triton X-100; 3. the free plasmid of NUHL30457; 4. 20ug of CR-HvKP-OMVs treated with DNase I and proteinase K; 5. 50ug of CR-HvKP-OMVs treated with DNase I and proteinase K. **(B)** transformants in LB plate with 5mg/l potassium Tellurite. **(C)** transformants in LB plate with 2mg/l Imipenem.

with ATCC 700603 ($p < 0.5$, by log-rank test) (Figure 6C). The results showed that the transformant was a highly pathogenic phenotype.

PCR and S1-PFGE analysis of 700,603 transformant strain

PCR confirmed the presence of virulence and antimicrobial-resistant genes in 700,603 transformants. Some genes were transferred to the *K. pneumoniae* ATCC 700603 recipient cells (Table 2). To determine whether CR-HvKP OMVs transferred plasmids to transformants, we compared the plasmid profiles of the CR-HvKP NUHL30457, ATCC 700603, and 700,603 transformants. The PFGE fingerprints showed that 700,603 and 700,603 t are from the same strain and have similar homologous structures (Figure 7A). The S1-PFGE results demonstrated that 700,603 T harbored two plasmids (Figure 7B). Compared with the plasmid profiles of the ATCC700603, the positions of the two plasmids of 700,603 t were changed. The possible cause of this change was the acquisition of virulence and drug resistance genes. Southern blotting experiments confirmed that the two plasmids of the transformant contained bla_{NDM-1} and *rmpA2* (Figures 7C,D). Combining S1-PFGE and Southern blotting results, the plasmid of the transformant contained both drug-resistant and virulence genes, revealing that OMVs of the CR-HVKP strain could transfer virulence and drug-resistant genes.

Growth curve measurements and stability of plasmids in 700,603 transformant

Based on the bacterial growth curves, we found that the 700,603 transformants grew slowly compared with ATCC700603, which might be attributed to their plasmids (Figure 8A).

To evaluate the stability of plasmids in the 700,603 transformants, we propagated the plasmid harboring 700,603 in antibiotic-free LB broth for 14 days. However, the plasmid was significantly unstable because plasmid was rapidly degraded within 4 days (Figure 8B).

Given that the transformant was unlikely to persist in an antibiotic-free medium, we conducted a serial passaging experiment in LB broth containing meropenem (2 mg/l) and potassium tellurite (5 mg/l) for 14 days. After evolution under positive selection, we analyzed 32 randomly selected clones in an LB plate containing meropenem (2 mg/l) and potassium tellurite (5 mg/l) for 14 consecutive days. Under antibiotic pressure, the plasmid became stable in host bacteria (Figure 8B). However, it still had some limitations. First, the structural diversity of the plasmid under different antibiotic pressures needed to be further explored. Second, the host species used in this study were limited. Third, the underlying mechanism leading to plasmid stability under positive selection still requires further investigation.

These results supported that the transformants had drug resistance-related and highly pathogenic phenotypes. Furthermore, these findings suggested that CR-HvKP OMVs could effectively transfer virulence and drug-resistant genes to the ATCC *K. pneumoniae* strain.

Discussion

CR-HvKP has been widely reported in Asian countries, severely threatening public health (Zhang et al., 2016; Mohammad Ali Tabrizi et al., 2018). Moreover, the rapidly increasing isolation rate of carbapenem-resistant *K. pneumoniae* worldwide (Rumbo et al., 2011) has brought great difficulties in controlling clinical infection (Schwechheimer and Kuehn, 2015). The successful persistence of carbapenem-resistant *K. pneumoniae* in clinical settings may be attributed to antimicrobial resistance and virulence. The continuous evolution of plasmids of hypervirulence or carbapenem resistance has led to the emergence of hypervirulent and carbapenem-resistant *K. pneumoniae*.

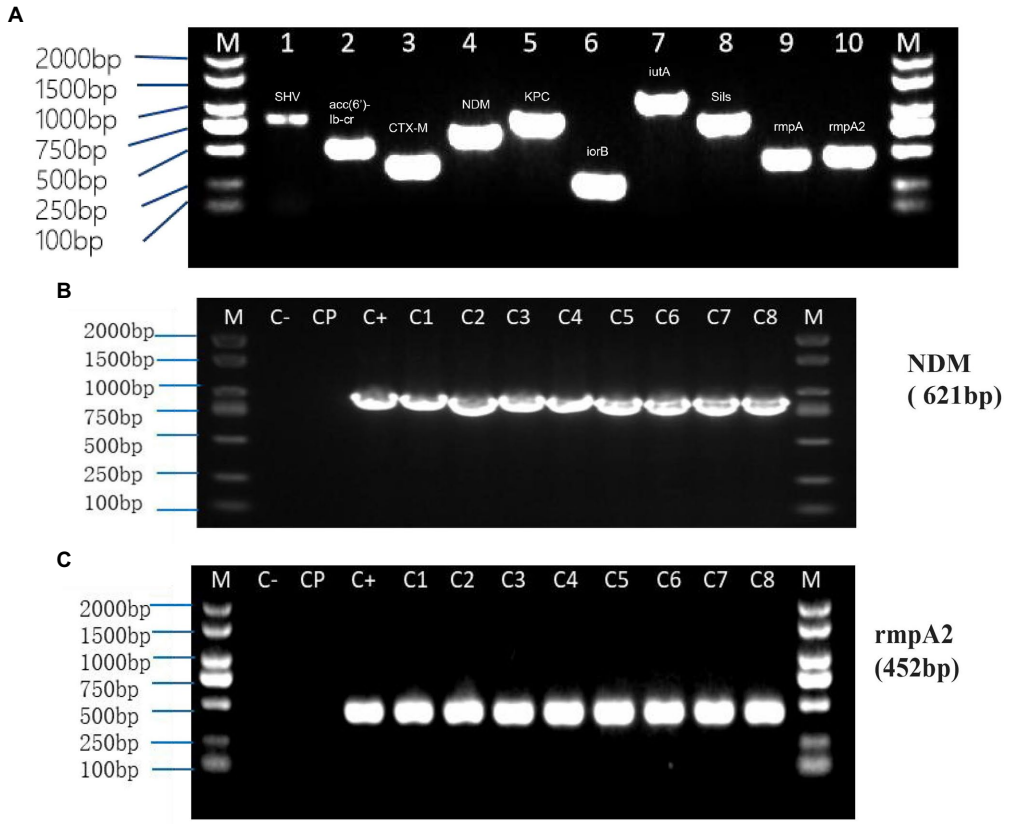

FIGURE 3
PCR from NUHL30457 omvs **(A)** and Colony-PCR from recipient cells treated with NUHL30457 omvs **(B,C)**. **(A)** NUHL30457omvs pcr, DNA gel showed PCR products with expected lengths. M: 2000bp size marker1.bla_{SHV} product~898bp 2. *acc(6')-Ib-cr* product~508bp 3.bla_{CTX-M} product~355bp 4. bla_{NDM} product~621bp5.bla_{KPC} product~798bp 6. *iroB* product~235bp7.*iutA* product~1,115bp 8. *silS* product~803bp9.*rmpA* product~434bp 10. *rmpA2* product~452bp **(B,C)**: Colony-PCR from recipient cells treated with NUHL30457 omvs，DNA gel showed PCR products with expected lengths. NOTE: M:2000bp size marker Colony-PCR (C_{1-8}), Control water (C−), untreated bacteria (Cp), Control water (C−), and untreated bacteria (Cp) did not show amplification.

TABLE 4 Antimicrobial resistance profiles.

Agent	NUHL30457		700,603 T		700,603	
	MIC	Interpretation	MIC	Interpretation	MIC	Interpretation
Ampicillin	≥256	R	≥256	R	≥256	R
Piperacillin/tazobactam	≥128/4	R	≥128/4	R	32/4	I
Ceftazidime	≥256	R	≥64	R	32	R
Cefepime	≥256	R	≥32	R	16	R
Aztreonam	256	R	64	R	32	R
Imipenem	≥64	R	≥64	R	≤1	S
Meropenem	≥64	R	4	R	≤1	S
Amikacin	≥256	R	≤2	S	≤ 1	S
Ciprofloxacin	≥32	R	≤0.25	S	≤0.25	S
Levofloxacin	≥32	R	1	S	≤ 1	S
Trimethoprim/sulfamethoxazole	≥4/76	R	≤2/38	S	≤2/38	S
Tigecycline	≤1	S	≤1	S	≤1	S

HGT is vital in promoting bacterial evolution, adaptation to environmental changes, and acquiring new metabolic capabilities (Daubin and Szöllősi, 2016). OMVs are a new mechanism to mediate the transmission of drug-resistant genes among bacteria (Husnik and McCutcheon, 2018; Soler and Forterre, 2020). Earlier reports have shown that DNA is incorporated into the lumen by

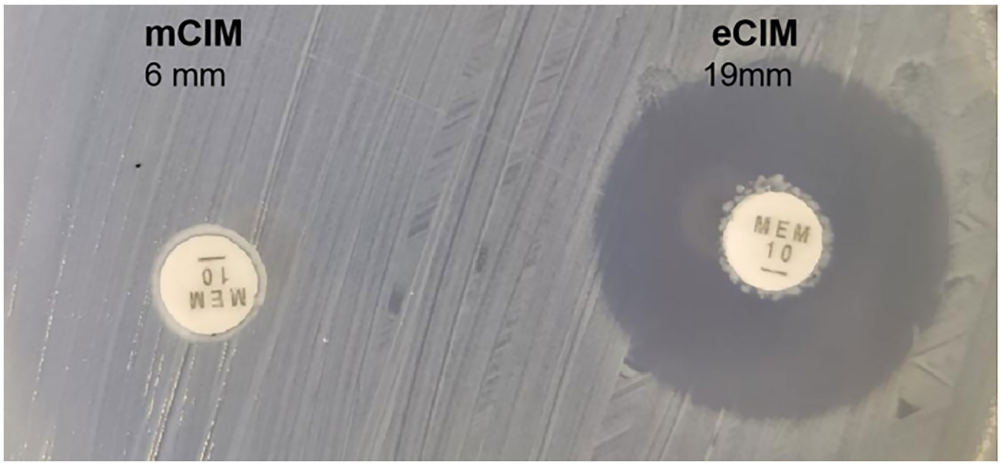

FIGURE 4
Meropenem discs of mCIM and eCIM tests of transformants. Notes:left: the inhibition zone diameter of mCIM was 6mm; right: the inhibition zone diameter of eCIM was 19mm.

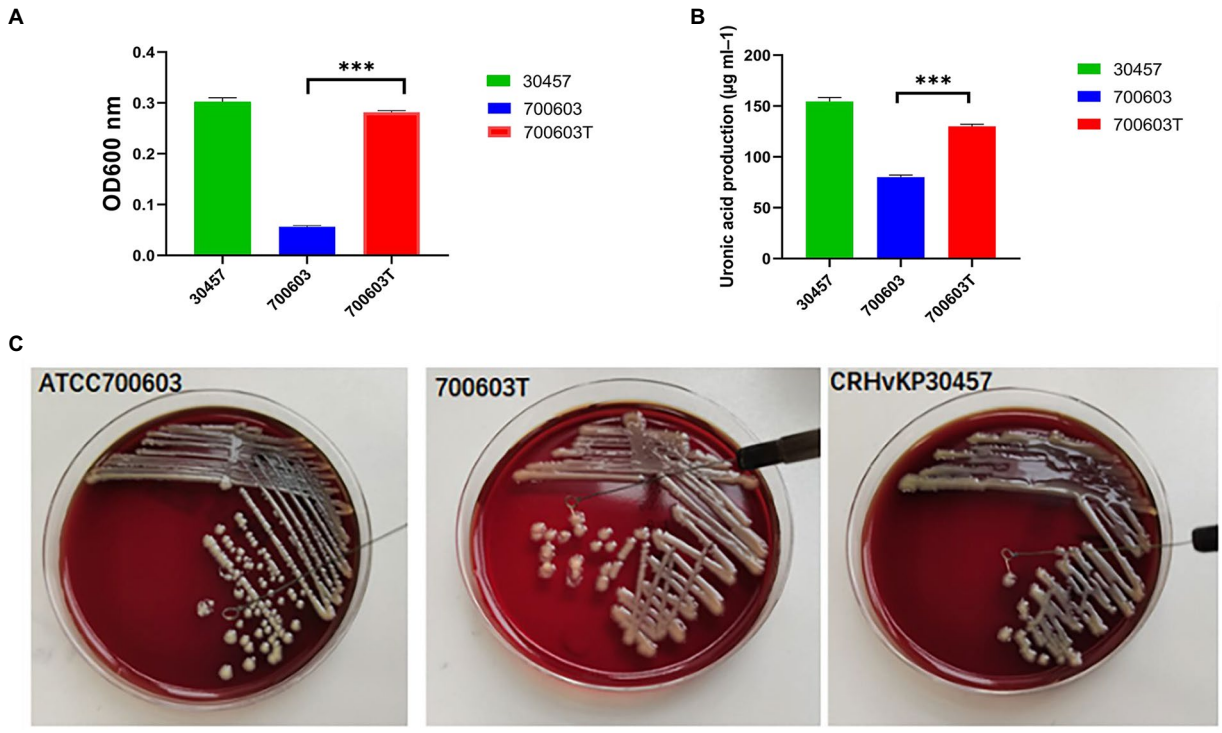

FIGURE 5
Mucoviscosity **(A)**, uronic acid production **(B)**, and string tests **(C)** of the 700,603 transformant strain.Two-way ANOVA tests were performed for statistical analysis. ***, $p<0.001$.

OMVs and then transported to recipient cells (Rumbo et al., 2011; Kalra et al., 2016). Recent findings demonstrate that OMVs secreted by *K. pneumoniae* have been involved in HGT, allowing the spread of resistance genes in microbial communities (Wang et al., 2019). Hua et al. have demonstrated that hvKp-OMVs facilitate virulence genes transfer, allowing an increased virulence level of ESBL-producing cKp (Hua et al., 2022). A recent and detailed study has shown that OMVs derived from *K. pneumoniae* can efficiently deliver virulence plasmids into other *K. pneumoniae* strains, even carbapenem-resistant strains (Wang et al., 2022). Recently, the continuous evolution of plasmids of hypervirulence or carbapenem resistance has led to the emergence of CR-HvKP

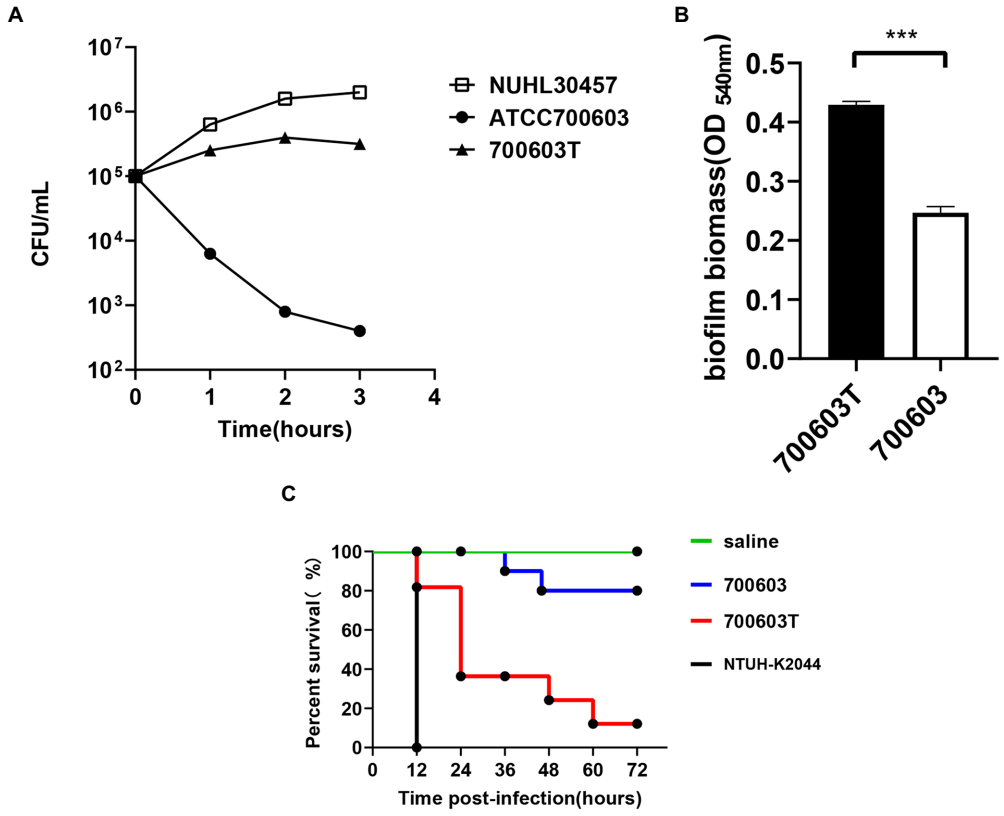

FIGURE 6
Virulence characteristics of transformants. **(A)** The serum resistance level of the 700,603 transformant strain. **(B)** The ability of the 700,603 transformant strain to form biofilm was evaluated by crystal violet assay. **(C)** The Mann–Whitney test was used for statistical analyses.***, $p<0.001$. Virulence potential of the 700,603 transformant strain in a *Galleria mellonella* infection model.

(Gu et al., 2018; Tian et al., 2021). In contrast, it remains unclear whether virulence and drug-resistant plasmids can be co-transmitted through OMVs. Our present study provided experimental evidence on the co-delivery of virulence and drug-resistant genes by CR-HVKP OMVs.

The CP-hvKP strain NUHL30457 was collected from a burn patient and exhibited three typical features of hvKP: hypermucoviscosity phenotype, serum resistance, and antiphagocytosis (Liu et al., 2019). In addition, WGS has demonstrated that four complete plasmids are obtained (Liu et al., 2019).

Firstly, OMVs were isolated from CR-HvKP NUHL30457 (K2, ST86). TEM and DLS analyses revealed the spherical morphology of the vesicles, which was consistent with earlier findings, with a similar diameter to the OMVs derived from *K. pneumoniae* ATCC 10031 (Dell'Annunziata et al., 2020).

Secondly, our study demonstrated that CR-HvKP delivered genetic material, incorporated DNA within the OMVs, and protected it from degradation by extracellular exonucleases. Our present findings and some early investigations (Rumbo et al., 2011; Bielaszewska et al., 2020; Hua et al., 2022) showed that the DNA inside OMVs was not affected by nucleases, which might be present in the environment or the host tissues. This process favors the interflow of genetic material or the horizontal transfer of DNA, thus probably conferring extra merits for gene dissemination to those OMV-releasing microorganisms.

Thirdly, the CR-HvKP NUHL30457 strain plasmids harbored blakpc-2, blaNDM-1 genes, and the virulence plasmid pLVPK carried rmpA2 genes. However, such virulence plasmids cannot self-transfer due to the absence of transfer modules (Liu et al., 2019). Therefore, we performed transformation experiments by isolating OMVs from CR-HvKP NUHL30457 to determine whether CR-HvKP OMVs could co-transfer virulence and antimicrobial-resistant plasmids.

The vesicular lumen DNA was delivered to the recipient cells after determining the presence of virulence and carbapenem-resistant genes in the CR-HvKP OMVs. After contact with OMVs, the recipient cell *K. pneumoniae* ATCC strain acquired and expressed resistance to carbapenem and potassium tellurite, proving the OMVs' ability to carry both virulence and antimicrobial-resistant genes and promoting intraspecies HGT. The transformation did not occur when cells were incubated with the free plasmid, suggesting that vesicles could represent a physiological mechanism that exceeded environmental limits (exonuclease degradation, dilution of gene material, and

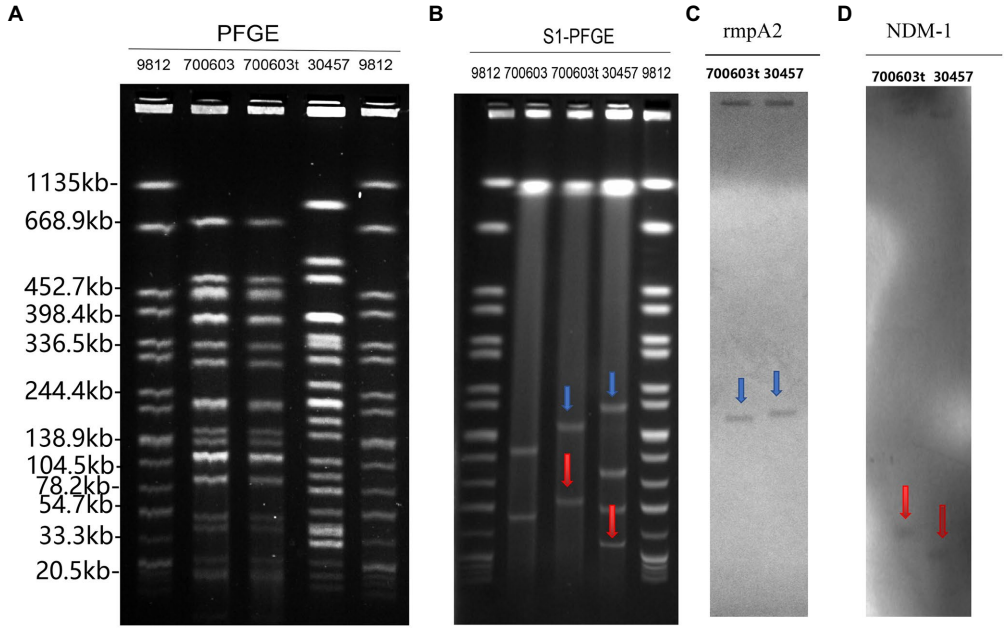

FIGURE 7
PFGE, *S1*-PFGE and Southern hybridization analysis of 700,603 transformant strain **(A)** PFGE, Clonal relatedness was established using *XbaI*-PFGE. **(B)** *S1*-PFGE: *S1* nuclease digestion of genomic DNA of *K. pneumoniae* strains was followed by PFGE. Plasmid bands are shown as linearized fragments on the gel. **(C)** Southern blot hybridization of the marker gene (rmpA2) of the virulence plasmid, marked with a blue arrow. **(D)** Southern blot hybridization of bla_{NDM-1} gene, marked with a red arrow. Lane 9,812, reference standard strain Salmonella serotype Braenderup H9812 restricted with *XbaI*.

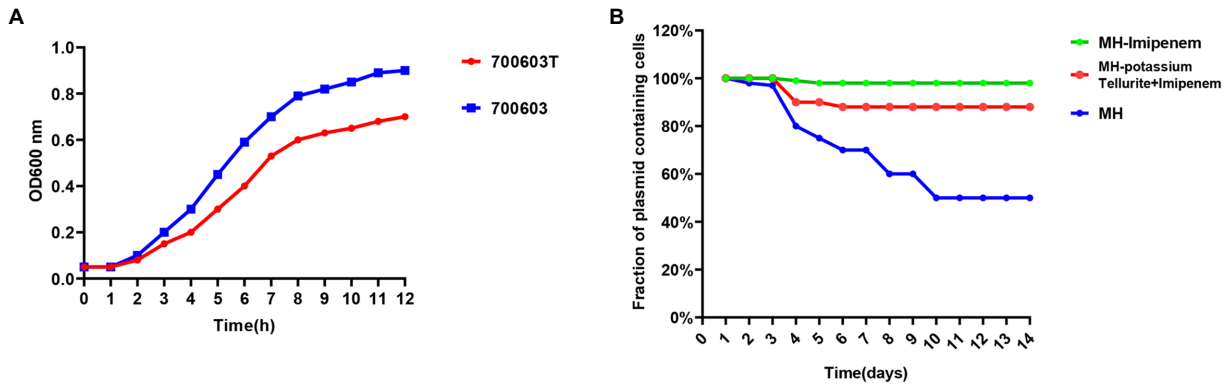

FIGURE 8
Growth curve measurements and stability of plasmids in 700,603 transformant. **(A)** Growth curves of the700603 transformant strain; **(B)** stability of plasmids in the 700,603 transformant strain in antibiotic and antibiotic-free medium.

long-distance transfer) and was related to the donor/recipient cell (state of competence, high vesicle-OM affinity, and correlation phylogenetics) (Dell'Annunziata et al., 2021).

Importantly, S1-PFGE and Southern hybridization analysis of the 700,603 transformant strain showed that the transformant contained both drug-resistant and virulence plasmids. Under antibiotic pressure, the plasmid became stable in the host bacteria. Furthermore, it revealed that OMVs of the CR-HvKP strain could transfer virulence and drug-resistant genes *via* plasmids. Our results supported that the transformants had drug resistance-related and highly pathogenic phenotypes. Furthermore, it suggested that CR-HvKP OMVs could simultaneously stably and effectively co-transfer virulence and drug-resistant genes to ATCC *K. pneumoniae*.

The emergence of CR-HvKP causes high mortality in clinical patients, suggesting that it is urgently necessary to clarify the molecular mechanism underlying the rapid global dissemination. However, there were several main limitations of this study. First, it was unclear what was the specific content of CR-HvKP OMVs. Second, the particular situation of its proteomics and nucleiomics was unknown. Third, it remained undetermined whether changing the structure of vesicles could

block this transmission mode. These questions will be investigated in future studies.

The innovation of our article is that we selected a strain of CRHVKP as the research object. The strain and secreted-OMVs carried both virulence plasmid and drug-resistant plasmid. Through the conjugation experiment of OMVs, we screened the transformant CRHVKP on the plate of imipenem plus potassium tellurite. It was proved that our CRHVKP-OMVs transmitted both virulence plasmid and drug-resistant plasmid, transforming the sensitive KP strain into the CRHVKP strain. In summary, the formation mechanism of CRHVKP is expounded from various perspectives. Studies show that HVKP-OMVs can transfer virulence plasmids to CRKP strains to form CRHVKP (Wang et al., 2022). It can also transfer virulence and drug-resistant plasmids to sensitive KP strains from CRHVKP-OMVs to form CRHVKP. In the present study, we aimed to clarify the role of CRHvKP-OMVs in transmitting CR-HvKP among *K. pneumoniae*. Collectively, our findings provided valuable insights into the evolution of CR-HvKP.

Data availability statement

The original contributions presented in the study are included in the article/supplementary material, further inquiries can be directed to the corresponding authors.

Author contributions

WZ and YL designed the study. PiL and WaL performed the experiments. T-XX, YJ, LF, and PeL performed the analysis. PeL, D-DW, and WeL drafted the manuscript. All authors contributed to the article and approved the submitted version.

Funding

Financial support was provided by the National Natural Science Foundation of China (82102411 and 81860368), the Natural Science foundation of Jiangxi Province (20202ACBL206025 and 20202ACBL206023), Jiangxi Province Double Thousand Plan scientific and technological innovation High-end Talent Project Research projects (jsxq2019201102), and The first affiliated hospital of Nanchang University Young Talents Scientific Research Breeding Fund (YFYPY202114).

Conflict of interest

The authors declare that the research was conducted in the absence of any commercial or financial relationships that could be construed as a potential conflict of interest.

Publisher's note

All claims expressed in this article are solely those of the authors and do not necessarily represent those of their affiliated organizations, or those of the publisher, the editors and the reviewers. Any product that may be evaluated in this article, or claim that may be made by its manufacturer, is not guaranteed or endorsed by the publisher.

References

Bielaszewska, M., Daniel, O., Karch, H., and Mellmann, A. (2020). Dissemination of the $Bla_{ctx\text{-}M\text{-}15}$ gene among Enterobacteriaceae via outer membrane vesicles. *J. Antimicrob. Chemother.* 75, 2442–2451. doi: 10.1093/jac/dkaa214

Chatterjee, S., Mondal, A., Mitra, S., and Basu, S. (2017). Acinetobacter Baumannii transfers the $Bla_{ndm\text{-}1}$ gene via outer membrane vesicles. *J. Antimicrob. Chemother.* 72, 2201–2207. doi: 10.1093/jac/dkx131

Chutkan, H., Macdonald, I., Manning, A., and Kuehn, M. J. (2013). Quantitative and qualitative preparations of bacterial outer membrane vesicles. *Methods Mol. Biol.* 966, 259–272. doi: 10.1007/978-1-62703-245-2_16

Daubin, V., and Szöllősi, G. J. (2016). Horizontal gene transfer and the history of life. *Cold Spring Harb. Perspect. Biol.* 8:A018036. doi: 10.1101/cshperspect.a018036

De Gelder, L., Ponciano, J. M., Joyce, P., and Top, E. M. (2007). Stability of a promiscuous plasmid in different hosts: no guarantee for a Long-term relationship. *Microbiology (Reading)* 153, 452–463. doi: 10.1099/mic.0.2006/001784-0

Dell'annunziata, F., Cp, I., Dell'aversana, C., Greco, G., Coppola, A., Martora, F., et al. (2020). Outer membrane vesicles derived from *Klebsiella Pneumoniae* influence the Mirna expression profile in human bronchial epithelial Beas-2b cells. *Microorganisms* 8:1985. doi: 10.3390/microorganisms8121985

Dell'annunziata, F., Dell'aversana, C., Doti, N., Donadio, G., Dal Piaz, F., Izzo, V., et al. (2021). Outer membrane vesicles derived from *Klebsiella Pneumoniae* are a driving force for horizontal gene transfer. *Int. J. Mol. Sci.* 22:8732. doi: 10.3390/ijms22168732

Du, F. L., Huang, Q. S., Wei, D. D., Mei, Y. F., Long, D., Liao, W. J., et al. (2020). Prevalence of Carbapenem-resistant *Klebsiella Pneumoniae* co-Harboring Bla_{kpc}-carrying plasmid and Plvpk-like virulence plasmid in bloodstream infections. *Front. Cell. Infect. Microbiol.* 10:556654. doi: 10.3389/fcimb.2020.556654

Extremina, C. I., Costa, L., Aguiar, A. I., Peixe, L., and Fonseca, A. P. (2011). Optimization of processing conditions for the quantification of enterococci biofilms using microtitre-plates. *J. Microbiol. Methods* 84, 167–173. doi: 10.1016/j.mimet.2010.11.007

Gu, D., Dong, N., Zheng, Z., Lin, D., Huang, M., Wang, L., et al. (2018). A fatal outbreak of St11 Carbapenem-resistant Hypervirulent *Klebsiella Pneumoniae* in a Chinese hospital: a molecular epidemiological study. *Lancet Infect. Dis.* 18, 37–46. doi: 10.1016/S1473-3099(17)30489-9

Hua, Y., Wang, J., Huang, M., Huang, Y., Zhang, R., Bu, F., et al. (2022). Outer membrane vesicles-transmitted virulence genes mediate the emergence of new antimicrobial-resistant Hypervirulent *Klebsiella Pneumoniae*. *Emerg. Microb. Infect.* 11, 1281–1292. doi: 10.1080/22221751.2022.2065935

Husnik, F., and Mccutcheon, J. P. (2018). Functional horizontal gene transfer from bacteria to eukaryotes. *Nat. Rev. Microbiol.* 16, 67–79. doi: 10.1038/nrmicro.2017.137

Kalra, H., Drummen, G. P., and Mathivanan, S. (2016). Focus on extracellular vesicles: introducing the next small big thing. *Int. J. Mol. Sci.* 17:170. doi: 10.3390/ijms17020170

Lan, P., Jiang, Y., Zhou, J., and Yu, Y. (2021). A global perspective on the convergence of Hypervirulence and Carbapenem resistance in *Klebsiella Pneumoniae*. *J. Glob. Antimicrob. Resist.* 25, 26–34. doi: 10.1016/j.jgar.2021.02.020

Lee, C. R., Lee, J. H., Park, K. S., Jeon, J. H., Kim, Y. B., Cha, C. J., et al. (2017). Antimicrobial resistance of Hypervirulent *Klebsiella Pneumoniae*: epidemiology,

Hypervirulence-associated determinants, and resistance mechanisms. *Front. Cell. Infect. Microbiol.* 7:483. doi: 10.3389/Fcimb.2017.00483

Li, K., Wong, D. K., Hong, K. Y., and Raffai, R. L. (2018). Cushioned-density gradient ultracentrifugation (C-Dguc): a refined and high performance method for the isolation, characterization, and use of Exosomes. *Methods Mol. Biol.* 1740, 69–83. doi: 10.1007/978-1-4939-7652-2_7

Liu, Y., Liu, P. P., Wang, L. H., Wei, D. D., Wan, L. G., and Zhang, W. (2017). Capsular polysaccharide types and virulence-related traits of epidemic Kpc-producing *Klebsiella Pneumoniae* isolates in a Chinese university hospital. *Microb. Drug Resist.* 23, 901–907. doi: 10.1089/mdr.2016.0222

Liu, Y., Long, D., Xiang, T. X., Du, F. L., Wei, D. D., Wan, L. G., et al. (2019). Whole genome assembly and functional portrait of Hypervirulent extensively drug-resistant Ndm-1 and Kpc-2 co-producing *Klebsiella Pneumoniae* of capsular serotype K2 and St86. *J. Antimicrob. Chemother.* 74, 1233–1240. doi: 10.1093/jac/dkz023

Mclaughlin, M. M., Advincula, M. R., Malczynski, M., Barajas, G., Qi, C., and Scheetz, M. H. (2014). Quantifying the clinical virulence of *Klebsiella Pneumoniae* producing Carbapenemase *Klebsiella Pneumoniae* with a galleria Mellonella model and a pilot study to translate to patient outcomes. *BMC Infect. Dis.* 14:31. doi: 10.1186/1471-2334-14-31

Mohammad Ali Tabrizi, A., Badmasti, F., Shahcheraghi, F., and Azizi, O. (2018). Outbreak of Hypervirulent *Klebsiella Pneumoniae* harbouring $Bla_{(Vim-2)}$ among mechanically-ventilated drug-poisoning patients with high mortality rate in Iran. *J. Glob. Antimicrob. Resist.* 15, 93–98. doi: 10.1016/j.jgar.2018.06.020

Paczosa, M. K., and Mecsas, J. (2016). *Klebsiella Pneumoniae*: going on the offense with a strong Defense. *Microbiol. Mol. Biol. Rev.* 80, 629–661. doi: 10.1128/MMBR.00078-15

Palacios, M., Miner, T. A., Frederick, D. R., Sepulveda, V. E., Quinn, J. D., Walker, K. A., et al. (2018). Identification of two regulators of virulence that are conserved in *Klebsiella Pneumoniae* classical and Hypervirulent strains. *MBio* 9, E01443–E01418. doi: 10.1128/Mbio.01443-18

Pomakova, D. K., Hsiao, C. B., Beanan, J. M., Olson, R., Macdonald, U., Keynan, Y., et al. (2012). Clinical and phenotypic differences between classic and Hypervirulent Klebsiella pneumonia: an emerging and under-recognized pathogenic variant. *Eur. J. Clin. Microbiol. Infect. Dis.* 31, 981–989. doi: 10.1007/s10096-011-1396-6

Redondo-Salvo, S., Fernández-López, R., Ruiz, R., Vielva, L., De Toro, M., Rocha, E. P. C., et al. (2020). Pathways for horizontal gene transfer in bacteria revealed by a global map of their plasmids. *Nat. Commun.* 11:3602. doi: 10.1038/s41467-020-17278-2

Rumbo, C., Fernández-Moreira, E., Merino, M., Poza, M., Mendez, J. A., Soares, N. C., et al. (2011). Horizontal transfer of the Oxa-24 Carbapenemase gene via outer membrane vesicles: a new mechanism of dissemination of Carbapenem resistance genes in *Acinetobacter Baumannii*. *Antimicrob. Agents Chemother.* 55, 3084–3090. doi: 10.1128/AAC.00929-10

Schwechheimer, C., and Kuehn, M. J. (2015). Outer-membrane vesicles from gram-negative bacteria: biogenesis and functions. *Nat. Rev. Microbiol.* 13, 605–619. doi: 10.1038/nrmicro3525

Shi, Q., Lan, P., Huang, D., Hua, X., Jiang, Y., Zhou, J., et al. (2018). Diversity of virulence level phenotype of Hypervirulent *Klebsiella Pneumoniae* from different sequence type lineage. *BMC Microbiol.* 18:94. doi: 10.1186/S12866-018-1236-2

Shon, A. S., Bajwa, R. P., and Russo, T. A. (2013). Hypervirulent (Hypermucoviscous) *Klebsiella Pneumoniae*: a new and dangerous breed. *Virulence* 4, 107–118. doi: 10.4161/Viru.22718

Soler, N., and Forterre, P. (2020). Vesiduction: the fourth way of Hgt. *Environ. Microbiol.* 22, 2457–2460. doi: 10.1111/1462-2920.15056

Tenover, F. C., Arbeit, R. D., Goering, R. V., Mickelsen, P. A., Murray, B. E., Persing, D. H., et al. (1995). Interpreting chromosomal DNA restriction patterns produced by pulsed-field gel electrophoresis: criteria for bacterial strain typing. *J. Clin. Microbiol.* 33, 2233–2239. doi: 10.1128/jcm.33.9.2233-2239.1995

Tian, D., Wang, M., Zhou, Y., Hu, D., Hy, O., and Jiang, X. (2021). Genetic diversity and evolution of the virulence plasmids encoding Aerobactin and Salmochelin in *Klebsiella Pneumoniae*. *Virulence* 12, 1323–1333. doi: 10.1080/21505594.2021.1924019

Tsai, Y. M., Wang, S., Chiu, H. C., Kao, C. Y., and Wen, L. L. (2020). Combination of modified carbapenem inactivation method (mCIM) and EDTA-CIM (eCIM) for phenotypic detection of carbapenemase-producing Enterobacteriaceae. *BMC Microbiol.* 20:315. doi: 10.1186/s12866-020-02010-3

Turnbull, L., Toyofuku, M., Hynen, A. L., Kurosawa, M., Pessi, G., Petty, N. K., et al. (2016). Explosive cell Lysis as a mechanism for the biogenesis of bacterial membrane vesicles and biofilms. *Nat. Commun.* 7:11220. doi: 10.1038/ncomms11220

Wang, S., Gao, J., and Wang, Z. (2019). Outer membrane vesicles for vaccination and targeted drug delivery. *Wiley Interdiscip. Rev. Nanomed. Nanobiotechnol.* 11:E1523. doi: 10.1002/Wnan.1523

Wang, Z., Wen, Z., Jiang, M., Xia, F., Wang, M., Zhuge, X., et al. (2022). Dissemination of virulence and resistance genes among *Klebsiella Pneumoniae* via outer membrane vesicle: an important plasmid transfer mechanism to promote the emergence of Carbapenem-resistant Hypervirulent *Klebsiella Pneumoniae*. *Transbound. Emerg. Dis.* 69, E2661–E2676. doi: 10.1111/Tbed.14615

Xu, C., Dong, N., Chen, K., Yang, X., Zeng, P., Hou, C., et al. (2022). Bactericidal, anti-biofilm, and anti-virulence activity of vitamin C against Carbapenem-resistant Hypervirulent *Klebsiella Pneumoniae*. *Iscience* 25:103894. doi: 10.1016/j.isci.2022.103894

Yang, X., Dong, N., Chan, E. W., Zhang, R., and Chen, S. (2021). Carbapenem resistance-encoding and virulence-encoding conjugative plasmids in *Klebsiella Pneumoniae*. *Trends Microbiol.* 29, 65–83. doi: 10.1016/j.tim.2020.04.012

Yaron, S., Kolling, G. L., Simon, L., and Matthews, K. R. (2000). Vesicle-mediated transfer of virulence genes from Escherichia Coli O157:H7 to other enteric bacteria. *Appl. Environ. Microbiol.* 66, 4414–4420. doi: 10.1128/AEM.66.10.4414-4420.2000

Zhan, L., Wang, S., Guo, Y., Jin, Y., Duan, J., Hao, Z., et al. (2017). Outbreak by Hypermucoviscous *Klebsiella Pneumoniae* St11 isolates with Carbapenem resistance in a tertiary hospital in China. *Front. Cell. Infect. Microbiol.* 7:182. doi: 10.3389/Fcimb.2017.00182

Zhang, Y., Jin, L., Ouyang, P., Wang, Q., Wang, R., Wang, J., et al. (2020). Evolution of Hypervirulence in Carbapenem-resistant *Klebsiella Pneumoniae* in China: a multicentre, molecular epidemiological analysis. *J. Antimicrob. Chemother.* 75, 327–336. doi: 10.1093/jac/dkz446

Zhang, R., Lin, D., Chan, E. W., Gu, D., Chen, G. X., and Chen, S. (2016). Emergence of Carbapenem-resistant serotype K1 Hypervirulent *Klebsiella Pneumoniae* strains in China. *Antimicrob. Agents Chemother.* 60, 709–711. doi: 10.1128/AAC.02173-15

frontiers | Frontiers in Microbiology

TYPE Original Research
PUBLISHED 04 January 2023
DOI 10.3389/fmicb.2022.993240

OPEN ACCESS

EDITED BY
Yongfei Hu,
China Agricultural University,
China

REVIEWED BY
Juan Li,
Chinese Academy of Sciences (CAS), China
Valentine Usongo,
Health Canada,
Canada

*CORRESPONDENCE
Ibrahim Bitar
✉ ibrahimbitar5@gmail.com

SPECIALTY SECTION
This article was submitted to Antimicrobials, Resistance and Chemotherapy, a section of the journal Frontiers in Microbiology

RECEIVED 13 July 2022
ACCEPTED 06 December 2022
PUBLISHED 04 January 2023

CITATION
Bitar I, Papagiannitsis CC, Kraftova L, Marchetti VM, Petinaki E, Finianos M, Chudejova K, Zemlickova H and Hrabak J (2023) Implication of different replicons in the spread of the VIM-1-encoding integron, In110, in Enterobacterales from Czech hospitals. *Front. Microbiol.* 13:993240. doi: 10.3389/fmicb.2022.993240

Implication of different replicons in the spread of the VIM-1-encoding integron, In110, in Enterobacterales from Czech hospitals

Ibrahim Bitar[1,2]*, Costas C. Papagiannitsis[3], Lucie Kraftova[1,2], Vittoria Mattioni Marchetti[1,2], Efthymia Petinaki[3], Marc Finianos[1,2], Katerina Chudejova[1,2], Helena Zemlickova[4,5] and Jaroslav Hrabak[1,2]

[1]Department of Microbiology, Faculty of Medicine, University Hospital in Pilsen, Charles University, Pilsen, Czechia, [2]Biomedical Center, Faculty of Medicine, Charles University, Pilsen, Czechia, [3]Department of Microbiology, University Hospital of Larissa, Larissa, Greece, [4]National Reference Laboratory for Antibiotics, National Institute of Public Health, Prague, Czechia, [5]Department of Medical Microbiology, 3rd Faculty of Medicine, Charles University, Prague, Czechia

Background: VIM metallo-β-lactamases are enzymes characterized by the ability to hydrolyze all β-lactams. Usually, *bla*$_{VIM}$-like genes are carried by class 1 integrons. In the Czech Republic, only sporadic cases of VIM-producing Enterobacterales have been reported in which those isolates carried the VIM-1 carbapenemase-encoding integron In110. However, during 2019–2020, an increased number was reported. Therefore, the aim of the current study was to characterize the genetic elements involved in the increased spread of *bla*$_{VIM}$ genes.

Materials and methods: 32 VIM-producing Enterobacterales collected between 2019 and 2020 were subjected to: antimicrobial susceptibility testing, integron analysis, and short reads sequencing. Based on the results, 19 isolates were selected as representative and sequenced using Sequel I platform.

Results: The 32 VIM-producing isolates exhibited variations in the MICs of carbapenems. Based on short-read data, 26 of the 32 sequenced isolates harbored the *bla*$_{VIM-1}$ allele while six isolates carried the *bla*$_{VIM-4}$ gene. The most prevalent was the In110 integron (n=24) and two isolates carried the In4873 class 1 integron. The *bla*$_{VIM-4}$ allele was identified in class 1 integrons In1174 (n=3), In416 (n=1), In2143 (n=1) and In2150. Long reads sequencing revealed that the *bla*$_{VIM}$ was carried by: pKPC-CAV1193-like (n=6), HI1 (pNDM-CIT; n=4), HI2 (n=3), FIB (pECLA; n=2) and N (n=1) incompatibility groups. Two *bla*$_{VIM}$-carrying plasmids could not be typed by the database, while another one was integrated into the chromosome.

Conclusion: We observed the spread of VIM-encoding integrons, mainly of In110, among Enterobacterales isolated from Czech hospitals, but also an increased number of novel elements underlining the ongoing evolution.

10.3389/fmicb.2022.993240

KEYWORDS

Enterobacterales, whole-genome sequencing, *bla*$_{VIM-1}$, *bla*$_{VIM-4}$, In110, plasmids, integrons

Introduction

Mobile elements, such as integrons, transposons and plasmids, have played an important role in the spread of antimicrobial resistance genes among Enterobacterales. Integrons are genetic elements able to acquire and express genes in the form of cassettes. They can move due to their association with insertion sequences, transposons and plasmids (Mazel and Davies, 1999). Class 1 integrons, which are the most common integrons among clinical isolates, have been involved in the dissemination of more than 60 different gene cassettes conferring resistance to almost all antimicrobial categories (Mazel, 2006). One of the most recently characterized cassettes encodes VIM metallo-β-lactamases (MβLs), which are enzymes characterized by the ability to hydrolyze all β-lactams, including carbapenems (Laraki et al., 1999). Usually, *bla*$_{VIM}$-like genes are carried by class 1 integrons, like In-e541 identified in Greece (Miriagou et al., 2003), In110 and In113 in Spain (Tato et al., 2010) or In416 in Italy (Colinon et al., 2007).

In the Czech Republic, only sporadic cases of VIM-producing Enterobacterales have been reported (Papousek et al., 2017; Papagiannitsis et al., 2018), from 2011 till 2015. Interestingly, those isolates carried the VIM-1 carbapenemase-encoding integron In110 (*bla*$_{VIM-1}$-*aacA4-aadA1*; Lombardi et al., 2002). However, during 2019–2020, an increased number of VIM-producing Enterobacterales was isolated from Czech hospitals. Therefore, the aim of the current study was to characterize the genetic elements involved in the increased spread of *bla*$_{VIM}$ genes, and to examine if In110 was the only/main integron associated with the expression of VIM carbapenemases.

Materials and methods

Bacterial isolates, susceptibility testing and confirmation of carbapenemase production

In 2019 and 2020, Czech hospitals referred a total of 32 VIM-producing Enterobacterales isolates with a meropenem MIC of >0.125 μg/ml (2012; using *E.coli* ATCC 25922 as a quality control strain) to the National Reference Laboratory for antibiotics. However, five of those isolates have been previously published as they carried an *mcr*-like gene (Bitar et al., 2020). Species identification was confirmed by matrix-assisted laser desorption ionization-time of flight mass spectrometry (MALDI-TOF MS) using MALDI Biotyper software (Bruker Daltonics, Bremen, Germany). All isolates were tested for carbapenemase production by the MALDI-TOF MS meropenem hydrolysis assay (Rotova et al., 2017). Additionally, the presence of carbapenemase-encoding genes (*bla*$_{KPC}$, *bla*$_{VIM}$, *bla*$_{IMP}$, *bla*$_{NDM}$, and *bla*$_{OXA-48}$-like) was confirmed by PCR amplification (Poirel et al., 2004; Ellington et al., 2007; Naas et al., 2008; Yong et al., 2009). PCR products were sequenced as described below. Isolates positive for *bla*$_{VIM}$-like genes were further studied.

Antimicrobial susceptibility was performed using broth microdilution according to European Committee on Antimicrobial Susceptibility Testing (EUCAST) (2012) guidelines. Susceptibility data were interpreted according to the criteria (version v12.0) of the EUCAST.[1]

Integron analysis

Variable regions of class 1 integrons with *bla*$_{VIM}$-like genes were amplified in two parts, from the 5′conserved segment (5′CS) to carbapenemase-encoding cassette and from carbapenemase-encoding cassette to the 3′CS (Papagiannitsis et al., 2013). Whole-gene arrays were sequenced using an ABI 3500 sequencer (Applied Biosystems, Foster City, CA). The integron database, Integrall[2] (Moura et al., 2009) was used to analyze and assign integron sequences.

Short-read whole genome sequencing

All VIM-producing Enterobacterales were sequenced, using the Illumina MiSeq platform (Illumina Inc., San Diego, CA, United States). The genomic DNAs of the clinical isolates were extracted using the DNA-Sorb-B kit (Sacace Biotechnologies S.r.l., Como, Italy). Multiplexed DNA libraries were prepared using the Nextera XT library preparation kit, and 300-bp paired-end sequencing was performed on the Illumina MiSeq platform (Illumina Inc., San Diego, CA, United States) using the MiSeq v3 600-cycle reagent kit. Initial paired-end reads were quality trimmed using the Trimmomatic tool v0.33 (Bolger et al., 2014) and then, assembled by use of the de Bruijn graph-based *de novo* assembler SPAdes v3.14.0 (Bankevich et al., 2012).

1 http://www.eucast.org/

2 http://integrall.bio.ua.pt/

Long-read whole genome sequencing

Based on the results of short-read sequencing (see below), 19 VIM producers were selected to for long-read sequencing, to help close the whole plasmid sequences. These isolates were selected as representatives of all different hospitals, bacterial species, STs, replicon profiles and bla_{VIM} alleles.

Genomic DNA was extracted from the clinical isolates using NucleoSpin Microbial DNA kit (Macherey–Nagel, Germany). Whole genome sequencing (WGS) was performed on the Sequel I platform (Pacific biosciences, Menlo Park, CA, United States). Microbial multiplexing protocol was used for the library preparation according to the manufacturer instructions for Sheared DNA. DNA shearing was performed using the Megaruptor 2 (Diagenode, Liege, Belgium) using long hydropores producing 10 kb long inserts. No size selection was performed during the library preparation. The Microbial Assembly pipeline offered by the SMRT Link v9.0 software was used to perform the assembly and circularization with minimum seed coverage of 30X. Assembled sequences were annotated using the NCBI Prokaryotic Genome Annotation Pipeline (PGAP).

Nucleotide sequence accession numbers

The nucleotide sequences of the genomes and plasmids were deposited and are available in GenBank (Supplementary Table S1) under the BioProject number PRJNA772913.

Results

VIM-producing Enterobacterales

During 2019–2020, a total of 32, Enterobacterales isolates with a meropenem MIC of >0.125 μg/ml were referred to the National reference laboratory for antibiotics from 15 laboratories. Among them, 23 isolates were identified to be *Enterobacter cloacae* complex, 5 were identified to be *Citrobacter freundii*, and 3 were identified to be *Klebsiella pneumoniae*. The one remaining VIM-producing isolate belonged to the bacterial species *Klebsiella michiganensis*.

All 32 VIM-producing isolates exhibited resistance to piperacillin, piperacillin-tazobactam and cephalosporins, while the variations in the MICs of aztreonam and carbapenems that were observed (Supplementary Table S1) might reflect the presence of additional resistance mechanisms in some of the isolates. Twenty-six of the VIM-producing isolates also exhibited resistance to tetracycline, 25 were resistant to chloramphenicol, 23 were resistant to gentamicin, 19 were resistant to ciprofloxacin, 3 were resistant to tigecycline, 6 were resistant to amikacin, whereas three of the isolates were resistant to colistin.

Analysis of short-read sequencing results and VIM-encoding integrons

Based on short-read data, 26 of the 32 sequenced isolates harbored the bla_{VIM-1} allele (Tables 1, 2), while the remaining six isolates carried the bla_{VIM-4} gene. The bla_{VIM-4} gene was identified among 3\u00B0*C. freundii*, 1 *K. pneumoniae* and 2 *E. hormaechei* isolates. Moreover, characterization of the regions flanking the VIM-encoding genes by PCR mapping and sequencing data showed that bla_{VIM}-like genes were located in six main types of class 1 integrons (Figures 1, 2). The most prevalent was the In110 integron identified in 24 VIM-1-producing isolates. The two remaining VIM-1-producing isolates, which belonged to *K. pneumoniae* ST54, carried the In4873 class 1 integron. In4873 integron, which is an In416-like element identified for the first time in Greece (Papagiannitsis et al., 2016), included the bla_{VIM-1}, *aacA7*, *dfrA1*, *aadA1* and *smr2* gene cassettes. On the other hand, the bla_{VIM-4} allele was identified in class 1 integrons In1174 ($n=3$), In416 ($n=1$), In2143 ($n=1$) and In2150 (Tables 1, 2). The class 1 integron In1174 includes an array of *aacA4* and bla_{VIM-4} gene cassettes. The In416 element, which was firstly reported in Italy (Colinon et al., 2007), comprises bla_{VIM-4}, *aacA7*, *dfrA1*, *aadA1* and *smr2* gene cassettes. Additionally, the In2143, which was a novel class 1 integron carrying bla_{VIM-4}, *aacA7* and *aacC2c* gene cassettes, was found in a ST108 *E. hormaechei* isolate. Finally, the novel integron In2150, which comprised bla_{VIM-4}, *aacA7*, *smr2* cassettes, was identified in ST674 *C. freundii* isolate (Cfr-56322cz). Beside species-specific chromosomal β-lactamases, most of the clinical isolates also carried genes encoding TEM-1 penicillinases ($n=14$) and/or OXA-1 oxacillinases ($n=13$). Nine out of 22 *Enterobacter* isolates harboured the $bla_{CTX-M-15}$ gene, while the bla_{SHV-12} gene was found among 2 isolates. Additionally, 2 out of 3 *K. pneumoniae* co-carried the carbapenemase-encoding gene bla_{KPC-2}. All sequenced isolates exhibited a wide variety of resistance genes conferring resistance to aminoglycosides, sulfonamides, trimethoprim, streptomycin, fosfomycin (low-level resistance), fluoroquinolones, chloramphenicol, tetracyclines, colistin, erythromycin and/or rifampicin (Tables 1, 2).

WGS data revealed that most of the isolates belonging to *E. cloacae* complex isolates belonged to sequence types ST92 ($n=8$), ST106 ($n=5$), and ST190 ($n=2$; Tables 1, 2). The remaining seven *Enterobacter* isolates were ST25, ST92, ST108, ST252, ST421, ST764, and the novel STs 1734 and 1735. The isolates belonging to *C. freundii* species were assigned to ST95 ($n=2$), ST9 ($n=1$), and ST673 ($n=1$) and ST674 ($n=1$). ST673 and ST674 were novel STs. The *K. pneumoniae* isolates included two STs. The VIM-1 producers belonged to ST54, while the VIM-4-producing *K. pneumoniae* was ST11. Finally, the *K. michiganensis* (closely related to *K. oxytoca*) isolate was assigned to ST226.

Localization of VIM-encoding integrons

Based on short-read data, 19 VIM-producing isolates were selected to be sequenced by the Sequel I platform, to close plasmid

10.3389/fmicb.2022.993240

TABLE 1 WGS data of the 19 isolates sequenced using both short (illumina) and long reads sequencing platform (PacBio).

Isolate	Species	ST	VIM plasmid size	Inc	Integron type	Other replicons	Resistance genes
48212*	*E. cloacae complex*	106	55,220	pKPC-CAV1193-like	In110	Col(pHAD28), IncFIB(pECLA), IncHI2	*mcr-9*, *aac(6′)-IIc*, *aadA2b*, *aph*(6)-*Id*, *dfrA19*, *catA2*, *sul1*, *sul2*, *tetD*, *aac(6′)-Ib-cr*, *qnrA1*, *ere*(*A*), bla_{SHV}-12, bla_{TEM-1b}
							qnrS1, bla_{TEM-1a}, bla_{VIM-1}, *aac(6′)-Ib3*
48411	*E. hormaechei*	1734	171765	IncFIB(pECLA)	In110	Col(pHAD28)	*aacA4*, *aadA1*, *dfrA14*, bla_{VIM-1}, *catA2*, bla_{VIM-1B}, *strA*, *strB*, *tetA*, *qnrS1*,*qacE*, *sul1*, *sul2*, *fosA*
48880*	*E. cloacae complex*	764	2,62,616	IncHI2	In416	Col(pHAD28), IncFIB(pECLA), IncFII(pECLA), IncR	*mcr-9.2*, *aac(6′)-II*, *aadA22*, *dfrA1*, *sul1*, *tetA*, bla_{VIM-4}
48946*	*E. cloacae complex*	106	55,222	pKPC-CAV1193-like	In110	Col(pHAD28), IncFIB(pECLA), IncHI2	*mcr-9*, *aac(6′)-IIc*, *aadA2b*, *aph(3″)-Ib*, *aph*(6)-*Id*, *dfrA19*, *catA2*, *sul1*, *sul2*, *tetD*, *ere*(*A*), bla_{TEM-1b}, bla_{SHV-12}
							aac(6′)-Ib3, *qnrS1*, bla_{TEM-1a}, bla_{VIM-1},
48947	*E. hormaechei*	190	55220	pKPC_49790_ VIM_1	In110	IncHI2	*aacA4 (n=2)*, *aac(3)-IIa*, *aadA1*, *aadA2b*, *catA1*, *catB3*, *dfrA14*, bla_{VIM-1}, $bla_{CTX-M-15}$, bla_{OXA-1}, bla_{TEM-1A}, bla_{TEM-1B}, *strA*, *strB*, *qnrB1*, *qnrS1*, *sul1*, *sul2*, *tetA*
49589	*E. hormaechei*	108	294454	IncHI2	In2143	IncFIB(pECLA), IncFII(pECLA), IncR	*aac(3)-Ib*, *aac(6′)-Il*, bla_{VIM-4}, *qacE (n=2)*, *qnrA1*, *sul1 (n=2)*, *tetB*, *aacA7*, *aacC2c*
49790*	*E. cloacae complex*	106	55,220	pKPC-CAV1193-like	In110	Col(pHAD28), IncFIB(pECLA), IncHI2	*mcr-9*, *aac(6′)-IIc*, *aadA2b*, *aph(3″)-Ib*, *aph*(6)-*Id*, *dfrA19*, *catA2*, *sul1*, *sul2*, *tetD*, *aac(6′)-Ib-cr*, *qnrA1*, *ere*(*A*), *bla*SHV-12, bla_{TEM-1b}, *aac(6′)-Ib3*, *qnrS1*, bla_{TEM-1a}, bla_{VIM-1},
54569	*E. hormaechei*	92	171616	IncFIB (pECLA),IncFII (peCLA)	In110	IncQ1, Col440I, ColpVC	*aacA4*, *aac(3)-IIa*, *aac(6′)-Ib3*, *aadA1*, *aph(3′)-Via*, bla_{VIM-1}, *bla*OXA-1, *catB3*, *dfrA14*, *fosA*, *qacE*, *sul1*

(Continued)

TABLE 1 (Continued)

Isolate	Species	ST	VIM plasmid size	Inc	Integron type	Other replicons	Resistance genes
57816	*E. hormaechei*	106	55220	pKPC-CAV1193	In110	IncFIB (pECLA), IncHI2, Col (pHAD28)	*aacA4, aac(6′)-Ib3, aac(6′)-IIc, aadA2b (n=2),bla*$_{VIM-1}$, *bla*$_{TEM-1A}$, *bla*$_{TEM-1B}$, *bla*$_{SHV-12}$, *catA2, dfrA19, ere(A),mcr-9, qnrS1, fosA, qacE (n=3), strA, strB, sul1 (n=3), sul2, tet(D)*
58983	*E. cloacae*	421	64556	untypable	In110	IncFIB (pECLA)	*aacA4 (n=2), aac(3)-IIa, aadA1 (n=2), bla*$_{VIM-1}$, *bla*$_{CTX-M-15}$, *bla*$_{OXA-1}$, *bla*$_{TEM-1B}$, *catA1, catB3, dfrA14, qacE, qnrB1, strA, strB, sul1, sul2, tetA, fosA*
59732	*E. hormaechei*	1735	54956	pKPC-CAV1193	In110	IncFIB (pECLA), Col (pHAD28)	*aacA4, aadA2b, aac(6′)-Ib3, bla*$_{VIM-1}$, *bla*$_{TEM-1A}$ *(n=2), qnrS1, fosA, qacE, sul1*
60214	*E. hormaechei*	92	311801	IncHI1 (pNDM-CIT)	In110	IncFIB (pECLA), IncFII (pECLA), Col (pHAD28)	*aacA4 (n=2), aac(6′)-Ib3, aac(3)-IIa, aadA1 (n=2), aph(3′)-Ia, catB3, bla*$_{VIM-1}$, *bla*$_{CTX-M-15}$, *bla*$_{OXA-1}$, *bla*$_{TEM-1B}$, *dfrA1, dfrA14, qnrB1, fosA, qacE, strA, strB, sul1, sul2, tet(A)*
51929*	*C. freundii*	95	3,69,945	IncHI2-/IncM1	In1174		*mcr-9, aac(6′)-II, aac(3)-I, aac(6′)-Ib3, ant(2″)-Ia, aadA1, aadA2b, aph(3′)-Ia, dfrA19, catA2, cmlA1, sul1, tetA, aac(6′)-Ib-cr, qnrA1, bla*$_{VIM-4}$
52323	*C. freundii*	9	318136	IncHI1 (pNDM-CIT)	In110		*aacA4, aac(6′)-Ib3, aadA1 (n=2), aph(3′)-Ia, bla*$_{VIM-1}$, *catA1, dfrA1, qnrB75, qacE, sul1, tet(A)*
56322	*C. freundii*	674	344532	IncHI1A(NDM-CIT), IncHI1B(NDM-CIT)	In2150		*aacA7, aac(3)-IId, aadA2, bla*$_{VIM-4}$, *bla*$_{TEM-1B}$, *dfrA12, qnrB75, qacE, sul1 (n=2), sul2, tetA*
56415	*C. freundii*	673	106850	untypable	In1174	IncHI2	*aacA4, aac(6′)-Ib3, aadA1, aadA2b (n=3), aadB (n=2), aph(3′)-Ia (n=2), bla*$_{VIM-4}$, *catA2, cmlA1, dfrA19, mcr-9, qacE (n=4), sul-1 (n=4),*

(Continued)

TABLE 1 (Continued)

Isolate	Species	ST	VIM plasmid size	Inc	Integron type	Other replicons	Resistance genes
51135	*K. pneumoniae*	11	chromosome	NA	In1174	IncFIB(K), IncM1	*aacA4, aac(6')-Ib3,* bla_{VIM-1},bla_{TEM-1B}, $bla_{SHV-182}$, *qacE, cmx, oqxA, oqxB, fosA*
59062	*K. pneumoniae*	54	56199	IncN	In4873	IncFIB (K) (pCAV1099-114), IncH1B (pNDM-MAR),IncC, IncFIB (pQil) IncFII(K)	*aacA7, aac(6')-Im, aadA22, aph(3')-Ia, aph(2'')-Ib,* bla_{VIM-1}, bla_{KPC-2}, *catA1, dfrA1, oqxAB, qnrS1, fosA, qacE, sul1, tet(D)*
53828	*K. michiganensis*	226	364473	IncHI1 (pNDM-CIT)	In110	IncFII(Yp)	*aacA4, aph(3')-Ia, aadA1 (n=2), dfrA1,* bla_{VIM-1}, *catA1, qacE, sul1, tetA*

*These isolates were already published in Bitar et al. (2020).

sequences. Analysis of long-read sequencing data revealed the presence of several bla_{VIM}-carrying plasmid sequences belonging to different Inc. groups and presenting diverse sizes (Table 1). Based on PlasmidFinder analysis of plasmid sequences, 16 out of 19 bla_{VIM}-carrying plasmids could be assigned to: pKPC-CAV1193-like ($n=6$), HI1 (pNDM-CIT; $n=4$), HI2 ($n=3$), FIB (pECLA; $n=2$) and N ($n=1$) incompatibility (Inc) groups (Figure 2). Two of the remaining bla_{VIM}-carrying plasmids could not be typed by the database, while in the ST11 *K. pneumoniae* isolate the VIM-4-encoding integron, In1174, was integrated into the chromosome.

All pKPC-CAV1193-like plasmids ($n=6$) carried the VIM-1 encoding integron In110. These plasmids, which were ~55,220-bp in size (except p59732CZ_VIM), were identical to plasmid p48212_VIM (Supplementary Figure S1) characterized previously from ST106 *E. hormaechei*, carrying *mcr-9* gene, isolated from a Czech hospital (Bitar et al., 2020). Plasmid p59732CZ_VIM lacked a 266-bp fragment in the ORF encoding a GNAT family N-acetyltransferase.

Also, three (p52323cz_VIM, p53828cz_VIM and p60214cz_VIM) out of four IncHI1 (pNDM-CIT) plasmids carried the In110. These plasmids were identical to VIM-1-encoding plasmid pLec-476cz (Supplementary Figure S2), which was previously characterized from a *Leclercia adecarboxylata* isolate (Papousek et al., 2017) recovered during a survey study focused on compliance with hand hygiene among the staff of a different Czech hospital in May 2011. On the other hand, the fourth IncHI1 (pNDM-CIT) plasmid (p56322_VIM), was carried by a ST674 *C. freundii* isolate. This plasmid harbored the VIM-4-encoding integron In2150. Plasmid p56322_VIM showed moderate similarity to IncHI1 plasmids, encoding VIM-1 (like p53828cz_VIM [72% coverage, 98.68% identity]), while the highest similarity was observed for the IncHI1 plasmid pRHBSTW-00135_2 (80% coverage, 100% identity; GenBank accession no. CP056828; Supplementary Figure S3) that was characterized from a wastewater influent sample collected in the United Kingdom. Of note was that plasmid pRHBSTW-00135_2 carried no resistance genes. p56322_VIM was composed of a partial IncHI1 backbone and a MDR region. Segments of the IncHI1 backbone, encoding proteins involved in the conjugative transfer system, were duplicated in the p56322_VIM plasmid. Furthermore, beside In2150, the MDR region contained the In27 integron, consisting of *dfrA12*, *gcuF* and *aadA2* gene cassettes, the bla_{TEM-1} and *aac*(3)-*IId* resistance genes, and regions conferring resistance to macrolides, mercury and chromate.

Two IncHI2 VIM-4-encoding plasmids (p48880_MCR_VIM and p51929_MCR_VIM), which also carried the *mcr-9* resistance gene, have been previously characterized (Bitar et al., 2020). The third IncHI2 plasmid, p49589_VIM, which was 294,454-bp in size, carried the novel VIM-4-encoding integron In2143. It exhibited moderate similarity to p48880_MCR_VIM (76% coverage, 99.48% identity) and p51929_MCR_VIM (76% coverage, 99.97% identity), while it was almost identical (99% coverage, 100% identity) to IncHI2 plasmid p48293_VIM (Supplementary Figure S4), which was previously sequenced from the *E. hormaechei* strain Ecl-48293co-producing KPC-2 and VIM-4 carbapenemases, during a study describing the ongoing spread of KPC-type producers in Czech hospitals (Kraftova et al., 2021). p49589_VIM was typed as sequence type 1 (ST1) following the IncHI2 pDLST scheme (Garcia-Fernandez and Carattoli, 2010). In agreement with other IncHI2 replicons, plasmid backbone was composed of regions responsible for replication (*repHI2*), conjugative transfer (*trh* genes), and plasmid maintenance (*par* gene). Additionally, similarly to other IncHI2 plasmids, it carried genes conferring resistance to tellurium (*terZABCDEF*), while genes conferring resistance to arsenic (*arsCBRH*) were not found. Moreover, one multidrug resistance (MDR) region was identified, in which the integron In2143 was embedded in a Tn*1696*-like transposon, also carrying a *qnrA1* resistance gene and a mercury (*mer*) resistance operon.

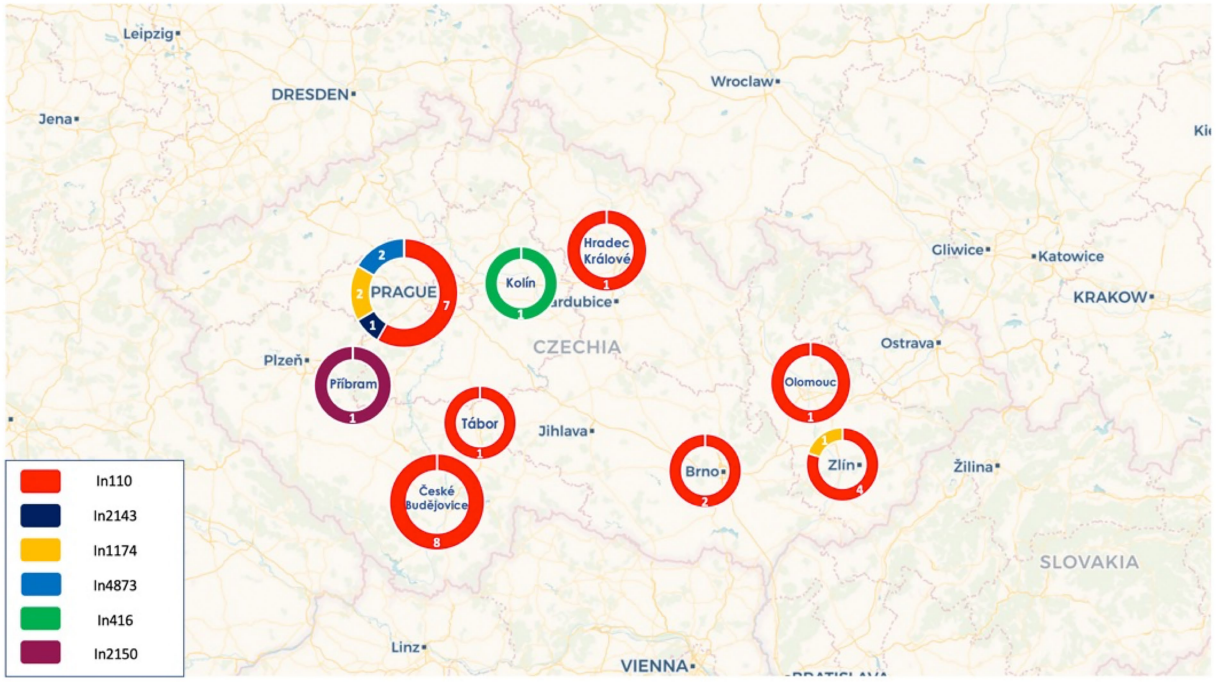

FIGURE 1
Distribution of the different integrons across the cities in the Czech Republic.

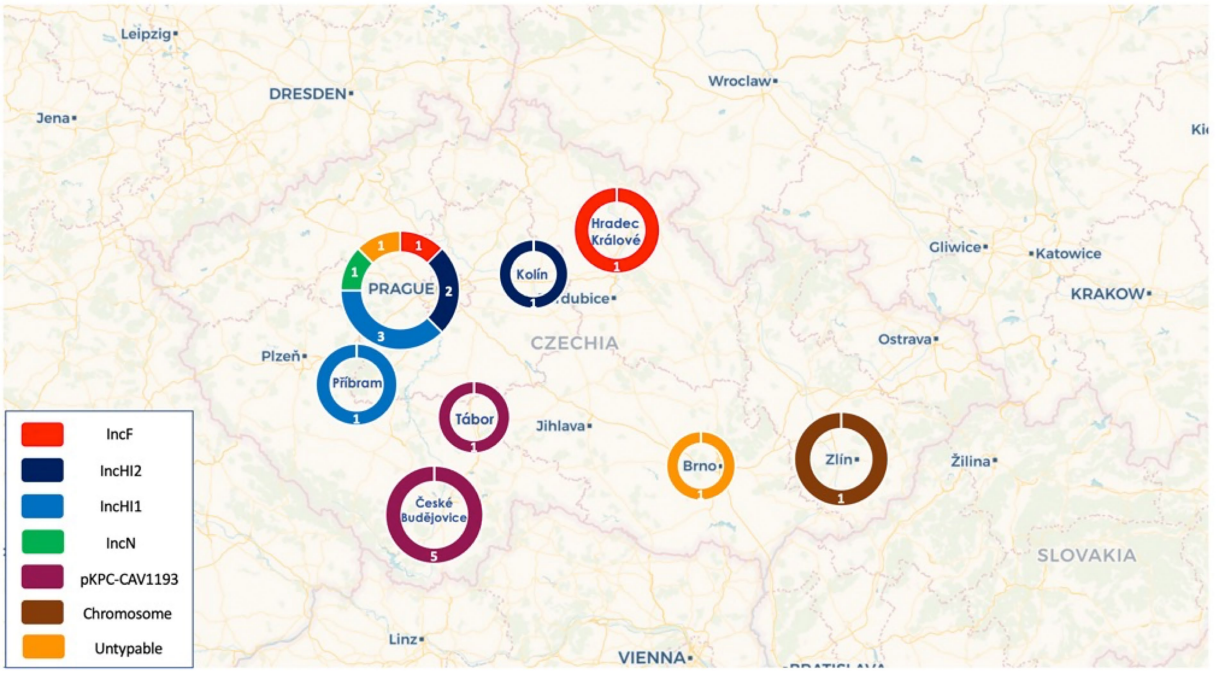

FIGURE 2
Distribution of the different plasmid types across the cities in the Czech Republic.

In IncFIB plasmids, p48411_VIM and p54569_VIM showed limited similarity (57% coverage, 100% identity) to each other (Supplementary Figure S5), despite being both typed as IncFIB (pECLA) by PlasmidFinder analysis. Plasmid p48411_VIM, which contained only the IncFIB replicon of pECL_A (Ren et al., 2010), seemed to be a fusion derivative of plasmids pLec-476cz

10.3389/fmicb.2022.993240

TABLE 2 WGS data of the isolates sequenced only using short reads sequencing platform (illumina).

Isolate	Species	ST	Replicons	*bla*VIM-positive Integron	Resistance genes
49049	*E. cloacae*	92	IncFIB(pECLA), IncFII(pECLA), IncQ1, ColpVC, Col440I	In110	*aac(6′)-Ib-cr, aac(3)-IIa, aph(3′)-VIa, aadA1, bla*$_{VIM-1}$, *bla*$_{ACT-16}$, *catB3, dfrA14, sul1, fosA, qacE*
51524	*E. cloacae*	92	IncFIB(pECLA), IncFII(pECLA), IncQ1, ColpVC, Col440I	In110	*aac(6′)-Ib-cr, aadA1, aac(3)-IIa, aph(3′)-VIa, bla*$_{VIM-1}$, *bla*$_{OXA-1}$, *bla*$_{ACT-16}$, *catB3, dfrA14, sul1, qacE, fosA*
52089	*E. cloacae*	92	IncFIB(pECLA), IncFII(pECLA), IncHI1A(NDM-CIT), IncHI1B(NDM-CIT), Col(pHAD28)	In110	*aac(6′)-Ib-cr, aac(3)-IIa, aadA1, aph(3′)-Ia, bla*$_{VIM-1}$, *bla*$_{CTX-M-15}$, *bla*$_{OXA-1}$, *bla*$_{TEM-1B}$, *catB3, dfrA1, dfrA14, strA, strB, sul1, sul2, tetA, qnrB1, qacE*
54680	*E. asburiae*	25	IncFIB(pECLA), IncFII(pECLA), IncHI2, IncHI2A	In110	*aac(6′)-Ib-cr, aac(3)-IIa, aadA24, arr-3, bla*$_{VIM-1}$, *bla*$_{CTX-M-15}$, *bla*$_{OXA-1}$, *bla*$_{TEM-1B}$, *bla*$_{ACT-6}$, *catA1, catB3, dfrA14, strA, strB, sul1, sul2, tetA, qnrB1, qacE, fosA*
54818	*E. cloacae*	92	IncFIB(pECLA), IncFII(pECLA), IncHI2, IncHI2A, IncQ1, ColpVC	In110	*aac(6′)-Ib-cr, aac(3)-IIa, aph(3′)-VIa, aadA1, bla*$_{VIM-1}$, *bla*$_{CTX-M-15}$, *bla*$_{OXA-1}$, *bla*$_{TEM-1B}$, *bla*$_{ACT-16}$, *catA1, catB3, dfrA14, strA, strB, sul1, sul2, tetA, qnrB1, qacE*
54822	*E. cloacae*	92	IncFIB(pECLA), IncFII(pECLA), IncQ1, ColpVC, Col440I	In110	*aac(6′)-Ib-cr, aac(3)-IIa, aph(3′)-VIa, aadA1, dfrA14, bla*$_{VIM-1}$, *bla*$_{OXA-1}$, *bla*$_{ACT-16}$, *catB3, sul1, qacE, fosA*
55614	*E. cloacae*	92	IncFIB(pECLA), IncFII(pECLA), IncQ1, ColpVC, Col440I	In110	*aac(6′)-Ib-cr, aac(3)-IIa, aph(3′)-VIa, aadA1, bla*$_{VIM-1}$, *bla*$_{OXA-1}$, *bla*$_{ACT-16}$, *catB3, dfrA14, sul1, qacE, fosA*
56501	*E. cloacae*	190	IncHI2, IncHI2A, pKPC-CAV1193, Col(pHAD28)	In110	*aac(6′)-Ib-cr, aac(3)-IIa, aadA1, aadA2b, bla*$_{VIM-1}$, *bla*$_{CTX-M-15}$, *bla*$_{OXA-1}$, *bla*$_{TEM-1B}$, *bla*$_{ACT-7}$, *catA1, catB3, dfrA14, strA, strB, sul1, sul2, tetA, qnrB1, qacE, fosA*
57689	*E. cloacae*	106	IncFIB(pECLA), IncFII(pECLA), IncHI2, IncHI2A, pKPC-CAV1193, Col(pHAD28)	In110	*aac(6′)-Ib-cr, aac(6′)-IIc, aph(6)-Id, aac(3)-IIa, aadA1, aadA2b, bla*$_{VIM-1}$, *bla*$_{CTX-M15}$, *bla*$_{OXA-1}$, *bla*$_{SHV-12}$, *bla*$_{TEM-1B}$, *bla*$_{ACT-15}$, *catA1, catB3, ereA, dfrA14, strA, strB, sul1, sul2, tetA, tetD, qnrB1, qnrS1, qacE, fosA*
61347	*E. cloacae*	1735	Col(pHAD28), pKPC-CAV1193, Col(pHAD28)	In110	*aac(6′)-Ib-cr, aadA2b, bla*$_{VIM-1}$, *bla*$_{TEM-1A}$, *bla*ACT-15, *sul1, qacE, fosA*
61503	*E. cloacae*	252	IncFIB(pECLA), IncFII(pECLA), repA(pENTd4a)	In110	*aac(6′)-Ib-cr, aac(3)-IIa, aadA1, bla*$_{VIM-1}$, *bla*$_{OXA-1}$, *bla*$_{ACT-3}$, *catBe, dfrA14, sul1, qnrE1, qacE, fosA1*

(Continued)

TABLE 2 (Continued)

Isolate	Species	ST	Replicons	*bla*VIM-positive Integron	Resistance genes
50714	*C. freundii*	673	IncFII(SARC14), IncN	In110	*aac(6′)-Ib-cr, aph(3″)-Ib, aadA1,* bla_{VIM-1}, bla_{CMY-78}, *dfrA14, sul1, sul2, qacE, qnrS1*
59343	*K. pneumoniae*	54	IncC, IncN, IncFIB(pQil), IncFII(K), IncFIB(K) (pCAV1099-114), IncHI1B(pNDM-MAR)	In4873	*aac(6′)-Im, aacA27, aph(3′)-Ia, aadA2,* bla_{VIM-1}, bla_{KPC-2}, $bla_{SHV-178}$, *catA1, dfrA1, sul1, tetD, qnrS1, qacE, oqxA, oqxB, fosA*

and pECL_A. It contained a 46,500-bp segment (1–32,410 and 157,676–171,765) being identical to a sequence of pLec-476cz including a part of the plasmidic backbone and a part of the MDR region, which contained the class 1 integron In110. The remaining 125,265-bp sequence, which contained a region encoding a type-F conjugative transfer system, carried regions responsible for resistance to tellurium, copper and silver, and a second MDR region carrying *dfrA14*, *catA2*, *sul2*, *strA*, *strB* and bla_{TEM-1} resistance genes. This MDR region resembled the MDR region in pECL_A and p60214_IncFII. The pECL_A-like plasmid, p60214_IncFII, was sequenced from a ST92 *E. hormaechei* isolate, characterized during this study. On the other hand, plasmid p54569_VIM was a derivative of pECL_A, which acquired a Tn*1721*-like transposition module (9986–24,830 bp) carrying In110 (Supplementary Figure S5). An identical transposition module has also been observed in plasmids p58983_VIM and pEncl-30969cz (as seen below). Direct repeats of 5 bp (TCCGG) were found at the boundaries of the Tn*3*-like element, suggesting its transposition into the pECL_A-like backbone. Unlike p48411_VIM, no *tra* region was found on p54569_VIM. Additionally, it contained both IncFIB and IncFII replicons of pECL_A (Ren et al., 2010).

The IncN plasmid p59062_VIM, which carried the VIM-1-encoding integron In4873, was typed as ST7 based on plasmid MLST (pMLST) scheme for rapid categorization of IncN plasmids (Garcia-Fernandez et al., 2011). It showed extensive similarity with other IncN plasmids (Supplementary Figure S6), like pTE_C_1 (83% coverage, 99.99% identity; GenBank accession no.MW574936), pNL194 (81% coverage, 99.22% identity; Miriagou et al., 2010) and p3846_IncN_VIM-1 (88% coverage, 100% identity; Marchetti et al., 2021). The In4873 integron was inserted between the genes, encoding EcoRII endonuclease and resolvase, of the IncN plasmidic backbone. Furthermore, a Tn*21* fragment consisting of *tniB* and *tniA* was found next to the 3′CS, 108 bp downstream of *orf5*, as in In2-like integrons. The *qnrS1* resistance gene was also found in p50962_VIM, located downstream of *fipA*.

The non-typeable plasmid p58983_VIM, which was characterized from a ST421 *E. cloacae* complex isolate, carried the VIM-1-encoding integron In110. It comprised a plasmidic backbone which was identical (100% coverage, 100% identity) to plasmid p54569CZ_2 (characterized from a ST92 *E. hormaechei* isolate in this study; Supplementary Figure S7). Additionally, it contained a MDR region being identical to the respective regions of plasmids p54569_VIM (characterized from a ST92 *E. hormaechei* isolate in this study) and pEncl-30969cz (sequenced from a VIM-1-producing ST92 *E. cloacae* isolated, in 2015, in a Czech hospital; Papagiannitsis et al., 2018). Similar to pEncl-30969cz, the MDR of p58983_VIM was a Tn*1721*-like transposon structure containing In110, a Tn*21* fragment, a Tn*3*-like transposon, and a *qnrB*-like gene conferring resistance to quinolones (Halova et al., 2014). Two copies of an IS*5075* element, which was shown previously to target the IRs of Tn*21*-like transposons (Partridge and Hall, 2003), disrupted the IRs of the Tn*3*-like. The remaining part of the Tn*21 mer* module was probably deleted due to insertion of the Tn*3*-like transposon, but in contrast to pEncl-30969cz the Tn*3*-like was in an opposite orientation. Target site duplications of 6 bp (CAATAC) were found at the boundaries of Tn*1721*-like transposon, suggesting its transposition into the p58983_VIM backbone.

The non-typeable plasmid p56415_VIM, which carried the VIM-4-encoding integron In1174, was composed of two parts: the plasmidic backbone and the MDR region. The plasmidic backbone was identical to plasmid p51929, which was characterized from a VIM-4-encoding *C. freundii* isolate (Cfr-51929cz; Bitar et al., 2020). Even though the plasmid p51929 carried no resistance genes, Cfr-51929cz also harbored the VIM-4-encoding integron In1174 in the *mcr-9*-positive plasmid (p51929_MCR_VIM that belonged to IncHI2 group). The MDR region of p56415_VIM consisted of a Tn*3*-like element carrying the In1174 integron (Supplementary Figure S8). The same Tn*3*-like transposon was inserted into the chromosome of the *K. pneumoniae* isolate Kpn51135cz (as seen below). Unlike Kpn51135cz, the IRmer of the Tn*3*-like element was intact, whilst the IRtnp was disrupted by IS*5075*. Direct repeats of 6 bp (AATATG) were found at the boundaries of the integrated segment, suggesting its transposition into the p56415-VIM plasmid.

Finally, in *K. pneumoniae* isolate Kpn51135cz, the VIM-4-encoding integron In1174 was localized in a Tn*3*-like transposon element that was integrated into the *K. pneumoniae* chromosome (Supplementary Figure S9). The IR of the Tn*3*-like *tnp* module and the IR of the *mer* module, at the boundaries of the

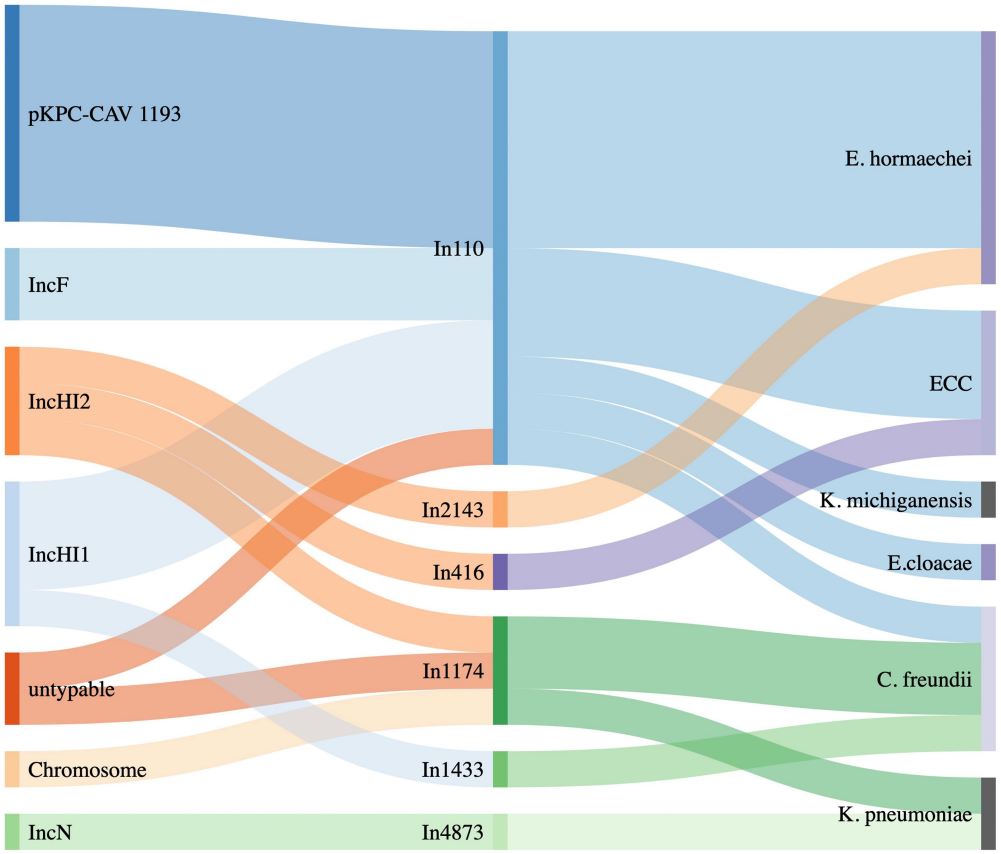

FIGURE 3
Sankey diagram showing the distribution of different integrons linking to the plasmid types (left) and to the bacterial species detected (right).

K. pneumoniae chromosome, were disrupted by two copies of the insertion sequences IS*4321*. Direct repeats of 5 bp (CTCAA) were found at the boundaries of the integrated segment, suggesting its transposition into the *K. pneumoniae* chromosome.

Discussion

In the current study, we characterized 32 VIM-producing Enterobacterales (including *E. cloacae*, *C. freundii*, *K. pneumoniae* and *K. michiganensis* isolates), which were isolated during the period of 2019–2020, in order to analyze the genetic determinants involved in the dissemination of bla_{VIM} alleles in various Czech hospitals. Our findings showed the presence of two bla_{VIM} variants, $bla_{VIM\text{-}1}$ ($n = 26$) and $bla_{VIM\text{-}4}$ ($n = 6$), carried by a significant number of integrons. The main VIM-1-encoding integron, identified during this study, was In110 ($n = 24$), while the In4873 was found in two ST54 *K. pneumoniae* isolates. On the other hand, three VIM-4-producing isolates included the In1174 integron, one isolate carried the In416, and the two remaining isolates carried novel integron structures. The In110 integron has been previously reported from isolates of Czech origin (Papousek et al., 2017; Papagiannitsis et al., 2018). Additionally, the presence of other integron types and the emergence of novel integron structures demonstrates the ongoing evolution of genetic determinants involved in the spread of resistance. Integrons usually carry more than one resistance gene, conferring resistance to multiple antimicrobial classes. Therefore, integrons are associated with the emergence of MDR bacteria and the fact of co-selection.

Moreover, the analysis of WGS data showed that bla_{VIM}-positive integrons were carried by several plasmids belonging to different Inc. groups (pKPC-CAV1193-like, HI1, HI2, FIB, N and non-typeable) and presenting diverse sizes (Table 1; Figure 3). Also, in one *K. pneumoniae* isolate, belonging to ST11, the VIM-4-encoding integron, In1174, was integrated into the chromosome (Supplementary Figure S9). Another interesting finding is the emergence of hybrid plasmids, such as p48411_VIM and p54569_VIM. The plurality of different plasmids, carrying bla_{VIM} alleles, and the emergence of hybrid plasmids are two features widening the spectrum of species that these resistance determinants could be disseminated. Also, of note was the characterization of plasmids being identical to VIM-1-encoding plasmid pLec-476cz (Supplementary Figure S2), which was previously characterized from a *L. adecarboxylata* isolate (Papousek et al., 2017) recovered during a survey study focused on compliance with hand hygiene among the staff of a different Czech hospital in May 2011. This data

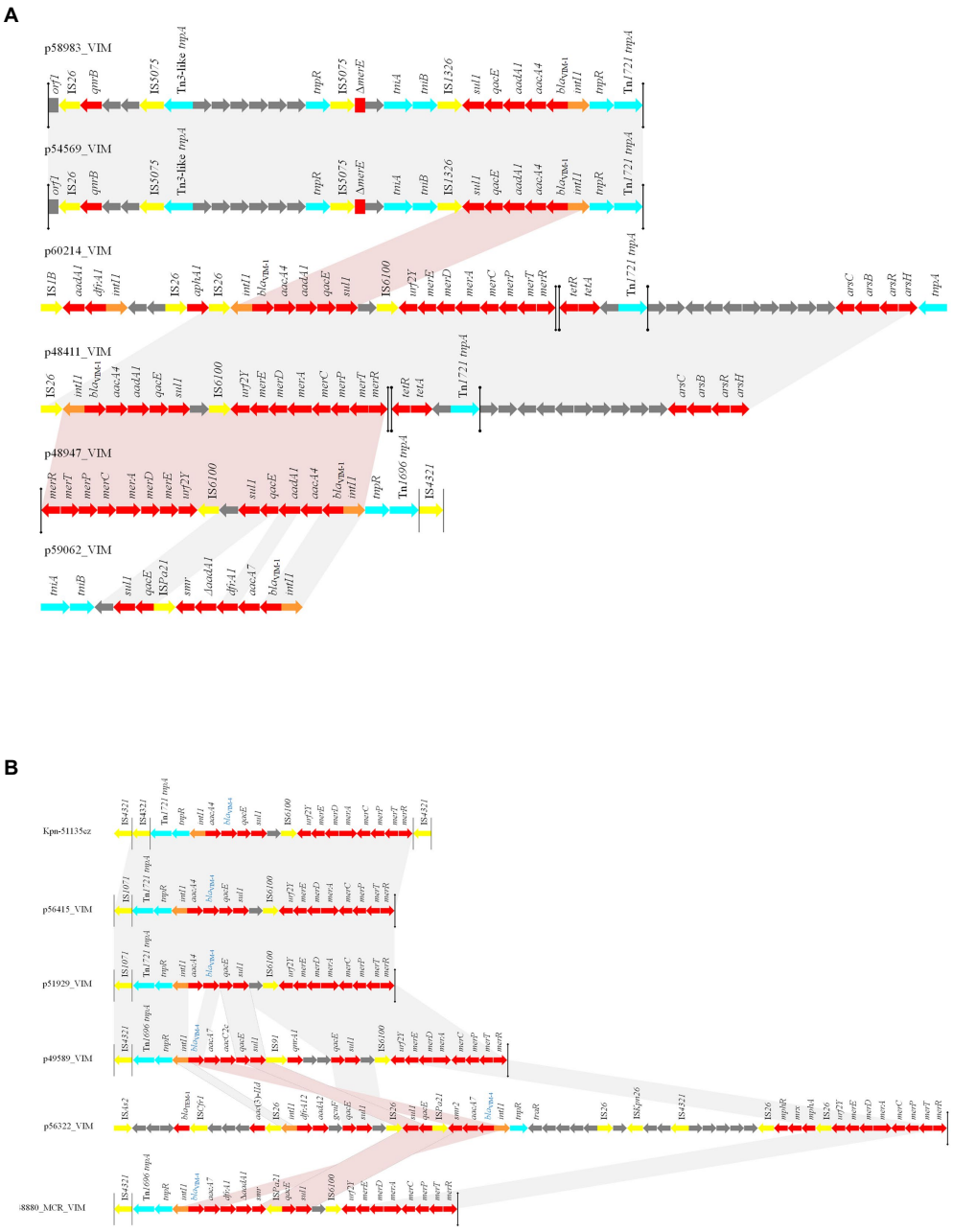

FIGURE 4
Linear comparisons of **(A)** VIM-1- **(B)** VIM-4- encoding MDR regions characterized from Enterobacterales isolated from Czech hospitals, during 2019–2020. Arrows show the direction of transcription of open reading frames (ORFs). Resistance genes are shown in red. IS elements and transposases are shown in yellow and aqua, respectively. *intI1* genes are shaded orange. The remaining genes are shown in gray. Homologous segments (representing ≥99% sequence identity) are indicated by light gray shading, while pink shading shows inverted homologous segments.

is worrying, since it highlights the hidden source, and the continuous spread of resistance determinants, and especially of carbapenemase-encoding genes, in Czech hospitals.

Finally, analysis of MDR regions revealed an increased divergence among these sequences (Figure 4). However, we observed the same VIM-1-encoding MDR region in IncHI1 (pNDM-CIT) plasmids (like p60214_VIM) and the IncFIB (pECLA) plasmid p48411_VIM, while a part of this structure was found in pKPC-CAV1193-like plasmids (like p48947_VIM). The presence of the same MDR region in plasmids of different Inc. groups may be the outcome of homologous recombination events. Also, we observed the presence of an identical transposition module in the IncFIB (pECLA) plasmid p54569_VIM and the non-typeable plasmid p58983_VIM. A totally different structure was identified in the IncN plasmid p59062_VIM. Regarding the VIM-4-encoding structures, we observed the presence of an

identical transposition module in the IncHI2 plasmid p51929_MCR_VIM, the non-typeable plasmid p56415_VIM and in the chromosome of the ST11 *K. pneumoniae* isolate Kpn51135cz. A similar transposition module, differing by acquisition of a different VIM-4-encoding integron (In2143 in p49589_VIM unlike In1174 in p56415_VIM) and of *qnrA1* resistance gene, was found in IncHI2 plasmid p49589_VIM. The presence of the same transposition modules into different replicons indicates the functional role of the specific transposons. On the other hand, totally diverse MDR regions were identified in IncHI1 (pNDM-CIT) plasmid p56322 and IncHI2 plasmid p48880_MCR_VIM.

One limitation of the study is not investigating the ability of the detected plasmids to conjugate. This is due to the high diversity in plasmids detected and to the different conjugation dynamics between *in-vitro* and *in-vivo*. This difference is prevalent for example to IncR and pKPC-CAV1193-like plasmids. The *in-vitro* conjugation assay for these two plasmids detected has a very low conjugation rate if any (Sheppard et al., 2016; Bitar et al., 2020) yet epidemiological results state the high ability of these plasmids to conjugate.

Of note, all pKPC-CAV1193 plasmids carried the In110 integrons which seems to be spread in Cesky Budejovice implying an outbreak of this plasmid in the city (Figures 1, 2). Moreover, all IncF and most of IncHI1 plasmids (except for one plasmid carrying In1433 integron; Figure 3) also carried In110 integrons. The IncHI2 plasmids carried different types of integrons such as In2143, In416 and In1174 (which was also found on the chromosome and on one un-typable plasmid). Finally, IncN plasmid carried In4873. This shows, although there is dominance of In110, that there are multiple integrons responsible for the dissemination of bla_{VIM} irrespective of the plasmid type. Additionally, of interest is the association of In110 with multiple replicons (Figure 3).

Conclusion

During this study, we observed the spread of VIM-encoding integrons, mainly of In110, among Enterobacterales isolated from Czech hospitals, in 2019 and 2020. Additionally, we noticed the presence of multiple mechanisms, including (i) the functional acquisition of bla_{VIM}-carrying transposons, (ii) the acquisition of bla_{VIM}-carrying MDR regions *via* homologous recombination events (iii) the ongoing evolution of bla_{VIM}-carrying integrons, (iv) and the hidden spread of bla_{VIM}-carrying replicons, involved in the emergence and spread of MDR regions carrying carbapenemase-encoding genes. Thus, ongoing surveillance of carbapenem-resistance is of utmost importance to control the spread of these emerging pathogens.

Data availability statement

The datasets presented in this study can be found in online repositories. The names of the repository/repositories and accession number(s) can be found in the article/Supplementary material.

Author contributions

IB and CP designed the study, analyzed the data, and wrote the manuscript. KC collected the samples. IB, LK, HZ, VM, EP, and MF conducted the experiments. IB and JH secured the funding. All authors contributed to the article and approved the submitted version.

Funding

The study was supported by research project grant NU20J- 05-00033, provided by the Czech Health Research Council, and by the project National Institute of Virology and Bacteriology (Programme EXCELES, ID Project No. LX22NPO5103) - funded by the European Union - Next Generation EU.

Acknowledgments

We would like to thank the Czech participants of the "Working Group for Monitoring of Antibiotic Resistance" for providing the isolates. The participants information is detailed in Supplementary Table S2.

Conflict of interest

The authors declare that the research was conducted in the absence of any commercial or financial relationships that could be construed as a potential conflict of interest.

Publisher's note

Supplementary material

The Supplementary material for this article can be found online at: https://www.frontiersin.org/articles/10.3389/fmicb.2022.993240/full#supplementary-material

References

Bankevich, A., Nurk, S., Antipov, D., Gurevich, A. A., Dvorkin, M., Kulikov, A. S., et al. (2012). SPAdes: a new genome assembly algorithm and its applications to single-cell sequencing. *J. Comput. Biol.* 19, 455–477. doi: 10.1089/cmb.2012.0021

Bitar, I., Papagiannitsis, C. C., Kraftova, L., Chudejova, K., Mattioni Marchetti, V., and Hrabak, J. (2020). Detection of five mcr-9-carrying Enterobacterales isolates in four Czech hospitals. *mSphere* 5:e01008-20. doi: 10.1128/mSphere.01008-20

Bolger, A. M., Lohse, M., and Usadel, B. (2014). Trimmomatic: a flexible trimmer for Illumina sequence data. *Bioinformatics* 30, 2114–2120. doi: 10.1093/bioinformatics/btu170

Colinon, C., Miriagou, V., Carattoli, A., Luzzaro, F., and Rossolini, G. M. (2007). Characterization of the IncA/C plasmid pCC416 encoding VIM-4 and CMY-4 beta-lactamases. *J. Antimicrob. Chemother.* 60, 258–262. doi: 10.1093/jac/dkm171

Ellington, M. J., Kistler, J., Livermore, D. M., and Woodford, N. (2007). Multiplex PCR for rapid detection of genes encoding acquired metallo-beta-lactamases. *J. Antimicrob. Chemother.* 59, 321–322. doi: 10.1093/jac/dkl481

European Committee on Antimicrobial Susceptibility Testing (EUCAST). (2012). *EUCAST guidelines for detection of resistance mechanism and specific resistances of clinical and/or epidemiological importance. European committee on antimicrobial susceptibility testing*. Växjö, Sweden:EUCAST.

Garcia-Fernandez, A., and Carattoli, A. (2010). Plasmid double locus sequence typing for IncHI2 plasmids, a subtyping scheme for the characterization of IncHI2 plasmids carrying extended-spectrum beta-lactamase and quinolone resistance genes. *J. Antimicrob. Chemother.* 65, 1155–1161. doi: 10.1093/jac/dkq101

Garcia-Fernandez, A., Villa, L., Moodley, A., Hasman, H., Miriagou, V., Guardabassi, L., et al. (2011). Multilocus sequence typing of IncN plasmids. *J. Antimicrob. Chemother.* 66, 1987–1991. doi: 10.1093/jac/dkr225

Halova, D., Papousek, I., Jamborova, I., Masarikova, M., Cizek, A., Janecko, N., et al. (2014). Plasmid-mediated quinolone resistance genes in Enterobacteriaceae from American crows: high prevalence of bacteria with variable qnrB genes. *Antimicrob. Agents Chemother.* 58, 1257–1258. doi: 10.1128/AAC.01849-13

Kraftova, L., Finianos, M., Studentova, V., Chudejova, K., Jakubu, V., Zemlickova, H., et al. (2021). Evidence of an epidemic spread of KPC-producing Enterobacterales in Czech hospitals. *Sci. Rep.* 11:15732. doi: 10.1038/s41598-021-95285-z

Laraki, N., Galleni, M., Thamm, I., Riccio, M. L., Amicosante, G., Frere, J. M., et al. (1999). Structure of In31, a blaIMP-containing Pseudomonas aeruginosa integron phyletically related to In5, which carries an unusual array of gene cassettes. *Antimicrob. Agents Chemother.* 43, 890–901. doi: 10.1128/AAC.43.4.890

Lombardi, G., Luzzaro, F., Docquier, J. D., Riccio, M. L., Perilli, M., Coli, A., et al. (2002). Nosocomial infections caused by multidrug-resistant isolates of pseudomonas putida producing VIM-1 metallo-beta-lactamase. *J. Clin. Microbiol.* 40, 4051–4055. doi: 10.1128/JCM.40.11.4051-4055.2002

Marchetti, V. M., Bitar, I., Sarti, M., Fogato, E., Scaltriti, E., Bracchi, C., et al. (2021). Genomic characterization of VIM and MCR co-producers: the first two clinical cases, in Italy. *Diagnostics (Basel)* 11:0079. doi: 10.3390/diagnostics11010079

Mazel, D. (2006). Integrons: agents of bacterial evolution. *Nat. Rev. Microbiol.* 4, 608–620. doi: 10.1038/nrmicro1462

Mazel, D., and Davies, J. (1999). Antibiotic resistance in microbes. *Cell. Mol. Life Sci.* 56, 742–754. doi: 10.1007/s000180050021

Miriagou, V., Papagiannitsis, C. C., Kotsakis, S. D., Loli, A., Tzelepi, E., Legakis, N. J., et al. (2010). Sequence of pNL194, a 79.3-kilobase IncN plasmid carrying the blaVIM-1 metallo-beta-lactamase gene in Klebsiella pneumoniae. *Antimicrob. Agents Chemother.* 54, 4497–4502. doi: 10.1128/AAC.00665-10

Miriagou, V., Tzelepi, E., Gianneli, D., and Tzouvelekis, L. S. (2003). Escherichia coli with a self-transferable, multiresistant plasmid coding for metallo-beta-lactamase VIM-1. *Antimicrob. Agents Chemother.* 47, 395–397. doi: 10.1128/AAC.47.1.395-397.2003

Moura, A., Soares, M., Pereira, C., Leitao, N., Henriques, I., and Correia, A. (2009). INTEGRALL: a database and search engine for integrons, integrases and gene cassettes. *Bioinformatics* 25, 1096–1098. doi: 10.1093/bioinformatics/btp105

Naas, T., Cuzon, G., Villegas, M. V., Lartigue, M. F., Quinn, J. P., and Nordmann, P. (2008). Genetic structures at the origin of acquisition of the beta-lactamase Bla KPC gene. *Antimicrob. Agents Chemother.* 52, 1257–1263. doi: 10.1128/AAC.01451-07

Papagiannitsis, C. C., Dolejska, M., Izdebski, R., Giakkoupi, P., Skalova, A., Chudejova, K., et al. (2016). Characterisation of IncA/C2 plasmids carrying an In416-like integron with the blaVIM-19 gene from Klebsiella pneumoniae ST383 of Greek origin. *Int. J. Antimicrob. Agents* 47, 158–162. doi: 10.1016/j.ijantimicag.2015.12.001

Papagiannitsis, C. C., Paskova, V., Chudejova, K., Medvecky, M., Bitar, I., Jakubu, V., et al. (2018). Characterization of pEncl-30969cz, a novel ColE1-like plasmid encoding VIM-1 carbapenemase, from an Enterobacter cloacae sequence type 92 isolate. *Diagn. Microbiol. Infect. Dis.* 91, 191–193. doi: 10.1016/j.diagmicrobio.2018.01.024

Papagiannitsis, C. C., Studentova, V., Ruzicka, F., Tejkalova, R., and Hrabak, J. (2013). Molecular characterization of metallo-beta-lactamase-producing Pseudomonas aeruginosa in a Czech hospital (2009-2011). *J. Med. Microbiol.* 62, 945–947. doi: 10.1099/jmm.0.056119-0

Papousek, I., Papagiannitsis, C. C., Medvecky, M., Hrabak, J., and Dolejska, M. (2017). Complete nucleotide sequences of two VIM-1-encoding plasmids from Klebsiella pneumoniae and Leclercia adecarboxylata isolates of Czech origin. *Antimicrob. Agents Chemother.* 61:2648. doi: 10.1128/AAC.02648-16

Partridge, S. R., and Hall, R. M. (2003). The IS1111 family members IS4321 and IS5075 have subterminal inverted repeats and target the terminal inverted repeats of Tn21 family transposons. *J. Bacteriol.* 185, 6371–6384. doi: 10.1128/JB.185.21.6371-6384.2003

Poirel, L., Heritier, C., Tolun, V., and Nordmann, P. (2004). Emergence of oxacillinase-mediated resistance to imipenem in Klebsiella pneumoniae. *Antimicrob. Agents Chemother.* 48, 15–22. doi: 10.1128/AAC.48.1.15-22.2004

Ren, Y., Ren, Y., Zhou, Z., Guo, X., Li, Y., Feng, L., et al. (2010). Complete genome sequence of Enterobacter cloacae subsp. cloacae type strain ATCC 13047. *J. Bacteriol.* 192, 2463–2464. doi: 10.1128/JB.00067-10

Rotova, V., Papagiannitsis, C. C., Skalova, A., Chudejova, K., and Hrabak, J. (2017). Comparison of imipenem and meropenem antibiotics for the MALDI-TOF MS detection of carbapenemase activity. *J. Microbiol. Methods* 137, 30–33. doi: 10.1016/j.mimet.2017.04.003

Sheppard, A. E., Stoesser, N., Wilson, D. J., Sebra, R., Kasarskis, A., Anson, L. W., et al. (2016). Nested Russian doll-like genetic mobility drives rapid dissemination of the Carbapenem resistance gene blaKPC. *Antimicrob. Agents Chemother.* 60, 3767–3778. doi: 10.1128/AAC.00464-16

Tato, M., Coque, T. M., Baquero, F., and Canton, R. (2010). Dispersal of carbapenemase blaVIM-1 gene associated with different Tn402 variants, mercury transposons, and conjugative plasmids in Enterobacteriaceae and Pseudomonas aeruginosa. *Antimicrob. Agents Chemother.* 54, 320–327. doi: 10.1128/AAC.00783-09

Yong, D., Toleman, M. A., Giske, C. G., Cho, H. S., Sundman, K., Lee, K., et al. (2009). Characterization of a new metallo-beta-lactamase gene, Bla(NDM-1), and a novel erythromycin esterase gene carried on a unique genetic structure in Klebsiella pneumoniae sequence type 14 from India. *Antimicrob. Agents Chemother.* 53, 5046–5054. doi: 10.1128/AAC.00774-09

Frontiers in Microbiology

Explores the habitable world and the potential of microbial life

The largest and most cited microbiology journal which advances our understanding of the role microbes play in addressing global challenges such as healthcare, food security, and climate change.

Discover the latest Research Topics

See more →

Frontiers

Avenue du Tribunal-Fédéral 34
1005 Lausanne, Switzerland
frontiersin.org

Contact us

+41 (0)21 510 17 00
frontiersin.org/about/contact